Systematics and evolutionary history of proterosuchian archosauriforms

by

Martin D. Ezcurra

A thesis submitted to the University of Birmingham for the degree of

DOCTOR OF PHILOSOPHY

Supervisor: Dr Richard J. Butler

Co-supervisor: Dr Ivan Sansom

School of Geography, Earth and Environmental Sciences

University of Birmingham

March 2015

250 million years ago…

"Life found the way" Alan Grant paraphrasing Ian Malcom (*Jurassic Park, 1993*)

…to survive and bloom again

From right to left: Richard J. Butler, Roland B. Sookias and Martín D. Ezcurra with a complete skull of a not-fully-grown *Erythrosuchus africanus* (BP/1/5207). Johannesburg, South Africa (May 2014).

Table of contents

Acknowledgement of collaborative work

Chapters 1 to 4 have been already published in collaboration with colleagues (Chapter 1: Ezcurra et al., 2013; Chapter 2: Ezcurra et al., 2014; Chapter 3: Ezcurra and Butler, 2015a; Chapter 4: Ezcurra and Butler, 2015b). In all cases, I designed or co-designed the research projects, conducted the research (i.e. collected, analysed and interpreted data), and wrote up the results. I was lead author on all of the resultant publications. My collaborators contributed to funding and designing the research projects, and provided comments and feedback on interpretations and drafts of manuscripts. Chapter 5 was conducted solely by me. I estimate that >95% of this thesis is my own work.

Abstract

The vertebrate clade Archosauromorpha comprises archosaurs (e.g. dinosaurs, birds, crocodilians) and several morphologically disparate Permian and Triassic taxa (e.g. tanystropheids, rhynchosaurs, proterosuchids, erythrosuchids, proterochampsians). The evolutionary history of archosauromorphs is of particular interest because it includes the origins of two of the best-known and most distinctive extant tetrapod groups: crocodylians and birds. Substantial previous research efforts have been focused on the crown group Archosauria, and by contrast the origin and early evolutionary radiation of archosauromorphs is relatively poorly understood. This incomplete understanding stems from the poor anatomical knowledge currently available for most of the early species of the clade and the paucity of detailed systematic work conducted in recent decades. In this thesis, the anatomy, taxonomy and systematics of the Permo-Triassic non-archosaur archosauromorphs are revised, with special emphasis on the proterosuchian archosauriforms. A revision of the Permian archosauromorph record indicates that only four Permian species are known (*Protorosaurus speneri*, *Eorasaurus olsoni*, *Archosaurus rossicus*, *Aenigmastropheus parringtoni* gen. et sp. nov.), which have a wider palaeobiogeographic distribution than previously appreciated. Following re-examination of proterosuchid taxa in collections worldwide, it is here concluded that there are three valid proterosuchid species in the *Lystrosaurus* Assemblage Zone of South Africa (*Proterosuchus fergusi*, *Proterosuchus goweri* sp. nov, *Proterosuchus alexanderi* comb. nov.). This result indicates a greater species richness of earliest Triassic archosauriforms than previously appreciated, but also that archosauriform morphological disparity remained low in this time interval. Qualitative and quantitative analyses of cranial ontogenetic

variation in *Proterosuchus fergusi* found that the skull of this species became proportionally taller, the infratemporal fenestra larger, and the teeth more isodont and numerous but with smaller crowns through ontogeny. The skulls of juvenile specimens of *Proterosuchus fergusi* closely resemble those of adults of the more basal archosauromorph *Prolacerta broomi*, whereas adult specimens of *Proterosuchus* resemble adults of more derived archosauriforms (e.g. erythrosuchids, *Euparkeria capensis*). This observation underpins the novel hypothesis that ontogenetic modification events (e.g. heterochrony) may have been key drivers of the evolution of the general shape of the skull at the base of Archosauriformes. The most comprehensive quantitative phylogenetic analysis to date focused on non-archosaurian archosauromorphs recovered a polyphyletic "Prolacertiformes" and restricted the taxonomic content of Proterosuchidae to only six species that occur immediately either side of the Permo-Triassic boundary. Erythrosuchidae was recovered as monophyletic and composed of eight nominal species, and *Euparkeria capensis* was found as the sister-taxon of the clade that includes proterochampsians (doswelliids + proterochampsids) and archosaurs. Phytosaurs were recovered within the crown-group Archosauria, as the most basal pseudosuchians. The results obtained here suggest that the evolutionary history of the archosauriforms during the Early Triassic can be subdivided into a first phase characterized by the short-lived "disaster-clade" Proterosuchidae and a second phase that witnessed the initial morphological and probably palaeoecological diversification of the group. A third phase in archosauriform evolution is documented by the diversification of the group into multiple ecomorphotypes during the Middle to Late Triassic.

Chapter 1: Introduction

The vertebrate clade Archosauromorpha comprises archosaurs (e.g. dinosaurs, birds, crocodylians) and several morphologically disparate Permian and Triassic taxa (e.g. tanystropheids, rhynchosaurs, proterosuchids, erythrosuchids, proterochampsians). Archosauromorphs were highly abundant in terrestrial ecosystems during the Mesozoic, and diversified into numerous species and ecomorphotypes. The evolutionary history of archosauromorphs is of particular interest because it includes the origins of two of the best-known and most distinctive extant tetrapod groups, crocodylians and birds. Most research efforts have been focused on the crown group, Archosauria (e.g. Nesbitt, 2011), and by contrast the origin and early evolutionary radiation of archosauromorphs is relatively poorly understood.

The stratigraphically oldest known taxon that can be unambiguously referred to Archosauromorpha is *Protorosaurus speneri* from the middle Lopingian (late Permian) of Europe (Meyer, 1832; Gottmann-Quesada and Sander, 2009) and other Palaeozoic archosauromorphs are rare (Ezcurra et al., 2014; Chapter 2). The archosauromorph fossil record becomes considerably richer and has a global distribution following the Permo-Triassic mass extinction. Early Triassic archosauromorphs are represented by at least five different lineages (Ezcurra et al., 2014; Chapter 2), but this post-extinction record is dominated by the families Proterosuchidae and Erythrosuchidae, in terms both of numbers of fossil specimens and taxonomic richness (Ezcurra et al., 2013). Proterosuchids and erythrosuchids were displaced from their dominant position in archosauromorph assemblages by other non-archosaurian archosauromorphs and archosaurs during the Middle and Late Triassic (e.g. Gower and Sennikov, 2000; Nesbitt, 2011).

Proterosuchidae (Fig. 1.1) and Erythrosuchidae (Fig. 1.2) represent the most basal lineages of Archosauriformes, the latter being a subclade of Archosauromorpha that also includes euparkeriids, proterochampsids, doswelliids, phytosaurs and the crown-group Archosauria (Gauthier et al., 1988). Proterosuchids and erythrosuchids were historically combined within "Proterosuchia", for which there are approximately 30 nominal species (Charig and Reig, 1970; Charig and Sues, 1976). The taxonomy and systematics of proterosuchians have suffered historically from a lack of robust resolution, and the taxonomic composition of both families has been debated. Nevertheless, most recent authors employing cladistic phylogenetic techniques have concluded that Proterosuchia is non-monophyletic (e.g. Juul, 1994; Gower and Sennikov, 1997; Dilkes and Sues, 2009; Ezcurra et al., 2010; Nesbitt, 2011; see Chapter 5), and I hereafter refer to "Proterosuchia" in inverted commas to acknowledge that likely paraphyly. Uncertainties in our understanding of proterosuchian taxonomy, systematics and evolution is largely a result of the poor anatomical knowledge currently available for most of the early species of the clade and the paucity of detailed systematic work conducted in recent decades. The main aim of this thesis is therefore to improve our anatomical, taxonomic and phylogenetic knowledge of the earliest known archosauromorphs, with a special emphasis on the taxonomy and systematics of proterosuchian archosauriforms. This work is crucial to understanding the adaptive radiation of the clade during the Triassic and its subsequent dominance of large-bodied vertebrate niches in terrestrial ecosystems for the rest of the Mesozoic.

The first part of the thesis (Chapter 2) is focused on the Palaeozoic archosauromorph record, and reviews the anatomy, taxonomy and systematics of the stratigraphically oldest members of the group. Permian fossil occurrences that have

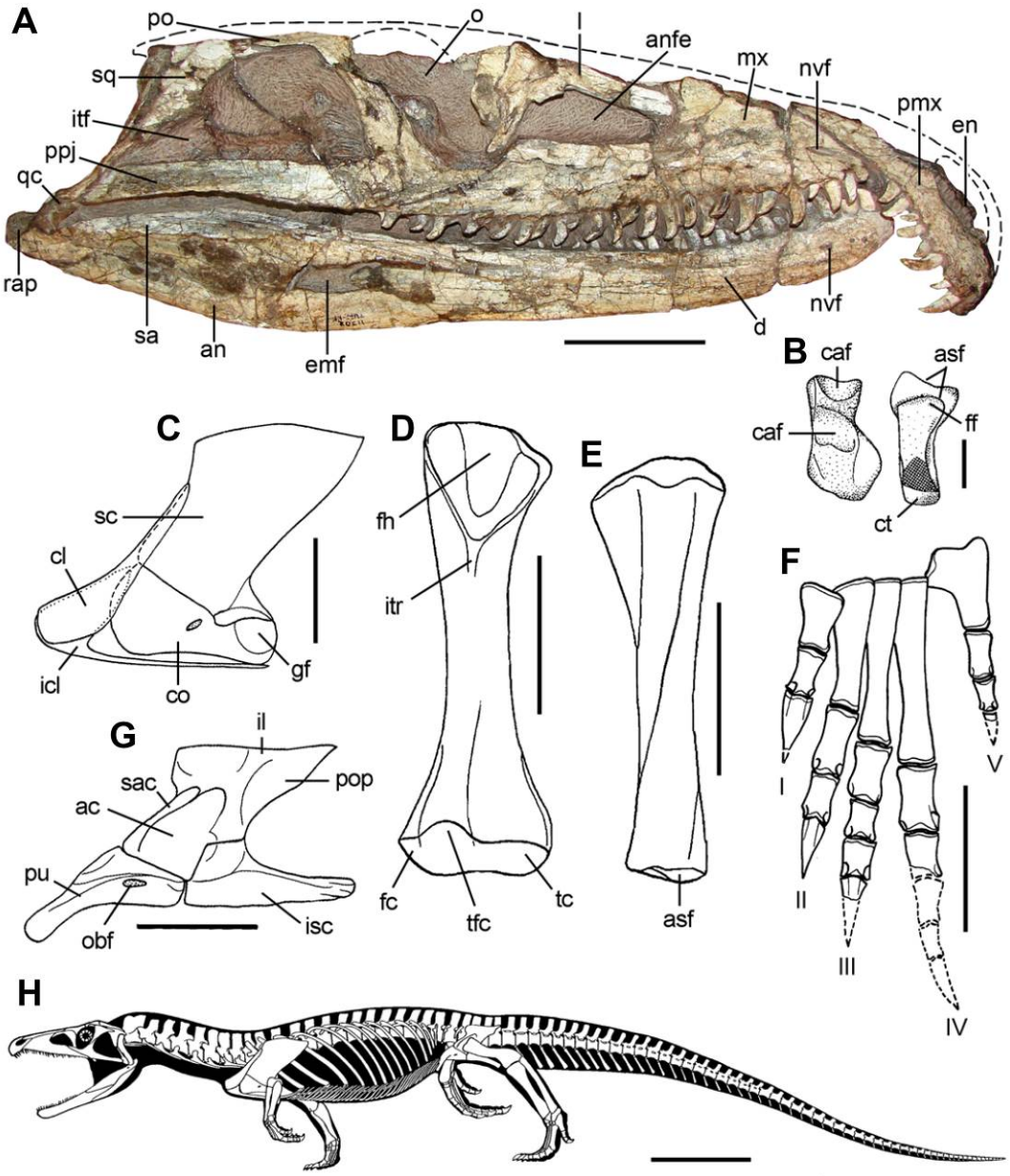

Figure 1.1. Selected bones and skeletal reconstruction of the proterosuchid *Proterosuchus fergusi*. (a) Skull in left lateral view (SAM-PK-11208; reversed to facilitate comparisons with Fig. 1.2a); (b) left astragalus (left) in distal view and left calcaneum (right) in proximal view; (c) articulated left pectoral girdle in lateral view; (d) left femur in ventral view; (e) left tibia in anterior view; (f) articulated left foot in dorsal view; (g) articulated left pelvic girdle in lateral view; (h) reconstruction of skeleton in lateral view. Abbreviations: I–V, pedal digit I–V; ac, acetabulum; an, angular; anfe, antorbital fenestra; asf, astragalar articular facet; caf, calcaneal articular facet; cl, clavicle; co, coracoid; ct, calcaneal tuber; d, dentary; emf, external mandibular fenestra; en, external naris; fc, fibular condyle; ff, fibular facet; fh, femoral head; gf, glenoid fossa; icl, interclavicle; il, ilium; isc, ischium; itf, infratemporal fenestra; itr, internal trochanter; l, lacrimal; mx, maxilla; nvf, neurovascular foramen; o, orbit; obf, obturator foramen; pmx, premaxilla; po, postorbital; pop, postacetabular process; ppj, posterior process of quadratojugal; pu, pubis; qc, quadrate distal condyles; rap, rtroarticular process; sa, surangular; sac, supraacetabular crest; sc, scapula; sq, squamosal; tc, tibial condyle; tfc, tibiofibular crest. Scale bars: 5 cm (a, c–f), 1 cm (b), 50 cm (h). Drawings (b–f) from Cruickshank (1972); reconstruction (h) from Parrish (1986), originally prepared by Gregory Paul.

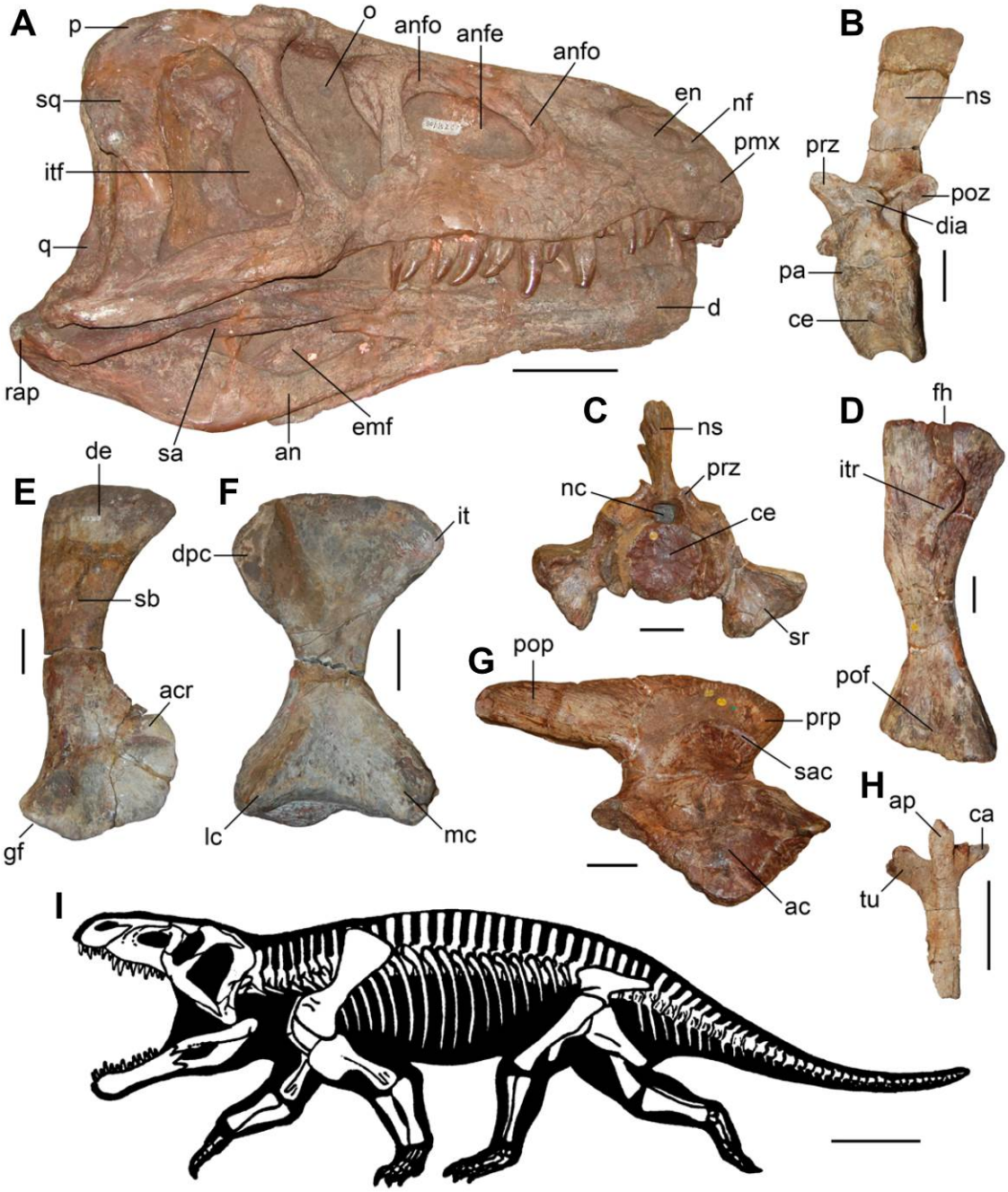

Figure 1.2. Selected bones and skeletal reconstruction of the erythrosuchid *Erythrosuchus africanus* (a, BP/1/5207; e, NHMUK3762a; b–d, f–h, NHMUK R3592). (a) Skull in right lateral view; (b) anterior dorsal vertebra in left lateral view; (c) first sacral vertebra in anterior view; (d) right femur in ventral view; (e) right scapula in lateral view; (f) right humerus in ventral view; (g) right ilium in lateral view; (h) proximal half of right anterior cervical rib in lateral view; (i) reconstruction of skeleton in lateral view. Abbreviations: ac, acetabulum; acr, acromion; an, angular; anfe, antorbital fenestra; anfo, antorbital fossa; ap, anterior process; ca, capitulum; ce, centrum; d, dentary; de, distal expansion; dia, diapophysis; dpc, deltopectoral crest; emf, external mandibular fenestra; en, external naris; fh, femoral head; gf, glenoid fossa; it, internal tuberosity; itf, infratemporal fenestra; itr, internal trochanter; lc, lateral distal condyle; mc, medial distal condyle; nc, neural canal; nf, narial fossa; ns, neural spine; o, orbit; p, parietal; pa, parapophysis; pmx, premaxilla; pof, popliteal fossa; pop, postacetabular process; poz, postzygapophysis; prp, preacetabular process; prz, prezygapophysis; q, quadrate; rap, retroarticular process; sa, surangular; sac, supraacetabular crest; sb, scapular blade; sq, squamosal; sr, sacral rib; tu, tuberculum. Scale bars: 10 cm (a), 5 cm (b–h), 50 cm (i). Reconstruction (i) modified from Gower (2003) by E. Lopez-Rolandi.

been referred to Lepidosauromorpha are also revisited in order to constrain temporally the lizard-crocodile split and, as a result, the origin of Archosauromorpha. The most abundant archosauromorph fossil material recovered from rocks deposited immediately after the Permo-Triassic extinction is the multiple mostly well-preserved proterosuchid specimens from the *Lystrosaurus* Assemblage Zone of South Africa (Charig and Sues, 1976; Ezcurra et al., 2013). This material is crucial to understanding the response of archosauromorphs to this mass extinction event. In Chapter 3, I reassess the taxonomy of the South African proterosuchid specimens in order to understand the taxonomic and morphological diversity present among earliest Triassic archosauriforms. The extensive sampling of well-preserved, three-dimensional skulls of the South African proterosuchid *Proterosuchus fergusi* represents a unique case among early archosauromorphs. This sampling is used in Chapter 4 to study the cranial changes that occurred in the ontogeny of *Proterosuchus fergusi*, with implications for understanding the role of heterochronic events in early archosauromorph evolution. Finally, the last section of the thesis (Chapter 5) is focused on the phylogenetic relationships of non-archosaurian archosauromorphs, with special emphasis on proterosuchian archosauriforms. The phylogenetic analysis conducted here represents the most exhaustive to date in terms of both taxonomic and character sampling. Several proterosuchian species are for the first time included here in a quantitative phylogenetic analysis, shedding new light on the diagnoses and taxonomic compositions of Proterosuchidae and Erythrosuchidae.

Chapter 2: The Permian archosauromorph record

2.1. Background

Saurians, or crown group diapsids, are highly taxonomically and morphologically diverse in extant ecosystems, with around 9,400 lepidosaur (snakes, lizards and rhynchocephalians) and 10,000 archosaur (birds and crocodilians) species, including cursorial, semi-aquatic, marine, fossorial and volant forms (Clements, 2007; Pyron et al., 2013). The stem-groups of Lepidosauria (non-lepidosaurian Lepidosauromorpha) and Archosauria (non-archosaurian Archosauromorpha) also include several morphologically disparate saurian lineages that were mostly restricted in time to the Triassic. These lineages formed important components of Triassic continental assemblages, and include kuehneosaurids, rhynchosaurs, proterosuchids, erythrosuchids, euparkeriids, doswelliids and proterochampsids (Dilkes, 1998; Evans, 2003; Ezcurra et al., 2013; Sookias and Butler, 2013; Sues et al., 2013; Trotteyn et al., 2013). However, the earliest (i.e. pre-Mesozoic) evolutionary history of Sauria is poorly known and there has been substantial debate regarding the late Paleozoic (i.e. Permian) record of the group (e.g. Parrington, 1956; Carroll, 1975, 1976; Ivachnenko, 1978; Gaffney, 1980; Reisz et al., 2000; Modesto and Reisz, 2002; Evans, 2003; Reisz and Modesto, 2007; Evans and Jones, 2010; Jones et al., 2013).

The best source of information on the early history of Sauria comes from the numerous fossils of the well-known basal archosauromorph *Protorosaurus speneri* from the Lopingian of Germany and England (Meyer, 1832; Evans and King, 1993; Gottmann-Quesada and Sander, 2009). Multiple less completely known specimens have also been argued to be Permian members of Sauria (e.g. Parrington's

"problematic reptile" from Tanzania, UMZC T836; Parrington, 1956). A better understanding of the Permian saurian record is fundamental for providing more accurate fossil constraints on the calibration of the crocodile-lizard (= bird-lizard) divergence, a major split within vertebrates that is of keen interest to molecular and evolutionary biologists and vertebrate palaeontologists alike (Reisz and Müller, 2004; Müller and Reisz, 2005; Benton and Donoghue, 2007; Sanders and Lee, 2007). A better knowledge of Permian saurians is also necessary to improve understanding of phylogenetic relationships among early members of Diapsida, an area of key interest because of the controversial systematic affinities of several possible saurian lineages including turtles, choristoderans and sauropterygians (e.g. Gregory, 1946; Rieppel and deBraga, 1996; deBraga and Rieppel, 1997; Platz and Conlon, 1997; Zardoya and Meyer, 1998; Rieppel and Reisz, 1999; Müller, 2004; Hill, 2005; Bhullar and Bever, 2009; Lyson et al., 2010, 2013; Lee, 2011; Shen et al., 2011; Neenan et al., 2013). New information on the Permian saurian record may also yield fresh insights into survivorship of this clade across the Permian-Triassic mass extinction and the dynamics of the dramatic saurian radiation in post-extinction ecosystems.

In this chapter, the Permian record of Sauria is revisited and reexamined to provide new information on the diversity, phylogeny, morphology, geographic distribution and physiology of Permian members of the clade, and the timing of the crocodile-lizard (or bird-lizard) split. Some Permian saurian specimens are fully or partially redescribed (e.g. UMZC T836; BP/1/4220; *Eorasaurus olsoni*) and a new genus and species of archosauromorph is erected, *Aenigmastropheus parringtoni*, for a specimen from the middle Lopingian of Tanzania. The new data offered here provides an improved understanding of early saurian and early archosauromorph evolutionary history, including calibration dates for molecular phylogenies.

2.2. Review of the Permian saurian record

Sauria comprises Lepidosauromorpha, Archosauromorpha, their most recent common ancestor, and all their extinct descendants (Gauthier et al., 1988). Several footprints and ichnotaxa potentially attributable to both lepidosauromorphs (e.g. *Ganasauripus ladinus*, *Paradoxichnium radeinensis*) and archosauromorphs (e.g. *Protochirotherium* isp., *Synaptichnium* isp.) have been described from Lopingian beds of southern Europe (Conti et al., 2000; Avanzini et al., 2011) and northern Africa (Hmich et al., 2006). However, here I focus solely on the body fossil record of Permian saurians.

2.2.1. *"Younginiformes"*

Several Lopingian diapsid species (all referred to at various points as "eosuchians") from South Africa (*Youngina capensis*: Broom, 1914; Gow, 1975), Tanzania (*Tangasaurus mennelli*: Haughton, 1924; Currie, 1982) and Madagascar (*Hovasaurus boulei*: Piveteau, 1926; Currie, 1981; *Acerosodontosaurus piveteaui*: Currie, 1980; Bickelmann et al., 2009; *Thadeosaurus colcanapi*: Carroll, 1981) have been considered by some authors to form a monophyletic Younginiformes (Currie, 1982; Benton, 1985; Evans, 1988) within Lepidosauromorpha (Gauthier, 1984; Benton, 1985; Evans, 1988; Gauthier et al., 1988). However, subsequent work has suggested that "Younginiformes" form a paraphyletic assemblage (Bickelmann et al., 2009), and these species are now widely accepted as basal non-saurian neodiapsids and therefore not lepidosauromorphs (e.g. Gaffney, 1980; Laurin, 1991; Jalil, 1997; Dilkes, 1998; Müller, 2004; Senter, 2004; Bickelmann et al., 2009; Reisz et al., 2010, 2011) (Fig. 2.1A). "Younginiformes" do not, therefore, represent Permian saurians.

2.2.2. *Other putative Permian lepidosauromorph records*

Five basal diapsid species (all referred to at various points as "eolacertilians") have been proposed as possible Permian lepidosauromorphs, and have often been identified as lizards: *Saurosternon bainii*, *Palaeagama vielhaueri*, *Paliguana whitei* and *Lacertulus bipes* from South Africa (Huxley, 1868; Broom, 1903, 1925; Carroll, 1975; Carroll and Thompson, 1982), the former three species forming the "Paliguanidae" of Carroll (1975), and *Lanthanolania ivakhnenkoi* from the Guadalupian (middle Permian) of Russia (Modesto and Reisz, 2002).

Among the South African specimens, the exact stratigraphic position of the type and only known specimen of *Saurosternon bainii* is poorly constrained (Huxley, 1868), but it is of definite Lopingian age (Carroll, 1975). By contrast, the type and only specimen of *Palaeagama vielhaueri* (Broom, 1926) cannot be stratigraphically constrained with certainty beyond a late Permian–Early Triassic age, although an Early Triassic age may be more likely (Carroll, 1975). The stratigraphic position of the type and only specimen of *Lacertulus bipes* is not constrained beyond Permian–Triassic (Carroll and Thompson, 1982). Whereas Carroll (1975) considered *Paliguana whitei* (Broom, 1903) to be of uncertain Lopingian –Triassic age, Kitching (Kitching, 1977) and Groenwald and Kitching (1995) listed this species as derived from the *Lystrosaurus* Assemblage Zone of Early Triassic age (Induan–?Olenekian; Damiani et al., 2000; Rubidge, 2005; Lucas, 2010).

Several of these species are of uncertain phylogenetic position. *Saurosternon bainii* and *Palaeagama vielhaueri* were assigned to Lepidosauromorpha by Gauthier et al. (1988), whereas Evans (2003) considered *Saurosternon bainii* as a possible basal lepidosauromorph and *Palaeagama vielhaueri* as an indeterminate diapsid.

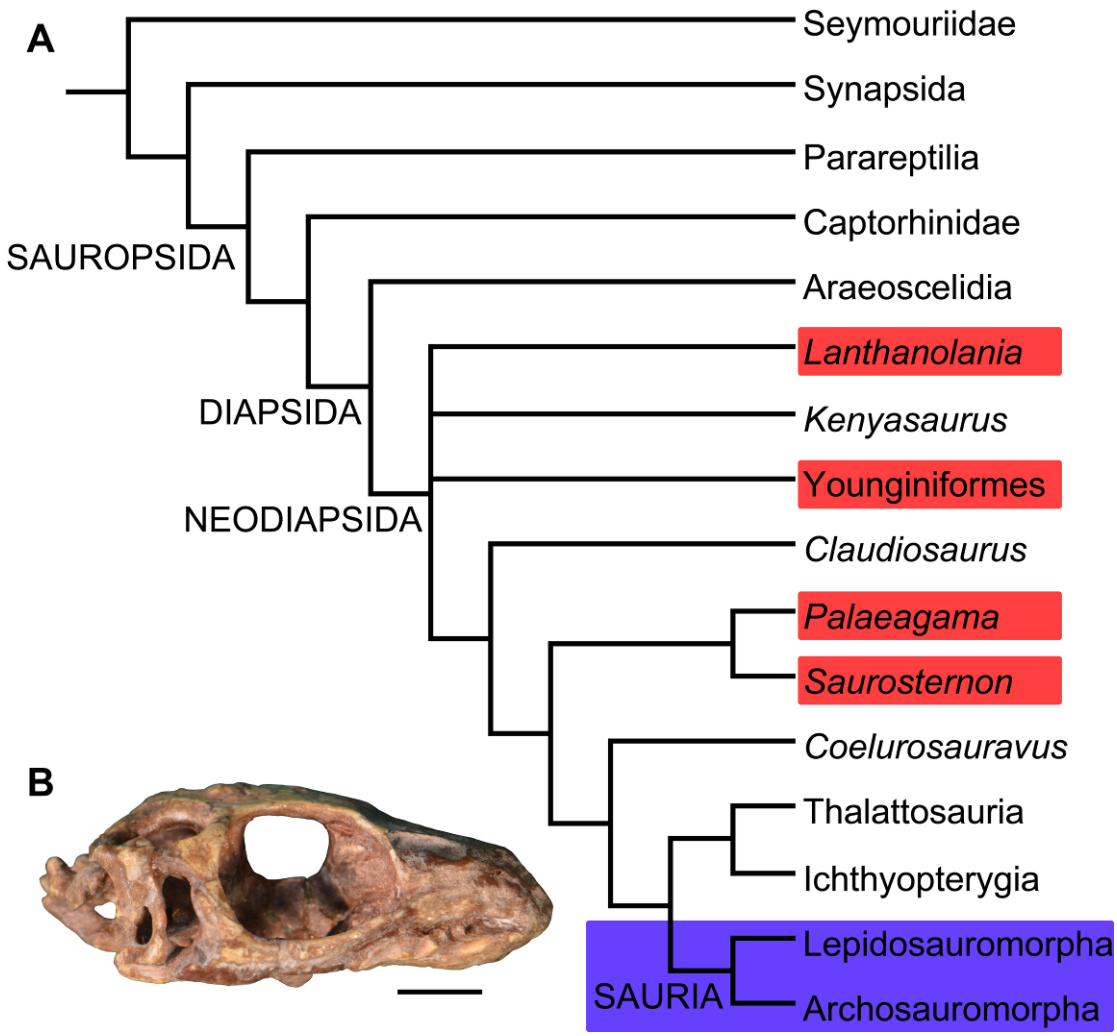

Figure 2.1. Simplified phylogenetic relationships of Diapsida. (A) Phylogenetic positions of Sauria (blue box) and several species previously considered as Permo-Triassic lepidosauromorphs (red boxes), based upon the phylogenetic analysis of Bickelmann et al. (2009) (illustration simplified) (B) Holotype (AM 3585) of *Paliguana whitei*, the oldest known lepidosauromorph from the Early Triassic of South Africa, in right lateral view. Scale bar equals 5 mm.

However, more recent quantitative phylogenetic analyses identified both species as non-saurian basal diapsids (Jones et al., 2013), possibly forming a monophyletic clade (Müller, 2004; Bickelmann et al., 2009) (Fig. 2.1A). These results do not therefore support the positions of *Saurosternon bainii* and *Palaeagama vielhaueri* within Sauria. *Lacertulus bipes* is not a squamate, but its phylogenetic relationships cannot be further determined because of the poor preservation of the specimen (Estes, 1983; Evans, 2003).

Paliguana whitei (Fig. 2.1B) possesses a quadrate conch (Evans, 1984; Evans and Borsuk-Białynicka, 2009; Evans and Jones, 2010; AM 201), a character widely accepted as a diagnostic feature of Lepidosauromorpha (Gauthier et al., 1988). As a result, Evans and Borsuk-Białynicka (2009) and Evans and Jones (2010) considered *Paliguana whitei* as referable to Lepidosauromorpha. In agreement with this hypothesis, the phylogenetic results of Chapter 5 recovered *Paliguana whitei* as a basal lepidosauromorph. However, as discussed above, *Paliguana whitei* is currently considered Early Triassic in age. Therefore, although *Paliguana whitei* is accepted as one of the oldest known lepidosauromorphs (Evans and Jones, 2010) it does not represent a Permian record of the group.

Finally, in the original description of the species *Lanthanolania ivakhnenkoi* from the Guadalupian of Russia, Modesto and Reisz (2002) recovered this species as a lepidosauromorph in some of the most parsimonious trees and as the sister-taxon of Sauria in others. These results suggested possible but uncertain saurian affinities. However, a more recent phylogenetic analysis recovered *Lanthanolania ivakhnenkoi* close to the base of Neodiapsida (Reisz et al., 2011) and outside Sauria, thus contradicting the possible inclusion of this species within Lepidosauromorpha or Sauria.

In summary, there is currently no Permian specimen that can unambiguously be assigned to Lepidosauromorpha. The earliest known member of Lepidosauromorpha (*Paliguana whitei*) comes from lowermost Triassic (Induan–?Olenekian) rocks that were deposited in the aftermath of the Permo-Triassic mass extinction.

2.2.3. *Permian records of Archosauromorpha*

Only three Permian species are currently considered as unambiguous members of Archosauromorpha: *Protorosaurus speneri* (Meyer, 1832) from Germany and England, and *Archosaurus rossicus* (Tatarinov, 1960) and *Eorasaurus olsoni* (Sennikov, 1997), both from Russia. In addition to these species, several incomplete specimens of Permian or possible Permian age have been considered as possible members of Archosauromorpha. This material includes a "problematic reptile" from Tanzania (Parrington, 1956), an isolated cervical vertebra from South Africa (Cruickshank, 1972), and some vertebral material from Uruguay (Dias-da-Silva et al., 2006). These three unambiguous Permian archosauromorphs and the additional possible records of the clade are discussed in more detail below.

"*Acanthotoposaurus bremneri*", based upon a single specimen (SAM-PK-K6888) from the Lopingian of South Africa, has been also considered an early member of Archosauromorpha (Evans and Heever, 1987). However, Reisz et al. (2000) provided a strong rebuttal to this interpretation and considered "*Acanthotoposaurus bremneri*" to be a subjective junior synonym of the "younginiform" *Youngina capensis* and, as a result, a non-saurian diapsid (see above). Another South African Lopingian taxon, *Heleosaurus scholtzi*, was suggested as a possible archosaur ancestor by Carroll (1976). However, *Heleosaurus* has never been

formally referred to Archosauromorpha, and Reisz and Modesto (2007) reinterpreted *Heleosaurus* as a varanopid synapsid, and thus non-diapsid. *Mesenosaurus romeri* from the Permian of Russia was reinterpreted by Ivachnenko (1978) as the oldest known archosaur, rather than a "pelycosaurian" synapsid as described by previous authors (Efremov, 1938; Romer and Price, 1940). However, additional specimens and new anatomical work have demonstrated that *Mesenosaurus romeri* is a varanopid synapsid (Reisz and Berman, 2001; Reisz et al., 2000).

2.2.3.1. *Protorosaurus speneri*. *Protorosaurus speneri* (Meyer, 1832) was a quadrupedal archosauromorph reaching a body length of 1.5–2 metres (Gottmann-Quesada and Sander, 2009), known from numerous specimens from the Lopingian Kupferschiefer Formation of Germany and England (Fig. 2.2). The first fossil specimen of *Protorosaurus speneri* was discovered in Germany in 1706, and Spener (1710) published a description of this specimen (identifying it as the remains of a Nile crocodile), making the taxon one of the first fossil reptiles ever described. Meyer (1830, 1832, 1856) identified the remains as those of a previously unknown extinct reptile, erected the new species *Protorosaurus speneri*, and published a monographic description. Subsequently, *Protorosaurus* remains were also recovered from England (Evans and King, 1993), and Gottman-Quesada and Sander (2009) recently published a full monographic redescription of *Protorosaurus speneri*, based on the abundant German material.

At least 28 *Protorosaurus speneri* specimens are known from the states of Thuringia and Hesse in central Germany. All of these German specimens come from the Kupferschiefer, part of the classic Permian Zechstein Group, which is divided into six cycles (Z1–Z6; e.g. Strohmenger et al., 1996). The Kupferschiefer forms part of

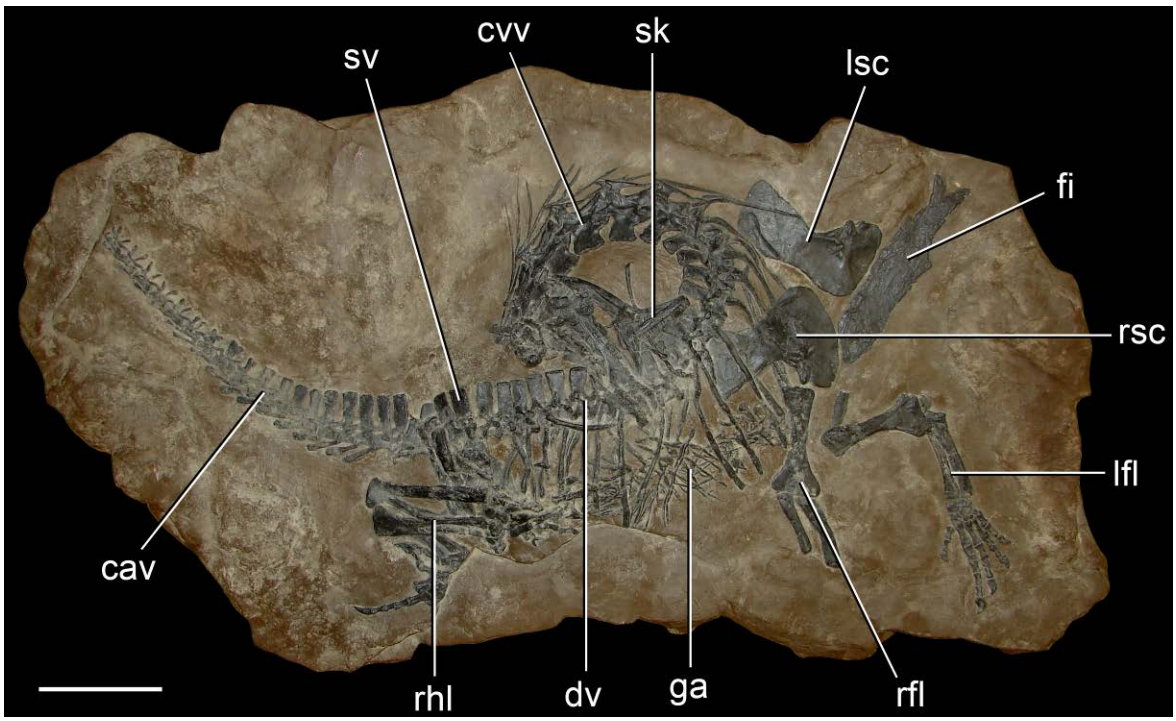

Figure 2.2. *Protorosaurus speneri*, a protorosaurian archosauromorph from the middle Lopingian of Western Europe. Axial skeleton primarily exposed in right lateral view (BSPG 1995 I 5, cast of WMSN P47361) collected near Münster, Germany. Abbreviations: cav, caudal vertebrae; cvv, cervical vertebrae; dv, dorsal vertebrae; fi, fisch; ga, gastralia; lfl, left forelimb; lsc, left scapula and coracoid; rfl, right forelimb; rhl, right hindlimb; rsc, right scapula and coracoid; sk, skull; sv, sacral vertebrae. Scale bar equals 10 cm.

the basal cycle of the Zechstein (Z1) and is a dark bituminous and calcareous shale deposited in a marine environment. The Kupferschiefer is often given as Tatarian (equivalent to the Wordian–Wuchiapingian) (e.g. Gottmann-Quesada and Sander, 2009) or Capitanian (e.g. Benton and Donoghue, 2007) in age. Brauns et al. (2003) reported a date of 257.3 ± 1.6 Ma (Lopingian: Wuchiapingian) for the Kupferschiefer based on a Re-Os geochronological study. The presence of the conodont *Mesogondolella britannica* in Kupferschiefer equivalents supports a middle Wuchiapingian age for the *Protorosaurus*-bearing levels (Legler et al., 2005; Legler and Schneider, 2008; Schneider pers. comm., 2012). *Protorosaurus* specimens from northwest England have been discovered in the Marl Slate (Evans and King, 1993), considered a lateral equivalent of the Kupferschiefer on the basis of independent geological data. A putative second species of *Protorosaurus* from England, *Protorosaurus huxleyi* (Hancock and Howse, 1870), was referred to the genus *Adelosaurus* by Evans (1988) and considered as a probable diapsid of uncertain affinities.

The phylogenetic position of *Protorosaurus speneri* within Archosauromorpha has been widely accepted and is uncontroversial (Gauthier, 1984; Benton, 1985; Evans, 1988; Laurin, 1991; Jalil, 1997; Benton and Allen, 1997; Dilkes, 1998; Rieppel et al., 2003; Gottmann-Quesada and Sander, 2009) and supported by the phylogenetic results of Chapter 5. *Protorosaurus speneri* has generally been considered to belong to a clade of otherwise Triassic archosauromorphs referred to either as Prolacertiformes or Protorosauria, although the composition and monophyly of this grouping is debated (see summary in Gottmann-Quesada and Sander, 2009). The phylogenetic results of Chapter 5 support referral of this species to Protorosauria, and suggest that “Prolacertiformes” is polyphyletic.

Sues and Munk (1996) briefly mentioned archosauromorph cranial and postcranial remains from fissure fill deposits at Korbach, in Hesse, central Germany, including “a *Protorosaurus*-like form and tooth-bearing jaw fragments of a large, as yet unidentifiable taxon”. The formation and infilling of this fissure was inferred to have taken place during the Z2 cycle of the Zechstein, indicating that these archosauromorph remains are slightly younger than *Protorosaurus speneri*. Unfortunately, more detailed descriptions of this material have not yet been published.

2.2.3.2. *Eorasaurus olsoni.* Sennikov (1997) erected *Eorasaurus olsoni* based on a sequence of cervico-dorsal vertebrae with one dorsal rib in articulation and some additional bone fragments (Figs. 2.3, 2.4). This material was collected from the bank of the Volga River in Tatarstan in European Russia during the 1930s. *Eorasaurus olsoni* comes from the upper substage of the Severodvinian regional stage (Sennikov, 1997, 2011). Recent magnetostratigraphic evidence suggests that the base of the Severodvinian stage is within the Capitanian (approximately middle Capitanian), but there exists uncertainty regarding the age of the upper boundary of the Severodvinian, which may be close to the Wuchiapingian–Changhsingian boundary (Taylor et al., 2009: fig. 8) or to the Capitanian–Wuchiapingian boundary (Taylor et al., 2009: p. 46). Accordingly, *Eorasaurus olsoni* is late Capitanian–Wuchiapingian in age and, as a result, roughly contemporaneous with (or possibly slightly older than) the middle Wuchiapingian *Protorosaurus speneri*.

Sennikov (1997) considered *Eorasaurus olsoni* to be closely related to *Protorosaurus speneri* and considered both taxa to be members of Protorosauridae. *Eorasaurus olsoni* was diagnosed by Sennikov on the basis of a combination of characters of the cervico-dorsal axial skeleton, such as moderately elongated and

strongly parallelogram-shaped vertebral centra, well-developed ridges situated below the diapophyses, absence of intercentra and three-headed anterior dorsal ribs (Sennikov, 1997: p. 95). Despite the importance of *Eorasaurus olsoni* as one of the oldest known archosauromorphs, this taxon has been largely ignored by subsequent authors. Sennikov (1997) provided a detailed description and drawings of *Eorasaurus olsoni*, and, as a result, a full redescription is not necessary here. However, the original description of the species is complemented with some additional observations and a few reinterpretations are provided based upon first hand examination of the specimens.

I agree with Sennikov (1997) in considering the holotype (PIN 156/109) and referred specimens (PIN 156/108, 110, 111) of *Eorasaurus olsoni* to belong to a single individual, because they possess the same mode of preservation and are congruent in size and morphology. The preserved bones of *Eorasaurus olsoni* are generally well preserved, but there are several broken areas and damaged surfaces. The vertebrae of *Eorasaurus olsoni* probably represent a continuous series of nine postaxial vertebrae, including middle (PIN 156/109; Fig. 2.3A–G) and posterior (PIN 156/108; Fig. 2.3H–L) cervical vertebrae and anterior dorsal vertebrae (PIN 156/110; Fig. 2.4A, B, E, F) (Table 2.1). The vertebrae of PIN 156/108 are interpreted as belonging to the posterior cervical series because the parapophyses are situated on the dorsal halves of the centra and the vertebrae of PIN 156/109 are identified as middle cervicals because the parapophyses are situated at mid-height on the anterior margins of the centra (Fig. 2.3: pa). By contrast, Sennikov (1997) originally interpreted the holotype vertebrae of PIN 156/109 as posterior cervical vertebrae and those of PIN 156/108 as more anterior cervicals. No traces of neurocentral sutures were observed in

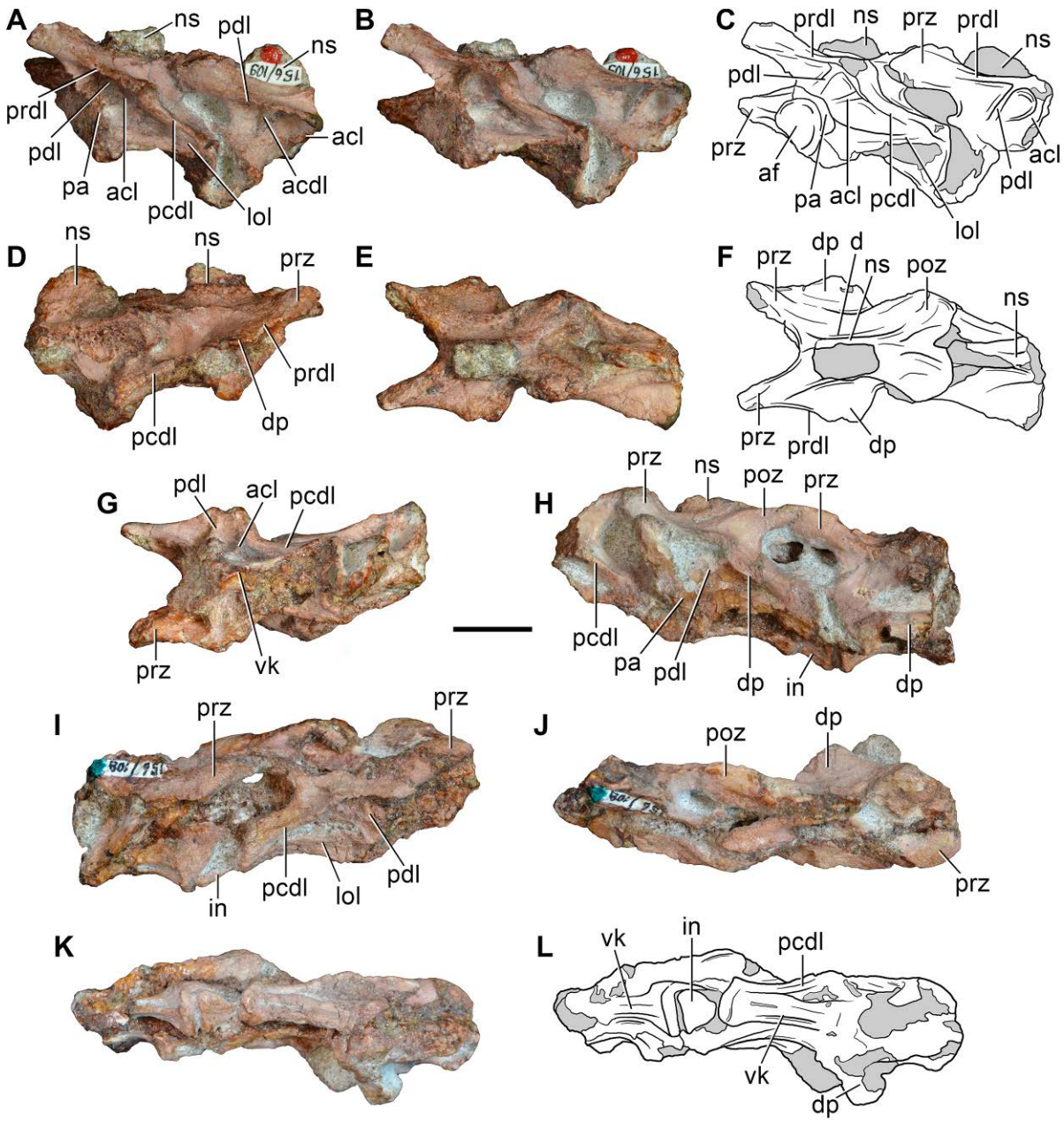

Figure 2.3. *Eorasaurus olsoni*, a possible early archosauriform from the late Guadalupian–early Lopingian of Russia. Middle (PIN 156/109: A–G) and posterior (PIN 156/108, holotype: H–L) cervical vertebrae in left lateral (A, H), left ventrolateral (B, C), right lateral (D, I), dorsal (E, F, J), and ventral (G, K, L) views. Abbreviations: acl, accessory lamina; af, anterior articular facet; d, depression; dp, diapophysis; in, intercentrum; lol, longitudinal lamina; ns, neural spine; pa, parapophysis; pcdl, posterior centrodiapophyseal lamina; pdl, paradiapophyseal lamina; poz, postzygapophysis; prdl, prezygodiapophyseal lamina; prz, prezygapophysis; vk, ventral keel. Scale bar equals 1 cm.

the vertebrae of *Eorasaurus olsoni*, suggesting that the specimen was not a juvenile when it died (Irmis, 2007).

The centra of the middle cervical vertebrae (PIN 156/109; Fig. 2.3A–G) possess low and well defined, median longitudinal ventral keels (Fig. 2.3: vk). The lateral surface of the centrum possesses a horizontal lamina that extends from the base of the parapophysis to the posterior margin of the centrum (Fig. 2.3: lol), resembling the condition of *Macrocnemus bassanii* (PIMUZ T4822) and *Tanystropheus longobardicus* (PIMUZ T2818). The lateral surface of the centrum immediately dorsal to the horizontal lamina is strongly concave, but the degree of concavity seems to be exaggerated due to the collapse of the cortical bone. The neural canal is considerably wider than tall in anterior view. Well-developed paradiapophyseal, posterior centrodiapophyseal and prezygodiapophyseal laminae extend away from the base of the diapophysis (Fig. 2.3: acdl, pcdl, pdl, prdl), as also occurs in the posterior cervical and/or dorsal vertebrae of the enigmatic neodiapsid *Helveticosaurus zollingeri* (PIMUZ T4352), numerous basal archosauromorphs (e.g. *Tanystropheus longobardicus*: Wild, 1973: figs. 52–54; *Protorosaurus speneri*: BSPG 1995 I 5, cast of WMSN P47361; *Spinosuchus caseanus*: Spielmann et al., 2009), and several basal archosauriforms and crown group archosaurs (e.g. *Erythrosuchus africanus*: NHMUK R3592, Gower, 2003; *Euparkeria capensis*: UMZC T921; *Bromsgroveia walkeri*: Butler et al., 2012; *Hypselorhachis mirabilis*: Butler et al., 2009; *Silesaurus opolensis*: Piechowski and Dzik, 2010; *Herrerasaurus ischigualastensis*: PVSJ 373, Novas, 1993). The posterior centrodiapophyseal lamina extends to the posterodorsal corner of the centrum and contacts in this area the horizontal lamina of the centrum.

The neural arch laminae delimit centrodiapophyseal and prezygapophyseal centrodiapophyseal fossae, but the postzygapophyseal centrodiapophyseal fossa is

Table 2.1. Measurements of the preserved bones of *Eorasaurus olsoni* (PIN 156/108, 109, 110) in millimetres. Values between brackets indicate incomplete measurements and the value given is the maximum measurable. The length along the zygapophyses is the maximum anteroposterior length between the anterior tips of the prezygapophyses and the posterior tips of the postzygapophyses. In PIN 156/110 the vertebrae were labeled as A or B, where A corresponds to the most anterior element in the specimen. Maximum deviation of the digital caliper equals 0.02 mm but measurements were rounded to the nearest 0.1 millimetre.

PIN 156/108	**Most anterior almost complete vertebra**		
	Centrum length	18.3	
	Anterior articular facet height	(8.4)	
	Anterior articular facet width	ca. 6.4	
	Posterior articular facet width	10.2	
	Maximum height of the vertebra	(21.8)	
	Length along zygapophyses	28.8	
	Length of base of neural spine	(11.4)	
	Intercentrum length	4.7	
	Intercentrum width	5.7	
PIN 156/109	**Most anterior almost complete vertebra**		
	Centrum length	16.9	
	Anterior articular facet height	10.0	
	Anterior articular facet width	9.2	
	Posterior articular facet height	10.4	
	Posterior articular facet width	ca. 9.8	
	Maximum height of the vertebra	(18.8)	
	Neural canal height	2.9	
	Neural canal width	6.7	
	Length along zygapophyses	28.2	
	Length of base of neural spine	11.0	
PIN 156/110	**Vertebra**	**A**	**B**
	Centrum length	16.5	-
	Anterior articular facet height	(8.4)	-
	Anterior articular facet width	(6.8)	-
	Maximum height of the vertebra	(17.4)	(11.0)
	Length along zygapophyses	(23.3)	ca. 21.2
	Transverse process width	(5.8)	11.5
	Transverse process length at distal end	-	7.6
	Neural spine length	(8.7)	(9.6)
	Anterior dorsal rib		
	Length	(23.9)	
	Anteroposterior proximal depth	(15.8)	
	Length tubercular facet	3.6	
PIN 156/111	**Long bone**	**A**	**B**
	Length	(46.4)	(38.7)

absent. The centrodiapophyseal fossa is subdivided by an accessory lamina that extends anteriorly from the posterior centrodiapophyseal lamina and contacts the base of the parapophysis and the paradiapophyseal lamina (Fig. 2.3: acl). This accessory lamina is not present in other basal diapsids and represents an autapomorphy of *Eorasaurus olsoni*. A ridge extends anteriorly from the base of the postzygapophysis onto the lateral surface of the neural arch, and curves ventrally, being positioned between the prezygapophysis and diapophysis but without reaching either of these structures. This ridge delimits the lateral margin of a shallow depression positioned next to the base of the neural spine (Fig. 2.3: d). A similar depression is also found in the cervical vertebrae of several basal archosauromorphs (e.g. *Protorosaurus speneri*: BSPG 1995 I 5; *Prolacerta broomi*: BP/1/2675; *Proterosuchus fergusi*: GHG 231). The base of the neural spine is transversely thin and not as wide as it appears in the drawing in the original description (Sennikov, 1997: fig. 1d). There is no evidence of intercentra in PIN 156/109 (Jalil, 1997).

The posterior cervical vertebrae (PIN 156/108) (Fig. 2.3H–L) possess a morphology that is very similar to that found in the middle cervical vertebrae, including the presence of a ventral longitudinal keel and the same suite of laminae on the centrum and neural arch. The accessory lamina that divides the centrodiapophyseal fossa is even more extensively developed laterally in the posterior cervical vertebrae than the middle cervicals. The neural arches of the posterior cervicals of PIN 156/108 each possess an incipient postzygapophyseal centrodiapophyseal fossa, consistent with their more posterior position in the axial series than the middle cervical vertebrae of PIN 156/109. There is no depression lateral to the base of the neural spine. Two intercentra are present in PIN 156/108 but were overlooked in the original description of the specimen. The presence of

intercentra resembles the condition observed in the postaxial cervical vertebrae of several basal archosauromorphs (e.g. *Macrocnemus bassanii*: PIMUZ T4822; *Trilophosaurus buettneri*: Spielmann et al., 2008: fig. 30; *Proterosuchus alexanderi*: NMQR 1484). By contrast, postaxial cervical intercentra are absent in *Tanystropheus longobardicus* (PIMUZ T2817), *Protorosaurus speneri* (Gottmann-Quesada and Sander, 2009), *Mesosuchus browni* (Dilkes, 1998) and *Howesia browni* (Dilkes, 1995). The intercentra are situated anterior to the most complete vertebrae of PIN 156/108 (Fig. 2.3: in). The intercentra are proportionally large and subtriangular in ventral view, with a transversely broad posterior margin and a tapering anterior end.

The general morphology of the anterior dorsal vertebrae (PIN 156/110) is congruent with that of the cervical vertebrae, but in the anterior dorsals the centrum is subrectangular in lateral view (Fig. 2.4A, B, E, F). The neural arches of the anterior dorsal vertebrae possess prezygodiapophyseal, posterior centrodiapophyseal and anterior centrodiapophyseal/paradiapophyseal laminae (Fig. 2.4: acdl, pcdl, prdl). It is not possible to determine whether or not the latter lamina reached the parapophysis because the relevant area is damaged. The centrodiapophyseal, prezygapophyseal centrodiapophyseal, and postzygapophyseal centrodiapophyseal fossae are present and the latter fossa is better developed than in the posterior cervical vertebrae (PIN 156/108). There is no accessory lamina subdividing the centrodiapophyseal fossa, contrasting with the condition in the cervical vertebrae (PIN 156/108, 109). The left transverse process of the third anterior dorsal vertebra of PIN 156/110 is complete and is very strongly developed laterally, with a transverse length to centrum length ratio of 0.70 (Fig. 2.4B: tp). This ratio resembles that observed in the anterior dorsal vertebrae of *Trilophosaurus buettneri* (0.84, Spielmann et al., 2008: fig. 37), *Proterosuchus alexanderi* (0.95, NMQR 1484) and *Erythrosuchus africanus* (0.85, NHMUK R3592).

By contrast, proportionally shorter transverse processes are present in the anterior dorsal vertebrae of *Youngina capensis* (0.46, BP/1/3859), early lepidosaurs (e.g. *Gephyrosaurus bridensis*: Evans, 1981: figs. 5, 6; *Planocephalosaurus robinsonae*, 0.18–0.25, Fraser and Walkden, 1984: figs. 5, 6), protorosaurs (*Protorosaurus speneri*, 0.38–0.45, BSPG 1995 I 5; *Tanystropheus longobardicus*, 0.46, SMNS 54628), *Macrocnemus bassanii* (0.56, PIMUZ T2472), *Mesosuchus browni* (approximately 0.5, Dilkes, 1998: p. 513) and *Prolacerta broomi* (0.55, BP/1/2675). The transverse process of *Eorasaurus olsoni* is slightly anteroposteriorly compressed close to its base, but possesses an overall subrectangular outline in dorsal view. There is no depression on the neural arch lateral to the base of the neural spine, similar to the condition in the posterior cervical vertebrae (PIN 156/108) but contrasting with condition in the middle cervical vertebrae (PIN 156/109).

The proximal half of the left dorsal rib is preserved in near articulation with the third vertebra of PIN 156/110 (Fig. 2.4A, B, E, F). The capitulum of this anterior dorsal rib lacks its distal end, but the process is relatively long. The tuberculum is complete and is very short. The articular facet of the tuberculum is flat and oval, with an acute posterior margin. The tuberculum is not well differentiated from the rest of the rib due to the presence of a thin lamina of bone that connects it with the capitulum (Fig. 2.4E: la). The lamina extends up to the same level as the articular facet of the tuberculum. An apparent notch between the capitulum and the lamina is the result of breakage. There is no conclusive evidence for the presence of a third articular facet on the anterior dorsal rib (contra Sennikov, 1997). Although the lamina between the capitulum and tuberculum resembles a similar lamina that houses the third articular facet in *Prolacerta broomi* (BP/1/2675), *Proterosuchus alexanderi* (NMQR 1484) and

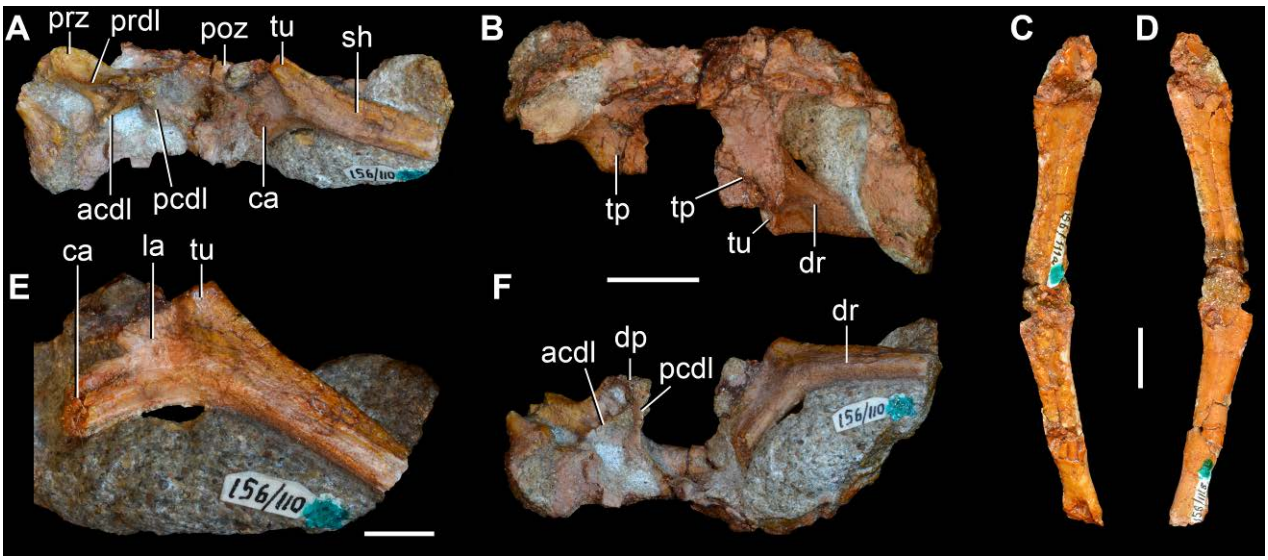

Figure 2.4. *Eorasaurus olsoni*, a possible early archosauriform from the late Guadalupian–early Lopingian of Russia. Anterior dorsal vertebrae and rib in articulation (PIN 156/110: A, B, F), close-up of the anterior dorsal rib (E), and probable long bones (PIN 156/111a, b: C, D) in left lateral (A, E), dorsal (B), and ventral (F) views. Abbreviations: acdl, anterior centrodiapophyseal lamina; ca, capitulum; dp, diapophysis; dr, anterior dorsal rib; la, lamina; pcdl, posterior centrodiapophyseal lamina; prdl, prezygodiapophyseal lamina; poz, postzygapophysis; prz, prezygapophysis; sh, shaft; tp, transverse process; tu, tuberculum. Scale bars equal 1 cm in (A–D, F) and 5 mm in (E).

Erythrosuchus africanus (Gower, 2003), the preserved portion of the lamina in PIN 156/110 lacks the transverse thickening that bears the facet in the those taxa.

PIN 156/111 is represented by two long bones (PIN 156/111a, 111b; Fig. 2.4C, D) and a small block of matrix with some unidentified partial bones (PIN 156/111). PIN 156/111a and 111b are interpreted as two limb bones in articulation. They do not seem to be rib shafts because they lack the curvature that would be expected for a rib and the proximal and distal ends of the bones are subequally expanded (contra Sennikov, 1997). Neither bone appears to be a femur and, as a result, they may represent a humerus and an ulna or radius. The long bones are strongly flattened, resembling the condition of the forelimb bones of protorosaurian archosauromorphs (e.g. *Tanystropheus longobardicus*: Wild, 1973). However, there are no clear features that would allow a confident identification of these bones; as a consequence, they are not very informative.

The morphology of *Eorasaurus olsoni* is congruent with that observed in basal archosauromorphs (e.g. presence of well developed prezygodiapophyseal and anterior and posterior centrodiapohyseal laminae, anterior dorsal zygapophyses close to the sagittal plane of the axial skeleton; cf. Sennikov, 1997). Indeed, the phylogenetic results of Chapter 5 recovered *Eorasaurus olsoni* as a derived archosauromorph within Archosauriformes.

The reexamination of the anatomy of *Eorasaurus olsoni* allowed a reinterpretation of some characters that were included in the original diagnosis of the species, including the supposed absence of intercentra and the presence of a dorsal rib with three articular facets. Accordingly, an emended diagnosis for the species is provided here. *Eorasaurus olsoni* is a small archosauromorph that differs from other diapsids in possessing the following combination of characters: presence of

prezygodiapophyseal and anterior and posterior centrodiapophyseal laminae; an accessory lamina that extends anteroventrally from the posterior centrodiapophyseal lamina and subdivides the centrodiapophyseal fossa (autapomorphic); strongly parallelogram-shaped middle and posterior cervical centra; and presence of postaxial cervical intercentra.

2.2.3.3. *Archosaurus rossicus.* Tatarinov (1960) described *Archosaurus rossicus* on the basis of fragmentary cranial and postcranial remains from the latest Vyatkian Gorizont in the Vladamir region, European Russia (Newell et al., 2010). *Archosaurus rossicus* comes from the upper fossil assemblage at the Vyazniki locality, which is interpreted to represent the youngest Permian beds of the Permo-Triassic European Russian sucession and also includes dvinosaurid temnospondyls, microsaurs, anthracosaurs, pareiasaurs, therocephalians, and dicynodonts (Sennikov, 1988a; Gower and Sennikov, 2000; Benton et al., 2004; Sennikov and Golubev, 2006, 2012; Newell et al., 2010). The Vyatkian Gorizont has been recently correlated with the Lopingian of the international stratigraphic scale (Newell et al., 2010, 2012).

Sennikov (1988a) subsequently referred to *Archosaurus rossicus* an additional dentary from the same general locality as the holotype and paratypes, as well as two isolated elements from a second locality. These referrals were based on the presence of congruent proterosuchid morphology. Sennikov (1988a) also revised the taxonomic status of *Archosaurus rossicus* (see also Gower and Sennikov, 2000; Sennikov, 2008). However, I note that some caution is warranted with regard to the assignment of the paratype and referred specimens from the type locality to *Archosaurus rossicus* given that they come from three different geographical points and different stratigraphic levels within a geographically large locality with a stratigraphic thickness of around

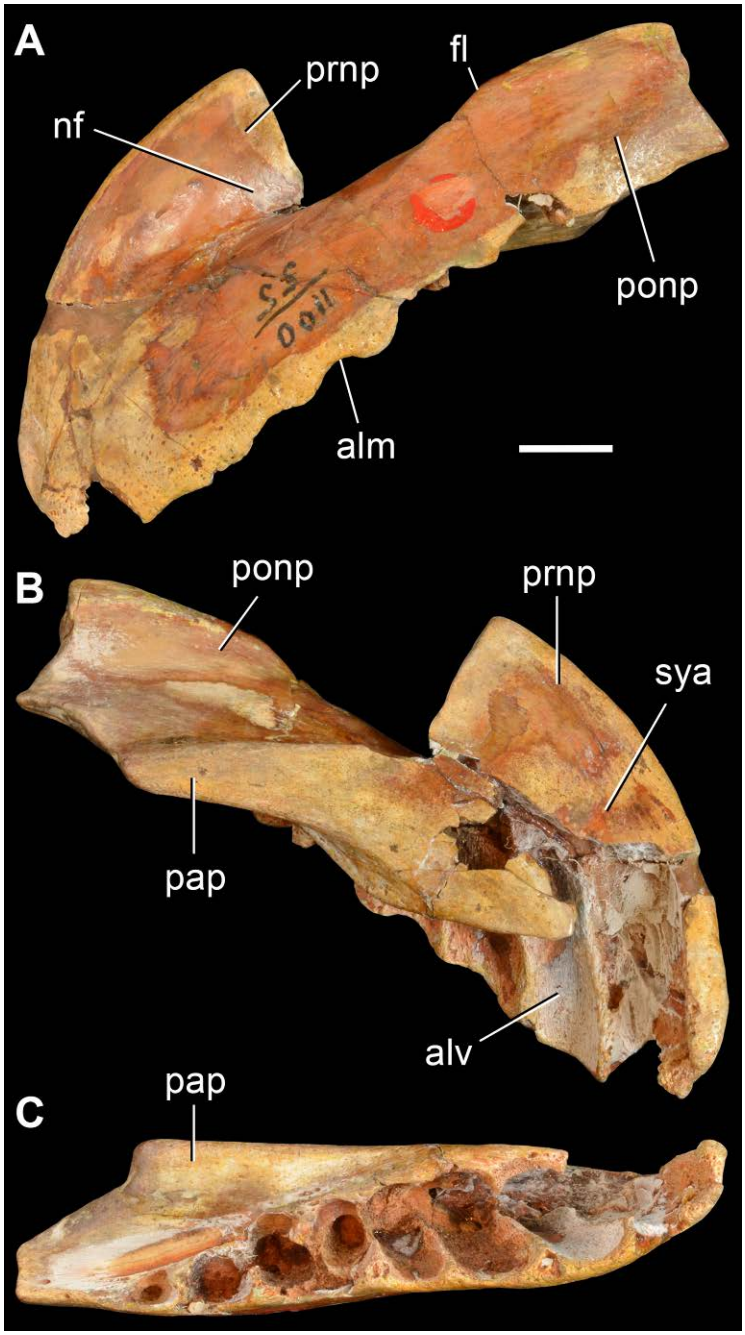

Figure 2.5. *Archosaurus rossicus*, a proterosuchid archosauriform from the latest Permian of Russia. Left premaxilla (PIN 1100/55, holotype) in lateral (A), medial (B) and ventral (C) views. Abbreviations: alm, alveolar margin; alv, alveolus; fl, lateral flange; nf, narial fossa; pap, palatal process; ponp, postnarial process; prnp, prenarial process; sya, symphyseal area. Scale bar equals 1 cm.

Table 2.2. Measurements of the holotype of *Archosaurus rossicus* (PIN 1100/55) in millimetres. Values between brackets indicate incomplete measurements and the value given is the maximum measurable. Maximum deviation of the digital caliper equals 0.02 mm but measurements were rounded to the nearest 0.1 millimetre.

Premaxilla		
	Length	(83.3)
	Height of the premaxillary body	19.8
	Length of the premaxillary body	73.6
	Maximum height	(34.6)
	Length first alveolus	11.1
	Length second alveolus	7.8
	Length third alveolus	8.3
	Length fourth alveolus	6.7
	Length fifth alveolus	5.6
	Length sixth alveolus	6.3
	Length seventh alveolus	7.1
	Length eighth alveolus	5.4

25 metres (Sennikov pers. comm., 2013). In addition to the holotype premaxilla (PIN 1100/55; Fig. 2.5; Table 2.2), I consider that the only previously referred specimens of *Archosaurus rossicus* that can be confidently identified as referable to Archosauriformes are the left dentary (PIN 1100/78), skull roof (PIN 1100/48) and possibly a tooth crown (PIN 1100/85). In addition, the cervical vertebrae (PIN 1100/66, 66a, 66b) referred by Tatarinov (1960) to *Archosaurus rossicus* possess a morphology that is very similar to and congruent with that of the cervical vertebrae of *Proterosuchus alexanderi* (NMQR 1484), and therefore they also possibly belong to an archosauriform.

The bone identified as a squamosal (PIN 1100/84a) and referred to *Archosaurus rossicus* by Tatarinov (1960) does not possess a morphology congruent with that of a squamosal. For example, it lacks a facet for articulation with the quadrate head and possesses a tuberosity on the posterodorsal border of the supposed supratemporal fenestra. Moreover, the anterior process is unusually transversely thick. Accordingly, I doubt the identification of this bone and, as a result, its archosauriform affinities.

The holotype premaxilla of *Archosaurus rossicus* (Fig. 2.5) differs from most basal archosauromorphs in that the first four premaxillary alveoli open lateroventrally (Fig. 2.5C), contrasting with the mostly ventrally opening anterior alveoli of *Prolacerta broomi* (BP/1/471), *Sarmatosuchus otschevi* (PIN 2865/68-9), *Tasmaniosaurus triassicus* (UTGD 54655) and *Erythrosuchus africanus* (NHMUK R3592). In addition, the angle formed between the anterior margin of the premaxillary body and the alveolar margin is more acute in *Archosaurus rossicus* than in *Proterosuchus fergusi* (RC 59, SAM-PK-11208) and "*Chasmatosaurus*" *yuani* (IVPP

V36315, V4067). Accordingly, the holotype specimen of *Archosaurus rossicus* is diagnostic and, as a result, the genus and species can be considered valid.

Archosaurus rossicus has been widely accepted as a proterosuchid archosauriform (Tatarinov, 1960; Charig and Sues, 1976; Sennikov, 1988a; Gower and Sennikov, 2000), and quantitative phylogenetic support for this position has been recovered by Nesbitt (2011) and by the phylogenetic analysis of Chapter 5.

2.2.3.4. Putative proterosuchian from the late Permian of South Africa.

Cruickshank (1972) reported that all known specimens of the early archosauriform *Proterosuchus* came from the lowermost Triassic *Lystrosaurus* Assemblage Zone of South Africa, with one possible exception: a cervical vertebra (BP/1/4220; Fig. 2.6; Table 2.3) collected from the Lopingian upper *Cistecephalus* Assemblage Zone. BP/1/4220 was collected in May 1969 at the farm Gegund 532 near Harrismith in Free State. Cruickshank (1972: table 1) identified BP/1/4220 as ?*Proterosuchus* sp. and figured the specimen (Cruickshank, 1972: fig. 4a). Subsequently, Reisz et al. (2000) briefly noted that they could not find any evidence of archosauromorph features in BP/1/4220. Additionally, Reisz et al. (2000: 443) cast doubt on the exact providence of the specimen and concluded that it could be Triassic rather than Permian in age, but without providing supporting evidence.

Re-examination of BP/1/4220 revealed a morphology that does not conform to that expected for a basal archosauriform (cf. Reisz et al., 2000). However, I did observe some unusual features not reported in any other tetrapod that I am aware of. Because no detailed description of the specimen has ever been published, BP/1/4220 is described in detail for the first time and its possible phylogenetic position is reassessed.

BP/1/4220 (Fig. 2.6) is an almost complete vertebra that is not an axis because the transverse processes are well-developed, but may have belonged to the middle cervical series based on the presence of a parallelogram-shaped centrum in lateral view (the anterior articular surface is positioned distinctly dorsal to the posterior surface) and a diapophysis that is placed well below the neural arch (ventral to the level of the dorsal margin of the centrum). The vertebra is notochordal, with an open notochordal canal that is wider than tall and which completely pierces the centrum (Fig. 2.6: nc). Series of concentric bony laminae surround the notochordal canal, indicating the partial resorption of the notochord during life. In addition, the neurocentral suture is obliterated, suggesting that the animal was not a juvenile at the time of its death (Irmis, 2007), and that the presence of an open notochordal canal is therefore not a result of an early ontogenetic stage. The persistence of an open notochordal canal in a non-juvenile individual resembles the condition in multiple lineages of basal reptiliomorphs, parareptiles, basal synapsids, basal sauropsids, basal lepidosauromorphs, and the new archosauromorph species *Aenigmastropheus parringtoni* from the Lopingian of Tanzania (Vaughn, 1955; Watson, 1957; Moss, 1972; Evans, 1981; Reisz, 1981; Fraser and Walkden, 1984; Evans and Haubold, 1987; Rieppel, 1989a; Colbert and Olsen, 2001; Bickelmann et al., 2009, see below).

The anterior and posterior articular surfaces of the centrum are wider than tall. The anterior and posterior borders of the centrum are strongly beveled on their ventral margin in lateral view (Fig. 2.6: be), indicating the probable presence of small intercentra. The centrum is slightly transversely compressed at mid-length, and has a spool-shape in ventral view. The ventral surface of the centrum is mostly planar and well differentiated from the lateral surfaces. The lateral surfaces of the centrum are concave in ventral view and possess shallow and poorly defined fossae. The centrum

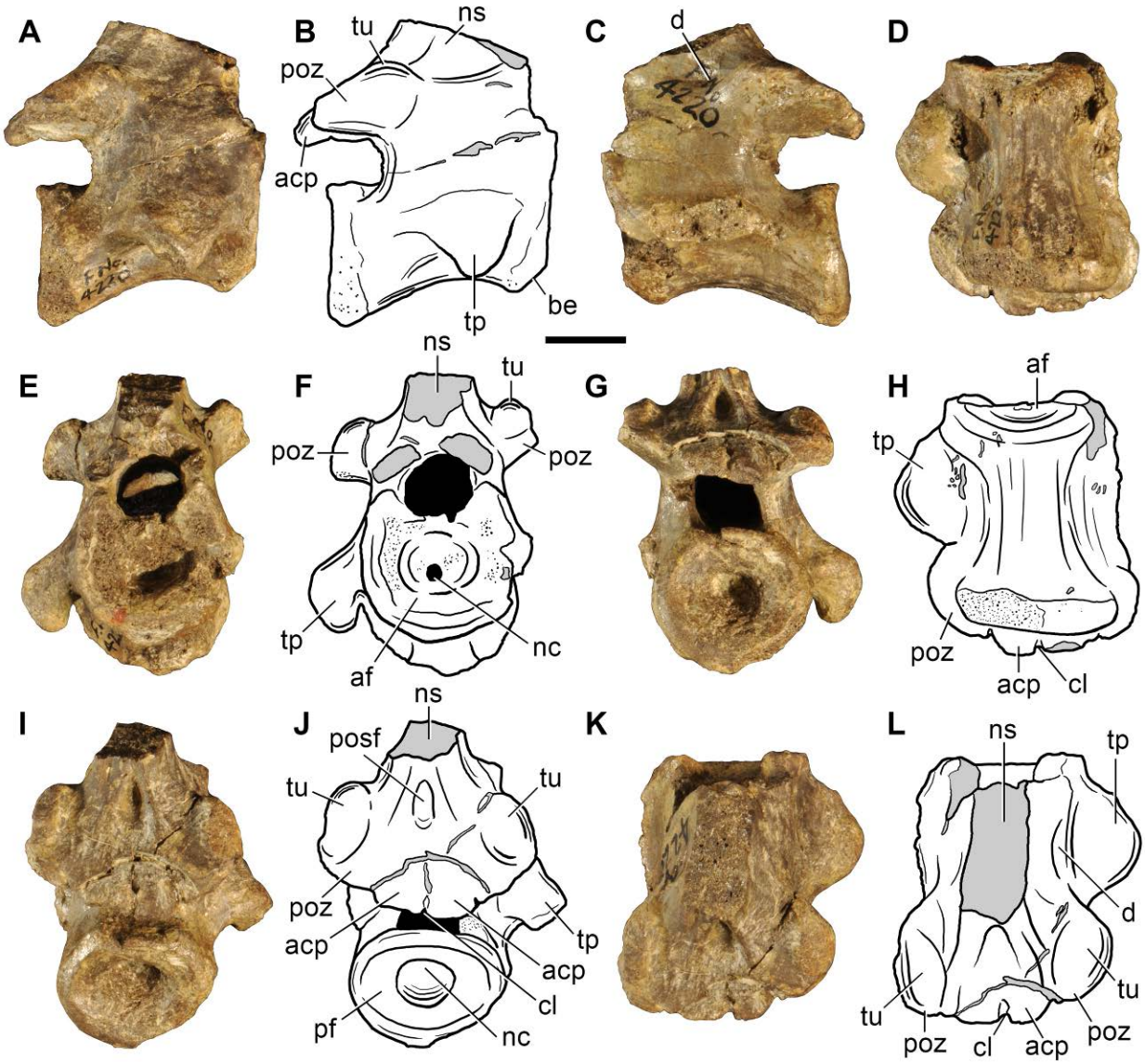

Figure 2.6. Indeterminate reptiliomorph from the late Permian–Early Triassic of South Africa. Cervical vertebra (BP/1/4220) in right lateral (A), left lateral (C), ventral (D, H), anterior (E, F), posterior (G), posterodorsal (I, J) and dorsal (K, L) views. Abbreviations: acp, accessory (interpostzygapophyseal) process; af, anterior facet; be, ventral beveling; cl, median cleft; d, depression; nc, notochordal canal; ns, neural spine; tu, tuberosity; pf, posterior facet; poz, postzygapophysis; posf, postspinal fossa; tp, transverse process. Scale bar equals 1 cm.

lacks parapophyses and it is likely that the parapophyses would have been placed on the intercentrum, as occurs in several basal amniotes (e.g. *Procolophon trigoniceps*: deBraga, 2003). Subcentral foramina are absent in BP/1/4220.

In the neural arch, the transverse processes are robust and directed posterolaterally and slightly ventrally. BP/1/4220 completely lacks any development of centrodiapophyseal or paradiapophyseal laminae, contrasting with the condition observed in some caudatans, "pelycosaurian" synapsids, basal diapsids and archosauromorphs (see below). The postzygapophyses are separated from the posterior end of the centrum by a tall and deep notch in lateral view. Only the bases of the prezygapophyses are preserved and they are well separated transversely from one another, as is also the case for the postzygapophyses. The presence of broadly separated zygapophyses contrasts with the condition observed in the cervical vertebrae of most archosauromorphs and some "pelycosaurian" synapsids, in which the zygapophyses are placed close to each other in dorsal view (e.g. *Ophiacodon* sp.: MCZ 1426; *Prolacerta broomi*: BP/1/2675; *Protorosaurus speneri*: ZMR MB R2173). The neural arch lacks a prezygodiapophyseal lamina, contrasting with the condition observed in the varanopid *Apsisaurus witteri* (Laurin, 1991: fig. 6; sensu Reisz et al., 2010) and several archosauromorphs (e.g. *Tanystropheus longobardicus*: SMNS 54628; *Protorosaurus speneri*: BSPG 1995 I 5; *Erythrosuchus africanus*: NHMUK R3592; *Garjainia prima*: PIN 2394/5-16).

The articular facets of the postzygapophyses of BP/1/4220 are oval, anteroposteriorly long and transversely wide, and face ventrally and slightly laterally. The dorsal surfaces of the postzygapophyses possess thick, rounded tuberosities (Fig. 2.6: tu) that resemble the epipophyses present in the cervical vertebrae of dinosaurs (Langer and Benton, 2006), the tanystropheids *Macrocnemus bassanii* (PIMUZ

Table 2.3. Measurements of the preserved bones of BP/1/4220 in millimetres. Values between brackets indicate incomplete measurements and the value given is the maximum measurable. The length along the zygapophyses is the maximum anteroposterior length between the anterior tips of the prezygapophyses and the posterior tips of the postzygapophyses. Maximum deviation of the digital caliper equals 0.02 mm but measurements were rounded to the nearest 0.1 millimetre.

Cervical vertebra		
	Centrum length	28.5
	Anterior articular facet height	20.6
	Anterior articular facet width	20.3
	Posterior articular facet height	17.7
	Posterior articular facet width	20.1
	Maximum height of the vertebra	(38.5)
	Length along zygapophyses	(28.8)
	Length of base of neural spine	18.6
	Width of neural spine	9.4
	Width along postzygapophyses	26.4
	Width of accessory processes	13.2
Rib		
	Length	(109.5)

T4822) and *Tanystropheus longobardicus* (SMNS 54630, 54654), and derived rhynchosaurs (Montefeltro et al., 2013). However, in contrast to the latter taxa, in BP/1/4220 the tuberosity is situated not on the posterior half of the postzygapophysis, but at the level of the anterior margin of its articular facet. The tuberosity possesses a rugose surface, which may suggest a tendinous attachment.

The neural arch possesses two posteriorly directed median or interpostzygapophyseal processes between the postzygapophyses that lack their most posterior ends (Fig. 2.6: acp). Despite being damaged posteriorly, the interpostzygapophyseal processes project further posteriorly than do the postzygapophyses. The position of these interpostzygapophyseal processes in BP/1/4420 is similar to the transpostzygapophyseal lamina of trilophosaurids (Spielmann et al., 2009) and the accessory intervertebral articular processes of some saurians (i.e. the non-homologous hyposphene of archosauriforms and the zygosphene of squamate lepidosauromorphs and sauropterygians) (Romer, 1956). The interpostzygapophyseal processes of BP/1/4220 are oval, posteriorly and slightly ventrally oriented, and separated from one another by a deep but transversely narrow median cleft (Fig. 2.6: cl). The presence of a cleft between the interpostzygapophyseal processes and the posterior extension of the processes beyond the level of the postzygapophyses differs from the morphology of the archosauromorph hyposphene and is in complete contrast with the depressed morphology of the lepidosauromorph zygosphene. No articular facet is discernable on the preserved portions of the interpostzygapophyseal processes of BP/1/4220. The interpostzygapophyseal processes of BP/1/4220 also differ from the accessory articular processes of tangasaurids (e.g. *Hovasaurus*: Currie, 1981), which are vertically oriented and placed dorsal to the postzygapophyses at the base of the neural spine, and from those of

diadectomorphs and seymouriamorphs (Sumida, 1991), in which the accessory processes are medioventral projections of the postzygapophyses. The presence of a median cleft and the possible absence of articular facets in the interpostzygapophyseal processes of BP/1/4220 resemble the condition present in the transpostzygapophyseal lamina of trilophosaurids (Spielmann et al., 2009), but in the latter taxa the lamina does not extend posteriorly beyond the level of the posterior margin of the postzygapophysis. Accordingly, the condition observed in BP/1/4220 does not match with the morphology of any other tetrapod of which I am aware.

The neural spine is transversely thick at its base and moderately expanded anteroposteriorly (Fig. 2.6: ns). The neural arch possesses a shallow depression lateral to the base of the neural spine on its left side (Fig. 2.6: d). This condition resembles that observed in some "pelycosaurian" synapsids (e.g. *Apsisaurus witteri*: Laurin, 1991) and archosauromorphs (e.g. *Protorosaurus speneri*: BSPG 1995 I 5; *Prolacerta broomi*: BP/1/2675), but contrasts with the deeper and better-defined depressions of the araeoscelidians *Araeoscelis gracilis* (Vaughn, 1955) and *Petrolacosaurus kansensis* (Reisz, 1981). Nevertheless, this depression is absent on the right side of the neural arch of BP/1/4220. The neural spine possesses a very deep and transversely wide postspinal fossa that is well defined laterally by sharp edges forming the posterolateral corners of the neural spine (Fig. 2.6: posf). The postspinal fossa is not completely preserved dorsally, but it is shallow at its most dorsal preserved portion suggesting that it would have extended only along the ventral portion of the neural spine. The postspinal fossa is subtriangular in posterior view.

Three indeterminate bone fragments and a possible fragment of rib shaft are also preserved in BP/1/4220. The possible rib shaft possesses a plate-like end that

becomes rod-like, with an elliptical cross-section, towards the other end of the bone. No articular facet is preserved on this fragment of bone.

I am unable to recognize any synapomorphies that would allow assignment of BP/1/4220 to Archosauromorpha (see also Reisz et al., 2000), Lepidosauromorpha or Sauria. Indeed, BP/1/4220 differs from several archosauromorphs (e.g. the new archosauromorph species *Aenigmastropheus parringtoni*, see below: UMZC T836; *Prolacerta broomi*: BP/1/2675; *Proterosuchus fergusi*: GHG 231) in possessing postzygapophyses that are strongly divergent posteriorly (although this condition is present in *Trilophosaurus* and rhynchosaurs; see below) and the absence of laminae on the neural arch (laminae are also absent in rhynchosaurs; see below). BP/1/4220 further differs from saurians in the absence of parapophyses on the centrum and the extreme transverse thickness of the neural spine at its base. As a result, the assignment of BP/1/4220 to Archosauromorpha by Cruickshank (1972) is not followed here.

BP/1/4220 possesses a striking combination of features unknown in any amniote that I am familiar with (e.g. notochordal centrum, thick and anterodorsally oriented neural spine, large tubercle on the dorsal surface of the postzygapophysis, interpostzygapophyseal processes). Although BP/1/4220 appears to represent a distinct amniote taxon I do not erect a new species for it due to the highly incomplete nature of the specimen. BP/1/4220 can be unambiguously assigned to Reptiliomorpha (diadectomorphs + amniotes) based on the presence of a large pleurocentrum (with a reduced intercentrum, if present; cf. Romer, 1956). However, I could not identify any feature that would allow the specimen to be assigned to a less inclusive reptiliomorph clade. BP/1/4220 was not included in the phylogenetic analysis conducted here because of its highly incomplete condition, and because of the absence of some major amniote clades in the taxonomic sample of the analysis (e.g. parareptiles). In

summary, BP/1/4220 is interpreted as belonging to Reptiliomorpha, and it may represent a previously unrecognized reptiliomorph lineage within the Lopingian of South Africa.

2.2.3.5. Specimens identified as either varanopid "pelycosaurs" or basal archosauromorphs from the Permo-Triassic of Uruguay. Piñeiro et al. (2003) described multiple isolated dorsal and caudal vertebrae from the Buena Vista Formation of northwestern Uruguay. This sedimentary unit was deposited during the Lopingian and probably also during the Early Triassic as part of the infill of the Paraná Basin (Bossi and Navarro, 1991). Piñeiro et al. (2003) assigned the vertebrae to varanopid "pelycosaurs", noting strong resemblances to the Permian species *Mycterosaurus longiceps* and *Mesenosaurus romeri*.

Subsequently, Dias-da-Silva et al. (2006) stated that the identification of "pelycosaurian" synapsids in the Buena Vista Formation was unwarranted and that the isolated vertebrae described by Piñeiro et al. (2003) closely resembled those of the basal archosauromorph *Prolacerta broomi*. Dias-da-Silva et al. (2006) concluded that the vertebrae reported from the Buena Vista Formation may belong to a basal archosauromorph or to another kind of diapsid. At the same time, Dias-da-Silva et al. (2006) pointed out that the other tetrapods (i.e. temnospondyl and procolophonoid remains) collected from the Buena Vista Formation (Marsicano et al., 2000; Piñeiro et al., 2004) are not strongly indicative of a Lopingian age.

The re-examination of the isolated vertebrae described by Piñeiro et al. (2003) (FC-DPV 1182, 1183, 1189, 1194, 1199, 1200 and 1333) does not reveal the presence of any archosauromorph synapomorphies in these specimens (e.g. there are no anterior or posterior centrodiapophyseal or prezygodiapophyseal laminae). The

overall morphology of these vertebrae is congruent with the vertebrae of basal archosauromorphs (e.g. *Prolacerta broomi*; see also Dias-da-Silva et al., 2006), but also with those of some varanopid "pelycosaurs" (Piñeiro et al., 2003). As a result, I do not support an unambiguous assignment of these vertebrae to Archosauromorpha. Nevertheless, recently published specimens from the Buena Vista Formation have been assigned to archosauromorphs and are probably closely related to protorosaurs and proterosuchids (Ezcurra et al., 2015a).

In sum, although the Buena Vista Formation yields archosauromorph remains, the current poor stratigraphic constraints on its age mean that the putative Permian age of specimens from this unit is ambiguous.

2.2.3.6. "Problematic reptile" from the late Permian of Tanzania. Parrington (1956) described the remains (several vertebrae and some fragmentary forelimb elements) of an enigmatic Permian specimen (UMZC T836) collected in the Ruhuhu Valley of Tanzania. He highlighted the apparent contrast between the primitive appearance of the forelimb bones and the more derived appearance of the vertebrae, with neural arch laminae ("buttresses") and articular rib facets resembling those of archosaurs. Parrington (1956) concluded that the bones of UMZC T836 did not bear close resemblances to any known synapsid, and suggested instead that the specimen might have close affinities with archosaurs because of the vertebral morphology and the presence of hollow limb bones and an ectepicondylar groove on the humerus.

Subsequently, Hughes (1963) noted that the vertebrae of UMZC T836 were not as archosaurian in appearance as Parrington originally thought and that laminae on the neural arch also occur in "pelycosaurian" synapsids. Hughes (1963) further noted that a notochordal centrum is present in "pelycosaurs", but is unknown among

archosaurs. However, Hughes (1963) concluded that the combination of a derived vertebral column and a primitive limb structure occurs in proterosuchian archosauromorphs, and suggested that UMZC T836 might possibly be an “incipient proterosuchian” (i.e. a proterosuchian ancestor). Reig (1970) noted that the vertebrae of UMZC T836 were transitional between those of “pelycosaurs” and archosaurs. Charig and Sues (1976) listed this specimen as a possible member of Proterosuchidae in their review of “Proterosuchia”, but also highlighted the skepticism raised by Hughes (1963) as to the archosaurian affinities of UMZC T836. Gower and Sennikov (2000) noted that UMZC T836 is probably indeterminate, but could possibly be archosaurian. Most recently, Ezcurra et al. (2013) indicated that UMZC T836 is likely not referable to Archosauriformes (the archosauromorph clade that includes proterosuchians).

Parrington (1956) reported that he collected UMZC T836 in the Ruhuhu Valley of Tanzania in 1933. These fossil-bearing levels correspond to locality B35 of Stockley (1932), which is located near the town of Ruanda in the Songea District of southern Tanzania (Stockley, 1932: plate 38; [147]: fig. 1) (Fig. 2.7). Stockley (1932) considered locality B35 to be part of the “Lower Bone Bed”, corresponding to his K6 horizon of the Songea Series. The K6 horizon is currently assigned to the Usili Formation (formerly the Kawinga Formation) of the Songea Group of the Ruhuhu Basin. Wopfner et al. (1991) and Sidor et al. (2010) described the Usili Formation as a 260 metres thick fluviolacustrine succession made up of a lowermost conglomeratic interval that is approximately 5 metres thick, grading up into a trough cross-bedded, coarse-grained, sandstone-dominated interval that is 25–40 metres thick, overlain by massive nodular siltstone and laminated mudstone beds with minor ribbon sandstones forming the bulk of the succession.

Sidor et al. (2010) recognized a single tetrapod faunal assemblage in the Usili Formation, which includes, in addition to UMZC T836, temnospondyls, pareiasaurs, gorgonopsians, therocephalians, cynodonts, and dicynodonts (Schlüter and Kohring, 1997; Gay and Cruickshank, 1999; Angielczyk et al., 2009; Sidor et al., 2010). In particular, the locality from which UMZC T836 was collected also yielded an isolated maxilla of a dicynodont listed by Parrington (1956) as cf. "*Esoterodon*" *uniseries* (UMZC T969), as well as other dicynodont (UMZC T779, T1170) and gorgonopsid (UMZC T882, T883) remains (Parrington, 1956; Kemp, 1969; UMZC catalogue and unpublished field notes of Parrington in UMZC collections). Parrington (1956) proposed that locality B35 is equivalent in age to the South African horizons that yield *Endothiodon* (currently known in the late *Pristerognathus*, *Tropidostoma*, and early *Cistecephalus* assemblage zones of South Africa: Rubidge, 1995, 2005; Fröbisch, 2009; Sidor et al., 2010; Angielczyk et al., 2014) because of the presence of cf. "*Esoterodon*" *uniseries* ("*Esoterodon*" is currently considered to be a junior synonym of *Endothiodon*; Cox, 1964). More recently, Angielczyk *et al*. (2014) considered that the common presence of the dicynodonts *Dicynodon huenei* and possibly *Katumbia parringtoni* allow a direct correlation between the faunistic associations of the Usili Formation and the Zambian Upper Madumabisa Mudstone. As a result, the well-supported correlation of the Upper Madumabisa Mudstone with the rocks of the *Cistecephalus* Assemblage Zone in the South African Karoo Basin implies that the Usili Formation can be considered a lateral equivalent of the *Cistecephalus* Assemblage Zone (Angielczyk et al., 2014), constrained to the middle–late Wuchiapingian (ca. middle Lopingian, 260–255 Ma; Gradstein et al., 2012).

Several authors commented on the phylogenetic relationships of UMZC T836 following the original description of Parrington (1956). However, a detailed

redescription, illustrations and comparisons of the specimen are currently lacking. The unusual combination of archosauromorph-like features and amniote plesiomorphies recognized in UMZC T836 by Parrington (1956) led me to revisit its anatomy and phylogenetic relationships, and allowed me to recognize this specimen as a new taxon, *Aenigmastropheus parringtoni* gen. et sp. nov.

Systematic Palaeontology

AMNIOTA Haeckel, 1866

DIAPSIDA Osborn, 1903 sensu Laurin (1991)

SAURIA Gauthier, 1984 sensu Gauthier et al. (1988)

ARCHOSAUROMORPHA Huene, 1946 sensu Dilkes (1998)

Aenigmastropheus gen. nov.

urn:lsid:zoobank.org:act:354E966B-CDA9-4509-84F5-2F130E23B2B5

Aenigmastropheus parringtoni sp. nov.

urn:lsid:zoobank.org:act: 78DF791F-C4F4-4592-8C3E-D333C8C91E58

(Appendix 2: figures S2.1–S2.5)

Etymology. The generic name ("enigmatic vertebra") is derived from the Latin word *aenigma* (enigmatic) and the Greek word *stropheus* (vertebra) in allusion to the problematic taxonomic history of the holotype specimen. The specific name honours the British palaeontologist Dr. F. R. Parrington for his contribution to the

understanding of Permo-Triassic amniotes and his discovery and initial description of the holotype specimen.

Holotype. UMZC T836, partial postcranial skeleton including five posterior cervical–anterior dorsal vertebrae, distal half of the right humerus, fragment of probable left humeral shaft, proximal end of the right ulna, and three indeterminate fragments of bone (one of which may represent part of a radius) (Appendix 2: figs. S2.1–S2.5).

Diagnosis (combined generic and specific diagnosis). *Aenigmastropheus parringtoni* is a medium-sized archosauromorph saurian distinguished from other amniotes by the following combination of features: posterior cervical and anterior dorsal vertebrae notochordal, with well-developed anterior and posterior centrodiapophyseal and prezygodiapophyseal laminae, and sub-triangular neural spines in lateral view; humerus with a strong diagonal ridge on the anterior surface of the shaft (autapomorphy); humerus with strongly developed capitellum (radial condyle) and trochlea (ulnar condyle) and without entepicondylar and ectepicondylar foramina; ulna with strongly developed olecranon process forming a single ossification with the rest of the bone.

Locality. Locality B35 of Stockley, close to the road near Ruanda, Songea District, Ruhuhu Valley, southern Tanzania (Stockley, 1932; Parrington, 1956) (Fig. 2.7).

Horizon and Age. Usili Formation (formerly the Kawinga Formation), deposited during the middle–late Wuchiapingian (middle Lopingian; Angielczyk et al., 2014), Songea Group, Ruhuhu Basin.

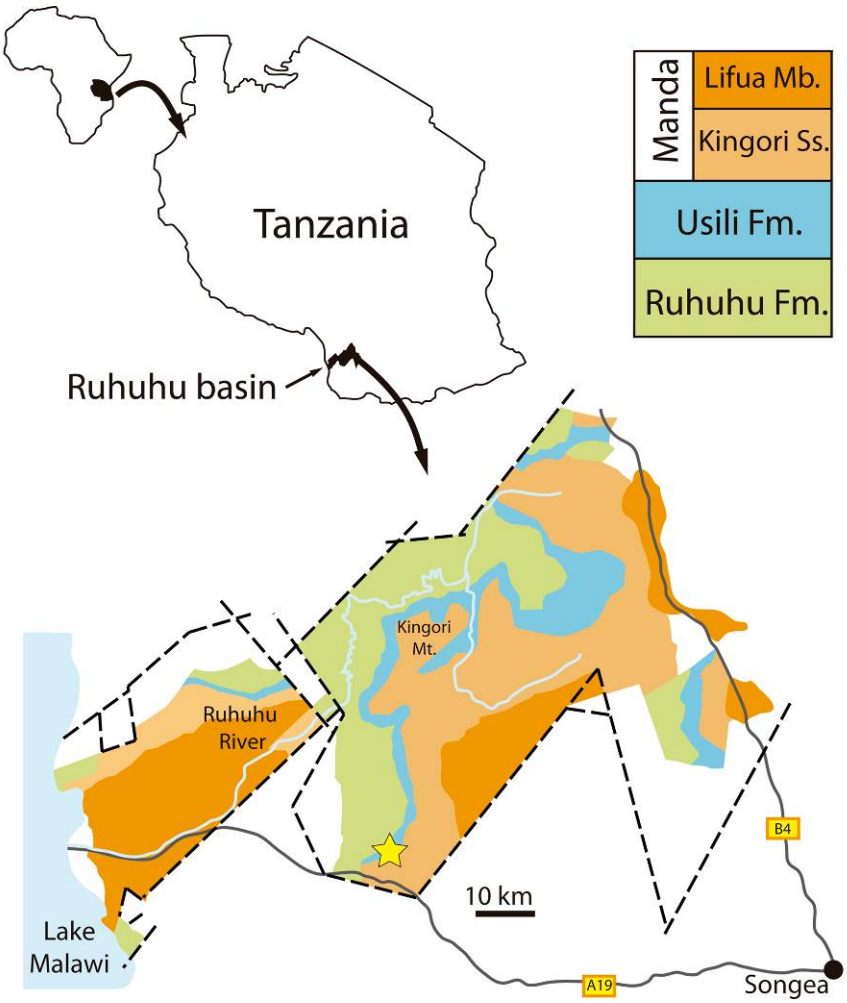

Figure 2.7. Type locality of *Aenigmastropheus parringtoni* in the Ruhuhu Basin, southwestern Tanzania, Africa. Star indicates the approximate geographic and stratigraphic occurrence of *Aenigmastropheus parringtoni* (locality B35). Abbreviations: Fm, formation; Mb, member; Mt, mountain; Ss, sandstone. Figure modified from Nesbitt et al. (2013a).

Comments. *Aenigmastropheus* possesses a striking combination of features that complicates assessment of its phylogenetic relationships (see Discussion and Chapter 5). However, these features also support its distinctiveness from other amniotes, including diapsids and "pelycosaur" synapsids. The combination of posterior centrodiapophyseal and prezygodiapophyseal laminae, zygapophyses that are positioned close to each other medially, and the absence of an entepicondylar foramen in the distal end of the humerus distinguish *Aenigmastropheus* from non-archosauromorph sauropsids. *Aenigmastropheus* differs from the enigmatic neodiapsid *Helveticosaurus zollingeri* due to the presence of low neural arches with subtriangular neural spines in the cervico-dorsal transition region, well-developed distal condyles of the humerus and a well-developed olecranon process on the proximal end of the ulna. Within Archosauromorpha, *Aenigmastropheus* differs from other basal members of the group due to the presence of notochordal vertebrae, a strongly developed olecranon process as part of a single ossification with the rest of the ulna (convergently acquired in some crown archosaurs) and a thick posteroventral ridge along the humeral shaft. The latter character is an autapopmorphy of *Aenigmastropheus parringtoni* among basal diapsids. *Aenigmastropheus parringtoni* is described in detail in Appendix 2.

2.3. Discussion

2.3.1. *Timing of the crocodile-lizard (or bird-lizard) divergence and recommendations for molecular calibrations*

The revision of the Permian saurian record presented in this chapter indicates that only four species can be considered as well-supported pre-Mesozoic members of the group: the approximately contemporaneous early–middle Lopingian *Protorosaurus speneri*, *Aenigmastropheus parringtoni* and *Eorasaurus olsoni* and the latest Permian *Archosaurus rossicus* (Table 2.4). Other supposed saurian taxa are identified as more basal diapsid forms (e.g. *Saurosternon*, *Youngina*) or as indeterminate reptiliomorphs (e.g. BP/1/4220), or as of Early Triassic or indeterminate late Permian–Early Triassic age. All the Permian saurian taxa recognized here can be assigned to Archosauromorpha and, as a result, there is no fossil record of Lepidosauromorpha prior to the Early Triassic (*Paliguana whitei*). The radioisotopic estimate for the age of *Protorosaurus* establishes a minimum divergence time for the crocodile-lizard split (origin of Sauria; equivalent to the bird-lizard split).

Following the explicit five-point protocol for fossil calibrations proposed by Parham et al. (2012), the following recommendations are made for molecular biologists wishing to use fossil data to calibrate the crocodile-lizard (or bird-lizard) split: (1) the split can be calibrated on the basis of the voucher specimen NHMW 1943 I 4, an almost complete skeleton missing the skull, lectotype of *Protorosaurus speneri* Meyer 1830 (see Gottmann-Quesada and Sander [2009] for designation of lectotype material); (2) *Protorosaurus speneri* is universally considered and strongly supported as a non-archosaurian member of Archosauromorpha upon the basis of the explicit morphological phylogenetic analyses conducted here, and many other studies

Table 2.4. List of specimens/species previously considered as pre-Mesozoic saurians and their age and current taxonomic assignment. Permian specimens/species currently supported as saurian are highlighted in bold font.

	Age	**Occurrence**	**Reported taxonomic assignment**	**Revised taxonomic assignment**
Aenigmastropheus parringtoni	**middle–late Wuchiapingian, middle Lopingian**	**Tanzania**	**"Proterosuchia" (Charig and Sues, 1976)**	**Archosauromorpha, ?Protorosauria**
Archosaurus rossicus	**Changhsingian, latest Permian**	**Russia**	**Proterosuchidae (Tatarinov, 1960; Nesbitt, 2011)**	**Archosauriformes, Proterosuchidae**
BP/1/4220	Late Permian–Early Triassic	South Africa	?*Proterosuchus* sp. (Cruickshank, 1972)	Reptiliomorpha
Buena Vista Fm specimens	Late Permian–Early Triassic	Uruguay	Synapsida (Piñeiro et al., 2003) and Archosauromorpha (Ezcurra et al., 2015a)	Amniota and Archosauromorpha, respectively
Eorasaurus olsoni	**late Capitanian–Wuchiapingian, late Guadalupian–early Lopingian**	**Russia**	**Archosauromorpha, Protorosauria (Sennikov, 1997)**	**Archosauromorpha, ?Archosauriformes**
Lanthanolania ivakhnenkoi	late Wordian, middle Guadalupian	Russia	Lepidosauromorpha / sister-taxon of Sauria (Modesto and Reisz, 2002); non-saurian Neodiapsida (Reisz et al., 2011)	Non-saurian Neodiapsida
Lacertulus bipes	Late Permian–Early Triassic	South Africa	Lepidosauromorpha (Carroll and Thompson, 1982); non-squamate Diapsida (Estes, 1983; Evans, 2003)	Non-squamate Diapsida
Palaeagama vielhaueri	Late Permian–Early Triassic	South Africa	Lepidosauromorpha (Carroll, 1975; Gauthier et al., 1988); non-saurian Neodiapsida (Müller, 2004)	Non-saurian Neodiapsida
Paliguana whitei	Early Triassic	South Africa	Lepidosauromorpha (Carroll, 1975, 1976; Evans, 1988)	Lepidosauromorpha
Protorosaurus speneri	**middle Wuchiapingian, middle Lopingian**	**Germany and England**	**Archosauromorpha Protorosauria (Benton, 1985; Gottmann-Quesada and Sander, 2009)**	**Archosauromorpha, Protorosauria**
Saurosternon bainii	Late Permian	South Africa	Lepidosauromorpha (Carroll, 1975; Gauthier et al., 1988); non-saurian Neodiapsida (Müller, 2004)	Non-saurian Neodiapsida

(Gauthier, 1984; Benton, 1985; Evans, 1988; Laurin, 1991; Jalil, 1997; Benton and Allen, 1997; Dilkes, 1998; Rieppel et al., 2003; Gottmann-Quesada and Sander, 2009; Ezcurra et al., 2014); (3) results of morphological phylogenetic analyses for major saurian relationships are generally consistent with molecular analyses, with the exception of the highly controversial phylogenetic position of turtles (e.g. Gregory, 1946; Rieppel and deBraga, 1996; deBraga and Rieppel, 1997; Platz and Conlon, 1997; Zardoya and Meyer, 1998; Rieppel and Reisz, 1999; Müller, 2004; Hill, 2005; Bhullar and Bever, 2009; Lyson et al., 2010, 2013; Lee, 2011; Shen et al., 2011; Neenan et al., 2013). However, because the earliest fossil turtle remains are Late Triassic in age (Li et al., 2008) the problematic position of turtles has no impact on the calibration proposed here; (4) NHMW 1943I4 comes from the locality Glücksbrunn in Thuringia, central Germany, and is from the Kupferschiefer (cycle Z1) of the Zechstein Group; (5) as discussed above, the Kupferschiefer is dated as 257.3 ± 1.6 Ma (Lopingian: Wuchiapingian) based on a Re-Os geochronological study (Brauns et al., 2003). This age is consistent with biostratigraphic data from the conodont *Mesogondolella britannica* supporting a middle Wuchiapingian age (Legler et al., 2005; Legler and Schneider, 2008; Schneider pers. comm., 2012).

These data suggest a minimum or hard calibration date for the crocodile-lizard split of 255.7 Ma (the youngest date for the Kupferschiefer suggested by geochronology). This is younger than the minimum calibration date proposed by Benton and Donoghue (2007), who proposed a calibration of 259.7 Ma, based on their interpretation of the Kupferschiefer as older (Capitanian) in age, and slightly older than the 252 Ma calibration recommended by Reisz and Müller (2004).

A maximum or soft calibration date for the crocodile-lizard split is more difficult, and Benton and Donoghue (2007) proposed that *Apsisaurus* from the Archer

City Formation of Texas, dated as Asselian (298.9 ± 0.2 Ma to 295.5 ± 0.4 Ma; Gradstein et al., 2012) can be used to constrain the maximum date of divergence, and therefore recommended a maximum or soft calibration date of 299.1 Ma. However, *Apsisaurus* was recently re-interpreted as a varanopid synapsid (Reisz et al., 2010). Accordingly, I propose here that the basal neodiapsid *Lanthanolania ivakhnenkoi* be used to constrain the maximum divergence time of Sauria because it is the closest of the sister taxa to Sauria (Reisz et al., 2011) that is unambiguously older than the earliest known saurian fossils. *Lanthanolania* comes from the Wordian of Russia (Modesto and Reisz, 2002; Reisz et al., 2011) (268.8 ± 0.5 Ma to 265.1 ± 0.4 Ma; Gradstein et al., 2012) and implies a maximum calibration date of 269.3 Ma, which is around 30 Ma younger than the date previously recommended by Benton and Donoghue (2007).

2.3.2. *Ghost lineages and archosauriform divergence*

As discussed above, Archosauromorpha and Lepidosauromorpha diverged prior to 255.7–259.9 Ma (middle–late Wuchiapingian; [Gradstein et al., 2012; Roscher and Schneider, 2006]). This minimum divergence date matches that of the immediate successive outgroups of Sauria, such as "younginiforms" and tangasaurids (Reisz et al., 2011), implying the absence of an unambiguous ghost lineage for Sauria. A middle–late Wuchiapingian age for the origin of the group is consistent with dates estimated by some recent molecular clocks, such as those of Alfaro et al. (2009) of 257–292 Ma and Sanders and Lee (2007) of 249.5–269.1 Ma. Conversely, the age estimated here for the origin of Sauria is considerably younger than dates estimated by some other recent molecular clock analyses that have proposed a Cisuralian (early Permian) divergence data (e.g. 285–289 Ma by Hugall et al. [2007]; 276–295 Ma by

Shen et al. [2011]). As a result, the ghost lineage between the origin of Sauria (and several non-saurian neodiapsids) and the first appearance of the group in the fossil record would be of 21 to 40 million years based on the latter molecular estimates. This extensive ghost lineage could be explained by gaps in the fossil record or by errors in the estimations based on molecular evidence (such as a more rapid rate of molecular evolution than those expected by the molecular models). Accordingly, although the oldest known unambiguous members of Sauria are middle Lopingian in age, it would not be surprising to find early members of the group in Guadalupian rocks. Such discoveries would result in a considerably older minimum origin time for the group, as has also recently been documented for neodiapsid sauropsids (Reisz et al., 2011).

The recovery of the Russian *Eorasaurus olsoni* within Archosauriformes in the phylogenetic analysis (Ezcurra et al., 2014; Chapter 5) implies that it represents the oldest member of the group, also suggesting a minimum middle Wuchiapingian divergence time for rhynchosaurians, prolacertids, proterosuchids and the *Erythrosuchus* + *Euparkeria* clade. As a result, this phylogenetic position would indicate that archosauriforms are not a group that appeared immediately before the Permo-Triassic mass extinction event and, conversely, had already undergone substantial taxonomic diversification by the Lopingian, with the presence of proterosuchids and the *Eorasaurus* lineage. However, the fragmentary nature of the known specimens of *Eorasaurus olsoni* and the weak support for its position within archosauriforms (e.g. only one extra step is necessary to recover it outside Archosauriformes) suggests that the phylogenetic position recovered here for this taxon should be considered as tentative.

2.3.3. *Palaeobiogeography*

The presence of early archosauromorphs in the middle Lopingian of Germany, England, Russia and Tanzania indicates a broad geographical distribution for the group during the late Paleozoic, spanning from close to the palaeo-Equator (Germany) to a palaeolatitude of 30° N (Russian localities) in the northern hemisphere to high palaeolatitudes of 55° S (Tanzania) in southern Pangaea (Fig. 2.8; palaeomap generated using Fossilworks based upon data from the Paleobiology Database: Alroy, 2013). This broad palaeobiogeographic distribution during the Permian undermines previous hypotheses that proposed a dispersal event for archosauromorphs from Eurasia to southern high latitudes (southern Africa) following the Permo-Triassic mass extinction (Reisz et al., 2000). The occurrences of *Protorosaurus speneri* and *Aenigmastropheus parringtoni* imply either a northern–southern dispersal event or a wider palaeobiogeographic distribution for archosauromorphs during the Lopingian, which is not currently well documented in the fossil record. In addition, previous authors have discussed the presence of endemic taxa in the Usili Formation of Tanzania (e.g. Gay and Cruickshank, 1999; Maisch, 2002; Abdala and Allinson, 2005; Angielczyk, 2007; Weide et al., 2009; Sidor et al., 2010; Angielczyk et al., 2014), which yielded the holotype of *Aenigmastropheus parringtoni*. The occurrence of the basal archosauromorph *Aenigmastropheus parringtoni* in the Usilli Formation contrasts with the current absence of the group in the Lopingian of the Upper Madumabisa Mudstone of Zambia and the considerably better sampled *Cistecephalus* Assemblage Zone of the South African Karoo Basin. Thus, *Aenigmastropheus parringtoni* enlarges the list of endemic taxa for the Tanzanian unit (see Angielczyk et al., 2014) and contrasts with previous hypotheses of a more homogenous Pangaean fauna during the Lopingian (e.g. Colbert, 1973).

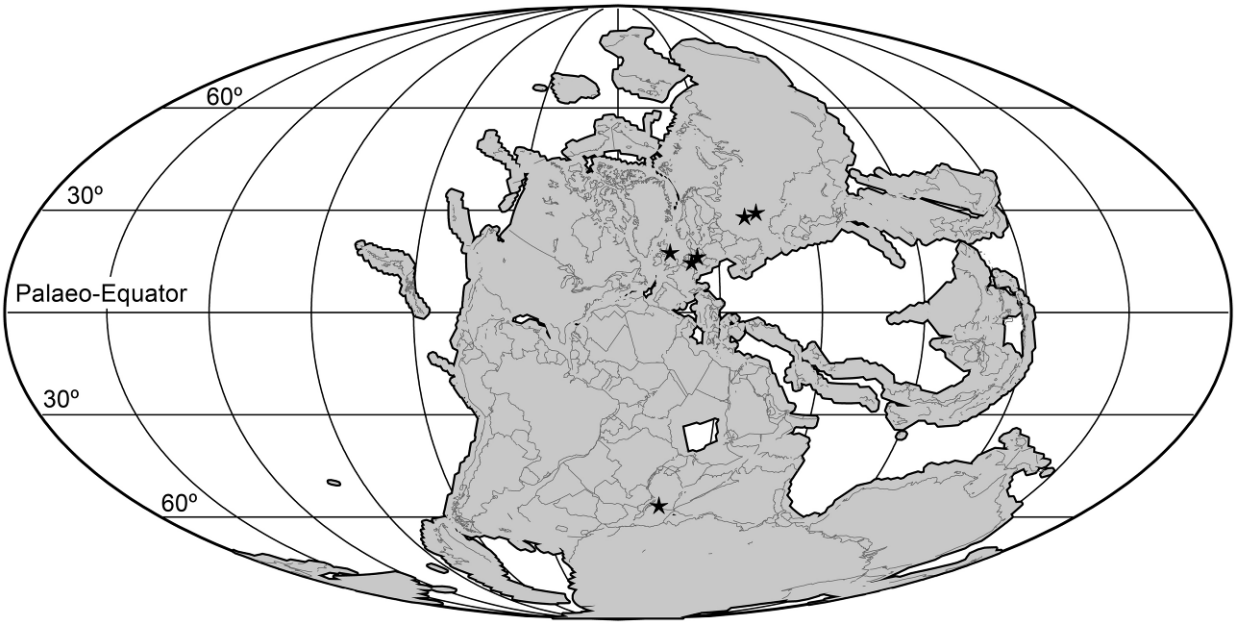

Figure 2.8. Palaeobiogeographical distribution of Archosauromorpha across Pangaea during the late Guadalupian–Lopingian. Black stars indicate archosauromorph records (palaeomap for 260 Ma downloaded from Fossilworks using data from the Paleobiology Database: Alroy, 2013).

Chapter 3: Taxonomy of proterosuchid specimens from the earliest Triassic of South Africa

3.1. Background

Historically, the most important source of information on the evolutionary history of Archosauriformes during the earliest Triassic has been the specimens of proterosuchids collected from the *Lystrosaurus* Assemblage Zone (AZ) (Palingkloof Member of the upper Balfour Formation and lower part of the Katberg Formation) of South Africa (Broom, 1903, 1932, 1946; Broili and Schröder, 1934; Haughton, 1924; Brink, 1955; Hoffman, 1965; Welman, 1998; Damiani et al., 2003; Smith and Botha, 2005; Botha-Brink et al., 2014). These specimens form the basis of knowledge of four nominal species, all of which have been synonymised as a single taxon, *Proterosuchus fergusi* Broom, 1903, by the most recent revisions (see Welman and Flemming, 1993; Welman, 1998). Proterosuchid material that has been referred to the genus *Proterosuchus* is the first 'new' vertebrate species (i.e. species not known from the Permian) to appear in the South African fossil record in the aftermath of the Permo–Triassic mass extinction, first occurring approximately 7 m above the boundary (Smith and Botha, 2005). In view of the importance of the South African proterosuchid material and the presence of abundant and well-preserved fossil specimens, it is surprising that their detailed anatomy remains undescribed. Here, I revisit and revise the taxonomy of the proterosuchid specimens from the *Lystrosaurus* AZ of South Africa based upon a comprehensive re-examination of available archosauriform specimens from this horizon, and provide a redescription of the holotype of *Proterosuchus fergusi*. The aim of this revision is to more completely

understand the taxonomic richness of archosauriforms in the immediate aftermath of the Permo-Triassic mass extinction and the implications for the early evolutionary history of the group.

3.2. *Taxonomic history of the South African* Lystrosaurus *AZ proterosuchids*

Broom (1903) described the first proterosuchid specimen from the *Lystrosaurus* AZ of South Africa (SAM-PK-591), a partial skull including parts of the snout, orbital region, and palate, represented by natural moulds and strongly weathered bone fragments. Despite the fragmentary and poorly preserved condition of SAM-PK-591, Broom (1903) recognized enough distinct features to use it as the holotype of the new genus and species *Proterosuchus fergusi* (Table 3.1). Huene (1908) coined the new, monotypic family Proterosuchidae for *Proterosuchus fergusi*.

Haughton (1924) described a second, more complete archosauriform skull (TM 201), erecting for it the new genus and species "*Chasmatosaurus vanhoepeni*", as well as the new family Chasmatosauridae. Haughton (1924) noted similarities between the maxillae and palates of *Proterosuchus fergusi* and "*Chasmatosaurus vanhoepeni*", but also differences including the presence in the latter of only one palatal tooth row and a much larger ectopterygoid with a long, posteriorly directed process lying against the jugal.

Broom (1932) reported a new archosauriform specimen that he referred to "*Chasmatosaurus vanhoepeni*" (no accession number was originally provided, but comparison of known proterosuchid specimens with the drawings presented by Broom indicates that is AMNH FR 2237). Broom (1932) concluded that *Proterosuchus fergusi* and "*Chasmatosaurus vanhoepeni*" were very closely related or potentially synonymous, but that this could not be fully assessed because of the very

Table 3.1. Summary of the taxonomic history of the proterosuchids from South Africa over the last 100 years.

Author	**Taxonomic scheme**
Broom (1903)	*Proterosuchus fergusi*
Haughton (1924)	*Proterosuchus fergusi*, "*Chasmatosaurus vanhoepeni*"
Broom (1932)	*Proterosuchus fergusi* ?= "*Chasmatosaurus vanhoepeni*"
Broili and Schröder (1934)	Same as Haughton (1924)
Broom (1946)	*Proterosuchus fergusi*, "*Chasmatosaurus vanhoepeni*", "*Chasmatosaurus*" sp., "*Elaphrosuchus rubidgei*"
Brink (1955)	"*Chasmatosaurus vanhoepeni*", "*Elaphrosuchus rubidgei*"
Hughes (1963)	*Proterosuchus fergusi* nomen dubium, "*Chasmatosaurus vanhoepeni*" (= "*Elaphrosuchus rubidgei*")
Hoffman (1965)	*Proterosuchus fergusi*, "*Chasmatosaurus vanhoepeni*", "*Chasmatosaurus*" *alexanderi*, "*Elaphrosuchus rubidgei*"
Charig and Reig (1970)	*Proterosuchus fergusi*, "*Chasmatosaurus vanhoepeni*" (= "*Chasmatosaurus*" *alexanderi*), "*Elaphrosuchus rubidgei*"
Cruickshank (1972)	*Proterosuchus fergusi nomen dubium*, "*Proterosuchus vanhoepeni*" (= "*Chasmatosaurus*" *alexanderi*, = "*Elaprhosuchus rubidgei*"), ?*Proterosuchus* sp.
Charig and Sues (1976)	*Proterosuchus fergusi*, "*Chasmatosaurus vanhoepeni*" (= "*Chasmatosaurus*" *alexanderi*), "*Elaphrosuchus rubidgei*", ?*Proterosuchus* sp.
Welman (1998)	*Proterosuchus fergusi* (= "*Chasmatosaurus vanhoepeni*", = "*Chasmatosaurus*" *alexanderi*, = "*Elaphrosuchus rubidgei*")
Ezcurra et al. (2013, 2014)	Same as Welman (1998)
This chapter	*Proterosuchus fergusi* (= "*Chasmatosaurus vanhoepeni*", = "*Elaphrosuchus rubidgei*"), *Proterosuchus alexanderi* comb. nov., *Proterosuchus goweri* sp. nov.

fragmentary condition of the holotype of *Proterosuchus fergusi*. Broili and Schröder (1934) described an almost complete skull (BSPG 1934 VIII 514) that they referred to "*Chasmatosaurus vanhoepeni*".

A small archosauriform skull (RC 59) was described by Broom (1946) as the new genus and species "*Elaphrosuchus rubidgei*". Broom (1946) distinguished "*Elaphrosuchus rubidgei*" from *Proterosuchus fergusi* based on differences in the shape of the maxilla, and from "*Chasmatosaurus vanhoepeni*" based on the different shapes of the premaxilla, infratemporal fenestra and interparietal, supposed absence of the postfrontal and the supposed presence of an external mandibular fenestra. In addition, Broom (1946) suggested that the specimen (BSPG 1934 VIII 514) described by Broili and Schröder (1934) might represent a different species from that of the holotype of "*Chasmatosaurus vanhoepeni*" (TM 201) and referred the former to "*Chasmatosaurus*" sp. Broom (1946) referred all of these South African taxa (*Proterosuchus fergusi*, "*Chasmatosaurus vanhoepeni*", "*Chasmatosaurus*". sp., "*Elaphrosuchus rubidgei*") to the family Proterosuchidae, together with "*Chasmatosaurus*" *yuani* Young, 1936 from the Jiucaiyuan Formation (*Lystrosaurus* AZ) of China. Broom (1946) also reported that the holotype (SAM-PK-591) of *Proterosuchus fergusi* had been lost.

Brink (1955) described a new skull of "*Chasmatosaurus vanhoepeni*" (NMQR 880, formerly NM C. 500) and agreed with Broom (1946) in considering "*Elaphrosuchus rubidgei*" to be valid. However, Brink (1955) considered BSPG 1934 VIII 514 referable to "*Chasmatosaurus vanhoepeni*" (Broili and Schröder, 1934; contra Broom, 1946). Hughes (1963) reviewed the early archosauriform fossil record and proposed that all the then known proterosuchid specimens from the *Lystrosaurus* AZ of South Africa belonged to a single species, "*Chasmatosaurus vanhoepeni*". As a

result, Hughes (1963) suggested that "*Elaphrosuchus rubidgei*" might be a juvenile individual (and thus a subjective junior synonym) of "*Chasmatosaurus vanhoepeni*". In addition, Hughes (1963: 234) considered *Proterosuchus fergusi* invalid and suggested that, given the fragmentary and poorly preserved condition of the holotype (SAM-PK-591), *Proterosuchus fergusi* was 'best forgotten!'

The fourth nominal proterosuchid species from South Africa, "*Chasmatosaurus*" *alexanderi*, was erected by Hoffman (1965) based on a fairly complete, previously undescribed proterosuchid skeleton (NMQR 1484, formerly NM C. 3016). Hoffman (1965) referred the specimens BSPG 1934 VIII 514 and NMQR 880 (both previously referred to "*Chasmatosaurus vanhoepeni*") to "*Chasmatosaurus*" *alexanderi*. Hoffman (1965) distinguished "*Chasmatosaurus*" *alexanderi* from "*Chasmatosaurus vanhoepeni*" on the basis of a less downturned premaxilla, an orbit with an oval outline and a lacrimal situated anteriorly to the prefrontal.

Charig and Reig (1970) provided the first comprehensive review of the Proterosuchia (i.e. Proterosuchidae + Erythrosuchidae). These authors considered *Proterosuchus fergusi* and "*Chasmatosaurus vanhoepeni*" to be specifically distinct, but suggested that they might ultimately prove to be congeneric. Charig and Reig (1970) considered "*Elaphrosuchus rubidgei*" a distinct and valid proterosuchid genus and species, but following detailed discussion (Charig and Reig, 1970: 150–154) they considered "*Chasmatosaurus*" *alexanderi* a subjective junior synonym of "*Chasmatosaurus vanhoepeni*". In the same year, Reig (1970) employed a taxonomic scheme for the South African proterosuchids congruent with that presented by Charig and Reig (1970).

Cruickshank (1972) published the most comprehensive currently available anatomical description of the South African proterosuchids based on multiple specimens. In his discussion of the taxonomy of the South African proterosuchids (which seems to have been written without being aware of the review of Charig and Reig [1970]), Cruickshank (1972) reported that the previously lost holotype of *Proterosuchus fergusi* (SAM-PK-591) had been relocated and that its palatal morphology was consistent with that in the specimens of "*Chasmatosaurus*" from South Africa. Moreover, Cruickshank (1972) suggested that the differences observed by Haughton (1924) between the palatal tooth morphology of the holotypes of "*Chasmatosaurus vanhoepeni*" (TM 201) and *Proterosuchus fergusi* (SAM-PK-591) are preservational artefacts. As a result, Cruickshank (1972) considered "*Chasmatosaurus*" to be a junior synonym of *Proterosuchus*. In addition, he stated that the fragmentary and poorly preserved condition of the holotype of *Proterosuchus fergusi* (SAM-PK-591) prevents the referral of other proterosuchians to that species, and concluded that *Proterosuchus* contained two species: *Proterosuchus fergusi* and "*Proterosuchus vanhoepeni*". Cruickshank (1972) provided a detailed rebuttal of the differences that Broom (1946) reported between "*Elaphrosuchus rubidgei*" and the other South African proterosuchid specimens, and he concluded that "*Elaphrosuchus rubidgei*" was a subjective junior synonym and juvenile specimen of "*Proterosuchus vanhoepeni*". In addition, Cruickshank (1972) discussed the taxonomic validity of "*Chasmatosaurus*" *alexanderi* and, based on similar grounds to those discussed by Charig and Reig (1970), he also considered this species a subjective junior synonym of "*Proterosuchus vanhoepeni*". Finally, Cruickshank (1972) also referred an isolated cervical vertebra and rib from the Lopingian of South Africa to ?*Proterosuchus* sp.,

potentially extending the range of this genus back in time beyond the Permo-Triassic boundary.

In a second comprehensive review of the Proterosuchia, Charig and Sues (1976) considered that the subjective synonymy of "*Chasmatosaurus*" with *Proterosuchus* should be rejected on the grounds of 'common sense, practicability and consideration for others', and maintained *Proterosuchus fergusi* and "*Chasmatosaurus vanhoepeni*" as distinct species. Charig and Sues (1976) accepted the synonymy of "*Chasmatosaurus*" *alexanderi* with "*Chasmatosaurus vanhoepeni*" previously proposed by Charig and Reig (1970) and Cruickshank (1972). However, they retained "*Elaphrosuchus rubidgei*" as a valid genus and species. Despite the arguments put forward by Charig and Sues (1976), most subsequent authors (e.g. Cruickshank, 1978, 1979; Benton and Clark, 1988; Sereno, 1991; Parrish, 1992; Clark et al., 1993; Welman and Flemming, 1993; Juul, 1994; Bennett, 1996; Gower, 1996; Gower and Sennikov, 1996, 1997) followed the taxonomic scheme proposed by Cruickshank (1972) and considered "*Chasmatosaurus*" a subjective junior synonym of *Proterosuchus.*

Welman and Flemming (1993) conducted a statistical analysis of the proterosuchid skulls from the *Lystrosaurus* AZ of South Africa (including the holotypes of the four nominal species) and concluded that all specimens represented members of a single ontogenetic series, in agreement with Cruickshank (1972). Subsequently, Welman (1998) provided detailed rebuttals to the differences proposed by previous authors for separation of the four nominal species. He also considered the holotype of *Proterosuchus fergusi* to be diagnostic and thus referred all known South African proterosuchids to this species as subjective junior synonyms (Welman 1998). All subsequent authors (e.g. Dilkes and Sues, 2009; Kear, 2009; Klembara and

Welman, 2009; Nesbitt et al., 2009; Ezcurra et al., 2010, 2013, 2014; Desojo et al., 2011; Nesbitt, 2011; Ezcurra, 2014) have followed the taxonomic interpretation proposed by Welman (1998). Finally, Reisz et al. (2000) and Ezcurra et al. (2013, 2014; see Chapter 2) provided evidence to dismiss the report by Cruickshank (1972) of ?*Proterosuchus* sp. in the Permian of South Africa.

3.3. Materials and Methods

3.3.1. *Studied specimens*

All of the known archosauriform specimens collected from the *Lystrosaurus* AZ of South Africa were studied directly (AMNH FR 2237, BP/1/3993, 4016, 4224, 4589, 6046, BSPG 1934-VIII-514, GHG unnumbered, 72, 231, 363, NMQR 880, 1484, 3570, RC 59, 846, SAM-PK-591, 11207, 11208, K139, K140, K9957, K10603, TM 201, UMZC T950; Tables 3.2 and 3.3), with the exception of the recently reported and as yet undescribed NMQR 3924 (Botha-Brink et al., 2014). In addition, all published proterosuchid specimens collected from the Jiucaiyuan Formation (*Lystrosaurus* AZ) of China were also studied ("*Chasmatosaurus*" *yuani*: IVPP V36315 [field number 90002], V4067, V2719). The relative ontogenetic stage of the South African specimens was estimated based on comparisons between their size and that of specimens for which the ontogenetic stage has previously been determined by histological sampling by Botha-Brink and Smith (2011) (e.g. SAM-PK-11208, K140). Unfortunately, it was not possible to study limb bone histology for most specimens, because they are represented mainly by cranial remains (e.g. BSPG 1934 VIII 514, BP/1/3993, 4016, GHG 231, RC 59, 846, SAM-PK-K10603, TM 201).

Table 3.2. Locality and previous and current taxonomic assignment of non-*Proterosuchus* archosauriform specimens from the *Lystrosaurus* AZ of South Africa.

Specimen	Locality	Previous assignment	Current assignment
AMNH FR 2237	Near Dewetsdorp, Xhariep Distrinct, Free State Province (Broom, 1932)	"*Chasmatosaurus vanhoepeni*" (Broom, 1932); *Proterosuchus fergusi* (Nesbitt, 2011)	Proterosuchidae indet. (distinct from "*Chasmatosaurus*" *yuani*)
BP/1/4589	Fairydale, Bethulie District, Free State Province	None	cf. Proterosuchidae (unprepared)
BP/1/6046	Barendskraal, Middelburg, Chris Hani District, Eastern Cape Province	*Proterosuchus fergusi* (Damiani et al., 2003)	cf. Proterosuchidae (unprepared)
GHG unnumbered	Sonja McDonald 952, Harrismith, Thabo Mofutsanyana District, Free State Province	None	cf. Proterosuchidae (unprepared)
GHG 72	Farm Kruisvlei 279 (28°31'45"S; 27°15'49"E), east of Winburg, Lejweleputswa District, Free State Province	*Proterosuchus fergusi* (Welman, 1998)	Proterosuchidae indet. (distinct from *Proterosuchus alexanderi* and *Proterosuchus goweri*)
NMQR 3570	Farm Vangfontein, Middelburg, Chris Hani District, Eastern Cape Province	Archosauriformes indet. (Modesto and Botha-Brink, 2008)	Archosauriformes indet. (distinct from *Proterosuchus* spp. and SAM-PK-K9957)
SAM-PK-11207	Barendskraal, Middelburg, Chris Hani District, Eastern Cape Province	*Proterosuchus fergusi* (Damiani et al., 2003)	Proterosuchidae indet.
SAM-PK-K139	Skerpioenkraal, Middelburg, Chris Hani District, Eastern Cape Province	None	Proterosuchidae indet.
SAM-PK-K9957	Heldemoed, Smithfield, Xhariep District, Free State Province	None	Archosauriformes indet.
UMZC T950	Harrismith, Thabo Mofutsanyane District, Free State Province	None	Archosauriformes indet.

3.3.2. *Quantitative analyses*

Post-mortem deformation and incomplete regions in most of the skulls of the South African proterosuchid sample mean that few measurements can be directly compared in all or most of the available specimens. As a result, it was not possible to conduct an exploratory analysis using quantitative morphometric data to shed light on the taxonomy of South African proterosuchids. Nevertheless, I did employ morphometric data to test the qualitative observations. The morphometric data set was composed of 160 linear measurements from each specimen, tooth count numbers for the premaxilla, maxilla and dentary, and the angle between the posterior margins of the proximal and distal ends of the quadrate. These data were collected from the South African proterosuchid specimens mentioned above and the three specimens of "*Chasmatosaurus*" *yuani*. A data subset was built, with the aims of prioritizing the putative diagnostic features recognized qualitatively within the South African proterosuchid specimens (e.g. quadrate angle, length of anterior process of maxilla; see below) and including the maximum possible number of specimens. The resultant subset was composed of nine specimens and five measurements, but two measurements were significantly correlated with one another (number of tooth positions in the maxilla and the length of the anterior process of the maxilla; Pearson's correlation coefficient=0.6687, seven d.f., P=0.049). As a result, one of them (maxillary tooth count) was pruned. The final data subset was composed of nine specimens and four characters (Appendix 3: table S1).

Measurements were normalized and transformed logarithmically following the protocol described by Lleonart et al. (2000) to remove information related to body size, including absolute size and allometric effects. A function to implement this normalization protocol was written for R, a freeware environment for statistical

Table 3.3. Locality and key previous taxonomic assignment of *Proterosuchus fergusi* specimens from the *Lystrosaurus* AZ of South Africa.

Specimen	Locality	Previous assignment
BP/1/3993	Farm Nooitgedacht 68, Bethulie District, Free State Province	'*Proterosuchus vanhoepeni*' (Cruickshank, 1972); *Proterosuchus fergusi* (Welman, 1998)
BP/1/4016	Farm Nooitgedacht 68, Bethulie District, Free State Province	*Proterosuchus fergusi* (Welman, 1998)
BP/1/4224	Bethulie Commonage, close to bridge over Orange River, Bethulie District, Free State Province	None
BSPG 1934 VIII 514	Rietfontein, on the bank of the Caledon River, between Bethulie and Aliwal North, Joe Gqabi or Xhariep District, Free State or Eastern Cape Province	"*Chasmatosaurus vanhoepeni*" (Broili and Schröder, 1934); *Proterosuchus fergusi* (Welman, 1998)
GHG 231	red mudstone on the farm Brakfontein 333 (32°12'01" S; 26°07'40" E), Cradock, Chris Hani District, Eastern Cape Province	*Proterosuchus fergusi* (Welman, 1998)
GHG 363	green mudstone on the farm Wilgeboshrivier 241 (31°45'44.32" S; 25°01'46.95" E), Middelburg, Chris Hani District, Eastern Cape Province	None
RC 59	Barendskraal, Middelburg, Chris Hani District, Eastern Cape Province	"*Elaphrosuchus rubidgei*" (holotype, Broom, 1946); "*Proterosuchus vanhoepeni*" (Cruickshank, 1972); *Proterosuchus fergusi* (Welman, 1998)
RC 846 (proposed neotype)	Farm Ruygte Valley 321, Middelburg, Chris Hani District, Eastern Cape Province	*Proterosuchus fergusi* (Welman, 1998)
SAM-PK-11208	Barendskraal, Middelburg, Chris Hani District, Eastern Cape Province	*Proterosuchus fergusi* (Damiani et al., 2003)
SAM-PK-K140	Visgat, Conway, Middelburg, Chris Hani District, Eastern Cape Province	"*Proterosuchus vanhoepeni*" (Cruickshank, 1972); *Proterosuchus fergusi* (Welman, 1998)
SAM-PK-K10603	Heldemoed, Smithfield, Xhariep District, Free State Province	None
TM 201	Harrismith, Thabo Mofutsanyane District, Free State Province	"*Chasmatosaurus vanhoepeni*" (holotype, Haughton, 1924); "*Proterosuchus vanhoepeni*" (Cruickshank, 1972); *Proterosuchus fergusi* (Welman, 1998)

computing and graphics (Appendix 4). This function normalizes measurements following the equation of Lleonart et al. (2000) only if the results of allometric regression are significant; if not, it normalizes measurements by dividing them by the independent variable (i.e. common ratio normalization). Total skull length was used as the independent variable for both normalizations. Total skull length could not be measured directly in BP/1/4016 and NMQR 1484 because the premaxilla is damaged in both specimens. Nevertheless, total skull length was estimated for both specimens using equations derived from exponential regressions between skull length and dentary length for BP/1/4016 and infratemporal fenestra length for NMQR 1484. These regressions were generated using data from the other proterosuchid specimens (P<0.0001, R^2=0.99) (Appendix 5). Quadrate angle was not normalized or transformed because its allometric regression was not significant (P=0.8736, R^2=0.0039) and there is no evidence that it is affected by absolute size. However, quadrate angle was divided by 100 to match the range of values obtained for the normalized and logarithmically transformed measurements (Appendix 3: table S2).

The transformed and normalized data subset was used to conduct a principal component analysis (PCA) in R. In addition, PERMANOVA analyses were employed to test for significant distinctions between specimens assigned to *Proterosuchus fergusi* and to the other three species, and between the four species recognized by qualitative data (i.e. *Proterosuchus fergusi*, *Proterosuchus alexanderi* comb. nov., *Proterosuchus goweri* sp. nov. and "*Chasmatosaurus*" *yuani*). Similarly, linear discriminant analyses (LDAs), generating jacknifed predictions, were conducted on a data set to distinguish between specimens of *Proterosuchus fergusi* and specimens of other proterosuchid species, and to distinguish specimens of the four different species recognized by qualitative evidence. T-tests (t.test function), PERMANOVAs (adonis

function), LDAs (lda function) and distribution tests (pnorn function; inferring a normal distribution) were also conducted in R and an alpha level of 0.05 was used in all statistical analyses. Degrees of freedom (d.f.) are reported for the first three mentioned analyses.

3.4. Results

3.4.1. Qualitative results

3.4.1.1. *Redescription of the holotype of* Proterosuchus fergusi *(SAM-PK-591)*

The holotype of *Proterosuchus fergusi* is redescribed in Appendix 6 with the aim of determining if it is a diagnostic specimen.

3.4.1.2. *Differences between the holotype of* Proterosuchus alexanderi comb. nov. *(NMQR 1484) and other South African proterosuchid specimens*

I agree here with Welman and Flemming (1993) and Welman (1998) that several features proposed by previous authors as differences between the holotype of *Proterosuchus alexanderi* (NMQR 1484) (Fig. 3.1) and other proterosuchids (Hoffman, 1965; Charig and Reig, 1970) can be explained by ontogenetic variation or are not inconsistent with the condition present in other South African specimens (e.g. shape of snout, frontals and orbits, position of the lacrimal, squamosal with shallow otic notches). Charig and Reig (1970) proposed that the 90º angle formed by the paraoccipital processes of the opisthotics of NMQR 1484 was distinct from the lower angle present in other proterosuchids. However, Welman (1998) argued that the different condition present in NMQR 1484 was an artefact result of post-mortem distortion. I was unable to recognise the presence of such distortion in NMQR 1484

(see below), but the 90º angle in this specimen falls within the variation observed in other South African proterosuchids (e.g. GHG 231). However, several notable differences do exist between NMQR 1484 and other South African proterosuchid specimens that I discuss in more detail here.

Length of the anterior process of the maxilla. The total anteroposterior length of the maxilla of NMQR 1484 is 2.26 times the length of the part of the bone that is placed anterior to the anteriormost border of the antorbital fenestra (i.e. the length of the anterior process). By contrast, in other South African proterosuchid specimens this ratio ranges from 2.53–3.11 (Table 3.4), indicating that their anterior processes are proportionally substantially shorter. In TM 201 (the holotype of "*Chasmatosaurus vanhoepeni*") it is not possible to measure the total length of the maxilla, but the shape of the anterior process of the maxilla closely resembles that of most other specimens of South African proterosuchids when it is rescaled to the same size, and is proportionally considerably shorter than that in NMQR 1484. The length of the anterior process of the maxilla cannot be determined in the holotype of *Proterosuchus fergusi* (SAM-PK-591) because the anterior portion of the bone is missing. In the Chinese "*Chasmatosaurus*" *yuani* (IVPP V4067) the ratio between the total length of the maxilla and the length of the anterior process falls within the range observed in all South African specimens (Table 3.4), with the exception of NMQR 1484. The ratio in NMQR 1484 differs significantly from that present in other proterosuchids in a distribution test (P=0.001).

The proportionally longer anterior process of the maxilla of NMQR 1484 is not a result of a shorter antorbital fenestra because the ratio between the length of the antorbital fenestra and length of the dentary are rather similar in NMQR 1484 (0.256)

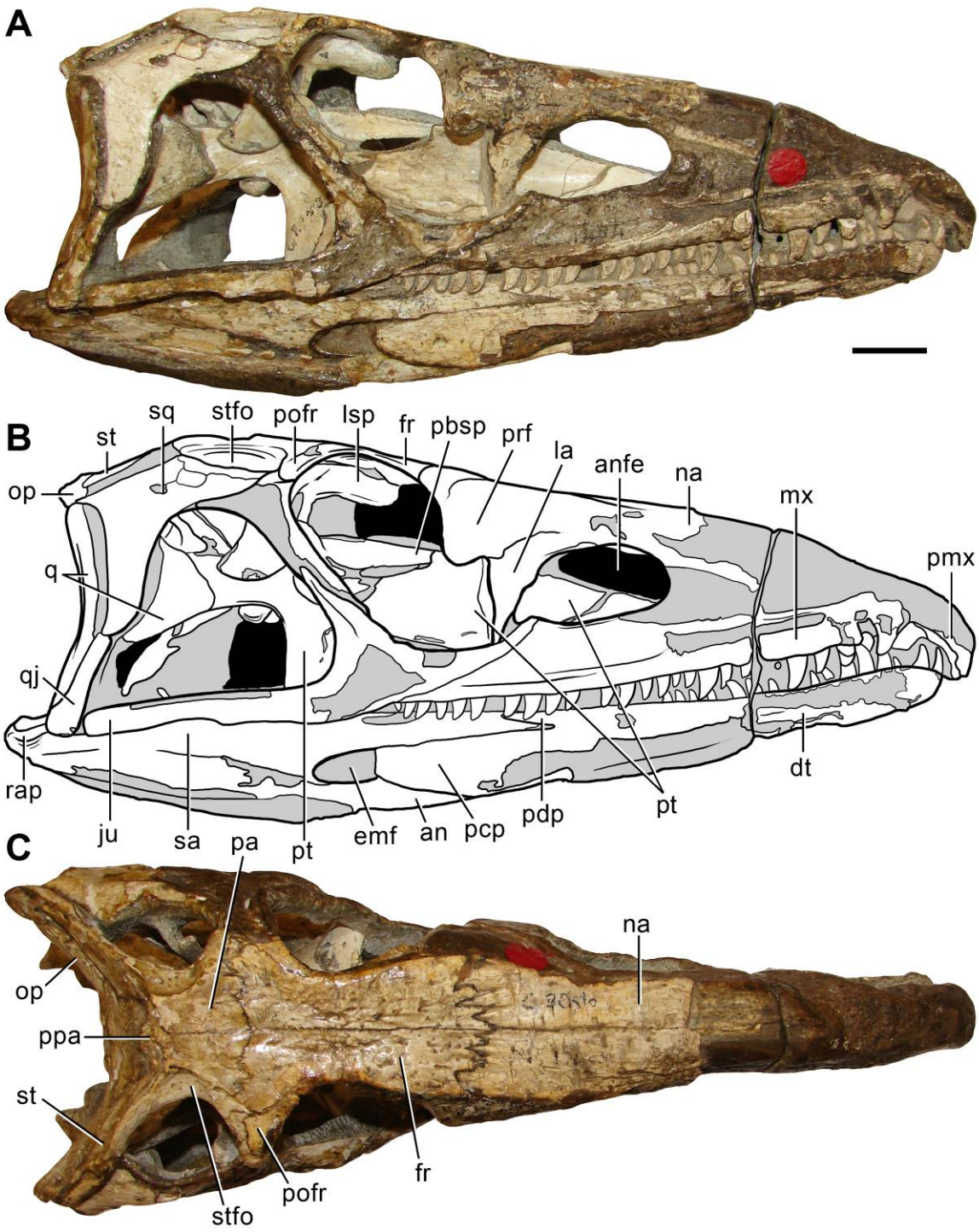

Figure 3.1. Skull of the holotype of *Proterosuchus alexanderi* (NMQR 1484). A, B, right lateral; and C, dorsal views. Abbreviations: an, angular; anfe antorbital fenestra; dt, dentary; emf, external mandibular fenestra; fr, frontal; ju, jugal; la, lacrimal; lsp, laterosphenoid; mx, maxilla; na, nasal; op, opisthotic; pa, parietal; pbsp, parabasisphenoid; pcp, posterocentral process; pdp, posterodorsal process; pmx, premaxilla; pofr, postfrontal; ppa, postparietal; prf, prefrontal; pt, pterygoid; q, quadrate; qj, quadratojugal; rap, retroarticular process; sa, surangular; sq, squamosal; st, supratemporal; stfo, supratemporal fossa. Scale bar equals 20 mm.

and in *Proterosuchus fergusi* (e.g. BSPG 1934 VIII 514: 0.258). In addition, NMQR 1484 possesses a proportionally higher maxillary tooth count than other proterosuchid specimens. When absolute body size and allometric effects are removed, the transformed and normalized value of the maxillary tooth count for NMQR 1484 is 1.50 and in other specimens ranges from 1.39–1.46 (BP/1/4016, SAM-PK-K140, SAM-PK-11208, NMQR 880, RC 846, BSPG 1934 VIII 514, IVPP V4067, GHG 231). The higher number of maxillary teeth in NMQR 1484 is probably a result of a proportionally longer anterior process of the maxilla (both characters are significantly correlated with each other, see Materials and Methods of this Chapter) rather than a shorter antorbital fenestra.

Ornamentation on the dorsal surface of the frontal. The dorsal surfaces of the frontals of NMQR 1484 are ornamented by a series of anastomosed shallow grooves and sub-circular pits with a random arrangement (Fig. 3.2A). By contrast, the dorsal surfaces of the frontals of other South African proterosuchids (e.g. BP/1/3993, 4016, 4224, BSPG 1934 VIII 514, GHG 231, NMQR 880, RC, 59, 846, SAM-PK-K10603) and the Chinese species "*Chasmatosaurus*" *yuani* (IVPP V4067) are almost flat or possess very shallow depressions, but lack grooves or pits (Fig. 3.2B–D). This condition is present in specimens both smaller and larger than NMQR 1484, indicating that the ornamentation present in the latter specimen cannot be explained only by ontogenetic variation.

Quadrate angle. The angle formed between the posterior margins of the proximal and distal ends of the quadrate is 149º in NMQR 1484 (holotype of *Proterosuchus alexanderi*) and NMQR 880 (holotype of *Proterosuchus goweri*). By contrast, in other

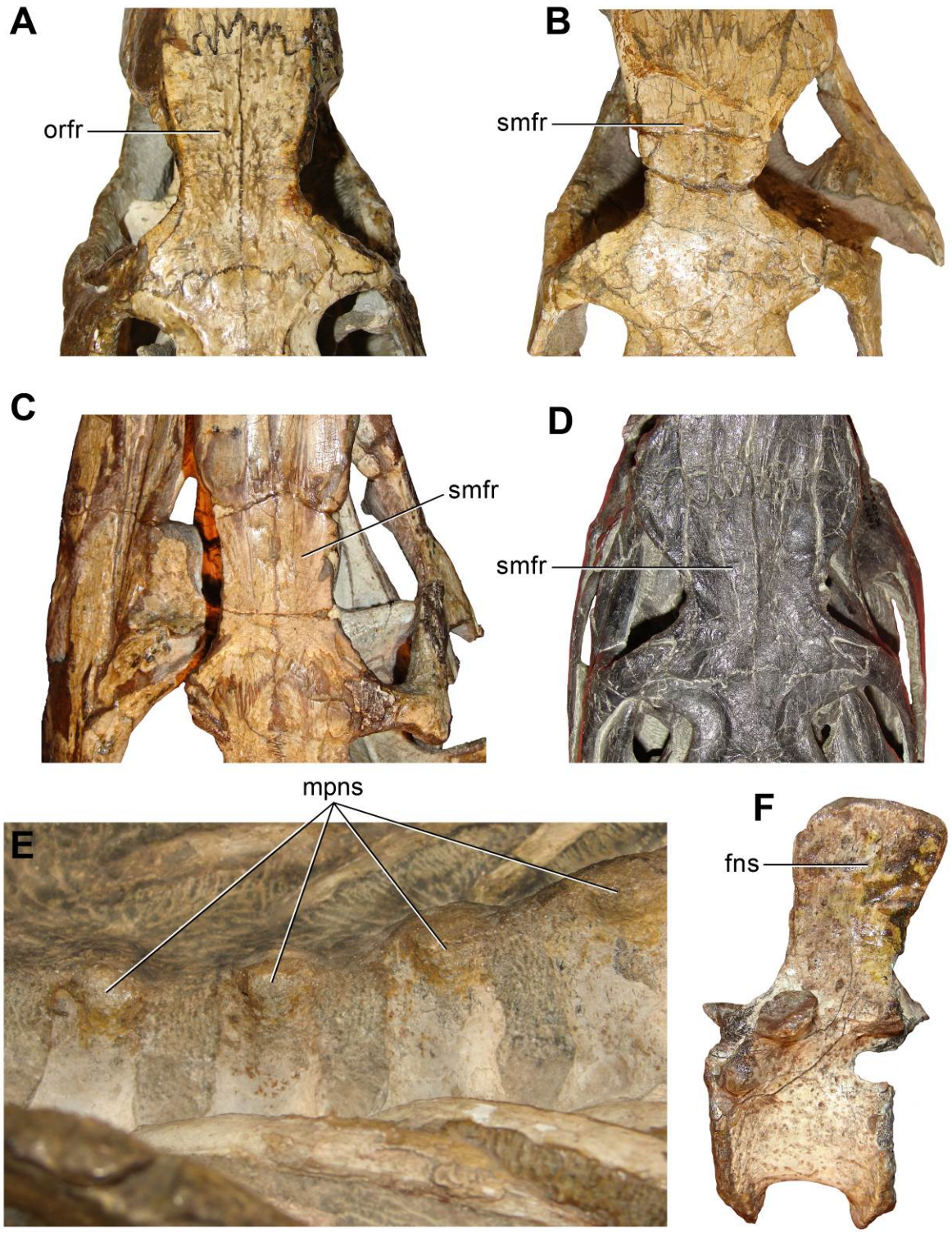

Figure 3.2. Comparison between the three species of *Proterosuchus* from South Africa. A, E, *Proterosuchus alexanderi* (NMQR 1484); B, *Proterosuchus goweri* (NMQR 880); and C, D, F, *Proterosuchus fergusi* (C, RC 59; D, SAM-PK-K10603; F, GHG 363). A–D, frontals in dorsal view; and E, presacral vertebrae 13–16; and F, anterior dorsal vertebra in left lateral views. Abbreviations: fns, flat neural spine; mpns, mammillary processes on neural spines; orfr, ornamented frontal; smfr, smooth frontal. Not to scale.

South African proterosuchid specimens this angle ranges from 120–127º (Table 3.4). In the Chinese "*Chasmatosaurus*" *yuani* this angle is 155º (IVPP V4067). A T-test recovered a significant difference in the quadrate angle between the group formed by NMQR 1484, NMQR 880 and "*Chasmatosaurus*" *yuani* and that formed by other South African proterosuchid specimens (2.71 d.f., P=0.0019).

The presence of a more vertical quadrate in NMQR 1484 than in other South African proterosuchids was previously recognized by Charig and Reig (1970), and subsequently dismissed as not informative by Welman (1998). Welman (1998) proposed that the nearly vertical orientation of the quadrate of NMQR 1484 was the result of a distortion pressure on the posteroventral end of the skull combined with an extreme position resulting from streptostylic cranial kinesis. However, the following alternative hypothesis is proposeed here. NMQR 1484 is represented by a fairly complete axial skeleton and some appendicular bones preserved in articulation (Hoffman, 1965: figs. 4, 5). Although preserved in articulation with the skull, the cervical series does not exhibit evidence of significant post-mortem deformation, contrasting with the expectation of the hypothesis of Welman (1998). Moreover, if deformation affected the posteroventral end of the skull, the retroarticular processes should show evidence of deformation. However, no such deformation is present; indeed, the processes possess a morphology very similar to that present in other South African proterosuchid specimens (BP/1/3993, 4016, BSPG 1934 VIII 514, RC 846, SAM-PK-11208).

In addition, the relationship between the quadrate, quadratojugal and posterior process of the jugal is the same as in most South African proterosuchid specimens (e.g. BSPG 1934 VIII 514, RC 846, SAM-PK-11208, K10603), in which the posterior

Table 3.4. Selected cranial measurements and ratios of proterosuchid specimens.

Specimen	Taxonomic assignment	Maxilla-anterior process lengths ratio	Minimum height horizontal process-maxilla length ratio	Quadrate angle	Parietal-supratemporal fossa minimum widths ratio
BP/1/3993	*Proterosuchus fergusi*	2.53	0.123	-	3.4
BP/1/4016	*Proterosuchus fergusi*	2.70	0.121	124º	5.9
BP/1/4224	*Proterosuchus fergusi*	-	-	127º	4.6
BSPG 1934 VIII 514	*Proterosuchus fergusi*	2.83	0.131	120º	7.8
GHG 231	*Proterosuchus fergusi*	3.11	0.120	126º	3.4
IVPP V4067	"*Chasmatosaurus*" *yuani*	2.75	0.132	155º	4.6
NMQR 880	*Proterosuchus goweri*	2.62	0.152	149º	4.5
NMQR 1484	*Proterosuchus alexanderi*	2.26	0.124	149º	4.5
RC 59	*Proterosuchus fergusi*	2.93	0.069	-	4.2
RC 846	*Proterosuchus fergusi*	2.78	0.108	126º	3.8
SAM-PK-591	Proterosuchidae	-	0.098	-	-
SAM-PK-11208	*Proterosuchus fergusi*	2.68	0.121	125º	4.1
SAM-PK-K140	*Proterosuchus fergusi*	2.78	0.115	122º	-
SAM-PK-K10603	*Proterosuchus fergusi*	2.62	-	125º	3.0
TM 201	*Proterosuchus fergusi*	-	-	-	8.0

process of the jugal almost contacts the quadratojugal and the infratemporal fenestra is incipiently open posteroventrally. By contrast, if the skull was deformed as proposed by Welman (1998) it would be expected that the posterior process of the jugal would overlap the quadratojugal following the displacement of the quadrate-quadratojugal to acquire a nearly vertical orientation. Similarly, if the vertical orientation of the quadrate of NMQR 1484 is interpreted as result of an extreme kinetic position and the quadrate is forced to acquire a posteroventral orientation, as occurs in the vast majority of South African proterosuchid specimens (e.g. BP/1/3993, 4016, 4224, BSPG 1934 VIII 514, GHG 231, RC 846, SAM-PK-11208, K140, K10603), the posterior tip of the jugal would lie far away from the quadratojugal, clearly contrasting with the condition present in other proterosuchids. Moreover, the position of the palato-quadrate complex of NMQR 1484 is rather similar to that of RC 846 (proposed neotype of *Proterosuchus fergusi*), suggesting the absence of a considerable difference in the kinetic position of the skull. Accordingly, I was unable to identify evidence to support the hypothesis of Welman (1998) that NMQR 1484 suffered substantial deformation at its posteroventral end or that cranial kinesis can explain the differences in quadrate orientation and angle between its ends observed between this specimen and other South African proterosuchid specimens.

Mammillary processes in presacral neural spines. Some Early Triassic archosauromorphs possess lateral processes on the distal half of their neural spines in some vertebrae of the presacral series (e.g. *Prolacerta broomi*: BP/1/2675; *Boreopricea funerea*: PIN 3708/1; "*Chasmatosaurus*" *yuani*: IVPP V4067). These processes differ from the transverse expansion restricted to the distal tip of the neural spine (i.e. spine table) present in some archosauriforms (e.g. *Euparkeria capensis*:

SAM-PK-5867; *Riojasuchus tenuisceps*: PVL 3827; *Herrerasaurus ischigualastensis*: PVL 2566). Instead, they are formed by a gradual lateral development along the distal half of the neural spine and are distinctly separated from the distal end of the neural spine by a longitudinal cleft, resulting in a spine ending with three distal projections. The morphology of these processes is very similar to the mammillary processes of araeoscelidians (e.g. *Araeoscelis gracilis*: Vaughn, 1955; *Petrolacosaurus kansensis*: Reisz, 1981). As a result, the similar processes present in some Triassic archosauromorphs are also referred to here as mammillary processes, but they are almost certainly independently acquired structures.

NMQR 1484 possesses mammillary processes on the distal half of the neural spines in presacral vertebrae 5–16 (i.e. cervicals 5–9 and dorsals 1–7) (Fig. 3.2E), but the condition is unknown in presacral 4. In other South African proterosuchid specimens the presence of mammillary processes is rather variable along the presacral series 5–16. In SAM-PK-K140 (*Proterosuchus fergusi*) the mammillary processes are absent in presacrals 6 or 7, 7 or 8 and the anterior–middle dorsal vertebrae. In GHG 363 (*Proterosuchus fergusi*) the mammillary processes are present in the cervico-dorsal vertebrae (possibly cervical 8 or 9 to dorsal 1 or 2), but absent in two anterior dorsal vertebrae (probably belonging to dorsals 3–7) (Fig. 3.2F). In BP/1/3993 (*Proterosuchus fergusi*) mammillary processes are absent in two middle–posterior cervicals, which are identified as located posterior to cervical 4. In SAM-PK-11208 (*Proterosuchus fergusi*) cervicals 6–9 possess mammillary processes on the neural spines whereas they are absent in cervical 5 and the condition is unknown in the dorsal series. Accordingly, there is variation in the point within the presacral column at which the mammillary processes of the neural spines are absent (e.g. cervical 6/7 in SAM-PK-K140 and within the anterior dorsal series in GHG 363 and SAM-PK-

11208). However, in specimens of *Proterosuchus fergusi* that preserve the dorsal series (e.g. GHG 363, SAM-PK-K140, SAM-PK-11208) the mammillary processes are consistently absent posterior to the cervico-dorsal transition, contrasting with NMQR 1484 in which they extend into the middle dorsals. In the Chinese "*Chasmatosaurus*" *yuani* the mammillary processes of the neural spines are present in the posteriormost five cervical vertebrae and the first four dorsal vertebrae (probably presacrals 5–13) (IVPP V4067; MDE and Corwin Sullivan pers. obs.). However, taking into account the strong variation present in the distribution of the mammillary processes in *Proterosuchus fergusi*, it would not be surprising if further sampling blurred the discrete difference currently observed between specimens of *Proterosuchus fergusi* and NMQR 1484.

3.4.1.3. *Differences between the holotype of* Proterosuchus goweri *sp. nov.(NMQR 880) and other South African proterosuchids*

A number of anatomical features that differentiate NMQR 880 (Fig. 3.3) from other South African proterosuchids are here described and discussed, which allow me to recognise a new species of *Proterosuchus* for this specimen.

Dorsoventral minimum height of the horizontal process of the maxilla.

Quantitative analyses showed that the horizontal process of the maxilla of NMQR 880 is proportionally deeper than in other proterosuchids. In NMQR 880 the minimum height of the horizontal process of the maxilla is 15.2% of the total length of the maxilla. By contrast, in other South African and Chinese proterosuchid specimens this ratio ranges from 7–13.2% (Table 3.4). The ratio present in NMQR 880 differs significantly from the distribution of ratios present in other South African and Chinese

proterosuchid specimens (*P*=0.0192). NMQR 880 has a proportionally deeper horizontal process than that present in both smaller and larger specimens of *Proterosuchus fergusi*. As a result, this difference cannot be explained only by ontogeny.

Alveolar margin of the maxilla sigmoidal. The anterior two-thirds of the maxillary alveolar margin of NMQR 880 are concave and the posterior third is convex, resulting in a distinctly sigmoid ventral margin of the bone in lateral view (Fig. 3.3A, B). By contrast, in other specimens of South African proterosuchids (BP/1/3993, 4016, BSPG 1934 VIII 514, GHG 231, NMQR 1484, RC 59, 846, SAM-PK-11208, K10603, TM 201) and the Chinese "*Chasmatosaurus*" *yuani* (IVPP V36315, V4067) the alveolar margin of the maxilla is mostly straight or continuously slightly convex in lateral view (Fig. 3.4).

Edentulous portion equivalent in length to two tooth positions at the anterior end of the maxilla. The anterior end of the maxillary alveolar margin of NMQR 880 is edentulous, with a gap that would have housed two tooth positions (Fig. 3.3A, B: edm), resembling the condition present in "*Chasmatosaurus*" *yuani* (IVPP V4067). By contrast, in other South African proterosuchid specimens the alveolar margin of the maxilla has a gap equivalent to only one tooth position (e.g. BP/1/4016, NMQR 1484, RC 846, SAM-PK-11208, TM 201).

Quadrate angle. See discussion above for NMQR 1484.

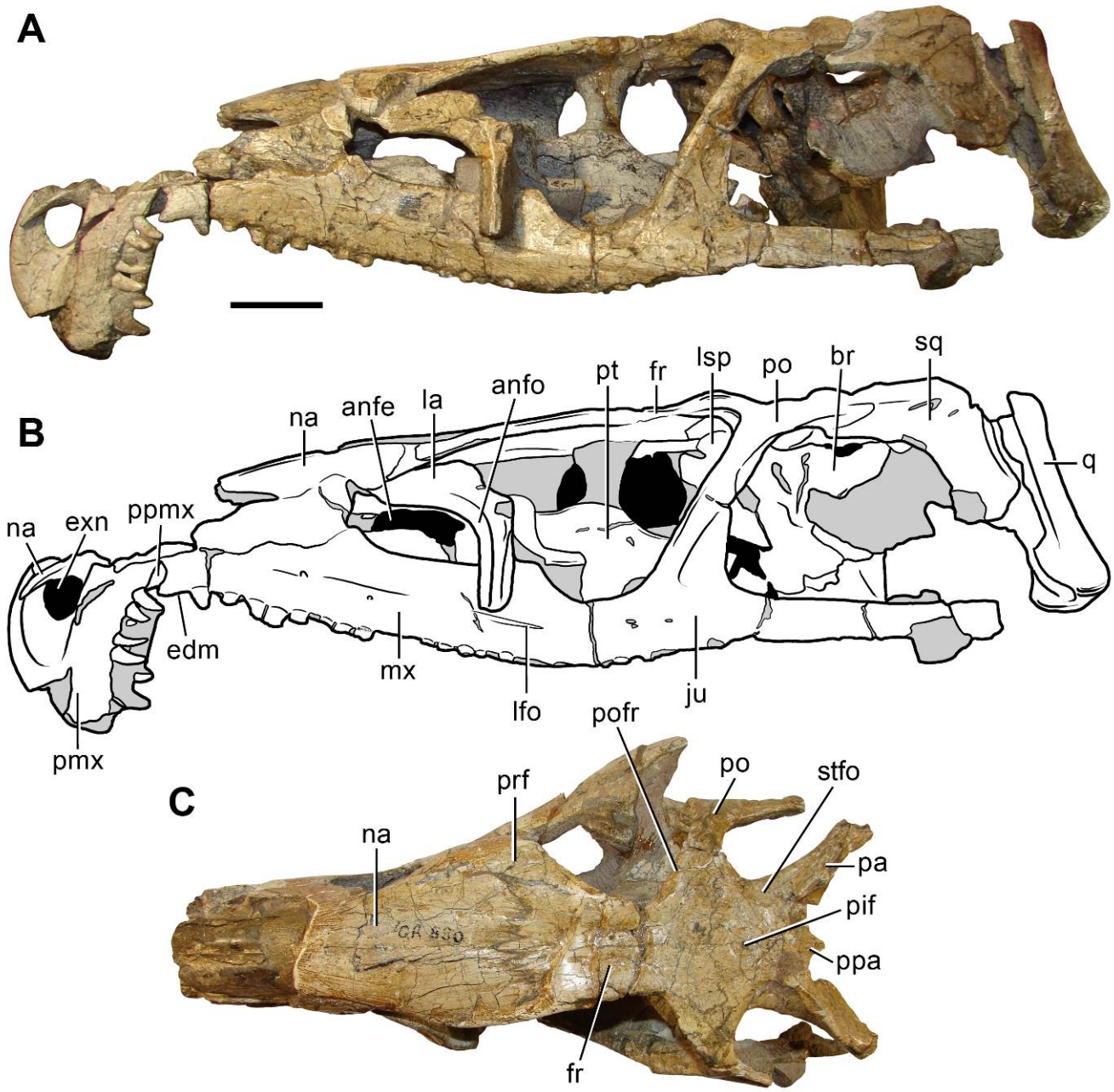

Figure 3.3. Skull of the holotype of *Proterosuchus goweri* (NMQR 880). A, B, left lateral; and C, dorsal views. Abbreviations: anfe, antorbital fenestra; anfo, antorbital fossa; br, braincase; edm, edentulous margin; exn, external naris; fr, frontal; ju, jugal; la, lacrimal; lfo, lateral foramen; lsp, laterosphenoid; mx, maxilla; na, nasal; pa, parietal; pif, pineal foramen; pmx, premaxilla; po, postorbital; pofr, postfrontal; ppa, postparietal; ppmx, palatal process of the maxilla; prf, prefrontal; pt, pterygoid; q, quadrate; sq, squamosal; stfo, supratemporal fossa. Scale bar equals 30 mm.

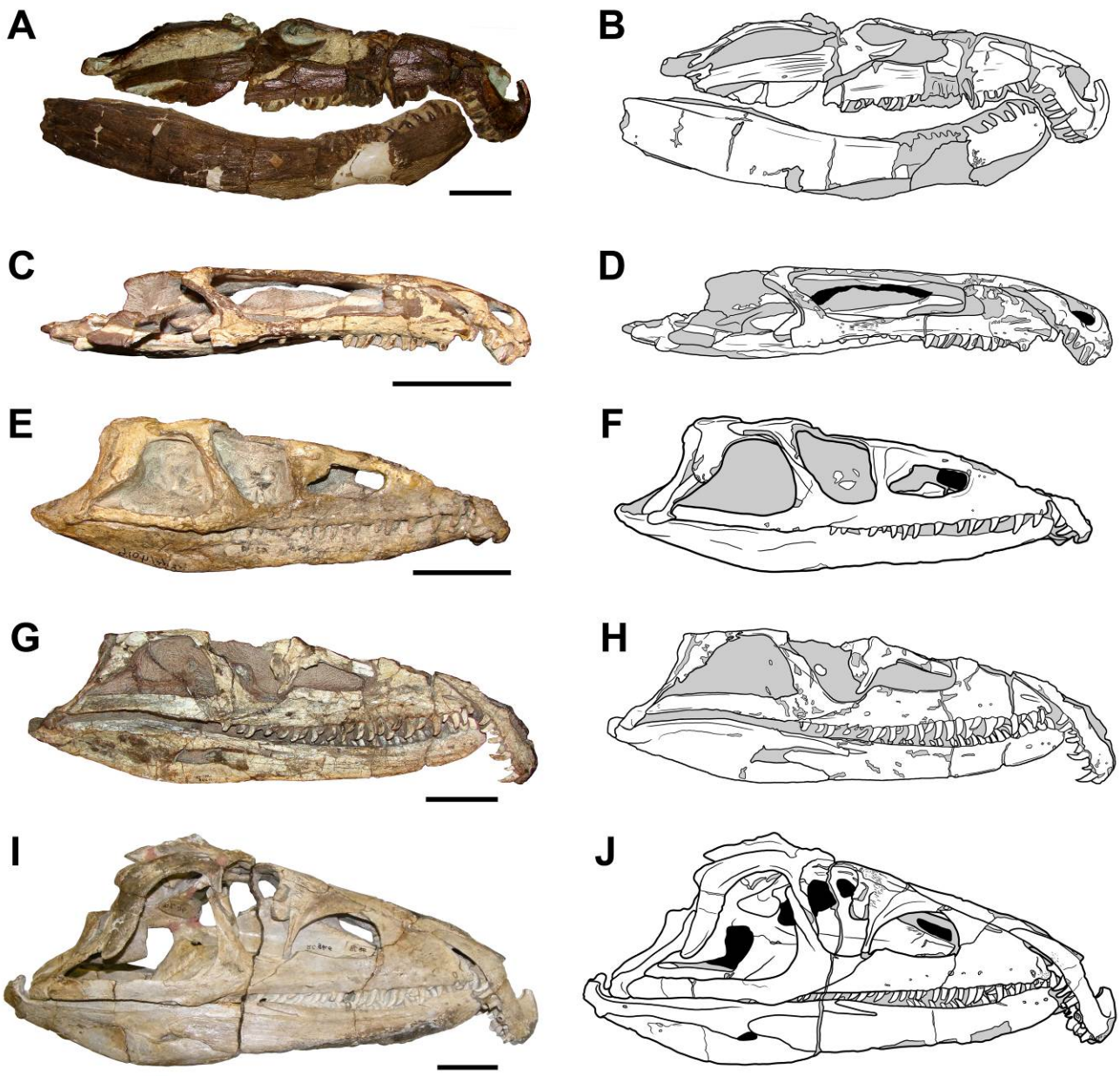

Figure 3.4. *Proterosuchus fergusi*. A–H, skull and lower jaw of referred specimens; and I–J, proposed neotype in lateral views. A, B, TM 201; C, D, RC 59; E, F, BP/1/4016 (reversed); G, H, SAM-PK-11208 (reversed); and I, J, RC 846. Scale bars equal 50 mm.

3.4.1.4. *Other differences among South African proterosuchid specimens*

There are two additional, non-ontogenetically-controlled, variable characters among the South African proterosuchid specimens that deserve discussion.

Quadratojugal-jugal bar. Broom (1932: fig. 1) and Broili and Schröder (1934: figs. 1, 2, 4, 6) interpreted the ventral border of the infratemporal fenestra of *Proterosuchus fergusi* as completely closed, but the position and shape of the jugal-quadratojugal contact was unknown to those authors. Cruickshank (1972: fig. 1) reached the same interpretation and suggested that the anterior process of the quadratojugal rested in a groove on the lateral surface of the posterior process of the jugal. This latter interpretation was followed by subsequent authors (e.g. Dilkes, 1998: character 35). Re-examination of South African proterosuchid specimens revealed that most individuals lack an anterior process on the quadratojugal and/or a jugal-quadratojugal suture (Fig. 3.5A). Accordingly, the lower temporal bar (= ventral border of the infratemporal fenestra) is incomplete, as also occurs in "*Chasmatosaurus*" *yuani* (IVPP V4067) and several non-archosauriform archosauromorphs (e.g. *Prolacerta broomi*, *Mesosuchus browni*, *Protorosaurus speneri*, *Azendohsaurus madagaskarensis*, *Tanystropheus longobardicus*; Dilkes, 1998; Flynn et al., 2010). Nevertheless, the posterior process of the jugal in proterosuchids is extremely long and may loosely contact the main body of the quadratojugal during extreme streptostylic kinetic movements. By contrast, in two specimens of *Proterosuchus fergusi*, BP/1/3993 and BP/1/4016, at least on one side of the skull the quadratojugal possesses a very small anterior process that articulates with the posterior process of the jugal, completely closing the ventral border of the infratemporal fenestra (Fig. 3.5B, C) (the right quadratojugal of BP/1/3993 seems to lack an anterior process,

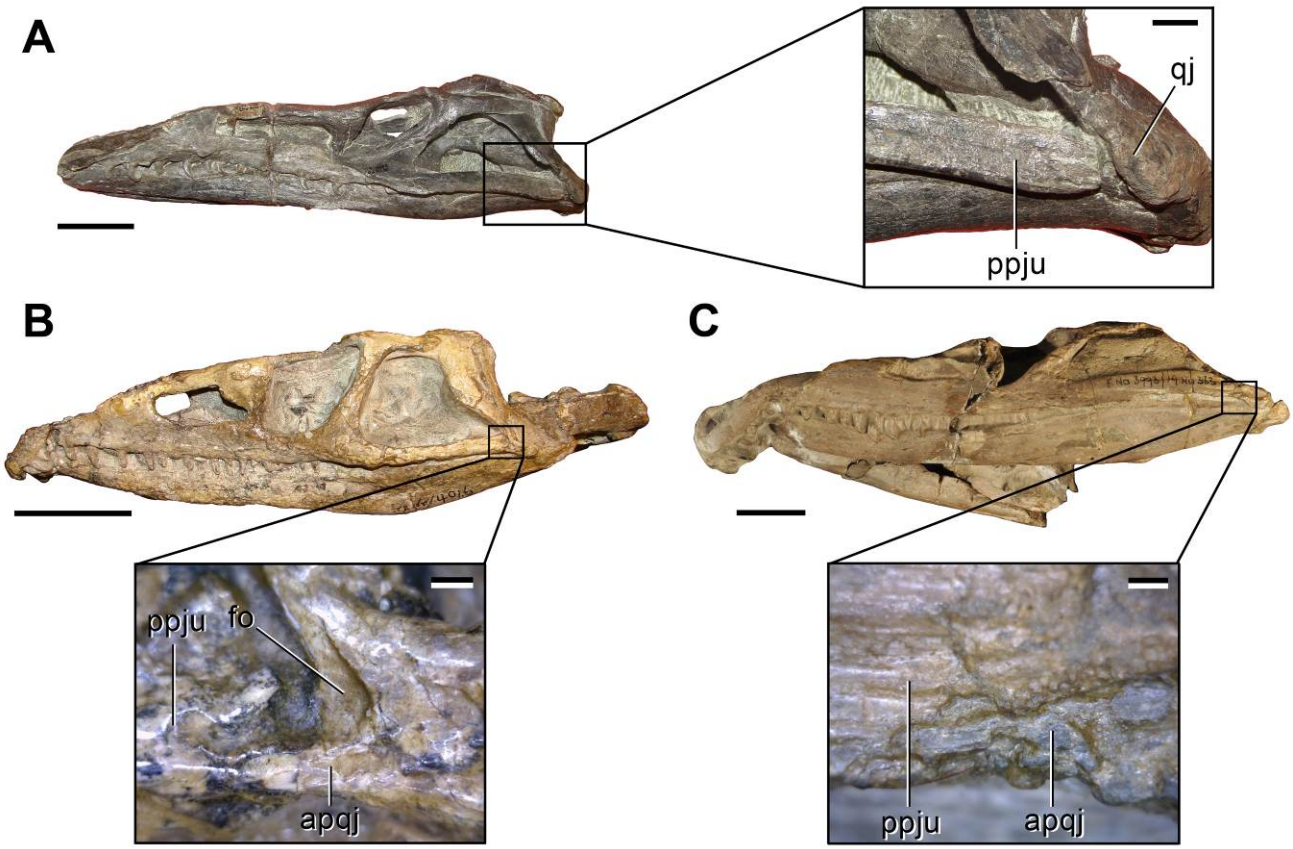

Figure 3.5. Close-ups of the posteroventral corner of the infratemporal fenestra in three referred specimens of *Proterosuchus fergusi* in lateral views. A, open lower temporal bar morphotype; and B, C, closed lower temporal bar morphotype. A, SAM-PK-K10603 (reversed); B, BP/1/4016; and C, BP/1/3993. Abbreviations: apqj, anterior process of the quadratojugal; fo, fossa; ppju, posterior process of the jugal; qj, quadratojugal. Scale bars in overall pictures of the skulls equal 50 mm, in the close-up of A equals 10 mm, and in the close-ups of B and C equal 10 mm.

resembling the open infratemporal fenestra present in other specimens of *Proterosuchus fergusi*). This morphology seems to be a very poorly developed version of the condition present in *Fugusuchus hejiapanensis*, erythrosuchids, *Euparkeria capensis*, proterochampsids, phytosaurs and archosaurs (Ewer, 1965; Romer, 1971a; Parrish, 1992; Gower, 2003; Nesbitt, 2011; Ezcurra et al., 2013). The anterior process of the quadratojugal (Fig. 3.5B, C: apqj) of BP/1/3993 and BP/1/4016 fits into a groove on the lateral surface of the posterior end of the posterior process of the jugal, as described by Cruickshank (1972). This condition would have hampered the palatoquadrate-quadratojugal of BP/1/3993 and BP/1/4016 from functioning as a separate unit to the lower temporal bar during kinetic streptostylic movements, contrasting with most South African proterosuchid specimens. Some specimens that are intermediate in size between BP/1/4016 and BP/1/3993 possess an incomplete lower temporal bar (e.g. NMQR 1484, SAM-PK-11208), suggesting that the closure of the ventral border of the infratemporal fenestra is not related to ontogenetic changes, but the condition might be also variable within the same individual (e.g. BP/1/3993).

Supratemporal fossa. Most specimens of South African proterosuchids have a transversely broad and shallow supratemporal fossa adjacent to the medial border of the supratemporal fenestra (Fig. 3.6C, D: bsfo), with the ratio of the minimum widths of the parietals versus the supratemporal fossa being below 6.0 (Table 3.4). By contrast, two specimens of *Proterosuchus fergusi* (BSPG 1934 VIII 514 and TM 201) possess transversely narrow and deep supratemporal fossae (Fig. 3.6A, B: ndfo), in which the ratio is higher than 7.5 (Table 3.4). In the single specimen of "*Chasmatosaurus*" *yuani* that preserves the posterior end of the skull roof (IVPP

V4067) the supratemporal fossa is broad and shallow, resembling the condition present in most South African specimens (Table 3.4).

Numerous non-ontogenetically variable features do not show any clear pattern that would allow different morphotypes to be distinguished. Such features appear to include the variability previously discussed in the jugal-quadratojugal bar (Fig. 3.5) and supratempral fossae (Fig. 3.6) on the parietals. The presence of a fully closed jugal-quadratojugal bar is present only in BP/1/3993 and BP/1/4016 (Fig. 3.5B, C), but I could not find other unique characters shared by these specimens that would allow a clearly distinct morphotype to be recognised based on these two individuals. It is interesting that BP/1/3993 and BP/1/4016 come from the same locality (although their relative stratigraphic positions within the *Lystrosaurus* AZ are not clear; Botha-Brink et al., 2014) and, as a result, the presence of a closed jugal-quadratojugal bar could represent regional and/or temporal variation. A larger sample and better stratigraphic resolution is needed to test this hypothesis.

The presence of narrow and deep supratemporal fossae in TM 201 and BSPG 1934 VIII 514 is a character that distinguishes these specimens from other South African proterosuchids and "*Chasmatosaurus*" *yuani*, including specimens of similar size (i.e. skull length >400mm, e.g. RC 846, IVPP V4067, GHG 231). However, the rest of the anatomy of TM 201 and BSPG 1934 VIII 514 is consistent with other specimens of *Proterosuchus fergusi* (e.g. RC 59, 846, BP/1/14016, 3993, GHG 231, SAM-PK-11208, K10603). It is interesting that the morphotype of narrow and deep supratemporal fossae is found only among large proterosuchid specimens (i.e. TM 201 and BSPG VIII 514). These specimens had probably reached sexual maturity because they are larger than SAM-PK-11208 (Fig. 3.7), which seems to have already reached this ontogenetic stage based on palaeohistological evidence (Botha-Brink and

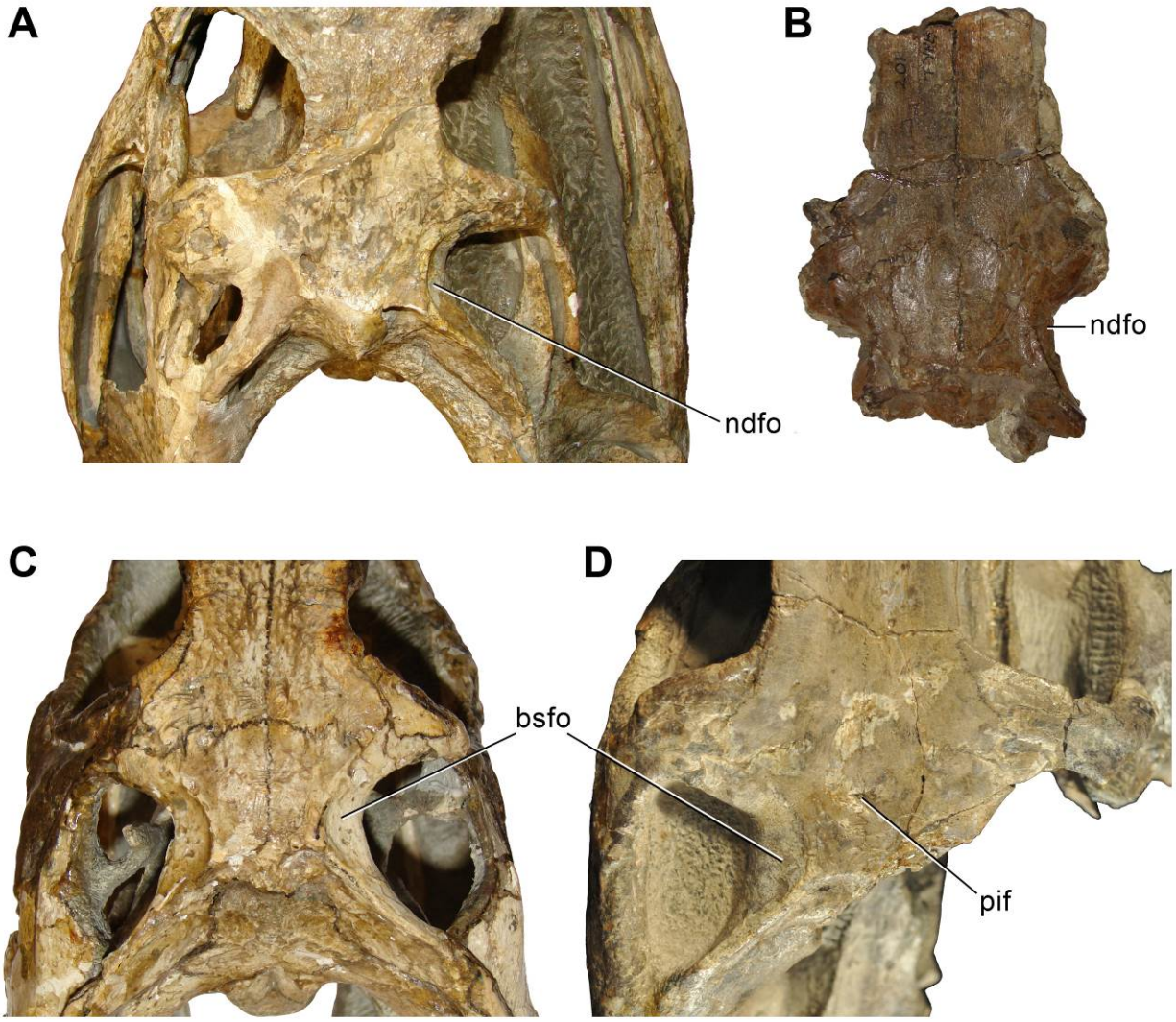

Figure 3.6. Comparison between *Proterosuchus* supratemporal fossa morphotypes. A, B, narrow and deep; and C, D, broad and shallow morphotypes in dorsal views. A, B, D, *Proterosuchus fergusi* (A, BSPG 1934 VIII 514; B, TM 201; D, BP/1/3993); and C, *Proterosuchus alexanderi* (NMQR 1484). Abbreviations: bsfo, broad and shallow supratemporal fossa; ndfo, narrow and deep supratemporal fossa; pif, pineal foramen. Not to scale.

Smith, 2011). By contrast, all known probable juvenile and sub-adult individuals (e.g. RC 59, BP/1/3993, 4016, 4224, SAM-PK-K140, K10603) possess broad and shallow supratemporal fossae (Fig. 3.7). The variation in the morphology of the supratemporal fossa does not therefore appear to be ontogenetically-controlled at the specific level. However, ontogenetic variation could still exist within a subsample of the species, if incomplete sampling means that medium sized individuals with narrow supratemporal fossae have not yet been discovered (green dashed line in Fig. 3.7). This would suggest the differentiation of two morphotypes occurring after sexual maturity, potentially representing a case of intraspecific adult dimorphism related to sexual differences (e.g. see Raath, 1990). The same kind of intraspecific variation in the width of the supratemporal fossa has been described in the archosauromorph *Prolacerta broomi* (Modesto and Sues, 2004), in which most specimens have a broad supratemporal fossa (BP/1/471, BP/1/4504a, BP/1/5066, BP/1/5375, SAM-PK-K10797, UMZC 2003.41R) and a few have a narrow fossa (BP/1/2675, GHG 431). Further studies should be conducted to determine if there is any size pattern in the distribution of these morphotypes in *Prolacerta broomi*. In any case, the variations observed in the jugal-quadratojugal bar and supratemporal fossae of the South Arican proterosuchids do not seem to be taxonomically informative within the currently available sample of South African proterosuchid specimens.

3.4.2. Quantitative results

The result of the PCA is consistent with the taxonomic scheme suggested by qualitative evidence, recovering a clear distinction between specimens assigned to *Proterosuchus fergusi* and those of the other three proterosuchid species (i.e.

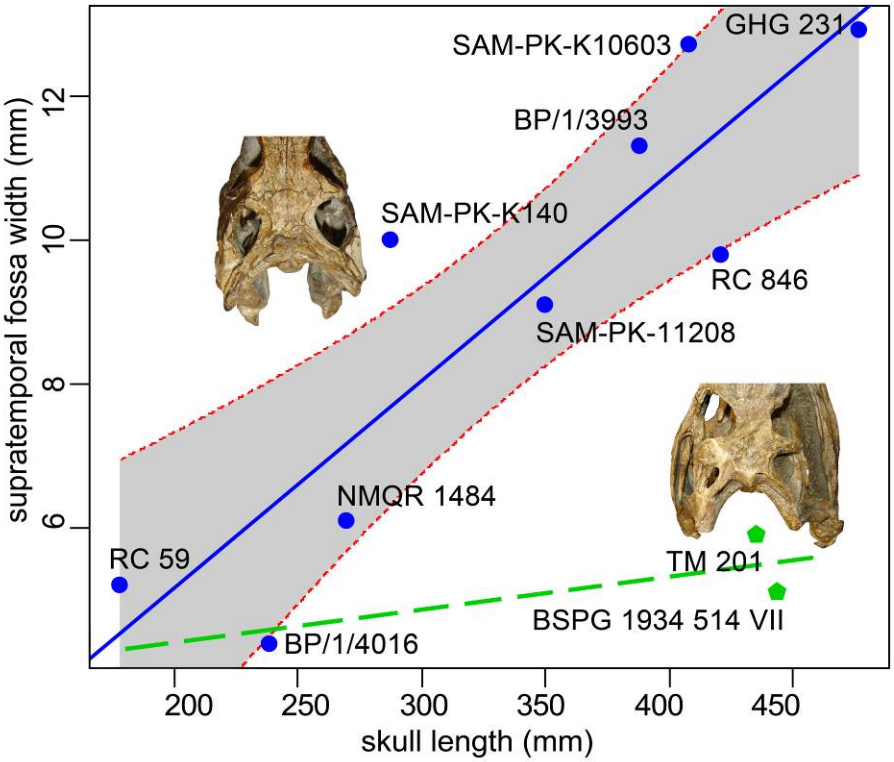

Figure 3.7. Bivariate plot between skull length and supratemporal fossa width in *Proterosuchus* spp. Blue dots and regression correspond to the broad and shallow supratemporal fossa morphotype, and the green dots correspond to the narrow and deep morphotype. Green dotted line is a qualitative 'regression' showing the probable change in slope if the condition in both morphotypes was similar in juvenile individuals. Green area represents the 95% confidence interval of the broad and shallow supratemporal fossa morphotype regression.

Proterosuchus alexanderi, *Proterosuchus goweri* and "*Chasmatosaurus*" *yuani*) (Fig. 3.8). PC1 (57.2%) mainly represents variation of the quadrate angle, PC2 (36.1%) mainly variation of the width of the supratemporal fossa, and PC3 (5.2%) and PC4 (1.5%) mainly variation of the length of the anterior process of the maxilla and the minimum height of the horizontal process of the maxilla (Appendix 3: table S3). Rotation coefficients of the PCA show that a different variable mainly drives the information in each component and, as a result, PC3 and PC4 do not represent random information (Appendix 3: table S3). The plot of PC1 versus PC2 shows a clear separation between specimens of *Proterosuchus fergusi* and those of the other three species of proterosuchids along PC1 (Fig. 3.8A). The continuously spread specimens along PC2 corresponds to what it is interpreted here as an intraspecifically variable character of, at least, *Proterosuchus fergusi* (width of the supratemporal fossa, see below), which does not fit significantly to a linear allometric regression. The plot of PC1 versus PC3 shows a better separation among *Proterosuchus alexanderi*, *Proterosuchus goweri* and "*Chasmatosaurus*" *yuani*, and the specimens of *Proterosuchus fergusi* are more closely clustered together than in PC2 (Fig. 3.8B). The three characters that are mainly responsible for the pattern observed in PC1 versus PC3 are not intraspecifically variable and fit significantly with a linear allometric regression. *Proterosuchus goweri* is distinguished from other species by the presence of a proportionally deeper horizontal process of the maxilla, which does not seem to be related with the presence of a sigmoid alveolar margin in lateral view. *Proterosuchus alexanderi* differs from other proterosuchid species in the presence of an anteroposteriorly longer anterior process of the maxilla, as described in the qualitative observations.

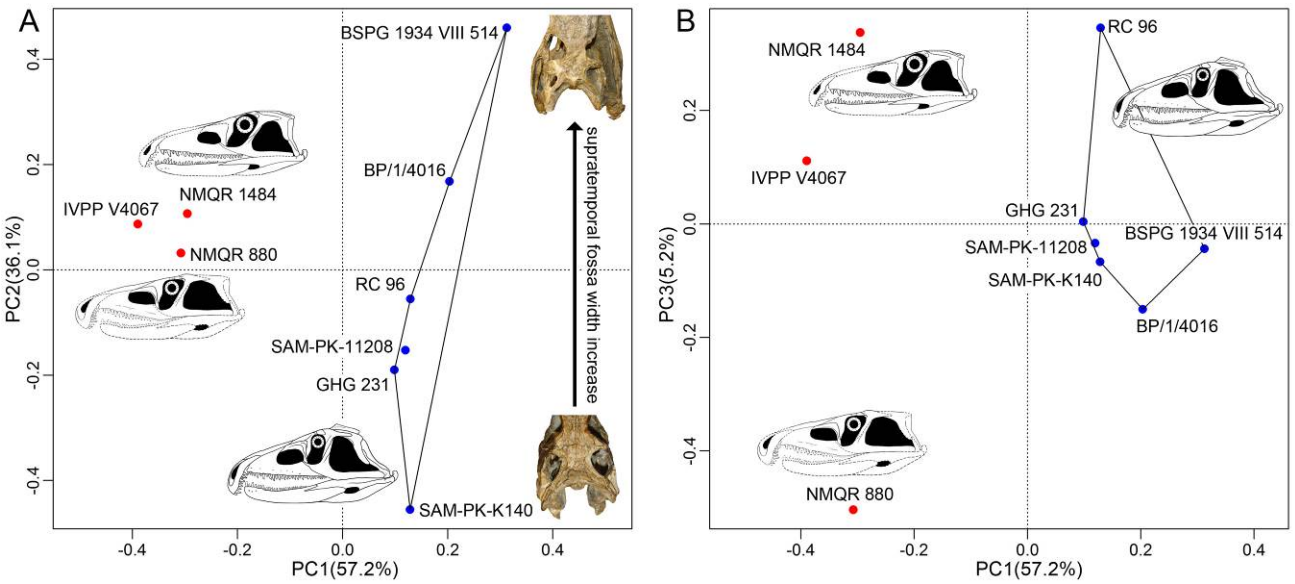

Figure 3.8. Bivariate plots showing results of the PCA. A, PC1 against PC2; and B, PC1 against PC3.

The result of the PCA is complemented by the results of the PERMANOVA analyses, which recovered a significant distinction between *Proterosuchus fergusi* and a group including the other three species (one d.f., P=0.012) and among the four species of proterosuchids (three d.f., P=0.036). In addition, two different LDAs were conducted. The first LDA employed two groups, namely *Proterosuchus fergusi* and other proterosuchid species (i.e. *Proterosuchus alexanderi* + *Proterosuchus goweri* + "*Chasmatosaurus*" *yuani*), and predicted with an accuracy of 100% the assignment of specimens to each respective group. The second LDA used four different groups, corresponding to each of the four species (i.e. *Proterosuchus fergusi*, *Proterosuchus alexanderi*, *Proterosuchus goweri* and "*Chasmatosaurus*" *yuani*). This analysis failed to assign correctly specimens of *Proterosuchus alexanderi*, *Proterosuchus goweri* and "*Chasmatosaurus*" *yuani*, but assigned specimens of *Proterosuchus fergusi* correctly with an accurancy of 83%. The failure in the assignment of specimens to the former three species of proterosuchids is probably because each species is represented by a single specimen in the analysis. Accordingly, the results of the three quantitative analyses were consistent with the taxonomy inferred from qualitative data, supporting a distinction of three different species in the proterosuchid sample from the *Lystrosaurus* AZ of South Africa.

3.4.3. Systematic Palaeontology

DIAPSIDA Osborn, 1903 sensu Laurin, 1991

SAURIA Macartney, 1802 sensu Gauthier, Kluge and Rowe, 1988

ARCHOSAUROMORPHA Huene, 1946 sensu Dilkes, 1998

ARCHOSAURIFORMES Gauthier, Kluge and Rowe, 1988

PROTEROSUCHIDAE Huene, 1908 sensu Ezcurra, Butler and Gower, 2013

Proterosuchus Broom, 1903

Figures 3.1–3.6, 3.9

1924 *Chasmatosaurus* Haughton, p. 93, 96, 97, pl. VII, VIII, figs. 57, 58.

1946 *Elaphrosuchus* Broom, p. 346, figs. 1, 2a.

Type species. *Proterosuchus fergusi* Broom, 1903.

Diagnosis. Proterosuchid archosauriforms (skull length reaching up to approximately 50 cm and total body length up to 3–3.5 m, based on the fairly complete referred specimen of "*Chasmatosaurus*" *yuani* [IVPP V4067] and a skull-total length equation estimated for extant crocodiles by Platt et al. [2009] that agrees with the ratios observed between skull-total length in the proterosuchid specimens IVPP V4067 and NMQR 1484) distinguished from other archosauromorphs on the basis of the following unique combination of characters (autapomorphies marked with an asterisk): (1) premaxilla with a prenarial process strongly tapering posteriorly from its base (not tapering in *Archosaurus rossicus*); (2) jugal with a subrectangular posterior process that forms the entire ventral border of the infratemporal fenestra, nearly contacting or contacting the quadratojugal* (but unknown in other potential proterosuchid genera, e.g. *Archosaurus rossicus*, *Tasmaniosaurus triassicus*, *Blomosuchus georgii*); (3) premaxillary, maxillary and dentary tooth counts are 5–9, 20–31 and 18–28, respectively (also present in *Prolacerta broomi* and the premaxilla of *Archosaurus rossicus*); and (4) presacral vertebrae with mammillary processes on the neural spines of cervicals 6 and 7* (mammillary processes are present from the

eighth cervical to the anterior dorsal vertebrae in *Prolacerta broomi* and, at least, on anterior dorsal vertebrae in *Boreopricea funerea*, unknown in *Archosaurus rossicus*).

Proterosuchus fergusi Broom, 1903

Figures 3.2C, D, F; 3.4; 3.5; 3.6A, B, D; 3.9A, B

1924 *Chasmatosaurus vanhoepeni* Haughton, p. 93, pl. VII, VIII, figs. 57, 58.

1946 *Elaphrosuchus rubidgei* Broom, p. 346, figs. 1, 2a.

1946 *Chasmatosaurus* sp. Broom, p. 346.

1972 *Proterosuchus vanhoepeni* Cruickshank, p. 91, 92, 94, pl. I, figs. 1–3, 4b, c, 5–10.

Holotype. SAM-PK-591, heavily weathered partial skull preserved in two blocks that fit together. The specimen is preserved as bones and natural moulds, including the distal tips of the palatal processes of both premaxillae, both septomaxillae, maxillae and nasals, right lacrimal and jugal, both vomers, palatines, pterygoids and ectopterygoids, parabasisphenoid, right dentary, possible right surangular, both splenials, angulars and hyoid bones (Appendix 6: Fig. S5.1). This specimen is considered here to not be diagnostic (see below).

Proposed neotype. RC 846 (referred to as RC 96 by Welman and Flemming [1993] and subsequent authors), large (42.1 cm total skull length) fairly complete skull and lower jaws, atlas, axis, partial third cervical and first three cervical ribs (Fig. 3.4I, J). A neotype for the species is proposed for the sake of taxononomic stability following the recommendations of Article 75.5 of the International Code of Zoological Nomenclature (ICZN).

Type localities. Farm Wheatlands, Tarkastad, Chris Hani District, Eastern Cape Province, South Africa (holotype); and Farm Ruygte Valley 321, Middelburg, Chris Hani District, Eastern Cape Province, South Africa (proposed neotype).

Type horizon. *Lystrosaurus* AZ (Induan–?early Olenekian; Damiani et al., 2000; Rubidge, 2005; Lucas, 2010), upper Balfour Formation or lower Katberg Formation, Beaufort Group, Karoo Supergroup.

Emended diagnosis. Proterosuchid archosauriform (skull length reaching up to approximately 50 cm and total body length up to 3–3.5 m) distinguished from other archosauromorphs on the basis of the following unique combination of characters: (1) premaxilla lacking a groove on the lateral surface of the main body (groove also absent in *Proterosuchus goweri* and *Archosaurus rossicus*, groove present in "*Chasmatosaurus*" *yuani*, unknown in *Proterosuchus alexanderi*); (2) ratio of total length of maxilla versus length of maxilla anterior to the antorbital fenestra greater than 2.5 (2.53–3.11) (also present in *Proterosuchus goweri* and "*Chasmatosaurus*" *yuani*, ratio lower in *Proterosuchus alexanderi*); (3) maxilla lacks an anterolaterally opening longitudinal groove adjacent to the anterior margin of the bone (groove also absent in *Proterosuchus goweri*, groove present in "*Chasmatosaurus*" *yuani*, unknown in *Proterosuchus alexanderi*); (4) minimum height of the horizontal process of maxilla is equal to or less than 13% of the total length of the maxilla (also present in *Proterosuchus alexanderi* and "*Chasmatosaurus*" *yuani*, ratio higher in *Proterosuchus goweri*); (5) maxillary alveolar margin straight to gently convex in lateral view (also present in *Proterosuchus alexanderi* and "*Chasmatosaurus*" *yuani*, alveolar margin is sigmoidal in *Proterosuchus goweri*); (6) quadrate with an angle

between the posterior margins of the proximal and distal ends of less than 130° (120°–127°) (angle higher in other proterosuchid species, unknown in *Archosaurus rossicus*); (7) presacral vertebrae with mammillary processes on the neural spines of at least cervicals 6 and 7 and absent on dorsals 4–7 (also present in "*Chasmatosaurus*" *yuani*, mammillary processes more posteriorly extended on the dorsal series in *Proterosuchus alexanderi*, unknown in *Proterosuchus goweri*); and (8) presence of postaxial intercentra (also present in *Proterosuchus alexanderi*, absent in "*Chasmatosaurus*" *yuani*, unknown in *Proterosuchus goweri*) (Fig. 3.9A, B).

Referred specimens. For each of the specimens referred here to *Proterosuchus fergusi*, I identify the characters that are present in that specimen that allow referral to the species. The condition of other characters in the diagnosis is uncertain in each case due to incomplete preservation.

BP/1/3993, medium-sized (38.8 cm total skull length) partial skull and lower jaws (lacking right temporal region and the posterior ends of the mandibular rami), axis and five anterior–middle postaxial cervical vertebrae (Fig. 3.5C). BP/1/3993 possesses character states 1–7 of the diagnosis of *Proterosuchus fergusi*.

BP/1/4016, small (ca. 24 cm total skull length) partial skull and lower jaws (lacking the anterior ends of the premaxillae and the anterior half of skull roof), first four cervical vertebrae and probable atlantal rib and postaxial cervical ribs (Figs. 3.4E, F; 3.5B). BP/1/4016 possesses character states 2 and 4–6 of the diagnosis of *Proterosuchus fergusi*.

BP/1/4224, small (ca. 23 cm total skull length) posterior half of skull and lower jaws, axis and one cervical rib. A ventral border of the infratemporal fenestra formed entirely by the posterior process of the jugal supports the assignment of

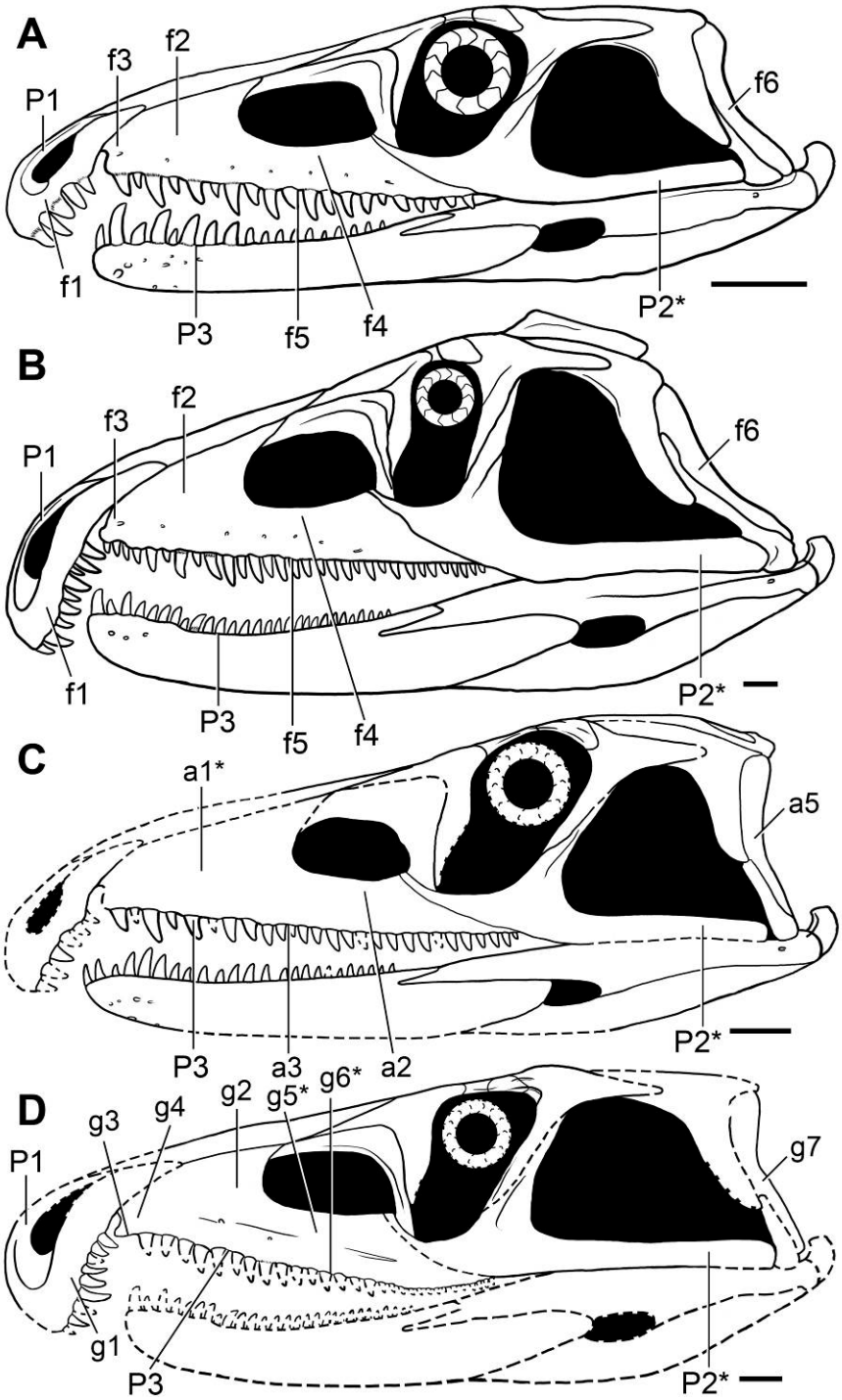

Figure 3.9. Skull and lower jaw reconstructions of *Proterosuchus* species from the *Lystrosaurus* AZ of South Africa. A, juvenile of *Proterosuchus fergusi* (based on RC 59 and BP/1/4016); B, adult of *Proterosuchus fergusi* (based on BSPG 1934 VIII 514, GHG 231, RC 846); C, *Proterosuchus alexanderi*; and D, *Proterosuchus goweri* in left lateral views. Abbreviations: a1, a2, a4, diagnostic characters 1, 2 and 4 of *Proterosuchus alexanderi*; P1–3, diagnostic characters 1–6 of *Proterosuchus*; g1–7, diagnostic characters 1–7 of *Proterosuchus goweri*; f1–6, diagnostic characters 1–6 of *Proterosuchus fergusi*. Characters with asterisks indicate autapomorphies. Scale bars equal 20 mm.

BP/1/4224 to Proterosuchidae and possibly *Proterosuchus*, but the character-state is unknown in the supposed proterosuchids *Archosaurus rossicus*, *Tasmaniosaurus triassicus* and *Blomosuchus georgii*. BP/1/4224 possesses character state 6 of the diagnosis of *Proterosuchus fergusi*.

BSPG 1934 VIII 514, large (43.5 cm total skull length) partial skull and complete lower jaws, first four cervical vertebrae with their ribs and intercentra. BSPG 1934 VIII 514 possesses character states 1–6 and 8 of the diagnosis of *Proterosuchus fergusi*.

GHG 231, large (47.7 cm total skull length) partial skull (lacking the left maxilla) and complete lower jaws, first seven cervical vertebrae, and atlantal, axial and fourth and fifth cervical ribs. A ventral border of the infratemporal fenestra formed entirely by the posterior process of the jugal supports the assignment of GHG 231 to Proterosuchidae and possibly *Proterosuchus*, but the character-state is unknown in the other supposed proterosuchids. GHG 231 possesses character states 1, 2 and 4–6 of the diagnosis of *Proterosuchus fergusi*.

GHG 363, large partial skull (snout only), three cervico-dorsal vertebrae with two right ribs in partial articulation, two middle dorsal vertebrae, one middle caudal vertebra, one posterior caudal vertebra, and interclavicle. GHG 363 possesses character states 1, 7 and 8 of the diagnosis of *Proterosuchus fergusi*.

RC 59, holotype of "*Elaphrosuchus rubidgei*" Broom, 1946, small (17.8 cm total skull length) partial skull and lower jaws (lacking prefrontals, lacrimals, left squamosal and quadratojugal, epipterygoids, and braincase), an atlantal neural arch and some cervical ribs (Fig. 3.4C, D). RC 59 possesses character states 1–5 of the diagnosis of *Proterosuchus fergusi*.

SAM-PK-11208, medium-sized (35.0 cm total skull length) partial skull and lower jaws (lacking most of the skull roof and with the left side severely damaged), axis, third and fourth cervical vertebrae in articulation, probable fifth cervical to first dorsal vertebrae in articulation, three anterior dorsal vertebrae in articulation, possible first sacral vertebra, and some long bone fragments (Fig. 3.4G, H). SAM-PK-11208 possesses character states 1–6 and 8 of the diagnosis of *Proterosuchus fergusi*.

SAM-PK-K140, small (28.7 cm total skull length) partial skull (lacking the skull roof and braincase) and lower jaws, first four cervical vertebrae in articulation, a series of seven middle cervical to anterior dorsal vertebrae, two middle dorsal vertebrae, sacral vertebrae (currently lost), several cervical and dorsal ribs and gastralia, right scapula (currently lost), left ulna, radius, carpus and hand, partial pelvic girdles (currently lost), partial hindlimbs, incuding well preserved left femur, right astragalus and calcaneum, and left foot in articulation, and a bone previously identified as an isolated osteoderm. SAM-PK-K140 possesses character states 1–2 and 4–8 of the diagnosis of *Proterosuchus fergusi*.

SAM-PK-K10603, large (ca. 41 cm total skull length) fairly complete skull and lower jaws (missing most of the premaxillae), and atlas (Fig. 3.5A). SAM-PK-K10603 possesses character states 2, 3, 5 and 6 of the diagnosis of *Proterosuchus fergusi*.

TM 201, holotype of "*Chasmatosaurus vanhoepeni*" Haughton, 1924, TM 201, large (ca. 44 cm total skull length) partial skull and lower jaws, including both premaxillae, maxillae, nasals, frontals, parietals, vomers and partial quadrates and opisthotics, right jugal, pterygoid, posterior process of the palatine and partial ectopterygoid, left squamosal, possible interparietal, supraoccipital, right dentary, angular, surangular and articular, anterior end of left dentary, and both splenials. TM

201 possesses character states 1, 3, 5 and possibly 2 of the diagnosis of *Proterosuchus fergusi*.

Referred horizon and localities. All referred specimens of *Proterosuchus fergusi* come from South Africa and are from the same general stratigraphic level (*Lystrosaurus* AZ) as the holotype, although precise stratigraphic details are generally not available. Localities are detailed in Table 3.3.

Comments. Welman (1998) considered SAM-PK-591 (the holotype of *Proterosuchus fergusi*) to be diagnostic and consistent in morphology with other South African proterosuchid specimens, and, as a result, retained *Proterosuchus fergusi* as a valid species and referred all other South African specimens to this taxon. However, Welman (1998) did not compare SAM-PK-591 with the Chinese species "*Chasmatosaurus*" *yuani*. Following restudy of SAM-PK-591 I was unable to find any character or character combination to distinguish this specimen from "*Chasmatosaurus*" *yuani*. By contrast, other South African proterosuchid specimens (e.g. NMQR 880, 1484, TM 201) can be clearly distinguished from "*Chasmatosaurus*" *yuani* using multiple cranial and postcranial features (e.g. "*Chasmatosaurus*" *yuani* is distinguished by the presence of a groove on the lateral surface of the premaxillary body, a diagonal shelf on the lateral surface of the anterior end of the maxilla, a non-bifurcated second sacral rib, and a more massive calcaneal tuber: IVPP V4067, V36315). Because SAM-PK-591 cannot be distinguished from "*Chasmatosaurus*" *yuani* or from the holotypes of other South African proterosuchids that are clearly distinct from "*Chasmatosaurus*" *yuani*, I here consider that the

holotype of *Proterosuchus fergusi* is not diagnostic, in agreement with some previous proposals (Hughes, 1963; Cruickshank, 1972).

Although the holotype of *Proterosuchus fergusi* is not diagnostic, I consider that in the interest of taxonomic stability it is desirable to retain the genus *Proterosuchus* and species *Proterosuchus fergusi*, because these taxonomic entities have been widely used in the scientific literature in the last 25 years (e.g. Clark et al., 1993; Juul, 1994; Gower and Sennikov, 1996, 1997, 2000; Welman, 1998; Modesto and Botha-Brink, 2008; Kear, 2009; Klembara and Welman, 2009; Nesbitt et al., 2009; Ezcurra et al., 2010, 2013, 2014; Botha-Brink and Smith, 2011; Desojo et al., 2011; Nesbitt, 2011; Botha-Brink et al., 2014; Ezcurra, 2014). A Google Scholar search recovers 232 citations that mention *Proterosuchus* during the timeframe 1990–2014. Moreover, *Proterosuchus* is a key taxon of the *Lystrosaurus* AZ of South Africa, and thus has important regional biostratigraphic significance. ICZN Article 75.5 recommends the erection of a neotype in the interest of taxonomic stability when the "taxonomic identity of a nominal species-group taxon cannot be determined from its existing name-bearing type (i.e. its name is a nomen dubium)". Accordingly, I provisionally retain the usage of *Proterosuchus* and *Proterosuchus fergusi* and propose RC 846 as a neotype for this species. RC 846 is one of the best preserved specimens of the hypodigm of *Proterosuchus fergusi*, probably represents an adult specimen, has no existing type status, can be differentiated from other proterosuchid species (e.g. *Archosaurus rossicus*, *Proterosuchus alexanderi*, *Proterosuchus goweri*, "*Chasmatosaurus*" *yuani*), and comes from the same district of the Eastern Cape Province as the holotype. I intend to appeal in the near future to the ICZN to use its plenary power [Art. 81] to set aside the existing name-bearing type of the species and designate a neotype.

With regards to "*Chasmatosaurus vanhoepeni*" and "*Elaphrosuchus rubidgei*", I could not find any taxonomically relevant character state or character combination that would distinguish their holotypes ("*Chasmatosaurus vanhoepeni*": TM 201; "*Elaphrosuchus rubidgei*": RC 59) from the proposed neotype or other referred specimens of *Proterosuchus fergusi*. By contrast, the combination of features present in *Proterosuchus fergusi* is also present in RC 59 and TM 201. I agree with Welman (1998) in considering the previously proposed differences between "*Elaphrosuchus rubidgei*" and other South African proterosuchid specimens (Broom, 1946; Brink, 1955; Hoffman, 1965; Charig and Reig, 1970; Charig and Sues, 1976) to be a consequence of the early ontogenetic stage of the specimen (the holotype of "*Elaphrosuchus rubidgei*" is approximately 37% of the size of the largest specimen of *Proterosuchus fergusi*, GHG 231). As a result, I consider "*Chasmatosaurus vanhoepeni*" and "*Elaphrosuchus rubidgei*" to be subjective junior synonyms of *Proterosuchus fergusi*, as previously proposed by Hughes (1963), Cruickshank (1972) and Welman (1998).

Proterosuchus alexanderi (Hoffman, 1965), comb. nov.

Figures 3.1; 3.2A, E; 3.6C; 3.9C

1965 *Chasmatosaurus alexanderi* Hoffman, p. 36, 38, figs. 2–5.

1998 *Proterosuchus fergusi* Welman, p. 341.

Holotype. NMQR 1484, small fairly complete skull (lacking most of the premaxillae) and postcranial axial skeleton (lacking the posterior half of the caudal series), and partial appendicular skeleton (Fig. 3.1).

Type locality. Farm Zeekoegat, 4 miles from Venterstad, Joe Gqabi District, Eastern Cape Province, South Africa (Hoffman, 1965).

Type horizon. *Lystrosaurus* AZ (Induan–?early Olenekian; Damiani et al., 2000; Rubidge, 2005; Lucas, 2010), upper Balfour Formation or lower Katberg Formation, Beaufort Group, Karoo Supergroup.

Emended diagnosis. Proterosuchid archosauriform distinguished from other archosauromorphs by the following combination of characters (autapomorphies marked with an asterisk): (1) ratio of total length of maxilla versus length of maxilla anterior to the antorbital fenestra less than 2.3*; (2) minimum height of the horizontal process of maxilla is equal to or less than 13% of the total length of the maxilla (also present in *Proterosuchus fergusi* and "*Chasmatosaurus*" *yuani*, ratio higher in *Proterosuchus goweri*); (3) maxillary alveolar margin straight to gently convex in lateral view (also present in *Proterosuchus fergusi* and "*Chasmatosaurus*" *yuani*, alveolar margin sigmoid in *Proterosuchus goweri*); (4) frontals with a dorsal surface ornamented by a series of anastomosed shallow grooves and sub-circular pits with a seemingly random arrangement*; (5) quadrate with an angle between the posterior margins of the proximal and distal ends greater than 145° (also present in *Proterosuchus goweri* and "*Chasmatosaurus*" *yuani*, angle lower in *Proterosuchus fergusi*); (6) presacral vertebrae with mammillary processes on the neural spines present in presacrals 14–16 (dorsals 5–7)*; (7) presence of postaxial intercentra (also present in *Proterosuchus fergusi*, absent in "*Chasmatosaurus*" *yuani*, unknown in *Proterosuchus goweri*); and (8) first and second sacral ribs distally subdivided* (unknown in *Proterosuchus fergusi* and *Proterosuchus goweri*) (Fig. 3.9C).

Comments. The skull length of the only known individual is approximately 27 cm with a preserved total length of around 1 m and an estimated total body length of approximately 1.5 m (using Platt et al. [2009] total length-snout-vent length equation). However, this specimen was probably not at adult body size at the time of death because its tooth count and cranial proportions are similar to those of sub-adult specimens of *Proterosuchus fergusi*, based on histological information for SAM-PK-K140 and SAM-PK-11208 (Botha-Brink and Smith, 2011).

The discussion provided above for several characters demonstrates that NMQR 1484 possesses several features that distinguish this specimen from other proterosuchids. Some features that were previously used to distinguish NMQR 1484 from other proterosuchids were not considered to result from intraspecific ontogenetic variation by Welman (1998), but rather from post-mortem deformation (e.g. quadrate angle). However, the restudy of the specimen leads me to reject the latter explanation. Accordingly, I consider NMQR 1484 as taxonomically distinguishable from other valid proterosuchid species and resurrect the species "*Chasmatosaurus*" *alexanderi* because NMQR 1484 is its type specimen. Because the genus "*Chasmatosaurus*" is a subjective junior synonym of *Proterosuchus* (see above), I propose here the new combination *Proterosuchus alexanderi*. A referral to the genus *Proterosuchus* may also be required for the Chinese proterosuchid species "*Chasmatosaurus*" *yuani*, but the hypodigm of the species is currently under revision and its taxonomic status will be discussed elsewhere.

Proterosuchus goweri sp. nov.

LSID. urn:lsid:zoobank.org:act:F97DB492-347B-462F-AD67-5924E6962DF0

Figures 3.2B; 3.3; 3.9D

Holotype. NMQR 880, partial skull with detached braincase, a right dorsal rib, and left tibia and fibula (Fig. 3.3).

Derivation of name. In honour of David J. Gower, in recognition of his contributions to the study and knowledge of proterosuchian archosauriforms.

Type locality. Farm Kruisvlei (Kruisvlei 1095 in Brink [1955] and Kruisvlei 279 in Welman [1998]), east of Winburg, Lejweleputswa District, Free State Province, South Africa (Brink, 1955).

Type horizon. *Lystrosaurus* AZ (Induan–?early Olenekian), upper Balfour Formation or lower Katberg Formation, Beaufort Group, Karoo Supergroup.

Diagnosis. Proterosuchid archosauriform (skull length of the only known individual ca. 39 cm and total body length estimated in 2.5–3 m using Platt et al. [2009] skull-total length equation) distinguished from other archosauromorphs by the following combination of characters (autapomorphies marked with an asterisk): (1) premaxilla lacking grooves on the lateral surface (also in *Proterosuchus fergusi* and *Archosaurus rossicus*, grooves present in "*Chasmatosaurus*" *yuani*, unknown in *Proterosuchus alexanderi*); (2) ratio of total length of maxilla versus length of maxilla anterior to the antorbital fenestra greater than 2.5 (2.62) (also in *Proterosuchus fergusi* and "*Chasmatosaurus*" *yuani*, ratio lower in *Proterosuchus alexanderi*); (3) maxilla with an edentulous anterior end, the length of which is equivalent to that of two tooth

positions (also present in "*Chasmatosaurus*" *yuani*, edentulous anterior end absent in *Proterosuchus alexanderi* and *Proterosuchus fergusi*); (4) maxilla lacking an anterolaterally opening longitudinal groove adjacent to the anterior margin (groove absent in *Proterosuchus fergusi*, groove present in "*Chasmatosaurus*" *yuani*, unknown in *Proterosuchus alexanderi*); (5) minimum height of the horizontal process of maxilla is equal to or greater than 15% of the total length of the maxilla*; (6) maxillary alveolar margin distinctly sigmoid in lateral or medial views, with a concave anterior two-thirds and a convex posterior third*; and (7) quadrate with an angle between the posterior margins of the proximal and distal ends greater than 145° (also present in *Proterosuchus alexanderi* and "*Chasmatosaurus*" *yuani*, angle lower in *Proterosuchus fergusi*) (Fig. 3.9D).

Comments. NMQR 880 can also be differentiated from other proterosuchids by a combination of non-ontogenetically related characters. As a result, I consider NMQR 880 taxonomically distinguishable from other proterosuchids and erect the new species *Proterosuchus goweri*. The absolute size, skull proportions and tooth counts of NMQR 880 resemble those of large and probably sexually mature specimens of *Proterosuchus fergusi* (e.g. SAM-PK-11208).

PROTEROSUCHIDAE gen. et sp. indet.

Material. AMNH FR 2237, large partial postcranial skeleton that includes probable cervical vertebrae 4 and 6–8, nine anterior–middle dorsal vertebrae, two anterior caudal vertebrae, several gastralia preserved in two blocks, right scapula and coracoid, possible interclavicle, right and possible left humeri, six carpals, proximal ends of

metacarpals I–IV, distal half of right femur, right tibia, fibula, and astragalus, calcaneum and centrale preserved in articulation; GHG 72, medium-sized partial postcranial skeleton, including middle and posterior cervical, several dorsal, both sacral, and anterior caudal vertebrae with several ribs and intercentra, both partial scapular girdles and forelimbs, pelvic girdle, proximal ends of both femora, and a few cranial remains; SAM-PK-11207, medium-sized fragmentary skull, including posterior process of left jugal, left quadratojugal, pterygoid and ectopterygoid, possible right palatine, basisphenoid and presacral vertebra in cross section; SAM-PK-K139, small partial skull with partial maxillae, nasals, pterygoids, dentaries, splenials and hyoids, left jugal and ectopterygoid and right palatine.

Horizon and localities. All specimens come from the same horizon: *Lystrosaurus* Assemblage Zone (Induan–?early Olenekian), upper Balfour Formation or lower Katberg Formation, Beaufort Group, Karoo Basin. Localities are detailed in Table 3.2.

Comments. AMNH FR 2237 was previously referred to "*Chasmatosaurus vanhoepeni*" by Broom (1932) and to *Proterosuchus fergusi* by Nesbitt (2011). Although the morphology of the preserved bones of the specimen is consistent with those of *Proterosuchus fergusi*, *Proterosuchus alexanderi*, and *Proterosuchus goweri*, there are no diagnostic features that would allow an unambiguous referral to any species of *Proterosuchus*. However, AMNH FR 2237 differs from "*Chasmatosaurus*" *yuani* in the presence of postaxial intercentra and a calcaneum with a dorsoventrally oriented cleft on the distal margin and a dorsoventrally compressed calcaneal tuber.

GHG 72 can be distinguished from *Proterosuchus alexanderi* by the presence of posterior cervical vertebrae without mammillary processes in the neural spines, and

sacral ribs that are undivided at their distal ends, and from "*Chasmatosaurus*" *yuani* by the presence of intercentra in the dorsal series. The morphology of the specimen is consistent with that of *Proterosuchus fergusi* and cannot be compared properly with that of *Proterosuchus goweri* because of the almost complete absence of overlapping bones.

SAM-PK-11207 is a proterosuchid because of the presence of a ventral border of the infratemporal fenestra formed entirely by a sub-rectangular posterior process of the jugal (see above). The morphology of SAM-PK-11207 is consistent with that of all of the species of *Proterosuchus*, but cannot be compared with that of *Archosaurus rossicus* because of the absence of overlapping bones.

SAM-PK-K139 can be referred to Proterosuchidae because of the combination of the following characters: concave ventral border of the antorbital fenestra (antorbital fenestra absent in *Prolacerta broomi* and ventral border straight in *Tasmaniosaurus triassicus*; Modesto and Sues, 2004; Ezcurra, 2014); more than 21 maxillary tooth positions (lower tooth count in *Kalisuchus rewanensis*, erythrosuchids and *Euparkeria capensis*; QM F8998; Ezcurra et al., 2010); tooth crowns with denticles (absent in *Prolacerta broomi*: Modesto and Sues, 2004); and an ankylothecodont tooth implantation. The morphology of SAM-PK-K139 is consistent with that of all of the species of *Proterosuchus*, but cannot be compared with that of *Archosaurus rossicus* because of the absence of overlapping bones. Although a high number of maxillary teeth is part of the diagnosis of *Proterosuchus*, together with other non-autapomorphic characters, its presence alone is not enough to assign SAM-PK-K139 to *Proterosuchus* because occurs in other basal archosauromorphs (e.g. *Prolacerta broomi*).

BP/1/4589, BP/1/6046 (mentioned by Damiani et al. [2003]) and an unnumbered GHG specimen are potentially additional proterosuchid specimens from the *Lystrosaurus* AZ of South Africa, but they are currently unprepared and precise taxonomic identification is not yet possible. The maxilla of the unnumbered GHG specimen differs from that of *Proterosuchus alexanderi* in having an anteroposteriorly short anterior process, and from that of *Proterosuchus goweri* in having a gently convex alveolar margin in lateral view. Botha-Brink et al. (2014: 300) briefly reported a new specimen (NMQR 3924) that was assigned to *Proterosuchus fergusi* on the basis of 'the skull roof and tooth morphology'. This specimen was not examined during this study and, as a result, its taxonomic status cannot be currently assessed by us.

3.5. Discussion

The revised taxonomy of the proterosuchid specimens of the *Lystrosaurus* AZ of South Africa has implications for our understanding of the early evolution of archosauriforms. Until now, only two archosauriform taxa were recognised in the *Lystrosaurus* AZ: *Proterosuchus fergusi* and an unnamed taxon distinct from, but similar to, the proterosuchid specimens discussed here, which is represented only by a partial maxilla (NMQR 3570; Modesto and Botha-Brink, 2008). In this chapter I conclude that there are three different species among the specimens previously assigned to *Proterosuchus fergusi* and, as a result, the minimum alpha taxonomic diversity of archosauriforms in the *Lystrosaurus* AZ of South Africa is four species. This contrasts with a lower taxonomic diversity in the younger *Cynognathus* AZ Subzones A and B of South Africa that currently possess one (*Garjainia madiba*) and

two (*Erythrosuchus africanus* and *Euparkeria capensis*) described species of archosauriform, respectively (Hancox, 2000; Ezcurra et al., 2013; Gower et al., 2014). This result is consistent with the pattern observed for tetrapods as a whole, where species richness and origination rates are higher in the *Lystrosaurus* AZ than in the *Cynognathus* AZ (Botha and Smith, 2006). Nevertheless, it cannot be ruled out that the currently low number of archosauriform species recognized in the *Cynognathus* AZ is a result of incomplete sampling or taphonomic/palaeoecological factors. Moreover, incomplete stratigraphic data for many of the proterosuchid specimens, particularly those collected historically, mean that it is currently unclear how many of the *Lystrosaurus* AZ species were sympatric and/or coeval.

Our new results suggest that the taxonomic radiation of archosauriforms was relatively fast, at least in South Africa, following the Permo-Triassic mass extinction event. Proterosuchid specimens seem to be restricted to the lowermost *Lystrosaurus* AZ and, as a result, the taxonomic radiation of proterosuchids in the Karoo Basin must have occurred relatively rapidly, assuming that their ghost lineages do not cross the Permo-Triassic boundary (Botha and Smith, 2006). The short temporal range of South African proterosuchids also suggests that the rapid taxonomic radiation was followed by a remarkably early disappearance of the proterosuchids from the Karoo Basin. Although several South African archosauriform species are recognized in the immediate aftermath of the mass extinction, all of these taxa are highly morphologically similar, either belonging to Proterosuchidae (*Proterosuchus* spp.) or being highly similar in morphology to this clade (NMQR 3570). Likewise, the earliest Triassic archosauriforms from China, India and Australia are also either proterosuchids or proterosuchid-like (Ezcurra et al., 2013; Ezcurra, 2014). Accordingly, the results of this chapter suggest a greater species richness of earliest

Triassic archosauriforms than previously appreciated, but that archosauriform morphological disparity remained low and did not expand much until the late Early Triassic (late Olenekian) to early Middle Triassic (early Anisian), when erythrosuchids, *Euparkeria* and poposauroid pseudosuchians are recorded for the first time (Gower and Sennikov, 2000; Butler et al., 2011).

Chapter 4: Post-hatchling cranial ontogeny of *Proterosuchus fergusi*

4.1. Background

The South African fossil reptile *Proterosuchus fergusi* (see Chapter 3) is unique among early archosauromorphs and archosauriforms, because it is known from an extensive, highly ontogenetically variable sample of well-preserved three-dimensional skulls (Ezcurra and Butler, 2015a; Chapter 3). Moreover, the cranial morphology of *Proterosuchus fergusi* is plesiomorphically similar in its general construction to basal members of other Permo-Triassic archosauromorph lineages (e.g. *Protorosaurus speneri*, *Macrocnemus bessani*, *Prolacerta broomi*, *Garjainia prima*, *Euparkeria capensis*: Gottmann-Quesada and Sander, 2009; Ezcurra et al., 2013, 2014; Sookias and Butler, 2013; Gower et al., 2014). By contrast, other Triassic basal archosauromorphs known from extensive and ontogenetically variable samples possess highly specialized skulls, and their ontogenetic trajectories are probably not useful models for understanding broader macroevolutionary processes (e.g. rhynchosaurids, proterochampsids: Langer et al., 2000a; Trotteyn et al., 2013). As a result, an understanding of ontogenetic changes during the development of *Proterosuchus fergusi* has the potential to shed light on the role of ontogenetic modification events (e.g. heterochrony) in the early evolutionary history of archosauromorphs, and the origin and diversification of archosauriforms.

Welman and Flemming (1993) conducted the first quantitative analysis of the cranial morphometrics of the South African proterosuchids, and demonstrated that all known specimens fitted well within a single ontogenetic series. The South African proterosuchid sample has improved in the last 20 years through the collection of new

fossil specimens, and the taxonomy of *Proterosuchus* has been revisited and substantially revised (Ezcurra and Butler, 2015a). Moreover, methodological advances over the same time interval have led to new approaches to analysing ontogeny in fossil species (e.g. ontograms: Brochu, 1992). As a result, a new, detailed study of the ontogeny of *Proterosuchus fergusi* is necessary and timely (Ezcurra and Butler, 2015b). I conduct here qualitative and quantitative analyses of the ontogeny of this species and discuss the implications for the early evolution of Archosauromorpha.

4.2. Materials and methods

4.2.1. *Studied specimens and available ontogenetic series*

The total number of fossil specimens of *Proterosuchus fergusi* available for study has increased since Welman and Flemming (1993), and three additional, recently collected, fairly complete skulls are available (BP/1/4224, SAM-PK-11208, K10603). The improved sampling means that seven skulls (BP/1/3993, BSPG 1934 VIII 514, GHG 231, RC 59, 846, SAM-PK-11208, K140) are currently available from which the complete length of the skull can be directly measured (i.e. length between the anterior tip of the premaxilla and the posterior tip of the cranio-mandibular joint). Based on these more complete specimens, it is possible to estimate the skull length of four additional partial skulls with good statistical support (R^2>0.99; see Appendix 5). As a result, it was possible to use skull length directly as a standard measurement for the allometric regressions conducted here, contrasting with the use of proxies of skull size by Welman and Flemming (1993).

The neotype of *Proterosuchus fergusi* proposed by Ezcurra and Butler (2015a) (RC 846) and 10 referred specimens (RC 59, BP/1/3993, 4016, 4224, SAM-PK-

11208, K140, K10603, BSPG-1934-VIII-514, TM 201 and GHG 231) were examined first hand (see Ezcurra and Butler 2015a; Chapter 3). Precise stratigraphic data is lacking for specimens collected more than 50 years ago (R. Smith pers. comm., 2012), but there exists consensus that all specimens studied were collected from the *Lystrosaurus* Assemblage Zone (earliest Triassic: Induan–early Olenekian) of South Africa (Welman, 1998). The smallest specimen available in the sample (RC 59: total skull length of 177.6 mm) has a skull length that is 37.2% of that of the largest specimen (GHG 231: total skull length of 477.0 mm) (Fig. 4.1). Similarly, the total body length and snout-vent length ratios between the smallest and largest sampled specimens of *Proterosuchus fergusi* are estimated between 35−37% (using equations described by Platt et al. [2009: dorsal cranial length versus total and snout-vent lengths] for the extant crocodile *Crocodylus moreletti* to estimate total and snout-vent lengths in the fossil species the ratios are 36.7% and 36.3%, respectively; and using an equation described by Webb and Messel [1978: total head length versus snout-vent length for the 13−60 cm size class] for the extant crocodile *Crocodylus porosus* the ratio is 35.6%). The broad size range present in the available sample suggests that it can be interpreted as a growth series and approximates the snout-vent length difference between hatchling and maximum adult size of some extant reptiles (e.g. the lepidosaur *Gambelia sila*; Germano and Williams, 2005: hatchlings are 36.4% of the adult length). However, the size range in the *Proterosuchus fergusi* sample is considerably lower than the skull length and snout-vent length ranges observed between hatchling and large adult individuals of some extant crocodiles (e.g. *Crocodylus moreletii*; Pérez-Higareda et al., 1991; Barrios-Quiroz and Casas-Andreu, 2010: hatchlings are 5.6-6.1% of the adult cranial length and 4.6-5.0% of the adult snout-vent length). The substantial differences in size range between *Proterosuchus*

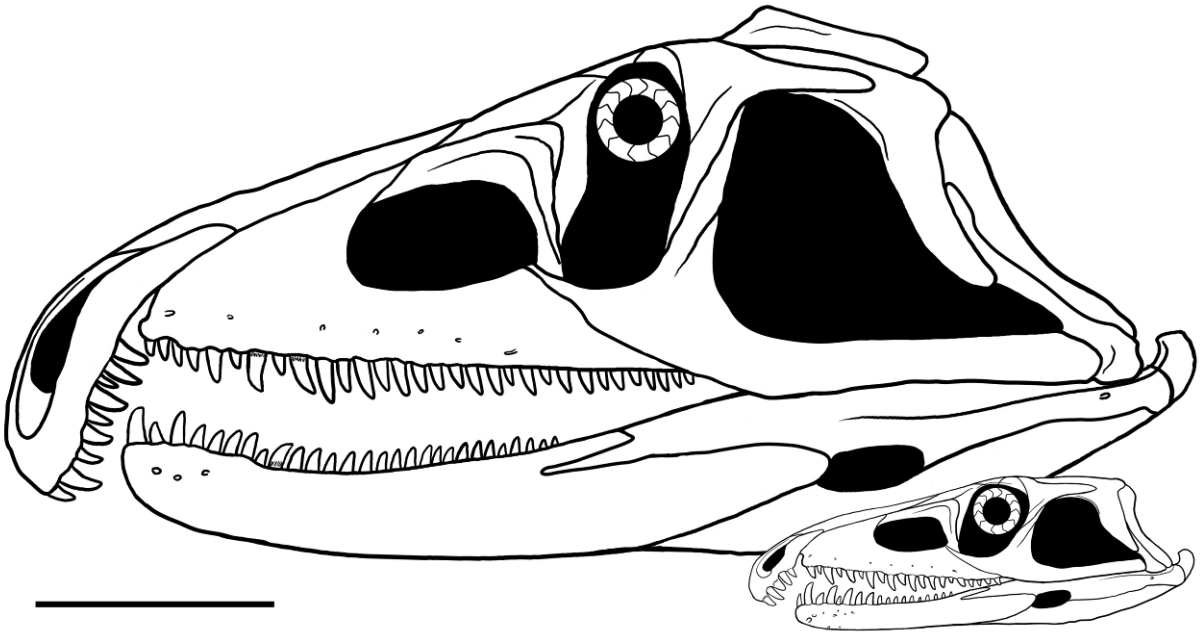

Figure 4.1. Cranial reconstructions of early juvenile and late adult individuals of the proterosuchid archosauriform *Proterosuchus fergusi*. The difference in size between the two skulls represents the size range of the ontogenetic sequence available in the present study. Scale bar equals 10 cm.

fergusi and some extant crocodiles are probably because the upper and lower limits of the size range of *Proterosuchus fergusi* have not yet been sampled, but it is also possible that this difference at least partially results from differing growth strategies. Most specimens of *Proterosuchus fergusi* consist solely of cranial remains. By contrast, osteohistological assessment of ontogenetic stage in fossil species generally requires postcranial remains (usually limb bones: Hutton, 1986; Games, 1990; Woodward and Moore, 1992; Chinsamy, 1993; Tucker, 1997; Erickson and Brochu, 1999; Erickson et al., 2003; Erickson, 2005). As a result, osteohistological information useful to determine ontogenetic stages is very limited for *Proterosuchus fergusi* and currently limited to two specimens (Botha-Brink and Smith, 2011). The osteohistology of hindlimb bones indicates that the specimen SAM-PK-K140 (total skull length of 287.0 mm: 60.2% of the maximum recorded skull length for the species) was a non-sexually mature individual that was growing relatively fast at the time of its death, with fibro-lamellar bone tissue and no lines of arrested growth (LAGs) (Botha-Brink and Smith, 2011). By contrast, SAM-PK-11208 (total skull length of 350.0 mm: 73.4% of the maximum recorded skull length for the species) possesses lamellar-zonal and parallel-fibered bone tissue with secondary remodelling and multiple LAGs, suggesting that it was a late sub-adult or adult individual at the time of its death (Botha-Brink and Smith, 2011). Botha-Brink and Smith (2011) suggested that the dramatic change in growth observed between SAM-PK-K140 and SAM-PK-11208 was because the latter specimen had reached sexual maturity. Accordingly, it can be hypothesized that the largest known individuals of *Proterosuchus fergusi* (e.g. BSPG-1934-VIII-514, TM 201, GHG 231) had reached or were close to the maximum size of the species because they are considerably larger than the probably already sexually mature SAM-PK-11208. By contrast, SAM-PK-

K140 and smaller specimens (e.g. RC 59, BP/1/4016, 4224) are considered to be juvenile individuals. In agreement with this idea, the neurocentral sutures are still visible in the postaxial cervical vertebrae of SAM-PK-K140, but these sutures cannot be discerned in the cervical vertebrae of SAM-PK-11208 and BSPG 1934 VIII 514. These sutures progressively close (a closed neurocentral suture has no trace on the surface of the bone sensu Brochu [1996]) in a posterior-anterior pattern along the axial series during the ontogeny of crocodiles and, as a result, it is a useful criterion to determine ontogenetic stages (Brochu, 1996) that has been widely applied to fossil archosaurs (see Irmis, 2007). Accordingly, the available sample seems to be adequate to examine ontogenetic changes during the post-hatchling development of *Proterosuchus fergusi*.

The skull reconstruction of the juvenile ontogenetic stage of *Proterosuchus fergusi* is based on RC 59 and BP/1/4016 and the reconstruction for the adult ontogenetic stage is based on BSPG 1934 VIII 514, GHG 231 and RC 846 (Ezcurra and Butler, 2015b) (Fig. 4.1).

4.2.2. *Qualitative analysis*

Examination of the growth series of *Proterosuchus fergusi* revealed variable characters within the sample that can be best explained as ontogenetic variation. Some of these characters cannot be measured or currently show discrete states (e.g. pattern of the sutures on the skull roof, appearance of a pineal fossa). As a result, these characters are discussed qualitatively.

4.2.3. *Quantitative analysis: allometric regressions*

Raw data for the allometric regressions consisted of 158 linear cranial measurements (plus skull length), the angle between the proximal and distal ends of the quadrate, and tooth counts of the tooth rows of the premaxilla, maxilla and dentary (Appendix 7). Measurements were taken first hand with a digital calliper with a maximum deviation of 0.02 mm, but measurements were rounded to the nearest 0.1 mm. Ninety-four of the original measurements were not considered for the allometric regressions because they could only be measured for three or fewer individuals (due to incomplete preservation). As a result, 68 variables were retained and $\log_{10}$-transformed to fit the linear power function before conducting the regression analyses (Gould, 1966).

One regression was calculated for each of the 68 variables using the standardised major axis (SMA) regression method implemented in the package Smatr version 3.2.6 for R (Warton et al., 2012; R Development Core Team, 2013). SMA regression was employed instead of ordinary least squared regression because it has been suggested to be the most appropriate method to study allometry in bivariate data (Warton et al., 2006; Smith, 2009). Some authors have employed the first axis of a principal component analysis (PCA) as proxy for body size in allometric regression analyses (e.g. Fernandez Blanco et al., 2015). However, PCA is not a reliable method for the present data set because of the low number of variables that could be measured for all or most of the specimens (PCA does not allow missing data). As a result, total skull length was used as the independent variable for all SMA regressions.

R^2 and p-values were obtained from each SMA regression. Variables were excluded from further consideration if their regression against skull length was statistically non-significant. For variables with a statistically significant fit, the allometric coefficient (K) (i.e. the slope of the regression) with its respective 90%

confidence intervals (CIs) was calculated and a statistical test (Pitman, 1939; Warton et al., 2006) was conducted to determine if the slope was significantly different from 1 (H_0=slope not different from 1). Growth was considered isometric if the allometric coefficient was not significantly different from 1. Conversely, the growth was considered allometric if the allometric coefficient was significantly ($p<0.05$) or marginally significantly ($0.05<p<0.10$) different from 1 (i.e. $K>1$ represents a positive allometry and $K<1$ represents a negative allometry).

After conducting the SMA regressions, the distribution of the slopes (and their lower and upper limits) was studied, first using all the variables, and second separating the variables into four different groups in order to determine differential patterns in different regions of the skull. These four groups consisted of length, height and width measurements, and variables concerning tooth morphology.

4.2.4. *Quantitative analysis: ontogram*

The vast majority of specimens of *Proterosuchus fergusi* are represented only by cranial remains. As a result, information that could be used to determine the relative ontogenetic stage of specimens, such as the sequence of closure of neurocentral sutures or fusion between other postcranial bones, as well as osteohistological data, is very limited. The aim of an ontogram is to show the sequence of maturity expressed by individuals relative to one another within an ontogenetic series (Brochu, 1992; Carr and Williamson, 2004; Tykoski, 2005; Carr, 2010; Frederickson and Tumarkin-Deratzian, 2014). The basic idea behind an ontogram is the same as a phylogenetic analysis, but species or supraspecific taxa are replaced with individuals and phylogenetically informative characters are replaced with ontogenetically variable characters.

An ontogram was constructed here to reconstruct the sequence of maturity of the *Proterosuchus fergusi* sample. The character list is composed of 20 characters, including 12 continuous and 8 discrete and discretised characters, scored across the 11 available specimens (Appendix 5). Maximum parsimony was chosen as the optimality criterion and the data matrix was analysed using TNT version 1.1 (Goloboff et al., 2008) using the implicit enumeration algorithm. Continuous characters (e.g. ratio between length of the premaxillary body and total length of the skull) were analysed as such, and as a result implied weights (with a concavity constant of 10) were used to mitigate the effects of disproportionate character-state transformations among these characters and reduce homoplasy (Goloboff et al., 2006). Zero length branches were collapsed following the search.

The analysis was conducted rooting the trees with the smallest available specimen (RC 59). A second, a posteriori analysis was conducted using a hypothetical root (= artificial embryo of Carr and Williamson [2004]) scored with supposed hatchling character-states to test the polarity reconstructed in the first analysis, resembling the protocol followed by Carr (2010) (Appendix 5). Hatchling character-states in the artificial embryo were inferred based upon the morphological trends observed among small specimens. In the case of the continuous characters, the scored ratios for the actual specimens seem to tend to 0 or 1 through ontogeny, respectively. As a result, the extreme values 0 and 1 were used as scorings for the artificial embryo depending on the tendency observed through ontogeny in the actual specimens. An artificial adult (sensu Carr and Williamson, 2004) was not used in this second analysis in order to decrease the number of a priori assumptions and leave the optimality criterion to choose character polarities (cf. a traditional phylogenetic analysis). As an additional test of the reconstructed sequence of maturity, total skull length was

optimized on the recovered most parsimonious trees (MPTs). Subsequently, a set of resampled trees was generated using 10,000 pseudoreplications of Monte Carlo randomizations. A statistical test, based on the number of values obtained from the simulated trees that presented a higher consistency index than the original value, was conducted in order to test if skull length fitted the MPTs significantly better than random, as is expected for an ontogram. The significance coefficient (α) for this statistical analysis was at the 0.05 level.

4.2.5. *Bivariate plots, thin plate spline analysis and general statistics*

The thin plate spline (= deformation grid) analysis showing changes in skull morphology through ontogeny of *Proterosuchus fergusi* was conducted following a basic geometric morphometric analysis using 21 landmarks on the reconstructed juvenile and adult stages, respectively (see Discussion). The geometric morphometric and thin plate spline analyses, bivariate plots, statistical parameters of slope distributions, and Shapiro-Wilk tests of normality distribution (α=0.05) were conducted and/or calculated in R (packages shapes version 1.1-9 and stats version 2.16.0).

4.3. Results

4.3.1. *Qualitative analysis*

The hypodigm of *Proterosuchus fergusi* possesses a high degree of anatomical variation. Some of these variations cannot be explained as ontogenetic changes, such as the closure of the infratemporal fenestra by a complete lower temporal bar in some specimens and a narrower supratemporal fossa in others (Ezcurra and Butler, 2015a).

However, at least three anatomical variations within the hypodigm of *Proterosuchus fergusi* can be explained as ontogenetic changes.

Isodont maxillary dentition. Anterior maxillary tooth crowns are distinctly distally curved and the posterior crowns are only very weakly distally curved in the smaller individuals of *Proterosuchus fergusi* (RC 59, BP/1/4016) (Fig. 4.2A, B). By contrast, the posterior maxillary tooth crowns are also strongly curved distally in medium to large-sized individuals (SAM-PK-K10603, RC 96, GHG 231). As such, the maxillary tooth series of larger individuals is more isodont (Charig and Reig, 1970) (Fig. 4.2C, D).

Skull roof sutures. The fronto-nasal, fronto-parietal and parietal-interparietal sutures are strongly interdigitated in small specimens, with the fronto-nasal and fronto-parietal sutures showing anteroposteriorly well-developed projections (RC 59, BP/1/4016, 4224). For example, the interdigitated fronto-parietal suture reaches posteriorly almost as far as the anteromedial margin of the supratemporal fossae in RC 59 (Fig. 4.3A). By contrast, in larger individuals these sutures still possess an interdigitated pattern, but have projections that are considerably less well-developed anteroposteriorly (SAM-PK-K10603, RC 96, BSPG 1934 VIII 514, TM 201, GHG 231) (Fig. 4.3B).

Pineal fossa. A pineal fossa on the dorsal surface of the frontals and parietals is only observed in large individuals of *Proterosuchus fergusi* (BP/1/3993, SAM-PK-K9957, SAM-PK-K10603, RC 96, TM 201, GHG 231) (Fig. 4.3B). In BPSG-1934-VIII-514 the dorsal surface of the parietals is damaged and, as a result, the condition of this

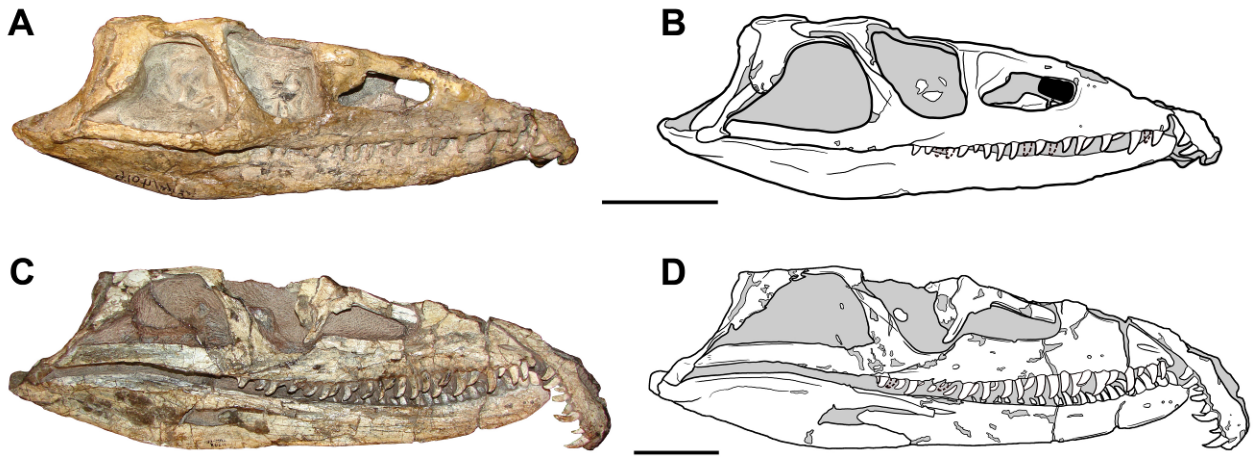

Figure 4.2. Juvenile (A, B: BP/1/4016, reversed) and adult (C, D: SAM-PK-11208, reversed) skulls of *Proterosuchus fergusi* in lateral view, showing the changes in number, shape and size of maxillary tooth crowns during ontogeny. Scale bars equal 5 cm.

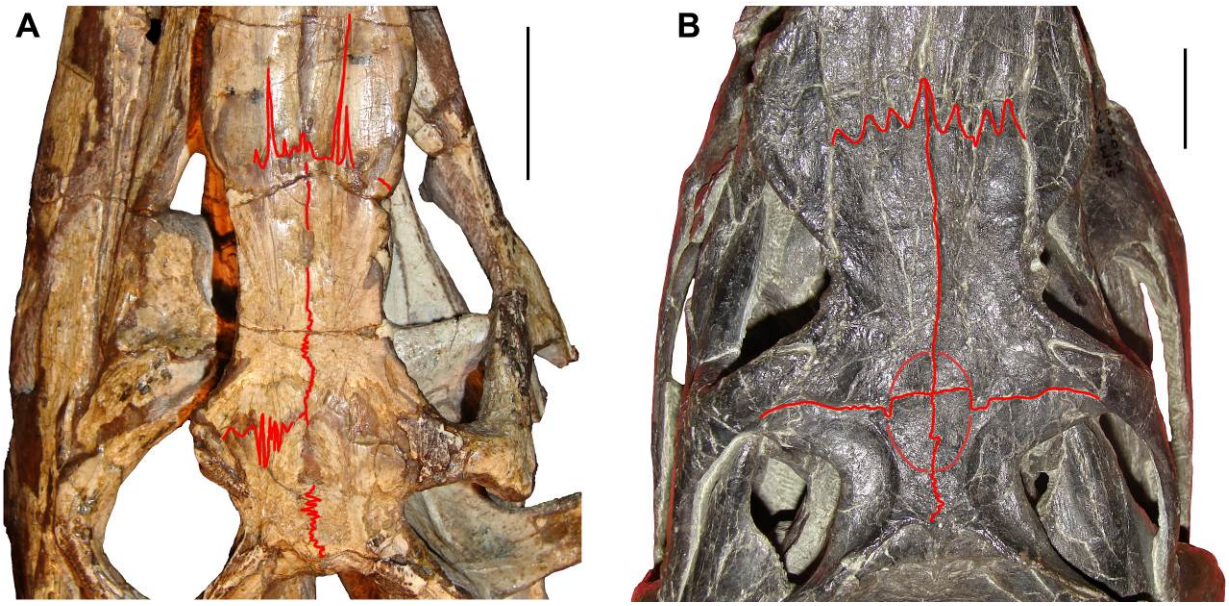

Figure 4.3. Orbital and temporal regions of skulls of a juvenile (A: RC 59) and a medium-sized (B: SAM-PK-K10603) specimen in dorsal views. Fronto-nasal, fronto-parietal, frontal-frontal and parietal-parietal sutures, and the pineal fossa are highlighted with lines. Scale bars equal 2 cm.

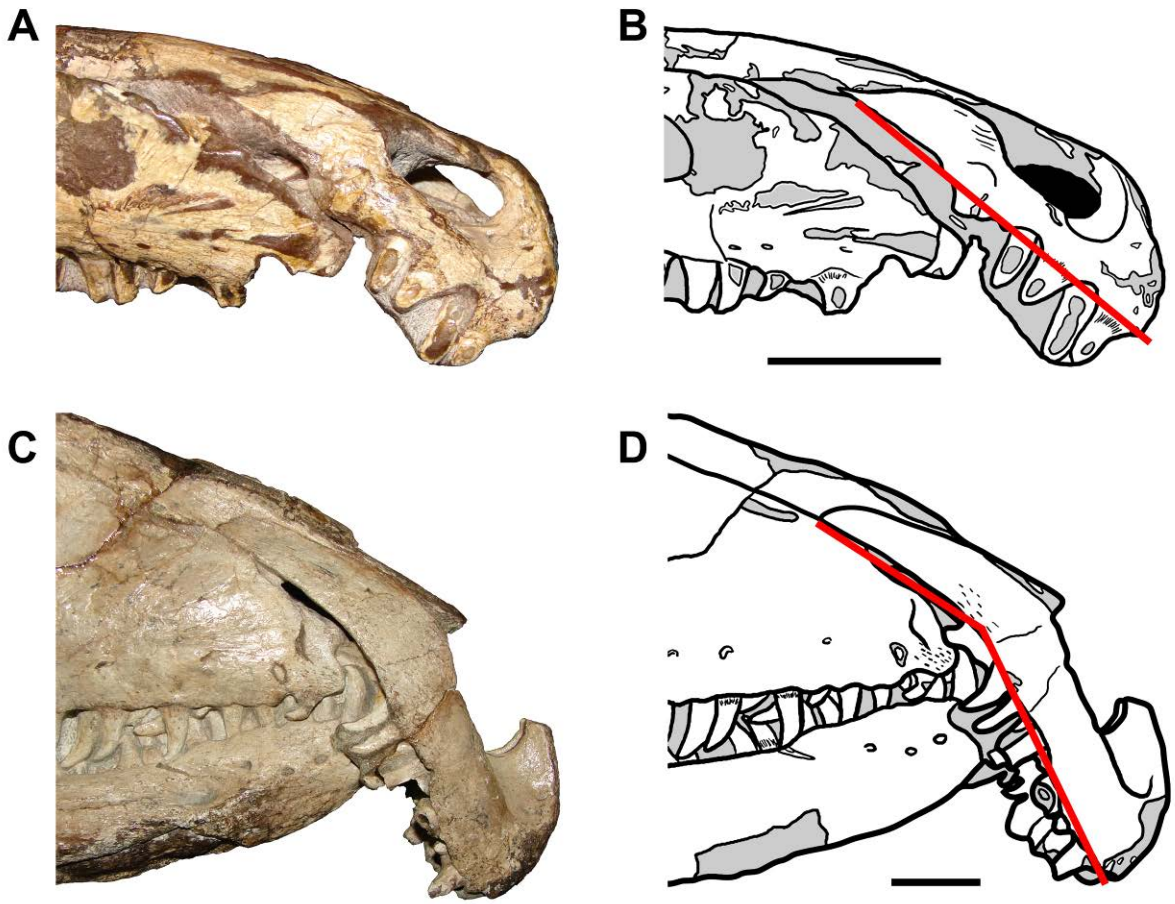

Figure 4.4. Anterior half of the snout of a juvenile (A, B: RC 59) and an adult (C, D: RC 846, neotype, reversed) of *Proterosuchus fergusi*. Lines show the changes in orientation of the postnarial process of the premaxilla with respect to the alveolar margin of the bone during ontogeny. Scale bars equal 2 cm.

feature cannot be determined. By contrast, in the smallest individuals of the ontogenetic series the skull roof lacks a pineal fossa (RC 59, BP/1/4016, 4224) (Fig. 4.3A).

Other changes. The main axis of the postnarial process of the premaxilla is subparallel to the alveolar margin of the bone in the smallest preserved specimen of *Proterosuchus fergusi* (RC 59) (Fig. 4.4A, B). By contrast, in all other specimens of the species the postnarial process is downturned with respect to the main axis of the alveolar margin (e.g. BP/1/3993, BSPG 1934 VIII 514, RC 846, SAM-PK-11208, TM 201) (Fig. 4.4C, D). This variation can be interpreted as either non-ontogenetically related or ontogenetically related because RC 59 is the only specimen with this morphotype. Nevertheless, the presence of this feature in the smallest known specimen of the growth series might indicate that the change in orientation of the postnarial process occurred very early in ontogeny. This hypothesis could be tested with a future improved sample of early juvenile specimens of *Proterosuchus fergusi*. Previous authors suggested that the pattern of tooth replacement of *Proterosuchus fergusi* changed during ontogeny (Broom, 1946). However, in agreement with Welman (1998), I was unable to recognize any clear change in this feature in the ontogenetic sequence. Similarly, no conclusive evidence was identified supporting the hypothesis of a migration of the internal choanae to a more posterior position during ontogeny (contra Welman and Flemming, 1993).

4.3.2. *Quantitative analysis*

Table 4.1 (and subsequent page). Results of the SMA regressions using total skull length as the independent variable. Abbreviations: (+), marginally significant positive allometry; (-), marginally significant negative allometry; +, positive allometry; -, negative allometry; =, isometry; CI, confidence interval; N, size of the variable.

Measurement	N	R^2	p-value (regression-test)	Slope	Lower limit (90% CI)	Upper limit (90% CI)	p-value (isometry-test)	Trend
Skull maximum height	5	0.9013	0.0136	1.5614	1.0312	2.3642	0.0848	(+)
Length anterior to antorbital fenestra	8	0.9627	<0.0001	1.0390	0.8920	1.2102	0.6445	=
Postorbital region maximum width	6	0.7119	0.0371	1.2538	0.7272	2.1619	0.4430	=
Premaxillary body length	7	0.9094	0.0008	1.2279	0.9392	1.6053	0.1850	=
Premaxillary body height	9	0.8714	0.0002	1.2245	0.9498	1.5786	0.1761	=
Number of premaxillary teeth	8	0.6498	0.0156	0.6983	0.4436	1.0994	0.1798	=
Largest premaxillary tooth length at base	7	0.7902	0.0074	1.1434	0.7650	1.7088	0.5408	=
Snout minimum width	9	0.9256	<0.0001	0.8868	0.7303	1.0766	0.2806	=
Maxilla length	8	0.9610	<0.0001	1.1000	0.9411	1.2856	0.2811	=
Maxilla horizontal process minimum height	10	0.9339	<0.0001	1.4498	1.2254	1.7154	0.0031	+
Maxilla length anterior to antorbtial fenestra	9	0.9560	<0.0001	1.0918	0.9401	1.2581	0.3036	=
Number of maxillary teeth	9	0.8386	0.0005	0.5323	0.4008	0.7070	0.0030	-
Largest maxillary tooth height	9	0.6910	0.0054	0.6598	0.4475	0.9727	0.0810	(-)
Largest maxillary tooth length at base	10	0.6201	0.0068	0.6045	0.4073	0.8972	0.0426	-
Antorbital fenestra length	6	0.9679	0.0004	0.9721	0.8041	1.1753	0.7682	=
Lacrimal length	4	0.9275	0.0369	0.9799	0.5764	1.6659	0.9249	=
Lacrimal height	6	0.7111	0.0349	1.3518	0.7834	2.3323	0.3184	=
Jugal anterior process height	10	0.7504	0.0012	1.3242	0.9589	1.8288	0.1458	=
Orbit length	7	0.8210	0.0049	0.8406	0.5790	1.2200	0.3986	=
Orbit height	6	0.9567	0.0007	1.8453	1.4808	2.2995	0.0033	+
Frontal length	8	0.9512	<0.0001	0.9001	0.7562	1.0714	0.2864	=
Frontals minimum width	9	0.7344	0.0032	0.9030	0.6293	1.2958	0.6162	=
Postfrontal oblique length	5	0.8219	0.0338	0.7680	0.4450	1.3256	0.3532	=
Postorbital length	7	0.8586	0.0026	1.4765	1.0586	2.0593	0.0634	(+)
Postorbital height	7	0.9860	<0.0001	0.8436	0.7586	0.9382	0.0231	-
Squamosal length	6	0.7033	0.0370	0.9523	0.5482	1.6541	0.8662	=
Squamosal height	8	0.9206	0.0002	1.2089	0.9686	1.5088	0.1480	=
Squamosal ventral process height	8	0.8810	0.0005	1.2891	0.9838	1.6891	0.1180	=
Squamosal ventral process base length	8	0.8310	0.0016	0.8916	0.6470	1.2287	0.5191	=
Infratemporal fenestra length	8	0.9611	<0.0001	1.4242	1.2187	1.6642	0.0042	+
Infratemporal fenestra height	6	0.9092	0.0032	1.3923	1.0152	1.9094	0.0888	(+)
Supratemporal fenestra length	10	0.8230	0.0002	1.1224	0.8541	1.4750	0.4588	=
Supratemporal fossa width	11	0.7965	0.0012	1.2118	0.8820	1.6649	0.2942	=
Quadrate height	5	0.8144	0.0360	1.2864	0.7376	2.2434	0.3814	=
Parietal length	10	0.8314	0.0002	1.0100	0.7736	1.3188	0.9468	=
Parietals maximum width	8	0.8912	0.0004	1.4396	1.1113	1.8648	0.0326	+
Parietals minimum width	10	0.9528	<0.0001	0.7445	0.6458	0.8584	0.0046	-
Width between paroccipital processes	6	0.7940	0.0171	1.3823	0.8668	2.2043	0.2202	=
Ectopterygoid width	5	0.8044	0.0391	1.1266	0.6374	1.9912	0.6717	=
Lower jaw length	7	0.9743	<0.0001	0.9830	0.8512	1.1352	0.8212	=
Dentary length	10	0.9915	<0.0001	1.0180	0.9582	1.0814	0.5981	=
Dentary anterior height	10	0.8966	<0.0001	0.8986	0.7285	1.1083	0.3734	=
Number of dentary teeth	6	0.7152	0.0338	0.4524	0.2631	0.7778	0.0300	-
Surangular height	9	0.6858	0.0058	0.9917	0.6706	1.4666	0.9697	=

Angular length	5	0.9576	0.0037	0.9604	0.7287	1.2660	0.7566	=
Angular height	8	0.7804	0.0036	0.9398	0.6533	1.3520	0.7566	=
Retroarticular process length	6	0.8086	0.0147	1.0272	0.6544	1.6125	0.9081	=
Retroarticular process width	5	0.9641	0.0029	1.0218	0.7922	1.3180	0.8560	=
Retroarticular process height	6	0.7650	0.0226	0.8948	0.5448	1.4697	0.6699	=

4.3.2.1. Allometric regressions. Nineteen of the original 68 variables failed the regression test ($p>0.05$) and these measurements were excluded because they do not show a significant relationship with size (as measured by skull length) (e.g. width of the supratemporal fenestra, angle between the proximal and distal ends of the quadrate, length and height of the external mandibular fenestra, and width and height of the supraoccipital). Thirty-six variables (73.5% of the variables with a significant regression) show a slope that does not significantly depart from K=1 (Figs. 4.5A, C, 4.6A; Table 4.1). Seven measurements show a positive allometric trend (14.3% of the variables with a significant regression), of which four are height measurements (Figs. 4.5B, D, 4.6B, 4.7C; Table 4.1). Six variables show a negative allometric trend (12.2% of the variables with a significant regression), of which four are variables describing tooth morphology (Fig. 4.7A, B, D; Table 4.1). The mean of all of the 49 recovered slopes is very close to K=1, because most of the variables are length and width measurements, and the means of the slopes of the length and width measurements are very close to K=1 (Table 4.2). The slopes of the variables related to height measurements have a mean of around K=1.2, and those related to tooth morphology have a slope of around K=0.7.

As a result, the length and width of the skull of *Proterosuchus fergusi* show a general pattern of isometric growth during ontogeny. For example, the length of the premaxilla, maxilla, frontal, orbit and dentary all show isometric growth (Table 4.1), implying that the elongated snout and enlarged premaxilla that are characteristic of proterosuchids did not significantly change its proportions during ontogeny. By contrast, the skull becomes proportionally taller through ontogeny, as demonstrated by the positive allometric growth of the maximum height of the skull, minimum height of the horizontal process of the maxilla, and heights of the orbit and

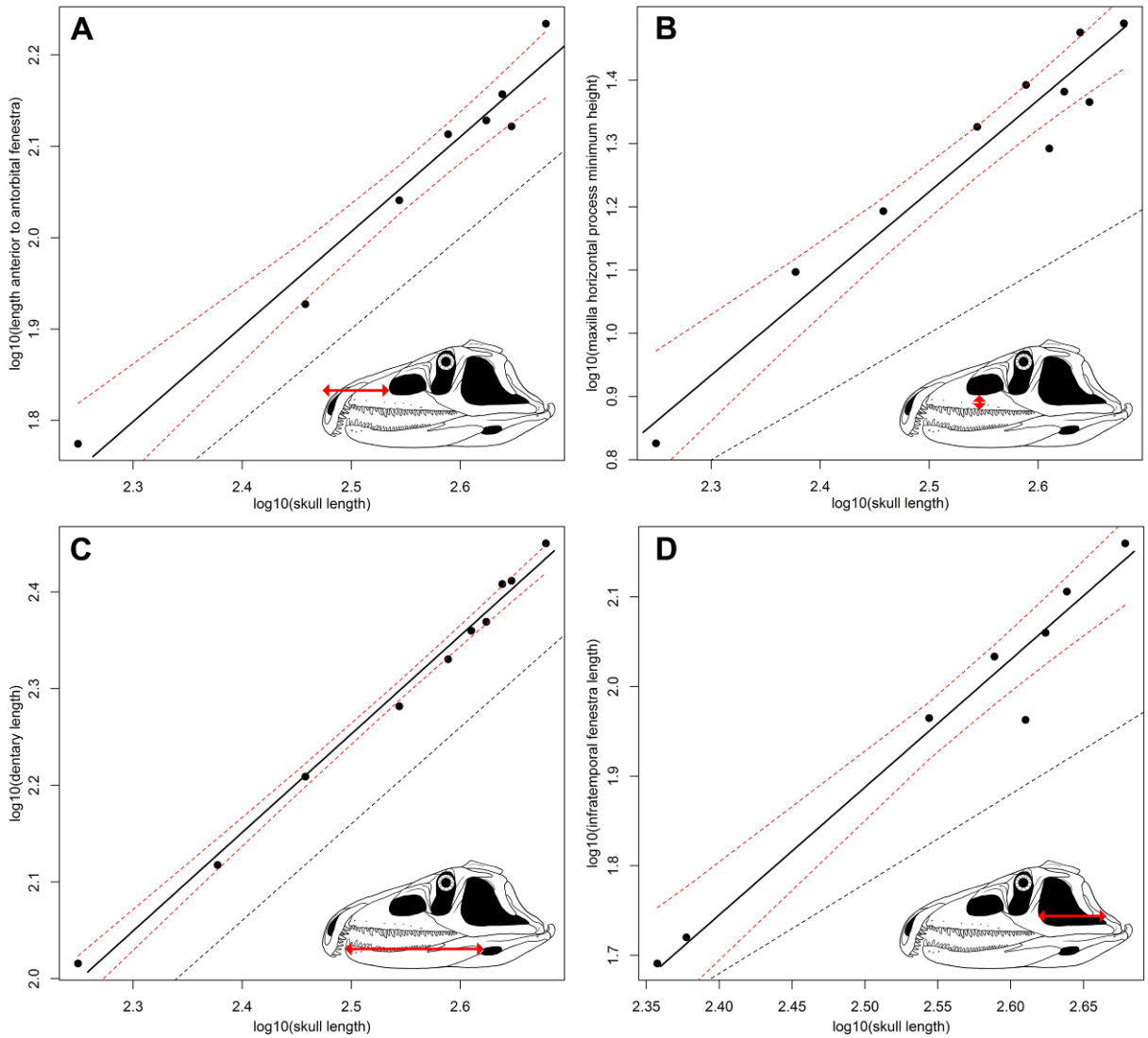

Figure 4.5. Bivariate plots showing isometric (A, C) and positive allometric (B, D) trends. Dotted lines show the limits of the 90% confidence intervals and a line with a slope equal to 1, respectively.

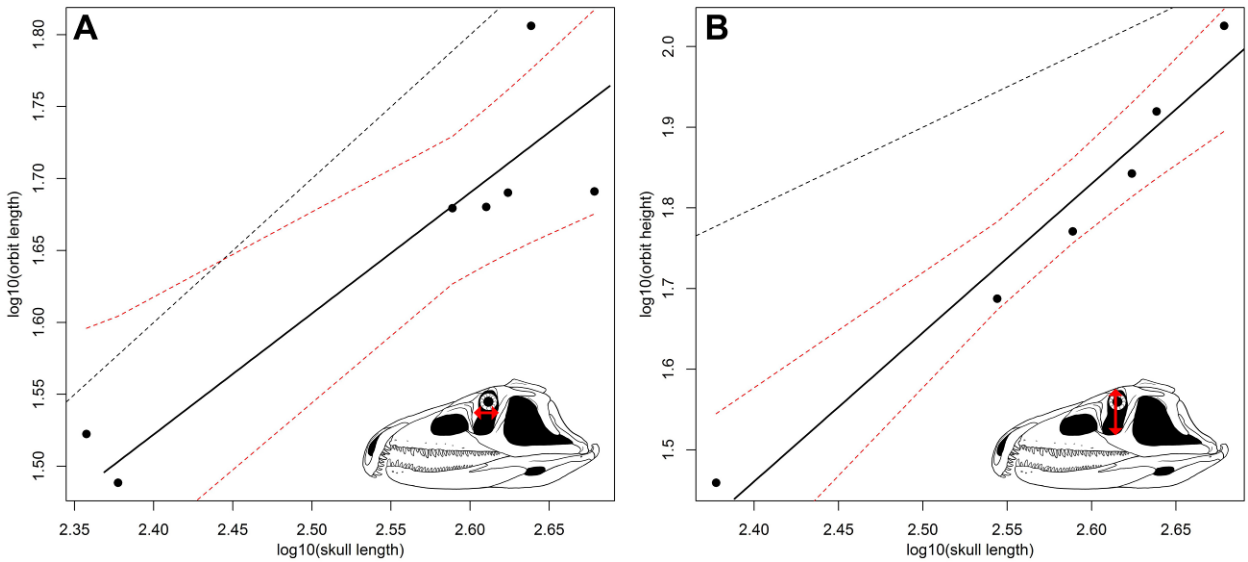

Figure 4.6. Bivariate plots showing the possible negative allometric trend of (A) the length of the orbit (A) and the positive allometric trend of the height of the orbit (B). Dotted lines show the limits of the 90% confidence intervals and a line with a slope equal to 1, respectively.

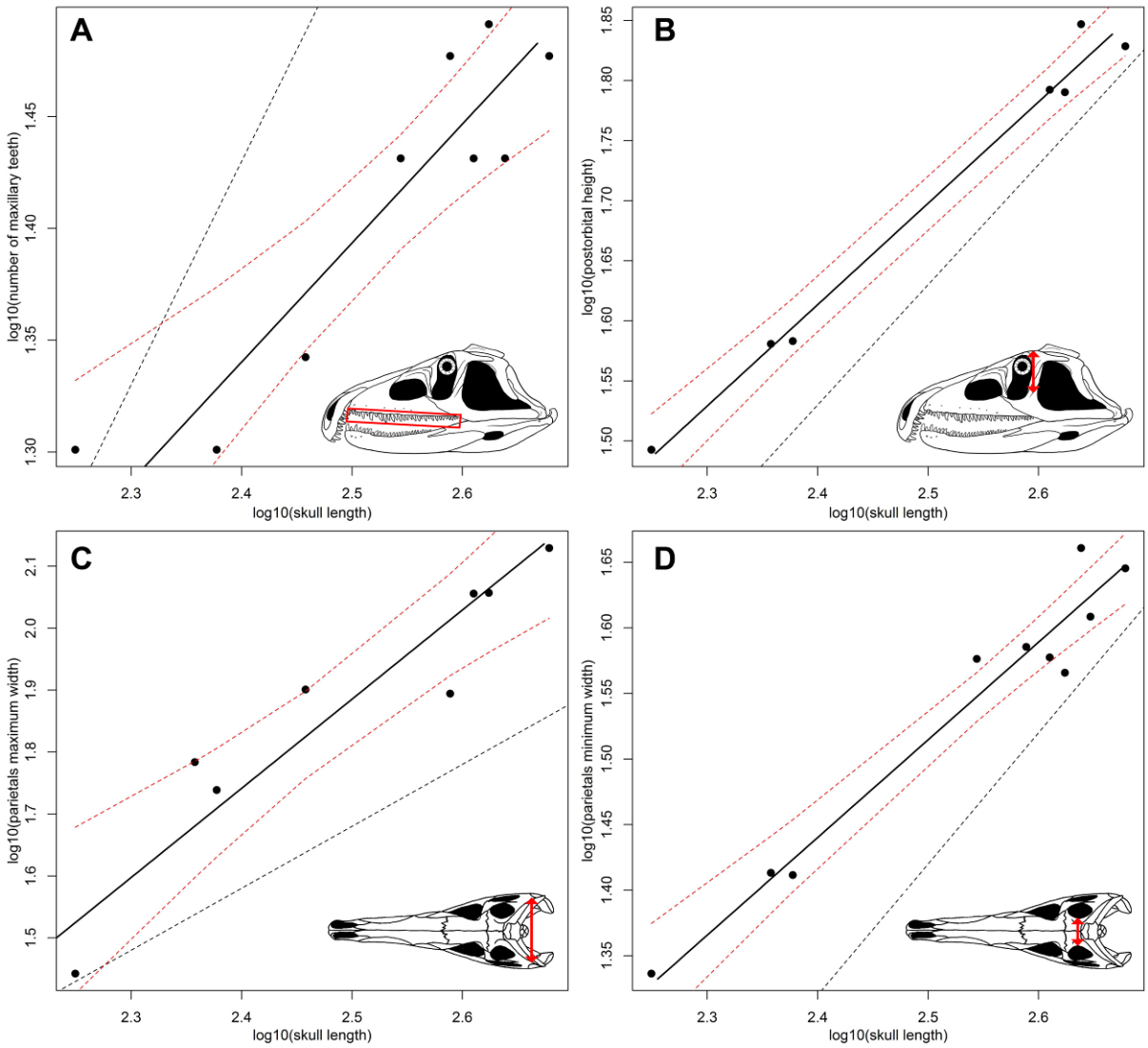

Figure 4.7. Bivariate plots showing negative (A, B, D) and positive (C) allometric trends. Dotted lines show the limits of the 90% confidence intervals and a line with a slope equal to 1, respectively.

Table 4.2. Statistical parameters of the distribution of slopes and their upper and lower limits. Abbreviations: N, size of the variable; sd=standard deviation.

Group	N	Mean	Upper limit mean	Lower limit mean	Median	Upper limit median	Lower limit median
All variables	49	1.0683 (sd=0.2796)	1.4840 (sd=0.4317)	0.7838 (sd=0.2367)	1.0218	1.4670	0.7650
Length	19	1.0413 (sd=0.17778)	1.3850 (sd=0.2603)	0.7982 (sd=0.1945)	1.0100	1.2860	0.8041
Height	15	1.2335 (sd=0.2811)	1.7203 (sd=0.4441)	0.8994 (sd=0.2421)	1.2864	1.6891	0.9498
Width	9	1.1078 (sd=0.2367)	1.6040 (sd=0.4879)	0.7803 (sd=0.1558)	1.1266	1.6649	0.7303
Teeth	6	0.6818 (sd=0.2428)	1.0272 (sd=0.3618)	0.4546 (sd=0.1663)	0.6318	0.9349	0.4254

Table 4.3. Results of the SMA regressions using the respective tooth-bearing bone lengths as independent variables. Abbreviations: -, negative allometry; CI, confidence interval; N, size of the variable.

Measurement	N	R^2	p-value (regression-test)	Slope	Lower limit (90% CI)	Upper limit (90% CI)	p-value (isometry-test)	Trend
Premaxillary tooth count	7	0.7015	0.0186	0.5390	0.3354	0.8662	0.0186	-
Maxillary tooth count	8	0.9022	0.0003	0.4923	0.3620	0.6696	0.0009	-
Dentary tooth count	6	0.6808	0.0432	0.4505	0.2546	0.7972	0.0351	-

infratemporal fenestra. Although the absolute number of tooth positions increases considerably through ontogeny for all the tooth-bearing bones (Ezcurra et al., 2013, see ontogram), the ratio between tooth counts and the lengths of the bones is significantly negative (Fig. 4.7A; Table 4.3). In addition, at least maxillary tooth crowns become proportionally apicobasally shorter and mesiodistally narrower during ontogeny.

4.3.2.2. Ontogram. The parsimony analysis yielded a single most parsimonious tree (MPT) with a fit score of 0.22015, a consistency index (CI) of 0.8598 and a retention index (RI) of 0.8724. The tree is fully resolved and its overall topology shows a general tendency of increase in body size towards its apex (Fig. 4.8). The smallest non-rooted specimens are found as successive sister-individuals of larger specimens at the base of the tree (BP/1/4016, 4224), and three of the four largest specimens are placed at the apex (BSPG 1934 VIII 514, RC 846, GHG 231). The resampling statistical test found that the total length of the skull fits significantly to the topology of the recovered MPT ($p=0.0013$). This result is in agreement with the a priori assumption that the ontogram shows a sequence of maturity (Brochu, 1992). The topology and optimization of the characters on the tree were not affected when the tree was rooted with an artificial embryo (i.e. RC 59 was still found as the least mature specimen). Several ambiguous ontomorphies (sensu Frederickson and Tumarkin-Deratzian, 2014) are optimized under accelerated transformations (ACCTRAN) for the nodes that include SAM-PK-K140 and SAM-PK-K10603, and more mature individuals, respectively. These ambiguous optimizations are a result of the multiple missing scorings present in BP/1/4224 and SAM-PK-K140.

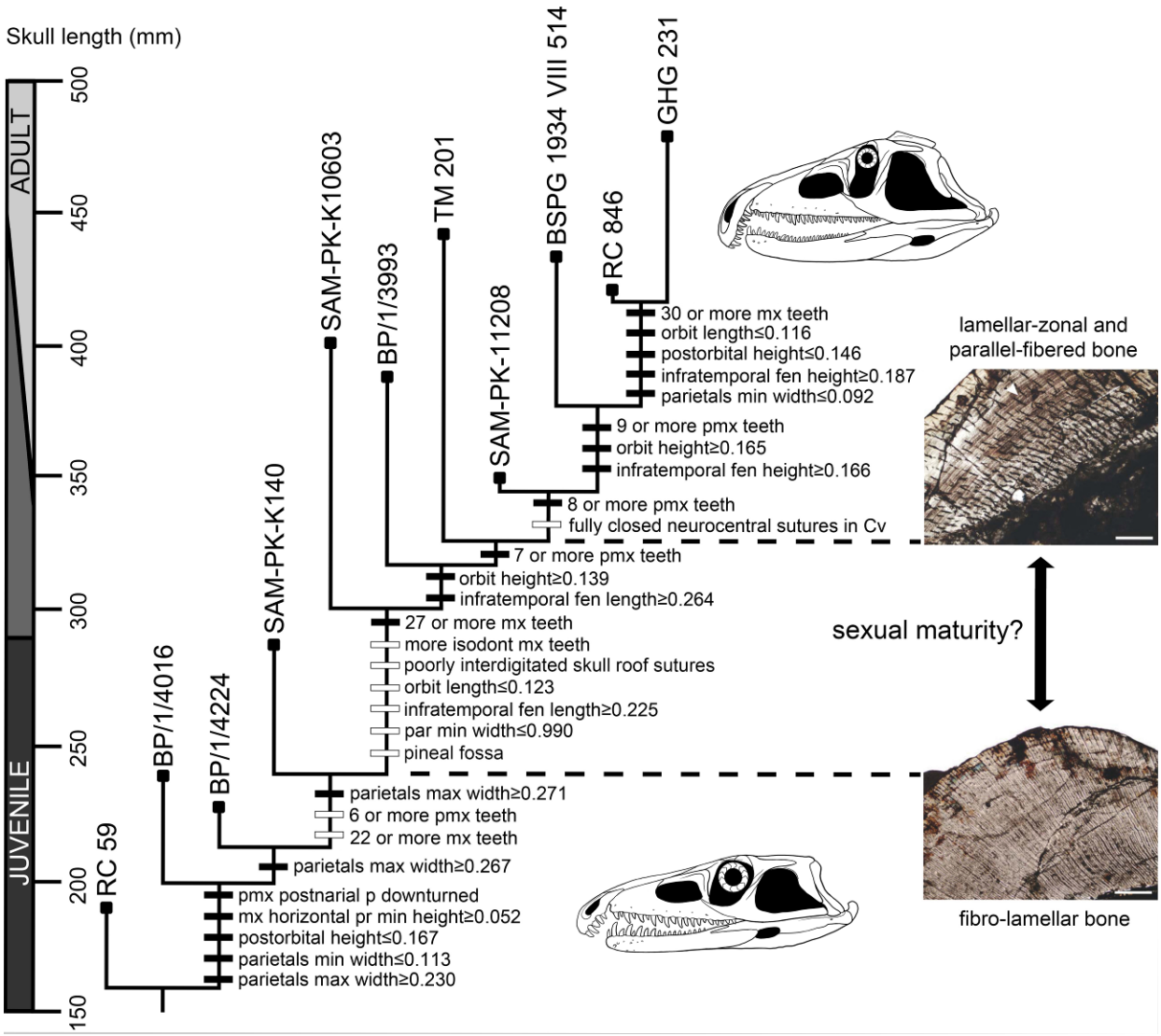

Figure 4.8. Single recovered most parsimonious ontogram showing the sequence of somatic maturity of the available ontogenetic sequence of *Proterosuchus fergusi*. Ontogenetic changes indicated with a black box are unambiguously optimized characters (synontomorphies) and changes indicated with a white box are characters optimized under an ACCTRAN optimization (possible ontomorphies). Upper thin-section shows the bone microstructure of the probable sexually mature SAM-PK-11208 and the lower thin-section shows the bone microstructure of the probably sexually immature SAM-PK-K140 (taken from Botha-Brink and Smith, 2011).

The sequence of optimization of the continuous characters on the tree is in general agreement with the results of the allometric regressions. Measurements with significant negative allometries show a decrease in their ratios with respect to the total length of the skull through the ontogram (e.g. parietals minimum width, postorbital height). Conversely, measurements with significant positive allometries show an increase of their ratios through ontogeny (e.g. maxillary horizontal process height, orbit height, infratemporal fenestra height, parietals maximum width, infratemporal fenestra length, infratemporal fenestra height).

Orbit length was recovered as having an isometric growth by the allometric regression analysis, but in the ontogram it optimizes with a tendency of decrease in its proportional size towards more mature individuals. This result suggests negative allometric growth for this measurement, which is in agreement with the low slope found in its SMA regression (K=0.8406). However, the relatively low regression coefficient (R^2=0.8210) and the low number of specimens that could be measured for this variable might have resulted in a negative allometric pattern being overlooked by the statistical test of isometry. The presence of a positive allometry in orbit height and a negative allometry in orbit length seems a likely explanation of the drastic modifications that occur in the shape and relative size of the orbit through the ontogeny of *Proterosuchus fergusi* (Fig. 4.1).

The numbers of tooth positions in the premaxilla and maxilla, which are correlated with the number of tooth positions in the dentary (R^2=0.9888), increase through ontogeny, from five to nine premaxillary teeth, 20 to 30−31 maxillary teeth, and 18 to 28 dentary teeth. Other ontogenetic changes recovered by the ontogram include a downturned postnarial process of the premaxilla with respect to the alveolar

margin of the bone, the appearance of a pineal fossa, more isodont maxillary tooth crowns (all strongly distally curved), less interdigitated sutures on the skull roof and completely closed neurocentral sutures in cervical vertebrae.

4.4. Discussion

4.4.1. *Comparisons with previous studies*

The increased number of specimens of *Proterosuchus fergusi* available when compared with the analysis of Welman and Flemming (1993) allowed the direct use of skull length as the independent variable, constituting a clear step forward in the analysis of allometric regressions. For example, the standard measurement (i.e. the proxy for overall size) most widely used by Welman and Flemming (1993) was the minimum width between both parietals. However, this analysis has demonstrated that this variable has a negative allometric trend with respect to skull length (K=0.7445, p=0.0046). Use of a variable with a negative allometric trend as the independent variable will tend to produce a systematic bias towards higher slope values.

The histogram showing the frequency of slopes recovered in this analysis shows that the highest frequencies are situated around K=1 (mean=1.0683, sd=0.2796, median=1.0218). As a result, the general tendency of the cranial allometric regressions in the skull of *Proterosuchus fergusi* is isometric (Fig. 4.9A; Table 4.2). The distribution of the slopes is slightly skewed towards values higher than 1, but a Shapiro-Wilk test failed to reject the null hypothesis of a normal distribution (p=0.8795). The mean of the distribution of slopes recovered by Welman and Flemming (1993) is 0.9093 (sd=0.4178) and the median is 0.8100. The histogram of slope frequencies of Welman and Flemming (1993) is strongly skewed towards values

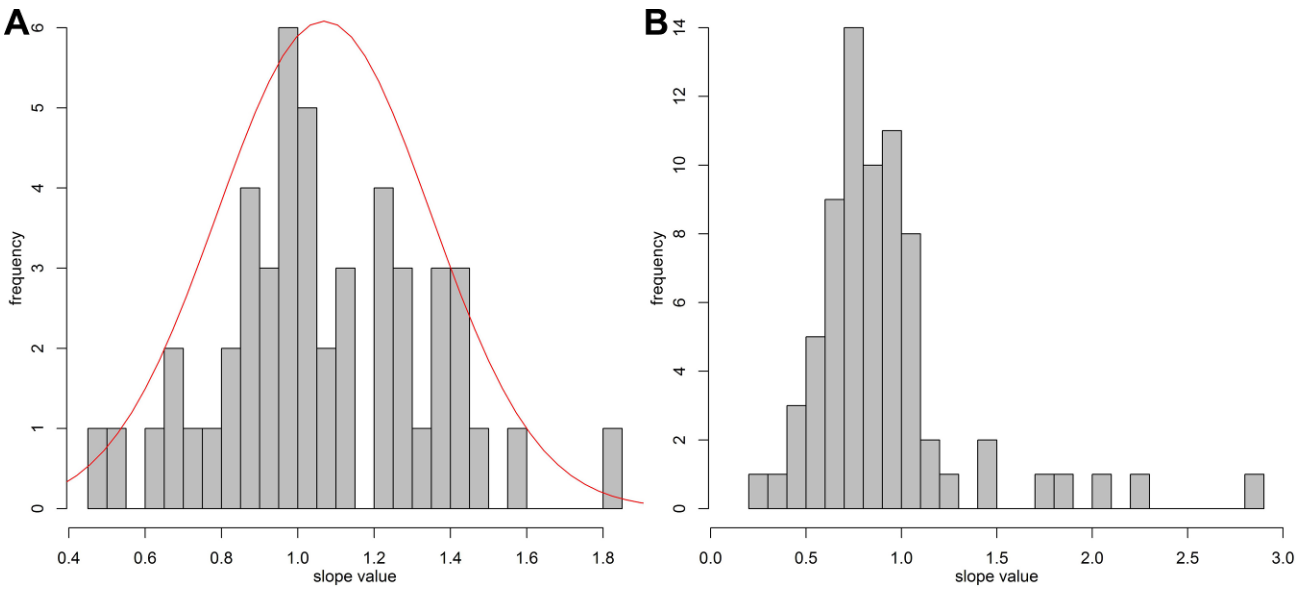

Figure 4.9. Histograms showing the distribution of slopes recovered in the present SMA regressions (A) and the analysis of Welman and Flemming (1993) (B). The line in (A) represents a normal distribution adjusted to the data set.

higher than 1 (Fig. 4.9B) and the Shapiro-Wilk test rejected the normality of the distribution of these slopes ($p<0.0001$), in contrast to the results of this chapter.

A second allometric analysis was conducted using the minimum width of the parietals as the independent variable in order to test the possible influence of this variable in the study of Welman and Flemming (1993). I employed the same variables as in the initial analysis, but replaced skull length with the minimum width of the parietals as the standard measurement. In this new analysis, 26 of the 49 regressions show a positive allometric trend, the mean of the slope values is 1.4111 (sd=0.3545) and the median is 1.3566. These results indicate a general positive allometric trend (which is probably the result of a systematic bias), contrasting with the general isometric trend recovered by the original analysis. For example, the length of the dentary was found to have a significant positive allometry in this alternative analysis ($K=1.3566$, $p=0.0095$), but a statistically well-supported isometric trend in the original analysis. The Shapiro-Wilk test failed to reject the null hypothesis of a normal distribution ($p=0.8011$), resembling the result of the original analysis but contrasting with the distribution of slope values recovered by Welman and Flemming (1993). A T-test found a significant difference between the slopes recovered using skull length versus minimum width of the parietals as alternative independent variables ($p<0.0001$). As a result, use of a different independent variable in the present study partially, but not completely (e.g. it does not explain the change in the shape of the distribution of the slope values), explains the differences between the results of the original analysis and the results recovered by Welman and Flemming (1993). Differences in specimen sampling, because of the addition of recently collected specimens and the effects of the recently revised taxonomy, and measurements may also contribute to the differences observed with the results of Welman and Flemming (1993).

4.4.2. *Sequence of somatic maturity in* Proterosuchus fergusi

The result of the ontogram is in agreement with osteohistological data that indicates that SAM-PK-11208 is a more mature individual than SAM-PK-K140 (Botha-Brink and Smith, 2011) (Fig. 4.8). In addition, Botha-Brink and Smith (2011) proposed that SAM-PK-11208 may have reached sexual maturity, whereas SAM-PK-K140 had not. Following these lines of evidence, the ontogram suggests that *Proterosuchus fergusi* reached sexual maturity in individuals with skull lengths that were at least 60.2−73.4% of the skull length of the largest individual currently known. Botha-Brink and Smith (2011) proposed that *Proterosuchus fergusi* possessed relatively rapid continuous growth, without LAGs, prior to reaching sexual maturity, and until reaching at least 67% of the maximum recorded skull length of the species. However, these authors slightly underestimated the maximum recorded skull length of *Proterosuchus fergusi*, and rapid continuous growth continued until reaching at least 60.2% of the maximum skull length (Fig. 4.8) and an estimated total body length of at least 60% of the maximum estimated total length of the species (based on the equation of Platt et al. [2009]). If the absence of LAGs in SAM-PK-K140 indicates that the specimen is younger than a year old, as has been widely interpreted for other archosauriforms (Botha-Brink and Smith, 2011), this would mean that the onset of sexual maturity was reached after the first year of life.

Similar growth timings are present in disparate diapsid reptiles, such as the ornithischian dinosaur *Maiasaura peeblesorum* (an individual younger than a year old was up to 50% of the maximum adult total body length; Horner et al., 2000) and the

varanoid lizard *Varanus niloticus* (a year old individual is around 40% of the maximum snout-vent adult length; de Buffrénil and Castanet, 2000).

Botha-Brink and Smith (2011) also suggested the possibility of extremely fast growth in the basal archosauromorph *Prolacerta broomi*, also known from the earliest Triassic of South Africa. They suggested that *Prolacerta broomi* may have reached maximum size within its first year of life (assuming that growth did not temporarily slow down or cease during the unfavourable growing season). However, although some archosauromorphs also grew rapidly in their first year of life (see above), first year growth rates are considerably lower in many other archosauromorph species (e.g. 15.7% of maximum total body length in extant crocodiles: Huchzermeyer, 2003; 15.3% of maximum femoral length in *Psittacosaurus lujiatunensis*: Erickson et al., 2009). As a result, rapid first year growth rates do not appear to be a general character of archosauromorphs – instead, this feature appears to be rather homoplastic within the group. Changes in growth strategies among archosauromorphs may have been influenced by non-phylogenetic, external factors (e.g. climate, interspecific competition) and it is striking that both archosauromorph species known from the *Lystrosaurus* AZ of South Africa for which information is available on growth rates (*Prolacerta broomi*, *Proterosuchus fergusi*) appear to have attained more than 60% of their maximum recorded size during the first year of life.

The result of the ontogram in combination with osteohistological evidence allows the interpretation that RC 59, BP/1/4016, 4224 and SAM-PK-K140 represent sexually immature (juvenile) individuals (skull length<300 mm) and SAM-PK-11208, BSPG 1934 VIII 514, RC 846 and GHG 231 represent sexually mature (adult) individuals (skull length≥350−444 mm) (Fig. 4.8). The ontogenetic stages of SAM-PK-K10603, BP/1/3993 and TM 201 are ambiguous because they are bracketed by the

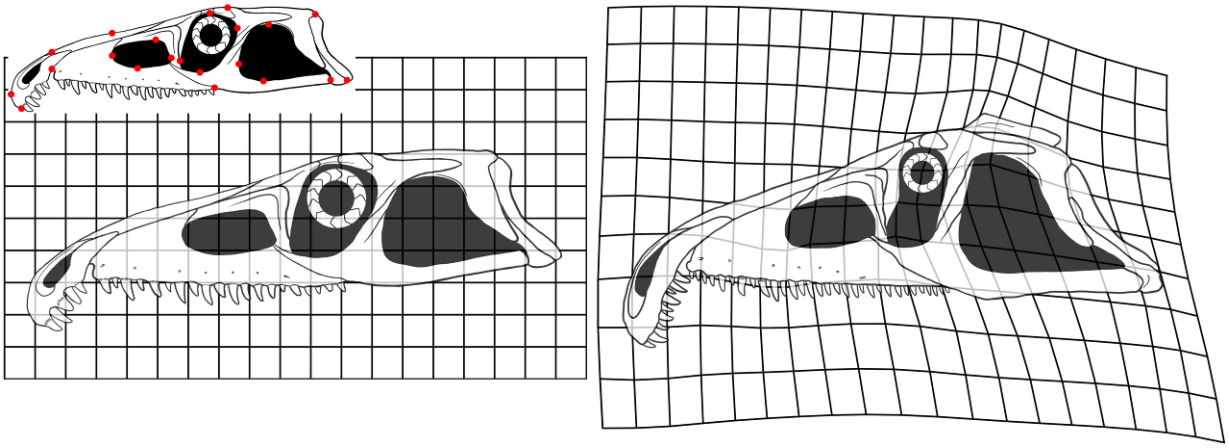

Figure 4.10. Position of the 21 landmarks (red dots) used for the basic geometric morphometric analysis (juvenile smaller skull on the upper left corner of the figure) and results of the thin plate spline analysis for the juvenile (left) and adult (right).

oldest immature and the youngest mature individuals. The earliest somatic changes recognized within the sampled ontogenetic sequence of *Proterosuchus fergusi* include a downturned postnarial process of the premaxilla with respect to the alveolar margin of the bone, increases in the minimum height of the maxillary horizontal process, maximum height of the postorbital and maximum width of the parietals, and a decrease in the minimum width of the parietals. During the somatic maturity of juvenile specimens the maximum width of the parietals continued to increase and the oldest recognized juvenile has six tooth positions in the premaxilla and 22 in the maxilla. Several changes are recognized in the ontogenetic sequence of specimens with an ambiguous ontogenetic stage, including the appearance of a more isodont maxillary dentition, 7 tooth positions in the premaxilla and 27 in the maxilla, poorly interdigitated skull roof sutures, pineal fossa, increases in the height of the orbit and length of the infratemporal fenestra, and decreases in the length of the orbit and minimum width of the parietals. Some of these changes may be correlated with the onset of sexual maturity. Somatic changes in the unambiguously recognized youngest sexually mature individual include the presence of 8 tooth positions in the premaxilla and fully closed neurocentral sutures in the cervical vertebrae. The latest changes recognized here during the ontogeny of *Proterosuchus fergusi* are the presence of 9 tooth positions in the premaxilla and 30 or more teeth in the maxilla, increase in the height of the orbit and infratemporal fenestra, and decreases in the length of the orbit, height of the postorbital, and minimum width of the parietals.

4.4.3. *Allometric growth patterns in* Proterosuchus fergusi *and possible palaeoecological implications*

The results of the allometric regressions suggest three main patterns during the ontogeny of *Proterosuchus fergusi*: isometric growth in the anteroposterior and transverse directions; positive allometric growth in a dorsoventral direction; and a negative allometric growth of the dentition. The result of the thin plate spline analysis showing changes between the skull reconstruction of a juvenile and an adult individual is in agreement with the results of the allometric regressions and the ontogram (Fig. 4.10). The areas that suffered stronger shape changes are located in the orbital and temporal regions. The adult thin plate spline shows relative anteroposterior and dorsoventral elongations in the area occupied by the infratemporal fenestra and a relative dorsoventral elongation in the area occupied by the orbit. Conversely, the area occupied by the orbit shows a relative anteroposterior shortening. No landmarks were placed on the tooth crowns, but a reduction in the size of the premaxillary and maxillary teeth is evident in a comparison of the reconstructions of the juvenile and adult skulls.

The changes in morphology observed between juvenile and adult individuals of *Proterosuchus fergusi* may have had implications for the palaeocology of the species. The presence in juveniles of a dorsoventrally lower and more gracile skull, with less numerous and proportionally larger teeth than in the adult forms may have resulted in different prey selections between juveniles and adults. This behavioural differentiation would have reduced the degree of intraspecific competition between the two ontogenetic stages. This hypothesis could be tested in the future with morphofunctional analyses that go beyond the scope of this paper.

Implications for early archosauromorph evolution

The role of ontogenetic modifications between ancestor-descendant species is mostly unknown among early archosauromorphs because of the scarce knowledge of the ontogenetic development of basal members of the clade. Indeed, heterochronic changes have been only explored in detail in the skull of hyperodapedontine rhynchosaurs among Permo-Triassic archosauromorphs (Benton and Kirkpatrick, 1989). However, the cranial morphology of hyperodapedontine rhynchosaurs is highly modified from the inferred ancestral archosauromorph condition, and it does not contribute considerably to shed light on the role of heterochronic changes in the early evolution of archosauromorphs and archosauriforms. The new information presented here for *Proterosuchus fergusi* provides the most detailed insight yet available into the ontogenetic development of an early archosauromorph species. However, the ontogenetic development of other early archosauromorph and archosauriform species remains poorly understood, greatly hampering detailed analyses of ontogenetically related evolutionary processes. The ontogenetic changes demonstrated here for *Proterosuchus fergusi* allow us to propose some novel hypotheses about the role of ontogenetic modification in the early archosauromorph radiation. These hypotheses can be tested by future more complete sampling of the ontogenetic trajectories of other basal archosauromorphs.

Juvenile specimens of *Proterosuchus fergusi* possess a dorsoventrally low skull, with a sub-circular orbit. This morphology closely resembles the generalised morphology present in adult specimens of protorosaurs (one of the most basal archosauromorph radiations) and *Prolacerta broomi* (Modesto and Sues, 2004; Gottmann-Quesada and Sander, 2009) (Fig. 4.11). By contrast, adult specimens of *Proterosuchus fergusi* possess a dorsoventrally deeper and more massive skull, with an anteroposteriorly compressed, suboval orbit. This morphology closely resembles the generalised skull

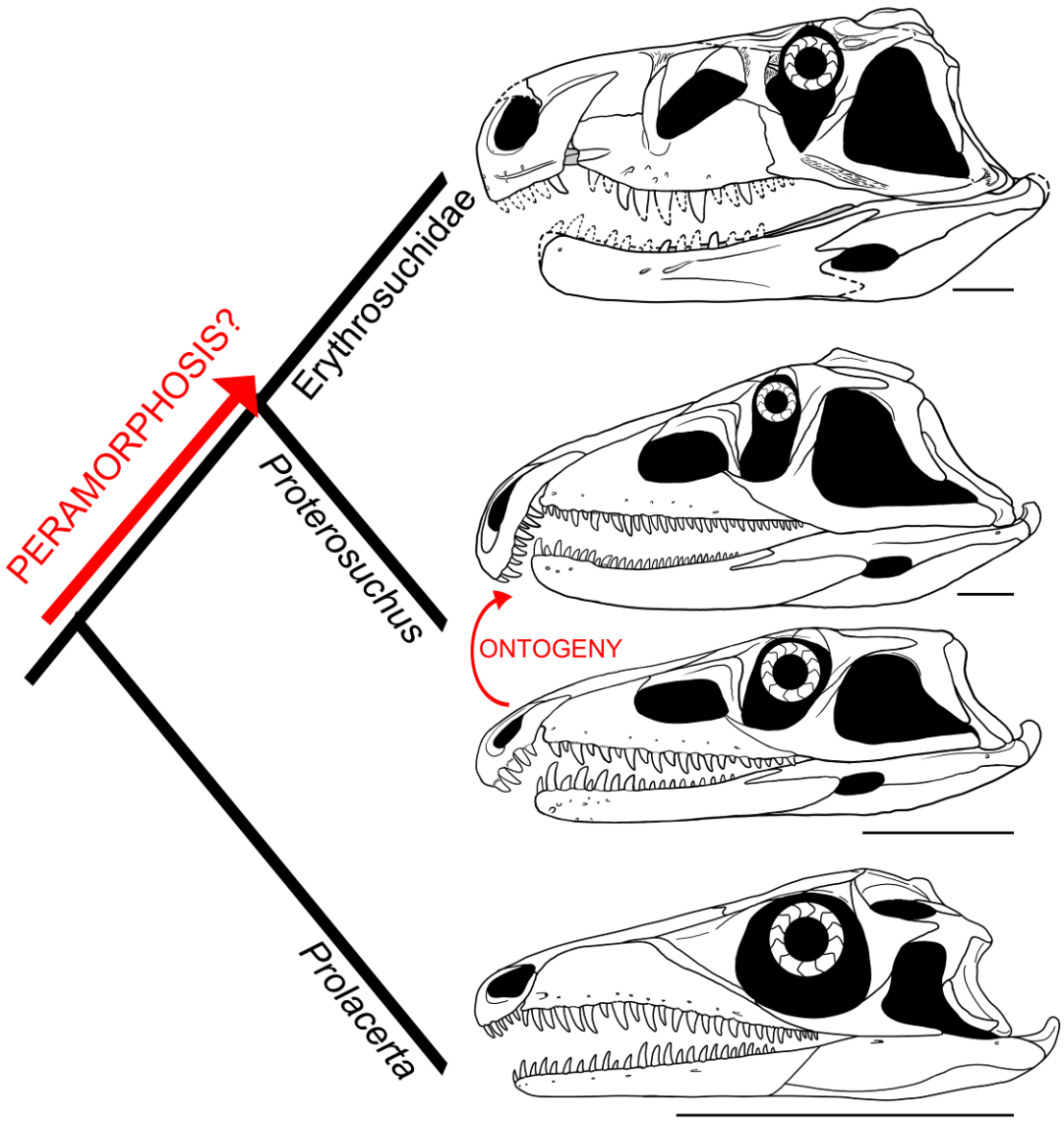

Figure 4.11. Simplified phylogenetic relationships in the non-archosauriform archosauromorph to archosauriform transition showing the possible direction of heterochronic changes that contributed to the evolution of overall skull shape. Note the similarities between the juvenile skull of *Proteorsuchus fergusi* and the adult of *Prolacerta broomi*, and the adult of *Proterosuchus fergusi* and an adult erythrosuchid (based on *Garjainia prima*). Scale bars equal 5 cm.

morphology of adult individuals of the more crownward archosauriforms Erythrosuchidae (e.g. *Garjainia prima, Erythrosuchus africanus*: Gower, 2003; Ezcurra et al., 2013) and *Euparkeria capensis* (Ewer, 1965).

In a phylogenetic context, this means that juveniles of *Proterosuchus fergusi* resemble the adults of early archosauromorphs, including a species repeatedly recovered as the sister-taxon of Archosauriformes in recent phylogenetic analyses (*Prolacerta broomi*; Modesto and Sues, 2004; Gottmann-Quesada and Sander, 2009; Ezcurra et al., 2014; Chapter 5). By contrast, the adults of diverse groups of basal archosauriforms are generally similar to one another in overall skull construction (Fig. 4.11). As a result, I hypothesize that ontogenetic modification events (probably peramorphosis) may have been the main drivers in the evolution of the general shape of the skull (dorsoventral height, shape of the orbit) at the base of Archosauriformes. This hypothesis implies that the probable major heterochronic processes are the opposite of those operating in the evolution of early birds, in which the paedomorphic skull morphology of adult birds resembles that of juvenile non-avian theropods (Bhullar et al., 2012). Accordingly, ontogenetic modification events between different species may have contributed to the occupation of a new region of morphospace by early archosauriforms around the Permo-Triassic boundary. The cranial morphospace of non-archosauriform archosauromorphs was limited to gracile and low skulls, possibly adapted to preying upon smaller animals (e.g. insects and small reptiles and synapsids). Massive and dorsoventrally deep skulls are documented for the first time in the archosauromorph evolution in basal archosauriforms (e.g. adult proterosuchids, erythrosuchids and *Euparkeria*) and this cranial morphology seems to have appeared independently several times in the lineage (e.g. ‘rauisuchians’, ornithosuchids, herrerasaurids; Sereno and Novas, 1993; Baczko and Ezcurra, 2013; Nesbitt et al.,

2013b). These massive skulls probably allowed the occupation of new niches, including the role of top predators in their respective ecosystems.

Chapter 5: Phylogenetic relationships of basal archosauromorphs

5.1. Background

The early evolution of the archosauromorphs during the Triassic is an excellent example of an adaptative radiation in the fossil record (Brusatte et al., 2008; Nesbitt, 2011). In the aftermath of the Permo-Triassic mass extinction, multiple, anatomically well diversified archosauromorph groups appear for the first time in the fossil record, including semi-aquatic or entirely aquatic forms (e.g. tanystropheids, doswelliids, proterochampsids, some poposauroids), highly specialized herbivores (e.g. trilophosaurids, rhynchosaurs), and massive predators (e.g. erythrosuchids, "rauisuchians"). As a result, the early evolution of archosauromorphs constitutes an excellent empirical case study to shed light on evolutionary radiations in deep time and the timing and processes of recovery of terrestrial faunas after a mass extinction. However, macroevolutionary studies of early archosauromorphs are strongly limited by the poor knowledge of their phylogenetic relationships (Ezcurra et al., 2013). Many early archosauromorph species have not been previously included in a quantitative phylogenetic analysis, and have been historically included within groups that are probably non-monophyletic as often conceived (e.g. "Prolacertiformes", Proterosuchidae: Dilkes, 1998; Modesto and Sues, 2004; Gottmann-Quesada and Sander, 2009; Ezcurra et al., 2010, 2013, 2014). In addition, the high-level phylogenetic relationships of the main lineages of archosauromorphs are highly debated and there is limited consensus between the results recovered by different studies (e.g. Dilkes, 1998; Modesto and Sues, 2004; Gottmann-Quesada and Sander, 2009; Ezcurra et al., 2014).

One of the main early archosauromorph groups that need an exhaustive phylogenetic study is “Proterosuchia”, which as historically conceived includes members of both Proterosuchidae and Erythrosuchidae (Reig, 1970; Charig and Reig, 1970; Charig and Sues, 1976; Ezcurra et al., 2013). Indeed, most proterosuchian species have not yet been included in quantitative phylogenetic analyses, and their phylogenetic positions among basal archosauriforms or within either Proterosuchidae or Erythrosuchidae is in state of flux (e.g. *Guchengosuchus shiguaiensis*, *Cuyosuchus rusconi*, *Chalishevia cothurnata*, *Shansisuchus kuyeheensis, Garjainia madiba*, “*Chasmatosaurus*” *yuani*, “*Blomosuchus georgii*”, *Vonhuenia friedrichi*, *Chasmatosuchus rossicus, Tasmaniosaurus triassicus, Kalisuchus rewanensis*). The proterosuchians represent the most basal known archosauriforms, and, as a result, an understanding of their phylogenetic relationships is crucial to attempts to reconstruct the interrelationships of more crownward archosauriforms and the early evolutionary history of Archosauriformes as a whole. However, the poor current phylogenetic understanding of the proterosuchians hampers the development of diagnoses for Proterosuchidae and Erythrosuchidae, and the taxonomic inclusiveness of these clades remains uncertain (Ezcurra et al., 2013). This chapter focuses on the phylogenetic relationships of non-archosaurian archosauromorphs, with a special emphasis on the interrelationships among taxa historically identified as proterosuchian archosauriforms.

5.2. Historical background of the phylogenetic relationships of “Proterosuchia”

The first discovered proterosuchian fossil was collected in the Lower Triassic Panchet Formation of India and described by Huxley (1865) as “*Ankistrodon indicus*”. This

species is based on a fragment of tooth-bearing bone interpreted by Huxley (1865) as a “thecodont saurian” with a tooth morphology closely resembling that of other carnivorous “thecodonts” and dinosaurs. During the early 20th century, Broom (1903) described the remains of a fossil reptile collected in the Lower Triassic part of the Karoo Basin of Eastern Cape Province, South Africa, and erected the new species *Proterosuchus fergusi*. He stated that *Proterosuchus* differed so greatly from any hitherto described species that it was difficult to decide its affinities (Broom, 1903: 162). However, mainly based on the morphology of the palatal teeth, Broom (1903: 163) concluded that *Proterosuchus* was a primitive “Rhynchocephalian” (conceived by Broom as a group of primitive reptiles including the likes of *Procolophon* and *Protorosaurus*) that showed “a considerable degree of specialisation along the line which gave rise to the early Crocodiles and Dinosaurs”. Two years later, the same author named *Erythrosuchus africanus* from the early Middle Triassic of South Africa and assigned it to the Phytosauria (Broom, 1905). Subsequently, Broom (1906) reviewed the classification of “Diaptosauria” (a group that included several amniote clades) and coined the new suborder or order Proterosuchia, within which he included *Proterosuchus*. Broom (1906) interpreted the Proterosuchia as more closely related to the Rhynchocephalia than to other Triassic diaptosaurian orders, such as Phytosauria and “Gnathodontia” (e.g. *Howesia*).

Huene (1908) considered Proterosuchia as a family-ranked group, resulting in the new taxon Proterosuchidae. Subsequently, Huene (1908) described a new and more complete *Erythrosuchus* specimen and proposed the new order “Pelycosimia”, within which he included *Erythrosuchus* and the derived rhynchosaur “*Scaphonyx*” (= *Hyperodapedon* sensu Langer et al., 2000b), among other taxa (Huene, 1911). Huene (1911) interpreted the “Pelycosimia” as closely related to pelycosaur synapsids.

However, Watson (1917) recognized *Erythrosuchus* as a member of the "Thecodontia" and coined the monospecific, family-ranked clade Erythrosuchidae. Subsequently, Huene (1920) agreed with this new interpretation and included the "Pelycosimia" within the order Thecodontia as a suborder.

Haughton (1924) described the new species "*Chasmatosaurus vanhoepeni*" from the same horizon as *Proterosuchus fergusi*, and assigned it to its own family, Chasmatosauridae. Williston (1925) considered the Proterosuchia as a non-thecodont order of diapsids. Subsequently, the suborder Erythrosuchia was erected by Goodrich (1930) in order to include only *Erythrosuchus*. Kuhn (1933) considered *Proterosuchus* to be closely related to the probable stem-crocodylomorphs *Dyoplax* and *Erpetosuchus*, whereas he interpreted *Erythrosuchus* and "*Chasmatosaurus*" as forming a group of closely related taxa together with the aetosaur "*Acompsosaurus*". Broili and Schröder (1934) also considered "*Chasmatosaurus*" and *Erythrosuchus* to be closely related.

Between the 1940s and 1960s several classifications were proposed that mostly agreed in considering proterosuchids and erythrosuchids as closely related taxa forming a single group (Proterosuchia or Proterosuchoidea, depending on the rank employed by each author) within a primitive stock of "thecodonts" (e.g. Romer, 1945, 1956; Huene, 1948, 1956; Hoffstetter, 1955; Kuhn, 1961; Reig, 1961). Ochev (1958) described *Garjainia prima* from the late Early Triassic of Russia and included it in its own family, Garjainiidae. Similarly, Huene (1960) described "*Vjushkovia*" *triplicostata* from the same horizon as *Garjainia prima* and erected the new family Vjushkoviidae, and Young (1964) described *Shansisuchus shansisuchus* from the Middle Triassic of China and coined the family Shansisuchidae. These families were included within the Proterosuchia, together with Proterosuchidae and

Erythrosuchidae, by some authors (e.g. Young, 1964; Reig, 1961; Kuhn, 1966). Tatarinov (1961) proposed that "*Vjushkovia*", *Garjainia*, *Dongusia*, and *Cuyosuchus* were junior synonyms of *Erythrosuchus*, a hypothesis that was followed by several other authors (e.g. Hughes, 1963; Ewer, 1965; Romer, 1966, 1972a; Cruickshank, 1972), but rejected by Young (1964), Charig and Reig (1970), and subsequent workers (e.g. Parrish, 1992; Sennikov, 1995a, b; Gower and Sennikov, 1996, 1997, 2000; Desojo et al., 2002; Ezcurra et al., 2010, 2013, 2014; Ezcurra, 2014; Ezcurra and Butler, 2015a, b).

Charig and Reig (1970) recognized the suborder Proterosuchia as composed of two families: Proterosuchidae ("*Chasmatosaurus*"-like forms) and Erythrosuchidae (*Erythrosuchus*-like forms). These authors included *Archosaurus*, "*Chasmatosaurus*", *Chasmatosuchus*, "*Elaphrosuchus*", and *Proterosuchus* within the Proterosuchidae, and *Garjainia*, *Erythrosuchus*, "*Vjushkovia*", *Shansisuchus*, and possibly *Cuyosuchus* within the Erythrosuchidae. Accordingly, Charig and Reig (1970) considered Shansisuchidae, Garjainiidae and Vjushkoviidae as junior synonyms of Erythrosuchidae, and Chasmatosauridae as a junior synonym of Proterosuchidae. Charig and Reig (1970) considered the proterosuchids as a primitive stock of "thecodonts" from which erythrosuchids evolved. In particular, "*Elaphrosuchus*" was depicted as more closely related to erythrosuchids than were other proterosuchids (Charig and Reig, 1970: fig. 6). Subsequently, Bonaparte (1982) proposed a more inclusive suborder Proterosuchia, being composed of two distinct infraorders: Proterochampsia and Rauisuchia. Within Proterochampsia, Bonaparte (1982) included Proterosuchidae, Cerritosauridae and Proterochampsidae, whereas "Rauisuchia" was composed of Erythrosuchidae and Rauisuchidae. From the late 1970s to early 1990s, multiple Early and Middle Triassic archosauriforms were described from Australia,

Russia and China (Camp and Banks, 1978; Ochev, 1979, 1980; Thulborn, 1979; Cheng, 1980; Wu, 1981; Peng, 1991; Sennikov, 1992, 1994), and most were assigned to either Proterosuchidae or Erythrosuchidae following the "*Chasmatosaurus*"-like and *Erythrosuchus*-like dichotomy.

Benton (1985) reported the first cladistic analysis of basal diapsids, including early archosauriforms, although it still was a fully explicit approach. Benton (1985) placed *Proterosuchus fergusi* either within Prolacertiformes or as the sister taxon of his conception of Archosauria (which in Benton's usage was a non-crown-group clade including *Erythrosuchus*, *Euparkeria* and "later archosaurs"), with *Erythrosuchus africanus* recovered as sister to all other archosaurs. The first numerical cladistic analysis to include "proterosuchians" was that of Gauthier (1986), who employed Proterosuchidae to root the tree in which he found Erythrosuchidae as the sister taxon of Proterochampsidae + Archosauria. Gauthier (1986: 42) restricted the usage of the term Archosauria to the crown group, and Gauthier et al. (1988) erected the new group Archosauriformes for the clade including all the descendants of the most recent common ancestor of Proterosuchidae, Erythrosuchidae, Proterochampsidae and Archosauria. Several subsequent analyses recovered broadly similar topologies to that of Gauthier (1986), including those of Benton and Clark (1988), Sereno and Arcucci (1990), Sereno (1991), Parrish (1993), Gower (2002) and Benton (2004), but the paraphyly of "Proterosuchia" in these studies was the outcome of choices (implicit or explicit) in rooting and not a result of the analyses (other than that erythrosuchids lie outside of non-proterosuchid, non-erythrosuchid archosauriforms when trees are rooted with proterosuchids). Juul (1994) and Bennett (1996) were the first authors to include both Proterosuchidae and Erythrosuchidae as part of the ingroup in numerical analyses, and, as a consequence, to test the phylogenetic position of proterosuchids

among archosauromorphs. The analyses of Juul (1994) and Bennett (1996) recovered proterosuchids and erythrosuchids as successive outgroups of all other archosauriforms, though proterosuchids and erythrosuchids were each represented either as a suprageneric taxon or by a single species, such that the monophyly of Proterosuchidae and of Erythrosuchidae were not tested. Parrish (1992) reported an analysis that included six proterosuchian species and an aggregate "other archosauriforms" in the ingroup and *Proterosuchus* as an outgroup. Within his monophyletic Erythrosuchidae, *Shansisuchus shansisuchus*, *Erythrosuchus africanus*, *Garjainia prima* and *Fugusuchus hejiapensis* were successive outgroups of a monophyletic "*Vjushkovia*", comprising "*Vjushkovia*" *triplicostata* (= *Garjainia triplicostata*) and "*Vjushkovia*" *sinensis* (= *Youngosuchus sinensis*) (Fig. 5.1A).

Gower and Sennikov (1996) reported a cladistic analysis based only on braincase characters, in which proterosuchians were recovered as monophyletic. Among proterosuchians, distinct proterosuchid and erythrosuchid clades were recognized, with *Fugusuchus hejiapensis* as well as *Proterosuchus fergusi* found as members of Proterosuchidae (contra Parrish, 1992). *Xilousuchus sapingensis*, "*Vjushkovia*" *triplicostata*, *Erythrosuchus africanus*, and *Shansisuchus shansisuchus* were recovered as members of Erythrosuchidae (Gower and Sennikov, 1996). Within Erythrosuchidae, Gower and Sennikov (1996) found sister taxon relationships for *Xilousuchus sapingensis* and "*Vjushkovia*" *triplicostata*, and for *Erythrosuchus africanus* and *Shansisuchus shansisuchus*. Gower and Sennikov (1997) added non-braincase characters and included a different taxon sampling and recovered a paraphyletic "Proterosuchia", with erythrosuchids more closely related to Archosauria than to proterosuchids (Fig. 5.1B). *Proterosuchus fergusi* was found as sister taxon to

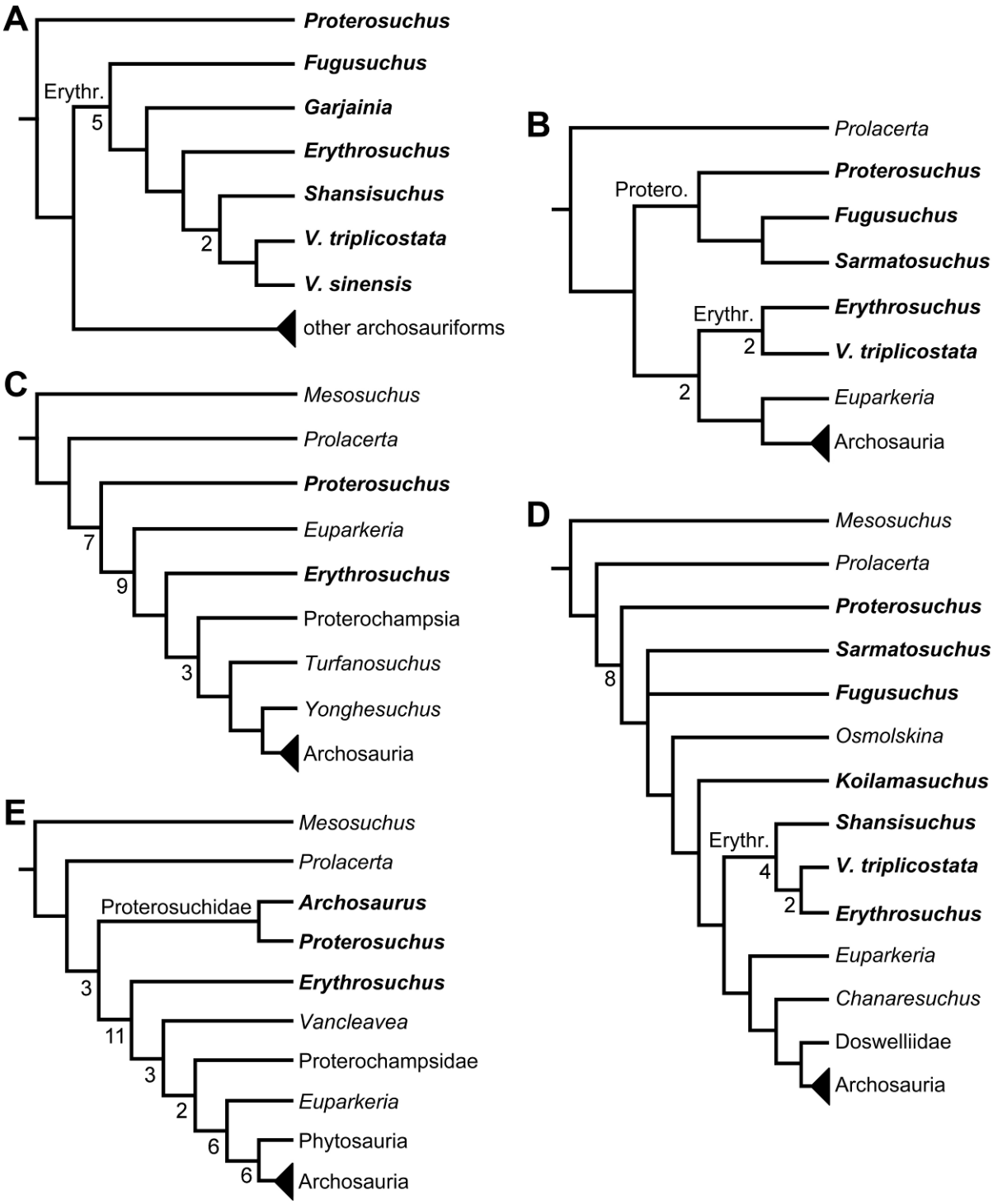

Figure 5.1. Phylogenetic trees depicting selected previous hypotheses of relationships for 'Proterosuchia'. (A) Single most parsimonious tree of Parrish (1992); (B) strict reduced consensus tree of Gower and Sennikov (1997); (C) single most parsimonious tree of Dilkes and Sues (2009); (D) strict consensus tree of Ezcurra et al. (2010); and (E) strict consensus tree of Nesbitt (2011). Bremer support (= Decay Index) values greater than one are indicated below each node (support values for the trees of Parrish 1992 and Gower and Sennikov 1997 were calculated using the original data matrices). Abbreviations: Erythr., Erythrosuchidae; Protero., Proterosuchidae. Bold font indicates putative proterosuchians.

the other putative proterosuchids *Fugusuchus hejiapensis* and *Sarmatosuchus otschevi*. Additionally, in contrast to the earlier study of Gower and Sennikov (1996), *Xilousuchus sapingensis* was recovered as an erythrosuchid in only some of their most parsimonious trees (Gower and Sennikov, 1997). Gower and Sennikov (2000) conducted a review of the Permo–Triassic archosauriforms from Russia and concluded that "*Vjushkovia*" was a junior synonym of *Garjainia*, in agreement with previous comments by Kalandadze and Sennikov (1985), Ochev and Shishkin (1988) and Sennikov (1995a, b), and that *Garjainia triplicostata* was probably also a junior synonym of *Garjainia prima*.

Recent work by Dilkes and Sues (2009) found results that differ from most previous phylogenetic analyses. Although *Proterosuchus fergusi* was recovered as the sister taxon of all other archosauriforms, *Euparkeria capensis* was found as the sister taxon of *Erythrosuchus africanus* and more crownward archosauriforms (Fig. 5.1C). Thus, Dilkes and Sues (2009) recovered a polyphyletic (rather than the more usual paraphyletic) "Proterosuchia". Subsequent revision of this dataset by Dilkes and Arcucci (2012) recovered a paraphyletic "Proterosuchia". Ezcurra et al. (2010) described the new early archosauriform *Koilamasuchus gonzalezdiazi* and expanded the taxonomic and character sample of the data matrix of Dilkes and Sues (2009), including characters employed in several previous archosauriform phylogenetic analyses (e.g. Dilkes, 1998; Gower and Sennikov, 1997). Among taxa sampled by Ezcurra et al. (2010), the taxonomic content of Proterosuchidae hypothesized by previous authors (e.g. *Proterosuchus*, *Sarmatosuchus* and *Fugusuchus*: Gower and Sennikov, 1997) was recovered as paraphyletic (or even polyphyletic because the specimen that it is now the holotype of *Koilamasuchus gonzalezdiazi* was interpreted originally as a proterosuchid: Bonaparte 1981), and the previously hypothesized

content of Erythrosuchidae (*Erythrosuchus africanus*, *Shansisuchus shansisuchus*, *Garjainia triplicostata*) was recovered as monophyletic (Fig. 5.1D). Ezcurra et al. (2010) recovered *Proterosuchus fergusi* as sister taxon to all other sampled archosauriforms, with *Sarmatosuchus otschevi* and *Fugusuchus hejiapensis* (considered as proterosuchids by Gower and Sennikov, 1996, 1997, 2000) being more closely related to other archosauriforms than to *Proterosuchus fergusi*. Ezcurra et al. (2010) also recovered *Koilamasuchus gonzalezdiazi* and the proposed euparkeriid *Osmolskina czatkowicensis* (Borsuk-Białynicka and Evans, 2003) as successive outgroups of Erythrosuchidae and more crownward archosauriforms. Erythrosuchidae was recovered as the sister-group of *Euparkeria capensis* and more crownward archosauriforms, in contrast to the results of Dilkes and Sues (2009) but in agreement with most other quantitative phylogenetic analyses of Archosauriformes (e.g. Juul, 1994; Bennett, 1996; Gower and Sennikov, 1997; Nesbitt et al., 2009; Nesbitt, 2011). Within Erythrosuchidae, Ezcurra et al. (2010) recovered *Shansisuchus shansisuchus* as the sister taxon of *Erythrosuchus africanus* + "*Vjushkovia*" (= *Garjainia*) *triplicostata*, contrasting with the internal relationships of Erythrosuchidae found by Gower and Sennikov (1996). Desojo et al. (2011) obtained broadly similar results to those of Ezcurra et al. (2010) using a similar data matrix.

Nesbitt (2011) recovered *Erythrosuchus africanus* and Proterosuchidae as successive outgroups of all non-proterosuchian archosauriforms, resembling most previous numerical analyses. Nesbitt (2011: 249) was the first to include the oldest known archosauriform, *Archosaurus rossicus*, in a numerical phylogenetic analysis and found it to be the sister taxon of *Proterosuchus fergusi* within a monophyletic Proterosuchidae (Fig. 5.1E). Nesbitt (2011) and Nesbitt et al. (2011) reinterpreted the Chinese taxon *Xilousuchus sapingensis*, once considered a member of

"Proterosuchia" (see above), as a poposauroid archosaur, a hypothesis followed by recent authors (e.g. Butler et al., 2011). Ezcurra et al. (2014) revised the Permian saurian record (see Chapter 2) and conducted a phylogenetic analysis including several basal archosauromorphs. These authors found *Proterosuchus fergusi* and *Archosaurus rossicus* within a monophyletic Proterosuchidae, in agreement with Nesbitt (2011). The enigmatic Permian diapsid *Eorasaurus olsoni* was recovered in a polytomy together with *Erythrosuchus africanus* and *Euparkeria capensis*, thus potentially representing the oldest known archosauriform (Ezcurra et al., 2014).

In summary, the systematic history of proterosuchians was turbulent through most of the 20th century, but the advent of numerical phylogenetic techniques gave rise to near-unanimous consensus regarding the non-monophyly of "Proterosuchia" (but see Gower and Sennikov 1996), with erythrosuchids being more closely related to Archosauria than to proterosuchids. However, this stability may be superficial because few proterosuchian species have been included in numerical phylogenetic analyses. Furthermore, the taxonomic contents and internal relationships of Proterosuchidae and Erythrosuchidae have not yet been tested thoroughly. It is important to note that quantitative support for many of the previously recovered relationships among putative proterosuchids and erythrosuchids is low in terms of decay indices, and that topology-based statistical tests of the (non)monophyly of Proterosuchidae, Erythrosuchidae and Proterosuchia have not been carried out.

5.3. Materials and Methods

5.3.1. *Objectives and taxonomic sample*

The aim of the present phylogenetic analysis is to generate a comprehensive higher-level phylogenetic hypothesis of basal archosauromorphs and shed light on the species-level interrelationships of taxa historically identified as proterosuchian archosauriforms (i.e. taxa usually considered as members either of Proterosuchidae or Erythrosuchidae; Charig and Reig, 1970; Charig and Sues, 1976; Ezcurra et al., 2013). As a result, the taxonomic sample is mainly focused on non-archosaurian archosauromorphs and, more specifically, on proterosuchians, which range stratigraphically from the Lopingian to the Upper Triassic. Six non-archosauromorph diapsids were included as outgroups: the early diapsid *Petrolacosaurus kansensis*, the basal neodiapsids *Youngina capensis* and *Acerosodontosaurus piveteaui*, and the early lepidosauromorphs *Paliguana whitei*, *Planocephalosaurus robinsonae* and *Gephyrosaurus bridensis*. All of these taxa have been consistently recovered outside Archosauromorpha in recent phylogenetic analyses (Müller, 2004; Bickelmann et al., 2009; Reisz et al., 2011; Ezcurra et al., 2014) and as a whole provide an exhaustive sample of early diapsid character states. The Carboniferous *Petrolacosaurus kansensis* has been repeatedly found to be more distantly related to archosauromorphs than are *Youngina capensis*, *Acerosodontosaurus piveteaui* and lepidosauromorphs (Müller, 2004; Senter, 2004; Bickelmann et al., 2009; Reisz et al., 2011; Ezcurra et al., 2014) and therefore was chosen here to root the phylogenetic trees.

The taxonomic sample of non-archosauriform archosauromorphs is chosen in order to test the higher-level phylogenetic relationships between relatively well-established groups (e.g. Rhynchosauria, Tanystropheidae) and several species with

problematic affinities, such as several taxa usually assigned to the likely non-monophyletic “Prolacertiformes”. A total of 19 taxa previously identified as non-archosauriform archosauromorphs are included, including three tanystropheids (*Macrocnemus bassani*, *Amotosaurus rotfeldensis*, *Tanystropheus longobardicus*), six rhynchosaurs (*Noteosuchus colletti*, *Mesosuchus browni*, *Howesia browni*, *Eohyosaurus wolvaardti*, *Rhynchosaurus articeps*, *Bentonyx sidensis*), eight taxa identified previously as protorosaurs/prolacertiforms (*Aenigmastropheus parringtoni*, *Protorosaurus speneri*, *Prolacertoides jimusarensis*, *Boreopricea funerea*, *Jesairosaurus lehmani*, *Prolacerta broomi*, *Kadimakara australiensis*, *Eorasaurus olsoni*), and the enigmatic but well-known *Trilophosaurus buettneri* and *Azendohsaurus madagaskarensis*. Non-proterosuchian archosauriforms are represented by 38 taxa, including four doswelliids (*Archeopelta arborensis*, *Tarjadia ruthae*, *Jaxtasuchus salomoni*, *Doswellia kaltenbachi*), all known proterochampsid species (see Trotteyn et al., 2013), three basal phytosaurs (*Paleorhinus* spp., *Nicrosaurus kapffi*, *Smilosuchus* spp.), seven basal ornithodirans (*Dimorphodon macronyx*, *Lagerpeton chanarensis*, *Marasuchus lilloensis*, *Lewisuchus admixtus*, *Silesaurus opolensis*, *Heterodontosaurus tucki*, *Herrerasaurus ischigualastensis*), two ornithosuchids (*Ornithosuchus longidens*, *Riojasuchus tenuisceps*), six basal suchians (*Aetosauroides scagliai*, *Gracilisuchus stipanicicorum*, *Turfanosuchus dabanensis*, *Prestosuchus chiniquensis*, *Batrachotomus kupferzellensis*, *Nundasuchus songeaensis*), and five archosauriforms that seem not to fit into any of the aforementioned clades (*Euparkeria capensis*, *Asperoris mnyama*, *Dorosuchus neoetus*, *Dongosuchus efremovi*, *Vancleavea campi*). The phytosaurs *Paleorhinus* spp. and *Smilosuchus* spp. are scored as supraspecific terminals because of the taxonomy

of both taxa is currently problematic, although both appear to represent monophyletic genera (Stocker and Butler, 2013).

The proterosuchian sample is intended to be the most comprehensive of the data set, representing a total of 24 terminals that sample all currently valid nominal species (Ezcurra et al., 2013). The holotype of *Proterosuchus fergusi* (SAM-PK-591) was considered as undiagnostic by Ezcurra and Butler (2015a, see Chapter 3) and, as a result, this specimen is included as an independent terminal in order to test this hypothesis. It is noteworthy that multiple proterosuchian species are included here for the first time in a quantitative phylogenetic analysis, namely "*Blomosuchus georgii*", *Vonhuenia friedrichi*, "*Ankistrodon indicus*", *Proterosuchus alexanderi*, *Proterosuchus goweri*, "*Chasmatosaurus*" *yuani*, *Kalisuchus rewanensis*, *Chasmatosuchus rossicus*, "*Gamosaurus lozovskii*", *Uralosaurus magnus*, *Shansisuchus kuyeheensis*, *Cuyosuchus huenei*, *Guchengosuchus shiguaiensis*, *Chalishevia cothurnata* and *Garjainia madiba*. Also included are an unnamed taxon represented by isolated dorsal vertebrae from the Early Triassic of southeastern Australia (Kear, 2009), a partial skeleton of a small erythrosuchid from the *Cynognathus* AZ of South Africa that was previously considered as possibly referable to *Erythrosuchus africanus* (Gower, 2003), and the probable pseudosuchian "*Dongusia colorata*" (Gower and Sennikov, 2000). "*Dongusia colorata*" is currently considered a nomen dubium (Young, 1964; Gower and Sennikov, 2000; Ezcurra et al., 2013), but it is included in this data matrix because it was originally considered an erythrosuchid. "*Crenelosaurus nigrosilvanus*", "*Exilisuchus tubercularis*", "*Ocolurtaia arquata*", "*Seemannia palaeotriadica*", and "*Shansisuchus heiyuekouensis*" represent five poorly informative proterosuchian species considered as nomina dubia (Gower and Sennikov, 2000; Ezcurra et al., 2010) and, as a result,

are not included in the analysis. An indeterminate species of "*Chasmatosaurus*" from the earliest Triassic of India (Satsangi, 1964) is also based on very fragmentary bones and is not also included. *Youngosuchus sinensis* (= "*Vjushkovia*" *sinensis*) was originally considered an erythrosuchid (Young, 1973a), but subsequently reassigned to a rauisuchian archosaur (Kalandadze and Sennikov, 1985). The first hand study of the only known specimen of *Youngosuchus sinensis* (IVPP V3239) supports the latter interpretation, but this species was not included in this analysis because of ongoing work to further prepare and restudy the specimen by J. Liu and C. Sullivan. Finally, the assignment of referred specimens to some species is problematic and one species is found here to be a subjective synonym of another ("*Gamosaurus lozovskii*" = *Chasmatosuchus magnus*, see below). As a result, the holotype and entire hypodigm (i.e. type specimens + referred specimens) of these species are scored separately as independent terminals, and the synonymous species are scored as either different terminals or as a single terminal following the hypothesis of synonymy, respectively. These alternative scorings allow the assignment of referred specimens of these species and the hypothesis of synonymy to be tested. The resultant taxonomic list of the data matrix is composed of 91 independent taxa, plus the holotype of *Proterosuchus fergusi*, three hypodigms that partially overlap the scorings present in their respective holotypes (*Kadimakara australiensis*, *Garjainia madiba* and *Uralosaurus magnus*) and one species that is probably a junior synonym of another and their combination ("*Gamosaurus lozovskii*" and "*Gamosaurus lozovskii*" + *Chasmatosuchus magnus*, respectively) (i.e. 97 operational taxonomic units).

The vast majority of species included in the archosauromorph taxonomic sample are Triassic in age, with the exception of four Lopingian (*Aenigmastropheus*

parringtoni, *Archosaurus rossicus*, *Eorasaurus olsoni* and *Protorosaurus speneri*) and two Early Jurassic (*Dimorphodon macronyx* and *Heterodontosaurus tucki*) species.

5.3.2. *Taxa with problematic hypodigms*

The assignment of the referred specimens of some of the species (*Kadimakara australiensis*, *Garjainia madiba* and *Uralosaurus magnus*) included in the current taxonomic sample is problematic. As a result, the holotype and the complete hypodigm (i.e. type and referred specimens) of these species were scored as independent terminals. The aim of these independent scorings is to test the effect that the referred material of the hypodigm has on the phylogenetic relationships of the species.

***Kadimakara australiensis*.** The holotype of *Kadimakara australiensis* is based on the postorbital region of a skull (QMF 6710) (Fig. 5.2A, B). A partial snout (QMF 6676) from the same locality was referred to the species (Fig. 5.2C, D), but with no clear association (Bartholomai, 1979). There are no overlapping bones between the specimens, and, as a result, their assignment to the same species is ambiguous. Nevertheless, the morphologies of both specimens are consistent with that of an animal similar to the non-archosauriform archosauromorph *Prolacerta broomi*. As such, the referral of QMF 6676 to *Kadimakara australiensis* can be considered a working hypothesis until there is more complete information that would allow it to be supported or rejected.

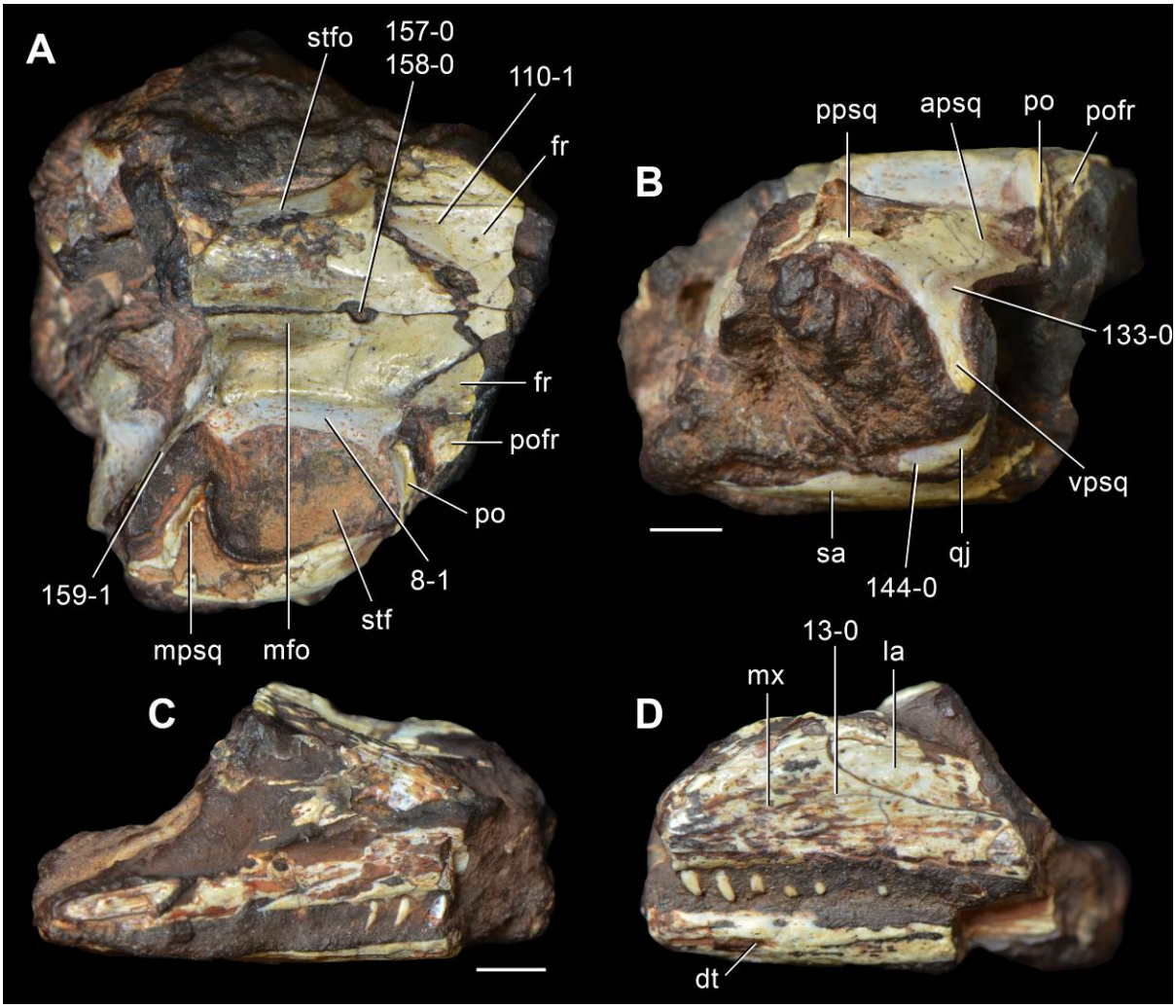

Figure 5.2. Holotype postorbital region of skull (QMF 6710) (A, B) and referred snout (QMF 6676) (C, D) of *Kadimakara australiensis* in dorsal (A), right lateral (B, C) and left lateral (D) views. Abbreviations: apsq, anterior process of the squamosal; dt, dentary; fr, frontal; la, lacrimal; mfo, median fossa; mpsq, medial process of the squamosal; mx, maxilla; po, postorbital; pofr, postfrontal; ppsq, posterior process of the squamosal; qj, quadratojugal; sa, surangular; stf, supratemporal fenestra; stfo, supratemporal fossa; vpsq, ventral process of the squamosal. Numbers refer to character states. Scale bars equal 2 mm.

***Garjainia madiba*.** Gower et al. (2014) recently described the new species *Garjainia madiba* from the upper Olenekian of South Africa. The holotype of the species (BP/1/5760) is based on cranial bones that probably belong to a single individual, and approximately 80 specimens were considered as paratypes and 16 as referred material (Gower et al., 2014). Most of the paratype and referred specimens of *Garjainia madiba* do not preserve overlapping features that can be compared with the holotype and, as a result, their assignment should be taken with caution. Nevertheless, all the bones referred to this species possess morphologies consistent with that of an animal very similar to *Garjainia prima* (Gower et al., 2014). As was the case for *Kadimakara australiensis*, the assignment of paratype and referred specimens to *Garjainia madiba* is taken here as a working hypothesis that will be tested in this phylogenetic analysis and by future discoveries of more complete, articulated specimens of the species.

***Uralosaurus magnus*.** Ochev (1980) erected the new species *Erythrosuchus magnus* from the Anisian of Russia based on a left pterygoid (PIN 2973/70). Ochev (1980) also referred to this species a right dentary (PIN 2973/71) and some isolated teeth from the type locality (PIN 2973/72−79), and tentatively referred some presacral vertebrae from other localities (Ochev, 1980; Gower and Sennikov, 2000). Subsequently, Sennikov (1995b) erected the new genus *Uralosaurus* and assigned *Erythrosuchus magnus* to it, resulting in the new combination *Uralosaurus magnus*. Sennikov (1995b) also referred to *Uralosaurus magnus* some cranial remains and caudal vertebrae from different localities to that of the holotype. All these elements possess an erythrosuchid-like morphology (Gower and Sennikov, 2000), but there are other species in the same stratigraphic horizon that may possess a similar morphology (e.g. *Dongusuchus efremovi*). Therefore, only the pterygoid, dentary and teeth from

the same locality are considered here as the hypodigm of *Uralosaurus magnus*. This hypothesis will be tested in the phylogenetic analysis and by subsequent discoveries of associated *Uralosaurus magnus* bones from the Donguz Gorizont. The overall morphologies of the bones and teeth of *Uralosaurus magnus* (PIN 2973/70−79) are very similar to those of other erythrosuchids (e.g. *Erythrosuchus africanus*) and it is difficult to find characters that may support the recognition of *Uralosaurus magnus* as a distinct taxon. There is a pair of blind and relatively shallow fossae placed immediately posterior to the final tooth socket along the alveolar margin of the referred dentary of *Uralosuchus magnus* (PIN 2973/71). These fossae are too shallow to have housed teeth and are not present in any other archosauriform of which I am aware. This condition may be related with the lower tooth count (eight alveoli) of PIN 2973/71 in comparison to the dentaries of other erythrosuchids (14−16 tooth positions in *Shansisuchus shansisuchus*: Young, 1964; 13−14 in *Garjainia prima*: PIN 2394/5-8, 5-9, 951/30; 14 in *Garjainia madiba*: NMQR 3051; ≥12 in *Erythrosuchus africanus*: BP/1/3893). It is not possible to determine here if these fossae are pathologic, but they may support the distinction of *Uralosaurus magnus* from other erythrosuchid species.

5.3.3. *Synonymous species and modified hypodigms*

The first hand study of some proterosuchian species as part of this research resulted in modifications to their taxonomy and hypodigms. The changes that have a direct impact on this phylogenetic analysis are discussed as follows.

***Archosaurus rossicus*.** As was discussed in Chapter 2, the specimens previously referred to *Archosaurus rossicus* cannot be unambiguously assigned to this species

(Ezcurra et al., 2014). As a result, the scorings of *Archosaurus rossicus* were limited to its holotype, in agreement with the decision taken in the phylogenetic analysis conducted by Nesbitt (2011).

"Blomosuchus georgii" and Vonhuenia friedrichi. Two supposed proterosuchid species have been named from the same locality (Spasskoe I) of the Early Triassic Vokhmian Gorizont of Russia: "*Blomosuchus georgii*" and *Vonhuenia friedrichi* (Sennikov 1992). The holotype of "*Blomosuchus georgii*" consists of an isolated partial parabasisphenoid that lacks most of the cultriform process and part of the intertuberal plate and the dorsolateral surface of the bone (PIN 1025/348) (Fig. 5.3A). Subsequently, Sennikov (1995b) referred to "*Blomosuchus georgii*" some isolated postcranial bones from the same locality. The holotype of *Vonhuenia friedrichi* is an isolated posterior cervical vertebra (PIN 1025/11) (Fig. 5.3D−F). An isolated parabasisphenoid, some vertebrae and other fragmentary postcranial bones collected in the type locality were referred to *Vonhuenia friedrichi* (Sennikov 1992, 1995b).

The isolated partial parabasisphenoid (PIN 1025/14) referred to *Vonhuenia friedrichi* (Fig. 5.3B) was distinguished from the holotype of "*Blomosuchus georgii*" (PIN 1025/348) because of the presence of a proportionally longer parabasisphenoid body and differences in the shape of the basipterygoid processes (Sennikov, pers. comm. 2013). However, the breakage of the median region of the intertuberal plate gives the artificial appearance that the body of the parabasisphenoid is anteroposteriorly shorter along the median line in the holotype of "*Blomosuchus georgii*" than it is in PIN 1025/14. The right basipterygoid process of PIN 1025/14 is completely missing and only the base of the left process is preserved, with the latter having a strongly weathered surface. The position of the base of the basipterygoid

process is identical in the holotype of "*Blomosuchus georgii*" and PIN 1025/14, and the orientation and shape of the distal articular surface of the basipterygoid process cannot be determined in PIN 1025/14. Accordingly, no substantial difference is recognised here between the holotype of "*Blomosuchus georgii*" and PIN 1025/14. As a result, both specimens probably belong to the same species. The morphologies of both parabasisphenoids are almost identical and cannot be distinguished from those of *Proterosuchus fergusi* (BP/1/3993), *Proterosuchus alexanderi* (NMQR 1484; Fig. 5.3C), *Proterosuchus goweri* (NMQR 880) and *Fugusuchus hejiapanensis* (Gower and Sennikov, 1996). Therefore, "*Blomosuchus georgii*" is considered here a nomen dubium. Nevertheless, this species is included in the phylogenetic analysis in order to test the presence of proterosuchids in the Lower Triassic beds of Russia. The lack of anatomical overlap between the postcranial bones previously referred to "*Blomosuchus georgii*" and the parabasisphenoids combined with the presence of another nominal species of supposed proterosuchid (*Vonhuenia friedrichi*) at the same locality and horizon suggests that caution is warranted in the taxonomic assignment of these specimens. As a result, the scorings of "*Blomosuchus georgii*" are restricted here to the holotype (PIN 1025/348) and the parabasisphenoid PIN 1025/14 (previously referred to *Vonhuenia friedrichi*).

Similarly, there is no direct overlap between the isolated cervico-dorsal vertebra that represents the holotype of *Vonhuenia friedrichi* (PIN 1025/11) and the specimens referred to this taxon, with the probable exception of a single vertebra that also possesses a third rib articular facet (PIN 1025/419) (Fig. 5.3G–I). This condition is not present among all the referred vertebral specimens, which have only two articular facets for the ribs. This suggests that the other referred vertebrae are from different positions in the vertebral column than the holotype and PIN 1025/419. The

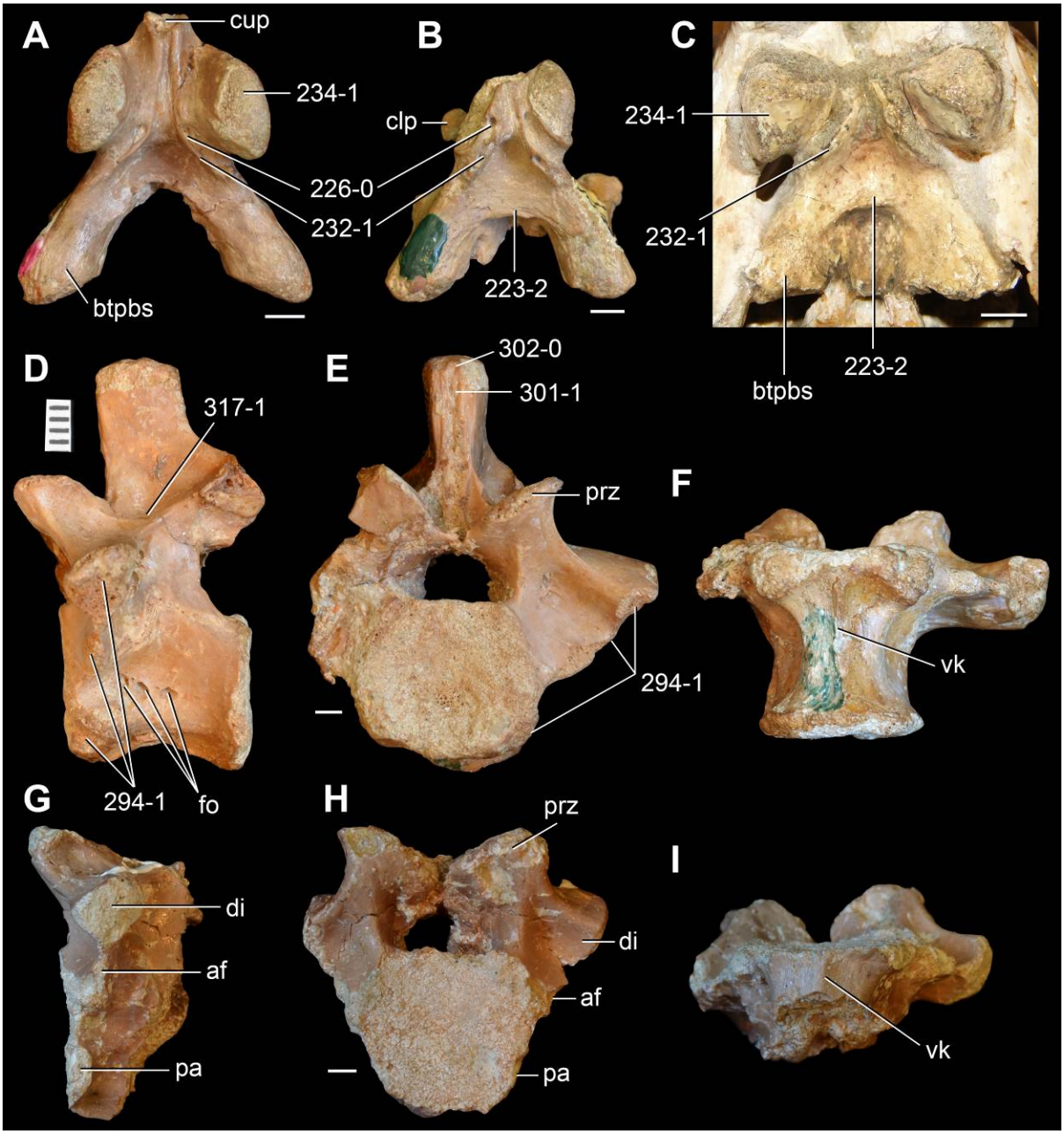

Figure 5.3. Holotype (PIN 1025/348) (A) and referred (PIN 1025/14) (B) parabasisphenoids of "*Blomosuchus georgii*", parabasisphenoid of *Proterosuchus alexanderi* (NMQR 1484) (C), and holotype (PIN 1025/11) (D−F) and referred (PIN 1025/419, reversed) (G−I) cervico-dorsal vertebrae of *Vonhuenia friedrichi* in ventral (A−C, F, I), left lateral (D), anterior (E, H) and right lateral (G) views. Abbreviations: af, accessory facet; btpbs, basal tubera of the parabasisphenoid; clp, clinoid process; cup, cultriform process; di, diapophysis; pa, parapophysis; prz, prezygapophysis; vk, ventral keel. Numbers refer to character states. Scale bars equal 2 mm in A, B, D−I and 4 mm in C.

latter specimen shares with the holotype (PIN 1025/11) the presence of prezygodiapophyseal and postzygodiapophyseal laminae, as well as a median longitudinal keel on the ventral surface of the centrum (Fig. 5.3: vk). This combination of features is not present in the cervico-dorsal vertebrae of other basal archosauromorphs and thus is diagnostic for *Vonhuenia friedrichi*. The other previously referred vertebrae do not possess this combination of features, although it may be because they are from a different region of the vertebral column than PIN 1025/11 and PIN 1025/419. As a result, the hypodigm of *Vonhuenia friedrichi* is restricted here to the holotype (PIN 1025/11) and a referred cervico-dorsal vertebra (PIN 1025/419).

Chasmatosuchus magnus* (= "*Jaikosuchus magnus*") *and "Gamosaurus lozovskii". Two supposed proterosuchids have been described from the upper Olenekian Yarenskian Gorizont of Russia: "*Gamosaurus lozovskii*" and *Chasmatosuchus magnus* (Ochev, 1979). The holotype of "*Gamosaurus lozovskii*" is an isolated partial anterior cervical vertebra (PIN 3361/13) (Ochev, 1979) (Fig. 5.4C, D), and Sennikov (1995b) referred to this species a middle (PIN 3361/213) and a posterior (PIN 3361/214) cervical vertebrae. The holotype of *Chasmatosuchus magnus* is an isolated anterior cervical vertebra (PIN 951/65), and Ochev (1979) referred to this species some vertebrae from the type horizon and the underlying Ustmylian Gorizont, as well as a fibula from the type locality and horizon. Subsequently, Sennikov (1990) erected the new genus "*Jaikosuchus*" for the species, resulting in the new combination "*Jaikosuchus*" *magnus.* He also restricted the referred material of this species to a single neural arch. "*Gamosaurus lozovskii*" is considered here a subjective junior synonym of *Chasmatosuchus* ("*Jaikosuchus*") *magnus* because the anterior cervical

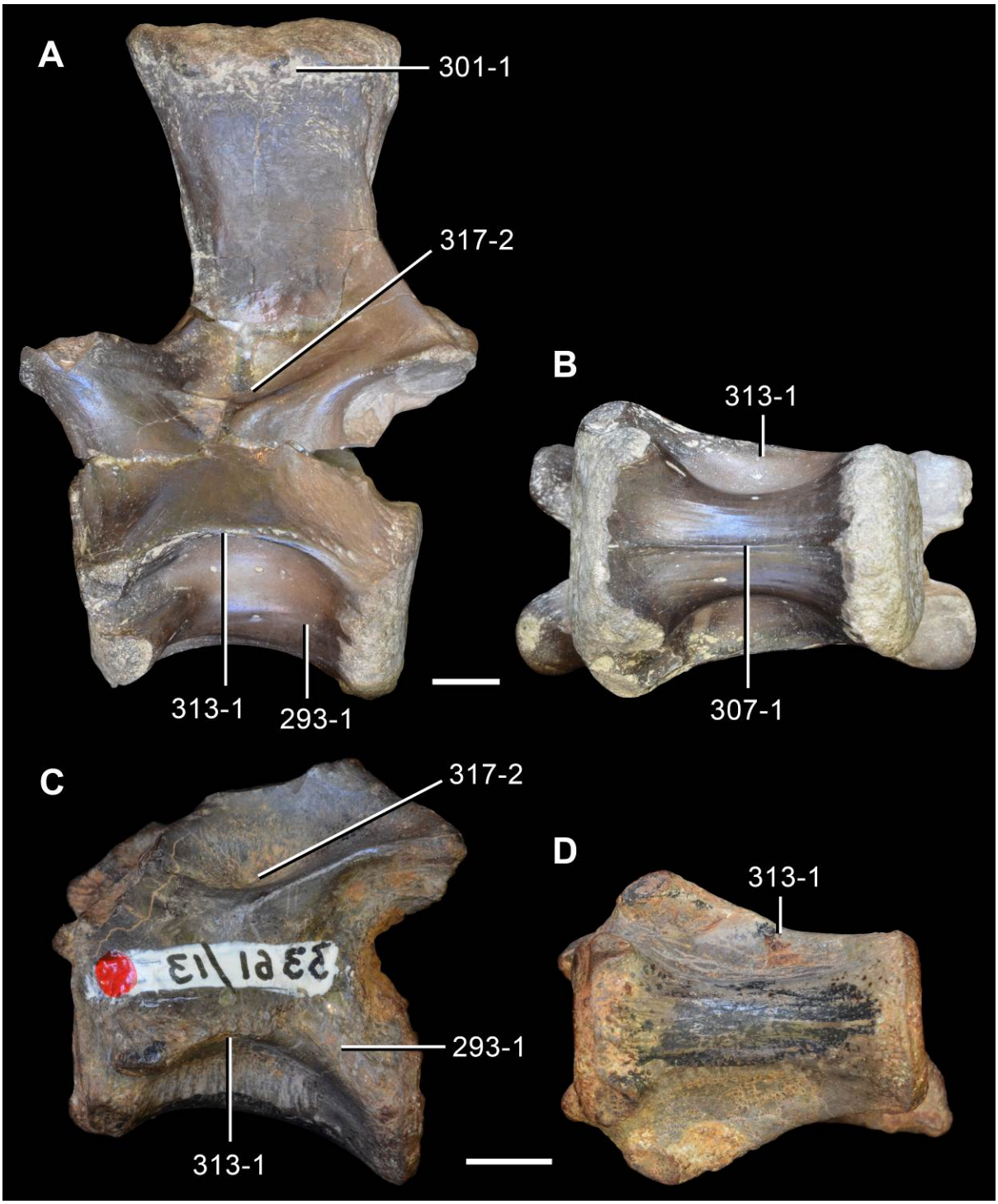

Figure 5.4. *Chasmatosuchus rossicus* referred middle cervical vertebra (PIN 3200/217) (A, B) and *Chasmatosuchus magnus* referred anterior cervical vertebra (PIN 3361/13, holotype of "*Gamosaurus lozovskii*", reversed) (C, D) in left lateral (A, C) and ventral (B, D) views. Numbers refer to character states. Scale bars equal 5 mm.

vertebrae of the former species are identical in morphology to the holotype of *Chasmatosuchus magnus* and they share the presence of a strongly developed tuberosity on the lateral surface of the centrum that extends posteriorly from the base of the diapophysis. This feature is not present in other basal archosauromorphs. In order to test this hypothesis of synonymy both species were scored as independent terminals in a first phylogenetic analysis and then merged together as a combined *Chasmatosuchus magnus* in a second phylogenetic analysis (see below).

Dorosuchus neoetus. The hypodigm of *Dorosuchus neoetus* is composed by the holotype right ilium, femur and tibia (PIN 1579/61, 67), which were found in articulation and thus represent a single individual, and several paratype specimens (PIN 1579/62−66, 68) that were collected from the same block as the holotype (Sennikov, 1989a, b; Sookias et al., 2014). In addition, an isolated partial left ilium (PIN 952/200) is also considered part of the paratype because is very similar in morphology to that of PIN 1579/66 (Sookias et al., 2014). Sookias et al. (2014) tentatively accepted the referal of a partial left pterygoid (PIN 1579/69) and a hemimandible (1579/70) to *Dorosuchus neoetus* by Sennikov (1995b, 2008), but they tested the effect that the inclusion of these two specimens may have on the phylogenetic relationships of the animal by conducting six alternative phylogenetic analyses. These two referred specimens were found in a different block from that of the type series (Sookias et al., 2014) and the presence of other basal archosauriforms that could possess a morphologically similar pterygoid and hemimandible in the same horizon as *Dorosuchus neoetus* (i.e. *Dongusuchus efremovi*, "*Dongusia colorata*") means that this referral should be treated with caution. As a result, I decided here not

to include the referred specimens of *Dorosuchus neoetus* when scorings this taxon; instead, *Dorosuchus neoetus* is scored based on the type series only.

***Dongusuchus efremovi*.** Sennikov (1988a) erected the new genus and species *Dongusuchus efremovi* based on an isolated complete left femur (PIN 952/15-1). Several additional postcranial bones have been subsequently referred to this species (Sennikov, 1988a, b, 1990, 1995). Recently, Niedźwiedzki et al. (2014) considered only four femora as demonstrably referred specimens (PIN 952/15-2−5), and the other previously referred specimens that cannot be compared directly with the holotype because they lack overlapping features were considered as equivocally referred specimens. Niedźwiedzki et al. (2014) conducted alternative phylogenetic analyses testing the effect that the inclusion of the equivocally referred specimens has on the phylogenetic position of the species. The results of these analyses showed that these equivocally referred specimens do not affect the position of *Dongusuchus efremovi* (Niedźwiedzki et al., 2014). In the present phylogenetic analysis the scorings for this species were based only upon the holotype and demonstrably referred specimens. As for *Dorosuchus neoetus*, the presence of other basal archosauriforms in the same horizon as *Dongusuchus efremovi* (e.g. *Dorosuchus neoetus*, "*Dongusia colorata*") means that caution is required in the referal of bones that do not overlap in morphology with the holotype (e.g. cervical vertebrae, forelimb elements).

***Kalisuchus rewanensis*.** The holotype of the supposed proterosuchid *Kalisuchus rewanensis* (Early Triassic, Australia) is an isolated left maxilla (QMF 8998), and multiple cranial and postcranial bones have been referred to the species (Thulborn, 1979). The referred specimens of *Kalisuchus rewanensis* that were available for study

at first hand (most of the bones figured by Thulborn [1979] are not currently housed in the QMF collection and should be considered lost at present, pers. obs. August 2012) possess a morphology consistent with that of a non-archosaurian archosauriform, but they do not possess a combination of apomorphies congruent with those expected in only one archosauriform subclade. As a result, the scorings for *Kalisuchus rewanensis* were based upon its holotype only, in order to avoid the artefacts that a chimaeric taxon composed of multiple non-closely-related taxa could potentially cause in character optimizations and ultimately in the tree topologies.

5.3.4. *Character sampling* and *scorings*

The character sampling of the phylogenetic analysis was built by combining the character lists of previous phylogenetic analyses focused on non-archosaurian archosauromorphs and basal archosaurs (e.g. Parrish, 1992; Gower and Sennikov, 1996, 1997; Dilkes, 1998; Ezcurra et al., 2010, 2014; Nesbitt, 2011; Desojo et al., 2011; Dilkes and Arcucci, 2012; Trotteyn and Ezcurra, 2014; Ezcurra et al., 2015b) after evaluating the independence between characters (repeated or partially non-independent characters were combined with one another). In addition, 96 new characters were added. The complete character list includes 560 characters, including 291 cranial (52%) and 269 postcranial (48%) characters (Appendix 8). The following 85 characters represent nested sets of homologies and, as a result, were treated as additive (= ordered): 1, 2, 7, 9, 10, 17, 19, 20, 21, 28, 29, 36, 40, 41, 49, 53, 64, 69, 73, 74, 116, 121, 146, 148, 149, 163, 168, 169, 177, 191, 213, 249, 252, 263, 267, 285, 305, 307, 311, 317, 323, 329, 330, 332, 340, 343, 348, 352, 354, 362, 382, 386, 388, 394, 395, 401, 406, 415, 417, 422, 426, 428, 431, 439, 445, 449, 450, 454, 455, 476, 481, 494, 501, 509, 515, 519, 520, 530, 532, 534, 537, 543, 544, 545 and 548.

Table 5.1 (and subsequent pages). Sources of scoring for each operation taxonomic unit. The specimen numbers listed here correspond to specimens studied at first hand.

Taxon	**Sources of scorings**
Petrolacosaurus kansensis	Peabody (1952); Reisz (1977, 1981)
Acerosodontosaurus piveteaui	MNHN 1908-32-57; Currie (1980); Bickelmann et al. (2009)
Youngina capensis	BP/1/2459, 3859; GHG K 106, RS 160; NHMUK R5481; SAM-PK-K6205, K7578, K7710, K8565; TM 1490, 3603; Broom (1914, 1921, 1922); Gow (1975); Evans (1987); Smith and Evans (1996); Dilkes (1998); Gardner et al. (2010)
Paliguana whitei	AM 3585; Carroll (1975)
Planocephalosaurus robinsonae	Multiple NHMUK specimens; Fraser (1982); Fraser and Walkden (1984); Fraser and Shelton (1988)
Gephyrosaurus bridensis	Evans (1980, 1981); Fraser and Shelton (1988)
Aenigmastropheus parringtoni	UMZC T836; Parrington (1956); Ezcurra et al. (2014)
Protorosaurus speneri	BSPG 1995 I 5 (cast of WMSN P47361), 1997 I 12 (cast), 1997 I 13 (cast), AS VII 1207; NHMW 1943I4; USNM 442453 (cast of NMK S 180); SMNS 55387 (cast of Simon/Bartholomäus specimen), 59345 (cast); ZMR MB R2171, R2172, R2173 (casts of specimens destroyed probably during WWII); Gottmann-Quesada and Sander (2009)
Amotosaurus rotfeldensis	SMNS 50691, 50830, 54783, 54784a, 54784b, 54810, 90540, 90543, 90544, 90552, 90559, 90563, 90564, 90566, 90599, 90600, 90601, several unnumbered specimens; Fraser and Rieppel (2006)
Macrocnemus bassanii	PIMUZ T2472, T4355, T4822; BSPG 1973 I 86 (cast of Besano II); Peyer (1937); Rieppel (1989b)
Tanystropheus longobardicus	PIMUZ T2189, T2793, T2817, T2818, T3901; SMNS 54147, 54626, 54628, 54630, 54631, 54632, 54654, 55341, 56289, 59380, 84821, SMNS unnumbered specimen; Wild (1973); Nosotti (2007)
Jesairosaurus lehmani	ZAR 06−15; Jalil (1997)
Azendohsaurus madagaskarensis	FMNH PR 2751; UA 7-20-99-653, 8-7-98-284, 8-22-97-91, 8-27-98-273, 8-29-97-151, 8-29-97-152, 8-29-97-160, 10603, 10604, UA unnumbered specimens; S. Nesbitt unpublished data; Flynn et al. (2010)
Trilophosaurus buettneri	USNM mounted skeleton; Gregory (1945); Parks (1969); Spielmann et al. (2008)
Noteosuchus colletti	AM 3591; Carroll (1976)
Mesosuchus browni	SAM-PK-5861, 5882, 6046, 6536, 7416, 7838; Haughton (1921); Carroll (1976); Dilkes (1998)
Howesia browni	NHMUK R5872 (cast), SAM-PK-5884−5886; Broom (1906); Carroll (1976); Dilkes (1995)
Eohyosaurus wolvaardti	SAM-PK-K10159; Butler et al. (in press)
Rhynchosaurus articeps	BATGM M20a, b; NHMUK R1236−41; SHRCM G3851, G07537; SHYMS 1−7; Benton (1990)
Bentonyx sidensis	BSPG 3D print of BRSUG 21200; unpublished pictures; Hone and Benton (2008); Langer et al. (2010b)
Eorasaurus olsoni	PIN 156/108−110; Sennikov (1997); Ezcurra et al. (2014)

Prolacertoides jimusarensis	IVPP V3233; Young (1973b)
Prolacerta broomi	BP/1/471, 2675, 2676, 4504a, 5066, 5375; GHG 431; SAM-PK-K10018, K10797; UMCZ 2003.41R; Gow (1975); Modesto and Sues (2004)
Kadimakara australiensis holotype	QM F6710; Bartholomai (1979)
Kadimakara australiensis combined	QM F6676, F6710; Bartholomai (1979)
Boreopricea funerea	PIN 3708/1; Tatarinov (1978); Benton and Allen (1997)
Archosaurus rossicus	PIN 1100/55; Tatarinov (1960); Ezcurra et al. (2014)
Proterosuchus fergusi holotype	SAM-PK-591; Broom (1903); Welman (1998)
Proterosuchus fergusi	BP/1/3993, 4016, 4224; BSPG 1934 VIII 514; GHG 231, 363; RC 59, 846; SAM-PK-11208, K140, K10603; TM 201; Broom (1903, 1946); Haughton (1924); Broili and Schröder (1934); Cruickshank (1972, 1979); Welman (1998); Ezcurra and Butler (2015a, b)
Proterosuchus goweri	NMQR 880; Brink (1955); Ezcurra and Butler (2015a)
Proterosuchus alexanderi	NMQR 1484; Hoffman (1965); Sereno (1991); Welman (1998); Klembara and Welman (2009); Ezcurra and Butler (2015a)
"*Chasmatosaurus*" *yuani*	IVPP V2719, 4067, 36315 (field number V90002); Young (1936, 1963, 1978)
"*Chasmatosaurus ultimus*"	IVPP V2301; Young (1958); Liu et al. (in press)
"*Ankistrodon indicus*"	GSI 2259; Huxley (1865)
Tasmaniosaurus triassicus	UTGD 54655; Camp and Banks (1978); Thulborn (1986); Ezcurra (2014)
"*Blomosuchus georgii*"	PIN 1025/14, 348; Ochev (1978); Sennikov (1992)
Vonhuenia friedrichi	PIN 1025/11, 419; Sennikov (1992)
Chasmatosuchus rossicus	PIN 2252/381, 3200/212, 217, 472, 2243/167, 2252/384, 386; Huene (1940)
Chasmatosuchus magnus	PIN 951/65; Ochev (1979)
"*Gamosaurus lozovskii*"	PIN 3361/13, 14, 94, 183, 213, 214; Ochev (1979); Sennikov (1995b)
C. magnus + *G. lozovskii*	PIN 951/65, 3361/13, 14, 94, 183, 213, 214; Ochev (1979); Sennikov (1995b)
"*Chasmatosuchus*" *vjushkovi*	PIN 2394/4; Ochev (1961)
SAM P41754 Long Reef	SAM P41754; Kear (2009)
Koilamasuchus gonzalezdiazi	MACN-Pv 18119; Bonaparte (1981); Ezcurra et al. (2010)
Kalisuchus rewanensis	QM F8998; Thulborn (1979)
Fugusuchus hejiapanensis	Unpublished photographs; Cheng (1980); Parrish (1992); Gower and Sennikov (1996)
Sarmatosuchus otschevi	PIN 2865/68; Sennikov (1994); Gower and Sennikov (1997)
Guchengosuchus shiguaiensis	IVPP V8808; Peng (1991)
Cuyosuchus huenei	MCNAM PV 2669; Rusconi (1951); Desojo et al. (2002)
GHG 7433MI	GHG 7433MI
Garjainia prima	PIN 2394/5, 951/8, 15, 23, 25, 27−30, 32−34, 36, 41, 42, 46, 50, 51, 54, 55, 63; Ochev (1958); Huene (1960); Gower (1996); Gower and Sennikov (1996)
Garjainia madiba holotype	BP/1/5760; Gower et al. (2014)
Garjainia madiba combined	BP/1/5760; BP and NMQR specimens reported by Gower et al. (2014); Gower et al. (2014)
Erythrosuchus africanus	AMNH 5594−5597, 19352, 19353; BP/1/2094, 2096, 2529, 2734, 3893, 4526, 4539, 4553, 4645, 4649, 4680, 5207; GHG AK-82-22; MNHN 1869-12; NHMUK R525, R533i,

	R2790, R3301, R3592, R3762−R3764, unnumbered specimens; NMQR 1473; SAM-PK-905, 912, 913, 930, 978, 1315, 3028, 3612, 7684, 11330, K1098, K1118, K10024, K10025; UMCZ T666, T700; Broom (1906); Brink (1955); Cruickshank (1978); Parrish (1992); Gower (1996, 1997, 2001, 2003)
Shansisuchus shansisuchus	IVPP V2504, 2505, unnumbered specimens; Young (1964); Parrish (1992); Gower (1996); Gower and Sennikov (1996)
Shansisuchus kuyeheensis	Cheng (1980)
Chalishevia cothurnata	PIN 2867/7, 18, 4366/1 (wrongly cited as PIN 4356/1 by Gower and Sennikov, 2000), 2, 3, 8; Ochev (1980); Sennikov (1995); Gower and Sennikov (2000)
"*Dongusia colorata*"	PIN 268/2; Huene (1940)
Uralosaurus magnus holotype	PIN 2973/70; Ochev (1980)
Uralosaurus magnus combined	PIN 2973/70−79; Ochev (1980)
Vancleavea campi	AMNH 30884 (casts); USNM 508519 (cast of GR 138); Long and Murry (1995); Hunt et al. (2005); Parker and Barton (2008); Nesbitt et al. (2009)
Asperoris mnyama	NHMUK R36615; Nesbitt et al. (2013a)
Euparkeria capensis	AMNH 2238, 2239, 5548, 19351; GPIT 1681/11); SAM-PK-1100, 3427, 5867, 5883, 6047A, 6047B, 6048−6050, 6557, 7411, 7659, 7696, 7700, 7702−7713, 7868, 10011, 10671, 13664−13667, K335, K8050, K8051, K8309, K10010, K10012, K10548; UMCZ T692, T921; Broom (1903); Haughton (1921); Ewer (1965); Gow (1970); Cruickshank (1979); Gower and Weber (1998); Senter (2003)
Dorosuchus neoetus	PIN 952/200, 1579/61−68; Sennikov (1989a, b, 1995b, 2008); Sookias et al. (2014)
Dongusuchus efremovi	PIN 952/15-1−5; Sennikov (1988a, b, 1990, 1995b); Niedźwiedzki et al. (2014)
Proterochampsa barrionuevoi	MACN-Pv 18165; PVL 2058, 2061, 2063; PVSJ 606; Reig (1959); Sill (1967); Trotteyn and Haro (2011); Trotteyn (2011); Dilkes and Arcucci (2012)
Proterochampsa nodosa	MCP 1694; Barberena (1982); Dilkes and Arcucci (2012)
Tropidosuchus romeri	PVL 4601, 4602, 4604, 4606; Arcucci (1990)
Cerritosaurus binsfeldi	UFRGS cast of CA unnumbered; unpublished photographs; Price (1946); Trotteyn et al. (2013)
Gualosuchus reigi	PULR 05; PVL 4576; Romer (1971a); Dilkes and Arcucci (2012); Trotteyn et al. (2013)
Chanaresuchus bonapartei	MCZ 4035, 4037, 4039; PULR 07; PVL 4575, 4586, 6244; Romer (1971a, 1972e); Cruickshank (1979); Sereno (1991); Trotteyn and Haro (2012)
Pseudochampsa ischigualastensis	PVSJ 567; Trotteyn and Haro (2012); Trotteyn et al. (2012); Trotteyn and Ezcurra (2014)
Rhadinosuchus gracilis	BSPG AS XXV 50, 51; Huene (1938); Ezcurra et al. (2015b)
Archeopelta arborensis	CPEZ-239a; Desojo et al. (2011)
Tarjadia ruthae	MCZ 4076, 4077, 9319, unnumbered specimen; PULR 063; Arcucci and Marsicano (1998)
Jaxtasuchus salomoni	SMNS 91002, 91083, 91352; Schoch and Sues (2013)
Doswellia kaltenbachi	USNM 25840, 186989, 214823, 244214; Weems (1980); Long and Murry (1995); Dilkes and Sues (2009)
Paleorhinus spp.	BSPG 1931 X 502, 1931 X 503; MNHN-ALM1;

	unpublished photographs of ZPAL specimens; Dutuit (1977); Fara and Hungerbühler (2000); Dzik (2001); Stocker (2010); Butler et al. (2014b)
Nicrosaurus kapffi	NHMUK R38036, 38037, 42743−42745; SMNS multiple specimens; Huene (1923); Hungerbühler (1998, 2000)
Smilosuchus spp.	MCZ 1029; UCMP 26699, 27200; USNM 18313; Camp (1930); Sereno (1991)
Ornithosuchus longidens	NHMUK R2409, R2410, R3142, R3143, R3149, R3562, R3622, R3916; Huene (1914); Walker (1964); Sereno (1991)
Riojasuchus tenuisceps	PVL 3814, 3826−3828; Bonaparte (1972)
Nundasuchus songeaensis	Nesbitt et al. (2014)
Turfanosuchus dabanensis	IVPP V3237; Young (1973c); Wu and Russell (2001)
Gracilisuchus stipanicicorum	CRILAR-Pv unnumbered specimen; MCZ 4116−4118; PULR 08; PVL 4597, 4612; Romer (1972b); Lecuona and Desojo (2011); Butler et al. (2014a)
Aetosauroides scagliai	MCP 13a-b-PV; PVL 2052, 2059, 2073; UFSM 11070a; Casamiquela (1960, 1961, 1967); Desojo and Ezcurra (2011)
Batrachotomus kupferzellensis	SMNS 52970, 80260, 80269, 80271, 80273, 80275, 80276, 80280, 80283, 80285, 80288, 80293, 80294, 80296, 80300, 80305, 80309, 80322, 91044, 91049, cast of MHI 1895; Gower (1999); Gower and Schoch (2009)
Prestosuchus chiniquensis	UFRGS-PV-0137-T, 0152-T, 0156-T, 0473-T, 0629-T; Barberena (1978); Nesbitt (2011); Mastrantonio et al. (2013)
Dimorphodon macronyx	NHMUK R41212-13, R1034, R1035; Padian (1983); Nesbitt (2011)
Lagerpeton chanarensis	MCZ 4121; PULR 06; PVL 4619; Romer (1971b, 1972c); Arcucci (1986); Sereno and Arcucci (1993)
Marasuchus lilloensis	PVL 3870−3872; Romer (1971b, 1972c); Bonaparte (1975); Sereno and Arcucci (1994)
Lewisuchus admixtus	PULR 01; Romer (1972d); Bittencourt et al. (2014)
Silesaurus opolensis	Multiple ZPAL specimens; Dzik (2003); Dzik and Sulej (2007); Piechowski and Dzik (2010); Langer et al. (2013); Kubo and Kubo (2014); Piechowski et al. (2014)
Heterodontosaurus tucki	AM 4765, unnumbered specimen; SAM-PK-K337, K1332; Crompton and Charig (1962); Santa Luca (1980); Norman et al. (2011); Porro et al. (2011); Sereno (2012)
Herrerasaurus ischigualastensis	MACN-Pv 18060; MCZ 4381, 7064; MLP 61-VIII-2-2, 61-VIII-2-3; PVL 2054, 2558, 2566; PVL 053, 104, 373, 380, 407; Reig (1963); Brinkman and Sues (1987); Novas (1986); Sereno and Novas (1992, 1993); Novas (1992, 1993); Sereno (1993); Ezcurra (2012)

The characters were scored in Mesquite 3.01 (Maddison and Maddison, 2015) based on first hand observations of approximately 95% of the selected terminals (Table 5.1, Appendix 9). Only five terminals were scored based on published bibliography: *Petrolacosaurus kansensis*, *Gephyrosaurus bridensis*, *Fugusuchus hejiapanensis*, *Shansisuchus kuyeheensis* and *Nundasuchus songeaensis*. The holotypes and only known specimens of *Fugusuchus hejiapanensis* and *Shansisuchus kuyeheensis* could not be studied at first hand because they were reported lost by the Geological Institute (Beijing, China) when access was requested in May 2013. Four taxa resulted redundant to other terminals (i.e. *Archosaurus rossicus* to South African species of *Proterosuchus*, "*Ankistrodon indicus*" to *Proterosuchus fergusi* and *Proterosuchus alexanderi*, "*Blomosuchus georgii*" to *Proterosuchus* spp. and "*Chasmatosaurus*" *yuani*, and "*Dongusia colorata*" to *Batrachotomus kupferzellensis*) but they were not excluded a priori from the analysis because the computational times of the searches will not be likely strongly affected.

Alternative analyses

The data matrix was built with the aim of conducting three alternative analyses:

Analysis 1 (holotypes only): in this analysis only the holotypes are included for species with problematic hypodigms. *Chasmatosuchus magnus* and its proposed junior subjective synonym "*Gamosaurus lozovskii*" are included as different terminals. The following four terminals are excluded from this analysis: *Kadimakara australiensis* combined, *Chasmatosuchus magnus* combined (i.e. *Chasmatosuchus magnus* + "*Gamosaurus lozovskii*"), *Garjainia madiba* combined and *Uralosaurus magnus* combined. The resultant data matrix includes 91 operational taxonomic units.

Analysis 2 (complete hypodigms): in this analysis the complete hypodigms are included for all species and a single terminal was used that combines both *Chasmatosuchus magnus* and "*Gamosaurus lozovskii*" (i.e. accepting the proposed synonymy of these species). Therefore, the following five terminals are excluded from this analysis: *Kadimakara australiensis* holotype, *Chasmatosuchus magnus*, "*Gamosaurus lozovskii*", *Garjainia madiba* holotype and *Uralosaurus magnus* holotype. The resultant data matrix includes 90 operational taxonomic units.

Analysis 3 (reduced analysis): in this analysis 21 terminals are pruned a priori because they represent nomina dubia or highly fragmentary taxa (usually represented by a single isolated bone), the inclusion of which led to major polytomies in the results of the previous two analyses. The pruned taxa were: *Eorasaurus olsoni*, *Kadimakara australiensis*, *Archosaurus rossicus*, *Proterosuchus fergusi* holotype, "*Ankistrodon indicus*", "*Blomosuchus georgii*", *Vonhuenia friedrichi*, *Chasmatosuchus rossicus*, *Chasmatosuchus magnus*, "*Gamosaurus lozovskii*", *Chasmatosuchus magnus* combined (i.e. *Chasmatosuchus magnus* + "*Gamosaurus lozovskii*"), "*Chasmatosuchus*" *vjushkovi*, Long Reef proterosuchid, *Kalisuchus rewanensis*, *Garjainia madiba* holotype, "*Dongusia colorata*", *Uralosaurus magnus* holotype, *Uralosaurus magnus* combined and *Dongosuchus efremovi*. These taxa are excluded because the alternative positions that they adopt in the different most parsimonious trees (MPTs) can cause ambiguities or artefacts in character optimizations that may affect the tree topologies. The main aim of analysis 3 is to allow other workers to use this data matrix in future studies easily, without requiring high amounts of computer memory and lengthy tree searches. The resultant data matrix includes 76 operational taxonomic units.

5.3.6. *Tree search, strict reduced consensus and tree support calculation methodologies*

The data matrices were analysed under equally-weighted parsimony using TNT 1.1 (Goloboff et al., 2008) in a computer with 128 GB RAM. A total of 1,800,000 trees were set to be retained in memory, which is the maximum number of trees possible that could be saved in that computer. A first search using the algorithms Sectorial Searches, Ratchet (perturbation phase stopped after 20 substitutions) and Tree Fusing (5 rounds) was conducted performing 1,000 replications in order to find all the tree islands. The best tree or trees obtained at the end of the replicates were subjected to a final round of TBR branch swapping. Zero length branches among any of the recovered MPTs were collapsed (rule 1 of Coddington and Scharff 1994).

As measures of tree support, decay indices (= Bremer support) were calculated and a bootstrap resampling analysis was conducted performing 10,000 pseudoreplicates. Both absolute and GC (i.e. difference between the frequency whereby the original group and the most frequent contradictory group are recovered in the pseudoreplicates) frequencies are reported. Taxa with high amounts of missing data may reduce node support values not as a result of a real low robustness of the node but because of ambiguous optimizations generated by unknown character states. Accordingly, a second round of decay indices was conducted following the a posteriori pruning of 49 terminals (Table 5.2), in which the percentage of missing data exceeded the mean of the missing data of the entire data matrix (this cutoff was decided arbitrarily as a compromise between retaining a representative subsample of terminals and aiming to reduce of missing data). Finally, alternative topologies of relationships between taxa were explored using heuristic tree searches under monophyly or non-monophyly constraints. This procedure aims to evaluate how many

Table 5.2 (and subsequent pages). Percentages of missing entries and polymorphisms present in the operational taxonomic units of the phylogenetic analysis. Terminals in bold were removed a posteriori to generate the series of strict reduced consensus trees and terminals indicated with an asterisk were removed a posteriori from the second round of decay indices and bootstrap resampling. Abbreviations: Amb. poly., polymorphisms due to ambiguities in scorings; Anat. poly., anatomical polymorphisms; Miss.ent., missing entries; Non-app., non-applicable characters.

Taxon	**Miss. ent.**	**Non-app.**	**Anat. poly**	**Amb. poly**
Petrolacosaurus kansensis	11.25	11.07	0.54	0.00
*Acerosodontosaurus piveteaui**	65.18	6.07	0.00	0.00
Youngina capensis	8.93	8.75	0.89	0.00
*Paliguana whitei**	84.29	2.86	0.00	0.00
Planocephalosaurus robinsonae	33.93	9.29	0.18	0.18
Gephyrosaurus bridensis	28.93	7.68	0.18	0.54
*Aenigmastropheus parringtoni**	94.29	0.00	0.00	0.18
Protorosaurus speneri	26.61	8.93	1.25	0.71
Amotosaurus rotfeldensis	51.61	6.25	0.54	0.36
Macrocnemus bassanii	34.11	8.57	0.71	0.00
Tanystropheus longobardicus	12.14	11.96	2.32	0.54
Jesairosaurus lehmani	48.04	8.21	0.71	0.89
Azendohsaurus madagaskarensis	10.00	7.86	0.71	0.36
Trilophosaurus buettneri	11.39	10.00	0.54	0.36
*Noteosuchus colletti**	73.75	2.68	0.18	0.36
Mesosuchus browni	11.07	7.68	0.18	0.36
Howesia browni	45.89	4.29	0.36	1.07
*Eohyosaurus wolvaardti**	78.75	1.43	0.00	0.71
Rhynchosaurus articeps	22.32	9.29	0.36	0.36
*Bentonyx sidensis**	63.04	5.89	0.00	0.18
Eorasaurus olsoni*	**96.25**	**0.00**	**0.18**	**0.18**
*Prolacertoides jimusarensis**	87.86	1.96	0.00	0.18
Prolacerta broomi	4.82	7.86	1.43	0.36
Kadimakara australiensis holotype*	88.21	0.54	0.00	0.36
Kadimakara australiensis combined*	83.93	2.68	0.00	0.71
Boreopricea funerea	45.89	4.64	0.00	0.71
Archosaurus rossicus*	**96.96**	**0.00**	**0.00**	**0.00**
Proterosuchus fergusi* holotype*	**91.25**	**0.18**	**0.00**	**0.71**
Proterosuchus fergusi	21.79	3.93	2.50	0.18
*Proterosuchus goweri**	63.04	1.07	0.00	0.71
Proterosuchus alexanderi	29.11	4.46	0.00	0.54
"Chasmatosaurus" yuani	23.04	5.36	1.07	1.43
*"Chasmatosaurus ultimus"**	91.07	0.00	0.00	0.36
"Ankistrodon indicus"*	**98.75**	**0.00**	**0.00**	**0.18**
*Tasmaniosaurus triassicus**	85.54	0.36	0.00	1.25
"Blomosuchus georgii"*	**97.50**	**0.00**	**0.00**	**0.18**
Vonhuenia friedrichi*	**96.96**	**0.36**	**0.00**	**0.00**
Chasmatosuchus rossicus*	**94.11**	**0.36**	**0.18**	**0.00**
Chasmatosuchus magnus*	**97.68**	**0.18**	**0.00**	**0.00**
"Gamosaurus lozovskii"*	**97.14**	**0.00**	**0.00**	**0.00**
C. magnus + G. lozovskii*	**96.43**	**0.18**	**0.00**	**0.00**
"Chasmatosuchus" vjushkovi*	**96.79**	**0.00**	**0.00**	**0.36**
SAM P41754 Long Reef*	**96.07**	**0.00**	**0.00**	**0.18**

*Koilamasuchus gonzalezdiazi**	94.46	0.36	0.00	0.71
Kalisuchus rewanensis*	**94.46**	**0.36**	**0.00**	**0.71**
*Fugusuchus hejiapanensis**	70.54	1.79	0.00	0.36
*Sarmatosuchus otschevi**	66.07	0.89	0.18	0.89
*Guchengosuchus shiguaiensis**	71.96	2.50	0.00	1.25
*Cuyosuchus huenei**	73.39	1.43	0.18	1.43
GHG 7433MI*	76.25	2.14	0.00	0.54
Garjainia prima	16.61	4.46	0.54	0.36
Garjainia madiba holotype*	94.46	0.18	0.00	0.18
Garjainia madiba combined	52.86	1.61	0.54	1.25
Erythrosuchus africanus	9.46	5.36	0.54	0.00
Shansisuchus shansisuchus	25.36	5.18	0.71	0.71
*Shansisuchus kuyeheensis**	88.04	0.36	0.00	0.36
*Chalishevia cothurnata**	86.43	0.36	0.00	0.36
"Dongusia colorata"*	**97.14**	**0.00**	**0.00**	**0.00**
Uralosaurus magnus* holotype	**98.21**	**0.54**	**0.00**	**0.00**
Uralosaurus magnus* combined	**95.36**	**0.54**	**0.00**	**0.00**
Vancleavea campi	31.07	8.04	0.18	0.36
*Asperoris mnyama**	84.29	1.43	0.00	0.89
Euparkeria capensis	6.43	2.50	1.79	0.18
*Dorosuchus neoetus**	84.64	0.18	0.00	0.00
Dongusuchus efremovi*	**95.54**	**0.18**	**0.00**	**0.00**
Proterochampsa barrionuevoi	31.61	6.07	0.36	1.07
*Proterochampsa nodosa**	69.29	1.79	0.00	0.36
Tropidosuchus romeri	24.64	3.57	0.54	1.07
*Cerritosaurus binsfeldi**	67.86	2.32	0.18	0.36
Gualosuchus reigi	31.43	3.93	0.71	0.54
Chanaresuchus bonapartei	11.25	4.46	1.79	0.00
Pseudochampsa ischigualastensis	43.39	3.04	0.00	0.89
*Rhadinosuchus gracilis**	84.29	0.36	0.18	0.89
*Archeopelta arborensis**	81.61	0.71	0.00	0.18
*Tarjadia ruthae**	92.50	0.18	0.00	0.36
*Jaxtasuchus salomoni**	71.07	1.07	0.18	1.07
Doswellia kaltenbachi	48.75	5.18	0.36	0.89
Paleorhinus spp.	53.75	3.75	1.25	0.36
Nicrosaurus kapffi	35.36	4.82	0.71	0.36
Smilosuchus spp.	12.14	5.36	0.54	0.18
Ornithosuchus longidens	31.61	3.04	0.36	0.36
Riojasuchus tenuisceps	13.93	3.39	0.54	0.54
*Nundasuchus songeaensis**	62.50	1.25	0.18	0.18
Turfanosuchus dabanensis	31.43	2.14	0.00	1.25
Gracilisuchus stipanicicorum	19.82	3.39	0.71	1.25
Aetosauroides scagliai	38.21	2.14	0.54	1.61
Batrachotomus kupferzellensis	18.93	3.21	0.36	0.36
Prestosuchus chiniquensis	9.82	3.04	0.36	0.36
Dimorphodon macronyx	45.54	7.50	0.36	0.36
*Lagerpeton chanarensis**	76.07	2.68	0.18	0.00
Marasuchus lilloensis	50.18	3.39	0.18	0.54
*Lewisuchus admixtus**	56.96	2.14	0.18	0.89
Silesaurus opolensis	22.68	6.43	0.00	0.71

Heterodontosaurus tucki	10.71	9.82	0.54	0.00
Herrerasaurus ischigualastensis	10.36	6.61	1.61	0.36
Mean (standard deviation)	56.49 (±32.00)	3.37(±3.13)	0.34(±0.51)	0.46(±0.40)
Median	62.5	2.68	0.18	0.36

additional steps are necessary to obtain these alternative topologies, such as those required to recover the monophyly of “Prolacertiformes”, “Proterosuchia” or previous taxonomically inclusive conceptions of Proterosuchidae.

The option of “pruned trees” in TNT was used to search for topologically unstable terminals among the recovered MPTs. The presence of multiple fragmentary species in the data matrix analysed here, specifically in analyses 1 and 2, may result in several polytomies in the strict consensus of the recovered MPTs. As a result, a series of strict reduced consensus trees (SRCTs) were generated from the recovered MPTs. These SRCTs were obtained by pruning a posteriori the terminals that were recovered in alternative positions among the MPTs (i.e. ‘wildcard taxa’), with the aim of resolving iteratively the strict consensus from the apex of the tree towards its root. This protocol results in a series of sequentially more resolved SRCTs that allow the phylogenetic positions of the ambiguously placed terminals to be constrained.

5.4. Results

The tree searches reached the maximum number of trees that could be retained in memory (1,800,000 MPTs) with the best score hit 1 time out of the 1,000 replications in analyses 1 and 2. The MPTs of analysis 1 are of 2,449 steps, with a consistency index (CI) of 0.3087 and a retention index (RI) of 0.6248, and the MPTs of analysis 2 are of 2,459 steps, with a CI of 0.3074 and a RI of 0.6226. Phylogenetic analysis 3 recovered three MPTs of 2,449 steps, with a CI of 0.3087, a RI of 0.6248, and the best score hit 1 time out of the 1,000 replications. The strict consensus tree of analysis 3 is very well resolved through the entire topology (Figs. 5.5−5.8). The topology of the strict consensus tree is identical in analyses 1 and 2, being completely resolved among

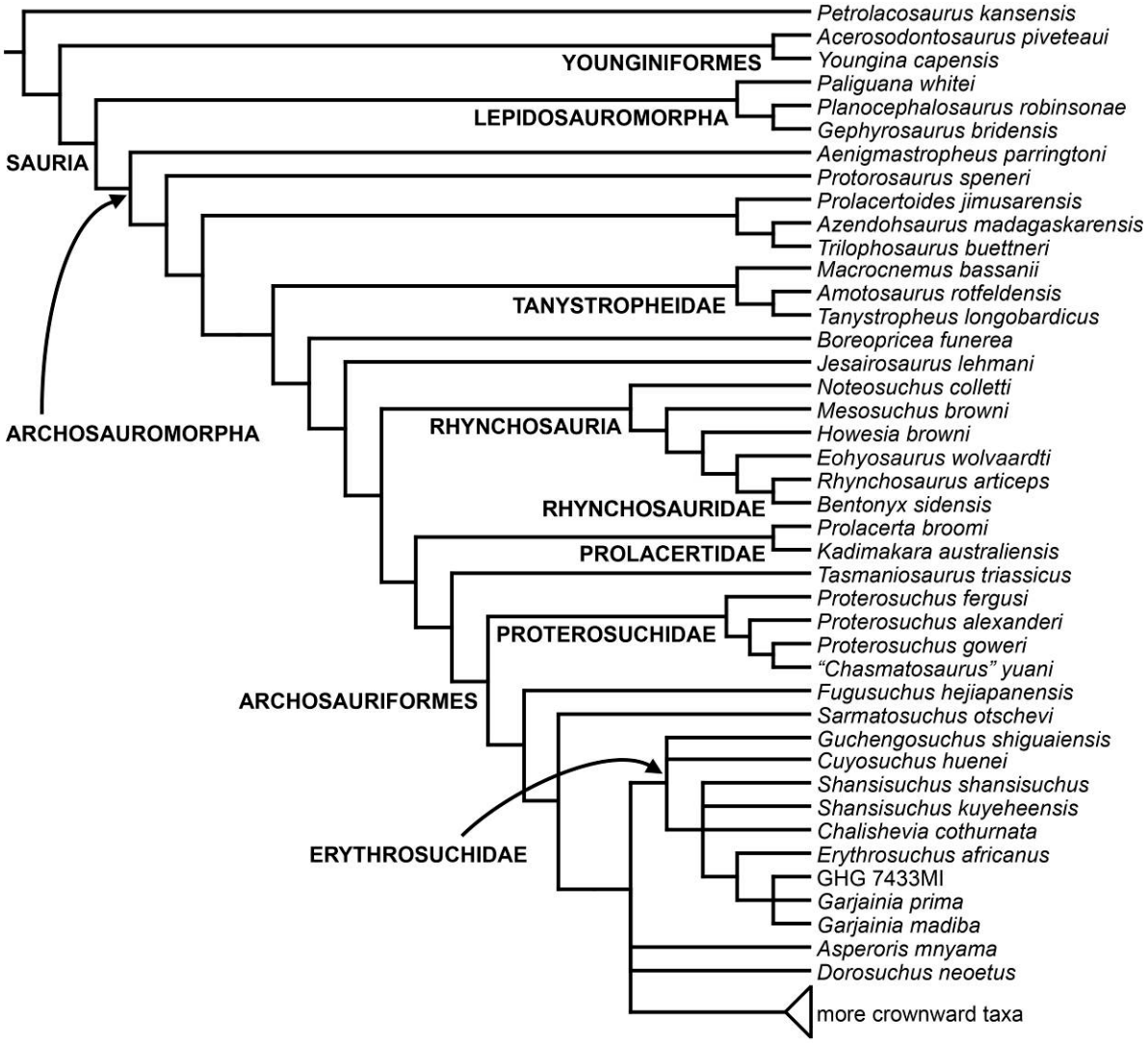

Figure 5.5. Strict consensus tree recovered from analysis 3 showing the phylogenetic relationships of basal archosauromorphs. *Euparkeria* and more crownward archosauriforms have been merged into "more crownward taxa" in this tree.

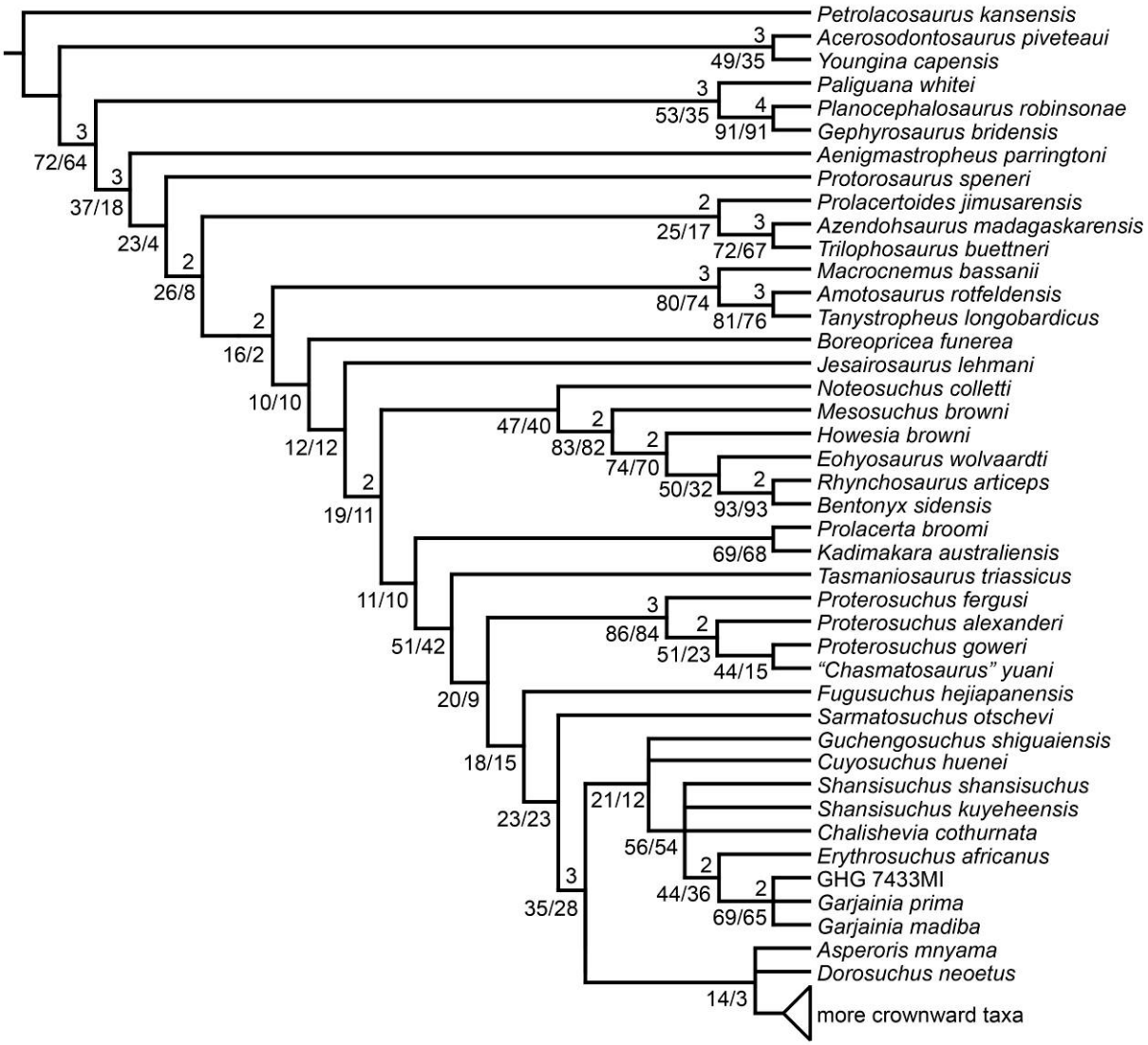

Figure 5.6. Node support values showed on the strict consensus tree recovered from analysis 3. Numbers above the nodes are Bremer supports above 1 and numbers below nodes are absolute (left) and GC (right) bootstrap frequencies. *Euparkeria* and more crownward archosauriforms have been merged into "more crownward taxa" in this tree.

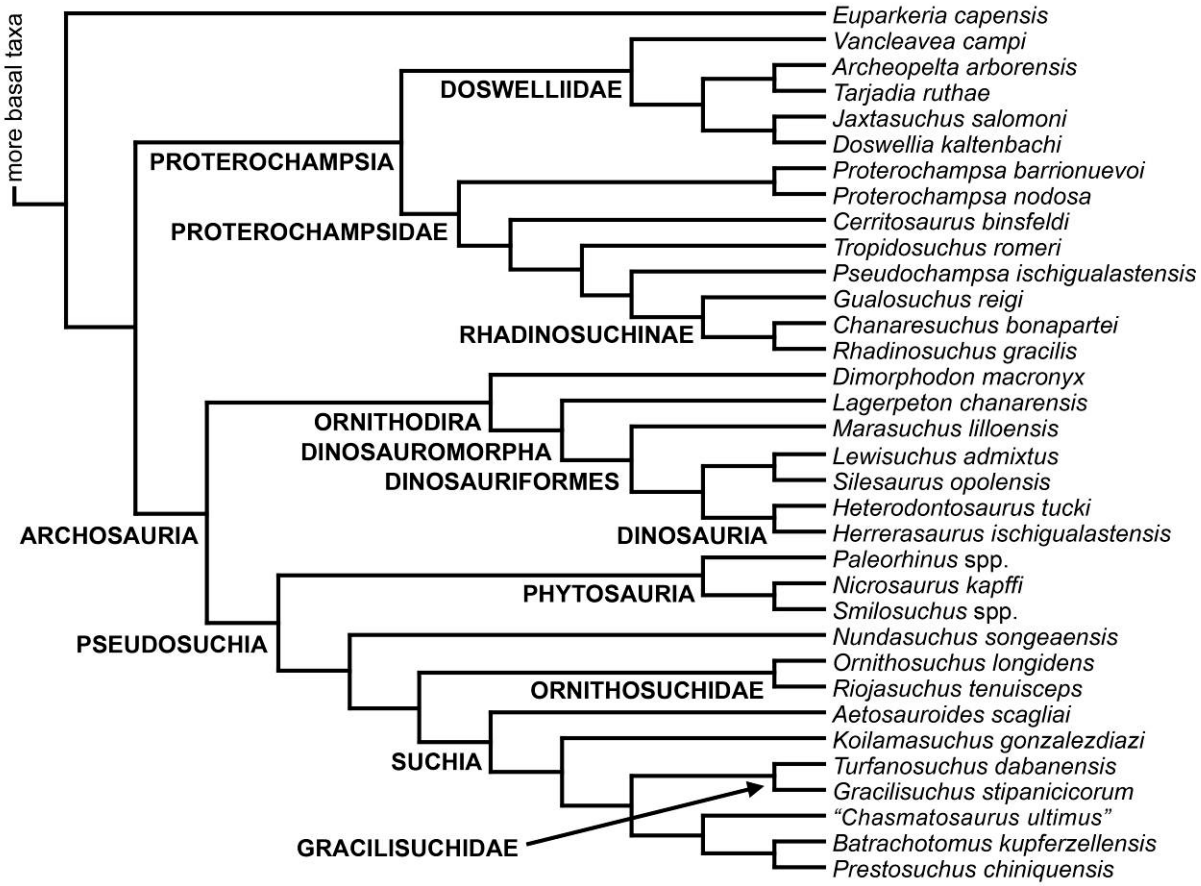

Figure 5.7. Strict consensus tree recovered from analysis 3 showing the phylogenetic relationships of basal archosauriforms. Taxa more basal than *Euparkeria* are not shown in this tree.

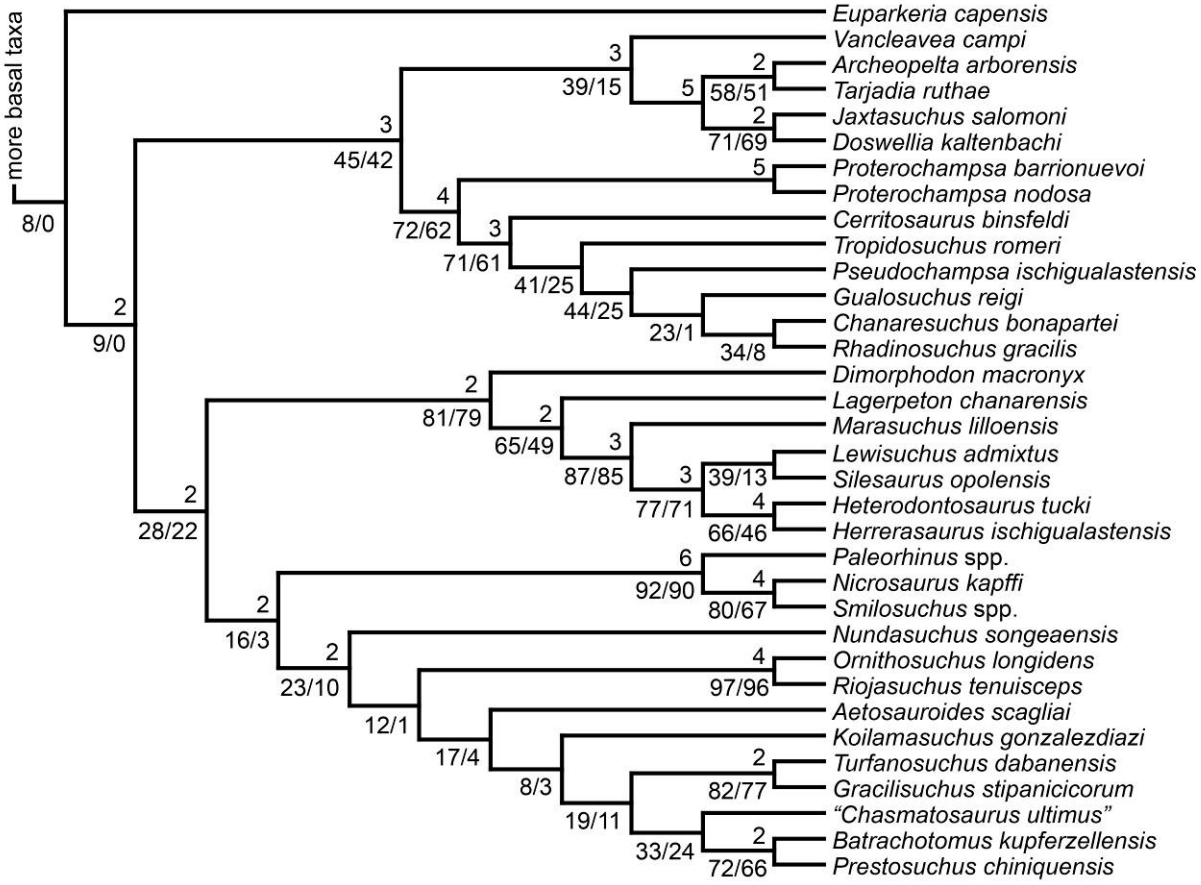

Figure 5.8. Node support values showed on the strict consensus tree recovered from analysis 3. Numbers above the nodes are Bremer supports above 1 and numbers below nodes are absolute (left) and GC (right) bootstrap frequencies. Taxa more basal than *Euparkeria* are not shown in in this tree.

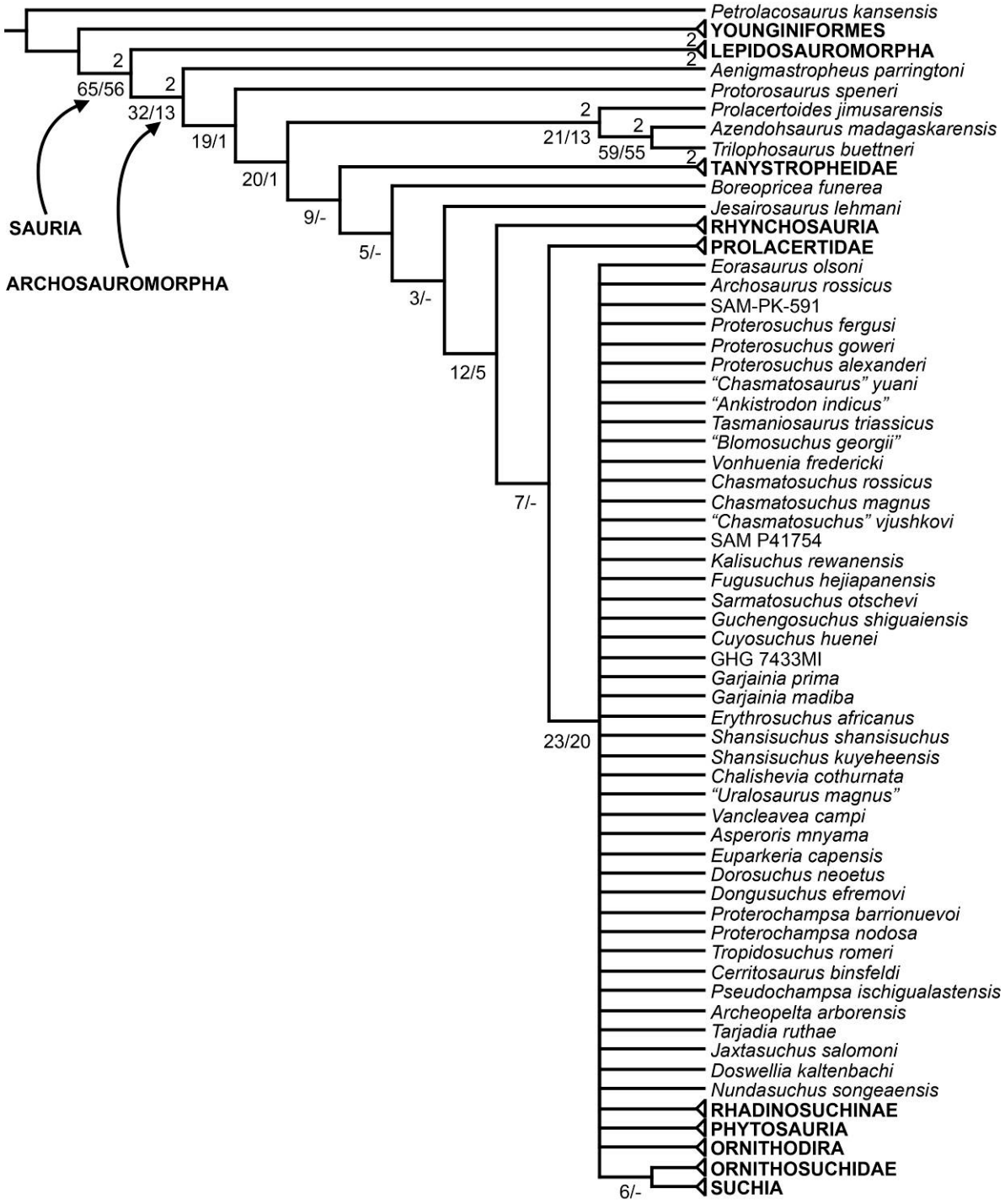

Figure 5.9. Strict consensus tree recovered from analyses 1 and 2. Numbers above the nodes are Bremer supports above 1 and numbers below nodes are absolute (left) and GC (right) bootstrap frequencies in analysis 2. Some clades have been condensed into suprageneric terminals to simplify the figure.

taxa usually considered as non-archosauriform diapsids and showing a massive polytomy among archosauriform species (Fig. 5.9). The topologies of the strict consensus trees of analyses 1–2 and 3 are completely consistent with each other. Regarding non-archosauriform diapsids, the Permian *Youngina capensis* and *Acerosodontosaurus piveteaui* are found to be more closely related to each other than to other diapsids, and, as a result, form together the clade Younginiformes (Figs. 5.5, 5.6). This clade is the sister taxon of the crown clade Sauria, which is composed of Lepidosauromorpha and Archosauromorpha (Gauthier et al., 1988). *Paliguana whitei* and the early rhynchocephalians *Planocephalosaurus robinsonae* and *Gephyrosaurus bridensis* are recovered within a monophyletic Lepidosauromorpha, with the latter two species as sister taxa to one another. The Lopingian *Aenigmastroepheus parringtoni* and *Protorosaurus speneri* are found as successive sister taxa of all other archosauromorphs. The enigmatic, Middle–Upper Triassic herbivorous species *Trilophosaurus buettneri* and *Azendohsaurus madagaskarensis* are found as more closely related to each other than to any other archosauromorph. This clade, Tanystropheidae, *Boreopricea funerea*, *Jesairosaurus lehmani*, Rhynchosauria and Prolacertidae are successive sister taxa of Archosauriformes. The only archosauriform clades that are resolved in the strict consensus trees of analyses 1 and 2 are Phytosauria, Ornithodira, Ornithosuchidae + Suchia and Rhadinosuchinae, which is a subclade of Proterochampsidae composed of *Gualosuchus reigi*, *Chanaresuchus bonapartei* and *Rhadinosuchus gracilis* (Fig. 5.9).

The “pruned trees” option found 16 and 15 terminals that are responsible for the lack of resolution among basal archosauriforms in analyses 1 and 2, respectively. These terminals possess in all cases a high amount of missing data (> 88%) (Table 5.2) and several of them are based on isolated bones (e.g. *Archosaurus rossicus*,

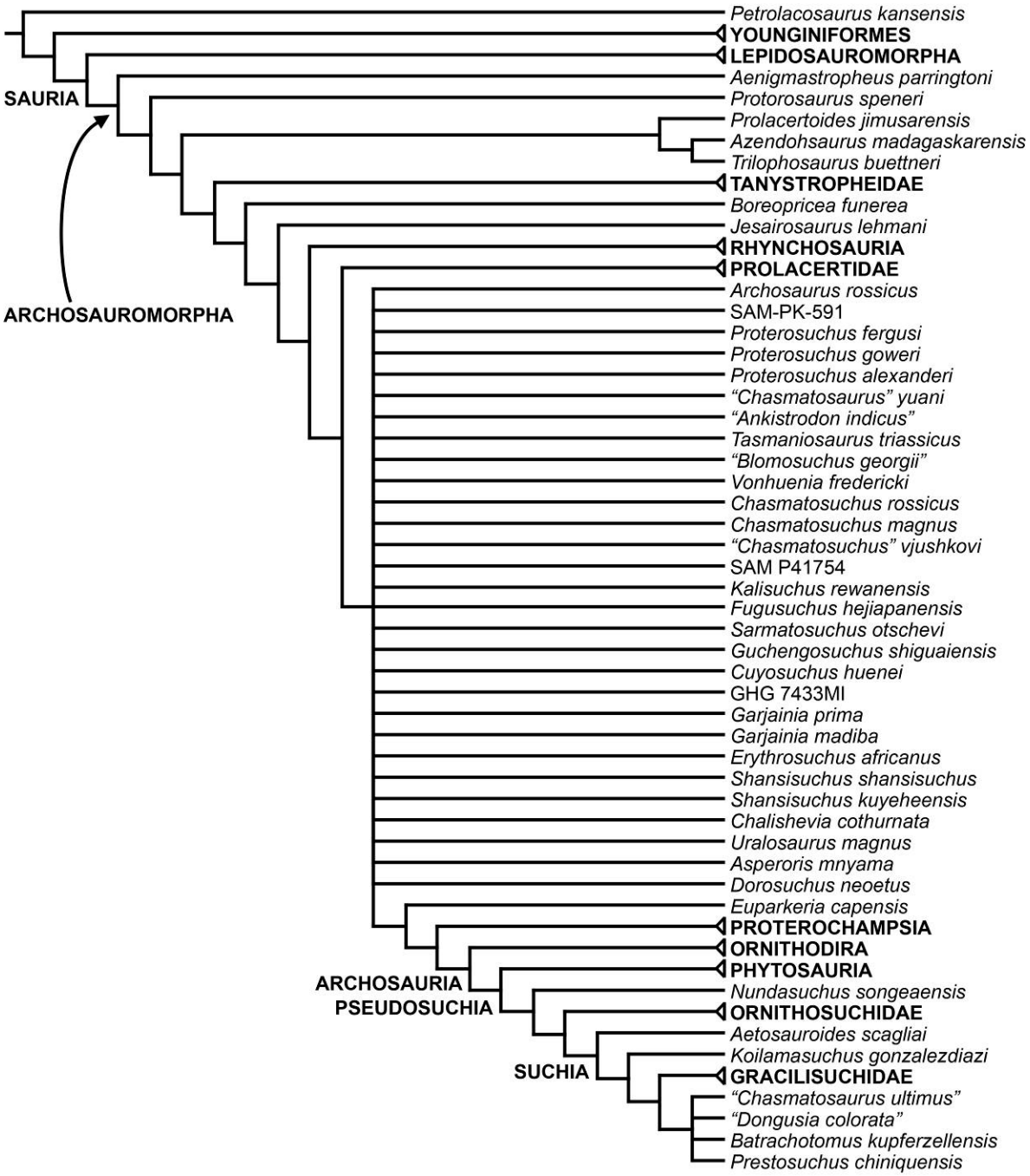

Figure 5.10. Frist strict reduced consensus tree recovered from analyses 1 and 2. Some clades have been condensed into suprageneric terminals to simplify the figure.

"*Ankistrodon indicus*", "*Blomosuchus georgii*", *Vonhuenia friedrichi*, "*Dongusia colorata*"). The SRCTs generated by the series of a posteriori prunings show the same topology in analyses 1 and 2 and are discussed together.

The first SRCT was generated after the a posteriori pruning of *Eorasaurus olsoni* and "*Dongusuchus efrmovi*" and resolved the interrelationships among *Euparkeria capensis* and more crownward archosauriforms (Fig. 5.10). A monophyletic clade (referred to here as Proterochampsia) formed by the supposedly semi-aquatic doswelliids and proterochampids is found as the sister taxon of Archosauria (i.e. Ornithodira + Pseudosuchia) (Figs. 5.7, 5.8). The bizarre, Late Triassic *Vanclavea campi* is recovered within this clade of semi-aquatic archosauriforms and as the most basal member of Doswelliidae. Phytosaurs are found within Archosauria and as the sister taxon of all other pseudosuchians. The recently described *Nundasuchus songeaensis* is found as the sister taxon of the clade formed by ornithosuchids and suchians. Several taxa previously identified as proterosuchians-—"*Chasmatosaurus ultimus*" from the Middle Triassic of China, "*Dongusia colorata*" from the Middle Triassic of Russia and *Koilamasuchus gonzalezdiazi* from the Middle–Late Triassic of Argentina—are found within Suchia. In particular, "*Dongusia colorata*" and *Koilamasuchus gonzalezdiazi* are placed within an unresolved clade nested within Suchia that is also composed of the loricatans *Prestosuchus chiniquensis* and *Batrachotomus kupferzellensis* (Fig. 5.10).

The second SRCT was generated after the a posteriori pruning of the taxa excluded in the first SRC and *Vonhuenia friedrichi*, *Chasmatosuchus rossicus*, *Chasmatosuchus magnus* (*Chasmatosuchus magnus* and "*Gamosaurus lozovskii*" in the case of analysis 1) and SAM P41754 (the "Long Reef proterosuchid") (Fig. 5.11). In this SRCT, all the taxa previously identified as erythrosuchids (with the exception

Figure 5.11. Second strict reduced consensus tree recovered from analyses 1 and 2. The light brown box indicates the monophyly of Erythrosuchidae. Some clades have been condensed into suprageneric terminals to simplify the figure.

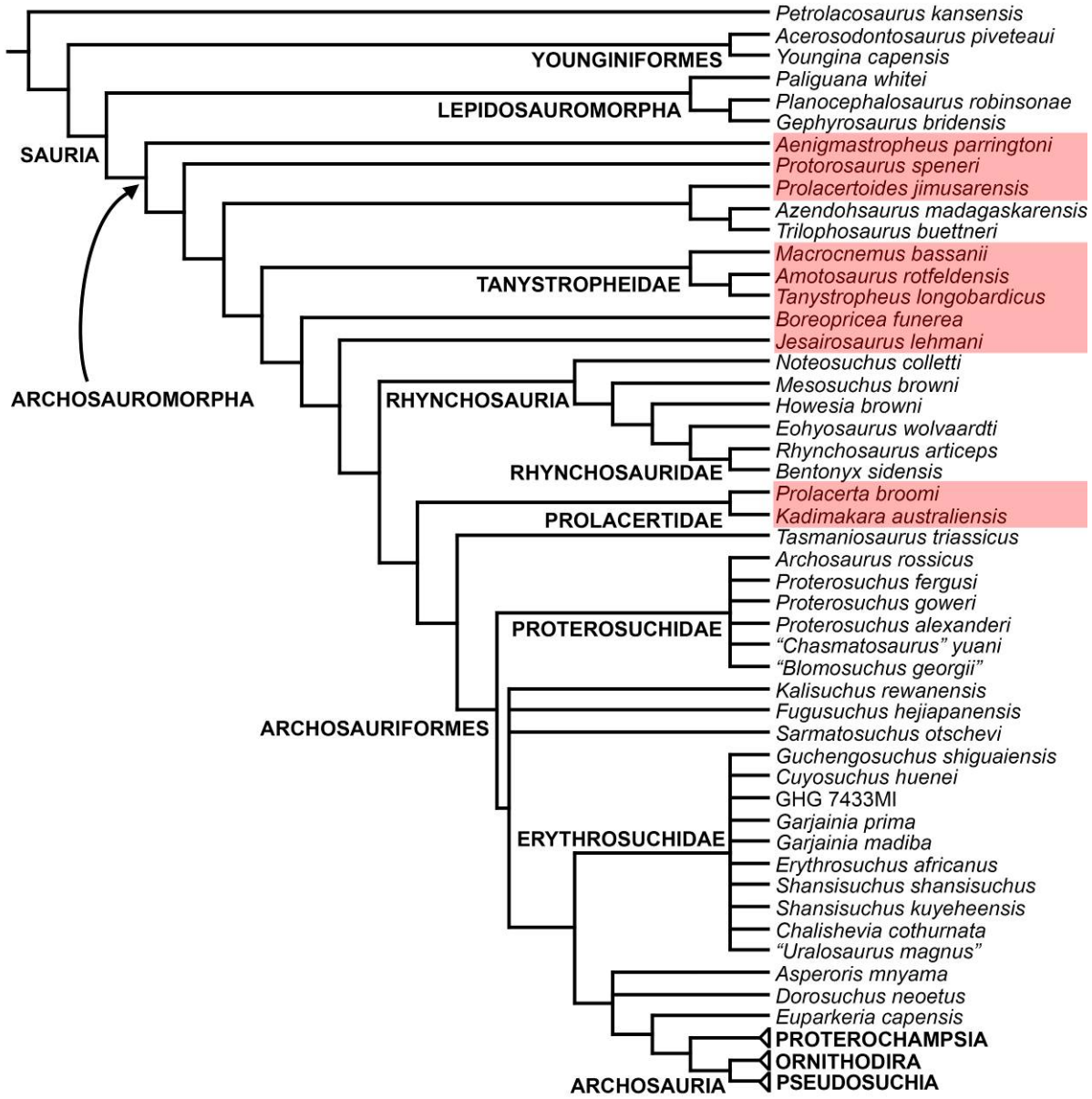

Figure 5.12. Third strict reduced consensus tree recovered from analyses 1 and 2. The red boxes indicate the polyphyly of “Prolacertiformes”. Some clades have been condensed into suprageneric terminals to simplify the figure.

of "*Dongusia colorata*", which was more recently reinterpreted as an archosaur; Charig and Reig, 1970; Gower and Sennikov, 2000) are recovered within a monophyletic Erythrosuchidae, including both species of *Garjainia*, both species of *Shansisuchus*, *Uralosaurus magnus*, *Chalishevia cothurnata*, *Erythrosuchus africanus*, *Cuyosuchus huenei*, *Guchengosuchus shiguaiensis* and the probable juvenile specimen of *Erythrosuchus africanus* (GHG 7433MI). Erythrosuchidae is the sister taxon of a trichotomy composed of *Dorosuchus neoetus*, *Asperoris mnyama* and the clade formed by *Euparkeria capensis* and more crownward archosauriforms.

The third SRCT was generated after the a posteriori pruning of the taxa excluded in the second SRC and SAM-PK-591 (the holotype of *Proterosuchus fergusi*), "*Chasmatosuchus*" *vjushkovi* and "*Ankistrodon indicus*" (Fig. 5.12). The aim of this SRCT is to completely resolve the interrelationships among the main clades of the tree. The Early Triassic *Tasmaniosaurus triassicus* is found as the sister taxon of Archosauriformes, which includes proterosuchids and more crownward taxa. Proterosuchidae is restricted to the latest Permian–Early Triassic *Archosaurus rossicus*, *Proterosuchus fergusi*, *Proterosuchus alexanderi*, *Proterosuchus goweri*, "*Chasmatosaurus*" *yuani* and "*Blomosuchus georgii*". Three taxa previously identified as proterosuchids—*Sarmatosuchus otschevi*, *Fugusuchus hejiapanensis* and *Kalisuchus rewanensis*—are found as more derived than proterosuchids and in a polytomy together with the clade formed by Erythrosuchidae and more crownward archosauriforms.

The fourth SRCT was generated after the a posteriori pruning of the taxa excluded in the first SRCT and SAM-PK-591 (the holotype of *Proterosuchus fergusi*),

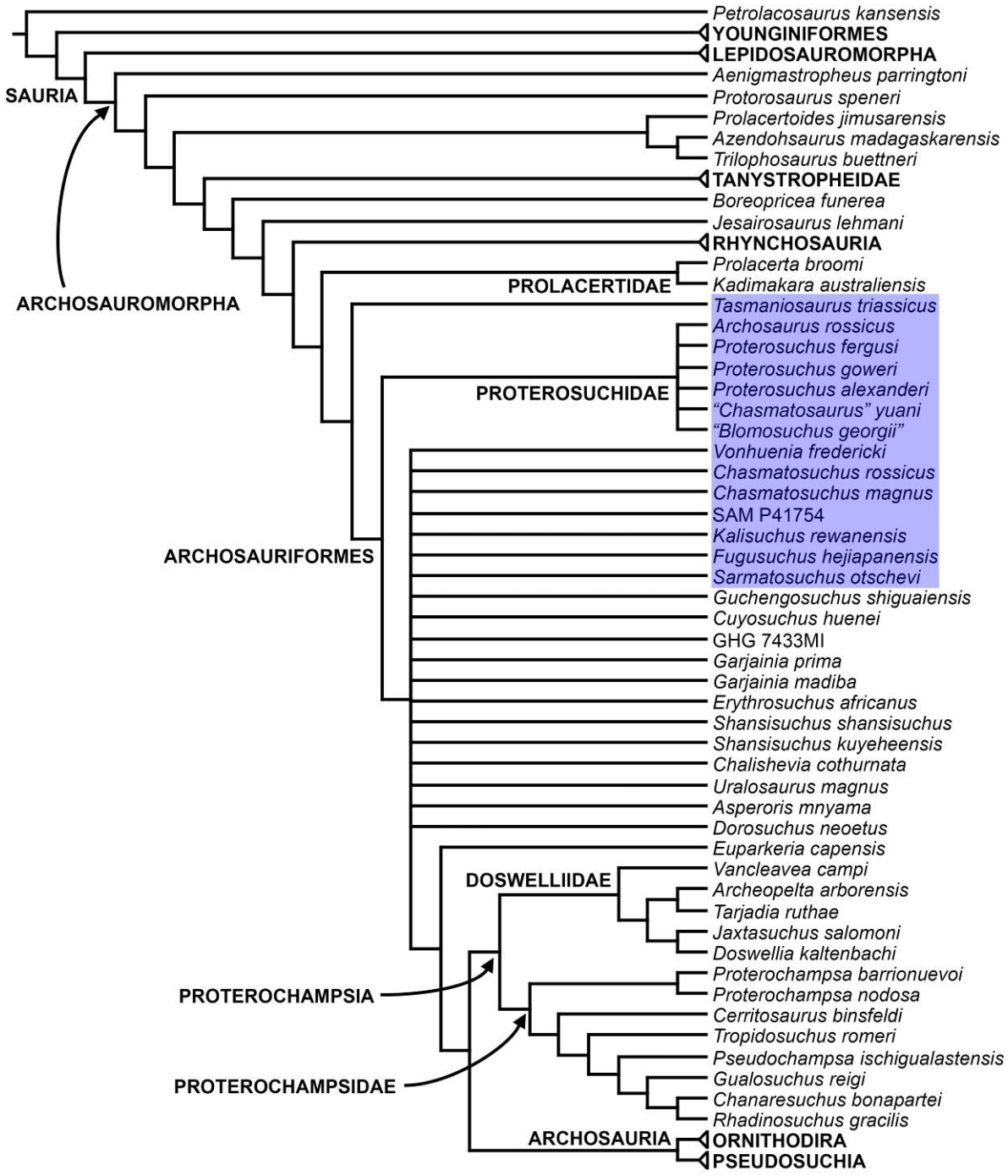

Figure 5.13. Fourth strict reduced consensus tree recovered from analyses 1 and 2. The blue box indicates the non-monophyly of archosauromorphs historically assigned to "Proterosuchidae". Some clades have been condensed into suprageneric terminals to simplify the figure.

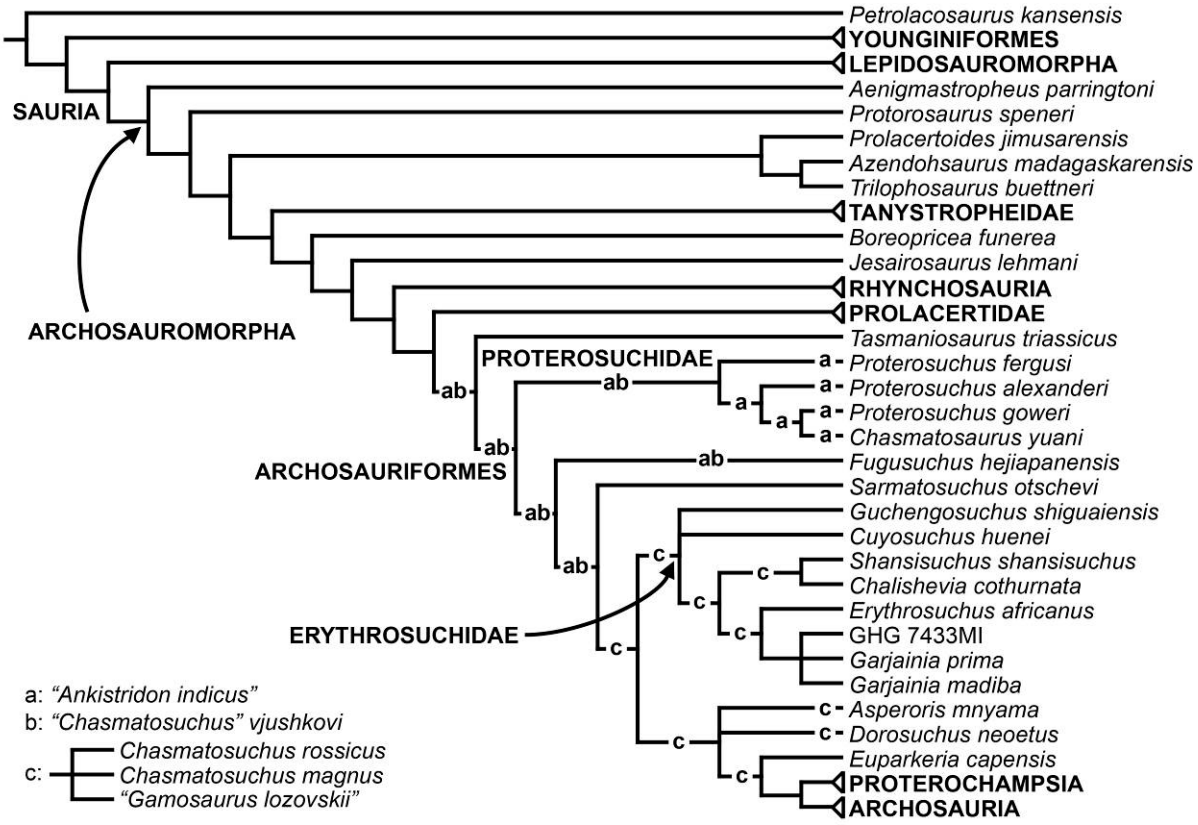

Figure 5.14. Fifth strict reduced consensus tree recovered from analyses 1 and 2. "a−c" indicates the alternative positions in which "*Ankistrodon indicus*", "*Chasmatosuchus vjushkovi*" and the genus *Chasmatosuchus* can be recovered in the most parsimonious trees. Some clades have been condensed into suprageneric terminals to simplify the figure.

"*Chasmatosuchus*" *vjushkovi* and "*Ankistrodon indicus*" (Fig. 5.13). The aim of this SRC is to constrain the phylogenetic positions of several taxa previously identified as proterosuchid. *Chasmatosuchus magnus* (*Chasmatosuchus magnus* and "*Gamosaurus lozovskii*" in the case of analysis 1), *Chasmatosuchus rossicus*, *Vonhuenia friedrichi* and SAM P41754 (the "Long Reef proterosuchid") are recovered as more derived than Proterosuchidae, as part of a massive polytomy that also includes *Kalisuchus rewanensis*, *Sarmatosuchus otschevi*, *Fugusuchus hejiapanensis*, *Dorosuchus neoetus*, *Asperoris mnyama* and erythrosuchids.

The fifth and final SRCT was generated after the a posteriori pruning of the taxa excluded in the third SRC and *Archosaurus rossicus*, "*Blomosuchus georgii*", *Kalisuchus rewanensis*, *Shansisuchus kuyeheensis*, *Uralosaurus magnus* and "*Dongusia colorata*" (Fig. 5.14). The aim of this SRC is to resolve the internal relationships of proterosuchids, erythrosuchids and suchians. Within Proterosuchidae, the South African *Proterosuchus fergusi*, *Proterosuchus alexanderi* and *Proterosuchus goweri* are successive sister species of the Chinese "*Chasmatosaurus*" *yuani*. Within Erythrosuchidae, *Cuyosuchus huenei* and *Guchengosuchus shiguaiensis* are recovered in a trichotomy together with a clade consisting of all other erythrosuchids. *Chalishevia cothurnata* and *Shansisuchus shansisuchus* are more closely related to each other than to other species and their clade is the sister taxon of the node including *Erythrosuchus africanus* and both species of *Garjainia*. The possible juvenile erythrosuchid from South Africa (GHG 7433MI) is found in an unresolved clade together with both species of *Garjainia*. Finally, within Suchia, "*Chasmatosaurus ultimus*" was recovered as the sister taxon of *Prestosuchus chiniquensis* and *Batrachotomus kupferzellensis* (Figs. 5.7, 5.8).

The strict consensus tree generated from the three MPTs recovered in analysis 3 shows an identical topology to that of the fifth SRCTs of analyses 1 and 2 (Figs. 5.5−5.8). As a result, the a priori pruning of the terminals in analysis 3 makes sense to allow future researchers to use this data matrix in reasonable computer times and using relatively low computer requirements. The diagnoses and unambiguous synapomorphy lists are reported in Appendix 10.

5.5. Discussion

The general structure of the phylogenetic trees recovered in this analysis agrees with those found by several previous workers (e.g. Sereno, 1991; Dilkes, 1998; Gottmann-Quesada and Sander, 2009; Ezcurra et al., 2010, 2014; Nesbitt, 2011). For example, tanystropheids, rhynchosaurs and prolacertids are found as successive sister taxa of Archosauriformes, resembling the results of Dilkes (1998), Gottmann-Quesada and Sander (2009) and Ezcurra et al. (2014), and proterosuchids and erythrosuchids are recovered as the most basal archosauriforms (Figs. 5.5, 5.6), in agreement with the topologies recovered by Ezcurra et al. (2010) and Nesbitt (2011). However, some results recovered here differ from those recently found by other researchers and are discussed as follows.

5.5.1. *The non-monophyly of "Prolacertiformes"*

Multiple gracile and long-necked Permian and Triassic archosauromorphs have been historically assigned to "Prolacertiformes" (Fig. 5.15), and some quantitative phylogenetic analyses have supported the monophyly of the group (Benton and Allen, 1997; Jalil, 1997). The most exhaustive quantitative analysis that tested the

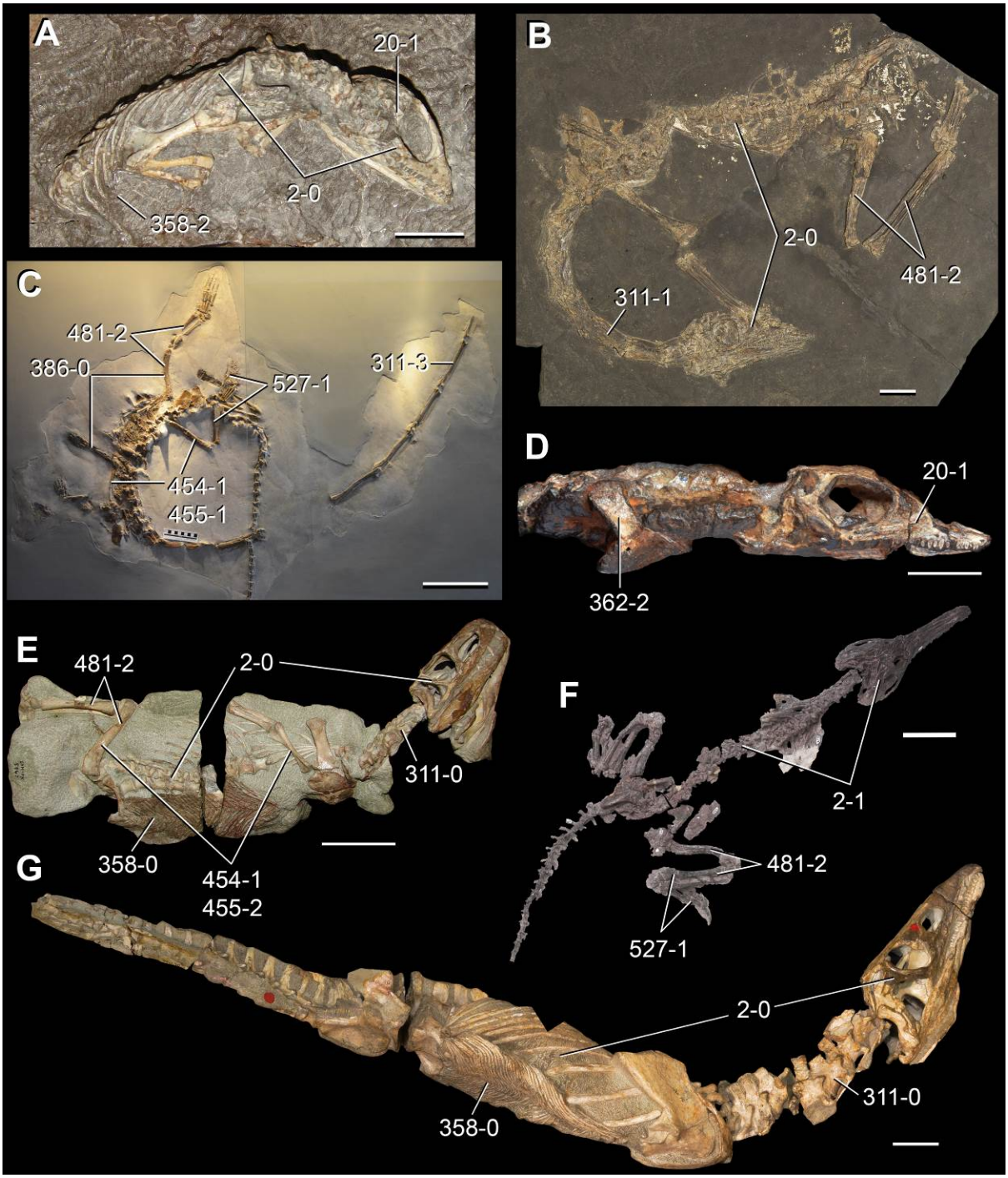

Figure 5.15. Partial skeletons of Permo-Triassic neodiapsids. *Youngina capensis* in left lateral view (SAM-PK-K8565, reversed) (A), *Macrocnemus bassanii* (PIMUZ T4355) (B), *Tanystropheus longobardicus* (PIMUZ T2817, reversed) (C), *Jesairosaurus lehmani* in right lateral view (ZAR 06) (D), *Euparkeria capensis* (SAM-PK-5867) (E), *Pseudochampsa ischigualastensis* in dorsal view (PVSJ 567) (F), and *Proterosuchus alexanderi* in left lateral view (NMQR 1484, reversed) (G). Numbers refer to character states. Scale bars equal 1 cm in A, D, 2 cm in B, 20 cm in C, and 5 cm in E−G.

monophyly of “Prolacertiformes” was conducted by Jalil (1997). This analysis found 14 genera within “Prolacertiformes”, namely *Protorosaurus*, *Prolacerta*, *Prolacertoides*, *Malutinisuchus*, *Kadimakara*, *Boreopricea*, *Malerisaurus*, *Jesairosaurus* and six very likely aquatic genera that are usually grouped within Tanystropheidae (*Trachelosaurus*, *Macrocnemus*, *Langobardisaurus*, *Cosesaurus*, *Tanystropheus*, *Tanytrachelos*). However, more recent quantitative analyses failed to recover a monophyletic “Prolacertiformes” sensu Jalil (1997) and recovered *Prolacerta broomi* as more closely related to archosauriforms than to *Protorosaurus speneri* (Dilkes, 1998; Modesto and Sues, 2004; Gottmann-Quesada and Sander, 2009; Ezcurra et al., 2014).

The results of the current phylogenetic analysis support the closer position of *Prolacerta broomi* to Archosauriformes than to *Protorosaurus speneri*. Moreover, most of the supposed prolacertiforms sampled by Jalil (1997) are recovered in a polyphyletic arrangement among non-archosauriform archosauromorphs (Fig. 5.12: red boxes). The only supposed prolacertiforms (sensu Jalil, 1997) recovered here in a monophyletic group are *Tanystropheus longobardicus* and *Macrocnemus bassanii*, which are included within Tanystropheidae together with *Amotosaurus rotfeldensis*. By contrast, *Prolacertoides jimusarensis* (and its probable close relatives *Trilophosaurus buettneri* and *Azendohsaurus madagaskarensis*), tanystropheids, *Boreopricea funerea* and *Jesairosaurus lehmani* are recovered as successive sister taxa, respectively, of the clade composed of Rhynchosauria and more crownward archosauromorphs.

Jalil (1997) recovered five synapomorphies for “Prolacertiformes” that are discussed below in the context of the present phylogenetic analysis.

1) Skull low and narrow with short and narrow post-orbital region. This character state is partially represented by characters 20 (antorbital length versus total length of the skull) and 22 (skull proportions at the level of the anterior border of the orbit) of the present phylogenetic analysis. Supposed prolacertiforms have an antorbital length that is 0.40−0.56 times the total length of the skull (e.g. *Jesairosaurus lehmani*: 0.47, ZAR 06; *Macrocnemus bessanii*: 0.56, PIMUZ T4822; *Prolacerta broomi*: 0.45, BP/1/471, SAM-PK-K10797) and the ratio present in immediate sister taxa of Archosauromorpha (e.g. *Youngina capensis*: 0.49, GHG K 106) and basal archosauriforms (*Proterosuchus fergusi*: 0.50−0.51, RC 846, SAM-PK-K11208) falls within this range. In addition, several basal archosauriforms also possess a narrow skull, being dorsoventrally taller than transversely broad at the level of the anterior border of the orbit (e.g. *Proterosuchus fergusi*: RC 846; *Garjainia prima*: PIN 2394/5-1). As a result, the presence of a low and narrow skull seems to not be restricted to supposed prolacertiforms.

2) Low and elongate cervical spine. Anteroposteriorly long and low cervical neural spines (character 321-1) are present in supposed prolacertiforms (e.g. *Protorosaurus speneri*, *Amotosaurus rotfeldensis*, *Macrocnemus bassanii*, *Tanystropheus longobardicus*, *Prolacerta broomi*, *Boreopricea funerea*), whereas basal archosauriforms possess dorsoventrally taller cervical neural spines (e.g. *Proterosuchus fergusi*: BSPG 1934 VII 514; *Proterosuchus alexanderi*: NMQR 1484; *Garjainia prima*: PIN 2394/5; *Euparkeria capensis*: SAM-PK-5867). The present phylogenetic analysis optimizes the presence of low and elongate cervical neural spines as a symplesiomorphy of Archosauromorpha, which is retained by prolacertiform-grade species and subsequently lost in *Trilophosaurus buettneri*, rhynchosaurs and archosauriforms.

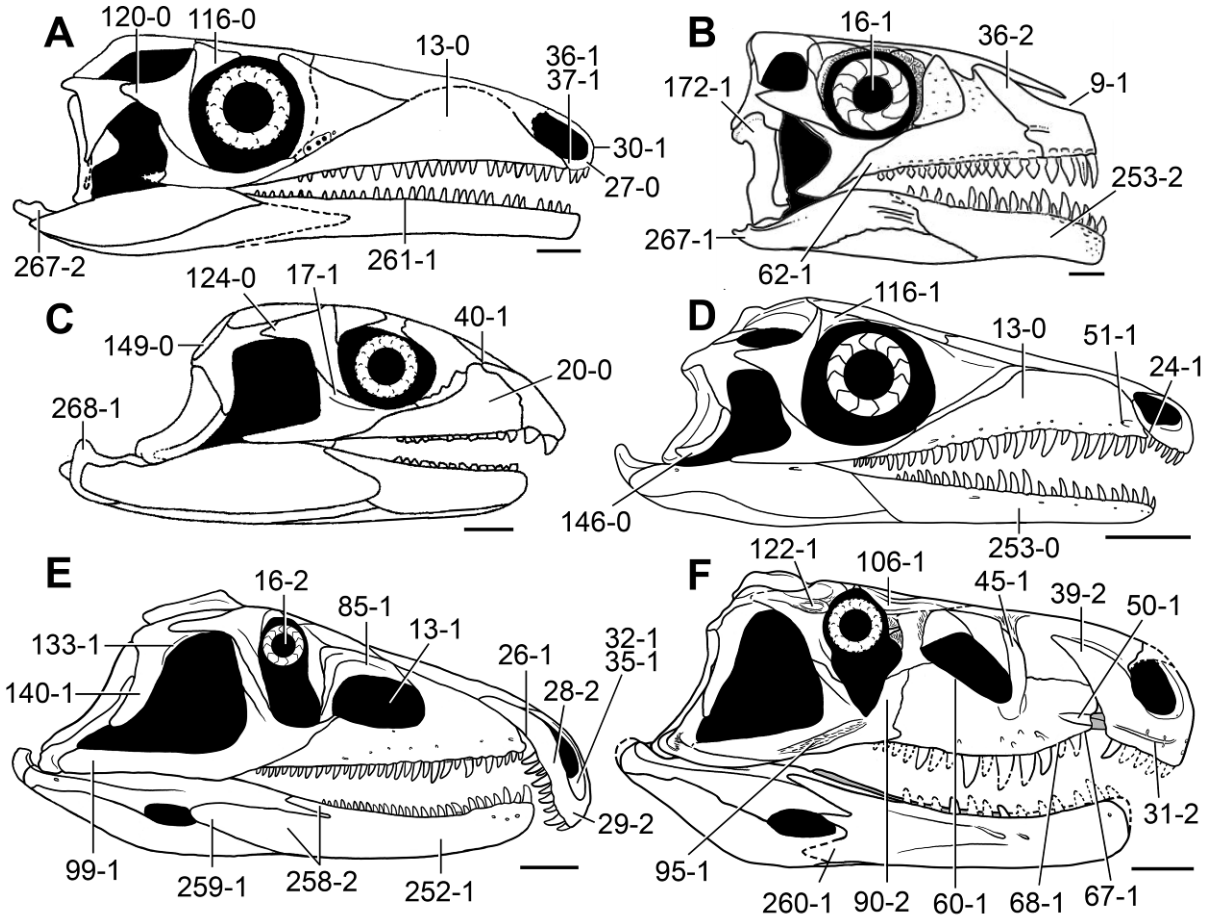

Figure 5.16. Reconstructions of the skull and lower jaw of Permo-Triassic archosauromorphs in lateral view. *Protorosaurus speneri* (A), *Azendohsaurus madagaskarensis* (B), *Mesosuchus browni* (C), *Prolacerta broomi* (D), *Proterosuchus fergusi* (E) and *Garjainia prima* (F). Numbers refer to character states. Scale bars equal 1 cm in A−D, and 5 cm in E, F. (A) modified from Gottmann-Quesada and Sander (2009), (B) modified from Flynn et al. (2010), and (C) modified from Dilkes (1998).

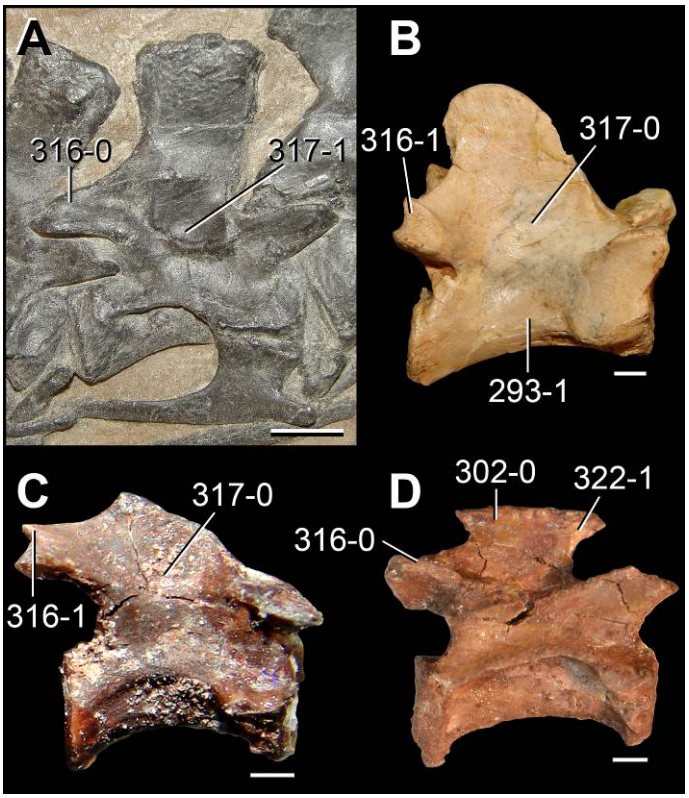

Figure 5.17. Middle and posterior cervical vertebrae of Permo-Triassic archosauromorphs in right lateral view. *Protorosaurus spneri* (BSPG 1995 I 5 [cast of WMSN P47361]) (A), *Tanystropheus longobardicus* (SMNS 54654) (B), *Boreopricea funerea* (PIN 3708/1) (C) and *Prolacerta broomi* (BP/1/2675) (D). Numbers refer to character states. Scale bars equal 1 cm in A, 5mm in B, and 2 mm in C, D.

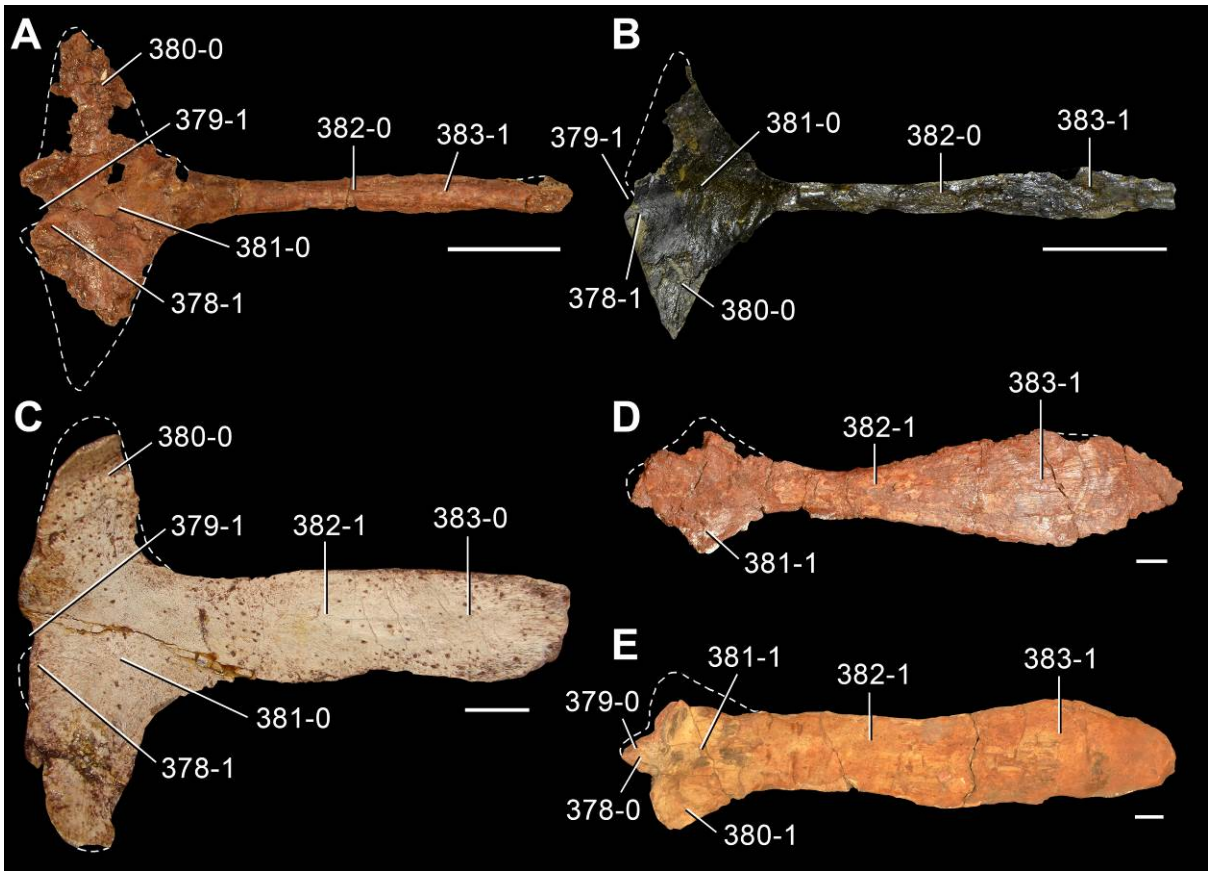

Figure 5.18. Interclavicles of Triassic archosauromorphs in ventral view. *Prolacerta broomi* (BP/1/2675) (A), *Tasmaniosaurus triassicus* (UTGD 54655) (B), *Proterosuchus fergusi* (GHG 363) (C), *Garjainia prima* (PIN 2394/5-34) (D) and *Parasuchus hislopi* (ISI R42) (E). Numbers refer to character states. Scale bars equal 1 cm.

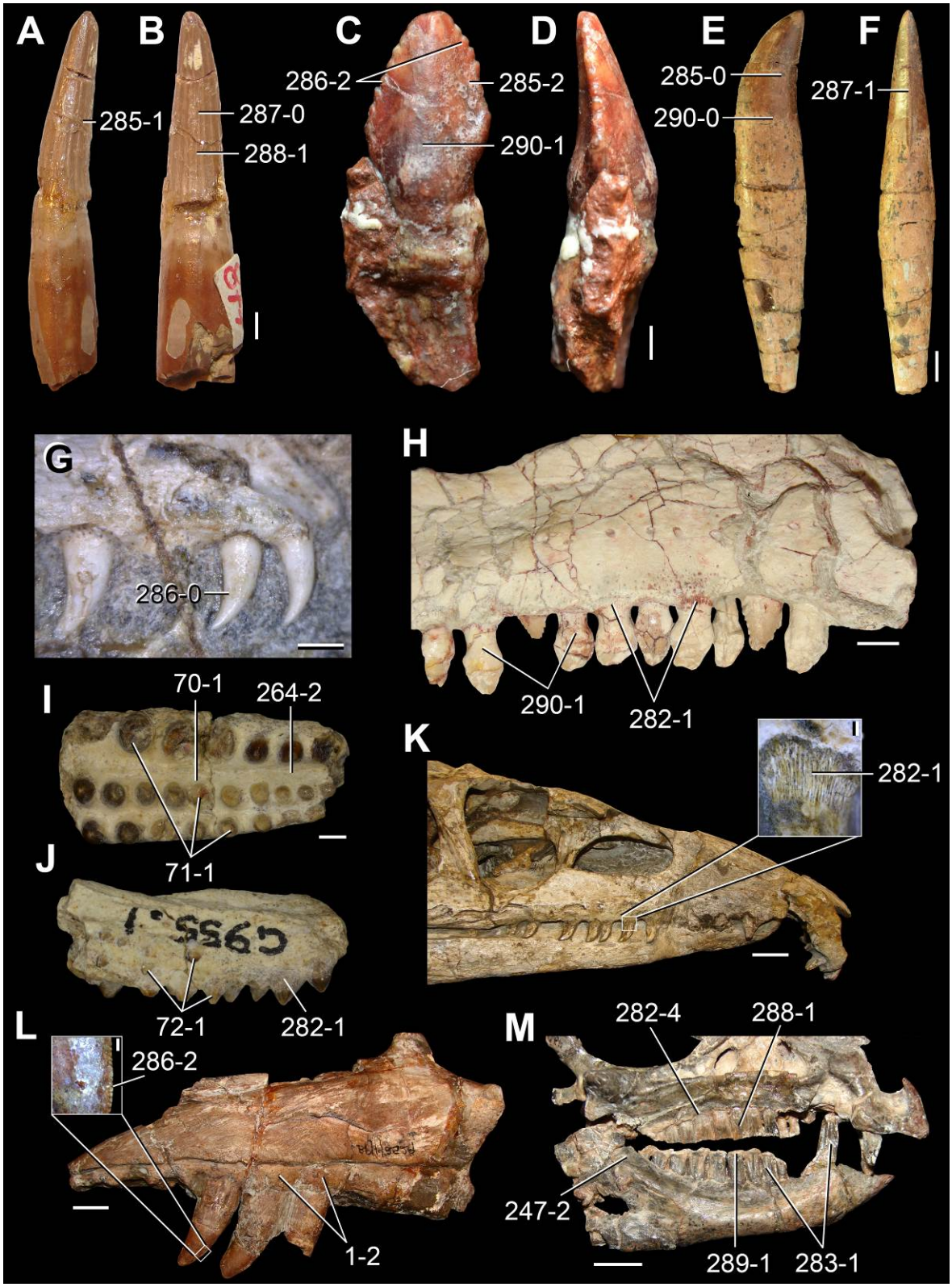

Figure 5.19. Teeth and tooth implantation in Triassic and Early Jurassic archosauromorphs. Isolated teeth of *Tanystropheus longobardicus* (SMNS 54147) (A, B), *Azendohsaurus laaroussi* (MNHN-ALM 424) (C, D) and *Chalishevia cothurnata* (PIN 4366/8) (E, F), and teeth in situ of *Prolacerta broomi* (BP/1/4504a) (G), *Azendohsaurus madagaskarensis* (UA 8-29-97-160) (H), "*Rhynchosaurus*" *brodiei* (WARMS G955) (I, J), *Proterosuchus fergusi* (BSPG 1934-VIII-514, reversed) (K), *Erythrosuchus africanus* (BP/1/2529, reversed) (L) and *Heterodontosaurus tucki* (SAM-PK-K1332) (M) in labial (A, C, E, G, H, K, M), mesial (B, D, F), occlusal (I), and lingual (J, L) views. Close-up of ankylothecodont tooth implantation in K and mesial denticles in L. Numbers refer to character states. Scale bars equal 2 mm in A, B, I, J, 1 mm in C, D, G, close-up of K, close-up of L, 5 mm in E, F, H, 2 cm in K, L, and 1 cm in M.

3) Long and slender cervical ribs. The supposed prolacertiforms *Protorosaurus speneri*, *Amotosaurus rotfeldensis*, *Macrocnemus bassanii* and *Tanystropheus longobardicus* possess very long cervical ribs, which are two times longer than their respective centra and oriented parallel to the neck (character 327-2). Nevertheless, basal archosauriforms also possess this character state (e.g. *Proterosuchus alexanderi*: NMQR 1484; *Euparkeria capensis*: SAM-PK-13665) and, as a result, it is optimized as an apomorphy of Archosauromorpha as a whole.

4) Lacrimal does not meet the nasal. This character state is as a result of the contact between the maxilla and prefrontal (character 59-1) and is widely distributed among basal saurians, including early lepidosauromorphs (Evans, 1980; Fraser, 1982), rhynchosaurs (e.g. *Mesosuchus browni*: SAM-PK-6536; *Rhynchosaurus articeps*: NHMUK R1236) and several supposed prolacertiforms (e.g. *Tanystropheus longobardicus*: Wild, 1973; *Jesairosaurus lehmani*: ZAR 08). By contrast, the lacrimal contacts the nasal in *Prolacerta broomi* (e.g. BP/1/471), basal archosauriforms (e.g. *Proterosuchus fergusi*: BSPG 1934 VII 514, RC 846; *Erythrosuchus africanus*: BP/1/5207; *Euparkeria capensis*: SAM-PK-5867) and apparently in *Protorosaurus speneri* (Gottmann-Quesada and Sander, 2009). Therefore, the absence of a contact between the lacrimal and nasal is optimized as a synapomorphy of the clade that includes tanystropheids and more crownward archosauromorphs, which is subsequently reversed in prolacertids and archosauriforms.

5) Loss of trunk intercentra. Most supposed prolacertiforms lack intercentra in the trunk series (e.g. *Protorosaurus speneri*: BSPG 1995 I 5; *Macrocnemus bassanii*: PIMUZ T4822; *Jesairosaurus lehmani*: ZAR 11, 13), but they may occur in the posterior dorsal series of some tanystropheids (e.g. *Amotosaurus rotfeldensis*: SMNS

90600). The absence of trunk intercentra is optimized as an apomorphy distributed among prolacertiform-grade level archosauromorphs and intercentra are reacquired in the clade that includes rhynchosaurs and more crownward archosauromorphs.

The presence of low and elongate cervical neural spines and absence of trunk intercentra are character states that are consistent with the hypothesis of monophyly of Prolacertiformes (sensu Jalil, 1997), but the other three supposed synapomorphies listed for the group are not consistent with this hypothesis. By contrast, multiple other character states are shared by some supposed prolacertiforms and more crownward archosauromorphs, but are absent in other supposed prolacertiforms (e.g. premaxilla with a postnarial process that forms most of the border of the external naris, 5 or more tooth positions in the premaxilla, maxilla without contact with prefrontal, labiolingual compression of the marginal dentition, pseudolagenar recess between the ventral surface of the ventral ramus of the opisthotic and the basal tubera, anterior and middle postaxial cervical neural spines without an anterior overhang, postaxial cervical vertebrae with epipophysis, and interclavicle without anterior process; Figs. 5.16−5.19). All these characters provide substantial evidence for the non-monophyly of “Prolacertiformes” sensu Jalil (1997) and 19 additional steps are necessary to recover the monophyly of the group under a topologically constrained search. In particular, some of the nodes that include some supposed prolacertiforms to the exclusion of others possess relatively high Bremer supports (>5; e.g. *Azendohsaurus* + Archosauriformes, Rhynchosauria + Archosauriformes, Prolacertidae + Archosauriformes) following the pruning of fragmentary taxa (Fig. 5.20). As a result, the hypothesis of monophyly of “Prolacertiformes” is rejected here. Instead, taxa previously identified as prolacertiforms form a polyphyletic assemblage distributed among the non-archosauriform archosauromorph region of the diapsid tree.

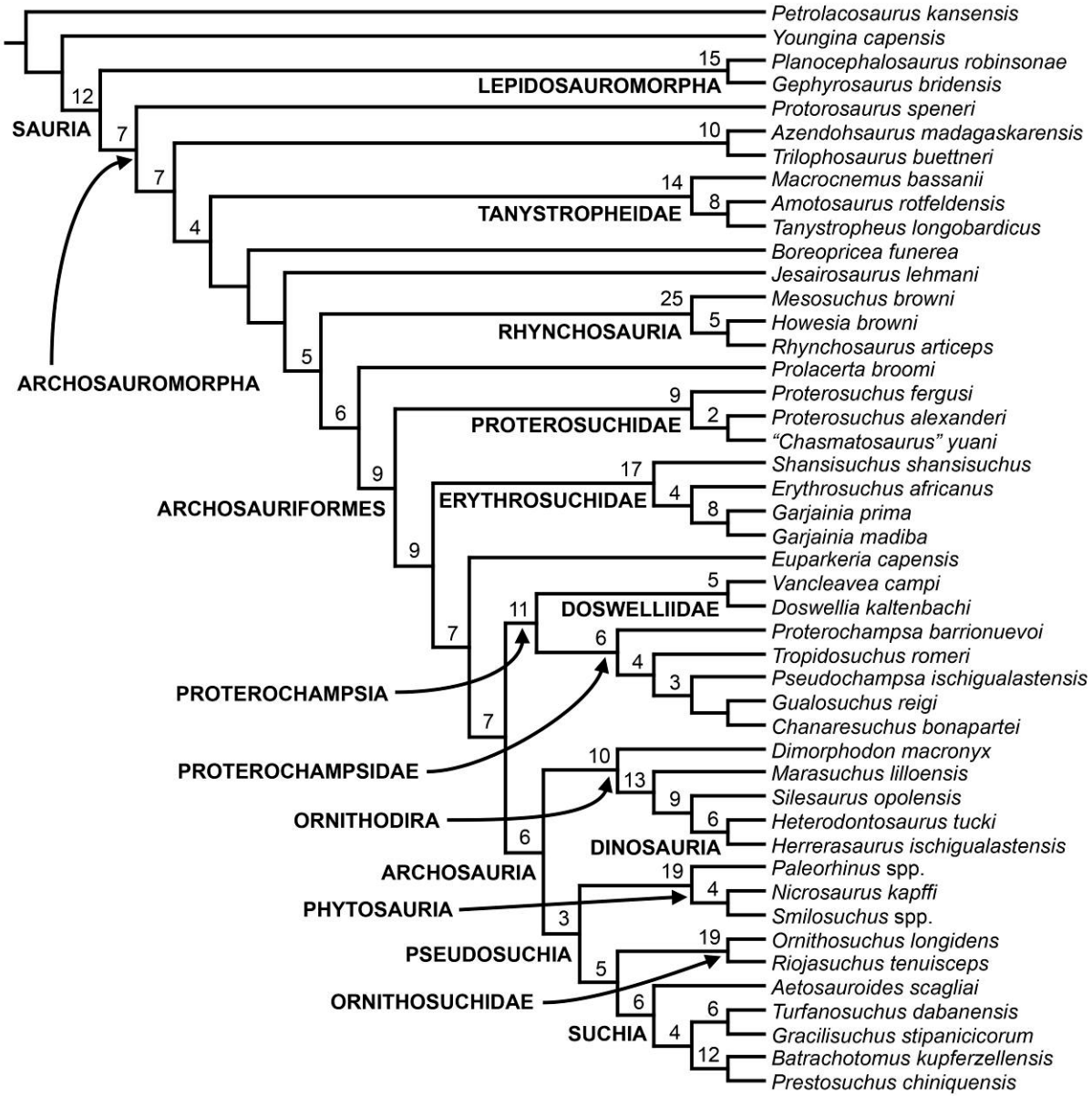

Figure 5.20. Bremer supports recovered after the pruning a posteriori of fragmentary terminals in analysis 3.

5.5.2. *The taxonomic content and monophyly of Proterosuchidae*

The 24 terminals sampled in this data matrix that were historically considered as proterosuchids are found as a polyphyletic assemblage, with different taxa being variously placed as the immediate sister taxon of archosauriforms (*Tasmaniosaurus triassicus*), very basal archosauriforms (e.g. *Proterosuchus* spp., *Kalisuchus rewanensis*, *Sarmatosuchus otschevi*) and even within the crown-group Archosauria ("*Chasmatosaurus ultimus*") (Fig. 5.13: blue box). In addition, the proterosuchid clade recovered in the quatitative analysis of Gower and Sennikov (1997) (i.e. *Proterosuchus* spp., *Fugusuchus hejiapanensis* and *Sarmatosuchus otschevi*) is recovered here as paraphyletic. *Fugusuchus hejiapanensis* and *Sarmatosuchus otschevi* are found to be successively more closely related, respectively, to erythrosuchids and more crownward archosauriforms than they are to *Proterosuchus* spp. This result is in agreement with that recovered by Ezcurra et al. (2010). Proterosuchidae sensu Gower and Sennikov (1997) was supported by three synapomorphies that are discussed as follows.

1) Downturned premaxilla. This character state (character 29-2) is restricted to rhynchosaurids (*Rhynchosaurus articeps* and *Bentonyx sidensis*), *Proterosuchus* spp., "*Chasmatosaurus*" *yuani*, *Archosaurus rossicus* and *Sarmatosuchus otschevi* among non-archosaurian archosauromorphs (Fig. 5.16). The condition present in rhynchosaurids has been clearly acquired independently from that of basal archosauriforms. As a result, the distribution of this character state is consistent with the monophyly of Proterosuchidae sensu Gower and Sennikov (1997). However, this character state optimizes in the current phylogenetic analysis as the plesiomorphic condition for Archosauriformes, and is subsequently lost in erythrosuchids and more derived archosauriforms.

2) Fully developed teeth tightly contacting alveolar bone. This condition describes an ankylothecodont tooth implantation (character 282-1) and is present in *Trilophosaurus buettneri*, rhynchosaurs, *Prolacerta broomi*, *Tasmaniosaurus triassicus* and several basal archosauriforms (Fig. 5.19). As a result, the current phylogenetic analysis optimizes the appearance of an ankylothecodont tooth implantation as a synapomorphy of the clade that includes rhynchosaurs and more crownward archosaromorphs, with the character state being retained by basal archosauriforms (e.g. *Proterosuchus* spp., *Sarmatosuchus otschevi*). Therefore, the distribution of this character state does not support the monophyly of Proterosuchidae sensu Gower and Sennikov (1997).

3) Cultriform process of the parabasisphenoid dorsoventrally constricted towards the base. The cultriform process of the parabasisphenoid continuously tapers anteriorly, without a dorsoventral constriction of its base, in *Proterosuchus fergusi* (BP/1/3993) and *Proterosuchus goweri* (NMQR 880). By contrast, the cultriform process is dorsoventrally compressed at its base in *Prolacerta broomi* (GHG 431, CT data), *Fugusuchus hejiapanensis* and *Euparkeria capensis* (character 228-1) (Gower and Sennikov, 1996). The latter condition is optimized as independently acquired by the three above-mentioned species and, as a result, is interpreted as a non-phylogenetically informative character in the current data set.

Therefore, the only synapomorphy of Proterosuchidae reported by Gower and Sennikov (1997) that is consistent in the current data set with their hypothesis of proterosuchid taxonomic content is the presence of a strongly downturned premaxillary body. However, there are at least eight character states in this analysis that favour a position of *Fugusuchus hejiapanensis* and *Sarmatosuchus otschevi* as more closely related to erythrosuchids and more crownward archosauriforms than to

Proterosuchus spp. (e.g. 15–22 tooth positions in the maxilla, basal tubera of the basioccipital partially connected to each other, occipital neck of the basioccipital distinctly separating the occipital condyle from the basioccipital body, intertuberal plate of the parabasisphenoid straight, parabasisphenoid oblique, with a posterodorsally-to-anteroventrally oriented main axis). Six additional steps are necessary to recover a monophyletic Proterosuchidae sensu Gower and Sennikov (1997) under a topologically constrained search.

Beyond the taxonomic content of Proterosuchidae suggested by the analysis of Gower and Sennikov (1997), there are multiple other taxa that have been historically identified as proterosuchids that are included here in a quantitative analysis for the first time. The majority of these taxa are found to not be members of Proterosuchidae and their phylogenetic positions are discussed in the following categories.

Immediate sister taxon of Archosauriformes. *Tasmaniosaurus triassicus* from the Lower Triassic of Australia has been historically considered a proterosuchid (Camp and Banks, 1978; Thulborn, 1986; Ezcurra et al., 2013; Ezcurra, 2014), but is recovered here as the sister taxon of Archosauriformes (Figs. 5.5, 5.6, 5.14). Three synapomorphies support the position of *Tasmaniosaurus triassicus* outside this clade (see synapomorphies of Archosauriformes, above). Three additional steps are necessary to place *Tasmaniosaurus triassicus* within Proterosuchidae, and two additional steps to place it within Archosauriformes, as the sister taxon of the clade composed of *Fugusuchus hejiapanensis* and more crownward archosauriforms.

Taxa more derived than proterosuchids. Several of the supposed proterosuchids are recovered here as more closely related to erythrosuchids and more crownward archosauriforms than to *Proterosuchus* spp. and other proterosuchids. *Kalisuchus rewanensis* is recovered in a polytomy together with *Fugusuchus hejiapanensis*,

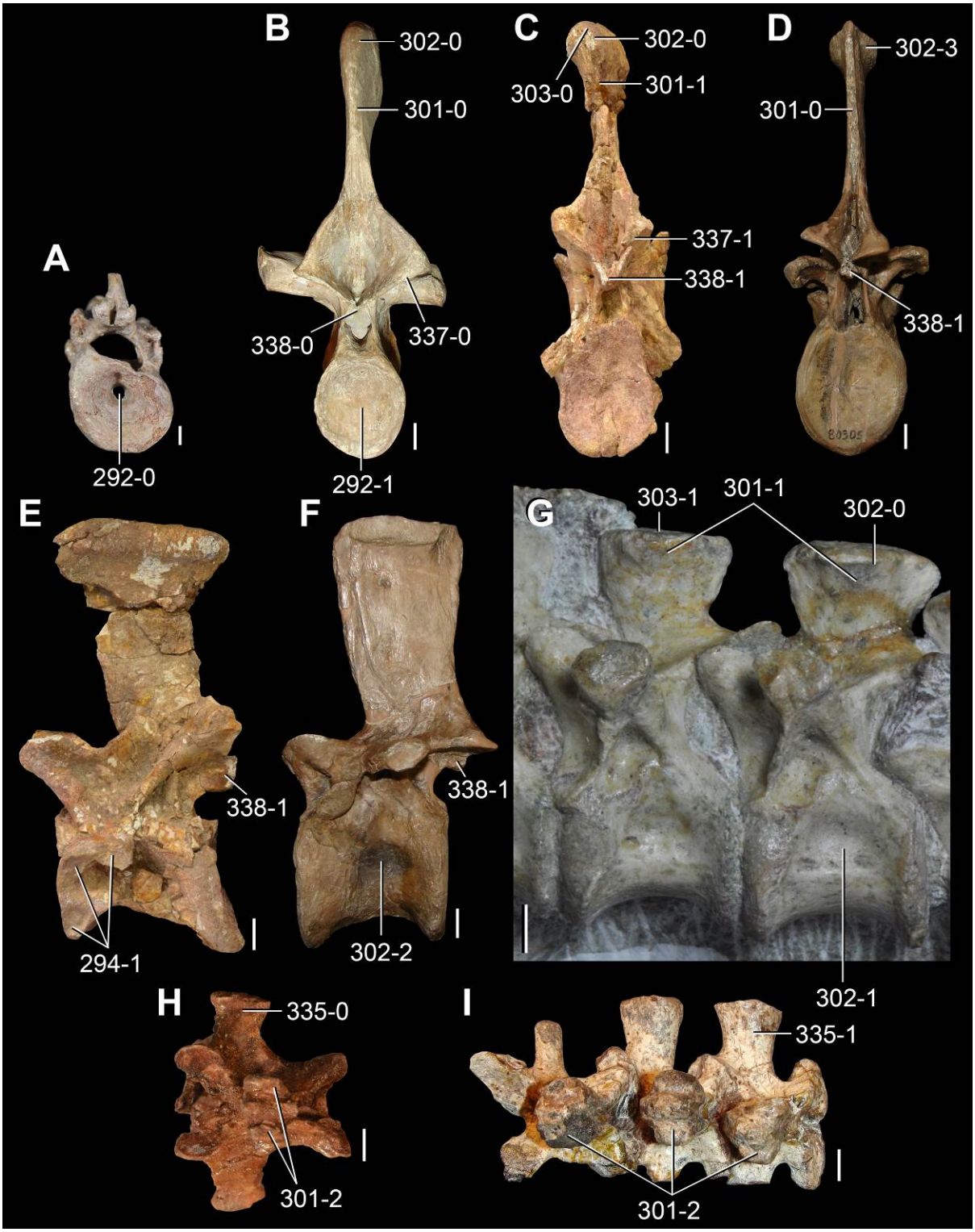

Figure 5.21. Presacral vertebrae of Permo-Triassic archosauromorphs in posterior (A−D), lateral (E−G), and dorsal (H, I) views. *Aenigmastropheus parringtoni* (UMZC T836) (A), *Tanystropheus longobardicus* (SMNS 55341) (B), *Guchengosuchus shiguaiensis* (IVPP V8808-10) (C, E), *Batrachotomus kupferzellensis* (SMNS 80296, reversed) (D, F), *Euparkeria capensis* (SAM-PK-6047A) (G), *Prolacerta broomi* (BP/1/2675) (H) and *Proterosuchus fergusi* (GHG 363) (I). Numbers refer to character states. Scale bars equal 2 mm in A, G, H, and 1 cm in B−F, I.

Sarmatosuchus otschevi and a clade that includes more crownward archosauriforms (Fig. 5.12). The presence of interdental plates along the entire alveolar margin of the premaxilla, maxilla and dentary (1:1→2) supports the position of *Kalisuchus rewanensis* as more derived among archosauriforms than proterosuchids. The "Long Reef proterosuchid" (SAM P41754; Kear, 2009) and *Vonhuenia friedrichi* are found as either the sister taxa of all archosauriforms with the exception of proterosuchids or as potential erythrosuchids (Fig. 5.13). These terminals are found as more derived than proterosuchids because of the presence of cervical and dorsal vertebrae with a gradual transverse expansion of the distal half of the neural spine that lacks mammillary processes (301:2→1) (Figs. 5.3, 5.21), and, in the case of *Vonhuenia friedrichi*, by the presence of a postzygodiapophyseal lamina in posterior cervical and/or anterior dorsal vertebrae (298:0→1) (Fig. 5.22). Only one additional step is necessary to place the "Long Reef proterosuchid" within Proterosuchidae and two extra steps are required to place *Vonhuenia friedrichi* within this clade. As a result, the non-proterosuchid affinities found here for *Vonhuenia friedrichi* bolster the hypothesis that it is a different taxon to the probably sympatric proterosuchid "*Blomosuchus georgii*".

Chasmatosuchus rossicus and *Chasmatosuchus magnus* are found in all the MPTs as more closely related to each other than to other basal archosauriforms. The *Chasmatosuchus* group is recovered either as the sister taxon of the clade formed by erythrosuchids and more crownward archosauriforms, within Erythrosuchidae, or as one of the sister taxa of the clade composed of *Euparkeria capensis* and more derived archosauriforms (Fig. 5.14). The position of *Chasmatosuchus* spp. as more derived than proterosuchids is supported by the presence of a posterior centrodiapophyseal lamina in cervical and/or anterior dorsal vertebrae (296:0→1) (Fig. 5.22) and the

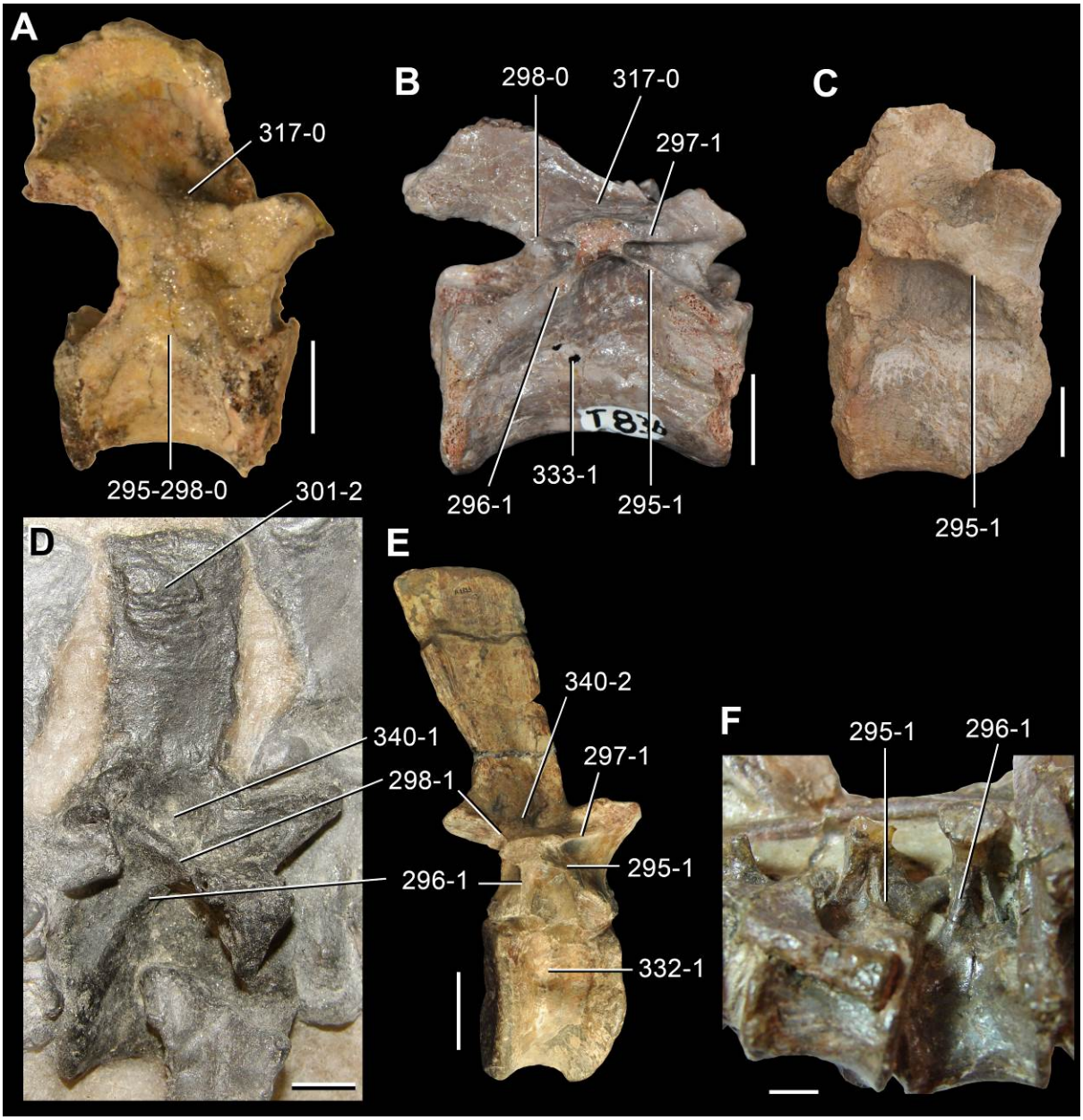

Figure 5.22. Dorsal vertebrae of Permo-Triassic neodiapsids in lateral (A−E) and ventrolateral (F) views. *Youngina capensis* (BP/1/3859) (A), *Aenigmastropheus parringtoni* (UMZC T836) (B), *Tarjadia ruthae* (PULR 63, reversed) (C), *Protorosaurus speneri* (BSPG 1995 I 5 [cast of WMSN P47361]) (D), *Erythrosuchus africanus* (NHMUK R3592) (E) and *Chanaresuchus bonapartei* (MCZ 4037) (F). Numbers refer to character states. Scale bars equal 2 mm in A, 5 mm in B, D, F, 1 cm in C, and 5 cm in E.

monophyly of the genus is supported by the presence of anterior and middle cervical vertebrae with a longitudinal tuberosity strongly developed as a prominent and thick, wing-like shelf extending posteriorly from the base of the transverse process (313:0→1), and postaxial cervical vertebrae with a deep pocket or pit immediately lateral to the base of the neural spine (317:1→2) (Fig. 5.4, 5.17, 5.22). Three additional steps are necessary to place both species of *Chasmatosuchus* within Proterosuchidae and two extra steps to force *Chasmatosuchus* to be non-monophyletic. When "*Gamosaurus lozovskii*" and *Chasmatosuchus magnus* are scored as different terminals, they are recovered in an unresolved clade together with *Chasmatosuchus rossicus* in all the MPTs. Therefore, this result supports the hypothesis that "*Gamosaurus lozovskii*" is a subjective junior synonym of *Chasmatosuchus magnus*. However, the internal relationships of this clade are not resolved because of the absence of diagnostic characters (Fig. 5.14).

"*Chasmatosaurus ultimus*" and *Koilamasuchus gonzalezdiazi* are found deeply nested within the crown-group Archosauria, as members of Suchia (Figs. 5.7, 5.8), which supports the non-proterosuchid affinities for these taxa as recently proposed by Ezcurra et al. (2010) and Liu et al. (in press). *Koilamasuchus gonzalezdiazi* shares with suchians the presence of dorsal vertebrae with a well-rimmed lateral fossa on the centrum below the neurocentral suture (332:1→2) (Fig. 5.21), humerus with an approximately symmetric proximal end in anterior view (391:1→0), and preacetabular process of the ilium longer than two-thirds of its height and not extending beyond the level of the anterior margin of the pubic peduncle (428:1→2), and with gracilisuchids and paracrocodylomorphs the presence of paramedian presacral dorsal osteoderms with a distinct anterior process on its anterior edge (557:0→1) (convergently present in *Vancleavea campi* and *Euparkeria capensis*).

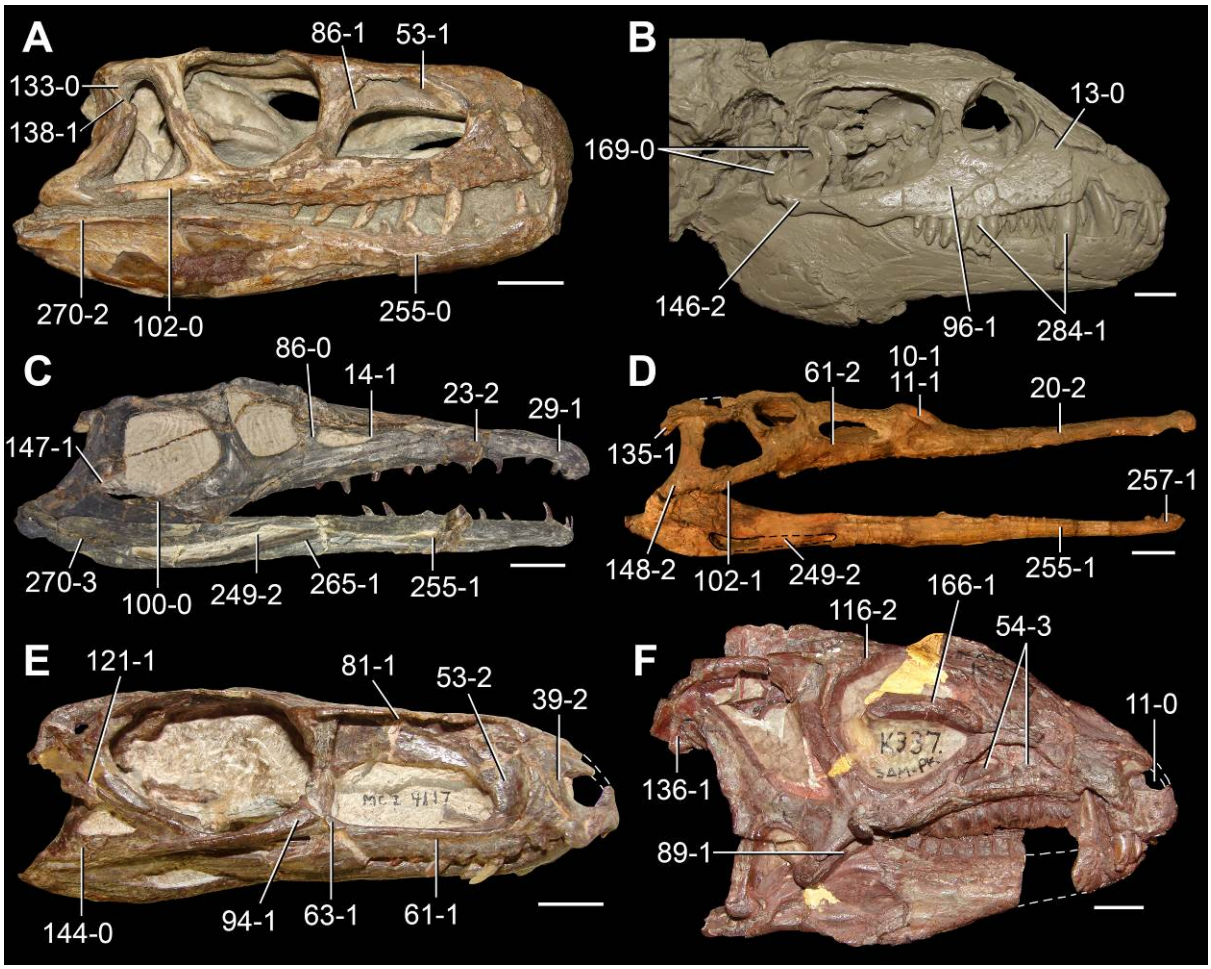

Figure 5.23. Skulls of Triassic and Early Jurassic archosauriforms in lateral view. *Euparkeria capensis* (SAM-PK-5867) (A), *Vancleavea campi* (USNM 508519 [cast of GR 138]) (B), *Gualosuchus reigi* (PVL 4576) (C), *Parasuchus hislopi* (ISI R42, reversed) (D), *Gracilisuchus stipanicicorum* (MCZ 4117) (E) and *Heterodontosaurus tucki* (SAM-PK-K337) (F). Numbers refer to character states. Scale bars equal 1cm in A, B, E, F, 2 cm in C, and 5 cm in D.

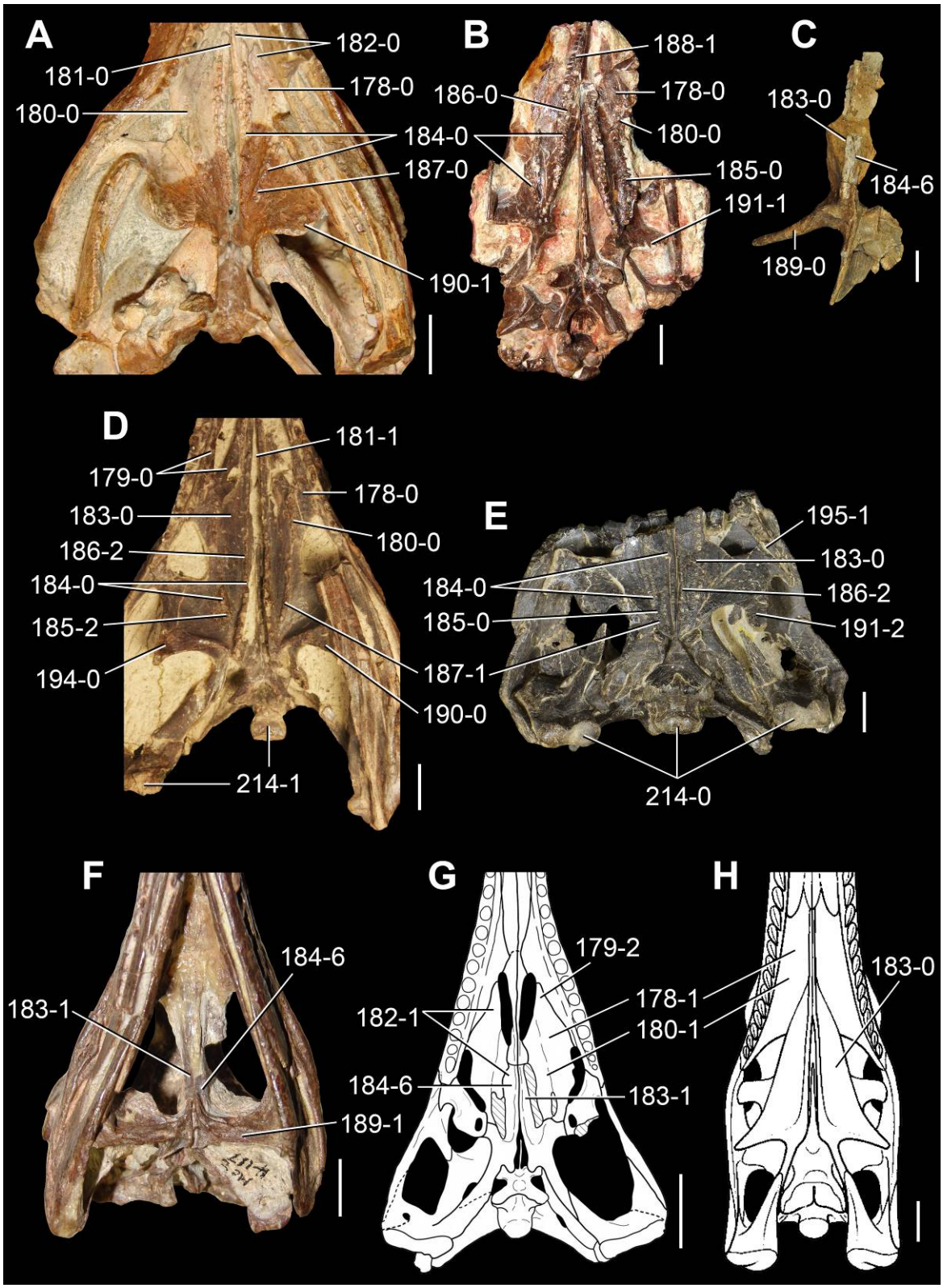

Figure 5.24. Skulls (A, B, D−H) and isolated pterygoid (C) of Permo-Triassic archosauromorphs in ventral view. *Mesosuchus browni* (SAM-PK-6536) (A), *Prolacerta broomi* (BP/1/5066) (B), *Erythrosuchus africanus* (NHMUK R3592) (C), *Chanaresuchus bonapartei* (PVL 4586) (D), *Doswellia kaltenbachi* (USNM 214823) (E), *Gracilisuchus stipanicicorum* (MCZ 4117) (F), *Paleorhinus angustifrons* (G) and *Herrerasaurus ischigualastensis* (H). Numbers refer to character states. Scale bars equal 1 cm in A, D−F, 5 mm in B, 5 cm in C, G, and 2 cm in H. (G) modified from Butler et al. (2013) and (H) modified from Sereno and Novas (1993).

Nevertheless, only one additional step is necessary to place *Koilamasuchus gonzalezdiazi* as the sister taxon of *Euparkeria capensis*, which is a more similar position to that recovered by Ezcurra et al. (2010). Five extra steps are required to place *Koilamasuchus gonzalezdiazi* within Proterosuchidae. Regarding "*Chasmatosaurus ultimus*", five synapomorphies support its position within Archosauria, including an antorbital fossa present on the ascending and horizontal processes of the maxilla, but not reaching the posteroventral corner of the fenestra (53:1→2) (Fig. 5.23), palatal process on the anteromedial surface of the maxilla meeting its counterpart at the midline (64:1→2), contact between vomer and maxilla (176:0→1), absence of palatine teeth (180:0→1) (Fig. 5.24), and dentary with a longitudinal groove approximately centred on the lateral surface (255:0→1) (Fig. 5.23). In addition, "*Chasmatosuchus ultimus*" is placed within Suchia in the present phylogenetic analysis because of the presence of a palatal process of the maxilla placed distinctly dorsal to the bases of the interdental plates (65:0→1), and dorsal margin of the anterior portion of the dentary dorsally expanded compared to the dorsal margin of the posterior portion (257:0→1) (Fig. 5.23). The position of "*Chasmatosaurus ultimus*" outside Proterosuchidae is very well supported and 15 additional steps are required to place it within Proterosuchidae under a topologically constrained search.

Unambiguous proterosuchids. The results of the present phylogenetic analysis restrict the unambiguous taxonomic content of Proterosuchidae to only five valid species: *Archosaurus rossicus*, "*Chasmatosaurus*" *yuani*, *Proterosuchus fergusi*, *Proterosuchus goweri* and *Proterosuchus alexanderi*. "*Blomosuchus georgii*" is also a member of Proterosuchidae, but it is considered here a nomen dubium. Thirteen synapomorphies diagnose Proterosuchidae in the present analysis (see

synapomorphies for Proterosuchidae, above) and the clade is well supported by bootstrap frequencies (>80%) and Bremer support (3 including all terminals and 9 excluding fragmentary terminals) (Figs. 5.6, 5.20). Twenty-three additional steps are required to force all taxa historically identified as proterosuchids to form a single monophyletic group. Interestingly, the topologically constrained search to generate a monophyletic group including all taxa historically identified as proterosuchids also results in a monophyletic Proterosuchia (i.e. Proterosuchidae + Erythrosuchidae). As a result, the hypothesis of a taxonomically inclusive Proterosuchidae, including all historically referred species, is rejected here.

The interrelationships within Proterosuchidae are completely unresolved when its six species are included in the strict consensus tree (Fig. 5.13). This is a result of the instability generated by *Archosaurus rossicus* and "*Blomosuchus georgii*", which are represented by a single premaxilla and a parabasisphenoid, respectively. The topology within Proterosuchidae is resolved in the strict reduced consensus tree generated after the a posteriori pruning of *Archosaurus rossicus* and "*Blomosuchus georgii*". In this consensus tree, *Proterosuchus goweri* is the sister taxon of "*Chasmatosaurus*" *yuani* and *Proterosuchus fergusi* and *Proterosuchus alexanderi* represent the successive sister taxa, respectively, of this clade (Fig. 5.5). The clade composed of *Proterosuchus alexanderi*, *Proterosuchus goweri* and "*Chasmatosaurus*" *yuani* is supported by four synapomorphies and that formed by the latter two species is supported by one character state (see synapomorphy list, above). Two additional steps are necessary to constrain a monophyletic group including only the South African species of the genus *Proterosuchus*.

The holotype of *Proterosuchus fergusi* (SAM-PK-591) is recovered in all possible positions within Proterosuchidae or alternatively as one of the most

immediate outgroups of Archosauriformes. This result bolsters the conclusion that this specimen cannot be distinguished from other proterosuchid species (Chapter 3; Ezcurra and Butler, 2015a).

Ambiguous proterosuchids. "*Chasmatosuchus*" *vjushkovi* and "*Ankistrodon indicus*" are recovered as proterosuchids in some of the MPTs (Fig. 5.14). However, they are also alternatively found immediately outside Archosauriformes or as more closely related to erythrosuchids and more crownward archosauriforms than to proterosuchids. The ambiguity in the phylogenetic position of these species among proterosuchian-grade archosauromorphs is a result of the lack of preservation of diagnostic characters rather than conflicting phylogenetic information. Indeed, the character states of "*Chasmatosuchus*" *vjushkovi* differ in only one scoring from those of *Proterosuchus* spp. (presence of an anteroposteriorly shallow base of the prenarial process of the premaxilla, character 35-0; Fig. 5.16) and scorings are identical between "*Ankistrodon indicus*" and *Proterosuchus* spp. Indeed, "*Ankistrodon indicus*" cannot be differentiated from *Proterosuchus* spp. and "*Chasmatosaurus*" *yuani* and is considered here a nomen dubium. It should be noted that "*Chasmatosuchus*" *vjushkovi* is not recovered in any of the MPTs as the sister taxon or within the clade composed of *Chasmatosuchus magnus* and *Chasmatosuchus rossicus* (Fig. 5.14). This result indicates that "*Chasmatosuchus*" *vjushkovi* does not belong to the genus *Chasmatosuchus*, which represents a group of more crownward archosauriforms. In summary, "*Chasmatosuchus*" *vjushkovi* and "*Ankistrodon indicus*" are potential members of Proterosuchidae, but more information is needed to test unambiguously this hypothesis.

5.5.3. *The taxonomic content and monophyly of Erythrosuchidae*

The eight species historically identified as erythrosuchid that were included in this analysis were recovered more closely related to each other than to other archosauromorphs, resulting in a monophyletic Erythrosuchidae (Fig. 5.11). The taxonomic content of Erythrosuchidae in this analysis consists of *Garjainia prima*, *Garjainia madiba*, *Erythrosuchus africanus*, *Guchengosuchus shiguaiensis*, *Shansisuchus shansisuchus*, *Shansisuchus kuyeheensis*, *Chalishevia cothurnata* and *Cuyosuchus huenei*. Four synapomorphies diagnose Erythrosuchidae in all the MPTs and four additional synapomorphies are recovered in only some MPTs (see synapomorphies for Erythrosuchidae, above). The Bremer support of Erythrosuchidae is 1 and the bootstrap resampling frequencies are also very low when all the terminals are included (Fig. 5.6), but after the pruning of fragmentary terminals the Bremer support of the group increases to 17 (Fig. 5.20). *Cuyosuchus huenei* and *Guchengosuchus shiguaiensis* are recovered as the most basal members of Erythrosuchidae, but their interrelationships are unresolved mainly because of the very limited overlapping elements between both taxa. *Shansisuchus shansisuchus*, *Shansisuchus kuyeheensis* and *Chalishevia cothurnata* are found in a polytomy together with the clade composed of *Erythrosuchus africanus* and *Garjainia* spp. This clade is supported by three synapomorphies in all the trees and six synapomorphies in only some trees (see synapomorphies of the *Shansisuchus shansisuchus* + *Garjainia prima* clade, above). *Shansisuchus shansisuchus* and *Chalishevia cothurnata* are recovered closer to each other than to other erythrosuchids in the strict reduced consensus tree after the a posteriori pruning of *Shansisuchus kuyeheensis* (Fig. 5.14). The *Shansisuchus shansisuchus* and *Chalishevia cothurnata* clade is supported by the presence of an antorbital fossa present on the ascending and horizontal processes of the maxilla, but not reaching the posteroventral corner of the fenestra (53:1→2), and

absence of an excavation immediately lateral to the base of the neural spine in postaxial cervical vertebrae (317:1→0).

Erythrosuchus africanus is found as more closely related to the genus *Garjainia* than to other erythrosuchids, in agreement with the result recovered by Ezcurra et al. (2010). By contrast, Parrish (1992) and Gower and Sennikov (1996) found *Erythrosuchus africanus* as more closely related to *Shansisuchus shansisuchus* than to *Garjainia prima* (= "*Vjushkovia*" *triplicostata*) (Fig. 5.1). Four synapomorphies support the *Erythrosuchus africanus* + *Garjainia* spp. clade in all the MPTs and eight other synapomorphies in only some of the MPTs (see synapomorphies for the *Erythrosuchus africanus* + *Garjainia prima* clade, above). Five additional steps are necessary to force a position for *Erythrosuchus africanus* as more closely related to *Shansisuchus* spp. and *Chalishevia cothurnata* than to *Garjainia* spp.

Parrish (1992) reported two synapomorphies supporting the position of *Erythrosuchus africanus* as more closely related to *Shansisuchus shansisuchus* than to *Garjainia prima*, which are discussed as follows in the context of the present phylogenetic analysis.

1) The external surface of the maxilla adjacent to the anterior and anterodorsal surfaces of the antorbital fenestra is recessed. Parrish (1992) described *Garjainia prima* as lacking an antorbital fossa on the maxilla, resembling the condition in *Fugusuchus hejiapanensis* and proterosuchids. However, *Garjainia prima* possesses an extensive antorbital fossa on the ascending process of the maxilla, but this fossa does not reach the base of the process as it occurs in *Erythrosuchus africanus* and *Shansisuchus shansisuchus* (character 53-1) (Fig. 5.16). As a result, although the observation of Parrish (1992) was not correct regarding *Garjainia prima*, the presence

of an antorbital fossa reaching the base of the ascending process of the maxilla is a feature that potentially supports the hypothesis that *Erythrosuchus africanus* is more closely related to *Shansisuchus shansisuchus* than to *Garjainia prima*.

2) Absence of a pineal foramen. Gower (2003) reported that there is no conclusive evidence for the presence or absence of a pineal foramen in available specimens of *Erythrosuchus africanus*. This observation is followed for the vast majority of specimens referred to *Erythrosuchus africanus*, but in NMQR 1473 this area of the skull is well preserved and there is no pineal foramen (character 157-2), resembling the condition in *Shansisuchus shansisuchus* (IVPP V2501, 2503, 2506, 2508). The holotype of *Garjainia prima* possesses a small, circular pit that is slightly displaced to the left of the sagittal midline of the skull (PIN 2394/5). This pit may represent an incipient pineal foramen, but this interpretation should be considered tentative. Beyond the presence or absence of a pineal foramen in *Garjainia prima*, this feature is absent in the most immediate outgroups of the clade composed of *Garjainia* spp., *Shansisuchus* spp. and *Erythrosuchus* (e.g. *Fugusuchus hejiapanensis*: Cheng, 1980; *Guchengosuchus shiguaiensis*: IVPP V8808-2; *Euparkeria capensis*: SAM-PK-5867). As a result, if a pineal foramen is present in *Garjainia prima* it may represent an autapomorphy of this taxon rather than a symplesiomorphy of Erythrosuchidae that is apomorphically lost in *Erythrosuchus africanus* and *Shansisuchus shansisuchus*.

Gower and Sennikov (1996) also found two synapomorphies supporting a closer relationship between *Erythrosuchus africanus* and *Shansisuchus shansisuchus* rather than with *Garjainia prima*. These two character states are discussed as follows.

1) Ventral ramus of the opisthotic recessed. Gower and Sennikov (1996) described the ventral ramus of the opithotic as poorly developed and recessed within the stapedial groove in *Erythrosuchus africanus* and *Shansisuchus shansisuchus*

(character 205-4). By contrast, in *Garjainia prima*, *Garjainia madiba*, *Fugusuchus hejiapanensis*, *Sarmatosuchus otschevi* and proterosuchids the ventral ramus of the opisthotic is better developed and well exposed in lateral view (Gower and Sennikov, 1996; Gower et al., 2014) (Fig. 5.25). As a result, the poor development of the ventral ramus of the opisthotic is in agreement with the hypothesis of a monophyletic *Erythrosuchus africanus* + *Shansisuchus shansisuchus* clade.

2) Medial margins of exoccipitals make contact for majority of their length. The exoccipitals contact each other on the floor of the endocranial cavity but diverge posteriorly on the dorsal surface of the occipital condyle in proterosuchids (e.g. *Proterosuchus goweri*: NMQR 880; *Proterosuchus alexanderi*: NMQR 1484; *Proterosuchus fergusi*: SAM-PK-K10603) *Fugusuchus hejiapanensis* (Gower and Sennikov, 1996), *Sarmatosuchus otschevi* (PIN 2865/68-1) and *Garjainia prima* (PIN 951/60) (character 208-1). By contrast, the exoccipitals form the entire floor of the posterior end of the endocranial cavity and meet along the dorsal surface of the occipital condyle in *Erythrosuchus africanus* and *Shansisuchus shansisuchus* (Gower and Sennikov, 1996; Gower, 1997). Therefore, this condition also support the potential position of *Erythrosuchus africanus* as more closely related to *Shansisuchus shansisuchus* than to *Garjainia prima*.

The discussion of the character states previously found as synapomorphies of the *Erythrosuchus africanus* and *Shansisuchus shansisuchus* clade indicates that three features support this hypothesis of relationship. However, the current analysis found twelve synapomorphies that support a monophyletic clade including *Erythrosuchus africanus* and *Garjainia* spp., but not *Shansisuchus shansisuchus* (see synapomorphies of the *Erythrosuchus africanus* + *Garjainia prima* clade, above). As a result, the character states shared by *Erythrosuchus africanus* and *Shansisuchus*

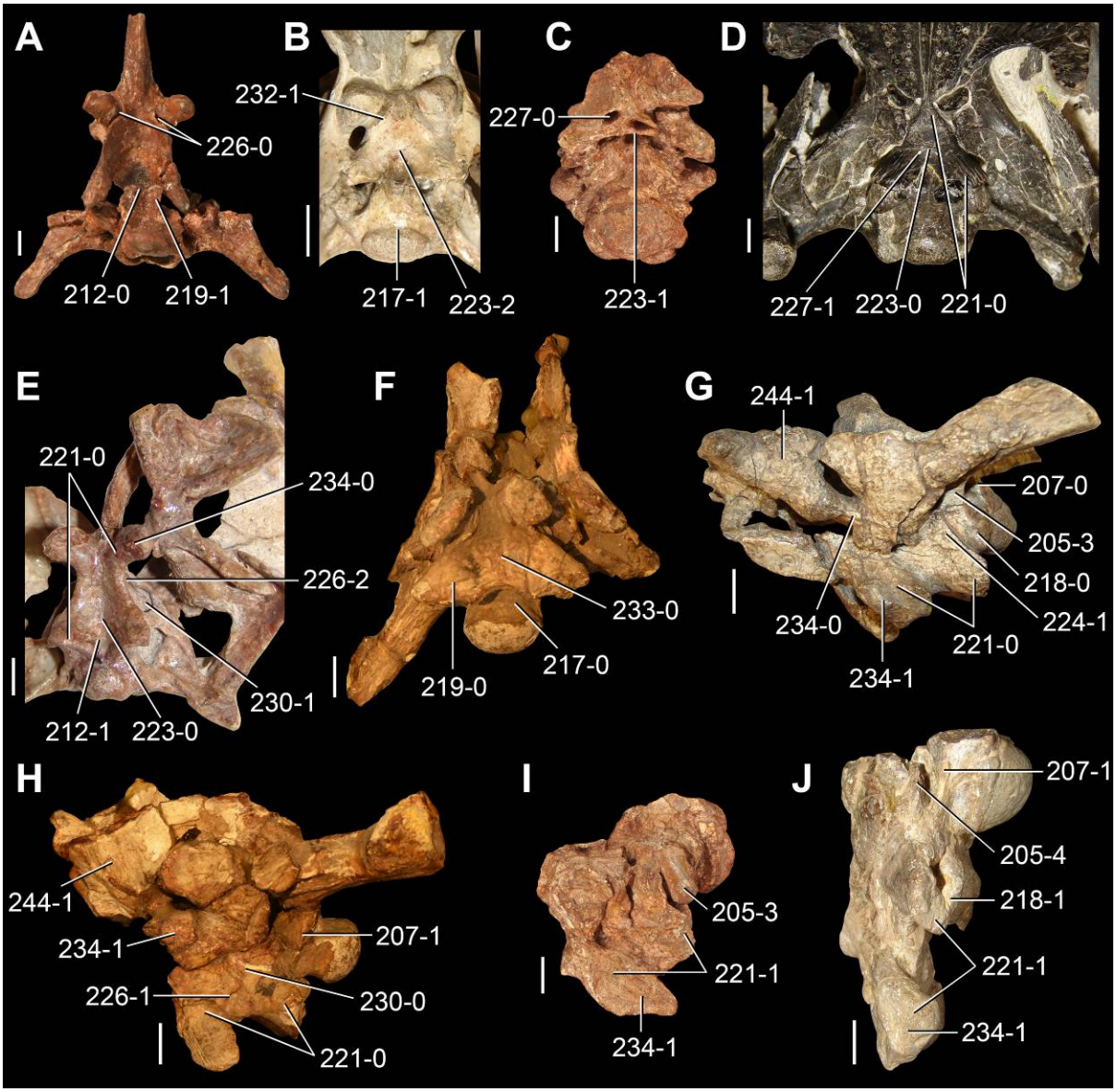

Figure 5.25. Braincases of Triassic archosauromorphs in ventral (A−F) and lateral (G−J) views. *Prolacerta broomi* (BP/1/2675) (A), *Proterosuchus alexanderi* (NMQR 1484) (B), *Garjainia madiba* (BP/1/5525) (C, I), *Doswellia kaltenbachi* (USNM 214823) (D), *Lewisuchus admixtus* (PULR 01) (E), *Parasuchus hislopi* (reversed, ISI R42) (F, H), *Proterosuchus goweri* (NMQR 880) (G) and *Batrachotomus kupferzellensis* (SMNS 80260) (J). Numbers refer to character states. Scale bars equal 2 mm in A, 1 cm in B, C, F−J, and 5 mm in D, E.

shansisuchus are interpreted here as independently acquired in these two species or as plesiomorphic for both species and subsequently lost in *Garjainia* spp.

GHG 7433MI is a probable juvenile erythrosuchid from the *Cynognathus* Assemblage Zone of South Africa that was tentatively referred to *Erythrosuchus africanus* by Gower (2003). The results of the present phylogenetic analysis do not support this assignment and, instead, found this specimen more closely related to *Garjainia* spp. than to other erythrosuchids. A detailed anatomical study of this specimen is necessary in order to determine confidently its taxonomic affinities, but two cranial synapomorphies support its probable referral to the genus *Garjainia* (see synapomorphies of *Garjainia*) and three additional steps are necessary to force a sister taxon relationship between GHG 7433MI and *Erythrosuchus africanus*. The monophyly of the genus *Garjainia* is very well supported in this analysis after the pruning of fragmentary terminals, with a Bremer support of 8 (Fig. 5.20).

5.5.4. *The phylogenetic positions of* Euparkeria *and Proterochampsidae*

Euparkeria capensis and the proterochampsids have been repeatedly found as the closest sister taxa of the crown group Archosauria since the first quantitative phylogenetic analyses (e.g. Benton and Clark, 1988; Sereno and Arcucci, 1990). One exception to this rather consensual hypothesis is the result recovered by Dilkes and Sues (2009), which placed *Euparkeria capensis* as the sister taxon of *Erythrosuchus africanus* and more crownward archosauriforms. However, this result has not been found again in more recent phylogenetic studies (e.g. Brusatte et al., 2010; Ezcurra et al., 2010; Desojo et al., 2011; Nesbitt, 2011; Dilkes and Arcucci, 2012). By contrast, the phylogenetic position of *Euparkeria capensis* and proterochampsids with respect to Archosauria is much more debated. Proterochampsids have been found as the sister

taxon of Archosauria and *Euparkeria capensis* as a more basal archosauriform by multiple, independent phylogenetic analyses in the last 30 years (e.g. Sereno, 1991; Parrish, 1993; Juul, 1994; Benton; 2004; Ezcurra et al., 2010; Desojo et al., 2011; Schoch and Sues, 2013) Nevertheless, Benton and Clark (1988) found *Euparkeria capensis* as the sister taxon of Archosauria and proterochampsids as more basal archosauriforms, and the same result was more recently recovered by Nesbitt (2011) and Dilkes and Arcucci (2012) (but phytosaurs were found outside Archosauria in the latter two analyses).

The present phylogenetic analysis recovered *Euparkeria capensis* as the sister taxon of the clade that includes proterochampsids and archosaurs (Figs. 5.7, 5.10, 5.20), resembling the topology most commonly recovered in previous studies. A total of twelve synapomorphies support this hypothesis (see synapomorphies for the Proterochampsia + Archosauria clade, above) and six of them were also sampled in the analysis of Nesbitt (2011), which placed *Euparkeria capensis* as the closest sister taxon of Archosauria. The scorings for these six characters are compared between both data matrixes as follows.

1) Postparietal absent as a separate ossification (character state 163-2). This character state is represented by character 146 of Nesbitt (2011). The scorings of this character by Nesbitt (2011) are congruent with those of the current study, with the exception that *Mesosuchus browni* is scored as lacking a postparietal here, in agreement with the scoring of Dilkes (1998: character 29). *Tasmaniosaurus triassicus*, proterosuchids, erythrosuchids, *Euparkeria capensis* and probably *Asperoris mnyama* possess a postparietal bone, which is lost in proterochampsids, doswelliids and archosaurs (Ewer, 1965; Cruickshank, 1972; Gower, 2003; Dilkes and Sues, 2009; Nesbitt, 2011; Nesbitt et al., 2013a; Ezcurra, 2014). As a result, the scorings for this

character support the hypothesis of *Euparkeria capensis* as more basal than proterochampsids and archosaurs.

2) Parabasisphenoid horizontal (character state 221-0). This character state is represented by character 97 of Nesbitt (2011), in which all the archosauromorphs sampled were scored as possessing a more vertical parabasisphenoid, with exception of *Mesosuchus browni*, *Prolacerta broomi* and *Proterosuchus fergusi*. The scorings for this character in the present analysis are generally in agreement with those of Nesbitt (2011). However, the bases of the basal tubera and the basipteryoid processes are placed at approximately the same level in lateral view in the parabasisphenoid of proterochampsids (e.g. *Chanaresuchus bonapartei*: MCZ 4037, PULR 07, PVL 4586; *Tropidosuchus romeri*: PVL 4601, 4606; *Proterochampsa barrionuevoi*: PVL 2063), *Doswellia kaltenbachi* (USNM 214823), phytosaurs (*Parasuchus hislopi*: ISI R42; *Paleorhinus angustifrons*: BSPG 1931 X 502; *Nicrosaurus kapffi*: NHMUK R42743), *Riojasuchus tenuisceps* (PVL 3827) and ornithodirans (e.g. *Marasuchus lilloensis*: PVL 3872; *Lewisuchus admixtus*: PULR 01; *Silesaurus opolensis*: Dzik, 2003; *Herrerasaurus ischigualastensis*: PVSJ 407) and these taxa, as a result, are scored as possessing a horizontal parabasisphenoid (Figs. 5.25, 5.26). The present phylogenetic analysis optimizes an oblique (= more vertical) parabasisphenoid as symplesiomorphic for erythrosuchids, *Dorosuchus neoetus* and *Euparkeria capensis*, whereas a horizontal parabasisphenoid is found as a synapomorphy of the clade that includes proterochampsians and archosaurs. An oblique parabasisphenoid is secondarily aquired by the doswelliid *Archeopelta arborensis* and suchian archosaurs.

3) Posterior surangular foramen (character state 273-1). This character state is represented by character 163 of Nesbitt (2011) and all non-archosaurian archosauromorphs were scored as having a posterior surangular foramen in his

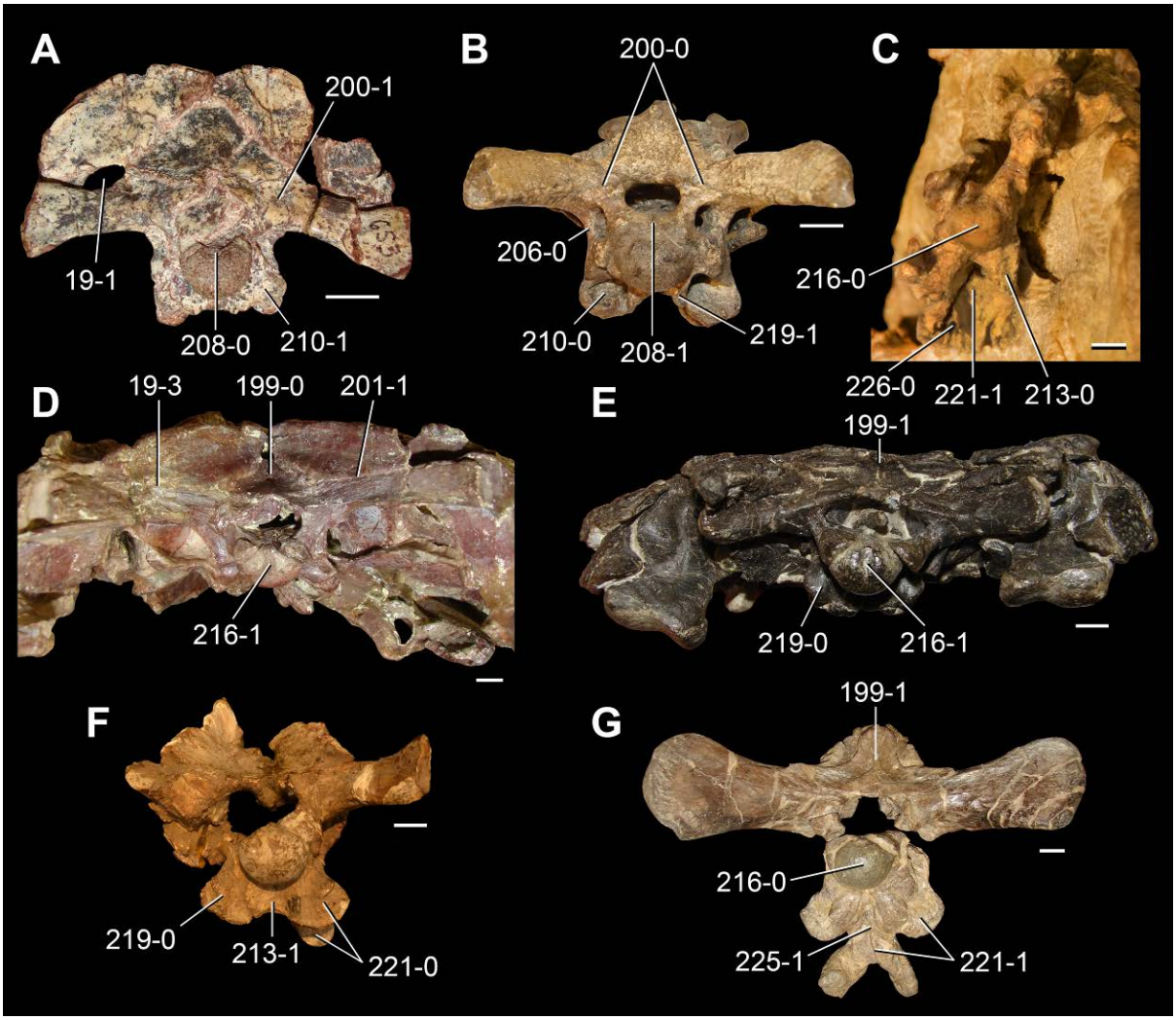

Figure 5.26. Braincases of Triassic archosauromorphs in occipital view. *Azendohsaurus madagaskarensis* (UA 7-20-99653) (A), *Proterosuchus goweri* (NMQR 880) (B), *Euparkeria capensis* (UMZC T692) (C), *Chanaresuchus bonapartei* (MCZ 4037) (D), *Doswellia kaltenbachi* (USNM 214823) (E), *Parasuchus hislopi* (ISI R42) (F) and *Batrachotomus kupferzellensis* (SMNS 80260) (G). Numbers refer to character states. Scale bars equal 1 cm in A, B, F, G, 2 mm in C, and 5 mm in D, E.

analysis. However, a broader variability regarding the absence and presence of this foramen is found among basal archosauromorphs in the current phylogenetic analysis. The presence of a posterior surangular foramen is recovered here as plesiomorphic for Archosauriformes, being retained by proterosuchids, some erythrosuchids and *Euparkeria capensis*. By contrast, this foramen is absent in proterochampsids (e.g. *Proterochampsa barrionuevoi*: Dilkes and Arcucci, 2012; *Gualosuchus reigi*: PULR 05, PVL 4576; the condition is polymorphic in *Chanaresuchus bonapartei*, being present in MCZ 4037 and absent in PULR 07 and PVL 4586), doswelliids (*Doswellia kaltenbachi*: USNM 214823) and several archosaurs (e.g. *Parasuchus hislopi*: ISI R42; *Nundasuchus songeaensis*: Nesbitt et al., 2014; *Turfanosuchus dabanensis*: IVPP V3237; *Gracilisuchus stipanicicorum*: MCZ 4117). As a result, the absence of the foramen is optimized as a synapomorphy of the clade that includes proterochampsians and archosaurs, being subsequently reacquired in different groups of archosaurs (e.g. dinosaurs: Sereno and Novas, 1993; phytosaurs, *Nicrosaurus kapffi*: NHMUK R38036, 42744; ornithosuchids: Walker, 1964; paracrocodylomorphs: Gower, 1999).

4) Cervical and dorsal vertebrae without gradual transverse expansion of the distal half of the neural spine (character state 301-0). This character state is not represented in the character list of Nesbitt (2011), but is related to the presence of a spine table in the presacral neural spines (characters 191 and 197 of Nesbitt, 2011). Nesbitt (2011) scored the presence of spine tables in the cervical and dorsal vertebrae of *Euparkeria capensis*, phytosaurs and non-poposauroid pseudosuchians, and only in the dorsal series of *Prolacerta broomi*, *Proterosuchus fergusi* and some basal dinosaurs. However, the presacral neural spines of *Euparkeria capensis* increase gradually in transverse width towards their distal ends and lack the abrupt transverse

expansion restricted to the distal end of the neural spine that forms a spine table in archosaurs (SAM-PK-5867, 6047A) (Fig. 5.21). Indeed, the condition in *Euparkeria capensis* is identical to that found in the cervical and dorsal vertebrae of multiple basal archosauriforms, including *Vonhuenia friedrichi* (PIN 1025/11) (Fig. 5.3D, E), *Chasmatosuchus rossicus* (PIN 3200/217), *Sarmatosuchus otschevi* (PIN 2865/68-13-19), *Cuyosuchus huenei* (MCNAM PV 2669), *Erythrosuchus africanus* (NHMUK R3592) and *Shansisuchus shansisuchus* (Wang et al., 2013). As a result, a gradual transverse expansion of the neural spine is scored as a different character (character 301) to the presence of a spine table (character 302) in this phylogenetic analaysis. In addition, the transverse expansions present in the middle–posterior cervical and dorsal vertebrae of *Prolacerta broomi* and *Proterosuchus* spp. clearly differ from the spine tables of archosaurs and the pair of distinct lateral projections of the neural spine in these taxa were referred to as mammillary processes by Ezcurra and Butler (2015a; see Chapter 3) because of their close resemblance to the structures present in araeoscelidians (e.g. *Petrolacosaurus kansensis*: Reiz, 1981).

Therefore, the presence of a gradual transverse expansion of the neural spine is found here as a symplesiomorphy of Archosauriformes, which is apomorphically lost in proterochampsids and archosaurs. On the other hand, the presence of spine tables in cervical and dorsal vertebrae is recovered as an apomorphy of Pseudosuchia.

5) Absence of postaxial cervical intercentra (character state 324-1). Nesbitt (2011) scored the presence of postaxial intercentra (character 177 of his data matrix) in *Mesosuchus browni*, *Prolacerta broomi*, *Proterosuchus fergusi*, *Erythrosuchus africanus* and *Euparkeria capensis*, and their absence in proterochampsids, *Vancleavea campi* and archosaurs. The scorings in Nesbitt (2011) are in agreement

with those of the present data matrix and support a more basal position for *Euparkeria capensis* than proterochampsids and archosaurs.

6) Large biceps process on the lateral surface of the coracoid (character state 373-1). This character state is represented by character 225 of Nesbitt (2011). Nesbitt (2011) scored the presence of a swollen tuber on the posteroventral portion of the coracoid in ornithosuchids, suchians and ornithodirans (with some absences in taxa deeply nested within those clades, e.g. poposaurids). The scorings of this character in the present analysis resemble those of Nesbitt (2011), but it is found here that a large, swollen biceps tubercle is also present in proterochampsids with well-preserved coracoids (*Gualosuchus reigi*: PVL 4576; *Chanaresuchus bonapartei*: MCZ 4035) (Fig. 5.27). Therefore, the presence of a large biceps process on the coracoid supports here the close relationship between proterochampsids and archosaurs.

Nesbitt (2011) found seven unambiguous synapomorphies in support of the hypothesis that *Euparkeria capensis* is more closely related to Archosauria than other basal archosauriforms. All of these characters are included in the current analysis and are discussed as follows.

1) Foramen on the medial side of the articular. Nesbitt (2011: character 159) scored the presence of a foramen on the medial side of the articular in *Euparkeria capensis*, phytosaurs, *Riojasuchus tenuisceps* and most suchians. However, this foramen is more broadly distributed among basal archosauriforms, being present in the proterosuchids *Proterosuchus fergusi* (RC 846) and *Proterosuchus alexanderi* (NMQR 1484), and the erythrosuchids *Garjainia madiba* (NMQR 3051) and *Erythrosuchus africanus* (Gower, 2003: 35) (character state 277-1). As a result, the presence of a medial foramen in the articular is optimized here as symplesiomorphic

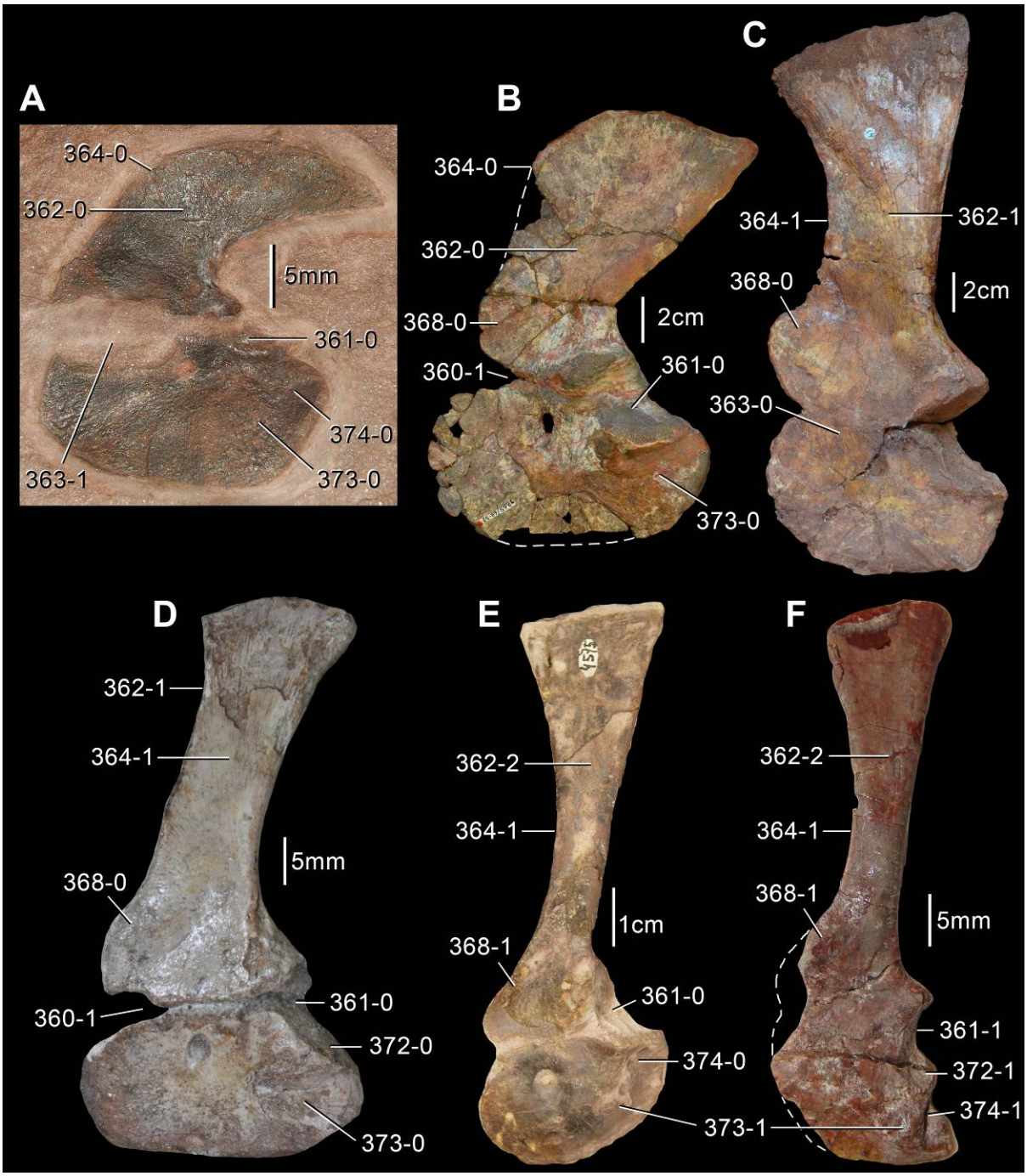

Figure 5.27. Scapulae and coracoids of Triassic archosauromorphs in lateral view. *Amotosaurus rotfeldensis* (SMNS 50830) (A), *Sarmatosuchus otschevi* (PIN 2865/68-37) (B), *Garjainia prima* (PIN 2394/5-32) (C), *Euparkeria capensis* (SAM-PK-5867, reversed) (D), *Chanaresuchus bonapartei* (PVL 4575) (E) and *Lewisuchus admixtus* (reversed, PULR 01) (F). Numbers refer to character states. Scale bars equal 5 mm in A, D, F, 2 cm in B, C, and 1 cm in E.

for Archosauriformes, being retained by *Euparkeria capensis* and pseudosuchians, and subsequently lost in proterochampsians and ornithodirans.

2) Distal ends of neural spines of the cervical vertebrae laterally expanded, and 3) neural spines of the dorsal vertebrae with a lateral expansion and a flat dorsal margin. See discussion above about the presence of a gradual transverse expansion of the neural spine in the presacral vertebrae.

4) Proximal end of the fibula, in proximal view, rounded or slightly elliptical. Nesbitt (2011: character 341) recognized the presence of a rounded to slightly elliptical fibula in proximal view in *Euparkeria capensis*, phytosaurs, ornithosuchids and several non-crocodylomorph suchians. By contrast, proterosuchids, erythrosuchids and proterochampsids were scored as having a transversely compressed proximal fibula. A more variable distribution of this character among archosaurs is recognized here, in which a transversely compressed proximal fibula (character state 490-1) is present in *Nicrosaurus kapffi* (Huene, 1923: fig. 54), *Turfanosuchus dabanensis* (IVPP V3237) and *Aetosauroides scagliai* (PVL 2073). As a result of the absence of a clear phylogenetic signal in this part of the tree, the optimization of this character is ambiguous at the base of Pseudosuchia and the transversely broad proximal end of the fibula of *Euparkeria capensis* is interpreted as autapomorphic.

5) Distal end of the fibula asymmetrical in lateral view. The presence of an asymmetric distal fibula in lateral view was recognized by Nesbitt (2011: character 345) to be present in *Euparkeria capensis*, phytosaurs, ornithosuchids and non-poposauroid basal suchians. The scorings for this character in the present phylogenetic analysis (character 496) are generally similar to those of Nesbitt (2011), but the inclusion of phytosaurs within Pseudosuchia produces an ambiguity for the

optimization of this character at the base of Archosauria because of the variable distribution of the feature among the most basal ornithodirans (e.g. a symmetric distal end of tibia in *Lagerpeton chanerensis* and an asymmetric distal end in *Marasuchus lilloensis*). The ambiguity in the optimization of this character is extended up to the clade that includes *Euparkeria* and more crownward archosauriforms.

6) The posterior corner of the dorsolateral margin of the astragalus dorsally overlaps the calcaneum much more than the anterior portion. Nesbitt (2011: character 360) found this character state to be present in *Euparkeria capensis* and all the archosaurs sampled in his analysis. However, this character state is only recognized here to be present in the ornithosuchid *Riojasuchus tenuisceps* (PVL 3827), whereas in other archosauromorphs the dorsolateral margin of the astragalus overlaps equally the anterior and posterior portions of the calcaneum (character state 505-0). Therefore, this character is not found to be phylogenetically informative in the present analysis.

7) Calcaneal tuber shaft proportions about the same or broader than tall. The scorings for the proportions of the shaft of the calcaneal tuber are congruent in both analyses. The only exception is that *Marasuchus lilloensis* is scored here as having a taller than broad calcaneal tuber (PVL 3870, character state 510-0) rather than approximately as tall as broad (Nesbitt, 2011: character state 376-1). *Euparkeria capensis* possesses a calcaneal tuber with a shaft that is approximately as tall as broad, resembling the condition in non-suchian pseudosuchians (Nesbitt, 2011) and some basal ornithodirans (e.g. *Asilisaurus kongwe*: Nesbitt et al., 2010) (Fig. 5.28). As a result, this character agrees with the hypothesis of a closer relationship between *Euparkeria capensis* and archosaurs, and a more basal position for proterochampsids.

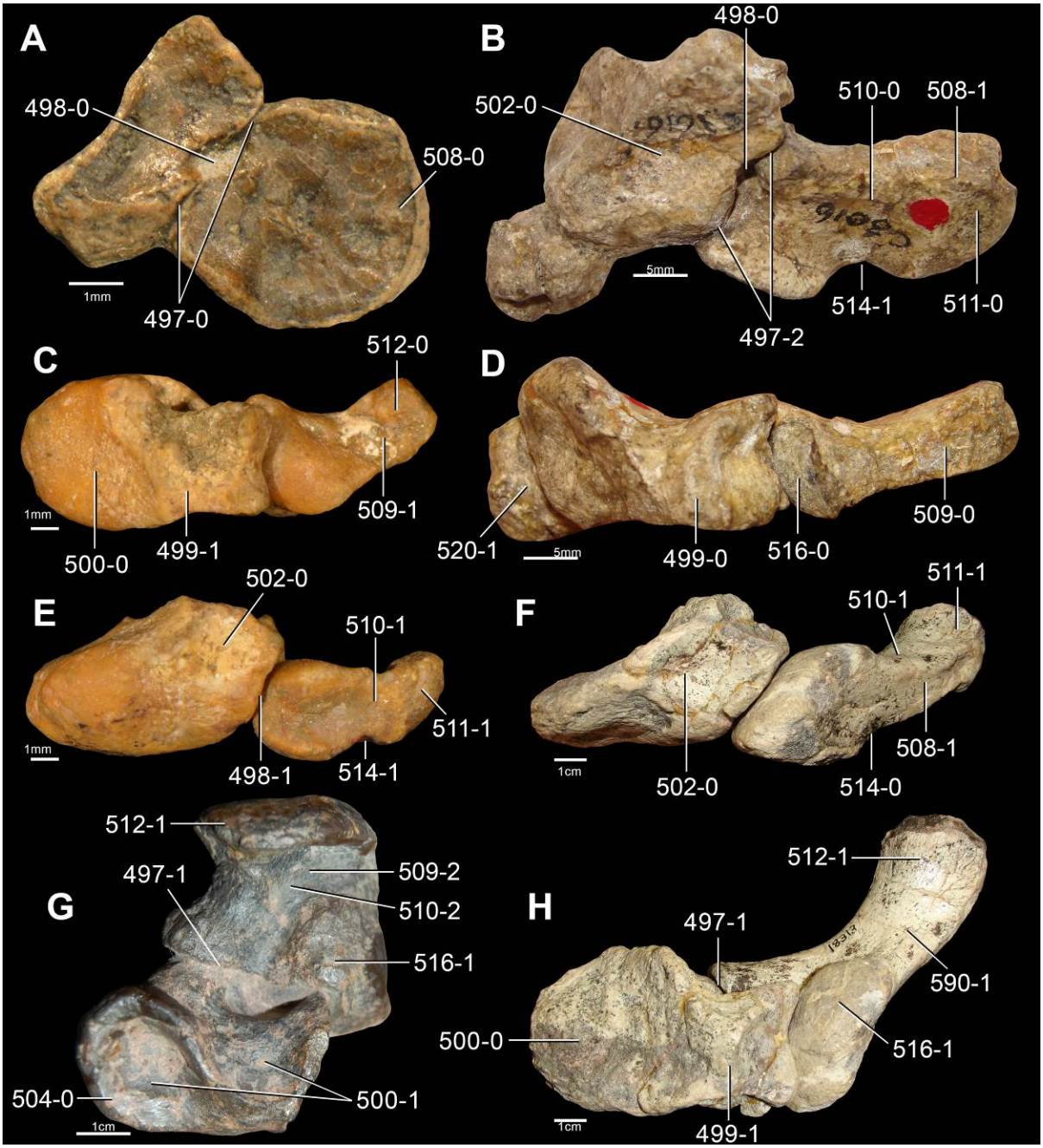

Figure 5.28. Proximal tarsals of Triassic archosauromorphs in anterior/dorsal (A, B, E, F) and proximal (C, D, G, H) views. *Macrocnemus bassanii* (PIMUZ T4822) (A), *Proterosuchus alexanderi* (NMQR 1484) (B, D), *Euparkeria capensis* (UMZC T692) (C, E), *Smilosuchus gregorii* (USNM 18313) (F, H) and *Aetosauroides scagliai* (PVL 2052) (G). Numbers refer to character states. Scale bars equal 1mm A, C, E, 5 mm B, D, and 1 cm F−H.

The revision of the currently available evidence in support of the position of either proterochampsids or *Euparkeria capensis* as the sister taxon of Archosauria clearly favours the hypothesis of a more basal position for *Euparkeria capensis* with respect to proterochampsids. Indeed, only one character is recognized here to provide unambiguous support for the alternative hypothesis. The strong support for the derived position of proterochampsians with respect to other non-archosaurian archosauriforms is indicated by a Bremer support of 7 (Fig. 5.20, after the exclusion of fragmentary taxa) and the 17 additional steps that are necessary to force the monophyly of a *Euparkeria* + Archosauria clade that excludes proterochampsids under a topologically constrained search.

It should be also noted here that *Dorosuchus neoetus* is found in all the MPTs as a more basal taxon than *Euparkeria capensis*, contrasting with the topology of Sookias et al. (2014), which found *Dorosuchus neoetus* as the immediate sister taxon of Phytosauria and Archosauria. Nevertheless, the result recovered here agrees with that of Sookias et al. (2014) in rejecting the monophyly of these two species within a taxonomically inclusive Euparkeriidae (see discussion about the taxonomic content of the group in Sookias and Butler, 2013). The different results between the phylogenetic analysis of Sookias et al. (2014) and those recovered here is mainly because of the decision taken here to exclude the tentatively referred specimens of *Dorosuchus neoetus* from this OTU rather than differences in scorings. The more derived position of *Euparkeria capensis* than *Dorosuchus neoetus* is supported by two braincase synapomorphies (see synapomorphies of the *Euparkeria capensis* + Archosauria clade, above) and the Bremer support is minimal and the bootstrap frequencies are relatively low (<50%). Two additional steps are necessary to recover *Euparkeria*

capensis as a more basal taxon than *Dorosuchus neoetus* or to force the monophyly of Euparkeriidae under topologically constrained searches.

5.5.5. *The phylogenetic position of Doswelliidae*

Doswellia kaltenbachi is a heavily armoured and probably semi-aquatic archosauriform from the Late Triassic of North America (Weems, 1980; Dilkes and Sues, 2009; Sues et al., 2013). The phylogenetic position of this species has been matter of debate with little consensus since its original description by Weems (1980) (Sues et al., 2013). The family Doswelliidae was monospecific for nearly 30 years following the description of its type genus. A monophyletic group of doswelliid species has been recognized only recently (Desojo et al., 2011) and currently includes six species from the Middle and Late Triassic of South America, North America and Europe (Heckert et al., 2012; Lucas et al., 2013; Schoch and Sues, 2013; Sues et al., 2013). All the quantitative phylogenetic analyses that have tested the position of *Doswellia kaltenbachi* or doswelliids as a whole agreed in their placement within Archosauriformes, being more derived than proterosuchids and erythrosuchids, but lying outside the crown-group Archosauria (Benton and Clark, 1988; Dilkes and Sues, 2009; Ezcurra et al., 2010; Desojo et al., 2011; Schoch and Sues, 2013). However, the doswelliids have been alternatively recovered as more closely related to archosaurs than to other archosauriforms (Desojo et al., 2011) or forming a clade with the also probably semi-aquatic proterochampsids and/or the fully aquatic *Vancleavea campi* (Benton and Clark, 1988; Dilkes and Sues, 2009; Ezcurra et al., 2010; Schoch and Sues, 2013).

The present phylogenetic analysis recovered all the supposed doswelliids of the taxonomic sample within a monophyletic group and more closely related to

Vancleavea campi and proterochampsids than to other archosauriforms (Figs. 5.7, 5.13). This result agrees partially with those found by some previous studies, but particularly matches the phylogenetic hypothesis recently proposed by Schoch and Sues (2013), in which *Vancleavea campi* is the most basal doswelliid and proterochampsids their immediate sister taxon. As a result, the families Proterochampsidae and Doswelliidae are included within the clade Proterochampsia.

Ezcurra et al. (2010) found two synapomorphies supporting the position of doswelliids (*Doswellia kaltenbachi* and *Vancleavea campi*) as more closely related to archosaurs than to *Chanaresuchus bonapartei*. These two character states are dicussed as follows.

1) Occipital condyle placed at the same level as the craniomandibular joint. The present phylogenetic analysis optimizes the presence of an occipital condyle placed anterior to the level of the craniomandibular joint (character 214-1) as an apomorphy of the clade that includes *Boreopricea funerea* and more crownward archosauromorphs. As a result, an occipital condyle placed at the same level as the craniomandibular joint is interpreted as independently and apomorphically acquired in *Doswellia kaltenbachi* (USNM 214823) and *Smilosuchus* spp. (UCMP 27200), and does not provide evidence for the non-monophyly of Proterochampsia (Fig. 5. 24).

2) Absence of a posterior groove on the astragalus. The posterior groove of the astragalus is present in all the archosauriforms sampled in the present analysis, with the exception of ornithodirans, *Vancleavea campi* and probably *Tropidosuchus romeri* (character 503-1). Therefore, the posterior groove of the astragalus is optimized as independently lost in these three taxa and is congruent with the hypothesis of monophyly of Proterochampsia.

In a subsequent analysis, Desojo et al. (2011) recovered four synapomorphies supporting a closer relationship between doswelliids and more crownward archosauriforms than with *Chanaresuchus bonapartei*. These four character states are discussed as follows.

1) Ventral process of the postorbital ends close to or at the ventral margin of the orbit. This character state cannot be evaluated in *Doswellia kaltenbachi* because this species lacks a distinct ventral process of the postorbital. As a result, the character is considered here inapplicable for *Doswellia kaltenbachi* and the condition is unknown in *Tarjadia ruthae*, *Archeopelta arborensis* and *Jaxtasuchus salomoni*. *Vancleavea campi* possesses a ventral process of the postorbital that ends well above the ventral margin of the orbit (Nesbitt et al., 2009), resembling the condition in the vast majority of basal archosauriforms. Therefore, the extension of the ventral process of the postorbital does not support the hypothesis of non-monophyly of Proterochampsia.

2) Ventral process of the squamosal anteroventrally projected and constricts the infratemporal fenestra at mid-height. This character state is restricted to phytosaurs, gracilisuchids and the dinosaur *Heterodontosaurus tucki* within the sample of the present phylogenetic analysis. By contrast, *Doswellia kaltenbachi* (USNM 214823) possesses a vertical ventral process of the squamosal, which represents the symplesiomorphic condition for Archosauriformes.

3) Posterior process of the squamosal ventrally curved. *Doswellia kaltenbachi* retains the symplesiomorphic condition for Archosauriformes of a straight posterior process of the squamosal (USNM 214823). In the present analysis, the presence of a ventrally curved posterior process of the squamosal is found as an independently derived state of both Pseudosuchia and Rhadinosuchinae (Fig. 5.23).

4) Absence of a semilunar depression on the parabasisphenoid. The condition of this character could not be determined for any doswelliid based on first hand observations of all the available specimens of the species sampled in the present phylogenetic analysis.

The discussion of the potential characters that may support the non-monophyly of Proterochampsia showed that there is no strong evidence for this hypothesis. Conversely, 15 synapomorphies support the monophyly of Proterochampsia (see synapomorphies of Proterochampsia, above) and the clade has a Bremer support of 3 when all the taxa are considered, increasing to 11 when fragmentary terminals are pruned a posteriori (Fig. 5.20). Fifteen additional steps are necessary to force doswelliids to be more closely related to archosaurs than to proterochampsids. The monophyly of Doswelliidae is supported by nine synapomorphies (see synapomorphies of Doswelliidae, above) and the Bremer support of the group is 3. Five additional steps are necessary to place *Vancleavea campi* as the sister taxon of all other proterochampsians and eleven additional steps to obtain the phylogenetic hypothesis recovered by Nesbitt (2011), in which *Vancleavea campi* is more basal than *Euparkeria capensis*, proterochampsids and archosaurs. As a result, the hypothesis that doswelliids are more closely related to archosaurs than to other archosauriforms is rejected here, as well as the hypothesis that *Vancleavea campi* is a more basal archosauriform than *Euparkeria capensis*, proterochampsids and archosaurs. Indeed, the observations and results of the present phylogenetic analysis strongly suggest the presence of a large monophyletic clade of semi-aquatic to aquatic basal archosauriforms composed of proterochampsids and doswelliids.

5.5.6. *The phylogenetic position of Phytosauria*

The vast majority of quantitative phylogenetic analyses of the last 30 years consistently found phytosaurs as basal pseudosuchians, and in many cases as the sister taxon of all other members of the clade (e.g. Gauthier, 1984; Benton and Clark, 1988; Sereno, 1991; Benton, 1999; Nesbitt and Norell, 2006; Nesbitt, 2007; Brusatte et al., 2010). However, Nesbitt (2011) found phytosaurs as the immediate sister taxon of Archosauria, and this result has been subsequent recovered by other studies that employed modified versions of this data set (e.g. Dilkes and Arcucci, 2012; Nesbitt and Butler, 2013; Nesbitt et al., 2014). The phylogenetic position of phytosaurs outside Archosauria has important evolutionary implications, such as for the origin of the crurotarsal ankle joint and the morphological disparity that the crown-group achieved during the Triassic (Nesbitt, 2011). In addition, the optimization of multiple characters at the base of Archosauria and its most immediate sister nodes are directly dependant on the position of phytosaurs.

In the present phylogenetic analysis, phytosaurs are found within the crown-group Archosauria and as the most basal pseudosuchians (Figs. 5.7, 5.10, 5.20). This result agrees with the majority of independent phylogenetic hypotheses of the last 30 years, but differs from that more recently found by Nesbitt (2011). The phylogenetic position of phytosaurs within Pseudosuchia is supported by 13 synapomorphies in this analysis (see synapomorphies of Pseudosuchia, above), but only three additional steps are necessary to force the placement of phytosaurs as the sister taxon of Archosauria under a topologically constrained search. The Bremer and bootstrap supports of Pseudosuchia are relatively low (Fig. 5.8) and the Bremer support remains low after the a posteriori pruning of fragmentary terminals (Fig. 5.20). The low support and number of additional steps necessary to force the alternative topology indicates that there is a substantial amount of conflicting evidence for the position of phytosaurs

within Archosauria. Nesbitt (2011) found 10 synapomorphies supporting the monophyly of archosaurs to the exclusion of phytosaurs. These character states are discussed as follows.

1) Palatal processes of the maxilla meet at the midline. The scorings of this character are congruent between both data matrices, with ornithodirans, ornithosuchids and suchians possessing a contact between the palatal processes of the maxillae at the median line (character 32-1 of Nesbitt [2011], character 64-2 of the present analysis). By contrast, in phytosaurs and more basal archosauriforms the palatal processes are less medially developed and lack such a contact. As a result, the distribution of this character state is consistent with the hypothesis that phytosaurs are the sister taxon of Archosauria.

2) Lagenar/cochlea recess present and elongated and tubular. The distribution of this character state among archosauriforms is consistent in both data matrixes, in which an elongated and tubular cochlea recess is restricted to suchians and ornithodirans (character 118-1 of Nesbitt [2011], character 211-1 of the present analysis). The condition in ornithosuchids is unknown, and the cochlea recess is absent or short in phytosaurs and non-archosaur archosauriforms. Therefore, this character state also supports the hypothesis that phytosaurs are the sister taxon of Archosauria.

3) External foramen for abducens nerves within prootic only. The scorings for this character are consistent in both data matrixes (character 122 of Nesbitt [2011], character 236 of the present analysis) and potentially support a more basal position of phytosaurs than it is recovered here. However, the optimization of this character is ambiguous at the base of Archosauria in the current analysis because in *Euparkeria capensis* the passage of the abducens nerves occurs through a foramen between the

prootic and parabasisphenoid, resembling the condition in phytosaurs, whereas in erythrosuchids the passage is only within the prootic (Gower and Sennikov, 1996), resembling the condition in suchians and ornithodirans (Nesbitt, 2011).

4) Antorbital fossa present on the lacrimal, dorsal process of the maxilla and the dorsolateral margin of the posterior process of the maxilla (the ventral border of the antorbital fenestra). The antorbital fossa is present in the horizontal (= posterior) process of the maxilla in all ornithodirans, ornithosuchids, basal phytosaurs (e.g. *Parasuchus hislopi*: ISI R42), and suchians sampled here (character 53-2/3), but it is restricted to the ascending process of the bone in *Euparkeria capensis* and most proterochampsians (Fig. 5.23). A similar distribution of these character states was found by Nesbitt (2011: character 137), but becaue of the presence of only relatively derived phytosaurs in his data matrix all the species sampled there were scored as lacking an antorbital fossa on the horizontal process of the maxilla. As a result, the distribution of this character is not unambiguously consistent with the non-archosaurian position of phytosaurs.

5) Posteroventral portion of the coracoid possesses a "swollen" tuber. This character was discussed above and showed to be present in proterochampsians, ornithodirans, ornithosuchids and suchians. As a result, the absence of a swollen biceps tubercle is interpreted in this analysis as an apomorphic reversal of phytosaurs. If phytosaurs are actually the sister taxon of Archosauria, this character would still not provide unambiguous support for this hypothesis. The optimization of the character would be ambiguous in the clade that includes proterochampsians and more crownward archosauriforms because of the absence of a well-developed biceps tubercle in *Euparkeria capensis* and phytosaurs and its presence in proterochampsians.

6) Lateral tuber on the proximal portion of the ulna. The distribution of the states of this character is congruent in both analyses (character 237 of Nesbitt [2011], character 404 of the present analysis) and is consistent with a non-archosaurian position of phytosaurs..

7) Longest metacarpal versus longest metatarsal ratio <0.5. It is not possible to score confidently this character for any phytosaur, ornithosuchid or suchian sampled in this data matrix because of lack of preservation (character 245 of Nesbitt [2011], character 415 of the present analysis). As a result, it could not be determined here if this character state supports any of the hypotheses of relationship for phytosaurs discussed here.

8) Anteromedial tuber of the proximal portion of the femur. The distribution of the states of this character is congruent in both analyses (character 300 of Nesbitt [2011], character 461 of the present analysis) and is consistent with a non-archosaurian position of phytosaurs..

9) Tibial facet of the astragalus divided into posteromedial and anterolateral basins. The scorings of this character are rather similar in both analyses (character 366 of Nesbitt [2011], character 500 of the present analysis). The main difference in the scorings is the absence of a subdivided tibial facet into posteromedial and anterolateral basins in *Marasuchus lilloensis* (PVL 3871). In addition, *Nundasuchus songeaensis* possesses a gently flexed tibial facet in the astragalus that closely resembles in morphology that of *Smilosuchus* spp. (Nesbitt et al., 2014: fig. 11g–l) and, therefore, this species is scored here as lacking a divided facet. As a result, the presence of a subdivided tibial facet in the astragalus is optimized here as an autapomorphy of *Lagerpeton chanarensis* and a synapomorphy of the clade composed

of ornithosuchids and suchians (Fig. 5.28). It does not therefore support a non-archosaurian position of phytosaurs.

10) Calcaneal tuber orientation, relative to the transverse plane, between 50º and 90º posteriorly. The distribution of the states of this character is congruent in both analyses (character 377 of Nesbitt [2011], character 509 of the present analysis) and is consistent with a non-archosaurian position of phytosaurs (Fig. 5.28).

The discussion of the character states that supported the position of phytosaurs as the sister taxon of Archosauria in Nesbitt (2011) demonstrates that there is a lot of congruence between the scorings of both data matrices and several characters may support this hypothesis. However, several other apomorphic features favour in this analysis the inclusion of phytosaurs within Archosauria (e.g. posttemporal fenestra smaller than the supraoccipital but does not develop as a small foramen; posterior process of the squamosal ventrally curved; anterior ramus of the pterygoid transversely narrow along its entire extension; posteroventral process of the dentary contributes to the border of the external mandibular fenestra; articular with a ventromedially directed process; spine table in the distal end of the postaxial cervical and dorsal neural spines; fibular condyle projecting distally distinctly beyond the tibial condyle in the distal end of the femur; area of attachment of the iliofibularis muscle in the fibula placed on a hypertrophied tubercle; calcaneal tuber approximately as broad as or broader than tall at midshaft; calcaneal tuber with a expanded distal end in proximal or distal view; pedal unguals strongly transversely compressed, with a sharp dorsal keel; Figs. 5.21, 5.23, 5.24, 5.26, 5.28, 5.29). Therefore, although the most parsimonious hypothesis found here is the monophyly of a traditional Archosauria, this result is not well supported and much more work is needed in the

Figure 5.29. Femora of Triassic archosauromorphs in medial (A, C, E, G, I−K) and posterior/ventral (B, D, F, H, L) views. *Tanystropheus longobardicus* (SMNS unnumbered) (A, B), *Prolacerta broomi* (BP/1/2676) (C, D), *Proterosuchus fergusi* (SAM-PK-K140) (E, F), *Erythrosuchus africanus* (NHMUK R3592) (G, H), *Chanaresuchus bonapartei* (MCZ 4035) (I), *Jaxtasuchus salomoni* (SMNS 91002) (J) and *Aetosauroides scagliai* (PVL 2073) (K reversed, L). Numbers refer to character states. Scale bars equal 2 cm in A, B, E, F, K, L, 5 mm in C, D, 5 cm in G, H, and 1 cm in I, J.

reconstruction of the higher-level phylogenetic relationships of phytosaurs. The discovery of new Early and Middle Triassic basal archosaurs and their immediate sister taxa may shed light on this issue.

5.5.7. *Macroevolutionary implications*

The phylogenetic analysis conducted here includes the most exhaustive sampling of non-archosaurian Permo-Triassic archosauromorphs published so far and its results have important implications for understanding the timing and mode of early archosauromorph evolution. The origin and early evolution of archosauromorphs during the Permian have been already discussed in Chapter 2 and the macroevolutionary implications of the results of this phylogenetic analysis are discussed here for the Triassic in a chronostratigraphic context (Fig. 5.30).

The diversity of non-archosauriform archosauromorph lineages. The higher-level taxonomic diversity of non-archosauriform archosauromorphs has been usually considered to be mainly restricted to two taxonomically diverse groups, namely "Prolacertiformes" and Rhynchosauria. However, a broadly polyphyletic "Prolacertiformes" sensu Jalil (1997) is recovered in the phylogenetic analysis conducted here, in which supposed prolacertiform species are found distributed among seven different linages of non-archosauriform archosauromorphs. Therefore, the temporal calibration of the topology recovered here implies that at least ten different archosauromorph clades crossed the Permo-Triassic boundary (Fig. 5.31). These different lineages of non-archosauriform archosauromorphs show a rather disparate morphology during the Triassic, including gracile, long-necked aquatic forms (e.g. tanystropheids), bulky and long-necked terrestrial herbivores

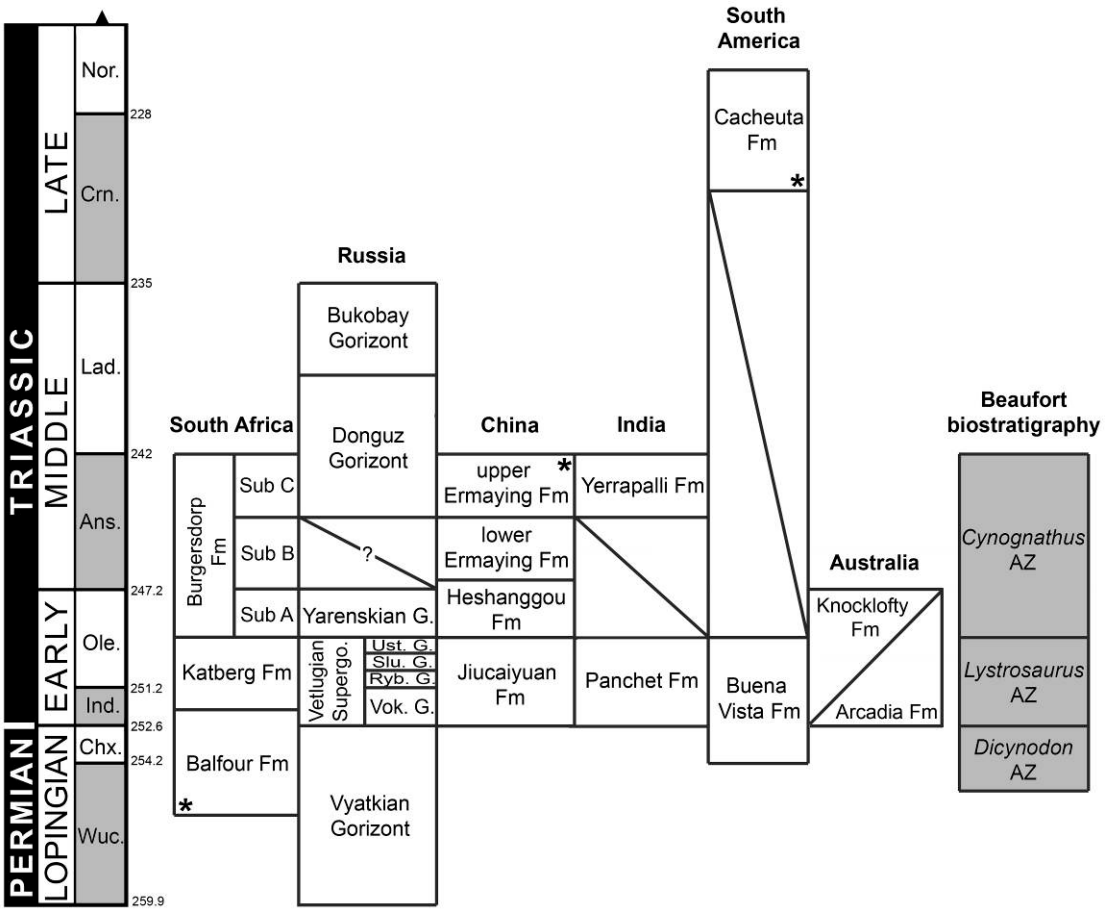

Figure 5.30. Chronostratigraphic diagram of proterosuchian-bearing units (sensu Ezcurra et al., 2013, 2015a). Ages of South African units based on Rubidge (2005) and Rubidge et al. (2013); Russian units based on Newell et al. (2010, 2012); Chinese and Indian units based on Lucas (2010) and Liu et al. (2013); South American units based on Piñeiro et al. (2003) and Spalleti et al. (2008); and Australian units based on Ezcurra (2014) and Warren and Hutchinson (1990). Asterisks indicate radioistopically dated boundaries. It should be noted that the lower Ermaying and Heshanggou formations of China, and the South American, Indian and Australian units belong to different basins, respectively. Russian Gorizonts (= Horizonts) include several formations and basins. Abbreviations: Ans, Anisian; AZ, Assemblage Zone; Chx, Changhsingian; Crn, Carnian; Fm, Formation; G, Gorizont; Ind, Induan; Lad, Ladinian; Nor, Norian; Ole, Olenekian; Ryb, Rybinskian; Slu, Sludkian; Sub, Subzone; Supergo, Supergorizont; Ust, Ustmylian; Vok, Vokhmian; Wuc, Wuchiapingian. Geological timescale after Gradstein et al. (2012).

(*Trilophosaurus* and *Azendohsaurus*), gracile and long-necked predatory species (e.g. prolacertids), and hyperspecialized herbivores (rhynchosaurs). This palaeoecological diversity among basal archosauromorphs seems to exceed that present in non-archosaurian archosauriforms, which are mainly represented by crocodile-like (e.g. proterosuchids, proterochampsids, doswelliids) and massive (e.g. erythrosuchids) predatory clades. These observations should be tested in the future by quantitative macroevolutionary analyses.

Proterosuchidae as a short-lived "disaster" clade and the biotic recovery after the Permo-Triassic mass extinction. The biochron of the proterosuchids has been previously suggested to to range from the latest Permian (*Archosaurus rossicus*) to the late Anisian ("*Chasmatosaurus ultimus*") (Charig and Reig, 1970; Charig and Sues, 1976; Gower and Sennikov, 2000; Ezcurra et al., 2013). However, proterosuchids are much more restricted temporally and taxonomically in the present phylogenetic analysis than previously thought. Proterosuchids are known from the latest Permian of Russia and the earliest Triassic (Induan) of South Africa, Russia, China, and probably India (Figs. 5.30, 5.31). As a result, current evidence indicates that proterosuchids are a short-lived clade that is documented in the fossil record for a period of probably less than 3 million years. In particular, proterosuchids are restricted to a short stratigraphic section 5−14 metres above the Permo-Triassic boundary in the *Lystrosaurus* AZ of South Africa, and they disappear during the first recovery phase of the extinction event (Smith and Botha-Brink, 2014). The proterosuchid-bearing levels of Russia and China are not as well stratigraphically constrained as those of South Africa (Gower and Sennikov, 2000), and it is possible that the biostratigraphic ranges of the proterosuchids in these horizons are also limited to the first few metres above the

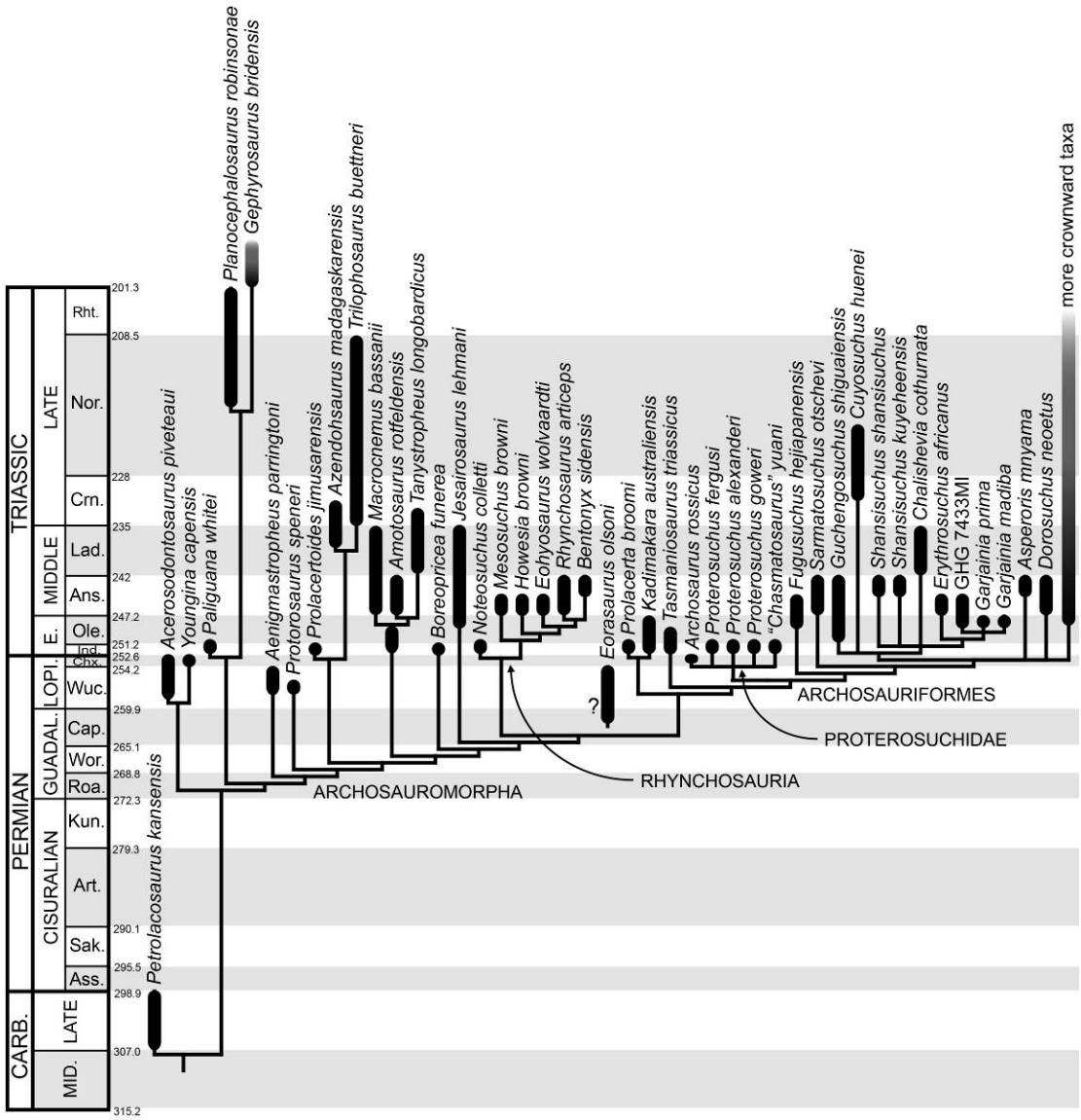

Figure 5.31. Time-calibrated phylogenetic tree of basal archosauromorphs recovered in this analysis. *Euparkeria* and more crownward archosauriforms have been merged into "more crownward taxa" in this tree. The length of the vertical bar representing each terminal taxon represents chronostratigraphical uncertainty rather than true stratigraphical range. Abbreviations: Ans, Anisian; Art, Artinskian; Ass, Asselian; Carb, Carboniferous; Cap, Capitanian; Chx, Changhsingian; Crn, Carnian; E., Early; Guadal, Guadalupian; Ind, Induan; Kun, Kungurian; Lad, Ladinian; Lopi, Lopingian; Mid, Middle; Nor, Norian; Ole, Olenekian; Rht, Rhaetian; Roa, Roadian; Sak, Sakmarian; Wor, Wordian; Wuc, Wuchiapingian. Geological timescale after Gradstein et al. (2012).

Permo-Triassic boundary. Therefore, the proterosuchids potentially represent a component of the first recovery phase of the extinction event, which in the case of the archosauriforms seems to be characterized by a high taxonomic diversity of rather morphologically similar species (Ezcurra and Butler, 2015a; Chapter 3). The biostratigraphic range of the proterosuchids closely resembles, but it is even more chronostratigraphically restricted than, that of the dicynodont genus *Lystrosaurus* (Smith and Botha-Brink, 2014).

The presence of morphologically disparate archosauriform groups is documented during the Olenekian for the first time in the fossil record, including "intermediate" forms between proterosuchids and erythrosuchids (e.g. *Chasmatosuchus rossicus*, *Kalisuchus rewanensis*), erythrosuchids (e.g. *Garjainia madiba*, *Garjainia prima*) and ctenosauriscid archosaurs (e.g. *Vytshegdosuchus zbeshartensis*, *Ctenosauriscus koeneni*) (Gower and Sennikov, 2000; Butler et al., 2011). However, the occurrence of ctenosauriscids that are deeply nested within Archosauria indicates that, at least, all other non-archosaurian archosauriform clades should have been present by that time (Butler et al., 2011). There is no current evidence that the initial diversification of archosauriforms occurred immediately after the mass extinction event (i.e. during the *Lystrosaurus* Assemblage Zone) and this diversification was probably delayed between 1 and 5 million years after the mass extinction. As a result, the evolutionary history of the archosauriforms during the Early Triassic can be subdivided into a first phase characterized by the short-lived "disaster-clade" Proterosuchidae and a second phase that witnessed the initial morphological and probably palaeoecological diversification of the group.

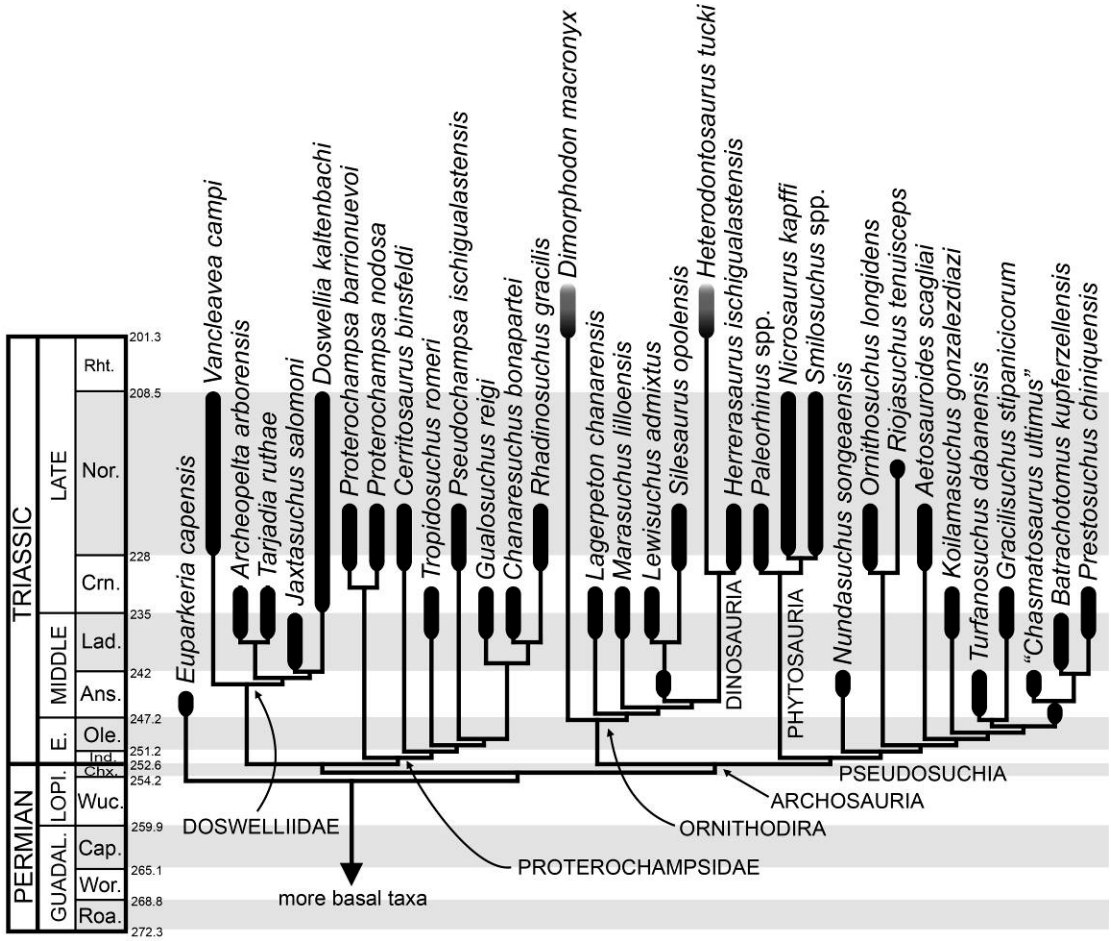

Figure 5.32. Time-calibrated phylogenetic tree of basal archosauromorphs recovered in this analysis. Taxa more basal than *Euparkeria* are not shown in in this tree. The length of the vertical bar representing each terminal taxon represents chronostratigraphical uncertainty rather than true stratigraphical range. Abbreviations: Ans, Anisian; Cap, Capitanian; Chx, Changhsingian; Crn, Carnian; E., Early; Guadal, Guadalupian; Ind, Induan; Lad, Ladinian; Lopi, Lopingian; Nor, Norian; Ole, Olenekian; Rht, Rhaetian; Roa, Roadian; Wor, Wordian; Wuc, Wuchiapingian. Geological timescale after Gradstein et al. (2012).

Proterochampsia: a diverse clade of basal archosauriforms with aquatic adaptations. The present phylogenetic analysis recovered a taxonomically rich monophyletic group of basal archosauriforms with aquatic adaptations, which is composed of at least 15 nominal species (13 of them sampled in the current analysis) (Trotteyn et al., 2013; Sues et al., 2013). The members of this clade possess characters that have been previously interpreted as evidence of a semi-aquatic (e.g. dorsally facing external nares and orbits; Romer, 1971a; Trotteyn et al., 2013; Sues et al., 2013) to a fully aquatic mode of life (e.g. reduced limbs; Nesbitt et al., 2009). This large, monophyletic Proterochampsia indicates that the invasion of continental aquatic niches by non-archosaurian or non-phytosaur archosauriforms was more successful than previously thought and probably restricted to a single lineage. Previous hypotheses of semi-aquatic habits for proterosuchids and erythrosuchids have been recently considered unlikely based on palaeohistological evidence (Botha-Brink and Smith, 2011). The morphological and taxonomic diversification of proterochampsians is probably part of a third phase in archosauriform evolution during the Triassic, which also included the invasion of the marine realm by some poposauroids (Nesbitt et al., 2013b) and the appearance of herbivorous clades, such as the aetosaurs (Desojo et al., 2013), in the late Middle to Late Triassic (Fig. 5.32). These three phases during the early evolution of archosauriforms lead to the numerical dominance of the group by the latest Triassic, which seems to have been enhanced during the Early Jurassic by the empty niches left by the Triassic-Jurassic mass extinction (Brusatte et al., 2008).

Conclusions

The results obtained in this thesis have important implications for the understanding of the anatomy, post-hatchling development, taxonomy and systematics of basal archosauromorphs. The most informative Permian archosauromorph is *Protorosaurus speneri* from the middle Lopingian of Western Europe (Chapter 2). A historically problematic specimen from the Lopingian of Tanzania is redescribed and identified as a new genus and species of basal archosauromorph: *Aenigmastropheus parringtoni* gen. et sp. nov. The supposed protorosaur *Eorasaurus olsoni* from the Lopingian of Russia is partially redescribed and recovered among Archosauriformes. Thus, this species potentially represents the oldest known member of the group, but the phylogenetic support for this position is low. The assignment of *Archosaurus rossicus* from the latest Permian of Russia to the archosauromorph clade Proterosuchidae is supported, resembling the result found in a recent quantitative phylogenetic analysis (Nesbitt, 2011). In agreement with previous studies, no valid Permian record for Lepidosauromorpha is supported here, and I also reject some of the previous referrals of Permian specimens to Archosauromorpha, such as the supposed occurrence of the genus *Proterosuchus* in the Lopingian of South Africa (contra Cruickshank, 1972). Therefore, the revision of the Palaeozoic archosauromorph record conducted here suggests a minimum fossil calibration date for the crocodile-lizard split of 255.7 Ma. The occurrences of basal archosauromorphs in the northern (30ºN) and southern (55ºS) parts of Pangaea imply a wider palaeobiogeographic distribution for the group during the Lopingian than previously appreciated.

As a result of the comprehensive re-examination of all known proterosuchid specimens from the *Lystrosaurus* Assemblage Zone of South Africa (Chapter 3), as

well as examination of other proterosuchid taxa in collections worldwide, it is concluded here that the holotype of *Proterosuchus fergusi* is undiagnostic. Therefore, a neotype (RC 846) is proposed for the species. "*Chasmatosaurus vanhoepeni*" and "*Elaphrosuchus rubidgei*" are considered subjective junior synonyms of *Proterosuchus fergusi*, resembling the taxonomic conclusions reached by Welman (1998). Nevertheless, in contrast with Welman (1998), "*Chasmatosaurus*" *alexanderi* is considered a valid species, for which the new combination *Proterosuchus alexanderi* comb. nov. is proposed. A third species, *Proterosuchus goweri* sp. nov., is erected on the basis of a single specimen (NMQR 880). All three species recognized here are taxonomically distinct from a previously described archosauriform maxilla from the lower *Lystrosaurus* Assemblage Zone (Modesto and Botha-Brink, 2008). As a result, a minimum of four archosauriform species are recognised following the Permo-Triassic mass extinction in South Africa. These results suggest a greater species richness of earliest Triassic archosauriforms than previously appreciated, but that archosauriform morphological disparity remained low and did not expand until the late Early Triassic to early Middle Triassic.

The excellent sample currently available of *Proterosuchus fergusi* provides a unique opportunity to understand early archosauriform cranial ontogeny. Qualitative and quantitative analyses of cranial ontogenetic variation were conducted on an ontogenetic sequence (Chapter 4), in which the smallest individual is 37% of the size of the largest one and osteohistological evidence published by Botha-Brink and Smith (2011) suggests that four of eleven collected specimens had not reached sexual maturity. Through ontogeny the skull of *Proterosuchus fergusi* became proportionally taller, the infratemporal fenestra larger, and the teeth more isodont and numerous but with smaller crowns. The sequence of somatic maturity supports relatively high

growth rates during early ontogeny. The skull of juvenile specimens of *Proterosuchus fergusi* closely resembles adults of the more basal archosauromorph *Prolacerta broomi*, whereas adult specimens resemble adults of more derived archosauriforms (e.g. erythrosuchids, *Euparkeria capensis*). As a result, a plausible hypothesis is that ontogenetic modification events (e.g. heterochrony) may have been key drivers of the evolution of the general shape of the skull at the base of Archosauriformes. These changes may have contributed to the occupation of a new morphospace by the clade around the Permo-Triassic boundary.

The quantitative phylogenetic analysis of this thesis was focused on non-archosaurian archosauromorphs and is the most comprehensive conducted so far in terms of both taxonomic and character sampling (Chapter 5). This analysis found a polyphyletic "Prolacertiformes" (sensu Jalil, 1997), in which the supposed prolacertiforms *Protorosaurus speneri*, *Prolacertoides jimusarensis*, tanystropheids, *Boreopricea funerea* and *Jesairosaurus lehmani* are recovered as successive sister taxa, respectively, of the clade composed of Rhynchosauria and more crownward archosauromorphs. *Prolacerta broomi* and its closely related species *Kadimakara australiensis* are recovered as more closely related to archosauriforms than to any other supposed prolacertiform, in agreement with the most recent phylogenetic hypotheses (e.g. Dilkes, 1998; Modesto and Sues, 2004; Gottmann-Quesada and Sander, 2009; Ezcurra et al., 2014). The broadly polyphyletic "Prolacertiformes" (sensu Jalil, 1997) recovered here implies that at least ten different archosauromorph clades crossed the Permo-Triassic boundary.

The 24 supposed proterosuchid terminals sampled in this analysis are found as a polyphyletic assemblage, being variously placed as the immediate sister taxon of archosauriforms (*Tasmaniosaurus triassicus*), very basal archosauriforms (e.g.

unambiguous proterosuchids, *Kalisuchus rewanensis*, *Sarmatosuchus otschevi*) or even within the crown-group Archosauria ("*Chasmatosaurus ultimus*"). The unambiguous taxonomic content of Proterosuchidae is restricted here to only five valid species: *Archosaurus rossicus*, "*Chasmatosaurus*" *yuani*, *Proterosuchus fergusi*, *Proterosuchus goweri* and *Proterosuchus alexanderi*. "*Blomosuchus georgii*" is also a member of Proterosuchidae, but is considered here a nomen dubium. Proterosuchidae is diagnosed by 13 synapomorphies and support metrics for the clade are strong. "*Chasmatosuchus*" *vjushkovi* and "*Ankistrodon indicus*" are recovered within Proterosuchidae in some of the most parsimonious trees, but also alternatively as more crownward archosauriforms than unambiguous proterosuchids. The topology within Proterosuchidae is unresolved when its six unambiguous species are included. Nevertheless, after the a posteriori pruning of *Archosaurus rossicus* and "*Blomosuchus georgii*", *Proterosuchus goweri* is recovered as the sister-taxon of "*Chasmatosaurus*" *yuani* and *Proterosuchus fergusi* and *Proterosuchus alexanderi* represent their successive sister taxa, respectively.

The eight supposed erythrosuchid species included in this analysis were recovered more closely related to each other than to other archosauromorphs, resulting in a monophyletic Erythrosuchidae. *Cuyosuchus huenei* and *Guchengosuchus shiguaiensis* are recovered as the most basal members of the clade. *Shansisuchus shansisuchus*, *Shansisuchus kuyeheensis* and *Chalishevia cothurnata* are found in a polytomy together with the clade composed of *Erythrosuchus africanus* and *Garjainia* spp. Eight apomorphies diagnose Erythrosuchidae and the support metrics for the monophyly of the clade are very high after the a posteriori pruning of fragmentary taxa.

Euparkeria capensis is found as the sister-taxon of the clade that includes proterochampsids and archosaurs, resembling the topologies most commonly recovered in previous studies (e.g. Sereno, 1991; Parrish, 1993; Juul, 1994; Benton; 2004; Ezcurra et al., 2010; Desojo et al., 2011; Schoch and Sues, 2013). A total of twelve synapomorphies support this topology and low evidence was found in support of the recently recovered alternative hypothesis that *Euparkeria capensis* is more derived than proterochampsids. All the supposed doswelliids of the taxonomic sample of this analysis were recovered within a monophyletic group and more closely related to *Vancleavea campi* and proterochampsids than to other archosauriforms, in agreement with some recent phylogenetic proposals (e.g. Schoch and Sues, 2013). In addition, the bizarre aquatic archosauriform *Vancleavea campi* is found as the most basal member of Doswelliidae. The families Doswelliidae and Proterochampsidae form the clade Proterochampsia.

Phytosaurs were found within the crown-group Archosauria and as the most basal pseudosuchians. This result agrees with numerous independent phylogenetic hypotheses recovered over the last 30 years, but differs from that more recently found by Nesbitt (2011). The phylogenetic position of phytosaurs within Pseudosuchia is supported by 13 synapomorphies in this analysis, but there is a high amount of conflicting evidence and only three additional steps are necessary to force the placement of phytosaurs as the sister taxon of Archosauria under a topologically constrained search. Therefore, the phylogenetic position of phytosaurs is not well supported here and needs considerable further research.

The results obtained in this thesis indicate that proterosuchids are a short-lived clade that is documented in the fossil record for probably less than 3 million years. The proterosuchids potentially represent a component of the first recovery phase from

the Permo-Triassic mass extinction event, which in the case of the archosauriforms seems to be characterized by a high taxonomic diversity of rather morphologically similar species. Morphologically disparate archosauriform groups are documented for the first time in the fossil record during the Olenekian, including "intermediate" forms between proterosuchids and erythrosuchids, erythrosuchids and ctenosauriscid archosaurs (e.g. *Vytshegdosuchus zbeshartensis*, *Ctenosauriscus koeneni*) (Gower and Sennikov, 2000; Butler et al., 2011). There is no current evidence that the initial morphological diversification of archosauriforms occurred immediately after the mass extinction event and it was probably delayed by between 1 and 5 million years after it. As a result, the evolutionary history of the archosauriforms during the Early Triassic can be subdivided into a first phase characterized by the short-lived, "disaster-clade" Proterosuchidae and a second phase that witnessed the initial morphological and probably palaeoecological diversification of the group. A third phase in archosauriform evolution documents the diversification of the group into multiple ecomorphotypes during the late Middle to Late Triassic, which included the invasion of the marine realm by some poposauroids (Nesbitt et al., 2013) and continental aquatic systems by proterochampsians (Trotteyn et al., 2013; Sues et al., 2013), and the appearance of herbivorous (e.g. aetosaurs; Desojo et al., 2013) and flying species (e.g. pterosaurs; Dalla Vecchia, 2013). These three phases of early archosauriform evolution recognized here led to the numerical dominance of the group by the latest Triassic, which seems to have been further enhanced during the Early Jurassic by the empty niches left by the Triassic-Jurassic mass extinction.

Acknowledgements

I thank my supervisor Richard Butler for offering me this line of research and continuous advice and encouragement during the last three years. Richard has considerably improved each chapter of this thesis with his comments and suggestions. I am also very thankful for all the comments and very critical suggestions of my external co-supervisor David Gower. His comments enriched all the chapters of this thesis. I thank Roland Sookias for discussions about basal archosauromorph anatomy and systematics and help during our collection visits in the last three years. I appreciate the comments of my internal co-supervisor Ivan Sansom, which were very useful during the second half of my PhD.

I thank Isabella von Lichtan for preparing casts of some of the bones of *Tasmaniosaurus triassicus*. I also thank Max Banks for allowing me to visit him at his house in Hobart (Tasmania) and providing useful information and discussion about the discovery of *Tasmaniosaurus* and the geology of the Crisp and Gunn's Quarry. I appreciate discussion with Garry Davidson about the geology and biostratigraphy of the Knocklofty Sandstone Formation. I thank Roland Sookias for his help in the field in Tasmania. I thank Fernando Abdala for unpublished pictures of RC 846 and Bhart-Anjan Bhullar for allowing me access to unpublished CT data of the same specimen. I thank technical staff of the QM for additional preparation conducted on specimens of *Kalisuchus rewanensis*. I thank Mathew Lowe and Jennifer Clack (UMZC) for the loan of the holotype of *Aenigmastropheus* and permission to carry out histological sampling, and Renate Liebreich (BSPG) for preparing a mould and cast of the sampled limb bone prior to sectioning. The loan of the *Prolacerta* specimen GHG 431 was possible thanks to Ellen de Kock (GHG). I highly appreaciate the comments and

suggestions of the two examiners that I had during my viva: Michael Benton and Jason Hilton. Their comments helped to improve the final version of this thesis. I thank Andrey Sennikov for discussion and providing useful information about the locality of *Archosaurus rossicus*. Discussions with Sterling Nesbitt, Bruce Rubidge, Christian Kammerer, Jennifer Botha-Brink, Fernando Abdala, Grzegorz Niedźwiedzki, Jörg Schneider, Michael Szurlies, Juan Carlos Cisneros, Federico Agnolín, Julia Desojo, Oliver Rauhut, Adriana López-Arbarello and Christian Foth are appreciated and were very useful at different stages of this research. The comments and suggestions of reviewers during the peer-review process of the chapters of this thesis were very useful and are greatly appreciated, including those of Gabriela Sobral, Marc Jones, Hans-Dieter Sues, Sterling Nesbitt, Steve Brusatte and Mark Webster. I thank Kenneth Angielczyk for sharing unpublished information about the biostratigraphy and age of the Usili Formation.

I thank the following curators, researchers and collection managers that provided access to specimens under their care for the purpose of this research: Billy de Klerk (AM); Carl Mehling and Steve Brusatte (AMNH); Matt Williams (BATGM); Bernhard Zipfel, Bruce Rubidge, Jonah Choiniere and Fernando Abdala (BP); Markus Moser and Oliver Rauhut (BSPG); Graciela Piñeiro, Alejandra Rojas and Andrea Corona (FC-DPV); William Simpson (FMNH); Ellen de Kock (GHG); curatorial staff of the GSI (Kolkata); Saswati Bandyopadhyay and Dhurjati Sengupta (ISI); Jun Liu and Corwin Sullivan (IVPP); Alejandro Kramarz and Stella Alvarez (MACN); Daniela Shwarz-Wings (MB); Susana Devinvenzi González (MCNAM);; Jessica Cundiff (MCZ); Ronan Allain (MNHN); Sandra Chapman and Lorna Steel (NHMUK); Elize Butler and Jennifer Botha-Brink (NM); Heinz Furrer (PIMUZ); Andrey Sennikov (PIN); Claudia Malabarba (PUCS/MCP); Emilio Vaccari (PULR);

Jaime Powell (PVL); Ricardo Martínez (PVSJ); Kristen Spring and technical staff (QM); Mary-Anne Binnie (SAM); Sheena Kaal and Roger Smith (SAM-PK); Daniel Lockett (SHRCM and SHYMS); Rainer Schoch (SMNS); Heidi Fourie (TM); Kevin Padian, Pat Holroyd and Randall Irmis (UCMP); César L. Schultz (UFRGS); Mathew Lowe and Jennifer Clack (UMZC); Michael Brett-Surman and Hans-Dieter Sues (USNM); Max Langer (USP); Isabella von Lichtan (UTGD); and Jon Radley (WARMS).

My research was primarily supported by the Emmy Noether Programme of the Deutsche Forschungsgemeinschaft (BU 2587/3-1 to Richard Butler), with additional support from the College of Life and Environmental Sciences (University of Birmingham), a Marie Curie Career Integration Grant (PCIG14-GA-2013-630123 to Richard Butler), and a National Geographic Young Explorers Grant. Access to the free version of TNT 1.1 was possible due to the Willi Henning Society. I thank the Synthesis Program that funded my visit to the collection of vertebrate palaeontology of the Museum National d'Historie Neturelle in Paris, and the Doris and Samuel P. Welles Fund funded my visit to the University of California, Museum of Paleontology in Berkeley. Grants from the Jurassic Foundation and the Society of Vertebrate Paleontology (Jackson School of Geosciences Student Member Travel Grant) also contributed in this research.

I thank Mariana Grassetti for leaving everything behind to share with me a year in Birmingham and give me her daily companionship. This thesis would not have been possible without all the encouragement of my parents during my childhood and the years that I have been in Europe conducting this research.

References

Abdala, F. and Allinson, M. 2005. The taxonomic status of *Parathrinaxodon proops* (Therapsida: Cynodontia), with comments on the morphology of the palate in basal cynodonts. Palaeontologia Africana 41: 45–52.

Alfaro, M. E., Santinia, F., Brock, C., Alamillo, H., Dornburg, A., Rabosky, D. L., Carnevale, G. and Harmon, L. J. 2009. Nine exceptional radiations plus high turnover explain species diversity in jawed vertebrates. Proceedings of the National Academy of Sciences 106: 13410–1341.

Alroy, J. 2013. Online paleogeographic map generator. http://paleodb.org/?a=mapForm

Angielczyk, K. D. 2007. New specimens of the Tanzanian dicynodont "*Cryptocynodon*" *parringtoni* von Huene, 1942 (Therapsida, Anomodontia), with an expanded analysis of Permian dicynodont phylogeny. Journal of Vertebrate Paleontology 27: 116–131.

Angielczyk, K. D., Sidor, C. A., Nesbitt, S. J., Smith, R. M. H. and Tsuji, L. A. 2009. Taxonomic revision and new observations on the postcranial skeleton, biogeography, and biostratigraphy of the dicynodont genus *Dicynodontoides,* the senior subjective synonym of *Kingoria* (Therapsida, Anomodontia). Journal of Vertebrate Paleontology 29: 1174–1187.

Angielczyk, K. D., Steyer, J.-S., Sidor, C. A., Smith, R. M. H., Whatley, R. L. and Tolan, S. 2014. Permian and Triassic dicynodont (Therapsida: Anomodontia) faunas of the Luangwa Basin, Zambia: taxonomic update and implications for dicynodont biogeography and biostratigraphy. In: The Early Evolutionary History

of the Synapsida, Kammerer, C. F., Angielczyk, K. D. and Fröbisch, J. (eds.). Springer, Dordrecht: 93−138.

Arcucci, A. 1986. Nuevos materiales y reinterpretacion de *Lagerpeton chanarensis* Romer (Thecodontia, Lagerpetonidae nov.) del Triasico Medio de la Rioja, Argentina. Ameghiniana 23: 233–242.

Arcucci, A. 1990. Un nuevo Proterochampsidae (Reptilia-Archosauriformes) de la fauna local de Los Chañares (Triasico Medio), La Rioja, Argentina. Ameghiniana 27: 365–378.

Arcucci, A. and Marsicano, C. A. 1998. A distinctive new archosaur from the Middle Triassic (Los Chañares Formation) of Argentina. Journal of Vertebrate Paleontology 18: 228–232.

Avanzini, M., Bernardi, M. and Nicosia, U. 2011. The Permo-Triassic tetrapod faunal diversity in the Italian Southern Alps. In: Earth and Environmental Sciences, Dar, I. A. (ed.). InTech, Rijeka and Shangai: 591−608.

Baczko, M. B. von and Ezcurra, M. D. 2013. Ornithosuchidae. In: Anatomy, Phylogeny and Palaeobiology of Early Archosaurs and their Kin, Nesbitt, S. J., Desojo, J. B. and Irmis, R. B. (eds.). Geological Society, London, Special Publication 379: 187–202.

Bakker, R. T. and Galton, P. M. 1974. Dinosaur monophyly and a new class of vertebrates. Nature 248: 168–172.

Barberena, M. C. 1978. A huge thecodont skull from the Triassic of Brazil. Pesquisas 9: 62–75.

Barberena, M. C. 1982. Uma nova espécie de *Proterochampsa*, *P. nodosa* sp. nov. do Triássico do Brasil. Anais da Academia Brasileira de Ciências 54: 127–141.

Barrios-Quiroz, G. and Casas-Andreu, G. 2010. Crecimiento con diferentes dietas en crías de C*rocodylus moreletii* Dumeril Bibron and Dumeril 1851 (Crocodylia: Crocodylidae) en cautiverio, Tabasco, México. Revista Latinoamericana de Conservación 1: 104–111.

Bartholomai, A. 1979. New lizard-like reptiles from the Early Triassic of Queensland. Alcheringa 3: 225−234.

Bassani, F. 1886. Sui fossili e sull'eta degli schisti bituminosi triasici di Besano in Lombardia. Atti Societa Italiana di Scienze Naturali, Milano 29: 15−72.

Bennett, S. C. 1996. The phylogenetic position of the Pterosauria within the Archosauromorpha. Zoological Journal of the Linnean Society 118: 261–308.

Benton, M. J. 1983. The Triassic reptile *Hyperodapedon* from Elgin: functional morphology and relationships. Philosophical Transactions of the Royal Society of London B 302: 605–717.

Benton, M. J. 1984. The relationships and early evolution of the Diapsida. Symposia of the Zoological Society of London 52: 575–96.

Benton, M. J. 1985. Classification and phylogeny of the diapsid reptiles. Zoological Journal of the Linnean Society 84: 97–164.

Benton, M. J. 1990. The species of *Rhynchosaurus*, a rhynchosaur (Reptilia, Diapsida) from the Middle Triassic of England. Philosophical Transactions of the Royal Society of London B 328: 213–306.

Benton, M. J. 1999. *Scleromochlus taylori* and the origin of dinosaurs and pterosaurs. Philosophical Transactions of the Royal Society of London B 354: 1423−1446.

Benton, M. J. 2004. Origin and relationships of Dinosauria. In: The Dinosauria, 2nd Edition, Weishampel, D. B., Dodson, P. and Osmólska, H. (eds). University of California Press, Berkeley: 7–24.

Benton, M. J. and Clark, J. M. 1988. Archosaur phylogeny and the relationships of the Crocodylia. In: The Phylogeny and Classification of the Tetrapods. Volume 1. Amphibians, Reptiles, and Birds, Benton, M. J. (ed.). Clarendon Press, Oxford: 295–338.

Benton, M. J. and Kirkpartrick, R. 1989. Heterochrony in a fossil reptile: juveniles of the rhynchosaur *Scaphonyx fischeri* from the Late Triassic of Brazil. Palaeontology 32: 335−353.

Benton M. J. and Allen J. L. 1997. *Boreopricea* from the Lower Triassic of Russia, and the relationships of the prolacertiform reptiles. Palaeontology 40: 931−953.

Benton, M. J. and Donoghue, P. C. J. 2007. Paleontological evidence to date the tree of life. Molecular Biology and Evolution 24: 26–53.

Benton, M. J., Tverdokhlebov, V. P. and Surkov, M. V. 2004. Ecosystem remodelling among vertebrates at the Permo-Triassic boundary in Russia. Nature 432: 97–100.

Berman, D. S. and Reisz, R. R. 1982. Restudy of *Mycterosaurus longiceps* (Reptilia, Pelycosauria) from the Lower Permian of Texas. Annals of the Carnegie Museum 51: 423–453.

Bhullar, B.-A. S. and Bever, G. S. 2009. An archosaur-like laterosphenoid in early turtles (Reptilia: Pantestudines). Breviora 518: 1–11.

Bhullar, B.-A. S., Marugán-Lobón, J., Racimo, F., Bever, G., Rowe, T., Norell, M. and Abzhanov, A. 2012. Birds have paedomorphic dinosaur skulls. Nature 487: 223–226.

Bickelmann, C., Müller, J. and Reisz, R. R. 2009. The enigmatic diapsid *Acerosodontosaurus piveteaui* (Reptilia: Neodiapsida) from the Upper Permian of

Madagascar and the paraphyly of “younginiform” reptiles. Canadian Journal of Earth Sciences 46: 651−661.

Bittencourt, J. S., Arcucci, A. B., Maricano, C. A. and Langer, M. C. 2014. Osteology of the Middle Triassic archosaur *Lewisuchus admixtus* Romer (Chañares Formation, Argentina), its inclusivity, and relationships amongst early dinosauromorphs. Journal of Systematic Palaeontology 13: 189−219.

Bonaparte, J. F. 1967. Dos nuevas ‘faunas’ de reptiles triásicos de Argentina. Gondwana Stratigraphy, 1 Gondwana Symposium, Mar del Plata: 283–325.

Bonaparte, J. F. 1970. Annotated list of the South American Triassic tetrapods. Proceedings and Papers of the 2 Gondwana Symposium: 665–682.

Bonaparte, J. F. 1972. Los tetrápodos del sector superior del a Formación Los Colorados, La Rioja, Argentina. (Triásico Superior) I Parte. Opera Lilloana 22: 13–56.

Bonaparte, J. F. 1975. Nuevos materiales de *Lagosuchus talampayensis* Romer (Thecodontia - Pseudosuchia) y su significado en el origen de los Saurischia. Chañarense inferior, Triásico Medio de Argentina. Acta Geologica Lilloana 13: 5−90.

Bonaparte, J. F. 1976. *Pisanosaurus mertii* Casimiquela and the origin of the Ornithischia. Journal of Paleontology 50: 808–820.

Bonaparte, J. F. 1981. Nota sobre una nueva fauna del Triásico Inferior del Sur de Mendoza, República Argentina, correspondiente a la zona de *Lystrosaurus* (Dicinodontia-Proterosuchia). 2º Congreso Latinoamericano de Paleontología (Porto Alegre), Annais 1: 277–288.

Bonaparte, J. F. 1982. Classification of the Thecodontia. Géobios, Mémoire Spécial, 6: 99–112.

Bonaparte, J. F. 1986. Les Dinosaures (Carnosaures, Allosauridés, Sauropodes, Cetiosauridés) du Jurassique Moyen de Cerro Cóndor (Chubut, Argentine). Annales de Paléontologie 72: 247−289.

Bonaparte, J. F. 1991. The Gondwanan theropod families Abelisauridae and Noasauridae. Historical Biology 5: 1−25.

Borsuk-Białynicka, M. and Evans, S. E. 2003. A basal archosauriform from the Early Triassic of Poland. Acta Palaeontologica Polonica 48: 649–653.

Borsuk−Białynicka, M. and Evans, S. E. 2009. A long−necked archosauromorph from the Early Triassic of Poland. Palaeontologia Polonica 65: 203–234.

Bossi, J. and Navarro, R. 1991. Geología del Uruguay. Departamento de Publicaciones, Universidad de la República, Montevideo, Uruguay: 996 pp.

Botha, J. and Smith, R. M. H. 2006. Rapid vertebrate recuperation in the Karoo Basin of South Africa following the end-Permian extinction. Journal of African Earth Sciences 45: 502–514.

Botha-Brink, J. and Smith, R. M. H. 2011. Osteohistology of the Triassic archosauromorphs *Prolacerta*, *Proterosuchus*, *Euparkeria*, and *Erythrosuchus* from the Karoo Basin of South Africa. Journal of Vertebrate Paleontology 31: 1238–1254.

Botha-Brink, J., Huttenlocker, A. K. and Modesto, S. P. 2014. Vertebrate paleontology of Nooitgedacht 68: a *Lystrosaurus maccaigi*-rich Permo-Triassic boundary locality in South Africa. In: Early Evolutionary History of the Synapsida, Kammerer, C. F., Angielczyk, K. D. and Fröbisch, J. (eds). Vertebrate Paleobiology and Paleoanthropology Series, Springer Dordrecht Heidelberg, New York, London: 289–304.

Brauns, C. M., Pätzold, T., and Haack, U. 2003. A Re–Os study bearing on the age of the Kupferschiefer at Sangerhausen (Germany). XVth Intern Congress on Carboniferous and Permian Stratigraphy. Utrecht, The Netherlands, Abstracts: 66.

Brink, A. S. 1955. Notes on some thecodonts. Navorsinge van die Nasionale Museum Bloemfontein 1: 141–148.

Brinkman, D. B. and Sues, H.–D. 1987. A staurikosaurid dinosaur from the Upper Triassic Ischigualasto Formation of Argentina and the relationships of the Staurikosauridae. Palaeontology 30: 493−503.

Brochu, C. A. 1992. Ontogeny of the postcranium in crocodylomorph archosaurs. Unpublished M.A. thesis, The University of Texas at Austin, Austin: 340 pp.

Brochu, C. A. 1996. Closure of neurocentral sutures during crocodilian ontogeny: implications for maturity assessment in fossil archosaurs. Journal of Vertebrate Paleontology 16: 49–62.

Broili, F. and Schröder, J. 1934. Beobachtungen an Wirbeltieren der Karroo Formation. V. Über *Chasmatosaurus vanhoepeni* Haughton. Sitzungsberichte der Bayerischen Akademie der Wissenschaften, Mathematisch-naturwissenschaftliche Abteiliung 3: 225–264.

Broom, R. 1903. On a new reptile (*Proterosuchus fergusi)* from the Karroo beds of Tarkastad, South Africa. Annals of the South African Museum 4: 159–164.

Broom, R. 1905. Notice of some new reptiles from the Karoo Beds of South Africa. Records of the Albany Museum 1: 331–337.

Broom, R. 1906. On the South African diaptosaurian reptile *Howesia*. Proceedings of the Zoological Society of London 1906: 591–600.

Broom, R. 1913. On the South-African pseudosuchian *Euparkeria* and allied genera. Proceedings of the Zoological Society of London 1913: 619–633.

Broom, R. 1914. A new thecodont reptile. Proceedings of the Zoological Society of London 1914: 1072–1077.

Broom, R. 1921. On the structure of the reptile tarsus. Proceedings of the Zoological Society 1921: 143−155.

Broom, R. 1922. An imperfect skeleton of *Youngina capensis*, Broom, in the collections of the Transvaal Museum. Annals of the Transvaal Museum 8: 273−277.

Broom, R. 1925. On the origin of lizards. Proceedings of the Zoological Society of London 1925: 1−16.

Broom, R. 1926. On a nearly complete skeleton of a new eosuchian reptile (*Palaeagama vielhaueri*, gen. et sp. nov.). Proceedings of the Zoological Society of London 1926: 487−492.

Broom, R. 1932. On some South African pseudosuchians. Annals of the Natal Museum 7: 55–59.

Broom, R. 1946. A new primitive proterosuchid reptile. Annals of the Transvaal Museum 20: 343–346.

Brusatte, S. P., Benton, M. J., Ruta, M. and Lloyd, G. T. 2008. Superiority, competition, and opportunism in the evolutionary radiation of dinosaurs. Science 321: 1485–1488.

Brusatte, S. L., Benton, M. J., Desojo, J. B. and Langer, M. C. 2010. The higher-level phylogeny of Archosauria (Tetrapoda: Diapsida). Journal of Systematic Palaeontology 8: 3-47.

Brusatte, S. L., Niedźwiedzki, G. and Butler, R. J. 2011. Footprints pull origin and diversification of dinosaur stem lineage deep into Early Triassic. Proceedings of the Royal Society of London, Biological Sciences 278: 1107–1113.

Buffrénil, V. de and Castanet, J. 2000. Age estimation by skeletochronology in the Nile Monitor (*Varanus niloticus*), a highly exploited species. Journal of Herpetology 34: 414−424.

Bulanov, V. V. and Sennikov, A. G. 2010. New data on the morphology of Permian gliding weigeltisaurid reptiles of Eastern Europe. Paleontological Journal 44: 682−694.

Butler, R. J. 2005. The 'fabrosaurid' ornithischian dinosaurs of the Upper Elliot Formation (Lower Jurassic) of South Africa and Lesotho. Zoological Journal of the Linnean Society 145: 175–218.

Butler, R. J., Barrett, P. M., Abel, R. L. and Gower, D. J. 2009. A possible ctenosauriscid archosaur from the Middle Triassic Manda Beds of Tanzania. Journal of Vertebrate Paleontology 29: 1022–1031.

Butler, R. J., Brusatte, S. L., Reich, M., Nesbitt, S. J., Schoch, R. R. and Hornung, J. J. 2011. The sail-backed reptile *Ctenosauriscus* from the latest Early Triassic of Germany and the timing and biogeography of the early archosaur radiation. PLoS ONE 6: e25693.

Butler, R. J., Barrett, P. M. and Gower, D. J. 2012. Reassessment of the evidence for postcranial skeletal pneumaticity in Triassic archosaurs, and the early evolution of the avian respiratory system. PLoS ONE 7: e34094.

Butler, R. J., Sullivan, C., Ezcurra, M. D., Liu, J., Lecuona, A. and Sookias, R. B. 2014a. New clade of enigmatic early archosaurs yields insights into early

pseudosuchian phylogeny and the biogeography of the archosaur radiation. BMC Evolutionary Biology 14: 128.

Butler, R. J., Rauhut, O. W. M., Stocker, M. R. and Bronowicz, R. 2014b. Redescription of the phytosaurs *Paleorhinus* ("*Francosuchus*") *angustifrons* and *Ebrachosuchus neukami* from Germany, with implications for Late Triassic biochronology. Zoological Journal of the Linnean Society 170: 155–208.

Butler, R. J., Ezcurra, M. D., Montefeltro, F. C., Samathi, A. and Sobral, G. In press. A new species of basal rhynchosaur (Diapsida: Archosauromorpha) from the early Middle Triassic of South Africa, and the early evolution of Rhynchosauria. Zoological Journal of the Linnean Society.

Camp, C. L. 1930. A study of the phytosaurs with description of new material from western North America. Memoirs of the University of California 10: 1–161.

Camp, C. L. and Banks, M. R. 1978. A proterosuchian reptile from the Early Triassic of Tasmania. Alcheringa 2: 143–158.

Campione, N. E. and Reisz, R. R. 2010. *Varanops brevirostris* (Eupelycosauria: Varanopidae) from the Lower Permian of Texas, with discussion of varanopid morphology and interrelationships. Journal of Vertebrate Paleontology 30: 724−746.

Carr, T. D. 2010. A taxonomic assessment of the type series of *Albertosaurus sarcophagus* and the identity of Tyrannosauridae in the *Albertosaurus* bonebed from the Horseshoe Canyon Formation (Campanian-Maastrichtian, Late Cretaceous). Canadian Journal of Earth Sciences 47: 1213–1226.

Carr, T. D. and Williamson, T. E. 2004. Diversity of late Maastrichtian Tyrannosauridae (Dinosauria: Theropoda) from western North America. Zoological Journal of the Linnean Society 142: 479–523.

Carrano, M. T., Sampson, S. D. and Forster, C. A. 2002. The osteology of *Masiakasaurus knopfleri*, a small abelisauroid (Dinosauria: Theropoda) from the Late Cretaceous of Madagascar. Journal of Vertebrate Paleontology 22: 510−534.

Carroll, R. L. 1975. Permo-Triassic 'lizards' from the Karroo. Palaeontologia Africana 18: 71–87.

Carroll, R. L. 1976. *Noteosuchus*—the oldest known rhynchosaur. Annals of the South African Museum 72: 37–57.

Carroll, R. L. 1981. Plesiosaur ancestors from the Upper Permian of Madagascar. Philosophical Transactions of the Royal Society of London B 293: 315–383.

Carroll, R. L. and Thompson, P. 1982. A bipedal lizardlike reptile from the Karroo. Journal of Paleontology 56: 1−10.

Casamiquela, R. M. 1960. Noticia preliminar sobre dos nuevos estagonolepoideos Argentinos. Ameghiniana 2: 3–9.

Casamiquela, R. M. 1961. Dos nuevos estagonolepoideos Argentinos (de Ischigualasto, San Juan). Revista de la Asociación Geológica Argentina 16: 143−203.

Casamiquela, R. M. 1967. Materiales adicionales y reinterpretación de *Aetosauroides scagliai* (de Ischigualasto, San Juan). Revista del Museo de La Plata 5: 173–196.

Case, E. C. 1928. A cotylosaur from the Upper Triassic of western Texas. Journal of Washington Academy of Science 18: 177−178.

Charig, A. J. and Reig, O. A. 1970. The classification of the Proterosuchia. Biological Journal of the Linnean Society 2: 125–171.

Charig, A. J. and Sues, H.-D. 1976. Proterosuchia. In: Handbuch der Paläoherpetologie 13, Kuhn, O. (ed.). Gustav Fischer, Stuttgart: 11–39.

Chatterjee, S. 1985. *Postosuchus*, a new thecodontian reptile from the Triassic of Texas and the origin of tyrannosaurs. Philosophical Transactions of the Royal Society of London B 309: 395–460.

Chatterjee, S. 1987. A new theropod dinosaur from India with remarks on the Gondwana-Laurasia connection in the Late Triassic. In: Gondwana 6: Stratigraphy, Sedimentology and Paleontology, McKenzie, G. D. (ed.). Geophysical Monograph 41: 183−189.

Cheng, Z. W. 1980. Vertebrate fossils. In: Mesozoic stratigraphy and paleontology of the Shan-Gan-Ning Basin 2. Publishing House of Geology, Beijing: 114–171.

Chinsamy, A. 1993. Bone histology and growth trajectory of the prosauropod dinosaur *Massospondylus carinatus* Owen. Modern Geology 18: 319−321.

Cisneros, J. C. 2008. Phylogenetic relationships of procolophonid parareptiles with remarks on their geological record. Journal of Systematic Palaeontology 6: 345−366.

Clark, J. M., Welman, J., Gauthier, J. A. and Parrish, J. M. 1993. The laterosphenoid bone of early archosauriforms. Journal of Vertebrate Paleontology 13: 48–57.

Clark, J. M., Sues, H.-D. and Berman, D. S. 2000. A new specimen of *Hesperosuchus agilis* from the Upper Triassic of New Mexico and the interrelationships of basal crocodylomorph archosaurs. Journal of Vertebrate Paleontology 20: 683–704.

Clark, J. M., Xu, X., Forster, C.A. and Wang, Y. 2004. A Middle Jurassic 'sphenosuchian' from China and the origin of the crocodylian skull. Nature 430: 1021–1024.

Clements, J. F. 2007. The Clements Checklist of the Birds of the World, 6th Edition. Cornell University Press, New York: 864 pp.

Coddington, J. A. and Scharff, N. 1994. Problems with zero-length branches. Cladistics 10: 415-423.

Colbert, E. H. 1973. Continental drift and the distributions of fossil reptiles. In: Implications of Continental Drift for the Earth Sciences, Tailing, D. H. and Runcorn, S. K. (eds.). Academic Press, London: 395–412.

Colbert, E. H. and Olsen, P. E. 2001. A new and unusual aquatic reptile from the Lockatong Formation of New Jersey (Late Triassic, Newark Supergroup). American Museum Novitates 3334: 1–24.

Conti, M. A., Leonardi, G., Mietto, P. and Nicosia, U. 2000. Orme di tetrapodi non dinosauriani del Paleozoico e Mesozoico in Italia. In: Dinosauri in Italia. Le orme giurassiche dei Lavini di Marco (Trentino) e gli altri resti fossili italiani, Leonardi, G. and Mietto, P. (eds.). Accademia Editoriale, Pisa: 297−320.

Cooper, M. R. 1984. Reassessment of *Vulcanodon karibaensis* Raath (Dinosauria: Saurischia) and the origin of Sauropoda. Palaeontologia Africana 25: 203–231.

Cope, E. D. 1869. Synopsis of the extinct Batrachia, Reptilia and Aves of North America. Transactions of the American Philosophical Society 14: 1–252.

Coria, R. A. and Salgado, L. 2000. A basal Abelisauria Novas 1992 (Theropoda–Ceratosauria) from the Cretaceous of Patagonia, Argentina. GAIA 15: 89−102.

Cox, C. B. 1964. On the palate, dentition, and classification of the fossil reptile *Endothiodon* and related genera. American Museum Novitates 2171: 1–25.

Cox, C. B. 1965. New Triassic dicynodonts from South America, their origins and relationships. Philosophical Transactions of the Royal Society of London B 248: 457–516.

Crompton, A. W. and Charig, A. J. 1962. A new ornithischian from the Upper Triassic of South Africa. Nature 196: 1074−1077.

Cruickshank, A. R. I. 1972. The proterosuchian thecodonts. In: Studies in Vertebrate Evolution, Joysey, K. A. and Kemp, T. S. (eds.). Oliver and Boyd, Edinburgh: 89–119.

Cruickshank, A. R. I. 1978. The pes of *Erythrosuchus africanus* Broom. Zoological Journal of the Linnean Society 62: 161–177.

Cruickshank, A .R. I. 1979. The ankle joint in some early archosaurs. South African Journal of Science 75: 168–178.

Currie, P. 1980. A new younginid (Reptilia: Eosuchia) from the Upper Permian of Madagascar. Canadian Journal of Earth Sciences 17: 500–511.

Currie, P. 1981. *Hovasaurus boulei*, an aquatic eosuchian from the Upper Permian of Madagascar. Palaeontologia Africana 24: 99–168.

Currie, P. 1982. The osteology and relationships of *Tangasaurus mennelli* Haughton (Reptilia, Eosuchia). Annals of the South African Museum 86: 247–265.

Currie, P. J. 1995. New information on the anatomy and relationships of *Dromaeosaurus albertensis* (Dinosauria: Theropoda). Journal of Vertebrate Paleontology 15: 576−591.

Dalla Vecchia, F. B. 2006. A new sauropterygian reptile with plesiosaurian affinity from the Late Triassic of Italy. Rivista Italiana di Paleontologia e Stratigrafia 112: 207−225.

Dalla Vecchia, F. B. 2013. Triassic pterosaurs. In: Anatomy, Phylogeny and Palaeobiology of Early Archosaurs and their Kin, Nesbitt, S. J., Desojo, J. B. and Irmis, R. B. (eds.). Geological Society, London, Special Publication 379: 119–155.

Damiani, R. J., Neveling, J., Hancox, P. J. and Rubidge, B. 2000. First trematosaurid temnospondyl from the *Lystrosaurus* Assemblage Zone of South Africa and its biostratigraphic implications. Geological Magazine 137: 659–665.

Damiani, R. J., Modesto, S. and Yates, A. 2003. Barendskraal, a diverse amniote locality from the *Lystrosaurus* Assemblage Zone, Early Triassic of South Africa. Palaeontologia Africana 39: 53–62.

Daudin, F. M. 1802. Histoire Naturelle, Générale et Particulière des Reptiles; ouvrage faisant suit à l'Histoire naturell générale et particulière, composée par Leclerc de Buffon; et rédigee par C.S. Sonnini, membre de plusieurs sociétés savantes. Volume 2. F. Dufart, Paris: 432 pp.

deBraga, M. 2003. The postcranial skeleton, phylogenetic position and probable lifestyle of the Early Triassic reptile *Procolophon trigoniceps.* Canadian Journal of Earth Sciences 40: 527–556.

deBraga, M. and Reisz, R. R. 1995. A new diapsid reptile from the uppermost Carboniferous (Stephanian) of Kansas. Palaeontology 38: 199–212.

deBraga, M. and Rieppel, O. 1997. Reptile phylogeny and the relationships of turtles. Zoological Journal of the Linnean Society 120: 281–354.

Desojo, J. B. and Ezcurra, M. D. 2011. A reappraisal of the taxonomic status of *Aetosauroides* (Archosauria: Aetosauria) specimens from the Late Triassic of South America and their proposed synonymy with *Stagonolepis*. Journal of Vertebrate Paleontology 31: 596–609.

Desojo, J. B., Arcucci, A. B. and Marsicano, C. A. 2002. Reassessment of *Cuyosuchus huenei*, a Middle-Late Triassic archosauriform from the Cuyo Basin, west-central Argentina. In: Upper Triassic Stratigraphy and Paleontology,

Heckert, A. B. and Lucas, S. G. (eds.). New Mexico Museum of Natural History and Science Bulletin 21: 143–148.

Desojo, J. B., Ezcurra, M. D. and Schultz, C. L. 2011. An unusual new archosauriform from the Middle–Late Triassic of southern Brazil and the monophyly of Doswelliidae. Zoological Journal of the Linnean Society 161: 839–871.

Desojo, J. B., Heckert, A. B., Martz, J. W., Parker, W. G., Schoch, R. R., Small, B. J. and Sulej, T. 2013. Aetosauria: A clade of armoured pseudosuchians from the Upper Triassic continental beds. In: Anatomy, Phylogeny and Palaeobiology of Early Archosaurs and their Kin, Nesbitt, S. J., Desojo, J. B. and Irmis, R. B. (eds.). Geological Society, London, Special Publication 379: 203–239.

Dias-da-Silva, S., Modesto, S. P. and Schultz, C. L. 2006. New material of *Procolophon* (Parareptilia: Procolophonidae) from the Lower Triassic of Brazil, with remarks on the ages of the Sanga do Cabral and Buena Vista formations of South America. Canadian Journal of Earth Sciences 43: 1685−1693.

Dilkes, D. W. 1995. The rhynchosaur *Howesia browni* from the Lower Triassic of South Africa. Palaeontology 38: 665–685.

Dilkes, D. W. 1998. The Early Triassic rhynchosaur *Mesosuchus browni* and the interrelationships of basal archosauromorph reptiles. Philosophical Transactions of the Royal Society of London B 353: 501–541.

Dilkes, D. W. and Sues, H.-D. 2009. Redescription and phylogenetic relationships of *Doswellia kaltenbachi* (Diapsida: Archosauriformes) from the Upper Triassic of Virginia. Journal of Vertebrate Paleontology 29: 58–79.

Dilkes, D. W. and Arcucci, A. B. 2009. Revision of *Proterochampsa barrionuevoi* and Proterochampsidae (Reptilia; Archosauriformes) from the Late Triassic of Argentina and Brazil. Journal of Vertebrate Paleontology 29: 88A.

Dilkes, D. W. and Arcucci, A. B. 2012. *Proterochampsa barrionuevoi* (Archosauriformes: Proterochampsia) from the Late Triassic (Carnian) of Argentina and a phylogenetic analysis of Proterochampsia. Palaeontology 55: 853−885.

Dutuit, J.-M. 1977. *Paleorhinus magnoculus*, phytosaure du Trias supérieur de l'Atlas Marocain. Géologie Méditerranéenne 4: 255–268.

Dzik, J. 2001. A new *Paleorhinus* fauna in the early Late Triassic of Poland. Journal of Vertebrate Paleontology 21: 625−627.

Dzik, J. 2003. A beaked herbivorous archosaur with dinosaur affinities from the early Late Triassic of Poland. Journal of Vertebrate Paleontology 23: 556−574.

Dzik, J. and Sulej, T. 2007. A review of the early Late Triassic Krasiejów biota from Silesia, Poland. Palaeontologia Polonica 64: 3−27.

Efremov, J. A. 1938. Some new Permian reptiles of the USSR. Comptes Rendus of the Academy of Sciences USSR Paleontology 19: 121−126.

Emmons, E. 1856. Geological Report on the Midland Counties of North Carolina. George P. Putnam, Raleigh: 118 pp.

Erickson, G. M. 2005. Assessing dinosaur growth patterns: a microscopic revolution. Trends in Ecology and Evolution 20: 677–684.

Erickson, G. M. and Brochu, C. M. 1999. How the 'terror crocodile' grew so big. Nature 398: 205–206.

Erickson, G. M., Ricqlès, A. de, Buffrénil, V. de, Molnar, R. E. and Bayless, M. K. 2003. Vermiform bones and the evolution of gigantism in *Megalania* – how a reptilian fox became a lion. Journal of Vertebrate Paleontology 23: 966–970.

Erickson, G. M., Makovicky, P. J., Inouye, B. D., Zhuo, C. and Gao, K. 2009. A life table for *Psittacosaurus lujiatunensis*: initial insights into ornithischian dinosaur population biology. Anatomical Record 292: 1514–1521.

Estes, R. 1983. Sauria terrestria, Amphisbaenia. Handbuch der Paläoherpetologie 10A, Stuttgart: 249 p.

Evans, S. E. 1980. The skull of a new eosuchian reptile from the Lower Jurassic of South Wales. Zoological Journal of the Linnean Society 70: 203–264.

Evans, S. E. 1981. The postcranial skeleton of *Gephyrosaurus bridensis* (Eosuchia: Reptilia). Zoological Journal of the Linnean Society 73: 81–116.

Evans, S. E. 1984. The classification of the Lepidosauria. Zoological Journal of the Linnean Society 82: 87–100.

Evans, S. E. 1987. The braincase of *Youngina capensis* (Reptilia: Diapsida; Permian). Neues Jahrbuch für Geologie und Paläontologie Monatshefte 1987: 293−203.

Evans, S. E. 1988. The early history and relationships of the Diapsida. In: The Phylogeny and Classification of the Tetrapods, Benton, M. J. (ed.). Oxford University Press, Oxford: 221−253.

Evans, S. E. 2003. At the feet of the dinosaurs: the early history and radiation of lizards. Biological Reviews 78: 513–551.

Evans, S. E. and Haubold, H. 1987. A review of the Upper Permian genera *Coelurosauravus*, *Weigeltisaurus* and *Gracilisaurus* (Reptilia: Diapsida). Zoological Journal of the Linnean Society 90: 275–303.

Evans, S. E. and Heever, J. A. van den. 1987. A new reptile (Reptilia: Diapsida) from the Upper Permian *Daptocephalus* zone of South Africa. South African Journal of Science 83: 724−730.

Evans, S. E. and King, M. S. 1993. A new specimen of *Protorosaurus* (Reptilia: Diapsida) from the Marl Slate (Late Permian) of Britain. Proceedings of the Yorkshire Geological Society 49: 229–234.

Evans, S. E. and Borsuk-Białynicka, M. 2009. A small lepidosauromorph reptile from the Early Triassic of Poland. Palaeontologia Polonica 65: 179–202.

Evans, S. E. and Jones, M. E. H. 2010. The origins, early history and diversification of lepidosauromorph reptiles. In: New Aspects of Mesozoic Biodiversity, Bandyopadhyay, S. (ed.). Springer-Verlag, Lecture Notes in Earth Science 132: 27−44.

Ewer, R. F. 1965. The anatomy of the thecodont reptile *Euparkeria capensis* Broom. Philosophical Transactions of the Royal Society of London B 751: 379–435.

Ezcurra, M. D. 2006. A review of the systematic position of the dinosauriform archosaur *Eucoelophysis baldwini* from the Upper Triassic of New Mexico, USA. Geodiversitas 28: 649−684.

Ezcurra, M. D. 2012. Sistemática, biogeografía y patrones macroevolutivos de los dinosaurios terópodos del Triásico Tardío y Jurásico Temprano. Tesis de Licenciatura, Universidad de Buenos Aires, Buenos Aires: 512 pp.

Ezcurra, M. D. 2014. The osteology of the basal archosauromorph *Tasmaniosaurus triassicus* from the Lower Triassic of Tasmania, Australia. PLoS ONE 9: e86864.

Ezcurra, M. D. and Butler, R. J. 2015a. Taxonomy of the proterosuchid archosauriforms (Diapsida: Archosauromorpha) from the earliest Triassic of

South Africa, and implications for the early archosauriform radiation. Palaeontology 58: 141−170.

Ezcurra, M. D. and Butler, R. J. 2015b. Post-hatchling cranial ontogeny in the Early Triassic diapsid reptile *Proterosuchus fergusi*. Journal of Anatomy.

Ezcurra, M. D., Lecuona, A. and Martinelli, A. 2010. A new basal archosauriform diapsid from the Lower Triassic of Argentina. Journal of Vertebrate Paleontology 30: 1433–1450.

Ezcurra, M. D., Butler, R. J. and Gower, D. J. 2013. 'Proterosuchia': the origin and early history of Archosauriformes. In: Anatomy, Phylogeny and Palaeobiology of Early Archosaurs and their Kin, Nesbitt, S. J., Desojo, J. B. and Irmis, R. B. (eds.). Geological Society, London, Special Publication 379: 9–33.

Ezcurra, M. D., Scheyer, T. M. and Butler, R. J. 2014. The origin and early evolution of Sauria: reassessing the Permian saurian fossil record and the timing of the crocodile-lizard divergence. PLoS ONE 9: e89165.

Ezcurra, M. D., Velozo, P., Meneghel, M. and Piñeiro, G. 2015a. Early archosauromorph remains from the Permo-Triassic Buena Vista Formation of north-eastern Uruguay. PeerJ 3: e776.

Ezcurra M. D., Desojo J. B. and Rauhut O. W. M. 2015b. Redescription and phylogenetic relationships of the proterochampsid *Rhadinosuchus gracilis* (Diapsida: Archosauriformes) from the early Late Triassic of southern Brazil. Ameghiniana: preprint.

Fara, E. and Hungerbühler, A. 2000. *Paleorhinus magnoculus* from the Upper Triassic of Morocco: a juvenile primitive phytosaur (Archosauria). Comptes Rendus de l'Académie des Sciences, Paris, Sciences de la Terre et des Planètes 331: 831–836.

Fernandez Blanco, M. V., Bona, P., Olivares, A. I. and Desojo, J. B. 2015. Ontogenetic variation in the skulls of *Caiman*: the case of *Caiman latirostris* and *Caiman yacare* (Alligatoridae, Caimaninae). Herpetological Journal 25: 65−73.

Flynn, J. J., Parrish, J. M., Rakotosamimanana, B., Simpson, W. F., Whatley, R. L. and Wyss, A. R. 1999. A Triassic fauna from Madagascar, including early dinosaurs. Science 286: 763–765.

Flynn, J. J., Parrish, J. M., Rakotosamimanana, B., Ranivoharimanana, L., Simpson, W. F. and Wyss, A. R. 2000. New traversodontids (Synapsida: Eucynodontia) from the Triassic of Madagascar. Journal of Vertebrate Paleontology 20: 422–427.

Flynn, J. J., Nesbitt, S. J., Parrish, J. M., Ranivoharimanana, L. and Wyss, A. R. 2010. A new species of *Azendohsaurus* (Diapsida: Archosauromorpha) from the Triassic Isalo Group of southwestern Madagascar: cranium and mandible. Palaeontology 53: 669–688.

Fox, R. C. and Bowman, M. C. 1966. Osteology and relationships of *Captorhinus aguti* (Cope) (Reptilia: Captorhinomorpha). The University of Kansas Paleontological Contributions, Series Vertebrata 11: 1−79

Fraas, O. 1877. *Aëtosaurus ferratus* Fr. Die gepanzerte Vogel-Escheaus dem Stubensandstein bei Stuttgart. Württembergische naturwissenschaftliche Jahreshefte 33: 1–22.

Fraser, N. C. 1982. A new rhynchocephalian from the British Upper Triassic. Palaeontology 25: 709–725.

Fraser, N. C. and Walkden, G. M. 1984. The postcranial skeleton of the Upper Triassic sphenodontid *Planocephalosaurus robinsonae*. Palaeontology 27: 575–595.

Fraser, N. C. and Shelton, C. G. 1988. Studies of tooth implantation in fossil tetrapods using high-resolution X-radiography. Geological Magazine 125: 117−122.

Fraser, N. C., and Rieppel, O. 2006. A new protorosaur (Diapsida) from the Upper Buntsandstein of the Black Forest, Germany. Journal of Vertebrate Paleontology 26: 866–871.

Fraser, N. C., Grimaldi, D. A. and Olsen, P. E. 1996. A Triassic Lagerstätte from eastern North America. Nature 380: 615−619.

Fraser, N. C., Padian, K., Walkden, G. M. and Davis, A. L. M. 2002. Basal dinosauriform remains from Britain and the diagnosis of the Dinosauria. Palaeontology 45: 79−95.

Frederickson, J. A. and Tumarkin-Deratzian, A. R. 2014. Craniofacial ontogeny in *Centrosaurus apertus*. PeerJ 2: e252.

Fröbisch, J. 2009. Composition and similarity of global anomodont-bearing tetrapod faunas. Earth Science Reviews 95: 119–175.

Gaffney, E. S. 1980. Phylogenetic relationships of the major groups of amniotes. In: The Terrestrial Environment and the Origin of Land Vertebrates, Panchen, A. L. (ed.). Academic Press, London: 593–610.

Galton, P. M. 1976. Prosauropod dinosaurs (Reptilia: Saurischia) of North America. Postilla 169: 1−98.

Galton, P. M. 1990. Basal Sauropodomorpha-Prosauropoda. In: The Dinosauria, Weishampel, D. B., Dodson, P. and Osmólska, H. (eds.). University of California Press, Berkeley: 320−344.

Games I. 1990. Growth curves for the Nile crocodile as estimated by skeletochronology. In: Crocodiles, Proceedings of the 10th Working Meeting of

the Crocodile Specialist Group, IUCN, Volume 1, The World Conservation Union Gland: 111–121.

Gardner, J. D. 2003. The fossil salamander *Proamphiuma cretacea* Estes (Caudata; Amphiumidae) and relationships within the Amphiumidae. Journal of Vertebrate Paleontology 23: 769−782.

Gardner, N. M., Holliday, C. M. and O'Keefe, F. R. 2010. The braincase of *Youngina capensis* (Reptilia, Dipsida): new insights from high-resolution CT scanning of the holotype. Palaeontologia Electronica 13: 19A.

Gauthier, J. A. 1984. A cladistic analysis of the higher categories of the Diapsida. Berkeley: PhD thesis, University of California: 564 pp.

Gauthier, J. A. 1986. Saurischian monophyly and the origin of birds. Memoirs of the California Academy of Sciences 8: 1–55.

Gauthier, J. A., Kluge, A. G. and Rowe, T. 1988. Amniote phylogeny and the importance of fossils. Cladistics 4: 105–209.

Gay, S. A. and Cruickshank, A. R. I. 1999. Biostratigraphy of the Permian tetrapod faunas from the Ruhuhu Valley, Tanzania. Journal of African Earth Sciences 29: 195–210.

Germano, D. and Williams, D. F. 2005. Population ecology of blunt-nosed leopard lizards in high elevation foothill habitat. Journal of Herpetology 39: 1–18.

Gervais, P. 1858. Description de I'*Aphelosaurus latevensis*, saurien fossile des schistes Permiens de Lodeve. American Science and Nature 10: 233−235.

Goloboff, P. A., Mattoni, C. and Quinteros, Y. S. 2006. Continuous characters analyzed as such. Cladistics 22: 589–601.

Goloboff, P. A., Farris, J. S. and Nixon, K. C. 2008. TNT, a free program for phylogenetic analysis. Cladistics 24: 774–786.

Goodrich, E. S. 1930. Studies n the Structure and Development of Vertebrates. Macmillan, London: 837 pp.

Gottmann-Quesada, A. and Sander, P. M. 2009. A redescription of the early archosauromorph *Protorosaurus spenseri* Meyer, 1832 and its phylogenetic relationships. Palaeontographica Abteilung A 287: 123–220.

Gould, S. J. 1966. Allometry and size in ontogeny and phylogeny. Biological Reviews 41: 587–640.

Gow, C. E. 1970. The anterior of the palate of *Euparkeria*. Palaeontologia Africana 13: 61−62.

Gow, C. E. 1975. The morphology and relationships of *Youngina capensis* Broom and *Prolacerta broomi* Parrington. Palaeontologia Africana 18: 89–131.

Gower, D. J. 1996. The tarsus of erythrosuchid archosaurs, and implications for early diapsid phylogeny. Zoological Journal of the Linnean Society 116: 347–375.

Gower, D. J. 1997. The braincase of the early archosaur *Erythrosuchus.* Journal of Zoology 242: 557–576.

Gower, D. J. 1999. Cranial osteology of a new rauisuchian archosaur from the Middle Triassic of southern Germany. Stuttgarter Beiträge zur Naturkunde B 280: 1−49.

Gower, D. J. 2001. Possible postcranial pneumaticity in the last common ancestor of birds and crocodilians: evidence from *Erythrosuchus* and other early archosaurs. Naturwissenschaften 88: 119–122.

Gower, D. J. 2002. Braincase evolution in suchian archosaurs (Reptilia: Diapsida): evidence from the rauisuchian *Batrachotomus kupferzellensis*. Zoological Journal of the Linnean Society 136: 49–76.

Gower, D. J. 2003. Osteology of the early archosaurian reptile *Erythrosuchus africanus* Broom. Annals of the South African Museum 110: 1–84.

Gower, D. J. and Sennikov, A. G. 1996. Morphology and phylogenetic informativeness of early archosaur braincases. Palaeontology 39: 883–906.

Gower, D. J. and Sennikov, A. G. 1997. *Sarmatosuchus* and the early history of the Archosauria. Journal of Vertebrate Paleontology 17: 60–73.

Gower, D. J. and Weber, E. 1998. The braincase of *Euparkeria*, and the evolutionary relationships of birds and crocodilians. Biological Reviews 73: 367–411.

Gower, D. J. and Sennikov, A. G. 2000. Early archosaurs from Russia. In: The Age of Dinosaurs in Russia and Mongolia, Benton, M. J., Kurochkin, E. N., Shishkin, M. A. and Unwin, D. M. (eds.). Cambridge University Press, Cambridge: 140–159.

Gower, D. J. and Schoch, R. 2009. Postcranial anatomy of the rauisuchian archosaur *Batrachotomus kupferzellensis*. Journal of Vertebrate Paleontology 29: 103–122.

Gower, D. J., Hancox, P. J., Botha-Brink, J., Sennikov, A. G. and Butler, R. J. 2014. A new species of *Garjainia* Ochev, 1958 (Diapsida: Archosauriformes: Erythrosuchidae) from the Early Triassic of South Africa. PLoS ONE 9: e111154.

Gradstein, F. M., Ogg, J. G., Schmitz, M. D. and Ogg, G. 2012. The Geologic Time Scale 2012. Boston, Elsevier: 1176 pp.

Gregory, J. T. 1945. Osteology and relationships of *Trilophosaurus*: University of Texas, Publication 4401: 273−359.

Gregory, W. K. 1946. Pareiasaurs versus placodonts as near ancestors to turtles. Bulletin of the American Museum of Natural Historty 86: 275−326.

Groenewald, G. H. and Kitching, J. W. 1995. Biostratigraphy of the *Lystrosaurus* Assemblage Zone. In: Rubidge, B. S. (ed.). Biostratigraphy of the Beaufort Group (Karoo Supergroup). South African Committee for Stratigraphy, Biostratigraphic Series 1: 35–39.

Haeckel, E. 1866. Generelle Morphologie der Organismen. Allgemeine Grundzüge der organischen Formen-Wissenschaft, mechanisch begründet durch die von Charles Darwin reformirte Deszendenz Theorie. Zweiter Band: Allgemeine Entwicklungsgeschichte der Organismen. Verlag von Georg Reimer, Berlin: 462 pp.

Hancock, A. and Howse, R. 1870. On *Proterosaurus speneri*, von Meyer, and a new species, *Proterosaurus huxleyi*, from the Marl-Slate of Midderidge, Durham. Quarterly Journal of the Geological Society 26: 565−572.

Hancox, P. J. 2000. The continental Triassic of South Africa. Zentralblatt für Geologie und Paläontologie Teil I 1998: 1285–1324.

Haughton, S. H. 1921. On the reptilian genera *Euparkeria* Broom, and *Mesosuchus* Watson. Transactions of the Roygal Society of South Africa 10: 81−88.

Haughton, S. H. 1924. On a new type of thecodont from the Middle Beaufort Beds. Annals of the Transvaal Museum 11: 93–97.

Heckert, A. B. and Lucas, S. G. 1999. A new aetosaur from the Upper Triassic of Texas and the phylogeny of aetosaurs. Journal of Vertebrate Paleontology 19: 50–68.

Heckert, A. B., Lucas, S. G., Rinehart, L. F., Celesky, M. D., Spielmann, J. A. and Hunt, A. P. 2010. Articulated skeletons of the aetosaur *Typothorax coccinarum* Cope (Archosauria: Stagonolepididae) from the Upper Triassic Bull Canyon Formation (Revueltian: early–mid Norian), eastern New Mexico, USA. Journal of Vertebrate Paleontology 30: 619–642

Heckert, A. B., Lucas, S. G. and Spielmann, J. A. 2012. A new species of the enigmatic archosauromorph *Doswellia* from the Upper Triassic Bluewater Creek Formation, New Mexico, USA. Palaeontology 55: 1333–1348.

Hill, R. V. 2005. Integration of morphological data sets for phylogenetic analysis of Amniota: the importance of integumentary characters and increased taxonomic sampling. Systematic Biology 54: 530–547.

Hillenius, W. J. 2000. Septomaxilla of nonmammalian synapsids: soft-tissue correlates and a new functional interpretation. Journal of Morphology 245: 29–50.

Hmich, D., Schneider, J. W., Saber, H., Voigt, S., and El Wartiti, M. 2006. New continental Carboniferous and Permian faunas of Morocco: implications for biostratigraphy, palaeobiogeography and palaeoclimate. In: Non–Marine Permian Biostratigraphy and Biochronology, Lucas, S. G., Cassinis, G. and Schneider, J. W. (eds.). Geological Society, London, Special Publication 265: 297–324.

Hoffman, A. C. 1965. On the discovery of a new thecodont from the Middle Beaufort Beds. Navorsinge van die Nasionale Museum Bloemfontein 2: 33–40.

Hoffstetter, R. 1955. Thecodontia. In: Traité de Paléontologie, Vol. 5: Amphibiens, Reptiles, Oiseaux, Piveteau, J. (ed.). Masson et Cie, Paris: 665–694.

Holmes, R. B. 1977. The osteology and musculature of the pectoral limb of small captorhinids. Journal of Morphology 152: 101−140.

Hone, D. W. E. and Benton, M. J. 2008. A new genus of rhynchosaur from the Middle Triassic of south-west England. Palaeontology 51: 95–115.

Horner, J. R., Ricqlés, A. de and Padian, K. 2000. Long bone histology of the hadrosaurid dinosaur *Maiasaurua pebblesorum*: growth dynamics and physiology based on an ontogenetic series of skeletal elements. Journal of Vertebrate Paleontology 20: 115–129.

Huchzermeyer, F. W. 2003. Crocodiles: Biology, Husbandry and Diseases. CABI Publishing, London: 352 pp.

Huene, F. von. 1908. Die Dinosaurier der europäischen Triasformation mit Berücksichtigung der aussereuropäischen Vorkommnisse. Geologische und Paläontologische Abhandlungen Supplement 1: 1–419.

Huene, F. von. 1911. Über *Erythrosuchus*, Vertreter der neuen Reptil-Ordnung Pelycosimia. Geologische und Paläontologische Abhandlungen, Neue Folge, 10: 67–122.

Huene, F. von. 1914. Beitrage zur Geschichte der Archosaurier. Geologische und Palaeontologische Abhandlungen, Neue Folge, 13: 1−53.

Huene, F. von. 1920. Osteologie von *Aetosaurus ferratus* O. Fraas. Acta Zoologica 1: 465–491.

Huene, F. von. 1923. Neue Beiträge zur Kenntnis der Parasuchier. Jahrbuch der Preussischen Geologischen Landesanstalt 42: 59–160.

Huene, F. von. 1938. Die fossielen Reptilien des südamerikanischen Gondwanalandes. Neues Jahrbuch für Mineralogie, Geologie und Paläontologie, Abteilung B, 1938: 142–151.

Huene, F. von. 1940. Eine Reptilfauna aus der ältesten Trias Nordrusslands. Neues Jahrbuch für Mineralogie, Geologie und Paläontologie: Beilagen-Band 84: 1–23.

Huene, F. von. 1942. Die fossilen Reptilien des südamerikanischen Gondwanalandes. Ergebnisse der Sauriergrabungen in Südbrasilien, 1928/1929. C.H. Becksche Verlagsbuchhandlung, München.

Huene, F. von. 1946. Die grossen Stämme der Tetrapoden in den geologischen Zeiten. Biologisches Zentralblatt 65: 268–275.

Huene, F. von. 1948. Short review of the lower tetrapods. Royal Society of South Africa, Special Publication (Robert Broom Commemorative Volume): 65–106.

Huene, F. von. 1956. Paläontologie und Phylogenie der Niederen Tetrapoden. Fischer, Jena: 716 pp.

Huene, F. von. 1960. Ein grosser Pseudosuchier aus der Orenburger Trias. Palaeontographica Abteilung A 114: 105–111.

Hugall, A. F., Foster, R. and Lee, M. S. 2007. Calibration choice, rate smoothing, and the pattern of tetrapod diversification according to the long nuclear gene RAG-1. Systematic Biology 56: 543–563.

Hughes, B. 1963. The earliest archosaurian reptiles. South African Journal of Science 59: 221–241.

Hungerbühler, A. 1998. Cranial anatomy and diversity of the Norian phytosaurs from southwest Germany. Unpublished PhD thesis, University of Bristol, Bristol: 464 pp.

Hungerbühler, A. 2000. Heterodonty in the European phytosaur *Nicrosaurus kapffi* and its implications for the taxonomy utility and functional morphology of phytosaur dentitions. Journal of Vertebrate Paleontology 20: 31–48.

Hungerbühler, A. and Hunt, A. P. 2000. Two new phytosaur species (Archosauria, Crurotarsi) from the Upper Triassic of Southwest Germany. Neues Jahrbuch für Geologie und Paläontologie, Monatshefte, 2000: 467–484.

Hunt, A. P. 1989. A new ornithischian dinosaur from the Bull Canyon Formation (Upper Triassic) of east-central New Mexico. In: Dawn of the Age of Dinosaurs in the American Southwest, Lucas, S. G. and Hunt, A. P. (eds.). New Mexico Museum of Natural History, Albuquerque: 355–358.

Hunt, A. P. and Lucas, S. G. 1991. A new Rhynchosaur from the Upper Triassic of West Texas, and the Biochronology of Late Triassic Rhyncosaurs. Palaeontology 34: 927–938.

Hunt, A. P. and Lucas, S. G. 1993. A new phytosaur (Reptilia: Archosauria) genus from the uppermost Triassic of the western United States and its biochonological significance. In: The nonmarine Triassic, Lucas, S. G. and Morales, M. (eds.). New Mexico Museum of Natural History and Science Bulletin, Albuquerque: 193–196.

Hunt, A. P., Lucas, S. G. and Spielmann J. A. 2005. The holotype specimen of *Vancleavea campi* from Petrified Forest National Park, Arizona, with notes on the taxonomy and distribution of the taxon. New Mexico Museum of Natural History and Science Bulletin 29: 59–66.

Hutchinson, J. R. 2001. The evolution of pelvic osteology and soft tissues on the line to extant birds. Zoological Journal of the Linnean Society 131: 123–168.

Hutton, J. M. 1986. Age determination of living Nile crocodiles from the cortical stratification of bone. Copeia 1986: 332–341.

Huxley, T. H. 1859. Postscript to: On the sandstones of Morayshire (Elgin & c.) containing reptilian remains; and on their relations to the Old Red Sandstone of that county (by R. I. Murchison). Quarterly Journal of the Geological Society of London 15: 435−436.

Huxley, T. H. 1865. On a collection of vertebrate fossils from the Panchet Rocks, Ranigunj, Bengal. Memoir of the Geological Survey of India 3: 1–24.

Huxley, T. H. 1868. On *Saurosternon Bainii*, and *Pristerodon McKayi*, two new fossil lacertillian reptiles from South Africa. Geological Magazine 5: 201–205.

Huxley, T. H. 1877. The crocodilian remains found in the Elgin sandstones, with remarks on ichnites of Cummingstone. Memoirs of the Geological Survey of the United Kingdom Monograph III 3: 1–51.

Irmis, R. B. 2007. Axial skeleton ontogeny in the Parasuchia (Archosauria: Pseudosuchia) and its implications for ontogenetic determination in archosaurs. Journal of Vertebrate Paleontology 27: 350–361.

Irmis, R. B., Nesbitt, S. J., Padian, K., Smith, N. D., Turner, A. H., Woody, D. and Downs, A. 2007. A Late Triassic dinosauromorph assemblage from New Mexico and the rise of dinosaurs. Science 317: 358−361.

Ivachnenko, M. F. 1978. The Permian and Triassic procolophonians from the Russian platform. Akademiya Nauk SSSR, Paleontologicheskiy Institut, Trudy, 164: 1−80.

Jalil, N.-E. 1997. A new prolacertiform diapsid from the Triassic of North Africa and the interrelationships of the Prolacertiformes. Journal of Vertebrate Paleontology 17: 506–525.

Jones, M. E. H., Anderson, C. L., Hipsley, C. A., Müller, J., Evans, S. E. and Schoch R. R. 2013. Integration of molecules and new fossils supports a Triassic origin for Lepidosauria (lizards, snakes, and tuatara). BMC Evolutionary Biology 13: 208.

Juul, L. 1994. The phylogeny of basal archosaurs. Palaeontologia Africana 31: 1–38.

Kalandadze, L. L. and Sennikov, A. G. 1985. New reptiles from the Middle Triassic of the southern Cis-Urals. Paleontological Journal 1985: 777–784. [In Russian]

Kear, B. P. 2009. Proterosuchid archosaur remains from the Early Triassic Bulgo Sandstone of Long Reef, New South Wales. Alcheringa 33: 331–337.

Kemp, T. S. 1969. On the functional morphology of the gorgonopsid skull. Philosophical Transactions of the Royal Society of London B 256: 1–83.

Kent, D. V., Santi Malnis, P., Colombi, C. E., Alcober, O. A. and Martínez, R. N. 2014. Age constraints on the dispersal of dinosaurs in the Late Triassic from

magnetochronology of the Los Colorados Formation (Argentina). Proceedings of the National Academy of Sciences 111: 7958−7963.

Kischlat, E.-E. 2000. Tecodôncios: a aurora dos arcossáurios no Triássico. In: Paleontologia do Rio Grande do Sul, Holz, M. and De Ross, L. F. (eds.). CIGO/UFRGS, Brasil: 273–316.

Kitching, J. W. 1977. The distribution of the Karroo vertebrate fauna. Bernard Price Institute for Palaeontological Research Memoir 1: 1–131.

Klembara, J. and Welman, J. 2009. The anatomy of the palatoquadrate in the Lower Triassic *Proterosuchus fergusi* (Reptilia, Archosauromorpha) and its morphological transformation within the archosauriform clade. Acta Zoologica 90: 275−284.

Krebs, B. 1974. Die Archosaurier. Die Naturwissenschaften 61: 17–24.

Kubo, T. and Kubo, M. O. 2014. Dental microwear of a Late Triassic dinosauriform, *Silesaurus opolensis*. Acta Paleontologica Polonica 59: 305−312.

Kuhn, O. 1933. Fossilium catalogus. 1: Animalia. Pars 58: Thecodontia. W. Junk, Berlin: 32 pp.

Kuhn, O. 1961. Die Familien der rezenten und fossilen Amphibien und Reptilien. Meisenbach KG, Bamberg: 79 pp.

Kuhn, O. 1966. Die Reptilien, System und Stammesgeschichte. Krailling bei München, Oeben: 154 pp.

Langer, M. C. 2005. Studies on continental Late Triassic tetrapod biochronology. II. The Ischigualastian and a Carnian global correlation. Journal of South American Earth Sciences 19: 219−239.

Langer, M. C. and Schultz, C. L. 2000. A new species of the Late Triassic rhynchosaur *Hyperodapedon* from the Santa Maria Formation of south Brazil. Palaeontology 43: 633–652.

Langer, M. C. and Benton, M. J. 2006. Early dinosaurs: a phylogenetic study. Journal of Systematic Palaeontology 4: 309−358.

Langer, M. C., Ferigolo, J. and Schultz, C. L. 2000a. Heterochrony and tooth evolution in hyperodapedontine rhynchosaurs (Reptilia, Diapsida). Lethaia 33: 119–128.

Langer, M. C., Boniface, M., Cuny, G. and Barbieri, L. 2000b. The phylogenetic position of *Isalorhynchus genovefae*, a Late Triassic rhynchosaur from Madagascar. Annales de Paléontologie 86: 101–127.

Langer, M. C., França, M. A. G. and Gabriel, S. 2007. The pectoral girdle and forelimb anatomy of the stem-sauropodomorph *Saturnalia tupiniquim* (Late Triassic, Brazil). In: Evolution and Palaeobiology of Early Sauropodomorph Dinosaurs, Barrett, P. M. and Batten, D. J. (eds.). Special Papers in Palaeontology 77: 113–137.

Langer M. C., Ezcurra, M. D., Bittencourt, J. and Novas, F. E. 2010a. The origin and early radiation of dinosaurs. Biological Reviews 85: 55−110.

Langer, M. C., Montefeltro, F. C., Hone, D. E., Whatley, R. and Schultz, C. L. 2010b. On *Fodonyx spenceri* and a new rhynchosaur from the Middle Triassic of Devon. Journal of Vertebrate Paleontology 30: 1884−1888.

Langer, M. C., Nesbitt, S. J., Bittencourt, J. S. and Irmis, R. B. 2013. Non-dinosaurian Dinosauromorpha. In: Anatomy, Phylogeny and Palaeobiology of Early Archosaurs and their Kin, Nesbitt, S. J., Desojo, J. B. and Irmis, R. B. (eds.). Geological Society, London, Special Publication 379: 157–186.

Laurenti, J. N. 1768. Specimen medicum, exhibens synopsin reptilium emendatam cum experimentis circa venena et antidota reptilium austriacorum. J. T. N. de Trattnern, Vienna: 214 pp.

Laurin, M. 1991. The osteology of a Lower Permian eosuchian from Texas and a review of diapsid phylogeny. Zoological Journal of the Linnean Society 101: 59–95.

Lecuona, A. and Desojo, J. B. 2011. Hind limb osteology of *Gracilisuchus stipanicicorum* (Archosauria: Pseudosuchia). Earth and Environmental Science Transactions of the Royal Society of Edinburgh 102: 105–128.

Lee, M. S. Y. 2011. Palaeontology: turtles in transition. Current Biology 23: 513–515.

Legler, B. and Schneider, J. W. 2008. Marine ingressions into the Middle/Late Permian saline lake of the Southern Permian Basin (Rotliegend, northern Germany) possibly linked to sea-level highstands in the Arctic rift system. Palaeogeography, Palaeoclimatology, Palaeoecology 267: 102–114.

Legler, B., Gebhardt, U. and Schneider, J. W. 2005. Late Permian non-marine–marine transitional profiles in the central Southern Permian Basin. International Journal of Earth Sciences 94: 851–862.

Linnaeus, C. 1758. Systema naturae per regna tria naturae, secundum classes, ordines, genera, species, cum characteribus, differentiis, synonymis, locis. Editio decima, reformata. Tomus 1. Laurentius Salvius, Stockholm: 824 pp.

Liu, J., Li, L. and Li, X. W. 2013. SHRIMP U-Pb zircon dating of the Triassic Ermaying and Tongchuang formations in Shanxi, China and its stratigraphic implications. Vertebrata PalAsiatica 51: 162−168.

Liu, J., Butler, R. J., Sullivan, C. and Ezcurra, M. D. In press. '*Chasmatosaurus ultimus*,' a putative proterosuchid archosauriform from the Middle Triassic, is an indeterminate crown archosaur. Journal of Vertebrate Paleontology.

Lleonart, J., Salat, J. and Torres, G. J. 2000. Removing allometric effects of body size in morphological analysis. Journal of Theoretical Biology 205: 85–93.

Long, R. A. and Murry, P. A. 1995. Late Triassic (Carnian and Norian) tetrapods from the southwestern United States. New Mexico Museum of Natural History and Science Bulletin 4: 1–254.

Lucas, S. G. 2010. The Triassic timescale based on non-marine tetrapod biostratigraphy and biochronology. In: The Triassic Timescale, Lucas, S. G. (ed.). Special Publication Geological Society 334, London: 447–500.

Lucas, S. G., Spielmann, J. A. and Hunt, A. P. 2013. A new doswelliid archosauromorph from the Upper Triassic of West Texas. In: The Triassic System, Tanner, L. H., Spielmann, J. A. and Lucas, S. G. (eds.). New Mexico Museum of Natural History and Science, Bulletin 61: 382−388.

Lyson, T. R., Bever, G. S., Bhullar, B.-A. S., Joyce, W. G. and Gauthier, J. A. 2010. Transitional fossils and the origin of turtles. Biology Letters 6: 830−833.

Lyson, T. R., Bever, G. S., Scheyer, T. M., Hsiang, A. Y. and Gauthier, J. A. 2013. Evolutionary origin of the turtle shell. Current Biology 23: 1113–1119.

Macartney, J. 1802. Lectures on comparative anatomy, translated from the French of G. Cuvier by William Ross, under the inspection of James Macartney. Longman and Rees, London, Volume I: 710 pp.

Maddison, W. P. and Maddison, D. R. 2015. Mesquite: a modular system for evolutionary analysis. Version 3.02 http://mesquiteproject.org

Maisch, M. W. 2002. Observation on Karoo and Gondwana vertebrates. Part 3: notes on the gorgonopsians from the Upper Permian of Tanzania. Neues Jahrbuch für Geologie und Paläontologie Monatshefte 2002: 237–251.

Makovicky, P. J. and Sues, H.-D. 1998. Anatomy and phylogenetic relationships of the theropod dinosaur *Microvenator celer* from the Lower Cretaceous of Montana. American Museum Novitates 3240: 1–27.

Marsh, O. C. 1889. Notice of gigantic horned Dinosauria from the Cretaceous. American Journal of Science 38: 173–175.

Marsicano, C., Perea, D. and Ubilla, M. 2000. A new temnospondyl amphibian from the Lower Triassic of South America. Alcheringa 24: 119−123.

Martínez, R. N., Sereno, P. C., Alcober, O. A., Colombia, C. E., Renne, P. R., Montañez, I. P. and Currie, B. S. 2011. A basal dinosaur from the dawn of the dinosaur era in southwestern Pangaea. Science 331: 206−210.

Mastrantonio, B. M., Schultz, C. L., Desojo, J. B. and Garcia, J. B. 2013. The braincase of *Prestosuchus chiniquensis* (Archosauria: Suchia). In: Anatomy, Phylogeny and Palaeobiology of Early Archosaurs and their Kin, Nesbitt, S. J., Desojo, J. B. and Irmis, R. B. (eds.). Geological Society, London, Special Publication 379: 425–440.

Mehl, M. G. 1915. The Phytosauria of the Trias. Journal of Geology 23: 129–165.

Mehl, M. G. 1928. *Pseudopalatus pristinus*, a new genus and species of phytosaurs from Arizona. University of Missouri Studies 3: 1–22.

Meyer, H. von .1830. *Protorosaurus*. Isis von Oken 1830: 517–519.

Meyer, H. von. 1832. Palaeologica zur Geschichte der Erde und ihrer Geschöpfe. Verlag von Siegmund Schmerber, Frankfurt am Main: 560 pp.

Meyer, H. von. 1856. Zur Fauna der Vorwelt. Saurier aus dem Kupferschiefer der Zechstein-Formation. Verlag Heinrich Keller vormals S. Schmerber'sche Buchhandlung, Frankfurt am Main: 1-24.

Meyer, H. von. 1860. Briefliche Mittheilung an Prof. Bronn. Neues Jahrbuch für Mineralogie, Geognosie, Geologie und Petrefakten-Kunde 1860: 556–560.

Meyer, H. von. 1861. Reptilien aus dem Stubensandstein des oberen Keupers. Palaeontographica 7: 253–346.

Modesto, S. P. and Reisz, R. R. 2002. An enigmatic new diapsid reptile from the Upper Permian of Eastern Europe. Journal of Vertebrate Paleontology 22: 851–855.

Modesto, S. P. and Sues, H.-D. 2004. The skull of the Early Triassic archosauromorph reptile *Prolacerta broomi* and its phylogenetic significance. Zoological Journal of the Linnean Society 140: 335–351.

Modesto, S. P. and Botha-Brink, J. 2008. Evidence of a second, large archosauriform reptile in the Lower Triassic Katberg Formation of South Africa. Journal of Vertebrate Paleontology 28: 914–917.

Montefeltro, F. C., Bittencourt, J. S., Langer, M. C. and Schultz, C. L. 2013. Postcranial anatomy of the hyperodapedontine rhynchosaur *Teyumbaita sulcognathus* (Azevedo and Schultz, 1987) from the Late Triassic of southern Brazil. Journal of Vertebrate Paleontology 33: 67–84.

Moss, J. L. 1972. The morphology and phylogenetic relationships of the Lower Permian tetrapod *Tseajaia campi* Vaughn (Amphibia: Seymouriamorpha). University of California Publications in Geological Sciences 98: 1−72.

Müller, J. 2004. The relationships among diapsid reptiles and the influence of taxon selection. In: Arratia, G., Wilson, M. V. H. and Cloutier, R. (eds.). Recent

Advances in the Origin and Early Radiation of Vertebrates. Dr Friedrich Pfeil, München: 379−408.

Müller, J. and Reisz, R. R. 2005. Four well-constrained calibration points from the vertebrate fossil record for molecular clock estimates. BioEssays 27: 1069−1075.

Müller, J., Berman, D. S, Henrici, A. C., Sumida, S. S. and Martens, T. 2006. The basal eureptile *Thuringothyris mahlendorffae* from the Lower Permian of Germany. Journal of Paleontology 80: 726−739.

Neenan, J. M., Klein, N. and Scheyer, T. M. 2013. European origin of placodont marine reptiles and the evolution of crushing dentition in Placodontia. Nature Communications 4: 1621.

Nesbitt, S. J. 2005. The osteology of the Middle Triassic pseudosuchian archosaur *Arizonasaurus babbitti*. Historical Biology 17: 19–47.

Nesbitt, S. J. 2007. The anatomy of *Effigia okeeffeae* (Archosauria, Suchia), theropod convergence, and the distribution of related taxa. Bulletin of the American Museum of Natural History 302: 1–84.

Nesbitt, S. J. 2011. The early evolution of archosaurs: relationships and the origin of major clades. Bulletin of the American Museum of Natural History 352: 1–292.

Nesbitt, S. J. and Norell, M. A. 2006. Extreme convergence in the body plans of an early suchian (Archosauria) and ornithomimid dinosaurs (Theropoda). Proceedings of the Royal Society of London B 273: 1045–1048.

Nesbitt, S. J. and Butler, R. J. 2013. Redescription of the archosaur *Parringtonia gracilis* from the Middle Triassic Manda Beds of Tanzania, and the antiquity of Erpetosuchidae. Geological Magazine 150: 225–238.

Nesbitt, S. J., Stocker, M. R., Small, B. J. and Downs, A. 2009. The osteology and relationships of *Vancleavea campi* (Reptilia: Archosauriformes). Zoological Journal of the Linnean Society 157: 814–864.

Nesbitt, S. J., Sidor, C. A., Irmis, R. B., Angielczyk, K. D., Smith, R. M. H. and Tsuji, L. A. 2010. Ecologically distinct dinosaurian sister-group shows early diversification of Ornithodira. Nature 464: 95−98.

Nesbitt, S. J., Liu, J. and Li, C. 2011. A sail-backed suchian from the Heshanggou Formation (Early Triassic: Olenekian) of China. Earth and Environmental Science Transactions of the Royal Society of Edinburgh 101: 271–284.

Nesbitt, S. J., Butler, R. J. and Gower, D. J. 2013a. A new archosauriform (Reptilia: Diapsida) from the Manda Beds (Middle Triassic) of southwestern Tanzania. PLoS ONE 8: e72753.

Nesbitt, S. J., Brusatte, S. L., Desojo, J. B., Liparini, A., de França, M. A. G., Weinbaum, J. C. and Gower, D. J. 2013b. Rauisuchia. In: Anatomy, Phylogeny and Palaeobiology of Early Archosaurs and their Kin, Nesbitt, S. J., Desojo, J. B. and Irmis, R. B. (eds.). Geological Society, London, Special Publication 379: 241–274.

Nesbitt, S. J., Flynn, J., Ranivohrimanina, L., Pritchard, A. and Wyss, A. 2013c. Relationships among the bizarre: the anatomy of *Azendohsaurus madagaskarensis* and its implications for resolving early archosauromroph phylogeny. Supplement to the online Journal of Vertebrate Paleontology: 184.

Nesbitt, S. J., Sidor, C. A., Angielczyk, K. D., Smith, R. M. H. and Tsuji, L. A. 2014. A new archosaur from the Manda beds (Anisian, Middle Triassic) of southern Tanzania and its implications for character state optimizations at Archosauria and Pseudosuchia. Journal of Vertebrate Paleontology 34: 1357−1382.

Newell, A. J., Sennikov, A. G., Benton, M. J., Molostovskaya, I. I., Golubev, V. K., Minikh, A. V. and Minikh, M. G. 2010. Disruption of playa-lacustrine depositional systems at the Permo-Triassic boundary: evidence from Vyazniki and Gorokhovets on the Russian Platform. Journal of the Geological Society of London 167: 695–716.

Newell, A. J., Benton, M. J., Kearsey, T., Taylors, G., Twitchett, R. J. and Tverdokhlebov, V. P. 2012. Calcretes, fluviolacustrine sediments and subsidence patterns in Permo-Triassic salt-walled minibasins of the south Urals, Russia. Sedimentology 59: 1659−1676.

Newton, E. T. 1894. Reptiles from the Elgin sandstone—description of two new genera. Philosophical Transactions of the Royal Society of London B 185: 573–607.

Nicholls, E. L. 1999. A reexamination of *Thalattosaurus* and *Nectosaurus* and the relationships of the Thalattosauria (Reptilia: Diapsida). PaleoBios 19: 1−29.

Niedźwiedzki, G., Sennikov, A. and Brusatte, S. L. 2014. The osteology and systematic position of *Dongusuchus efremovi* Sennikov, 1988 from the Anisian (Middle Triassic) of Russia. Historical Biology (advance online publication).

Norman, D. B., Crompton, A. W., Butler, R. J., Porro, L. B. and Charig, A. C. 2011. The Lower Jurassic ornithischian dinosaur *Heterodontosaurus tucki* Crompton and Charig, 1962: cranial anatomy, functional morphology, taxonomy and relationships. Zoological Journal of the Linnean Society 163: 182−276.

Nosotti, S. 2007. *Tanystropheus longobardicus* (Reptilia, Protorosauria): re-interpretations of the anatomy based on new specimens from the Middle Triassic of Besano (Lombardy, Northern Italy). Memorie della Societa Italiana di Scienze Naturali e del Museo Civico di Storia Naturale di Milano 35: 1–88.

Novas, F. E. 1986. Un probable terópodo (Saurischia) de la Formación Ischigualasto (Triásico superior), San Juan, Argentina. IV Congreso Argentino de Paleontología y Estratigrafía 2, Mendoza: 1−6.

Novas, F. E. 1989. The tibia and tarsus in Herrerasauridae (Dinosauria, *incertae sedis*) and the origin and evolution of the dinosaurian tarsus. Journal of Paleontology 63: 677−690.

Novas, F. E. 1992. Phylogenetic relationships of the basal dinosaurs, the Herrerasauridae. Palaeontology 35: 51−62.

Novas, F. E. 1993. New information on the systematics and postcranial skeleton of *Herrerasaurus ischigualastensis* (Theropoda: Herrerasauridae) from the Ischigualasto Formation (Upper Triassic) of Argentina. Journal of Vertebrate Paleontology 13: 400–423.

Novas, F. E. 1996. Dinosaur monophyly. Journal of Vertebrate Paleontology 16: 723−741.

O'Connor, P. M. 2006. Postcranial pneumaticity: an evaluation of soft-tissue influences on the postcranial skeleton and the reconstruction of pulmonary anatomy in archosaurs. Journal of Morphology 267: 1199–1226.

Ochev, V. G. 1958. New data concerning the pesudosuchians of the USSR. Doklady Akademi Nauk 123: 749–751. [In Russian]

Ochev, V. G. 1961. New thecodont from the Triassic of the Orenburg region of the Cis-Urals. Paleontological Journal 1961: 161–162. [In Russian]

Ochev, V. G. 1978. On the morphology of *Chasmatosuchus*. Paleontological Journal 1978: 98− 106. [In Russian]

Ochev, V. G. 1979. New Early Triassic archosaurs from eastern European Russia. Paleontological Journal 1979: 104–109. [In Russian]

Ochev, V. G. 1980. New archosaurs from the Middle Triassic of the southern Cis-Urals. Paleontological Journal 1980: 101–107. [In Russian]

Ochev, V. G. and Shishkin, M. A. 1988. Global correlation of the continental Triassic on the basis of tetrapods. International Geology Review 30: 163–176.

Osborn, H. F. 1903. The reptilian subclasses Diapsida and Synapsida and the early history of the Diaptosauria. Memoirs of the American Museum of Natural History 1: 449–507.

Owen, R. 1842. Report on British fossil reptiles. Report of the British Association for the Advancement of Science 11: 60–204.

Padian, K. 1983. Osteology and functional morphology of *Dimorphodon macronyx* (Buckland) (Pterosauria: Rhamphorhynchoidea) based on new material in the Yale Peabody Museum. Postilla 189: 1–44.

Parham, J. F., Donoghue, P. C. J., Bell, C. J., Calway, T. D., Head, J. J., Holroyd, P. A., Inoue, J. G., Irmis, R. B., Joyce, W. G., Ksepka, D. T., Patane, J. S. L., Smith, N. D., Tarver, J. E., van Tuinen, M., Yang, Z., Angielczyk, K. D., Greenwood, J, Hipsley, C. A., Jacobs, L., Makovicky, P. J., Müller, J., Smith, K. T., Theodor, J. M.. Warnock, R. C. M. and Benton, M. J. 2012. Best practices for justifying fossil calibrations. Systematic Biology 61: 346–359.

Parker, W. G. and Irmis, R. B. 2006. A new species of the Late Triassic phytosaur *Pseudopalatus* (Archosauria: Pseudosuchia) from Petrified Forest National Park, Arizona. In: A Century of Research at Petrified Forest National Park: Geology and Paleontology, Parker, W. G., Ash, S. R. and Irmis, R. B. (eds.). Museum of Northern Arizona, Flagstaff: 126–143.

Parker, W. G. and Barton, B. J. 2008. New information on the Upper Triassic archosauriform *Vancleavea campi* based on new material from the Chinle Formation of Arizona. Palaeontologia Electronica 11: 1–20.

Parks, P. 1969. Cranial anatomy and mastication of the Triassic reptile *Trilophosaurus* [M.S. thesis]: Austin, University of Texas: 100 pp.

Parrington, F. R. 1935. On *Prolacerta broomi*, gen. et sp. n. and the origin of lizards. Annals and Magazine of Natural History 16: 197–205.

Parrington, F. R. 1956. A problematic reptile from the Upper Permian. Annals and Magazine of Natural History 12: 333–336.

Parrish, J. M. 1986. Locomotor adaptations in the hindlimb and pelvis of the Thecodontia. Hunteria 1: 1–35.

Parrish, J. M. 1992. Phylogeny of the Erythrosuchidae (Reptilia: Archosauriformes). Journal of Vertebrate Paleontology 12: 93–110.

Parrish, J. M. 1993. Phylogeny of the Crocodylotarsi, with reference to archosaurian and crurotarsan monophyly. Journal of Vertebrate Paleontology 13: 287–308.

Parrish, J. M. 1994. Cranial osteology of *Longosuchus meadei* and the phylogeny and distribution of the Aetosauria. Journal of Vertebrate Paleontology 14: 196–209.

Peabody, F. E. 1952. *Petrolacosaurus kansensis* Lane, a Pennsylvanian reptile from Kansas. Paleontological Contributions of the University of Kansas, Vertebrata: 1−41.

Peng, J.-H. 1991. A new genus of Proterosuchia from the Lower Triassic of Shaanxi, China. Vertebrata PalAsiatica 29: 95–107.

Pérez-Higareda, G., Rangel-Rangel, A. and Smith, H. A. 1991. Maximum sizes of Morelet's and American crocodiles. Bulletin of the Maryland Herpetological Society 27: 34–37.

Peyer, B. 1937. Die Triasfauna der Tessiner Kalkalpen XII. *Macrocnemus bassanii* Nopcsa. Abhandlung der Schweizerische Palaontologische Geologischen Gesellschaft: 1−140.

Piechowski, R. and Dzik, J. 2010. The axial skeleton of *Silesaurus opolensis*. Journal of Vertebrate Paleontology 30: 1127–1141.

Piechowski, R., Tałanda, M. and Dzik, J. 2014. Skeletal variation and ontogeny of the Late Triassic Dinosauriform *Silesaurus opolensis*. Journal of Vertebrate Paleontology 34: 1383−1393.

Piñeiro, G., Verde, M., Ubilla, M. and Ferigolo, J. 2003. First basal synapsids ("pelycosaurs") from the Upper Permian-?Lower Triassic of Uruguay, South America. Journal of Paleontology 77: 389−392.

Piñeiro, G., Rojas, A. and Ubilla, M. 2004. A new procolophonoid (Reptilia, Parareptilia) from the Upper Permian of Uruguay. Journal of Vertebrate Paleontology 24: 814−821.

Pitman, E. T. G. 1939. A note on normal correlation. Biometrika 31: 9–12.

Piveteau, J. 1926. Paleóntologie de Madagascar, XIII — Amphibiens et reptiles Permiens. Annales de Paleóntologie 15: 55–178.

Platt, S. G., Rainwater, T. R., Thorbjarnarson, J. B., Finger, A. G., Anderson, T. A. and McMurry, S. T. 2009. Size estimation, morphometrics, sex ratio, sexual size dimorphism, and biomas of Morelet's crocodile in northern Belize. Caribbean Journal of Science 45: 80–93.

Platz, J. E. and Conlon, J. M. 1997. Reptile relationships turn turtle ... and turn back again. Nature 389: 245-46.

Porro, L. B., Butler, R. J., Barrett, P. M., Moore-Fay, S. and Abel, R. L. 2011. New heterodontosaurids specimens from the Lower Jurassic of southern Africa and the

early ornithischian dinosaur radiation. Earth and Environmental Transactions of the Royal Society of Edinburgh 101: 351–366.

Price, L. I. 1946. Sobre um novo pseudosuquio do Triássico Superior do Rio Grande do Sul. Boletim Divisão de Geología e Mineralogía 120: 1–38.

Pyron, R. A., Burbrink, F. T. and Wiens, J. J. 2013. A phylogeny and revised classification of Squamata, including 4161 species of lizards and snakes. BMC Evolutionary Biology 13: 93.

R Development Core Team. 2013. R: a language and environment for statistical computing. Vienna: R Foundation for Statistical Computing. ISBN 3–900051–07–0, available at http://www.R-project.org/.

Raath, M. A. 1990. Morphological variation in small theropods and its meaning in systematics: evidence from *Syntarsus rhodesiensis*. In: Dinosaur Systematics: Approaches and Perspectives, Carpenter, K. and Currie, P. J. (eds.). Cambridge University Press, San Diego: 91–105.

Rauhut, O. W. M. 2003. The interrelationships and evolution of basal theropod dinosaurs. Special Papers in Palaeontology 69: 1−213.

Reig, O. A. 1959. Primeros datos descriptivos sobre nuevos reptiles arcosaurios del Triásico de Ischigualasto (San Juan, Argentina). Revista de la Asociación Geológica Argentina 13: 257–270.

Reig, O. A. 1961. Acerca de la posición sistemática de la familia Rauisuchidae y del género *Saurosuchus* (Reptilia, Thecodontia). Publicaciones del Museo Municipal de Ciencias Naturales tradicional de Mar del Plata 1: 73–114.

Reig, O. A. 1963. La presencia de dinosaurios saurisquios en los “Estratos de Ischigualasto” (Mesotriásico superior) de las Provincias de San Juan y La Rioja (Republica Argentina). Ameghiniana 3: 3−20.

Reig, O. A. 1970. The Proterosuchia and the early evolution of the archosaurs; an essay about the origin of a major taxon. Bulletin of the Museum of Comparative Zoology 139: 229–292.

Reisz, R. R. 1977. *Petrolacosaurus*, the Oldest Known Diapsid Reptile. Science 196: 1091−1093.

Reisz, R. R. 1981. A diapsid reptile from the Pennsylvanian of Kansas. University of Kansas Publications of the Museum of Natural History 7: 1–74.

Reisz, R. R. and Berman, D. S. 2001. The skull of *Mesenosaurus romeri*, a small varanopseid (Synapsida: Eupelycosauria) from the Upper Permian of the Mezen River Basin, Northern Russia. Annals of Carnegie Museum 70: 113–132.

Reisz, R. R. and Dilkes, D. W. 2003. *Archaeovenator hamiltonensis*, a new varanopid (Synapsida: Eupelycosauria) from the upper Pennsylvanian of Kansas. Canadian Journal of Earth Sciences 40: 667–678.

Reisz, R. R. and Müller, J. 2004. Molecular timescales and the fossil record: a paleontological perspective. Trends in Genetics 20: 237–241.

Reisz, R. R. and Modesto, S. P. 2007. *Heleosaurus scholtzi* from the Permian of South Africa: a varanopid synapsid, not a diapsid reptile. Journal of Vertebrate Paleontology 27: 734–740.

Reisz, R. R., Modesto, S. P. and Scott, D. 2000. *Acanthotoposaurus bremneri* and the origin of the Triassic archosauromorph reptile fauna of South Africa. South African Journal of Science 96: 443–445.

Reisz, R. R., Laurin M. and Marjanović D. 2010. *Apsisaurus witteri* from the Lower Permian of Texas: yet another small varanopid synapsid, not a diapsid. Journal of Vertebrate Paleontology 30: 1628–1631.

Reisz, R. R., Modesto, S. P. and Scott, D. M. 2011. A new Early Permian reptile and its significance in early diapsid evolution. Proceedings of the Royal Society B 278: 3731−3737.

Renesto, S. 1992. The anatomy and relationships of *Endennasaurus acutirostris* (Reptilia: Neodiapsida) from the Norian (late Triassic) of Lombardy. Rivista Italiana di Paleontologia e Stratigrafia 97: 409–430.

Rieppel, O. 1989a. *Helveticosaurus zollingeri* Peyer (Reptilia, Diapsida): skeletal paedomorphosis; functional anatomy and systematic affinities. Palaeontographica A 208: 123–152.

Rieppel, O. 1989b. The hind limb of *Macrocnemus bassanii* (Nopcsa) (Reptilia, Diapsida): development and functional anatomy. Journal of Vertebrate Paleontology 9: 373−387.

Rieppel, O. and deBraga, M. 1996 Turtles as diapsid reptiles. Nature 384: 453–455.

Rieppel, O. and Reisz, R. 1999. The origin and evolution of turtles. Annual Review of Ecology and Systematics 30: 1–22.

Rieppel, O., Mazin, M. and Tchernov, E. 1999. Sauropterygia from the Middle Triassic of Makhtesh Ramon, Negev, Israel. Fieldiana, Geology, new series 40: 1−85.

Rieppel, O., Fraser, N. C. and Nosotti, S. 2003. The monophyly of Protorosauria (Reptilia, Archosauromorpha): a preliminary analysis. Atti della Societ`a Italiana di Scienze naturali e Museo civico di Storia naturale di Milano 144: 359–382.

Rieppel, O., Jiang, D. and Fraser, N. 2010. *Tanystropheus* cf. *T. longobardicus* from the early Late Triassic of Guizhou Province, southwestern China. Journal of Vertebrate Paleontology 30: 1082–1089.

Romer, A. S. 1944. The Permian cotylosaur *Diadectes tenuitectes*. American Journal of Science 242: 139−144.

Romer, A. S. 1945. Vertebrate Paleontology, 2nd edition. University of Chicago Press, Chicago: 687 pp.

Romer, A. S. 1956. Osteology of the Reptiles. University of Chicago Press, Chicago: 772 pp.

Romer, A. S. 1966. Vertebrate Paleontology, 3rd edition. Chicago, University of Chicago Press: 468 pp.

Romer, A. S. 1971a. The Chañares (Argentina) Triassic reptile fauna. XI: Two new long–snouted thecodonts, *Chanaresuchus* and *Gualosuchus*. Breviora 379: 1–22.

Romer, A. S. 1971b. The Chañares (Argentina) Triassic reptile fauna. XI. Two but new incompletely known long-limbed Pseudosuchians. Breviora 378: 1−10

Romer, A. S. 1972a. The Chañares (Argentina) Triassic reptile fauna. XVI. Thecodont classification. Breviora 395: 1–24.

Romer, A. S. 1972b. The Chañares (Argentina) Triassic reptile fauna. XIII. An early ornithosuchid pseudosuchian, *Gracilisuchus stipanicicorum*, gen. et sp. nov. Breviora 389: 1–24.

Romer, A. S. 1972c. The Chañares (Argentina) Triassic reptile fauna. XV. Further remains of the thecodonts *Lagerpeton* and *Lagosuchus*. Breviora 390: 1−7.

Romer, A. S. 1972d. The Chañares (Argentina) Triassic reptile fauna. XIV. *Lewisuchus admixtus* gen. et sp. nov., A further thecodont from the Chañares beds. Breviora 390: 1–13.

Romer, A. S. 1972e. The Chañares (Argentina) Triassic reptile fauna. XII. The postcranial skeleton of the thecodont *Chanaresuchus*. Breviora 385: 1–21.

Romer, A. S. and Price, L. I. 1940. Review of the Pelycosauria. Geological Society of America Special Paper 28: 1–538.

Roscher, M. and Schneider, J. W. 2006. Permo-Carboniferous climate; Early Pennsylvanian to Late Permian climate development of Central Europe in a regional and global context. Non-Marine Permian Biostratigraphy and Biochronology: In: Lucas, S. G., Cassinis, G. and Schneider, J.W. (eds.). Geological Society, London, Special Publication 265: 95–136.

Rowe, T. 1989. A new species of the theropod dinosaur *Syntarsus* from the Early Jurassic Kayenta Formation of Arizona. Journal of Vertebrate Paleontology 9: 125−136.

Rubidge, B. S. 1995. Biostratigraphy of the Beaufort Group (Karoo Supergroup). South African Committee for Stratigraphy, Biostratigraphic Series 1. Government Printer, Pretoria: 46 pp.

Rubidge, B. S. 2005. Re-uniting lost continents – fossil reptiles from the ancient Karoo and their wanderlust. South African Journal of Geology 108: 135–172.

Rubidge, B. S., Erwin, D. H., Ramezani, J., Bowring, S. A. and de Klerk W. J. 2013. High-precision temporal calibration of Late Permian vertebrate biostratigraphy: U-Pb zircon constraints from the Karoo Supergroup, South Africa. Geology 41: 363–366.

Rusconi, C. 1951. Laberintodontes triásicos y pérmicos de Mendoza. Revista del Museo de Historia Natural de Mendoza 5: 33–158.

Sanders, K. L. and Lee M. S. Y. 2007. Evaluating molecular clock calibrations using Bayesian analyses with soft and hard bounds. Biology Letters 3: 275−279.

Santa Luca, A. P. 1980. The postcranial skeleton of *Heterodontosaurus tucki* (Reptilia, Ornithischia) from the Stormberg of South Africa. Annals of the South African Museum 79: 159−211.

Satsangi, P. P. 1964. A note on *Chasmatosaurus* from the Panchet Series of Raniganj Coalfield, India. Current Science 33: 651–652.

Schlüter, T. and Kohring, R. 1997. The fossil record of the Karoo in East Africa: history, palaeoecology and biostratigraphy. Neues Jahrbuch für Geologie und Paläontologie, Abhandlung 204: 1–17.

Schoch, R. R. and Sues, H.-D. 2013. A new archosauriform reptile from the Middle Triassic (Ladinian) of Germany. Journal of Systematic Palaeontology 12: 113−131.

Sennikov, A. G. 1988a. The role of the oldest thecodontians in the vertebrate assemblage of Eastern Europe. Paleontological Journal 1988: 78–87. [In Russian]

Sennikov, A. G. 1988b. New rauisuchids from the Triassic of European Russia. Paleontologicheskiy Zhurnal 1988: 124−128. [In Russian]

Sennikov, A. G. 1989a. A new euparkeriid (Thecodontia) from the Middle Triassic of the Southern Preurals. Paleontologicheskiy Zhurnal 2: 71–78. [In Russian]

Sennikov, A. G. 1989b. A new euparkeriid (Thecodontia) from the Middle Triassic of the Southern Urals. Paleontological Journal 22: 66–73. [In Russian]

Sennikov, A. G. 1990. New data on the rauisuchids of eastern Europe. Paleontological Journal 1990: 3−16. [In Russian]

Sennikov, A. G. 1992. Oldest proterosuchids from the Triassic of eastern Europe. Doklady Akademii Nauk 326: 896–899. [In Russian]

Sennikov, A. G. 1994. The first Middle Triassic proterosuchid from eastern Europe. Doklady Akademii Nauk 336: 659–661. [In Russian]

Sennikov, A. G. 1995a. Diapsid reptiles from the Permian and Triassic of Eastern Europe. Paleontological Journal 1995: 75–83. [In Russian]

Sennikov, A. G. 1995b. Early thecodonts of Eastern Europe. Trudy Paleontologischeskogo Instituta RAN 263: 1–141. [In Russian]

Sennikov, A. G. 1997. An enigmatic reptile from the Upper Permian of the Volga River Basin. Paleontological Journal 31: 94–101.

Sennikov, A. G. 2005. A New Specialized Prolacertilian (Reptilia: Archosauromorpha) from the Lower Triassic of the Orenburg Region. Paleontological Journal 39: 199–209.

Sennikov, A. G. 2008. Archosauromorpha. In: Fossil vertebrates from Russia and adjacent countries, Fossil Reptiles and Birds Part 1, Ivakhnenko, M. F. and Kurochkin, E. N. (eds.). Russian Academy of Sciences Paleontological Institute, Moscow: 266–318. [In Russian]

Sennikov, A. G. 2011. New Tanystropheids (Reptilia: Archosauromorpha) from the Triassic of Europe. Paleontological Journal 45: 90−104.

Sennikov, A. G. and Golubev, V. K. 2006. Vyazniki biotic assemblage of the terminal Permian. Paleontological Journal 40: 475–481.

Sennikov, A. G. and Golubev, V. K. 2012. On the faunal verification of the Permo–Triassic boundary in continental deposits of eastern Europe: 1. Gorokhovets–Zhukov Ravine. Paleontological Journal 46: 313–323.

Senter, P. 2003. New information on cranial and dental features of the Triassic archosauriform reptile *Euparkeria capensis*. Palaeontology 46: 613–621.

Senter, P. 2004. Phylogeny of Drepanosauridae (Reptilia: Diapsida). Journal of Systematic Palaeontology 2: 257−268.

Sereno, P. C. 1986. Phylogeny of the bird-hipped dinosaurs (Order Ornithischia). National Geographic Resarch Exploration 2: 234−256.

Sereno, P. C. 1991. Basal archosaurs: phylogenetic relationships and functional implications. Society of Vertebrate Paleontology Memoir 2: 1–53.

Sereno, P. C. 1993. The pectoral girdle and forelimb of the basal theropod *Herrerasaurus ischigualastensis.* Journal of Vertebrate Paleontology 13: 425−450.

Sereno, P. C. 1999. The evolution of dinosaurs. Science 284: 2137−2147.

Sereno, P. C. 2005. The logical basis of phylogenetic taxonomy. Systematic Biology 54: 595–619.

Sereno, P. C. 2012. Taxonomy, morphology, masticatory function and phylogeny of heterodontosaurid dinosaurs. ZooKeys 226: 1–225.

Sereno, P. C. and Arcucci, A. B. 1990. The monophyly of crurotarsal archosaurs and the origin of bird and crocodile ankle joints. Neues Jahrbuch für Geologie und Paläontologie Abhandlungen 180: 21–52.

Sereno, P. C. and Novas, F. E. 1992. The complete skull and skeleton of an early dinosaur. Science 258: 1137−1140.

Sereno, P. C. and Wild, R. 1992. *Procompsognathus*: theropod, ‘‘thecodont’’ or both? Journal of Vertebrate Paleontology 12: 435−458.

Sereno, P. C. and Arcucci, A. B. 1993. Dinosaurian precursors from the Middle Triassic of Argentina: *Lagerpeton chanarensis*. Journal of Vertebrate Paleontology 13: 385–399.

Sereno, P. C. and Novas, F. E. 1993. The skull and neck of the basal theropod *Herrerasaurus ischigualastensis*. Journal of Vertebrate Paleontology 13: 451–476.

Sereno, P. C. and Arcucci, A.B. 1994. Dinosaurian precursors from the Middle Triassic of Argentina: *Marasuchus lilloensis*, gen. nov. Journal of Vertebrate Paleontology 14: 53–73.

Sereno, P. C., Forster, C. A., Rogers, R. R. y Monetta, A. M. 1993. Primitive dinosaur skeleton from Argentina and the early evolution of the Dinosauria. Nature 361: 64−66.

Sereno, P. C. Wilson, J. A., Larsson, H. C. E., Dutheil, D. B. and Sues, H.-D. 1994. Early Cretaceous dinosaurs from the Sahara. Science 266: 267–270.

Shen, X.-X., Liang, D., Wen, J.-Z. and Zhang, P. 2011. Multiple genome alignments facilitate development of NPCL markers: a case study of tetrapod phylogeny focusing on the position of turtles. Molecular Biology Evolution 28: 3237−3252.

Sidor, C. A., Angielczyk, K. D., Weide, D. M., Smith, R. M. H., Nesbitt, S. J., and Tsuji, L. A. 2010. Tetrapod fauna of the lowermost Usili Formation (Songea Group, Ruhuhu Basin) of southern Tanzania, with a new burnetiid record. Journal of Vertebrate Paleontology 30: 696–703.

Sill, W. D. 1967. *Proterochampsa barrionuevoi* and the early evolution of the Crocodilia. Bulletin of the Museum of Comparative Zoology 135: 415–446.

Smith, R. J. 2009. Use and misuse of the reduced major axis for line-fitting. American Journal of Physical Anthropology 140: 476–486.

Smith, R. M. H. and Evans, S. 1996. New Material of *Youngina*: Evidence of Juvenile Aggregation in Permian Diapsid Reptiles. Palaeontology 39: 289−303.

Smith, R. M. H. and Botha, J. 2005. The recovery of terrestrial vertebrate diversity in the South African Karoo Basin after the end-Permian extinction. Comptes Rendus Palevol 4: 623–636.

Smith, R. M. H. and Botha-Brink, J. 2014. Anatomy of a mass extinction: sedimentological and taphonomic evidence for drought-induced die-offs at the Permo-Triassic boundary in the main Karoo Basin, South Africa. Palaeogeography, Palaeoclimatology and Palaeoecology 396: 99–118.

Sömmerring, T. v. 1812. Über einen *Ornithocephalus*. Denkschriften der königlichen bayerischen Akademie der Wissenschaften, Mathematische-Physische Klasse 3: 89–158.

Sood, M. S. 1948. The anatomy of the vertebral column in serpentes. Proceedings of the Indian Academy of Sciences - Section B 28: 1−26.

Sookias, R. B. and Butler, R. J. 2013. Euparkeriidae. In: Anatomy, Phylogeny and Palaeobiology of Early Archosaurs and their Kin, Nesbitt, S. J., Desojo, J. B. and Irmis, R. B. (eds.). Geological Society, London, Special Publication 379: 35–48.

Sookias, R. B., Sennikov, A. G., Gower, D. J. and Butler, R. J. 2014. The monophyly of Euparkeriidae (Reptilia: Archosauriformes) and the origins of Archosauria: a revision of *Dorosuchus neoetus* from the Mid-Triassic of Russia. Palaeontology 57: 1177−1202.

Spalletti, L. A., Fanning, C. M. and Rapela, C. W. 2008. Dating the Triassic continental rift in the southern Andes: the Potrerillos Formation, Cuyo Basin, Argentina. Geologica Acta 6: 267–283.

Spener, C. M. 1710. Disquistio de crocodile in lapide scissile expresso, aliisque Lithozois. Misc Berol ad increment sci, ex scr Soc Regiae Sci exhibits ed I: 92−110.

Spielmann, J. A., Lucas, S. G., Rinehart, L. F. and Heckert, A. B. 2008. The Late Triassic archosauromorph *Trilophosaurus*. Bulletin of the New Mexico Museum of Natural Historty and Sciences 43: 1–177.

Spielmann, J. A., Lucas, S. G., Heckert, A. B., Rinehart, L. F. and Richards III, H. R. 2009. Redescription of *Spinosuchus caseanus* (Archosauromorpha: Trilophosauridae) from the Upper Triassic of North America. Palaeodiversity 2: 283–313.

Stocker, M. R. 2010. A new taxon of phytosaur (Archosauria: Pseudosuchia) from the Late Triassic (Norian) Sonsela Member (Chinle Formation) in Arizona, and a critical reevaluation of *Leptosuchus* Case, 1922. Palaeontology 53: 997–1022.

Stocker, M. R. and Butler, R. J. 2013. Phytosauria. In: Anatomy, Phylogeny and Palaeobiology of Early Archosaurs and their Kin, Nesbitt, S. J., Desojo, J. B. and Irmis, R. B. (eds.). Geological Society, London, Special Publication 379: 91–117.

Stockley, G. M. 1932. The geology of the Ruhuhu coalfields, Tanganyika Territory. The Quarterly Journal of the Geological Society of London 88: 610–622.

Storrs, G. W. and Gower, D. J. 1993. The earliest possible choristodere (Diapsida) and gaps in the fossil record of semi-aquatic reptiles. Journal of Geological Society 150: 1103–1107.

Strohmenger, C., Voigt, E. and Zimdars, J. 1996. Sequence stratigraphy and cyclic development of Basal Zechstein carbonate-evaporite deposits (Upper Permian, northwest Germany). Sedimentary Geology 102: 33−54.

Sues, H.-D. and Munk, W. 1996. A remarkable assemblage of terrestrial tetrapods from the Zechtsein (Upper Permian: Tatarian) near Korbach (northwestern Hesse). Paläontologische Zeitschrift 70: 213–223.

Sues, H.-D., Olsen, P. E., Carter, J. G. and Scott, D. M. 2003. A new crocodylomorph archosaur from the Upper Triassic of North Carolina. Journal of Vertebrate Paleontology 23: 329–343.

Sues, H.-D., Desojo, J. B. and Ezcurra, M. D. 2013. Doswelliidae: a clade of unusual armoured archosauriforms from the Middle and Late Triassic. In: Anatomy, Phylogeny and Palaeobiology of Early Archosaurs and their Kin, Nesbitt, S. J., Desojo, J. B., Irmis, R. B. (eds.). Geological Society, London, Special Publication 379: 49−58.

Sumida, S. S. 1991. Vertebral morphology, alternation of neural spine height, and structure in Permo-Carboniferous tetrapods, and a reappraisal of primitive modes of terrestrial locomotion. University of California Publication of Zoology 1: 221−135.

Tatarinov, L. P. 1960. Discovery of pseudosuchians in the Upper Permian of SSSR. Paleontological Journal 1960: 74–80. [In Russian]

Tatarinov, L. P. 1961. Pseudosuchians of the USSR. Paleontological Journal 1961: 117–132. [In Russian]

Tatarinov, L. P. 1978. Triassic prolacertilians of the USSR. Paleontological Journal 12: 505−514.

Taylor, G. K., Tucker, C., Twitchett, R. J., Kearsey, T., Benton, M. J., Newell, A. J., Surkov, M. V. and Tverdokhlebov, V. P. 2009. Magnetostratigraphy of Permian/Triassic boundarysequences in the Cis-Urals, Russia: no evidence for a major temporal hiatus. Earthand Planetary Science Letters 281: 36–47.

Thulborn, R. A. 1979. A proterosuchian thecodont from the Rewan Formation of Queensland. Memoirs of the Queensland Museum 19: 331–355.

Thulborn, R. A. 1986. The Australian Triassic reptile *Tasmaniosaurus triassicus* (Thecodontia: Proterosuchia). Journal of Vertebrate Paleontology 6: 123–142.

Trotteyn, M. J. 2011. The phylogenetic relationships and monophyly of Proterochampsidae. IV Congreso Latinoamericano de Paleontología de Vertebrados, San Juan, Argentina.

Trotteyn, M. J. and Haro, J. A. 2011. The braincase of a specimen of *Proterochampsa* Reig (Archosauriformes: Proterochampsidae) from the Late Triassic of Argentina. Palaontologische Zeitschrift 85: 1–17.

Trotteyn, M. J. and Haro, J. A. 2012. The braincase of *Chanaresuchus ischigualastensis* (Archosauriformes) from the Late Triassic of Argentina. Journal of Vertebrate Paleontology 32: 867–882.

Trotteyn, M. J. and Ezcurra, M. D. 2014. Osteology of *Pseudochampsa ischigualastensis* gen. et comb. nov. (Archosauriformes: Proterochampsidae) from the early Late Triassic Ischigualasto Formation of northwestern Argentina. PLoS ONE 9: e111388.

Trotteyn, M. J., Martinez, R. N. and Alcober, O. A. 2012. A new proterochampsid *Chanaresuchus ischigualastensis* (Diapsida, Archosauriformes) in the Early Late Triassic Ischigualasto Formation, Argentina. Journal of Vertebrate Paleontology 32: 485–489.

Trotteyn, M. J., Arcucci, A. B. and Raugust, T. 2013. Proterochampsia: an endemic archosauriform clade from South America. In: Anatomy, Phylogeny and Palaeobiology of Early Archosaurs and their Kin, Nesbitt, S. J., Desojo, J. B. and Irmis, R. B. (eds.). Geological Society, London, Special Publication 379: 59−90.

Tucker, A. D. 1997. Validation of skeletochronology to determine age of freshwater crocodiles (*Crocodylus johnstoni*). Marine and Freshwater Research 48: 343–351.

Tykoski, R. S. 2005. Osteology, ontogeny, and relationships of the coelophysoid theropods. PhD thesis, University of Texas at Austin, Austin: 553 pp.

Vaughn, P. P. 1955. The Permian reptile *Araeoscelis* restudied. Bulletin of the Harvard Museum of Comparative Zoology 113: 305–467.

Walker, A. D. 1964. Triassic reptiles from the Elgin area: *Ornithosuchus* and the origin of carnosaurs. Philosophical Transactions of the Royal Society of London B 248: 53−134.

Wang, R., Xu, S., Wu, X., Li, C. and Wang, S. 2013. A New Specimen of *Shansisuchus shansisuchus* Young, 1964 (Diapsida: Archosauriformes) from the Triassic of Shanxi, China. Acta Geologica Sinica 87: 1185−1197.

Warren, A. A. and Hutchinson, M. N. 1990. *Lapillopsis*, a new genus of temnospondyl amphibians from the Early Triassic of Queensland. Alcheringa 14: 149–158.

Warton, D. I., Wright, I. J., Falster, D. S. and Westoby, M. 2006. Bivariate linefitting methods for allometry. Biological Reviews 81: 259–291.

Warton, D. I., Wright, I. J., Falster, D. S. and Westoby, M. 2012. SMATR 3 – an R package for estimation and inference about allometric lines. Methodologies in Ecology and Evolution 2012: 257–259.

Watson, D. M. S. 1912. *Mesosuchus browni*, gen. et spec. nov. Records of the Albany Museum 2: 298–299.

Watson, D. M. S. 1917. A sketch classification of the Pre-Jurassic tetrapod vertebrates. Proceedings of the Zoological Society of London 1917: 167–186.

Watson, D. M. S. 1957. On *Millerosaurus* and the Early History of the Sauropsid Reptiles. Philosophical Transactions of the Royal Society of London B 240: 325−400

Webb, G. J. W. and Messel, H. 1978. Morphometric Analysis of *Crocodylus porosus* from the North Coast of Arnhem Land, Northern Australia. Australian Journal of Zoology 26: 1−27.

Wedel, M. J. 2007. What pneumaticity tells us about 'prosauropods', and vice versa. Special Papers in Palaeontology 77: 207−222.

Weems, R. E. 1980. An unusual newly discovered archosaur from the Upper Triassic of Virginia, USA. Transactions of the American Philosophical Society 70: 1–53.

Weide, D. M., Sidor, C. A., Angielczyk, K. D. and Smith, R. M. H. 2009. A new record of Procynosuchus delaharpeae (Therapsida: Cynodontia) from the Upper Permian Usili Formation, Tanzania. Palaeontologia Africana 44: 21−26.

Weinbaum, J. C. and Hungerbühler, A. 2007. A revision of *Poposaurus gracilis* (Archosauria: Suchia) based on two new specimens from the Late Triassic of the southwestern U.S.A. Paläontologische Zeitschrift 81: 131–145.

Weishampel, D. B. and Witmer, L. M. 1990. Heterodontosauridae. In: The Dinosauria, Weishampel, D. B., Dodson, P. and Osmólska, H. (eds.). University of California Press, Berkeley: 486–497.

Welman, J. 1998. The taxonomy of the South African proterosuchids (Reptilia, Archosauromorpha). Journal of Vertebrate Paleontology 18: 340–347.

Welman, J. and Flemming, A. F. 1993. Statistical analysis of the skulls of Triassic proterosuchids (Reptilia, Archosauromorpha) from South Africa. Palaeontologia Africana 30: 113–123.

Whiteside, D. I. and Marshall, J. E. A. 2008. The age, fauna and palaeoenvironment of the Late Triassic fissure deposits of Tytherington, South Gloucestershire, UK. Geological Magazine 145: 105–147.

Wild, R. 1973. Die Triasfauna dr Tessiner Kalkalpen. XXIII *Tanystropheus longobardicus* (Bassani) (Neue Ergebnisse). Abhandlungen Schweizerische Paläontologische Gesellschaft 95: 1–162.

Willistons, W. 1925. The osteology of the reptiles. Harvard University Press, Cambridge: 300 pp.

Wilson, J. A. 1999. Vertebral laminae in sauropods and other saurischian dinosaurs. Journal of Vertebrate Paleontology 19: 639–653.

Wilson, J. A., D'Emic, M. D., Ikejiri, T., Moacdieh, E. M. and Whitlock, J. A. 2011. A Nomenclature for Vertebral Fossae in Sauropods and Other Saurischian Dinosaurs. PLoS ONE 6: e17114.

Woodward, A. R. and Moore, C. T. 1992. *Alligator Age Determination*. Florida Game and Fresh Water Fish Commission Bureau of Wildlife Research, Final Report 7563.

Wopfner, H., Markwort, S. and Semkiwa, P. M. 1991. Early diagenetic laumontite in the Lower Triassic Manda Beds of the Ruhuhu Basin, southern Tanzania. Journal of Sedimentary Petrology 61: 65–72.

Wu, X. 1981. The discovery of a new thecodont from north-east Shensi. Vertebrata PalAsiatica 19: 122–132.

Wu, X.-C. and Chatterjee, S. 1993. *Dibothrosuchus elaphros*, a crocodylomorph from the Lower Jurassic of China and the phylogeny of the Sphenosuchia. Journal of Vertebrate Paleontology 13: 58–89.

Wu, X.-C. and Russell, A. P. 2001. Redescription of *Turfanosuchus dabanensis* (Archosauriformes) and new information on its phylogenetic relationships. Journal of Vertebrate Paleontology 21: 40–50.

Wu, X.-C., Liu, J. and Li, J.-L. 2001. The anatomy of the first archosauriform (Diapsida) from the terrestrial Upper Triassic of China. Vertebrata PalAsiatica 39: 251–265.

Yates, A. M. 2003. A new species of the primitive dinosaur *Thecodontosaurus* (Saurischia: Sauropodomorpha) and its implications for the systematics of early dinosaurs. Journal of Systematic Palaeontology 1: 1–42.

Young, C.-C. 1936. On a new *Chasmatosaurus* from Sinkiang. Bulletin of the Geological Society of China 15: 291–311.

Young, C.-C. 1958. On the occurrence of *Chasmatosaurus* from Wuhsiang, Shansi. Vertebrata PalAsiatica 2: 259−262.

Young, C.-C. 1963. Additional remains of *Chasmatosaurus yuani* Young from Sinkiang, China. Vertebrata PalAsiatica 7: 215–222.

Young, C.-C. 1964. The pseudosuchians in China. Palaeontologia Sincia new series C 151: 1–205.

Young, C.-C. 1973a. On the occurrence of *Vjushkovia* in Sinkiang. Memoirs of the Institute of Vertebrate Paleontology and Paleoanthropology 10: 38−52.

Young, C.-C. 1973b. *Prolacertoides jimusarensis*. Vertebrata PalAsiatica 11: 46−48.

Young, C.-C. 1973c. On a new pseudosuchian from Turfan, Sinking (Xinjiang). Memoirs of the Institute of Vertebrate Paleontology and Paleoanthropology, Academia Sinica, Series B 10: 15–37.

Young, C.-C. 1978. A complete skeleton of *Chasmatosaurus yuani* from Xinjinang. Memoirs of the Institute of Vertebrate Paleontology and Paleoanthropology, Academia Sinica, Series B 13: 26–46.

Zardoya, R. and Meyer, A. 1998. Complete mitochondrial genome suggests diapsid affinities of turtles. Proceeding of the National Academy of Sciences USA 95: 14226−14231.

Zittel, K. A. 1887−1890. Handbuch der Paläontologie. Abtheilung. I. Paläozoologie 3. R. Oldenbourg, Munich and Leipzig: 633−900.

Appendix 1

Institutional abbreviations

AM, Albany Museum, Grahamstown, South Africa; AMNH, American Museum of Natural History, New York, USA; BATGM; Bath Geology Museum, Bath, UK; BP, Evolutionary Studies Institute (formerly Bernard Price Institute for Palaeontological Research), University of the Witswatersrand, Johannesburg, South Africa; BRSUG, University of Bristol, Department of Geology, Bristol, United Kingdom; BSPG, Bayerische Staatssammlung für Paläontologie und Geologie, Munich, Germany; CA, Colégio Anchieta, Porto Alegre, Brazil; CPEZ, Coleção Municipal, São Pedro do Sul, Brazil; CRILAR, Centro Regional de Investigaciones y Transferencia Tecnológica de La Rioja, Paleontología de Vertebrados, Anillaco, La Rioja, Argentina; FC-DPV, Colección de Vertebrados Fósiles, Departamento de Paleontología, Facultad de Ciencias, Universidad de la República, Montevideo, Uruguay; FG, Paläontologische und Stratigraphische Sammlung an der TU Bergakademie Freiberg im Humboldt-Bau, Freiburg, Germany; FMNH, Field Museum of Natural History, Chicago, USA; GHG, Geological Survey, Pretoria, South Africa; GMB, Geological Institute, Beijing, China; GPIT, Paläontologische Sammlung der Universität Tübingen, Tübingen, Germany; GR, Ghost Ranch Ruth May Museum of Paleontology, New Mexico, USA; GSI, Geological Survey of India, Kolkata, India; IPB, Institut für Paläontologie, Universität Bonn, Bonn, Germany; IVPP, Institute of Vertebrate Paleontology and Paleoanthropology, Beijing, China; KUMNH, Kansas University Museum of Natural History, Lawrence, USA; MACN, Museo Argentino de Ciencias Naturales "Bernardino Rivadavia", Buenos Aires, Argentina; MCNAM, Museo de Ciencias Naturales y Antropológicas de Mendoza (J. C. Moyano), Mendoza, Argentina; MCP,

Museu de Ciências e Tecnologia da Pontifícia Universidade Católica do Rio Grande do Sul, Porto Alegre, Brazil; MCZ, Museum of Comparative Zoology, Cambridge, USA; MHI, Muschelkalkmuseum, Ingelfingen, Germany; MNHN, Muséum national d'Histoire naturelle, Paris, France; MLP, Museo de La Plata, La Plata, Argentina; MNHN, Muséum national d'Histoire naturelle, Paris, France; MSNM, Museo di Storia Naturale, Milano, Italy; Nat. Kab., Naturalienkabinett und Heimatmuseum, Waldenburg, Germany; NHMUK, The Natural History Museum, London, UK; NHMW, Naturhistorisches Museum Wien, Vienna, Austria; NM, National Museum, Bloemfontein, South Africa; NMK, Naturkundemuseum im Ottoneum, Kassel, Germany; PIMUZ, Paläontologisches Institut und Museum der Universität Zürich, Zurich, Switzerland; PIN, Paleontological Institute of the Russian Academy of Sciences, Moscow, Russia; PSM, Privatsammlung W. Munk, Walzbachtal, Germany; PULR, Paleontología, Universidad Nacional de La Rioja, La Rioja, Argentina; PVL, Paleontología de Vertebrados, Instituto 'Miguel Lillo', San Miguel de Tucumán, Argentina; PVSJ, División de Paleontología de Vertebrados del Museo de Ciencias Naturales y Universidad Nacional de San Juan, San Juan, Argentina; QM, Queensland Museum, Brisbane, Queensland, Australia; RC, Rubidge collection, Wellwood, Graaff-Reinet, South Africa; SAM, South Australian Museum, Adelaide, Australia; SAM-PK, Iziko South African Museum, Cape Town, South Africa; SHRCM, Shropshire County Museum, Ludlow, UK; SHYMS, Shrewsbury Borough Museum, Shrewsbury, UK; SMNS, Staatliches Museum für Naturkunde Stuttgart, Stuttgart, Germany; TM, Ditsong National Museum of Natural History (formerly Transvaal Museum), Pretoria, South Africa; TMM, Texas Memorial Museum, Austin, USA; UA, University of Antananarivo, Antananarivo, Madagascar; UCMP, University of California Museum of Paleontology, Berkeley, USA; UFRGS, Universidade Federal

do Rio Grande do Sul, Porto Alegre, RS, Brazil; UMZC, University Museum of Zoology, Cambridge, UK; USNM, National Museum of Natural History (formerly United States National Museum), Smithsonian Institution, Washington, D.C., USA; UTGD, School of Earth Sciences, University of Tasmania, Hobart, Australia; WARMS, Warwickshire Museum, Warwick, UK; WMsN, Westfälisches Museum für Naturkunde, Münster, Germany; YPM, Yale Peabody Museum, New Haven, Connecticut, USA; ZAR, Muséum national d'Histoire naturelle (Zarzaitine collection), Paris, France; ZMR MB, Museum für Naturkunde – Leibniz-Institut für Evolutions- und Biodiversitätsforschung, Berlin, Germany; ZPAL, Institute of Paleobiology of the Polish Academy of Sciences in Warsaw, Poland.

Appendix 2

Anatomical description of *Aenigmastropheus parringtoni* gen. et sp. nov.

Parrington (1956) apparently considered all the bones catalogued as UMZC T836 to belong to a single individual. The five preserved vertebrae do indeed possess a congruent morphology and similar size, consistent with belonging to a single individual (Figs. S2.1, S2.2; Table S2.1). The right humerus and ulna are also consistent in size with belonging to a single individual, and the trochanter (ulnar condyle) of the humerus fits quite well when articulated with the proximal articular facet of the ulna (Figs. S2.3, S2.5; Table S2.2). However, assessing the assignment of the axial and appendicular elements to a single individual is less straightforward. The ratio between the posterior widths of the centra and the maximum distal width of the humerus ranges between 0.29–0.33 in *Aenigmastropheus parringtoni*. This range is very similar to or overlaps the ratio observed in basal reptiliomorphs (e.g. 0.31 in the diadectomorph *Diadectes*: Romer, 1944), synapsids (e.g. 0.35–0.37 in the varanopid *Varanops*: TMM 43628-1 in Reisz et al. [2010]; 0.27–0.29 in *Ophiacodon mirus*: FMNH (WM) 671 in Romer and Price [1940]; 0.27–0.32 in *Dimetrodon loomsi*: FMNH (WM) 114 in Romer and Price [1940]) and diapsids (e.g. 0.38–0.41 in the archosauriform *Erythrosuchus africanus*: SAM-PK-905). Accordingly, this ratio supports the interpretation of Parrington (1956) that all the bones of UMZC T836 belong to a single individual.

The bones are generally well preserved, but possess some damaged surfaces, some of which possibly result from preparation with acetic acid. In a few areas the

cortical bone has collapsed or has broken away, and some degree of post-mortem distortion is evident in some elements (most notably in the vertebrae).

Five presacral **vertebrae** are preserved (Figs. S2.1, S2.2), and exhibit slight post-mortem distortion, with the left sides (e.g. zygapophyses and transverse processes) of some of the vertebrae having being displaced dorsally relative to the right side. Unfortunately, the prezygapophyses, transverse processes and neural spines are incomplete in all of the vertebrae. Parrington (1956: fig. 1) designated the vertebrae of UMZC T836 as specimens "1"–"5" for descriptive purposes (hereafter referred as vertebrae 1–5, retaining Parrington's original numbering), and these numbers are written on the left lateral surfaces of the elements. Although I cannot assess with confidence whether or not the preserved vertebrae represent a continuous series, vertebra 4 at least articulates well at its posterior end with vertebra 3 and vertebra 3 at its posterior end with vertebra 5. Thus, it is likely that these three were continuous elements. The interpretation of their order therefore differs from the numbering used by Parrington. In addition, all five of the vertebrae were likely close to one another within the axial series based on the similar positions of the parapophyses and the similar morphologies of the laminae of the neural arches. The parapophyses are placed primarily on the anterodorsal corners of the centra and extend only a short distance onto the base of the neural arch. Thus, as Parrington (1956) noted, these vertebrae likely correspond to the region of the cervico–dorsal transition. Vertebra 1 is here interpreted as the most anterior preserved element because of the relatively ventral position of the parapophysis. Vertebrae 2 and 4 most likely successively followed vertebra 1, because they possess slightly more dorsally placed parapophyses and similarly elongated centra. The most posterior preserved elements seem to be vertebrae 3 and 5, with vertebra 5 the most posterior of the two.

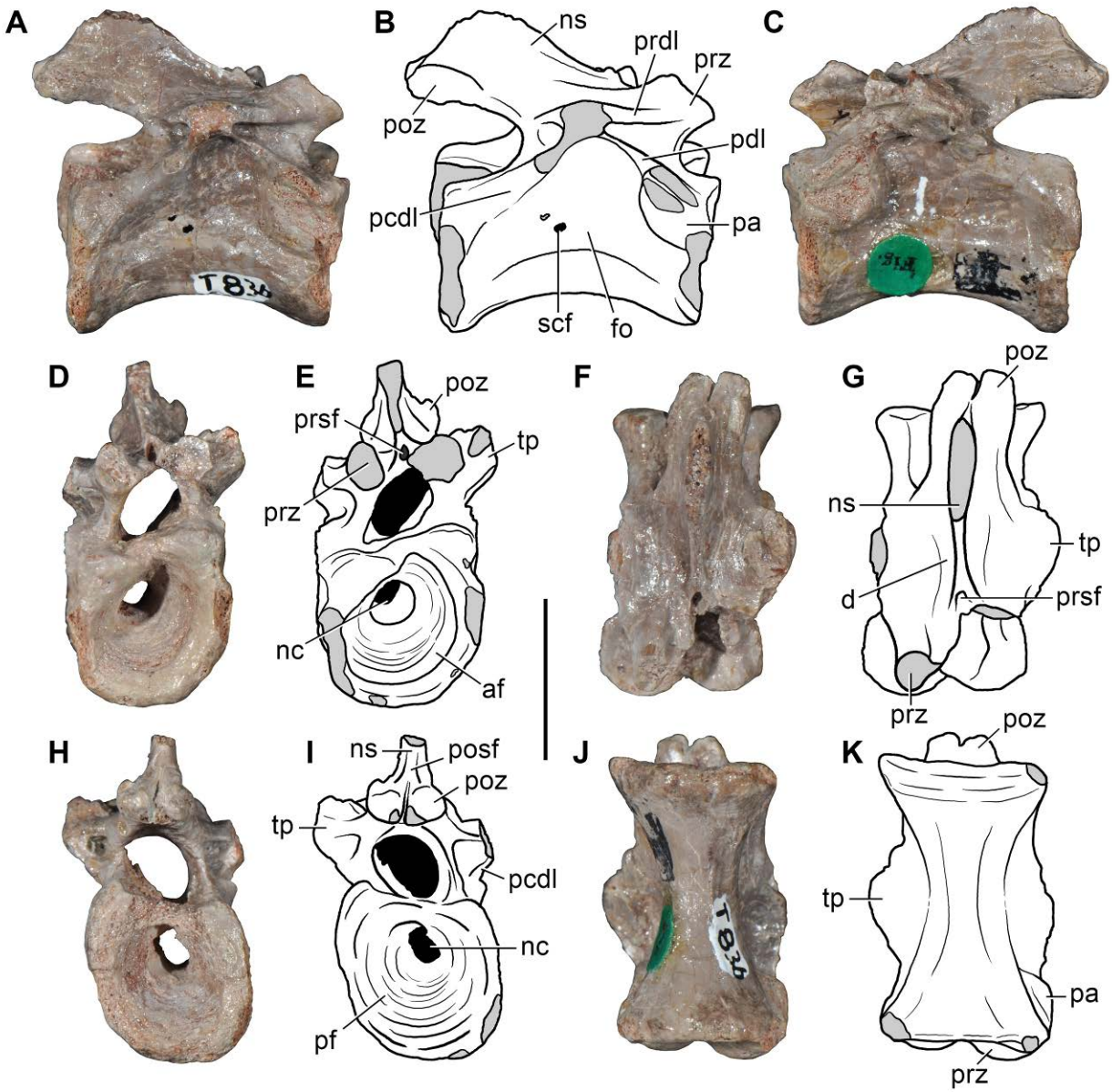

Figure S2.1. *Aenigmastropheus parringtoni*, an early archosauromorph from the middle Lopingian of Tanzania. Cervical vertebra (vertebra 1 sensu Parrington, 1956) (UMZC T836, holotype) in right lateral (A, B), left lateral (C), anterior (D, E), dorsal (F, G), posterior (H, I) and ventral (J, K) views. Abbreviations: af, anterior facet; d, depression; fo, lateral fossa; nc, notochordal canal; ns, neural spine; pa, parapophysis; pcdl, posterior centrodiapophyseal lamina; pdl, paradiapophyseal lamina; pf, posterior facet; posf, postspinal fossa; poz, postzygapophysis; prdl, prezygodiapophyseal lamina; prz, prezygapophysis; prsf, prespinal fossa; scf, subcentral foramen; tp, transverse process. Scale bar equals 1 cm.

These elements exhibit more dorsally positioned parapophyses and likely correspond to anterior dorsal vertebrae.

All the preserved vertebrae possess a completely open notochordal canal (Fig. S2.1: nc), but the notochordal canal is still connected to the neural canal through an hourglass-shaped opening in at least some elements (Parrington, 1956). This is best observed in vertebra 5, in which most of the neural arch is broken away. The neurocentral sutures are closed, without any trace of the suture remaining visible on the external surface. Thus, UMZC T836 was likely not a juvenile individual on the basis of the closed neurocentral sutures, but possibly also not fully-grown based upon the connected notochordal and neural canals (Parrington, 1956).

The centra are anteroposteriorly elongated, with a length to anterior height ratio of 1.61 in vertebra 1, 1.46 in vertebra 2, and 1.40 in vertebra 3 (Table S2.1), resembling the elongated cervical vertebrae of some basal synapsids (e.g. *Apsisaurus witteri*: Laurin, 1991) and several diapsids (e.g. *Protorosaurus speneri*: BSPG 1995 I 5; *Araeoscelis gracilis*: Vaughn, 1955; *Endennasaurus acutirostris*: Renesto, 1992; *Boreopricea funerea*: Benton and Allen, 1997; *Trilophosaurus buettneri*: Spielmann et al., 2008). Vertebrae 1 and 2 have sub-rectangular centra in lateral view. By contrast, in vertebrae 3 and 4 the posterior articular surface terminates in a more ventral position than the anterior one in lateral view. This condition would likely have resulted in a dorsally curved cervico–dorsal transition in lateral view, when the vertebrae were articulated with one another. The condition in vertebra 5 cannot be determined due to extensive damage to the posterior end of the centrum. In ventral view, the centra are hourglass-shaped, being transversely constricted at mid-length, as commonly occurs in many amniote lineages (Wedel, 2007). In lateral view, the ventral margin of the centrum is arched upwards. None of the preserved vertebrae

Table S2.1. Measurements of the preserved axial bones of *Aenigmastropheus parringtoni* nov. gen. et nov. sp. (UMZC T836) in millimetres. Values between brackets indicate incomplete measurements (due to post-mortem damage) and the value given is the maximum measurable. The length along the zygapophyses is the maximum anteroposterior length between the anterior tips of the prezygapophyses and the posterior tips of the postzygapophyses. Maximum deviation of the digital caliper is 0.02 mm but measurements were rounded to the nearest 0.1 millimetre.

Vertebrae (sensu Parrington, 1956)	**1**	**2**	**3**	**4**	**5**
Centrum length	16.4	16.5	15.17	16.6	(15.7)
Anterior articular facet height	10.2	11.3	11.2	(11.3)	11.5
Anterior articular facet width	(9.9)	10.8	11.4	(11.0)	10.4
Posterior articular facet height	11.6	(10.9)	10.9	10.8	(10.4)
Posterior articular facet width	10.2	11.0	11.3	11.3	(9.8)
Maximum height of the vertebra	(19.8)	(18.6)	(17.4)	(19.5)	(16.9)
Length along zygapophyses	(19.5)	(19.1)	(12.7)	(17.7)	(10.3)

possess a transversely thin median ventral keel, contrasting with the condition commonly found among the cervico–dorsal vertebrae of some basal parareptiles (e.g. *Millerosaurus pricei*: Watson, 1957; *Procolophon trigoniceps*: deBraga, 2003), some "pelycosaurian" synapsids (e.g. *Apsisaurus witteri*: Laurin, 1991; *Varanops brevirostris*: Campione and Reisz, 2010), araeoscelidians (e.g. *Petrolacosaurus kansensis*: Reisz, 1981; *Araeoscelis gracilis*: Vaughn, 1955) and some basal archosauromorphs (e.g. *Trilophosaurus buettneri*: Spielmann et al., 2008; *Euparkeria capensis*: SAM-PK-5867). Instead, the ventral surface of the centrum is flattened in vertebrae 3 to 5, with subtle longitudinal ridges laterally delimiting these planar ventral surfaces. In vertebrae 1 and 2 this flattening of the ventral surface is less well developed.

The ventral half of the lateral surface of the centrum is planar to very gently concave in all the vertebrae; more dorsally, the centrum possesses a deeper longitudinal fossa without well-defined margins, directly below the inferred position of the neurocentral suture (Fig. S2.1: fo). The presence of lateral fossae in the vertebral centrum has been also described for the dorsal vertebrae of probable choristoderan basal diapsids (e.g. *Pachystropheus rhaeticus*: Storrs and Gower, 1993) and the presacral vertebrae of numerous archosauriforms (e.g. *Koilamasuchus gonzalezdiazi*: Ezcurra et al., 2010; *Tarjadia ruthae*: Arcucci and Marsicano, 1998; *Erythrosuchus africanus*: NHMUK R3592; *Euparkeria capensis*: UMZC T692j; *Cuyosuchus huenei*: MCNAM PV 2669; *Pseudopalatus mccauleyi*: Irmis, 2007; *Arizonasaurus babbitti*: Nesbitt, 2005; *Aetosauroides scagliai*: Desojo and Ezcurra, 2011; *Marasuchus lilloensis*: PVL 3870; *Pantydraco caducus*: Yates, 2003).

Parrington (1956) described foramina that pierce the lateral faces of the centra (Fig. S2.1: scf). These foramina lie within the lateral fossae in UMZC T836. A pair of

foramina seems to be present on the right side of vertebra 1, but only the ventral margin of the most ventral foramen can be confidently identified as a natural border. Furthermore, it should be noted that Parrington (1956: fig. $1A_1$) only figured one foramen for this vertebra, which corresponds to the more ventral of the two openings currently present. Accordingly, the second "foramen" currently observed on vertebra 1 seems to be a break in the lateral surface of the centrum. The foramen of vertebra 1 is positioned slightly posterior to the mid-length of the centrum. No foramen is observed within the lateral fossa on the left side of the same vertebra. In vertebra 2 a well-defined circular foramen with well-preserved natural borders is present on the right side of the element, being of similar size and placed in the same position to that of vertebra 1. A circular foramen with well-defined natural borders is present on both right and left sides of vertebra 3, and is identical in position to the foramina of the more anterior elements, but the foramen on the left side is considerably smaller than that on the right side. In vertebra 4, a foramen is also present in the right side in an identical position to the foramina of the other vertebrae, but the pair of foramina figured by Parrington (1956) on the left side of this vertebra cannot be identified and the surface of the left side seems instead to be devoid of foramina. Finally, a foramen is observed on the left side of vertebra 5, but the condition on the right side cannot be assessed due to damage. Accordingly, the foramina are irregular in their occurrence on each vertebra (Parrington, 1956), but usually at least one foramen is present on at least one side of the centrum. The positions, sizes and shapes of the foramina are similar through the preserved vertebrae.

Parrington (1956) considered that these foramina would have had a nutritive function and were related to the persistence of the notochord. A foramen of similar shape and position to that of *Aenigmastropheus parringtoni* is present and termed a

subcentral foramen in several tetrapods, such as amphiumid caudatans (e.g. *Amphiuma means*: Gardner, 2003), "younginiforms" (e.g. *Acerosodontosaurus piveteaui*: Bickelmann et al., 2009), sauropterygians (e.g. *Bobosaurus forojuliensis*: Dalla Vechia, 2006), and basal lepidosauromorphs (e.g. *Gephyrosaurus bridensis*: Evans, 1981). Nevertheless, subcentral foramina occur in amniotes with both notochordal and non-notochordal vertebrae (e.g. sauropterygians: Dalla Vechia, 2006). Similar circular vascular foramina are also present in the non-notochordal vertebrae of extant lepidosaurs and crocodiles (Sood, 1948; Dalla Vechia, 2006; O'Connor, 2006; Butler et al., 2012), which sometimes occur within a lateral fossa that is associated with fat deposits (e.g. *Crocodylus acutus*: O'Connor, 2006). Accordingly, the nutritive function for the subcentral foramina in *Aenigmastropheus parringtoni* proposed by Parrington (1956) seems reasonable but their proposed association with the notochordal canal is ambiguous.

The anterior and posterior articular surfaces of the vertebrae are roughly sub-circular in outline, being slightly higher than wide in vertebra 2 and 5, and slightly wider than tall in vertebra 3. In all the vertebrae both anterior and posterior articular surfaces are strongly amphicoelous and the centrum is completely pierced by a notochordal canal positioned slightly dorsal to the center of the centrum in anterior or posterior view (Fig. S2.1: nc). The presence of a notochordal canal in *Aenigmastropheus parringtoni* resembles the condition observed in several basal reptiliomorphs (e.g. *Tseajaia campi*: Moss, 1972), parareptiles (e.g. *Millerosaurus pricei*: Watson, 1957; *Procolophon trigoniceps*: deBraga, 2003), basal synapsids (e.g. *Casea broilii*, *Archaeothyris florensis*, *Ophiacodon* sp., *Mycterosaurus longiceps*, *Mesenosaurus romeri*, *Aerosaurus wellesi*, *Varanops brevirostris*, *Varanodon agilis*, *Archaeovenator hamiltonensis*, *Apsisaurus witteri*: Romer and Price, 1940; Laurin,

Figure S2.2. *Aenigmastropheus parringtoni*, an early archosauromorph from the middle Lopingian of Tanzania. Cervico-dorsal vertebrae (UMZC T836, holotype) in right lateral (A–D), left lateral (E–H), anterior (I–L), posterior (M–P), dorsal (Q–T) and ventral (U–X) views. Vertebrae 2 (A, E, I, M, Q, U), 3 (C, G, K, O, S, W), 4 (B, F, J, N, R, V) and 5 (D, H, L, P, T, X) sensu Parrington (1956). Scale bar equals 1 cm.

1991; Campione and Reisz, 2010; Reisz et al., 2010: appendix S2), basal sauropsids (e.g. *Captorhinus aguti*: Fox and Bowman, 1966; *Coelurosauravus jaekeli*: Evans and Haubold, 1987; *Petrolacosaurus kansensis*: Reisz, 1981; *Araeoscelis gracilis*: Vaughn, 1955; *Acerosodontosaurus piveteaui*: Bickelmann et al., 2009; *Youngina capensis*: BP/1/3859), the enigmatic neodiapsids *Helveticosaurus zollingeri* (Rieppel, 1989a) and *Hypuronector limnaios* (Colbert and Olsen, 2001), and basal lepidosauromorphs (e.g. *Gephyrosaurus bridensis*: Evans, 1981; *Planocephalosaurus robinsonae*: Fraser and Walkden, 1984). The presence of a notochordal canal was described in the basal archosauromorph *Jesairosaurus lehmani* (Jalil, 1997), but unequivocal evidence for the presence of this feature could not be identified during direct restudy of the specimens of this taxon (in the holotype, ZAR 06, the center of an anterior dorsal centrum that is exposed in cross-section is filled by quartz crystals, whereas in ZAR 13 the exposed section of the dorsal vertebra possesses several trabeculae, but no notochordal canal).

The dorsal borders of the anterior articular surfaces of vertebrae 1, 3 and 4 possess a subtle notch at the midline, whereas in vertebrae 2 and 5 this border is not preserved due to damage. The centra do not possess beveled surfaces or facets for articulation with intercentra at the ventral margins of the articular surfaces, but it cannot be assessed with certainty whether intracentra were present or not. The parapophyses are not raised on peduncles, and they are oval, with the long axis being orientated posterodorsally in lateral view. The articular surfaces of the parapophyses are slightly concave and bounded by thick lips.

The most complete neural arches are preserved in vertebrae 1, 2 and 4. Vertebra 3 preserves the pedicles of the neural arch and the base of the prezygapophyses, whereas in vertebra 5 only parts of the neural arch pedicles are

available. In all of the available vertebrae of *Aenigmastropheus parringtoni*, the dorsoventral height of the neural arch, from its base up to the base of the neural spine, is lower than that of the centrum. A similar condition is usually found in the posterior cervical and anterior dorsal vertebrae of basal amniotes, such as the synapsids *Apsisaurus witteri* (Laurin, 1991) and *Varanops brevirostris* (Campione and Reisz, 2010), and the diapsids *Araeoscelis gracilis* (Vaughn, 1955), *Petrolacosaurus kansensis* (Reisz, 1981), *Youngina capensis* (BP/1/3859), *Prolacerta broomi* (BP/1/2675), *Tanystropheus longobardicus* (PIMUZ T2817), *Macrocnemus bassanii* (PIMUZ T2472) and *Protorosaurus speneri* (BSPG 1995 I 5). By contrast, in the basal lepidosaurs *Gephyrosaurus bridensis* (Evans, 1981) and *Planocephalosaurus robinsonae* (Fraser and Walkden, 1984) the neural arch is considerably higher than the centrum.

The neural canal of *Aenigmastropheus parringtoni* is oval in outline in the less-deformed vertebrae, being wider than tall. The base of the transverse process is anteroposteriorly short and dorsoventrally compressed, and did not extend onto the lateral margin of the prezygapophysis. A series of thin and well-developed laminae connect the transverse processes with other structures in all the preserved vertebrae (Parrington, 1956). A paradiapophyseal lamina connects the transverse process with the parapophysis (Fig. S2.1: pdl), whereas a posterior centrodiapophyseal lamina extends posteroventrally from the transverse process towards the posterodorsal corner of the centrum (Fig. S2.1: pcdl). The posterior centrodiapophyseal lamina becomes thicker and lower posteriorly. The paradiapophyseal and posterior centrodiapophyseal laminae bound a shallow concave depression that is separated from the lateral fossa of the centrum by a gently convex surface, and which can be recognized as a centrodiapophyseal fossa (Wilson et al., 2011). A prezygodiapophyseal lamina

connects the transverse process with the prezygapophysis (Fig. S2.1: prdl), and bounds together with the paradiapophyseal lamina a deep and sub-triangular prezygapophyseal centrodiapophyseal fossa that opens anterolaterally. The transverse process extends posteriorly as a thin ridge. However, this ridge cannot be identified as a postzygodiapophyseal lamina in a strict sense, because it does not reach the postzygapophysis (see Wilson, 1999), but it is topologically equivalent with such a feature. The ridge extending from the posterior end of the transverse process and the posterior centrodiapophyseal lamina bound a deep and sub-triangular depression, which is located in the same position as the postzygapophyseal centrodiapophyseal fossa of archosaurs (see Wilson et al., 2011). This depression is considerably shorter anteroposteriorly than the prezygapophyseal centrodiapophyseal fossa.

The presence of well-developed laminae in the neural arch is also observed in some caudatans, basal synapsids, basal diapsids and several archosauropomorphs. For example, the ophiacodontid synapsid *Ophiacodon* sp. (MCZ 1426), the basal diapsids *Acerosodontosaurus piveteaui* (MNHN 1908-32-57) and *Youngina capensis* (BP/1/3859), and the basal archosauriforms *Proterosuchus fergusi* (SAM-PK-K140, GHG 363) and "*Chasmatosaurus*" *yuani* (IVPP V2719) have paradiapophyseal or anterior centrodiapophyseal laminae. The amphiumid caudatan *Amphiuma means* (Gardner, 2003) has anterior and posterior centrodiapophyseal laminae (in *Amphiuma* the structures have been termed alar processes [sensu Gardner, 2003] but they are considered here as topologically equivalent to amniote laminae, although not homologous). The varanopid synapsid *Apsisaurus witteri* (Laurin, 1991: fig. 6; sensu Reisz et al., 2010) and the basal archosauromorphs *Prolacerta broomi* (BP/1/2675), *Tasmaniosaurus triassicus* (UTGD 54655) and *Sarmatosuchus otschevi* (PIN 2865/68) possess both prezygodiapophyseal and anterior centrodiapophyseal (or

paradiapophyseal) laminae. The basal archosauromorph *Trilophosaurus buettneri* possesses prezygodiapophyseal and postzygodiapophyseal laminae (USNM mounted skeleton, pers. obs.; S. Nesbitt pers. comm., 2013). Finally, the paradiapophyseal or anterior centrodiapophyseal, posterior centrodiapophyseal and prezygodiapophyseal laminae are all present, as in *Aenigmastropheus parringtoni*, in the enigmatic neodiapsid *Helveticosaurus zollingeri* (PIMUZ T4352), the basal archosauromorphs *Tanystropheus longobardicus* (SMNS 54628; Wild, 1973: fig. 52–54), *Protorosaurus speneri* (BSPG 1995 I 5), *Spinosuchus caseanus* (Spielmann et al., 2009) and *Macrocnemus bassanii* (PIMUZ T2472, 4822; although the presence of a posterior centrodiapophyseal lamina cannot be determined in this species), the basal archosauriforms *Erythrosuchus africanus* (NHMUK R3592; Gower, 2003), *Garjainia prima* (PIN 2394/5-16), *Shansisuchus shansisuchus* (Young, 1964: fig. 21) and *Euparkeria capensis* (UMZC T921), and several archosaurs (e.g. *Bromsgroveia walkeri*: Butler et al., 2012; *Hypselorhachis mirabilis*: Butler et al., 2009; *Silesaurus opolensis*: Piechowski and Dzik, 2010; *Herrerasaurus ischigualastensis*: PVSJ 373).

Only the bases of the prezygapophyses are preserved in vertebrae 1–4, and the prezygapophyses are missing completely in vertebra 5. The prezygapophyses are upturned in lateral view, being anterodorsally directed in all the vertebrae (Fig. S2.1: prz), which is in agreement with the wide notch formed by the postzygapophyses and the posterodorsal corner of the centra in lateral view. The prezygapophyses possess a thin, medially developed ridge that runs along the ventromedial edge of the articular surface in vertebrae 1 and 2, and along the mid-height of the structure in vertebrae 3 and 4. As a result, the prezygapophyses of vertebrae 1 and 2 are L-shaped in cross-section and those of vertebrae 3 and 4 are T-shaped. These ridges constrain transversely the space between the prezygapophyses at the midline to an extremely

narrow longitudinal notch. The most complete prezygapophysis, on the left side of vertebra 2, indicates that, at least in this vertebra, the prezygapophyses extended anteriorly beyond the anterior margin of the centrum.

The postzygapophyses are short in all the preserved vertebrae and poorly laterally distinguished from the base of the neural spine (Fig. S2.1: poz), resembling the condition observed in most archosauromorphs (e.g. *Protorosaurus speneri*: ZMR MB R2173; *Prolacerta broomi*: BP/1/2675; *Proterosuchus fergusi*: GHG 231) and some "pelycosaurian" synapsids (e.g. *Varanops brevirostris*: Campione and Reisz, 2010; *Ophiacodon* sp.: MCZ 1426). By contrast, the zygapophyses are laterally deflected from the rest of the neural arch in most basal sauropsids and lepidosaurs, such as *Araeoscelis gracilis* (Vaughn, 1955), *Petrolacosaurus kansensis* (Reisz, 1981), *Youngina capensis* (BP/1/3859), *Gephyrosaurus bridensis* (Evans, 1981) and *Planocephalosaurus robinsonae* (Fraser and Walkden, 1984). In vertebrae 1 and 2 the postzygapophyseal articular facets are mainly laterally facing, with only a slight ventral orientation (Parrington, 1956). This orientation of the postzygapophyseal articular facets would have mostly prevented lateral movement between the vertebrae in that region of the axial skeleton, which would probably correspond to the posterior end of the neck. By contrast, in vertebra 4 the articular facet of the preserved left postzygapophysis faces ventrolaterally, which would have allowed both lateral and dorsoventral movements among the vertebrae of this region, probably corresponding to the anterior end of the trunk. In vertebrae 1, 2 and 4 the postzygapophyses extend posteriorly beyond the posterior end of the centrum, but the condition cannot be assessed in vertebrae 3 and 5. The postzygapophyses are separated from one another along the posterior midline by a deep vertical furrow that does not extend dorsally along the neural spine.

The neural arches of vertebrae 1, 2 and 4 do not possess the depressions on both sides at the base of the neural spine (Fig. S2.1: d) that are usually observed in varanopid "pelycosaurs" (Berman and Reisz, 1982; Reisz and Dilkes, 2003; Campione and Reisz, 2010), araeoscelidians (Vaughn, 1955; Reisz, 1981) and some archosauromorphs (e.g. *Protorosaurus speneri*: BSPG 1995 I 5; *Mesosuchus browni*: SAM-PK-6046; *Prolacerta broomi*: BP/1/2675; *Proterosuchus fergusi*: GHG 231). The bases of the neural spines are anteroposteriorly long, extending from the base of the prezygapophyses up to a point just anterior to the posterior ends of the postzygapophyses. The preserved regions of the neural spines of vertebrae 1 and 2 suggest that the anterior portion of the anterior margin possessed a low angle to the long axis of the vertebra up to a point approximately level with the mid-length of the centrum. Beyond this point, the anterior margin became sharply upturned to form the neural spine (Fig. S2.1: ns). Unfortunately, the total height of the neural spine and the morphology of its distal end cannot be assessed in any of the preserved vertebrae.

The microstructure of the vertebrae can be observed due to breakages and damaged surfaces and its pattern varies in different regions of the axial elements. The articular face of the centrum possesses multiple layers of bone laminae distributed in a concentric pattern that follows the outline of the notochordal canal. These bone layers may represent successive sequences of ossification of the vertebral centrum along the internal surface of the notochordal canal, implying at least partial reabsorption of the notochord during ontogeny. Within the external borders of the centrum and along the neural arch a typical trabecular bone microstructure is visible.

The distal half of a right **humerus** is preserved, and has a well-preserved external bone surface (Fig. S2.3). The preserved portion of the shaft is roughly oval in cross-section, being slightly dorsoventrally deeper than anteroposteriorly wide (Table

S2.2). The outline of the shaft in cross-section is asymmetric, with convex ventral, dorsal and anterior margins. The posterior margin is slightly sigmoid due to the presence of a posterior depression extending proximodistally along the shaft that is ventrally bounded by a thick ridge (Fig. S2.3: pvr). This ridge rises from the central portion of the ventral surface of the shaft and extends more posteriorly towards its proximal end. It becomes thicker towards the proximal end of the bone; distally, the ridge does not reach the distal end of the humerus but fades out on the ventral surface. The posteroventral ridge observed in the humerus of *Aenigmastropheus parringtoni* does not appear to be homologous with that of basal synapsids (e.g. dicynodonts: Angielczyk et al., 2009), which connects the deltopectoral crest with the entepicondyle, because in basal synapsids the ridge is directed anteriorly towards its proximal end. A similar ridge is not present in basal diapsids (e.g. *Petrolacosaurus kansensis*: Reisz, 1981; *Araeoscelis gracilis*: MCZ 4383; *Youngina capensis*: BP/1/3859; *Protorosaurus speneri*: BSPG 1995 I 514; *Prolacerta broomi*: BP/1/2675). This ridge is identified here as autapomorphic for *Aenigmastropheus parringtoni*.

The distal end of the humerus of *Aenigmastropheus parringtoni* is strongly anteroposteriorly expanded, being around 3.6 times wider than the proximal end of the shaft at the point at which it is broken, resembling the condition in several amniotes (e.g. *Barasaurus besairiei*: Cisneros, 2008: fig. 3d; *Millerosaurus pricei*: Watson, 1957; *Varanosaurus acutirostris*, *Dimetrodon kempae*: Romer and Price, 1940; *Dicynodontoides* spp.: Angielczyk et al., 2009; *Captorhinus aguti*: Holmes, 1977; *Araeoscelis gracilis*: MCZ 4383; *Boreopricea funerea*: Benton and Allen, 1997; *Trilophosaurus buettneri*: Spielmann et al., 2008). In addition, the most proximal portion of the preserved shaft indicates that the bone was still tapering

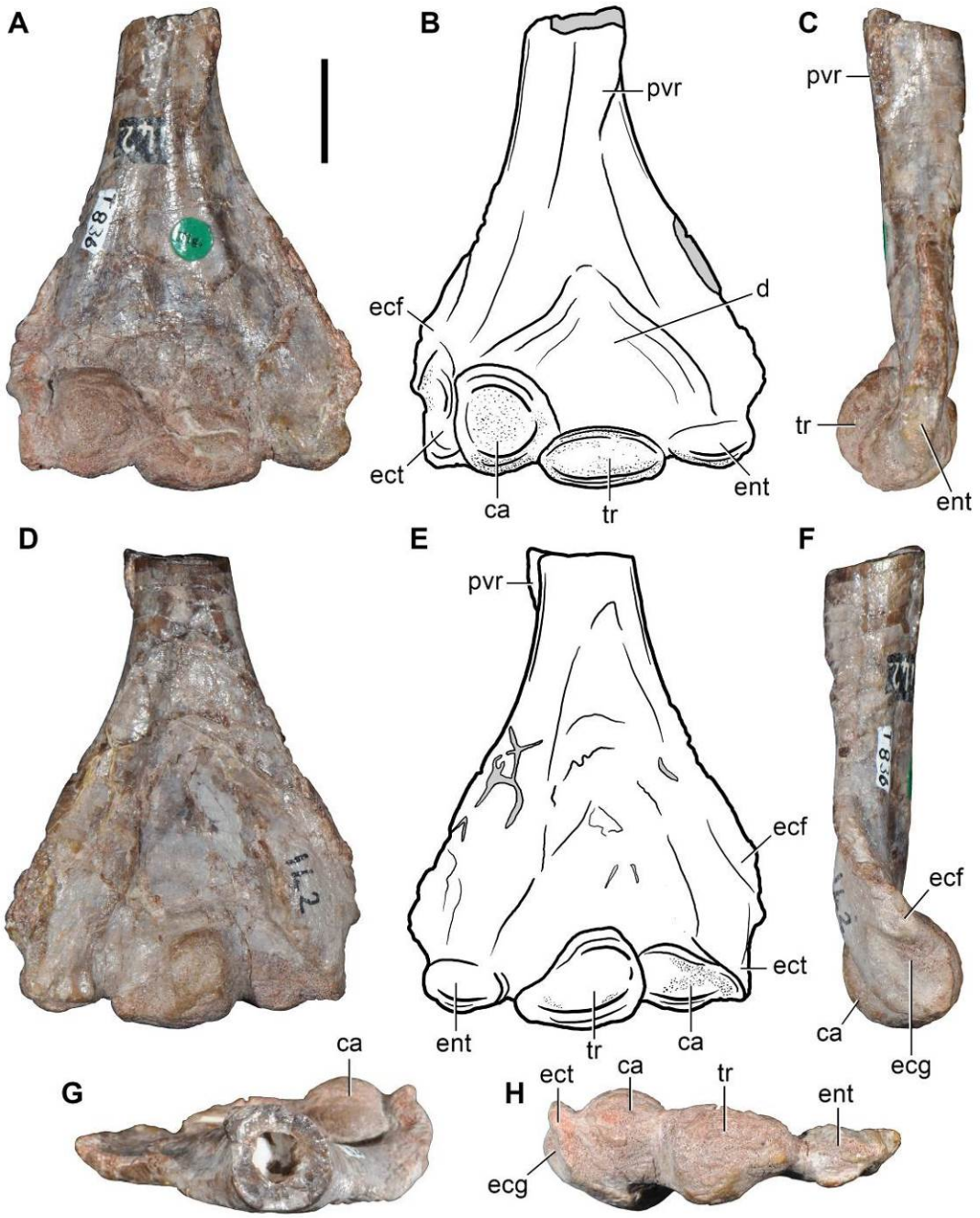

Figure S2.3. *Aenigmastropheus parringtoni*, an early archosauromorph from the middle Lopingian of Tanzania. Distal half of the right humerus (UMZC T836, holotype) in ventral (A, B), posterior (C), dorsal (D, E), anterior (F), proximal (G) and distal (H) views. Abbreviations: ca, capitellum (radial condyle); d, depression; ecf, ectepicondylar flange; ecg, ectepicondylar groove; ect, ectepicondyle; ent, entepicondyle; pvr, posteroventral ridge; tr, trochlea (ulnar condyle). Scale bar equals 1 cm.

proximally and the ratio of the anteroposterior width of the distal end to the minimum shaft width would have been even greater than currently preserved. By contrast, the dorsoventral thickness of the distal end of the bone is less than that of the shaft.

The distal end of the humerus possesses four well-developed and distinct distal articular condyles, which represent the entepicondyle, ectepicondyle, capitellum (radial condyle) and trochlea (ulnar condyle) (Fig. S2.3: ca, ect, ent, tr). The presence of four well-developed distal articular condyles resembles the condition in several basal amniotes (e.g. parareptiles: Watson, 1957; Cisneros, 2008; basal synapsids: Romer and Price, 1940; Cox, 1965; Angielczyk et al., 2009; captorhinids: Holmes, 1977; basal diapsids: Bulanov and Sennikov, 2010) and the basal archosauromorph *Trilophosaurus buettneri* (Spielmann et al., 2008). *Protorosaurus speneri* possesses at least three distinct distal condyles, which as preserved are considerably less well developed those of *Aenigmastropheus parringtoni*. Nevertheless, it is likely that the degree of development of the distal humeral condyles of *Protorosaurus speneri* is underestimated due to the strong compression that specimens suffered during fossilization (e.g. BSPG 1995 I 5, BSPG AS VII 1207). In other archosauromorphs only the ulnar and radial condyles are distinctly developed (e.g. *Boreopricea funerea*: Benton and Allen, 1997; *Malutinisuchus gratus*: Sennikov, 2005; *Tanystropheus longobardicus*: Wild, 1973; *Mesosuchus browni*: Dilkes, 1998; *Proterosuchus fergusi*: Cruickshank, 1972; *Erythrosuchus africanus*: Gower, 2003; *Euparkeria capensis*: Ewer, 1965).

The surfaces of the distal articular condyles are porous and covered by low striations, indicating that they were probably covered by hyaline cartilage that participated in a synovial elbow joint. The ventral surface of the humerus, proximal to the distal condyles, possesses a complex topography. Two ridge-like convexities

extend from the shaft in an inverted Y-shaped pattern. The thinner convexity is anterodistally directed and contacts the base of the ectepicondyle, whereas the thicker convexity is posterodistally directed and almost reaches the base of the entepicondyle. Both convexities and the capitellum and trochlea define a sub-triangular depressed area (Fig. S2.3: d), the depth of which appears to be exaggerated by damage and partial collapse of the cortical bone. This ventral depression would have housed the attachment area for the antebrachial ligaments (see Angielczyk et al., 2009). Both ectepicondylar and entepicondylar foramina are absent from the distal end of the humerus of *Aenigmastropheus parringtoni*. Either both foramina, or the entepicondylar foramen alone, occur widely among amniotes (e.g. parareptiles: Watson, 1957; Cisneros, 2008; basal synapsids: Romer and Price, 1940; Cox, 1965; Angielczyk et al., 2009; captorhinids: Holmes, 1977; basal diapsids: Romer, 1956). By contrast, the absence of both foramina from the humerus of *Aenigmastropheus parringtoni* is a condition shared with the enigmatic neodiapsid *Helveticosaurus zollingeri* (Rieppel, 1989a) and almost all archosauromorphs (e.g. *Mesosuchus browni*: Dilkes, 1998; *Hyperodapedon gordoni*: Benton, 1983; *Prolacerta broomi*: BP/1/2675; *Tanystropheus longobardicus*: Wild, 1973; *Macrocnemus bassanii*: PIMUZ T4355; *Protorosaurus speneri*: Gottmann-Quesada and Sander, 2009; *Boreopricea funerea*: Benton and Allen, 1997; *Trilophosaurus buettneri*: Spielmann et al., 2008; *Proterosuchus fergusi*: Cruickshank, 1972; *Erythrosuchus africanus*: Gower, 2003; *Euparkeria capensis*: SAM-PK-5867), with the exception of the putative protorosaurs *Czatkowiella harae*, which possesses an entepicondylar foramen (Borsuk–Białynicka and Evans, 2009), and *Jesairosaurus lehmani*, which possesses an ectepicondylar foramen (ZAR 09; Jalil, 1997).

The anterior margin of the distal end of the humerus, above the ectepicondyle, has a prominent supinator ridge or ectepicondylar flange (Fig. S2.3: ecf), which was likely the area of origin of the *M. supinator* (e.g. Benton, 1983). The posterior margin of the distal end of the bone is not completely preserved, but the available portion is very thin and suggests that only a small portion of bone has been lost. This posterior margin is folded ventrally, and delimits together with the thicker of the ventral convexities a proximodistally-extending concave depression that terminates a substantial distance from the base of the entepicondyle. The dorsal surface of the distal end of the humerus is mostly occupied by a large and sub-triangular depression that would have borne the origin of the *M. triceps humeralis medialis* (see Angielczyk et al., 2009). The depth of the central and proximal areas of this depression is exaggerated by damage with collapse of cortical bone. A raised shelf of bone that is continuous with the ectepicondyle delimits the anterior border of this dorsal depression and possesses a slightly rugose dorsal surface that would have housed the area for origin of the antebrachial extensor muscles (see Angielczyk et al., 2009). The posterior border of the depression is bounded by a faint posterodistally extending convexity that is continuous with the entepicondyle. The surface of the bone posterior to this convexity is slightly rugose, representing the area of origin of the antebrachial flexor muscles (see Angielczyk et al., 2009).

The ectepicondyle is the smallest of the distal condyles and is restricted to a rounded structure with a dorsoventrally oriented main axis. The anterior surface of the ectepicondyle possesses a shallow teardrop-shaped depression that corresponds to the ectepicondylar groove (Parrington, 1956) for the passage of the radial nerve (Romer and Price, 1940) (Fig. S2.3: ecg). This feature is widely distributed among amniotes (e.g. *Apsisaurus witteri*: Laurin, 1991; *Varanops brevirostris*: Campione and Reisz,

Table S2.2. Measurements of the preserved forelimb bones of *Aenigmastropheus parringtoni* nov. gen. et nov. sp. (UMZC T836) in millimetres. Values between brackets indicate incomplete measurements (due to post-mortem damage) and the value given is the maximum measurable. For the humerus the width is measured in the anteroposterior plane and the depth in the dorsoventral plane. Maximum deviation of the digital caliper is 0.02 mm but measurements were rounded to the nearest 0.1 millimetre. The perimeter close to mid-shaft was rounded to the nearest millimetre because the measurement cannot be made directly with the caliper.

Humerus		
	Length	(46.4)
	Width close to mid-shaft	9.5
	Depth close to mid-shaft	10.0
	Perimeter close to mid-shaft	32
	Distal width	34.1
	Distal depth	10.5
	Width of entepicondyle	7.6
	Depth of entepicondyle	5.9
	Width of capitellum	12.0
	Depth of capitellum	9.2
	Width of trochlea	8.9
	Depth of trochlea	8.7
	Width of ectepicondyle	3.3
	Depth of ectepicondyle	8.2
Ulna		
	Length	(37.5)
	Length of articular facet for humerus	15.5
	Width of articular facet for humerus	10.0
	Depth at distal broken surface	15.9
	Width at distal broken surface	4.8

2010; *Dimetrodon* sp.: SAM-PK-K8670; *Youngina capensis*: BP/1/3859; *Prolacerta broomi*: BP/1/2675; *Erythrosuchus africanus*: Gower, 2003) and the ectepicondylar groove of *Aenigmastropheus parringtoni* is considerably less well-developed than in some basal archosauromorphs (e.g. *Tanystropheus conspicuous*: Wild, 1973; *Trilophosaurus buettneri*: Spielmann et al., 2008: figs. 66–68; *Otischalkia elderae*: Hunt and Lucas, 1991), in which the passage is represented by a deep notch.

The trochlea (Fig. S2.3: tr), is a ball-shaped, proximoventrally-projecting condyle that articulated with the U-shaped proximal articular surface of the ulna. The capitellum is the widest and deepest of the condyles of the distal end (Fig. S2.3: ca). It possesses a slightly convex ventral articular surface and a strongly convex dorsal surface. In distal view, the capitellum has a comma-shaped outline, with a concavity on its posterodorsal margin. The entepicondyle (Fig. S2.3: ent) is smaller than the capitellum and trochlea, but larger than the ectepicondyle. It has an overall morphology that is very similar to that of the trochlea and its convex surface is dorsally oriented. The posterior surface of the entepicondyle possesses a small and deep oval concavity.

A fragment from the shaft of a long bone is interpreted as part of a probable left humerus (Fig. S2.4A, E, I, M, P, T). One of its ends is roughly sub-circular in cross-section and the opposite end is strongly compressed. The compressed end appears to have collapsed cortical bone on both of its main surfaces; it can thus be inferred to have had an originally sub-triangular cross-section. The size and shape of the end with a sub-circular cross-section is very similar to that of the shaft of the partial right humerus. Although this fragment of bone could belong to part of the left humeral shaft, it might also represent a fragment of tibial or femoral shaft.

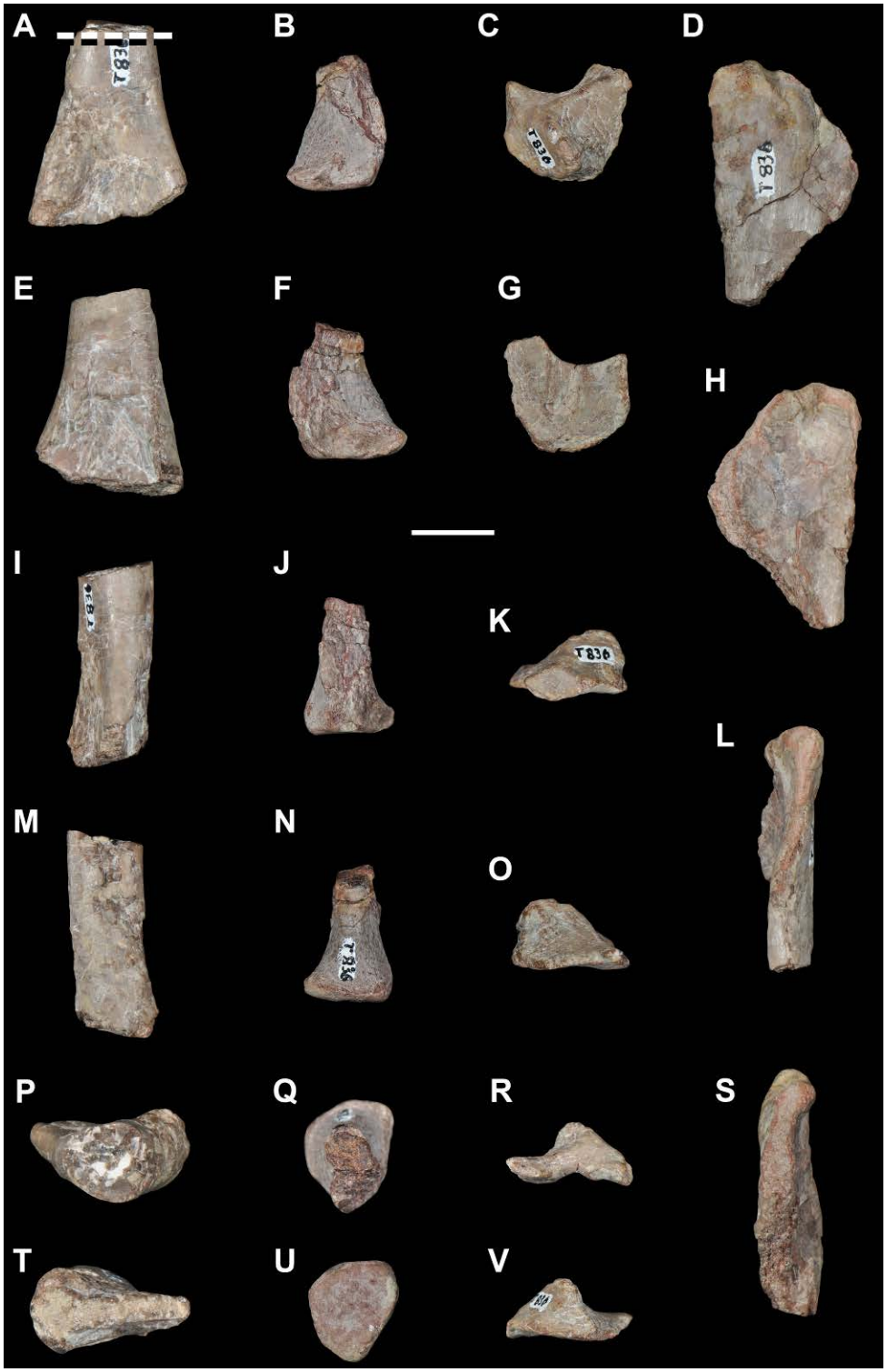

Figure S2.4. *Aenigmastropheus parringtoni*, an early archosauromorph from the middle Lopingian of Tanzania. Possible left humeral shaft (A, E, I, M, P, T), possible distal end of radius (B, F, J, N, Q, U) and two indeterminate bones (C, D, G, H, K, L, O, R, S, V) (UMZC T836, holotype) in several views. The dashed line indicates the area sampled for the palaeohistological study described in Ezcurra et al. (2014). Scale bar equals 1 cm.

The proximal end of the right **ulna** is preserved (Fig. S2.5). It has a well-preserved external bone surface, but the cortical bone on the posterior surface of the element distal to the olecranon process has collapsed, probably exaggerating the anteroposterior compression of the shaft (Fig. S2.5: ccb). This collapse is also evident in the constriction of the medullary space of the bone on the broken cross-section of the shaft (Fig. S2.5G). The ulna has a very large olecranon process (Fig. S2.5: ol), resembling the condition of some basal synapsids (e.g. *Ophiacodon navajovicus*, *Edaphosaurus boanerges*: Romer and Price, 1940; *Dinodontosaurus turpior*: Cox, 1965), basal sauropsids (e.g. *Captorhinus aguti*: Fox and Bowman, 1966; *Thuringothyris mahlendorffae*: Müller et al., 2006), the basal archosauromorphs *Protorosaurus speneri* (Gottmann-Quesada and Sander, 2009) and *Trilophosaurus buettneri* (Spielmann et al., 2008), and several archosaurs (e.g. *Typothorax coccinarum*: Heckert et al., 2010; *Fasolasuchus tenax*: PVL 3850; *Saturnalia tupiniqium*: MCP 3845-PV, Langer et al., 2007; *Eodromaeus murphi*: PVSJ 560). By contrast, the olecranon process is poorly developed or absent in varanopid synapsids (Campione and Reisz, 2010), "younginiforms" (e.g. *Youngina capensis*: Gow, 1975; *Acerosodontosaurus piveteaui*: Bickelmann et al., 2009), the neodiapsid *Helveticosaurus zollingeri* (PIMUZ T4352), and most basal archosauromorphs (e.g. *Prolacerta broomi*: Gow, 1975; *Tanystropheus longobardicus*: PIMUZ T2817; *Macrocnemus bassanii*: PIMUZ T4822; *Mesosuchus browni*: Dilkes, 1998).

The olecranon process of *Aenigmastropheus parringtoni* tapers gradually towards its apex, contrasting with that of at least some "pelycosaurian" synapsids, in which the process possesses an anteroposterior expansion towards its apex (e.g. *Dimetrodon* sp.: SAM-PK-K8670; *Ophiacodon* sp.: MCZ 1426). There are no traces

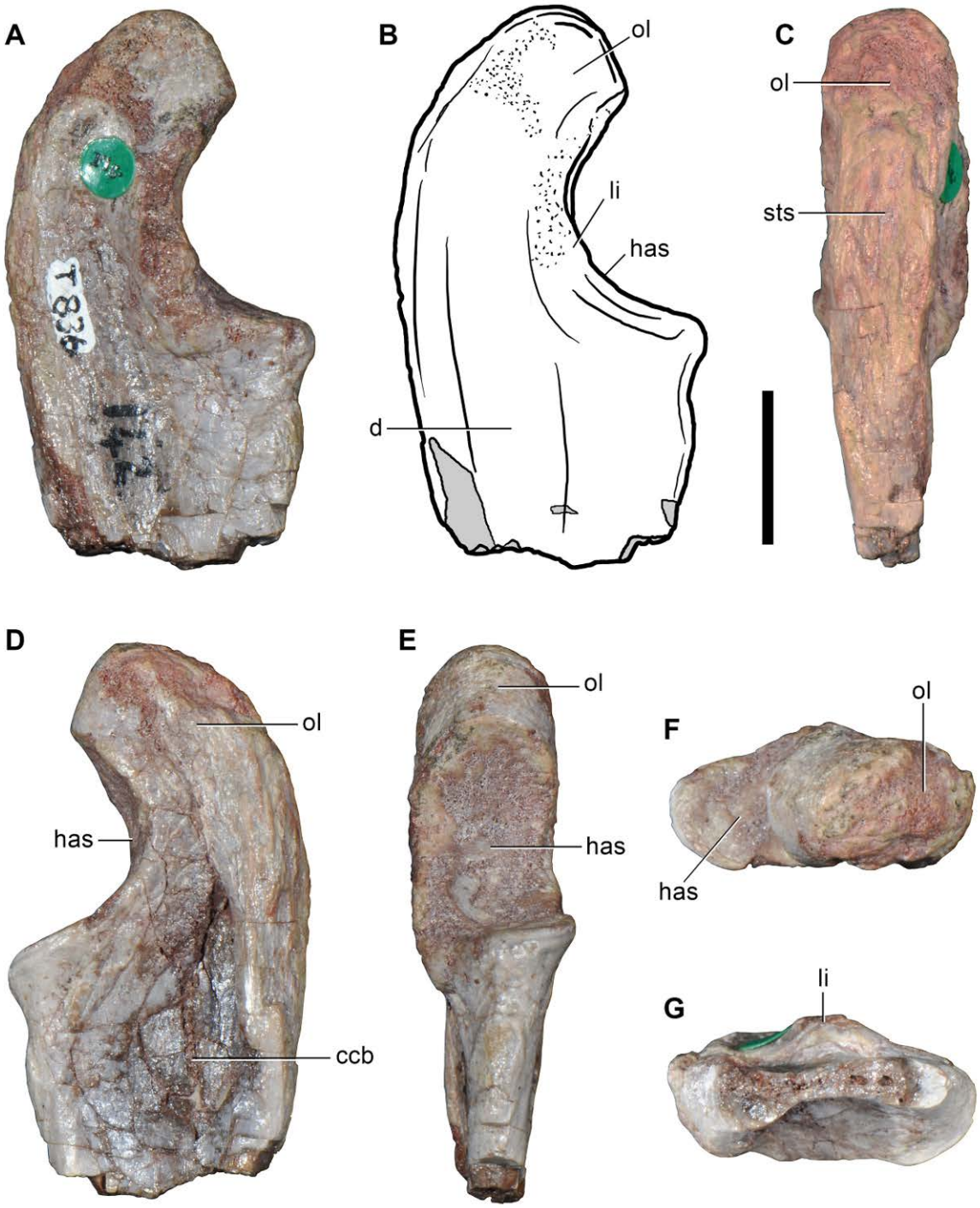

Figure S2.5. *Aenigmastropheus parringtoni*, an early archosauromorph from the middle Lopingian of Tanzania. Proximal end of the right ulna (UMZC T836, holotype) in anterior (A, B), dorsal (C), posterior (D), ventral (E), proximal (F) and distal (G). Abbreviations: ccb, collapsed cortical bone; d, depression; has, humeral articular surface; li, lip; ol, olecranon; sts, striated surface. Scale bar equals 1 cm.

of sutures in the olecranon of *Aenigmastropheus parringtoni*; thus, it seems that this structure formed a single ossification with the ulna. By contrast, in the basal archosauromorph *Protorosaurus speneri* the olecranon is developed as a separate ossification from the rest of the ulna (Gottmann-Quesada and Sander, 2009).

The proximal bone surface of the olecranon process is damaged. The olecranon process curves ventrally in order to form a U-shaped, large, oval and deeply concave ventral articular facet for the reception of the humeral trochlea (Fig. S2.5: has). The surface of this facet is porous and covered by faint striations, indicating that it was covered by hyaline cartilage in life. A thick lip bounds the anterior margin of the articular surface (Fig. S2.5: li). Dorsal to this lip, the olecranon has a concave longitudinal depression that extends distally along the anterior surface of the ulnar shaft (Fig. S2.5: d). The dorsal surface of the olecranon process is strongly convex and possesses a series of roughly longitudinal striations that represent the scars of the area of insertion of the *Mm. triceps* (Fig. S2.5: sts). The posterior surface of the olecranon possesses a longitudinal furrow, but this seems to be an artifact resulting from the collapse of the cortical bone. A lip also bounds the posterodistal border of the articular surface, but this lip is considerably lower than the anterior one. The ulnar shaft is strongly anteroposteriorly compressed, and the anterior and posterior longitudinal depressions (although the posterior depression has been exaggerated by damage) give the shaft a figure-of-eight-shaped cross-section at the point at which it is broken.

Parrington (1956) included the end of a bone with a planar articular surface among the indeterminate elements of UMZC T836, and this is here identified as a possible **radius** (Fig. S2.4B, F, J, N, Q, U). Although one of the borders of the bone has broken away, the preserved portion of the shaft suggests that it was oval in cross

section when complete. The bone clearly does not belong to a humerus, femur or tibia because it is proportionally too small. It does not appear to represent the distal end of an ulna because distal ulnae are usually considerably more compressed in amniotes. However, the morphology of this bone matches to that of a distal radius, particularly in possessing an expanded medial border, an approximately planar distal articular surface, and well-developed scars for probable ligament attachments. Indeed, the morphology of the distal articular surface in distal view is very similar to and matches that of the right radius of some amniotes (e.g. *Captorhinus aguti*: Holmes, 1977), with both tapering and more rounded borders. Nevertheless, the identity of this fragmentary bone cannot be established with certainty, nor can it be determined to which side it belonged.

Parrington (1956) also considered two other fragments of bone within UMZC T836 as indeterminate elements. One of the elements is a flattened and plate-like element (Fig. S2.4D, H, L, S). Four distinct borders can be recognized when the element is viewed perpendicular to its main plane. Two of these borders are broken margins, whereas the other two are damaged but maintain their overall shape. A short convex margin possesses a sub-triangular concavity that likely formed an articular area. A straight margin extends away from this short convex margin, and gradually increases in thickness, forming a low rounded tuberosity. One of the main surfaces of the bone is convex and the other one concave. This bone might represent part of a thickened cranial bone or a pectoral/pelvic girdle element.

A small, approximately pyramidal bone is also included among the indeterminate bones listed by Parrington (1956) (Fig. S2.4C, G, K, O, R, V). The bone is comma-shaped when it is viewed perpendicular to its main plane, but one of the tapering ends of the element in this view is broken away. Thus, the bone would

likely have had an “L”-shaped morphology when it was complete. One of the main surfaces of the element is planar, whereas the opposite surface bears a high and asymmetrically placed keel formed by two concave surfaces, one deeper than the other. The textures of the planar and the deepest concave surfaces suggest that they were articular surfaces. The remaining shallow concavity appears to be a non-articular surface. The morphology of this bone does not agree with that of a proximal end of a metacarpal or metatarsal because it does not have any process with a circular or oval cross section that could represent a shaft and the positions of the articular surfaces do not match the morphology expected for a metapodial. The size of the bone is very large relative to that expected for a carpal or distal tarsal bone. As such, I am unable to provide an identification for this element.

Appendix 3

Measurements employed in the quantitative analyses of Chapter 3

Table S1. Raw measurements used in the quantitative analyses and parameters recovered by the linear allometric regressions. *Abbreviations*: K, allometric coefficient; Mx h pr min height, maxilla horizontal process minimum height; Mx anterior pr length, maxilla anterior process length. Measurements between brackets were estimated based on equations derived from linear regressions.

Specimen/Allometric regression parametre	Skull length	Mx h pr min height	Mx anterior pr length	Supratemporal fossa width	Quadrate angle
BP/1/4016	(238.5)	12.5	38.2	4.4	124
NMQR 1484	(269.8)	16.4	56.7	6.1	149
SAM-PK-K140	287.0	15.6	48.6	10.0	122
SAM-PK-11208	350.0	21.2	60.7	9.1	125
NMQR 880	390.0	29.7	60.2	9.6	149
RC 846	420.6	24.1	80.1	9.8	126
BSPG 1934 VIII 514	435.0	29.9	75.5	5.9	120
IVPP V4067	436.0	28.4	78.3	10.2	155
GHG 231	477.0	30.9	82.5	12.9	126
K	-	1.3097	0.9891	0.4925	0.0255
R^2	-	0.9296	0.8779	0.4247	0.0039
p	-	<0.0001	0.0002	0.0572	0.8736

Table S2. Normalized and logarithmically transformed measurements used in the quantitative analyses. Abbreviations as in Table S1.

Specimen	Mx h pr min height	Mx anterior pr length	Supratemporal fossa width	Quadrate angle
BP/1/4016	1.3422	1.7673	-1.7340	1.2400
NMQR 1484	1.3900	1.8859	-1.6457	1.4900
SAM-PK-K140	1.3331	1.7924	-1.4579	1.2200
SAM-PK-11208	1.3535	1.8037	-1.5850	1.2500
NMQR 880	1.4383	1.7536	-1.6088	1.4900
RC 846	1.3046	1.8452	-1.6326	1.2600
BSPG 1934 VIII 514	1.3791	1.8050	-1.8676	1.2000
IVPP V4067	1.3555	1.8199	-1.6309	1.5500
GHG 231	1.3410	1.8040	-1.5679	1.2600

Table S3. Rotation coefficients recovered by the PCA for each variable. Abbreviations as in Table S1. The highest coefficient for each PC is indicated with an asterisk.

Variable	PC1	PC2	PC3	PC4
Mx h pr min height	-0.14441234	0.13405062	-0.51367787	-0.83505123*
Mx anterior pr length	-0.06253285	0.02536402	0.85638237*	-0.51191362
Supratemporal fossa width	-0.21852951	-0.97056224*	-0.04222709	-0.09203626
Quadrate angle	-0.96305741*	0.19848437	0.03100257	0.17934108

Appendix 4

Transformation and normalization of measurements

Function employed in Chapter 3 to transform and normalize measurements:

```
trans.log=function(table)
{
	Y.t=array()
	Y.t.log=array()
	Y.t.log.L=array()
	X0=mean(table[,1])
	d=dim(table)[1]
	e=dim(table)[2]-1

	xA=summary(lm(log(Ya)~log(X),data=table))
	xB=summary(lm(log(Yb)~log(X),data=table))
	xC=summary(lm(log(Yc)~log(X),data=table))
	xD=summary(lm(log(Yd)~log(X),data=table))

	b.scores=c(xA$coefficients[2,1],xB$coefficients[2,1],xC$coefficients[2,1],xD$coefficie
				nts[2,1])

	R.squared.scores=c(xA$r.squared,xB$r.squared,xC$r.squared,xD$r.squared)

	p.scores=c(xA$coefficients[2,4],xB$coefficients[2,4],xC$coefficients[2,4],xD$coefficie
				nts[2,4])

	for(j in 1:e)
	{
		for(i in 1:d)
		{
			if (p.scores[j]<0.05)
			{
				Y.t[i]=((X0/table[i,1])^b.scores[j])*table[i,j+1]
				 Y.t.log[i]=log10(Y.t[i])
			}
			if (p.scores[j]>0.05)
			 {
				Y.t[i]=table[i,j+1]/table[i,1]
				Y.t.log[i]=log10(Y.t[i])
			}
		}
		Y.t.log.L=list(transformed.values=Y.t.log)
		print(Y.t.log.L)
	}
	result=list(allometric.coefficient=b.scores, R2=R.squared.scores, p.value=p.scores)
	return(result)
}
```

Appendix 5

Total skull length estimations for Chapters 3 and 4

The lengths of the infratemporal fenestra and dentary were the variables with the highest R^2 values, and, as a result, were used to estimate total skull length for four specimens. Power function regressions were chosen over linear regression or other models because they were the models that best explained the data set.

BP/1/4016, 4224: estimation based on a power function regression between skull length and infratemporal fenestra length ($y=0.0189x^{1.4484}$, $R^2=0.9965$, $p<0.0001$).

SAM-PK-K10603 and TM 201: estimation based on an exponential regression between skull length and dentary length ($y=59.682^{e0.0033x}$, $R^2=0.9925$, $p<0.0001$).

Character list for the data matrix of the ontogram of Chapter 4

Characters 1−12 are continuous characters and were scored as the ratio between the measurement and the total length of the skull.

1. Premaxilla, body height. CONTINUOUS.
2. Skull, snout minimum width. CONTINUOUS.
3. Maxilla, minimum height of the horizontal process. CONTINUOUS.
4. Maxilla, tooth crowns length at base. CONTINUOUS.
5. Jugal, height of anterior process. CONTINUOUS.
6. Orbit, length. CONTINUOUS.
7. Orbit, height. CONTINUOUS.
8. Postorbital, height. CONTINUOUS.

9. Infratemporal fenestra, length. CONTINUOUS.
10. Infratemporal fenestra, height. CONTINUOUS.
11. Parietal, maximum width of both parietals. CONTINUOUS.
12. Parietal, minimum width of both parietals. CONTINUOUS.
13. Premaxilla, orientation of postnarial process with respect to alveolar margin: parallel (0); downturned (1).
14. Premaxilla, number of tooth positions: five (0); six (1); seven (2); eight (3); nine (4). ORDERED.
15. Maxilla, number of tooth positions: 20 (0); 22 (1); 27 (2); 30 (3); 31 (4). ORDERED. The number of dentary teeth was not included because it is strongly correlated with the number of maxillary teeth in an isometric growth pattern (K=1.0415) (R^2=0.9888).
16. Maxilla, curvature of tooth crowns: posterior tooth crowns poorly distally curved (0); isodont, all tooth crowns strongly distally curved (1).
17. Skull, sutures of skull roof: strongly interdigitated (0); poorly interdigitated (1).
18. Parietal, pineal fossa: absent (0); present (1).
19. Cervical vertebrae, neurocentral sutures: open, still visible (0); completely closed, no trace of suture (1). A closed suture has no trace of the suture on the surface of the bone (Brochu, 1996).
20. Hindlimb, long bone tissues: fibro-lamellar (0); lamellar-zonal and parallel-fibered (1).

TNT file of the data matrix of the ontogram of Chapter 4

```
nstates cont;
xread 'Data saved from TNT'
```

```
20 11
&[cont]
RC_59           0.034 0.121 0.038 0.023 0.036   ?    ?   0.175   ?    ?   0.156 0.122
BP_1_4224         ?    ?    ?    ?    ?   0.146   ?   0.167 0.215 0.155 0.267 0.113
BP_1_4016        0.036 0.098 0.052 0.019 0.037 0.129 0.121 0.160 0.220 0.154 0.230
0.108
SAM_PK_K140      0.053 0.119 0.054 0.020 0.044   ?    ?    ?    ?    ?   0.277   ?
SAM_PK_11208     0.050   ?   0.060 0.015 0.030   ?   0.139   ?   0.263 0.135   ?
0.107
BP_1_3993        0.046 0.096 0.063 0.019 0.042 0.123 0.152   ?   0.278   ?   0.202
0.099
SAM_PK_K10603      ?   0.102 0.048 0.013 0.055 0.117   ?   0.152 0.225   ?   0.279
0.092
RC_96           0.038 0.101 0.057 0.014 0.055 0.116 0.165 0.146 0.273 0.187 0.271
0.087
BSPG_1934_VIII_514  0.039 0.117 0.068 0.017 0.048 0.147 0.191 0.161 0.293 0.166
?   0.105
TM_201          0.038 0.097 0.052 0.013 0.036   ?    ?    ?    ?    ?    ?   0.091
GHG_231          0.044 0.098 0.064 0.013 0.031 0.103 0.222 0.141 0.302 0.220 0.282
0.092
&[num]
RC_59          000000??
BP_1_4224       ????00??
BP_1_4016       1?0000??
SAM_PK_K140     111???00
SAM_PK_11208    13210?11
BP_1_3993       113?11[01]?
SAM_PK_K10603   ??2111??
RC_96          1441111?
BSPG_1934_VIII_514 142?1?1?
TM_201          12??11??
GHG_231         143111??
;

Ccode
  +[/1  0      +[/1  1      +[/1  2      +[/1  3      +[/1  4
  +[/1  5      +[/1  6      +[/1  7      +[/1  8      +[/1  9
  +[/1  10     +[/1  11     ([/1  12     +[/1  13     +[/1  14
  ([/1  15     ([/1  16     ([/1  17        ([/1  18        ([/1    19   ;
piwe=10;
p/;
```

Scorings for the hypothetical root of the ontogram of Chapter 4

Root 01010101000100000000

Appendix 6

Redescription of the holotype of *Proterosuchus fergusi* (SAM-PK-591) of Chapter 3

The holotype skull is broken in a coronal section (i.e. in a horizontal plane) at the level of the palate, resulting in 'upper' and 'lower' blocks that articulate with each other. The upper block preserves the moulds of the premaxillae-nasals (the sutures between the bones cannot be determined in the moulds), maxillae, right lacrimal and jugal, partial septomaxillae and a probable cultriform process of the parabasisphenoid in cross section. The lower block preserves moulds and bone fragments of the lower jaws and hyoid apparatus, and both blocks preserve parts of the palatal bones.

Premaxilla. The premaxillae are represented only by the distal tips of the palatal processes, as well as a natural mould that probably represents the distal ends of the postnarial processes (Figs. S5.1A, B, S5.2B: pmx). The bone identified by Broom (1903: figs 1, 2) as a portion of the right premaxilla preserved immediately anterior to the right maxilla is reinterpreted here as a right septomaxilla. The preserved portions of the palatal processes are not very informative and it is not possible to determine if the premaxillae were strongly downturned as as in other basal archosauriforms (e.g. proposed neotype and referred specimens of *Proterosuchus fergusi*: Broili and Schröder, 1934; "*Chasmatosaurus*" *yuani*: Young, 1936; *Sarmatosuchus otschevi*: Gower and Sennikov, 1997). Moreover, the contact between the vomer and the premaxilla is exposed only in a coronal section through the skull in SAM-PK-591,

and, as a result, the contact cannot be readily compared with other proterosuchid specimens, in which the suture is exposed in ventral view.

Septomaxilla. Two plate-like bones are exposed in the most anterior preserved portion of SAM-PK-591 (Figs. S5.1A, B, S5.2B: spx). The right bone of this pair was originally identified as a partial premaxilla by Broom (1903: figs 1, 2). However, these bones do not represent the palatal processes of the premaxillae because they are situated immediately dorsal to the premaxilla-vomer contacts, extend considerably posterior to the anterior borders of the internal choanae, and are dorsoventrally taller than expected for the distal ends of premaxillary palatal processes. In addition, they are not continuous with the preserved portions of the palatal process of the premaxillae (which were not identified by Broom [1903]), which articulate with the vomers. These plate-like bones are re-identified here as a pair of septomaxillae because they are congruent in morphology with, and are situated in the same position as, the septomaxillae present in other proterosuchids (e.g. proposed neotype and referred specimens of *Proterosuchus fergusi*: BP/1/4016, BSPG 1934 VIII 514, RC 846; *Proterosuchus goweri*: NMQR 880).

The septomaxillae are partially exposed in transverse section (Fig. S5.2B: spx), as well as in lateral view (Fig. S5.1A, B: spx). However, the lateral surface of the right element is damaged and the posterior half of the left element is preserved as a natural mould only. The medial portions of the septomaxillae consist of sheets of bone that extend parallel to each other anteroposteriorly and are clearly separated from each other at the midline. The septomaxillae curve dorsally towards the midline, where they form nearly vertically oriented sheets; as a result, the exposed external surface of the bone is transversely concave and faces laterodorsally (Fig. S5.2B), as

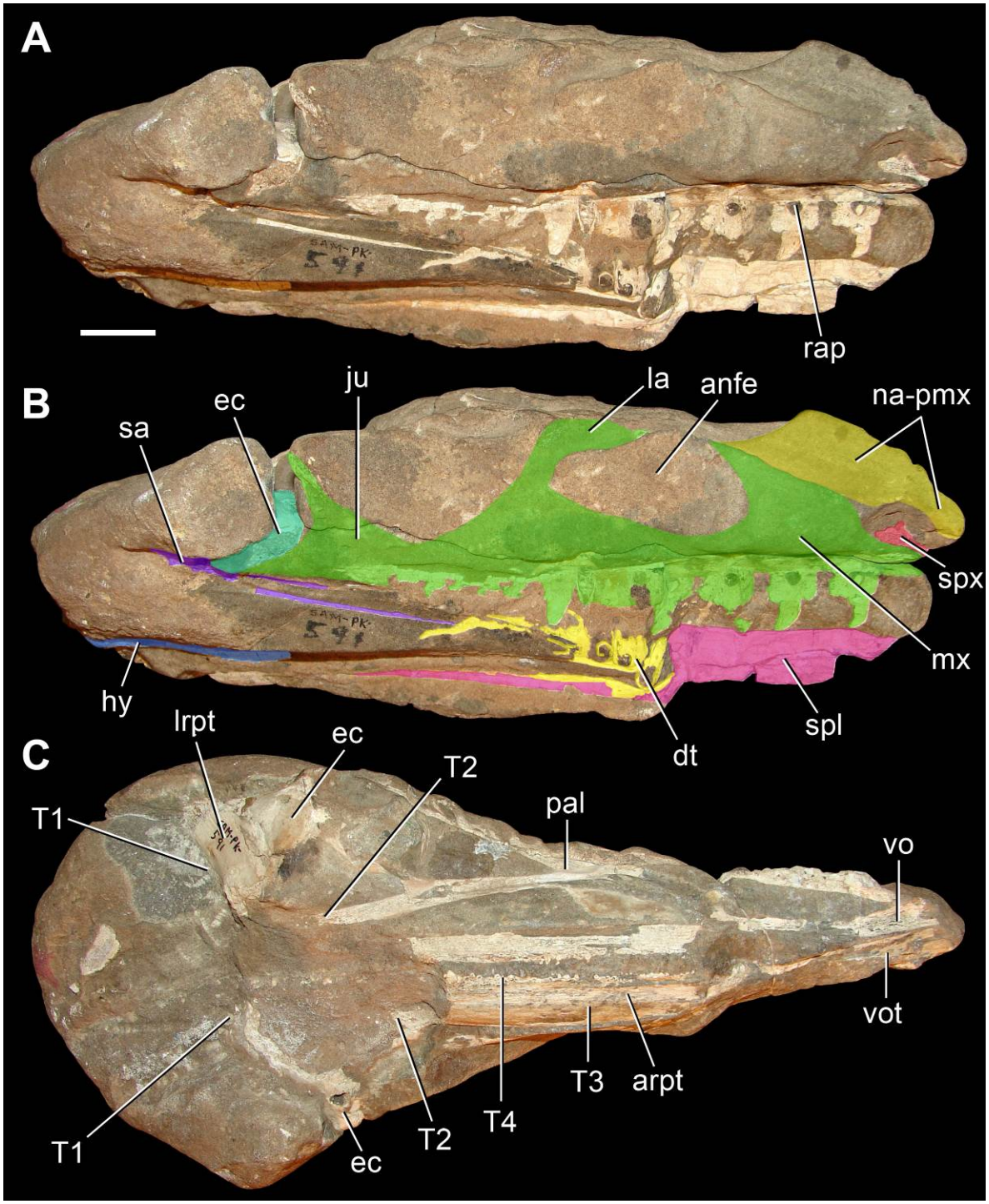

Figure S5.1. Holotype of *Proterosuchus fergusi* (SAM-PK-591). A, B, right lateral view of both blocks; and C, dorsal view of the lower block. Abbreviations: anfe, antorbital fenestra; arpt, anterior ramus of the pterygoid; dt, dentary; ec, ectopterygoid; hy, hyoid bone; ju, jugal; la, lacrimal; lrpt, lateral ramus of the pterygoid; mx, maxilla; na-pmx, nasal and/or premaxilla; pal, palatine; rap, reabsorption pit; sa, surangular; spl, splenial; spx, septomaxilla; T1–4, palatal tooth rows 1–4; vo, vomer; vot, vomerine teeth. Scale bar equals 20 mm.

also occurs in the proposed neotype and referred specimens of *Proterosuchus fergusi* (BP/1/4016; Fig. S5.2A) and *Proterosuchus goweri* (NMQR 880). This concave surface would have formed the base of the anterior portion of the nasolacrimal duct (Hillenius, 2000). The posterior end of the septomaxilla is directed posterodorsally in lateral view and seems to have extended adjacent to the dorsal margin of the anterior process of the maxilla.

Maxilla. Both maxillae are preserved, but preservation is mostly as natural moulds and both lack their anterior ends (Fig S5.1A, B: mx). Although the entire length of the anterior process of the maxilla cannot be determined, its preserved portion is relatively long, resembling the condition present in several non-archosaur archosauromorphs (e.g. *Prolacerta broomi*: BP/1/471; proposed neotype and referred specimens of *Proterosuchus fergusi*: BP/1/3993, 4016, BSPG 1934 VIII 514, GHG 231, SAM-PK-11208, RC 59, 846; "*Chasmatosaurus*" *yuani*: IVPP V4067, V36315). The anterior process of the maxilla tapers in dorsoventral height anteriorly, as a result of the anteroventral slope of its dorsal margin.

The moulds of both maxillae clearly preserve the anterior and ventral borders of the antorbital fenestra, but these borders are better defined on the right side of the skull. The antorbital fenestra is large with an approximately oval outline (Fig. S5.1B: anfe). The anterior border of the fenestra is formed by the maxilla and is continuously curved, but asymmetric, with the most anterior point of the fenestra situated ventral to its mid-height. The morphology of the anterior border of the antorbital fenestra is variable among South African proterosuchid specimens: some specimens (e.g. BP/1/3993) possess the condition present in SAM-PK-591, whereas in others (e.g. BP/1/4016) the most anterior point of the fenestra is positioned dorsal to its mid-

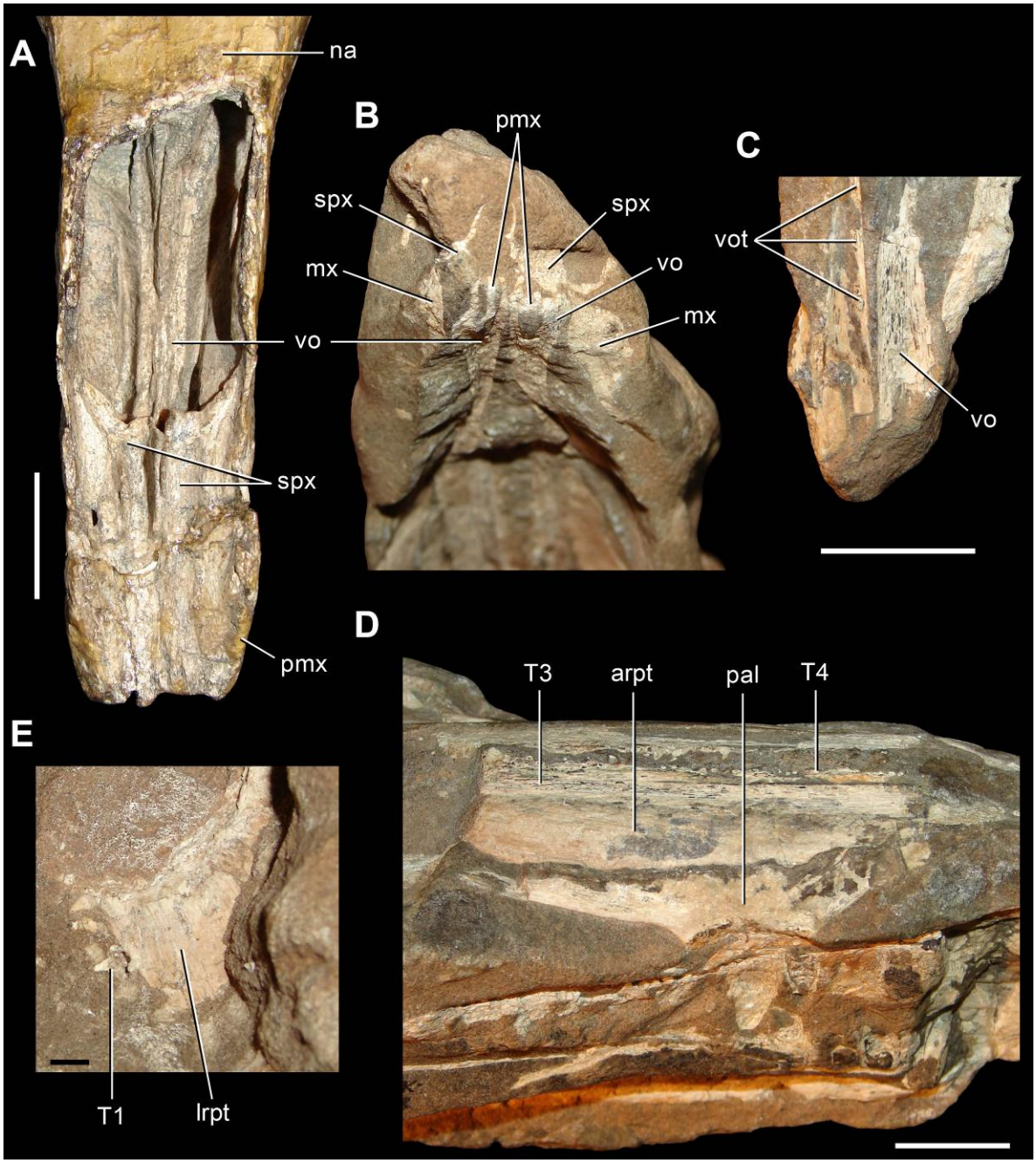

Figure S5.2. Proterosuchid palates. A, palate of a referred specimen (BP/1/4016); and B–E, holotype of *Proterosuchus fergusi* (SAM-PK-591). A, C, E, dorsal; B, anteroventral; and D, right dorsolateral views. Abbreviations: arpt, anterior ramus of the pterygoid; lrpt, lateral ramus of the pterygoid; mx, maxilla; na, nasal; pal, palatine; pmx, premaxilla; spx, septomaxilla; vo, vomer; vot, vomerine teeth; T1, 3, 4, palatal tooth rows 1, 3, 4. Scale bars equal 20 mm in A–D and 2 mm in E.

height. The ventral border of the antorbital fenestra formed by the maxilla is anteroposteriorly concave in lateral view, as occurs in several non-archosaur archosauriforms (e.g. proposed neotype and referred specimens of *Proterosuchus fergusi*: BP/1/3993, 4016, BSPG 1934 VIII 514, GHG 231, SAM-PK-11208, RC 59, 846; "*Chasmatosaurus*" *yuani*: IVPP V36315; *Erythrosuchus africanus*: BP/1/5207). By contrast, in *Tasmaniosaurus triasssicus* the ventral border of the antorbital fenestra is straight (UTGD 54655). It is not possible to determine the presence or absence of an antorbital fossa surrounding the fenestra in SAM-PK-591 due to the lack of preservation of the lateral surface of the maxilla.

The horizontal process of the maxilla (= 'main body' of the maxilla) posteriorly increases in dorsoventral height up until its point of contact with the lacrimal and jugal. Posterior to this point, the horizontal process tapers strongly in dorsoventral height towards its posterior end. The maxilla extends posteriorly as far as the level of the anteroposterior mid-point of the orbit, as also occurs in other proterosuchids (e.g. BP/1/4016, IVPP V2719, RC 846 [referred to as RC 96 by Welman and Flemming [1993] and subsequent authors, a number that actually corresponds to a dicynodont specimen; B. Rubidge, pers. comm., 2014], SAM-PK-1108). The ascending process of the maxilla is relatively short, posterodorsally directed, and tapers posteriorly, closely resembling the morphology present in other proterosuchids. It is not possible to determine the morphology of the suture between the ascending process of the maxilla and lacrimal.

The alveolar margin of the maxilla is gently convex ventrally in lateral view, resembling the condition present in most South African proterosuchid specimens (but see below). A total of 19–20 tooth positions are estimated to be present in the left maxilla, and 16–17 in the less complete right maxilla. If the missing anterior portions

of the maxillae are taken into account, the maxillary tooth count of SAM-PK-591 would exceed 20 tooth positions and thus fall within the range of variation observed in the proposed neotype and referred specimens of *Proterosuchus fergusi* (20–31 tooth positions; RC 59, 846). Most of the maxillary teeth of SAM-PK-591 are ankylosed to the maxilla through longitudinal bony ridges. A large, subtriangular nutrient dental pit is present at the base of each root.

Nasal. Only the natural moulds of the anteriormost ends of the nasals are preserved (Fig. S5.1A, B: na). The nasals are restricted to the dorsolateral surface of the snout and possess an extensive suture with the maxilla that extends from anteroventral to posterodorsal. The nasal morphology is consistent with that of other South African proterosuchid specimens (e.g. BP/1/3993, RC 846).

Lacrimal. A partial natural mould is preserved for the right lacrimal, but lacks the anterior three-quarters of the anterior process (Fig. S5.1A, B: la). The lacrimal is shaped like an inverted L, and forms the posterior and posterodorsal borders of the antorbital fenestra, as in other South African proterosuchid specimens (e.g. BP/1/3993, NMQR 880, 1484, RC 846, SAM-PK-11208), "*Chasmatosaurus*" *yuani* (IVPP V4067) and *Tasmaniosaurus triassicus* (UTGD 54655). The posterior border of the antorbital fenestra has a squared-off outline. The presence or absence of the flange of the lacrimal that extends into the posterodorsal corner of the antorbital fenestra in some South African proterosuchid specimens (e.g. BP/1/4016, SAM-PK-11208) cannot be determined. The ventral process of the lacrimal is directed slightly posteroventrally, rather than being vertical. It cannot be determined if the ventral process forms a contact at its ventral margin with only the jugal or with the jugal and

the maxilla. Although most of the anterior process of the lacrimal is missing, the presence of a short ascending process of the maxilla suggests that the anterior process of the lacrimal was relatively long, as in other South African proterosuchid specimens (e.g. BP/1/4016, NMQR 880, 1484, SAM-PK-11208) and "*Chasmatosaurus*" *yuani* (IVPP V4067).

Jugal. The right jugal is represented mostly by a natural mould, with the exception of the distal end of the dorsal process, of which some bone remains (Fig. S5.1A, B: ju). The preserved contour of the jugal resembles that of other South African proterosuchid specimens (e.g. BP/1/4016, NMQR 880, 1484, SAM-PK-11208). It is not possible to determine the shape of the suture between the maxilla and jugal and, as a result, whether the anterior process of the jugal participated in forming the border of the antorbital fenestra (contra Broom, 1903). Nevertheless, if SAM-PK-591 resembles other Early Triassic non-archosaur archosauromorphs (e.g. *Prolacerta broomi*: BP/1/471; "*Chasmatosaurus*" *yuani*: IVPP V4067; proposed neotype and referred specimens of *Proterosuchus fergusi*: RC 846, SAM-PK-11208, TM 201), the jugal would have formed an anteroposteriorly extensive diagonal suture with the horizontal process of the maxilla. The anteroposterior length of the orbit of SAM-PK-591 is approximately equal to that of the antorbital fenestra, as in NMQR 1484 and NMQR 880.

The dorsal process (= 'postorbital process') of the jugal tapers toward its distal end and is posterodorsally directed, as in other Triassic archosauriforms (e.g. *Prolacerta broomi*: BP/1/471; proposed neotype and referred specimens of *Proterosuchus fergusi*: BP/1/4016, RC 846, SAM-PK-11208; "*Chasmatosaurus*" *yuani*: IVPP V4067; *Garjainia prima*: PIN 2394/5). It is not possible to determine

how far ventrally the suture between the postorbital and the jugal extended, because in other Triassic archosauriforms the ventral end of the postorbital wraps around the lateral and anterior surfaces of the jugal, and this surface is not preserved in SAM-PK-591. Only the base of the posterior process of the jugal is preserved. As a result, the length of the posterior process cannot be determined, nor is it known if the infratemporal fenestra had a complete ventral border or not (cf. Broom, 1903). The mould of the base of the posterior process is laterally inflated with respect to the rest of the jugal and to the maxilla. This lateral inflation suggests the presence of a transverse expansion of the posterior part of the skull beginning at the very base of the posterior process of the jugal, as in other early archosauriforms (e.g. proposed neotype and referred specimens of *Proterosuchus fergusi*: BP/1/4016, RC 846, SAM-PK-11208; "*Chasmatosaurus*" *yuani*: IVPP V4067; *Garjainia prima*: PIN 2394/5; *Erythrosuchus africanus*: BP/1/5207).

Vomer. The vomers (= 'prevomers' of Broom [1903]) are broken in a coronal section and, as a result, parts of them are preserved in both the upper and lower blocks of SAM-PK-591 (Figs. S5.1C, S5.2B, C: vo). As exposed, the vomer contacts anteriorly the palatal process of the premaxilla, with the anterior margin of the vomer forming a concave U-shape into which the palatal process of the premaxilla articulates. The vomer is relatively transversely broad at its anterior end and becomes gradually transversely narrower towards its posterior end, acquiring a strap-like morphology along its posterior three-quarters. The vomer forms most of the medial border of the choana. It is not possible to determine the position of the suture of the vomer with the palatine, and as a result, the extent of the contribution of the palatine to the medial

border of the choana is unclear. Likewise, the position and shape of the vomer-pterygoid suture cannot be determined.

Posteriorly, the vomers diverge slightly from each other, resulting in an inter-vomerine vacuity along the posterior halves of the bones, as in other South African proterosuchid specimens (e.g. NMQR 880) and "*Chasmatosaurus*" *yuani* (IVPP V36315). However, as preserved, this vacuity appears to be larger at its posterior end than it was originally, because the anterior ends of the pterygoids, which would have contacted the posterior ends of the vomers medially and partially occluded the vacuity, are missing. In the portion of the right vomer that is preserved in the lower block there are at least three palatal teeth exposed in cross section (Fig. S5.2C: vot). These teeth are placed adjacent to the medial margin of the vomer and aligned in a row parallel to the longitudinal axis of the bone (Broom, 1903; Cruickshank, 1972; Welman, 1998). The vomerine teeth are ventrally oriented. These tooth positions are probably part of a single row of functional teeth that would have been continuous with those of the anterior ramus of the pterygoid, as reconstructed by Broom (1903) and Welman (1998: fig. 1).

Palatine. The palatines are both preserved partially as natural moulds, with some bone also present in each block (Figs. S5.1C, S5.2D: pal). The morphology of the palatine is consistent with that of other proterosuchids (e.g. RC 59). The anterolateral process is not preserved in either palatine, but the entire bone was probably tetraradiate. The posteromedial process is strongly anteroposteriorly elongated and tapers in transverse width posteriorly, but is considerably broader transversely than figured by Welman (1998: fig. 1) in his reconstruction of the palate of *Proterosuchus fergusi* (which was based on multiple South African specimens; i.e. NMQR 880,

1484, RC 59, SAM-PK-591, TM 201). The anteromedial process of the palatine is anteroposteriorly shorter than the posteromedial process and also tapers more strongly in transverse width. This morphology contrasts with the sub-rectangular anteromedial process reconstructed by Welman (1998: fig. 1). In addition, the lateral margin of the anteromedial process is anteroposteriorly concave, and is not straight as reconstructed by Welman (1998: fig. 1). The posterolateral process of the left palatine is preserved and is considerably longer than reconstructed by Welman (1998: fig. 1). Although there are several differences between the palatine of SAM-PK-591 and the reconstruction of the palatine of *Proterosuchus fergusi* by Welman (1998: fig. 1), the morphology of the palatine of SAM-PK-591 falls within the range of variation observed for other South African proterosuchid specimens.

As described by Broom (1903), palatine teeth are not visible in SAM-PK-591. However, their apparent absence is probably a result of the fact that the palatines are not sufficiently broken to expose the roots of the teeth in dorsal view, and the ventral surfaces of the bones are completely covered by matrix. As a result, it is not possible to determine the presence or absence of palatine teeth in this specimen.

Pterygoid. The right pterygoid is preserved mainly as bone, with parts present in both blocks, whereas the left pterygoid is preserved partly as bone in the lower block and partly as a natural mould in the upper block. Both pterygoids are represented by most of the anterior (= palatal) ramus, lacking its anterior tip and base (Figs. S5.1C, S5.2D: arpt), and part of the lateral (= ectopterygoid) ramus, missing its base (Figs. S5.1C, S5.2E: lrpt). The anterior ramus is transversely wide and well developed anteriorly, extending beyond the level of the posterior border of the choana, as in other South African proterosuchid specimens (e.g. NMQR 880, RC 59, TM 201; Welman, 1998;

contra Cruickshank, 1972). The anterior rami are separated from each other along their entire length, resulting in an interpterygoid vacuity, as occurs in other early archosauriforms (e.g. referred specimens of *Proterosuchus fergusi*: BSPG 1934 VIII 514, RC 59; "*Chasmatosaurus*" *yuani*: IVPP V36315; *Garjainia prima*: PIN 2394/5) and *Prolacerta broomi* (Gow, 1975; Modesto and Sues, 2004).

The exposed dorsal surface of the anterior ramus of the pterygoid is transversely convex and anteroposteriorly flat. The entire medial margin of the anterior ramus possesses a single row of fang-like palatal teeth, each of which is distally curved towards its apex. This tooth row corresponds to the tooth series T4 of Welman (1998) (Figs. S5.1C, S5.2D: T4). This tooth row is also present in *Prolacerta broomi* (BP/1/2675; Gow, 1975) and other proterosuchids (e.g. RC 59). Some teeth that belong to multiple rows of the tooth series T2 of Welman (1998) are preserved in SAM-PK-591 on small portions of the right and left pterygoids positioned close to the base of the lateral ramus (Broom, 1903) (Fig. S5.1C: T2). Several teeth that belong to the multiple rows of the tooth series T3 of Welman (1998) are present adjacent to the medial margin of the anterior ramus, as in other South African proterosuchid specimens (e.g. BSPG 1934 VIII 514, RC 59) and *Prolacerta broomi* (BP/1/2675) (Figs. S5.1C, S5.2D: T3). The T3 palatal teeth are generally poorly preserved in SAM-PK-591, being mainly exposed in cross section, and appear to be considerably more dispersed over the pterygoid than in other proterosuchid specimens (e.g. BSPG 1934 VIII 514, RC 59), but this is probably an artefact that results from the lack of exposure of several teeth on the exposed broken dorsal surface of the pterygoid (cf. Broom, 1903: fig. 3).

The lateral ramus of the pterygoid is best preserved on the left side. The ramus is posterolaterally and ventrally directed and possesses a single row of fang-like teeth,

each of which is distally curved toward its apex, that belong to the palatal tooth series T1 of Welman (1998) (Figs. S5.1C, S5.2E: T1), as also occurs in other South African proterosuchid specimens (e.g. RC 59, SAM-PK-11208) and *Prolacerta broomi* (BP/1/2675). The dorsal surface of the transverse ramus is transversely convex and possesses multiple narrow, low longitudinal striations on its anterolateral portion, adjacent to the contact with the ectopterygoid. The fracture of the right pterygoid shows that the anterior half of the ventral surface of the transverse ramus is strongly concave, as in other South African proterosuchid specimens (NMQR 880, RC 59, SAM-PK-11208). The posterior (= quadrate) ramus of the pterygoid is completely missing on both sides of the skull.

Ectopterygoid. Part of the main body and the base of the lateral flange are preserved as bone and natural moulds for each ectopterygoid, with the left being more complete than the right (Fig. S5.1: ec). Welman (1998: fig. 2) identified a quadrate as present on the right side of SAM-PK-591 close to the posterior border of the orbit, but I found no evidence for the presence of an anteriorly displaced quadrate in that area. Instead, part of the structure identified as a quadrate is here interpreted a cross section through the lateral flange of the right ectopterygoid (Welman, 1998: fig. 2a), and part is a natural mould of the lateral ramus of the right pterygoid (Welman, 1998: fig. 2b). The dorsal surface of the left ectopterygoid is subdivided into two convex surfaces separated by a shallow, semilunate and anteriorly curved depression. The ectopterygoid possesses a complex suture with the pterygoid, in which the ectopterygoid dorsally overlaps the pterygoid on the proximal half of the suture whereas the pterygoid dorsally overlaps the ectopterygoid along the distal portion of

the suture. This complex suture pattern is also present in some other Triassic archosauromorphs (Dilkes, 1998).

The lateral flange of the ectopterygoid is well developed transversely and strongly posteriorly curved, and has therefore a hook-like morphology as in other Triassic archosauriforms (e.g. *Garjainia prima*: PIN 2394/5). A cross section through the right lateral flange (Welman, 1998: fig. 2a: q) shows that the flange is dorsoventrally compressed. The lateral flange is situated immediately posterior to the level of the base of the ascending process of the jugal. The lateral flange formed a contact distally only with the posterior process of the jugal, as in other South African proterosuchids (e.g. SAM-PK-K10603; contra Broom, 1903; contra Cruickshank, 1972).

Parabasisphenoid. The cultriform process of the parabasisphenoid (identified as the vomer by Broom, 1903) is exposed in cross section, being situated within the interpterygoid vacuity. The cultriform process is U-shaped in cross section, with a deep dorsally opening notch. The cortical bone of the cultriform process is thin and the spongy bone area is relatively large, with thin trabeculae delimiting relatively large internal intertrabecular chambers.

Dentary. A small portion of the right dentary is preserved in cross section, including four partial teeth (Fig. S5.1A, B: dt). Part of the natural mould of the ventral border of the anterior half of the left dentary is also preserved. The morphology of the dentary teeth is consistent with that of the maxillary teeth.

Splenial. The posterior two-thirds of both splenials are partially preserved (Fig. S5.1A, B: spl). The splenial is a plate-like bone that increases in dorsoventral height posteriorly, as in other Triassic archosauriforms (e.g. proposed neotype and referred specimens of *Proterosuchus fergusi*: BSPG 1934 VIII 514; "*Chasmatosaurus*" *yuani*: IVPP V36315; *Tasmaniosaurus triassicus*: UTGD 54655). Along its anterior two-thirds, the splenial does not reach the ventral margin of the lower jaw, but it does reach the ventral margin at its posterior end. The lateral surface of the splenial is dorsoventrally concave and formed the internal wall of the Meckelian canal.

Post-dentary bones. Both angulars are partially preserved, and natural moulds of the surangulars and angulars are also present (Fig. S5.1A, B: sa). It is not possible to determine the presence or absence of an external mandibular fenestra. The preserved portions of the post-dentary bones are consistent in morphology with those of other South African proterosuchid specimens (e.g. BP/1/4016, NMQR 1484, RC 59, 846, SAM-PK-11208, K10603, TM 201).

Hyoid bones. Two bones identified as probable ceratobranchials of the hyoid apparatus are partially preserved on the sides of the lower block (Fig. S5.1A, B: hy). A third bone is exposed in cross-section close to the midline of the skull in the lower block and at the same dorsoventral level as the hyoid bones. This bone possesses a subcircular cross-section and its identity is unclear. However, it may represent a hyoid bone, although this interpretation would indicate that at least one of the other elements currently identified as hyoid bones has been misidentified.

Appendix 7

Complete list of measurements used in Chapter 4

Grey values=estimated measurements
NA=missing data

Measurement	RC 59	BPI/1/ 4224	BPI/1/ 4016	SAM-PK-K140	SAM-PK-11208	BPI/1/ 3993	SAM-PK-K10603	RC 846	BSPG-1934-VIII-514	TM 201	GHG 231	N
Skull_length	177.6	227.8	238.5	287.0	350.0	388.0	407.5	420.6	435.0	443.6	477.0	11
Skull_maximum_height	NA	NA	55.9	NA	71.1	NA	NA	126.6	127.2	NA	151.0	6
Length_anterior_to_antorbital_fenestra	59.5	NA	NA	84.6	109.9	129.8	NA	134.4	143.6	132.4	171.5	9
Postorbital_region_maximum_width	71.2	NA	77.4	124.1	NA	NA	134.0	127.1	255.0	NA	NA	7
Premaxilla_body_length	21.0	NA	NA	36.1	55.9	53.6	NA	53.2	NA	51.6	78.2	8
Premaxilla_body_height	6.0	NA	8.5	15.1	17.5	17.7	NA	15.7	17.1	17.0	20.9	10
Larger_pmx_tooth_height	9.2	NA	8.0	NA	13.2	NA	NA	13.0	11.3	NA	NA	6
Larger_pmx_tooth_length_at_base	2.2	NA	4.7	5.7	5.1	NA	NA	6.4	7.5	6.0	NA	8
Snout_minimum_width	21.5	NA	23.5	34.1	NA	37.3	41.4	42.3	51.0	43.1	46.8	10
Maxilla_length	96.7	NA	103.3	135.2	174.5	201.4	NA	222.7	229.0	NA	257.0	8
Maxilla_horizontal_process_minimum_height	6.7	NA	12.5	15.6	21.2	24.7	19.6	24.1	29.9	23.2	30.9	10
Maxilla_length_anterior_to_antorbtial_fenestra	33.0	NA	38.2	48.6	60.7	79.6	NA	80.1	75.5	87.1	82.5	10
Maxilla_horizontal_process_length	NA	NA	NA	NA	NA	NA	NA	141.1	149.0	NA	NA	3
Maxilla_ascending_process_height	NA	NA	NA	NA	NA	NA	NA	29.3	32.3	NA	NA	3
Maxilla_maximum_height	NA	NA	NA	NA	NA	NA	NA	57.9	NA	NA	NA	2
Maxillae_maximum_width	NA	NA	NA	NA	NA	NA	NA	64.6	NA	NA	NA	2
Larger_mx_tooth_height	8.0	NA	10.4	NA	13.8	14.6	13.1	15.6	11.2	12.3	15.6	10
Larger_mx_tooth_length_at_base	4.2	NA	4.6	5.8	5.4	7.5	5.3	6.3	7.6	5.8	6.6	11
Antorbital_fenestra_length	NA	NA	36.3	48.4	56.6	59.2	NA	66.2	66.0	NA	NA	6
Antorbital_fenestra_height	NA	NA	14.1	NA	NA	NA	NA	34.2	26.4	NA	NA	4
Nasal_length	NA	NA	NA	NA	NA	192.0	NA	195.0	NA	NA	187.0	4

Nasal_maximum_width	NA	NA	NA	NA	NA	33.6	NA	22.5	NA	NA	NA	3
Nasal_minimum_width	NA	NA	NA	NA	NA	27.9	NA	9.2	NA	20.5	NA	4
Lacrimal_length	NA	NA	40.5	NA	NA	NA	NA	61.7	78.0	NA	77.8	5
Lacrimal_height_(exposed_in_lateral_view)	NA	NA	27.1	NA	41.0	38.5	40.0	64.3	55.1	NA	NA	7
Lacrimal_anterior_process_length	NA	NA	NA	NA	NA	NA	NA	36.5	66.7	NA	NA	3
Lacrimal_ventral_process_height	NA	NA	NA	NA	NA	NA	15.0	24.7	36.8	NA	NA	4
Lacrimal_ventral_process_minimum_length	NA	NA	NA	NA	NA	NA	NA	3.4	8.5	NA	NA	3
Jugal_length	NA	NA	NA	NA	NA	NA	NA	183.3	NA	NA	NA	2
Jugal_height	NA	NA	NA	NA	NA	NA	NA	74.0	NA	NA	NA	2
Jugal_anterior_process_length	NA	NA	NA	NA	NA	NA	20.9	38.3	NA	NA	NA	3
Jugal_anterior_process_height	6.4	NA	8.9	12.8	10.6	16.4	22.6	23.2	21.1	16.0	15.0	10
Jugal_posterior_process_length	NA	NA	NA	NA	NA	NA	111.3	129.9	NA	NA	NA	3
Jugal_posterior_process_height_at_mid-length	NA	NA	NA	NA	NA	NA	12.9	13.0	NA	NA	NA	3
Jugal_ascending_process_height	NA	NA	NA	NA	NA	NA	46.5	56.1	NA	NA	NA	3
Prefrontal_length	NA	NA	50.3	NA	90.0	53.7	57.5	55.6	NA	NA	62.6	7
Prefrontal_width	NA	NA	10.9	NA	24.5	17.5	18.0	17.7	NA	NA	19.2	7
Prefrontal_height	NA	NA	23.7	NA	NA	33.3	31.0	NA	NA	NA	45.7	5
Orbit_length	NA	33.3	30.8	NA	NA	47.8	47.9	49.0	64.0	NA	49.1	8
Orbit_height	NA	NA	28.8	NA	48.7	59.0	NA	69.6	83.1	NA	106.1	7
Sclerotic_ring_plate_width	NA	NA	NA	NA	NA	NA	10.2	NA	NA	NA	NA	2
Sclerotic_ring_plate_length	NA	NA	NA	NA	NA	NA	NA	NA	NA	NA	NA	1
Frontal_length	34.2	36.7	38.4	NA	63.6	62.1	69.3	70.1	NA	NA	70.2	9
Frontals_minimum_width	18.7	25.9	23.5	NA	42.9	30.3	42.3	31.8	33.4	NA	49.8	10
Postfrontal_length_(oblique)	12.3	15.6	15.9	NA	NA	27.3	NA	NA	NA	NA	21.9	6
Postorbital_length	NA	30.3	30.9	42.5	38.0	53.9	74.0	NA	NA	NA	87.1	8
Postorbital_height	31.1	38.1	38.3	NA	NA	NA	62.0	61.7	70.3	NA	67.4	8
Postorbital_foramen_length	NA	NA	NA	NA	NA	NA	1.6	NA	NA	NA	NA	2
Postorbital_maximum_width	NA	NA	NA	NA	NA	NA	12.9	NA	NA	NA	NA	2
Postorbital_ascending_process_length	NA	NA	NA	NA	NA	NA	23.2	NA	26.3	NA	NA	3
Postorbital_posterior_process_length	NA	NA	NA	NA	NA	NA	46.4	42.5	NA	NA	NA	3
Postorbital_ventral_process_length	NA	NA	NA	NA	NA	NA	46.4	54.5	NA	NA	NA	3
Squamosal_length	NA	43.2	43.4	NA	68.2	54.8	NA	56.4	NA	NA	92.7	7
Squamosal_height	32.3	37.4	33.1	NA	51.5	NA	67.1	75.6	87.0	NA	97.9	9
Squamosal_ventral_process_height	22.6	30.5	23.9	NA	37.1	NA	45.4	61.4	64.6	NA	79.8	9

Squamosal_ventral_process_base_length	13.6	13.6	13.4	NA	23.6	NA	26.7	19.2	26.0	NA	28.0	9
Infratemporal_fenestra_length	NA	49.1	52.5	NA	92.2	108.0	91.8	114.8	127.6	NA	144.4	9
Infratemporal_fenestra_height	NA	35.5	36.9	NA	47.5	NA	NA	79.0	72.4	NA	105.0	7
Supratemporal_fenestra_length	13.1	24.5	17.9	34.3	26.4	32.8	33.5	37.2	39.4	NA	41.5	11
Supratemporal_fenestra_width	NA	15.6	7.5	22.4	NA	17.0	18.7	20.3	28.5	NA	18.7	9
Supratemporal_fossa_width	5.2	5.6	4.4	10.0	9.1	11.3	12.7	9.8	5.9	5.1	12.9	12
Quadratojugal_height_(laterally_exposed)	NA	NA	26.4	NA	NA	NA	31.9	85.3	63.8	NA	NA	5
Quadratojugal_length_at_ventral_margin	NA	NA	NA	NA	NA	NA	NA	14.7	16.4	NA	NA	3
Quadrate_height	NA	61.4	44.0	NA	78.8	83.7	NA	NA	120.8	NA	NA	6
Quadrate_foramen_height	NA	5.9	9.0	NA	NA	NA	9.3	NA	NA	NA	NA	4
Quadrate_foramen_width	NA	2.4	5.3	NA	NA	NA	6.9	NA	NA	NA	10.2	5
Quadrate_distal_end_width	NA	NA	NA	NA	NA	NA	46.9	NA	NA	41.4	NA	3
Quadrate_distal_end_length	NA	NA	NA	NA	NA	NA	NA	NA	NA	18.2	NA	2
Quadrate_lateral_distal_condyle_width	NA	NA	NA	NA	NA	NA	NA	NA	NA	26.0	NA	2
Quadrate_lateral_distal_condyle_depth	NA	NA	NA	NA	NA	NA	NA	NA	NA	15.1	NA	2
Quadrate_medial_distal_condyle_width	NA	NA	NA	NA	NA	NA	NA	NA	NA	NA	NA	1
Quadrate_medial_distal_condyle_depth	NA	NA	NA	NA	NA	NA	NA	NA	NA	13.8	NA	2
Parietal_length	43.7	40.3	52.5	52.1	79.0	70.4	71.0	94.5	106.8	NA	88.5	11
Parietal_length_up_to_transverse_crest	NA	NA	NA	NA	NA	NA	30.5	27.4	NA	NA	NA	3
Parietals_maximum_width	27.7	60.8	54.8	79.6	NA	78.4	113.7	114.0	NA	NA	134.7	9
Parietals_minimum_width	21.7	25.9	25.8	NA	37.7	38.5	37.8	36.8	45.8	40.6	44.2	11
Pineal_fossa_length	NA	NA	NA	NA	NA	2.7	12.1	7.1	NA	22.2	NA	5
Pineal_fossa_width	NA	NA	NA	NA	NA	3.9	9.0	7.2	NA	15.0	NA	5
Interparietal_height	NA	NA	NA	NA	NA	NA	9.3	NA	NA	NA	NA	2
Interparietal_width	3.6	NA	20.1	NA	NA	NA	8.0	8.8	NA	NA	11.2	6
Supraoccipital_height	NA	18.4	14.4	NA	17.2	NA	21.5	39.5	22.6	NA	NA	7
Supraoccipital_width	NA	23.1	26.2	NA	NA	NA	22.6	28.2	37.8	NA	23.7	7
Vomer_length	NA	NA	NA	NA	NA	NA	NA	NA	NA	NA	NA	1
Palatine_length	NA	NA	NA	NA	NA	NA	NA	NA	NA	NA	NA	1
Palatine_width	NA	NA	NA	NA	NA	NA	NA	NA	22.6	NA	NA	2
Palatal_indet_bone_length	NA	NA	NA	NA	NA	NA	NA	NA	NA	NA	NA	1
Palatal_indet_bone_width	NA	NA	NA	NA	NA	NA	NA	NA	24.3	NA	NA	2
Pterygoid_length	NA	NA	NA	NA	NA	177.0	NA	NA	294.0	170.6	NA	3
Pterygoid_width	NA	NA	NA	NA	NA	NA	NA	NA	NA	NA	NA	1

Pterygoid_height	NA	NA	NA	NA	NA	NA	NA	NA	NA	NA	NA	1
Pterygoid_quadrate_ala_length	NA	NA	NA	NA	NA	NA	NA	NA	100.5	NA	NA	2
Pterygoid_quadrate_ala_minimum_height	NA	NA	NA	NA	NA	NA	NA	NA	18.8	NA	NA	2
Pterygoid_transverse_ala_width	NA	NA	NA	NA	NA	NA	NA	NA	59.8	NA	NA	2
Pterygoid_transverse_ala_minimun_length	NA	NA	NA	NA	NA	NA	NA	NA	64.0	NA	NA	2
Pterygoid_palatal_ala_length	NA	NA	NA	NA	NA	NA	NA	NA	197.0	NA	NA	2
Pterygoid_palatal_ala_minimum_width	NA	NA	NA	NA	NA	NA	NA	NA	19.7	NA	NA	2
Ectopterygoid_length	NA	NA	NA	NA	NA	NA	41.5	47.4	NA	NA	NA	3
Ectopterygoid_width	14.0	NA	NA	NA	NA	25.1	34.8	39.6	NA	NA	NA	4
Ectopterygoid_lateral_process_length	NA	NA	NA	NA	NA	NA	NA	NA	NA	NA	NA	0
Ectopterygoid_lateral_process_height	NA	NA	NA	NA	NA	NA	18.5	NA	NA	NA	NA	1
Width_between_both_paroccipital_processes	NA	61.0	NA	NA	81.8	81.6	128.5	NA	133.6	NA	152.6	7
Exoccipital_height	NA	NA	NA	NA	NA	NA	NA	NA	NA	NA	NA	1
Exoccipital_width	NA	NA	NA	NA	NA	NA	NA	NA	NA	NA	NA	1
Foramen_magnum_height	NA	NA	NA	NA	7.6	NA	NA	10.1	8.2	NA	15.2	5
Foramen_magnum_width	NA	NA	10.7	NA	10.7	NA	NA	10.4	13.6	NA	16.2	6
Basioccipital_length	NA	NA	NA	NA	NA	NA	NA	NA	NA	NA	NA	1
Basioccipital_width	NA	NA	NA	NA	NA	NA	NA	NA	NA	NA	NA	1
Occipital_condyle_height	NA	NA	NA	NA	NA	NA	NA	NA	17.6	NA	15.8	3
Occipital_condyle_width	NA	NA	NA	NA	NA	NA	NA	9.4	20.9	NA	25.3	4
Basal_tubera_height	NA	NA	NA	NA	NA	NA	NA	NA	22.9	NA	NA	2
Basal_tubera_width_at_base	NA	NA	NA	NA	NA	NA	NA	NA	2.3	NA	NA	2
Width_between_basal_tuberae	NA	NA	NA	NA	NA	NA	NA	NA	55.2	NA	NA	2
Minimum_width_between_basal_tuberae	NA	NA	NA	NA	NA	NA	NA	NA	6.0	NA	NA	2
Basisphenoid_length_up_to_ basipterygoid_pr	NA	NA	NA	NA	NA	NA	NA	NA	22.2	NA	NA	2
Basisphenoid_maximum_width	NA	NA	NA	NA	NA	NA	NA	NA	50.0	NA	NA	2
Basipterygoid_process_length	NA	NA	NA	NA	NA	NA	NA	NA	NA	NA	NA	1
Basipterygoid_process_width	NA	NA	NA	NA	NA	NA	NA	NA	NA	NA	NA	1
Basisphenoid_recess_width	NA	NA	NA	NA	NA	NA	NA	NA	NA	NA	NA	1
Basisphenoid_central_pit_length	NA	NA	NA	NA	NA	NA	NA	NA	NA	NA	NA	1
Basisphenoid_central_pit_width	NA	NA	NA	NA	NA	NA	NA	NA	NA	NA	NA	1
Cultriform_process_length	NA	NA	NA	NA	NA	NA	NA	NA	NA	NA	NA	1
Prootic_length	NA	NA	NA	NA	NA	NA	NA	NA	NA	NA	NA	1
Prootic_height	NA	NA	NA	NA	NA	NA	NA	NA	NA	NA	NA	1

Epipterygoid_length	NA	NA	NA	NA	NA	NA	36.2	NA	NA	NA	NA	2
Epipterygoid_height	NA	NA	NA	NA	NA	NA	34.7	NA	NA	NA	NA	2
Epipterygoid_posterior_process_length	NA	NA	NA	NA	NA	NA	NA	NA	NA	NA	NA	1
Epipterygoid_anterior_process_length	NA	NA	NA	NA	NA	NA	NA	NA	NA	NA	NA	1
Laterosphenoid_length	NA	NA	NA	NA	NA	NA	NA	NA	NA	NA	NA	1
Laterosphenoid_height	NA	NA	NA	NA	NA	NA	NA	NA	NA	NA	NA	1
Laterosphenoid_width	NA	NA	NA	NA	NA	NA	NA	NA	NA	NA	NA	1
Stape_height	NA	NA	NA	NA	NA	NA	NA	NA	NA	NA	NA	1
Stape_width	NA	NA	NA	NA	NA	NA	3.2	NA	NA	NA	NA	2
Lower_jaw_length	178.1	NA	202.8	NA	317.0	352.0	NA	369.2	426.0	NA	441.0	8
Dentary_length	103.7	NA	131.1	161.8	191.3	214.0	229.0	234.0	256.0	258.0	282.0	11
Dentary_anterior_height	12.1	NA	12.6	18.5	19.6	24.5	19.8	22.1	25.9	25.5	26.9	11
Dentary_anterior_tooh_height	NA	NA	NA	NA	NA	NA	NA	NA	NA	NA	NA	1
Dentary_anterior_crown_height	NA	NA	NA	NA	NA	NA	NA	NA	NA	NA	NA	0
Dentary_anterior_crown_labiolingual_width	NA	NA	NA	NA	NA	NA	NA	NA	NA	NA	NA	0
Dentary_anterior_root_height	NA	NA	NA	NA	NA	NA	NA	NA	NA	NA	NA	1
Dentary_largest_crown_height	9.0	NA	NA	8.7	NA	NA	NA	NA	NA	NA	NA	3
Dentary_largest_crown_length_at_base	3.4	NA	NA	4.9	NA	NA	NA	NA	NA	NA	NA	3
Splenial_length	NA	NA	NA	NA	188.5	NA	NA	NA	251.0	NA	NA	3
Splenial_height	NA	NA	NA	NA	26.8	NA	22.8	NA	31.7	NA	NA	4
Surangular_height	15.7	NA	12.5	22.0	27.1	23.1	20.0	29.2	NA	29.8	34.1	10
Surangular+retroarticular_process_length	107.4	NA	96.0	NA	175.6	117.7	NA	239.6	NA	NA	260.0	7
Angular_length	89.4	NA	97.5	NA	164.6	177.4	NA	NA	192.0	NA	NA	6
Angular_height	11.2	NA	12.7	20.1	23.9	26.4	20.1	NA	22.7	21.8	NA	9
Prearticular_length	NA	NA	NA	NA	148.3	NA	156.5	NA	201.8	NA	NA	4
Prearticular_minimum_height	NA	NA	NA	NA	13.8	NA	13.6	NA	8.1	NA	NA	4
Prearticular_maximum_posterior_width	NA	NA	NA	NA	NA	NA	NA	NA	37.0	NA	NA	2
External_mandibular_fenestra_length	16.6	NA	9.9	22.3	34.3	NA	31.8	13.6	40.4	NA	44.5	9
External_mandibular_fenestra_height	7.0	NA	3.0	9.2	10.6	NA	NA	6.7	8.1	NA	15.5	8
Retroarticular_process_length	11.8	NA	12.8	NA	NA	20.7	NA	27.7	18.8	NA	32.8	7
Retroarticular_process_width	9.0	NA	11.6	NA	NA	18.7	NA	NA	24.9	NA	22.0	6
Retroarticular_process_height	7.1	NA	9.0	NA	NA	15.4	NA	17.8	15.1	NA	11.9	7
Lower_jaw_maximum_posterior_width	NA	NA	NA	NA	NA	NA	44.8	NA	NA	NA	NA	2
Hyoides_length	NA	NA	NA	NA	NA	NA	NA	NA	NA	NA	NA	1

Hyoides_minimum_width	NA	NA	NA	NA	NA	NA	NA	NA	7.3	NA	NA	2
Hyoides_maximum_anterior_width	NA	NA	NA	NA	NA	NA	8.8	NA	13.6	NA	NA	3
Number of pmx teeth	5	NA	NA	6	8	6	NA	9	9	7	9	9
Number of mx teeth	20	NA	20	22	27	30	27	31	27	NA	30	10
Number of dentary teeth	18	NA	NA	NA	24	NA	NA	28	25	22	28	7
Quadrate angle	NA	127	124	122	125	NA	125	126	120	NA	126	9

Results excluding low N and non-significant regressions

Measurement	N	R2	p-value (reg)	slope	Lower Limit (90% CI)	Upper Limit (90% CI)	p-value (isometry)	Trend	Groups		
Skull_maximum_height	5	0.9013	0.0136	1.5614	1.0312	2.3642	0.0848	(+)	Height	Isometric trends	35
Length_anterior_to_antorbital_fenestra	8	0.9627	<0,0001	1.0390	0.8920	1.2102	0.6445	=	Length	Possitive allometries	8
Postorbital_region_maximum_width	6	0.7119	0.0371	1.2538	0.7272	2.1619	0.4430	=	Width	Negative allometries	6
Premaxilla_body_length	7	0.9094	0.0008	1.2279	0.9392	1.6053	0.1850	=	Length		
Premaxilla_body_height	9	0.8714	0.0002	1.2245	0.9498	1.5786	0.1761	=	Height	(+) marginally significant possitive allometry (-) marginally significant negative allometry	
Larger_pmx_tooth_length_at_base	7	0.7902	0.0074	1.1434	0.7650	1.7088	0.5408	=	Teeth		
Snout_minimum_width	9	0.9256	<0,0001	0.8868	0.7303	1.0766	0.2806	=	Width		
Maxilla_length	8	0.9610	<0,0001	1.1000	0.9411	1.2856	0.2811	=	Length		
Maxilla_horizontal_process_min_height	10	0.9339	<0,0001	1.4498	1.2254	1.7154	0.0031	+	Height		
Maxilla_length_ant_to_antorbtial_fenestra	9	0.9560	<0,0001	1.0918	0.9401	1.2581	0.3036	=	Length		
Larger_mx_tooth_height	9	0.6910	0.0054	0.6598	0.4475	0.9727	0.0810	(-)	Teeth		
Larger_mx_tooth_length_at_base	10	0.6201	0.0068	0.6045	0.4073	0.8972	0.0426	-	Teeth		
Antorbital_fenestra_length	6	0.9679	0.0004	0.9721	0.8041	1.1753	0.7682	=	Length		
Lacrimal_length	4	0.9275	0.0369	0.9799	0.5764	1.6659	0.9249	=	Length		

Lacrimal_height_(exposed_in_lateral_view)	6	0.7111	0.0349	1.3518	0.7834	2.3323	0.3184	=	Height
Jugal_anterior_process_height	10	0.7504	0.0012	1.3242	0.9589	1.8288	0.1458	=	Height
Orbit_length	7	0.8210	0.0049	0.8406	0.5790	1.2200	0.3986	=	Length
Orbit_height	6	0.9567	0.0007	1.8453	1.4808	2.2995	0.0033	+	Height
Frontal_length	8	0.9512	<0,0001	0.9001	0.7562	1.0714	0.2864	=	Length
Frontals_minimum_width	9	0.7344	0.0032	0.9030	0.6293	1.2958	0.6162	=	Width
Postfrontal_length_(oblique)	5	0.8219	0.0338	0.7680	0.4450	1.3256	0.3532	=	Length
Postorbital_length	7	0.8586	0.0026	1.4765	1.0586	2.0593	0.0634	(+)	Length
Postorbital_height	7	0.9860	<0,0001	0.8436	0.7586	0.9382	0.0231	-	Height
Squamosal_length	6	0.7033	0.0370	0.9523	0.5482	1.6541	0.8662	=	Length
Squamosal_height	8	0.9206	0.0002	1.2089	0.9686	1.5088	0.1480	=	Height
Squamosal_ventral_process_height	8	0.8810	0.0005	1.2891	0.9838	1.6891	0.1180	=	Height
Squamosal_ventral_process_base_length	8	0.8310	0.0016	0.8916	0.6470	1.2287	0.5191	=	Length
Infratemporal_fenestra_length	8	0.9611	<0,0001	1.4242	1.2187	1.6642	0.0042	+	Length
Infratemporal_fenestra_height	6	0.9092	0.0032	1.3923	1.0152	1.9094	0.0888	(+)	Height
Supratemporal_fenestra_length	10	0.8230	0.0002	1.1224	0.8541	1.4750	0.4588	=	Length
Supratemporal_fossa_width	11	0.7965	0.0012	1.2118	0.8820	1.6649	0.2942	=	Width
Quadrate_height	5	0.8144	0.0360	1.2864	0.7376	2.2434	0.3814	=	Height
Parietal_length	10	0.8314	0.0002	1.0100	0.7736	1.3188	0.9468	=	Length
Parietals_maximum_width	8	0.8912	0.0004	1.4396	1.1113	1.8648	0.0326	+	Width
Parietals_minimum_width	10	0.9528	<0,0001	0.7445	0.6458	0.8584	0.0046	-	Width
Ectopterygoid_width	5	0.8044	0.0391	1.1266	0.6374	1.9912	0.6717	=	Width
Width_between_paroccipital_processes	6	0.7940	0.0171	1.3823	0.8668	2.2043	0.2202	=	Width
Lower_jaw_length	7	0.9743	<0,0001	0.9830	0.8512	1.1352	0.8212	=	Length
Dentary_length	10	0.9915	<0,0001	1.0180	0.9582	1.0814	0.5981	=	Length
Dentary_anterior_height	10	0.8966	<0,0001	0.8986	0.7285	1.1083	0.3734	=	Height
Surangular_height	9	0.6858	0.0058	0.9917	0.6706	1.4666	0.9697	=	Height
Angular_length	5	0.9576	0.0037	0.9604	0.7287	1.2660	0.7566	=	Length
Angular_height	8	0.7804	0.0036	0.9398	0.6533	1.3520	0.7566	=	Height
Retroarticular_process_length	6	0.8086	0.0147	1.0272	0.6544	1.6125	0.9081	=	Length
Retroarticular_process_width	5	0.9641	0.0029	1.0218	0.7922	1.3180	0.8560	=	Width
Retroarticular_process_height	6	0.7650	0.0226	0.8948	0.5448	1.4697	0.6699	=	Height
Number of pmx teeth	8	0.6498	0.0156	0.6983	0.4436	1.0994	0.1798	=	Tooth
Number of mx teeth	9	0.8387	0.0005	0.5323	0.4008	0.7070	0.0030	-	Tooth

Number of dentary teeth	6	0.7152	0.0338	0.4524	0.2631	0.7778	0.0300	-	Tooth
Number mx teeth vs. maxilla length	8	0.9022	0.0003	0.4923	0.3620	0.6696	0.0009	-	
Number pmx teeth vs. pmx body length	7	0.7015	0.0186	0.5390	0.3354	0.8662	0.0186	-	
Number dentary teeth vs. dentary length	6	0.6808	0.0432	0.4505	0.2546	0.7972	0.0351	-	

Results using the minimum width between both parietals as the independent variable

Measurement	slope	p-value (isometry)	Trend
Skull_length	1.3431	0.0046	+
Skull_maximum_height	1.8872	0.1213	=
Length_anterior_to_antorbital_fenestra	1.3592	0.0547	(+)
Postorbital_region_maximum_width	1.6778	0.0558	(+)
Premaxilla_body_length	1.7432	0.0050	+
Premaxilla_body_height	1.6491	0.0020	+
Larger_pmx_tooth_length_at_base	1.5038	0.1276	=
Snout_minimum_width	1.2099	0.0489	+
Maxilla_length	1.4117	0.0358	=
Maxilla_horizontal_process_minimum_height	1.9532	<0.0001	+
Maxilla_length_anterior_to_antorbtial_fenestra	1.4280	0.0413	+
Larger_mx_tooth_height	0.8798	0.6195	=
Larger_mx_tooth_length_at_base	0.8250	0.3635	=
Antorbital_fenestra_length	1.1830	0.4985	=
Lacrimal_length	1.1742	0.0485	+
Lacrimal_height_(exposed_in_lateral_view)	1.6047	0.2191	=
Jugal_anterior_process_height	1.8002	0.0274	+
Orbit_length	1.0807	0.5798	=
Orbit_height	2.2304	0.0094	+
Frontal_length	1.2613	0.0671	(+)
Frontals_minimum_width	1.1971	0.3886	=
Postfrontal_length_(oblique)	1.0419	0.8743	=
Postorbital_length	1.9922	0.0428	+
Postorbital_height	1.1338	0.0896	(+)
Squamosal_length	1.2938	0.3091	=
Squamosal_height	1.6047	0.0097	+
Squamosal_ventral_process_height	1.7111	0.0127	+
Squamosal_ventral_process_base_length	1.1836	0.2610	=
Infratemporal_fenestra_length	1.8238	0.0008	+

Isometric trends	22
Possitive allometries	26
Negative allometries	1

(+) marginally significant possitive allometry
(-) marginally significant negative allometry

Infratemporal_fenestra_height	1.7563	0.0762	(+)
Supratemporal_fenestra_length	1.4778	0.0228	+
Supratemporal_fossa_width	1.7458	0.0823	(+)
Quadrate_height	1.4592	0.1529	=
Parietal_length	1.3058	0.1058	=
Parietals_maximum_width	2.0669	0.0045	+
Ectopterygoid_width	1.6765	0.2461	=
Width_between_both_paroccipital_processes	1.7836	0.0889	(+)
Lower_jaw_length	1.2783	0.0265	+
Dentary_length	1.3566	0.0095	+
Dentary_anterior_height	1.2202	0.0911	(+)
Surangular_height	1.4169	0.1382	=
Angular_length	1.1539	0.2336	=
Angular_height	1.2290	0.2623	=
Retroarticular_process_length	1.3462	0.3541	=
Retroarticular_process_width	1.2951	0.0082	+
Retroarticular_process_height	1.1727	0.5995	=
Number of pmx teeth	0.9295	0.8012	=
Number of mx teeth	0.6731	0.0870	(-)
Number of dentary teeth	0.6133	0.1694	=

Appendix 8

Character list of the phylogenetic analysis of Chapter 5

(1) Skull and lower jaws, interdental plates: absent (0); present, but restricted to the anterior end of the dentary (1); present along the entire alveolar margin of the premaxilla, maxilla and dentary (2) (modified from Carrano et al., 2002), ORDERED.

(2) Skull, total length versus length of the presacral vertebral column: 0.22-0.45 (0); 0.53-0.59 (1); 0.94-0.98 (2) (modified from Sereno, 1991; Ezcurra et al., 2010: 113; Nesbitt, 2011: 134), CONTINUOUS, ORDERED. This character is inapplicable in taxa with an extremely elongated neck (e.g. *Tanystropheus longobardicus*).

Chanaresuchus bonapartei (PVL 4575): 0.53
Dimorphodon (Nesbitt, 2011: character 134): >0.50
Euparkeria (SAM-PK-5867): 0.38
Heterodontosaurus (SAM-PK-K1332): 0.34
Macrocnemus bassanii (PIMUZ T4355): ca. 0.22
Mesosuchus (SAM-PK-5882; Dilkes, 1998: fig. 23): 0.31
Petrolacosaurus (Reisz, 1981: fig. 1): 0.24
Prestosuchus chiniquensis (UFRGS-PV-0629-T): ca. 0.34
Prolacerta broomi (Gow, 1975: fig. 27): 0.27
Proterochampsa barrionuevoi (PVSJ 606): 0.96
Proterosuchus alexanderi (NMQR 1484): ca. 0.34
Protorosaurus (BSPG 1995 I 5, cast of WMsN P 47361, skull length based on lower jaw length between its anterior tip and anterior border of the glenoid fossa): 0.34
Pseudochampsa ischigualastensis (PVSJ 567): 0.59
Rhychosaurus articeps (NHMUK R1237, R1238): ca. 0.32
Tropidosuchus romeri (PVL 4601): ca. 0.44
Turfanosuchus dabanensis (IVPP V3237): ca. 0.29
Vancleavea campi (Nesbitt et al., 2009: fig. 18): ca. 0.28
Youngina (SAM-PK-K7710a): 0.36

Discretization by the cluster analysis: (1) 0.22-0.45; (2) 0.53-0.59; (3) 0.94-0.98. (5%=0.04). The first group is more inclusive than obtained in order to include several taxa with estimated ratio and proportionally small skulls.

(3) Skull, strongly dorsoventrally compressed skull with mainly dorsally facing antorbital fenestrae and orbits: absent (0); present (1) (Reig, 1959; Ezcurra et al., 2015b: 104).

(4) Skull, well developed nodular prominences on the lateral surface of maxilla, jugal, quadratojugal, squamosal and angular: absent (0); present (1) (Sill, 1967; Ezcurra et al., 2015b: 105).

(5) Skull, dermal sculpturing on the dorsal surface of the skull roof: absent (0); shallow or deep pits scattered across surface and/or low ridges (1); prominent ridges or tubercles on frontals, parietals, and nasals (2) (Dilkes and Arcucci, 2009; modified from Dilkes and Arcucci, 2012: 1).

(6) Skull, dorsal surface of nasals and/or frontals ornamented by ridges radiating from centres of growth: absent (0); present (1) (Romer, 1971a; Ezcurra et al., 2015b: 106). This character is inapplicable to taxa that lack ridges or tubercles on the dorsal surface of the skull roof.

(7) Skull, dorsal orbital margin: orbital margin of the frontal level with skull table or raised slightly (0); orbital margin of the frontal elevated above skull table (1); shelf/ridge elevated above skull table extends along the lateral surface of the lacrimal, prefrontal, frontal portion of orbital rim, and postorbital (2) (Dilkes and Sues, 2009; Ezcurra et al., 2010: 16; modified from Dilkes and Arcucci, 2012: 15, 20), ORDERED.

(8) Skull, supratemporal fossa immediately medial or anterior to the supratemporal fenestra on the dorsal surface of the skull roof: absent (0); present (1) (taken from Dilkes and Arcucci, 2012; Ezcurra et al., 2015b: 107). This character is inapplicable in taxa lacking supratemporal fenestrae.

(9) External naris, confluent with each other: absent (0); present (1) (Laurin, 1991: F2; Müller, 2004: 85; Reisz et al., 2010: 20; Ezcurra et al., 2010: 5; modified from Ezcurra et al., 2014: 20), ORDERED.

(10) External naris, anteroposterior position in the snout: terminal, on the anterior end of the snout (0); non-terminal, considerably posteriorly displaced, but posterior rim of the naris well anterior to the anterior border of the orbit (1); non-terminal, considerably posteriorly displaced and posterior rim of the naris approximately at level with the anterior border of the orbit (2) (Dilkes, 1998; Ezcurra et al., 2010: 5, in part; modified from Nesbitt, 2011: 139), ORDERED.

(11) External naris, directed: laterally (0); dorsally (1); anteriorly (2) (Sereno, 1991; Nesbitt, 2011: 140; modified from Dilkes and Arcucci, 2012: 6).

(12) External naris, shape: sub-circular (0); oval (1) (Dilkes, 1998: 12; Müller, 2004: 86; Ezcurra et al., 2014: 116).

(13) Antorbital fenestra: absent (0); present (1) (Juul, 1994; Dilkes, 1998: 5; Ezcurra et al., 2010: 3; Nesbitt, 2011: 136; Dilkes and Arcucci, 2012: 2; Ezcurra et al., 2014: 118).

(14) Antorbital fenestra, anterior margin: gently rounded (0); nearly pointed (1) (Benton and Clark, 1988; Nesbitt, 2011: 30). The character is not applicable to taxa that lack an antorbital fenestra.

(15) Secondary antorbital fenestra, immediately anterior to the antorbital fenestra: absent (0); present (1) (New character).

(16) Orbit, shape: anteroposteriorly longer than tall (0); subcircular (1); dorsoventrally taller than long (2) (Benton and Clark, 1988; modified from Nesbitt, 2011: 142).

(17) Orbit, elevated rim: absent or incipient (0); present, restricted to the ascending process of the jugal and sometimes also onto the ventral process of the postorbital (1); present, well-developed along the jugal, postorbital, frontal, prefrontal and lacrimal (2) (modified from Butler et al., in press), ORDERED.

(18) Infratemporal fenestra: present (0); absent (1) (Laurin, 1991: A2; Reisz et al., 2010: 40; modified from Ezcurra et al., 2010: 39).

(19) Posttemporal fenestra, size: larger than or subequal to the supraoccipital (0); smaller than the supraoccipital (1); developed as a small foramen (2); absent (3) (Sereno and Novas, 1993; Dilkes, 1998: 53, 54; Reisz et al., 2010: 59; Nesbitt, 2011: 141, in part; Ezcurra et al., 2014: 58), ORDERED.

(20) Snout, antorbital length (anterior tip of the skull to anterior margin of the orbit) versus total length of the skull: 0.29-0.40 (0); 0.43-0.62 (1); 0.70-0.76 (2) (Dilkes, 1998: 2; modified from Ezcurra et al., 2014: 113), CONTINUOUS, ORDERED.

Azendohsaurus madagaskarensis (Flynn et al., 2010: fig. 13a): 0.49
Bentonyx (BRSUG 27200): 0.33
Boreopricea (Tatarinov, 1978: 1b): 0.40
Cerritosaurus binsfeldi (CA s/n): 0.50
Chanaresuchus bonapartei (MCZ 4039): 0.54
Chanaresuchus bonapartei (MCZ 4037): 0.55
Chanaresuchus bonapartei (PVL 4586): 0.59
Chanaresuchus bonapartei (PVL 4575): 0.57
"*Chasmatosaurus*" *yuani* (IVPP V4067): 0.52
Erythrosuchus africanus (BP/1/5207): 0.52
Dimorphodon (Padian, 1983: fig. 5d): 0.72
Euparkeria (SAM-PK-5867): 0.47
Fugusuchus (Cheng, 1980: fig. 22): 0.43
Garjainia prima (PIN 2394/5): 0.55
Gephyrosaurus (Evans, 1980: fig. 1): 0.36
Gracilisuchus (MCZ 4117): 0.51
Gualosuchus reigi (PULR 05): 0.57
Gualosuchus reigi (PVL 4576): 0.55
Herrerasaurus (PVSJ 407): 0.57
Heterodontosaurus (AM unnumbered): 0.39
Heterodontosaurus (SAM-PK-K337): 0.38
Heterodontosaurus (SAM-PK-K1332): 0.37
Jesairosaurus lehmani (ZAR 06): ca. 0.47
Macrocnemus bessanii (PIMUZ T4822): 0.56

Mesosuchus (Dilkes, 1998: fig. 2c): 0.29
Nicrosaurus kapffi (SMNS 4379: Hungerbühler, 1998: table 2.2.1): 0.73
Nicrosaurus kapffi (SMNS 4378: Hungerbühler, 1998: table 2.2.1): 0.70
Nicrosaurus kapffi (SMNS 5727: Hungerbühler, 1998: table 2.2.1): 0.70
Nicrosaurus kapffi (SMNS 5726: Hungerbühler, 1998: table 2.2.1): 0.72
Ornithosuchus (Sereno, 1991: fig. 11a): 0.56
Paleorhinus magnoculus (MNHN-ALM1): 0.75
Paleorhinus sp. (Dzik, 2001: fig. 1b): 0.76
Petrolacosaurus (Reisz, 1981: fig. 2): 0.35
Planocephalosaurus (Fraser, 1981: fig. 1a): 0.35
Prestosuchus chiniquensis (UFRGS-PV-0156-T): 0.56
Prolacerta (BP/1/471): 0.45
Prolacerta (SAM-PK-K10797): 0.45
Proterochampsa barrionuevoi (Dilkes and Arcucci, 2012: fig. 4): 0.59
Proterochampsa barrionuevoi (PVL 2063): 0.62
Proterochampsa barrionuevoi (PVSJ 606): 0.58
Proterochampsa nodosa (MCP 1694-Pv): 0.61
Proterosuchus goweri (NMQR 880): 0.51
Proterosuchus fergusi (RC 846): 0.50
Proterosuchus fergusi (SAM-PK-11208): 0.51
Protorosaurus (USNM 442453, cast of NMK S 180): 0.56
Pseudochampsa ischigualastensis (PVSJ 567): 0.50
Rhynchosaurus articeps (SHYMS 3): ca. 0.34
Riojasuchus tenuisceps (PVL 3827): 0.50
Shansisuchus (Wang et al., 2013: fig. 2c): 0.49
Smilosuchus gregorii (UCMP 27200): 0.70
Smilosuchus adamanensis (Camp, 1930: fig. 11a): 0.72
Smilosuchus lithodendrorum (Camp, 1930: fig. 11c): 0.70
Tanystropheus longobardicus (Wild, 1973: fig. 10b): 0.52
Tropidosuchus romeri (PVL 4601): 0.49
Turfanosuchus dabanensis (IVPP V3237): ca. 0.50
Vancleavea campi (USNM 508579 cast of GR 138): 0.30-0.34
Youngina (GHG K 106): 0.49

Discretization by the cluster analysis: (1) 0.29-0.40, (2) 0.43-0.62; (3) 0.70-0.76. (5%=0.02).

(21) Snout, dorsoventral height at the level of the anterior tip of the maxilla versus dorsoventral height at the level of the anterior border of the orbit: 0.15-0.30 (0); 0.38-0.53 (1); 0.59-0.80 (2); 1.04 (3) (New character), CONTINUOUS, ORDERED.

Azendohsaurus madagaskarensis (Flynn et al., 2010: fig. 13a): 0.62
Batrachotomus kupferzellensis (Gower, 1999: fig. 2a): 0.78
Bentonyx (BRSUG 27200): 0.49
Boreopricea (Tatarinov, 1978: 1b): 0.48

Cerritosaurus binsfeldi (CA s/n): 0.39
Chanaresuchus bonapartei (MCZ 4037): 0.27
Chanaresuchus bonapartei (MCZ 4039): <0.22
Chanaresuchus bonapartei (PVL 4575): 0.15
Chanaresuchus bonapartei (PVL 4586): 0.21
"*Chasmatosaurus*" *yuani* (IVPP V4067): ca. 0.42
Dimorphodon (Padian, 1983: fig. 5d): 0.63
Erythrosuchus (BP/1/5207): 0.52
Euparkeria (SAM-PK-5867): ca. 0.71
Garjainia prima (PIN 2394/5): 0.70
Gephyrosaurus (Evans, 1980: fig. 1): 0.30
Gracilisuchus (MCZ 4117): ca. 0.54
Gualosuchus reigi (PULR 06): 0.26
Gualosuchus reigi (PVL 4576): 0.22
Herrerasaurus (PVSJ 407): 0.65
Heterodontosaurus (SAM-PK-K1332): 0.61
Macrocnemus bessanii (PIMUZ T4822): ca. 0.28
Mesosuchus (SAM-PK-6536): 0.50
Nicrosaurus kapffi (SMNS 4379: Hungerbühler, 1998: fig. 2.10): 1.04
Ornithosuchus (Sereno, 1991: fig. 11a): 0.52
Paleorhinus bransoni (Stocker, 2010: fig. 7a): 0.29
Petrolacosaurus (Reisz, 1981: fig. 2): 0.44
Planocephalosaurus (Fraser, 1981: fig. 1a): 0.45
Prestosuchus chiniquensis (UFRGS-PV-0156-T): 0.69
Prolacerta (BP/1/471): 0.42
Proterochampsa barrionuevoi (Dilkes and Arcucci, 2012: fig. 5a, b): 0.38
Proterochampsa barrionuevoi (PVL 2063): 0.41
Proterochampsa nodosa (MCP 1694-Pv): 0.59
Proterosuchus fergusi (RC 846): 0.39
Proterosuchus goweri (NMQR 880): <0.44
Rhynchosaurus articeps (SHYMS 1): ca. 0.44
Riojasuchus tenuisceps (PVL 3827): 0.73
Shansisuchus (Wang et al., 2013: fig. 2b): 0.59
Smilosuchus gregorii (UCMP 27200): 0.65
Smilosuchus adamanensis (Camp, 1930: fig. 11a): 0.72
Smilosuchus lithodendrorum (Camp, 1930: fig. 11c): 0.74
Trilophosaurus buettneri (Spielmann et al., 2008: fig. 20a, TMM 31025-207): 0.80
Turfanosuchus dabanensis (IVPP V3237): ca. 0.57
Vancleavea campi (USNM 508579 cast of GR 138): ca. 0.50

Discretization by the cluster analysis: (1) 0.15-0.30; (2) 0.38-0.53; (3) 0.59-0.80; (4) 1.04. (5%=0.04).

(22) Snout, proportions at the level of the anterior border of the orbit: transversely broader than dorsoventrally tall or subequal (0); dorsoventrally taller than

transversely broad (1) (Reisz and Dilkes, 2003: 53; Reisz et al., 2010: 7; modified from Ezcurra et al., 2014: 7).

(23) Snout, lateral margin of the snout anterior to the prefrontal: formed by the nasal (0); formed by the nasal and maxilla with gently rounded transition along the maxilla from the lateral to dorsal side of rostrum (1); formed by the nasal and maxilla with sharp edge along the maxilla between the lateral and dorsal sides of this bone (= box-like snout of Kischlat, 2000) (2) (Kischlat, 2000; Dilkes and Arcucci, 2012: 11). This character is inapplicable in taxa with an extensive contact between premaxilla and prefrontal (e.g. rhynchosaurids).

(24) Premaxilla-maxilla, suture: simple continuous contact (0); notched along the ventral margin (1) (Dilkes, 1998; Ezcurra et al., 2010: 7).

(25) Premaxilla-maxilla, subnarial foramen between the elements: absent (0); present and the border of the foramen is present on both the maxilla and the premaxilla (1); present and the border of the foramen is present on the maxilla but not on the premaxilla (2) (Benton and Clark, 1988; Nesbitt, 2011: 12).

(26) Premaxilla, alveolar margin does not reach the contact with the maxilla and forms a diastema (= subnarial gap): absent (0); present (1) (Nicholls, 1999; Müller, 2004: 116; Nesbitt, 2011: 11; Ezcurra et al., 2014: 117). This character is considered inapplicable in taxa without premaxillary teeth (e.g. *Trilophosaurus*).

(27) Premaxilla, main body size: small, the premaxillary body forms less than half of snout in front of the posterior border of the external nares (0); large, the premaxillary body forms half or more than half of snout in front of the posterior border of the external nares (1) (Rieppel et al., 1999; Müller, 2004: 1; Ezcurra et al., 2014: 115).

(28) Premaxilla, anteroposterior length of the main body versus its maximum dorsoventral height: 0.71 (0); 1.07-2.00 (1); 2.22-3.80 (2); 4.15-4.68 (3); >5.00 (4) (Bonaparte, 1991; modified from Nesbitt, 2011: 10), CONTINUOUS, ORDERED. This character is inapplicable in taxa with a premaxillary beak.

Aetosauroides scagliai (PVL 2059): >3.27
Archosaurus holotype (PIN 1100/55): 3.72
Asperoris (NHMUK R36615): 1.26
Azendohsaurus madagaskarensis (UA 8-7-98-284): 1.40
Azendohsaurus madagaskarensis (FMNH PR 2751): 1.25
Batrachotomus kupferzellensis (SMNS 52970): 1.51
Batrachotomus kupferzellensis (SMNS 80260): 1.83
Boreopricea (Tatarinov, 1978: 1b): 2.73
Cerritosaurus binsfeldi (CA s/n): ca. 1.50
Chanaresuchus bonapartei (MCZ 4039): 3.18
Chanaresuchus bonapartei (MCZ 4037): 3.19
Chanaresuchus bonapartei (PVL 4586): 4.15
Chanaresuchus bonapartei (PVL 4575): 3.27
"*Chasmatosaurus*" *yuani* (IVPP V4067): 3.49
"*Chasmatosaurus*" *yuani* (IVPP V36315): 4.37
Chasmatosuchus vjushkovi (PIN 2394/4): 2.78
Dimorphodon (NHMUK R41212-13): 4.68
Erythrosuchus (BP/1/5207): 1.50
Erythrosuchus (BP/1/4526): 1.65
Euparkeria (UMZC T692): 1.24
Euparkeria (SAM-PK-6047a): 1.24
Euparkeria (SAM-PK-13665): 1.66
Garjainia madiba (BP/1/6232N): 2.22
Garjainia madiba (BP/1/6232L): 2.83
Garjainia prima (PIN 2394/5): 1.82
Gephyrosaurus (Evans, 1980: fig. 29): 1.49
Gracilisuchus (MCZ 4117): 1.93
Gualosuchus reigi (PULR 05): 3.40
Gualosuchus reigi (PVL 4576): 3.22
Herrerasaurus (PVSJ 407): 1.22
Heterodontosaurus (AM unnumbered): 1.86
Heterodontosaurus (SAM-PK-K337): 1.49
Heterodontosaurus (SAM-PK-K1332): 1.91
Jesairosaurus lehmani (ZAR 06): ca. 6.89
Macrocnemus bessanii (PIMUZ T4822): 3.24
Mesosuchus (Dilkes, 1998: fig. 7a): 1.39
Nicrosaurus kapffi (SMNS 4379: Hungerbühler, 1998: fig. 2.10): 2.46
Ornithosuchus (NHMUK R2409): 3.20
Paleorhinus magnoculus (MNHN-ALM1): 15.8
Petrolacosaurus (Reisz, 1981: fig. 2): 3.00
Planocephalosaurus (Fraser, 1981: plate 70, fig. 1): 2.83
Prestosuchus chiniquensis (UFRGS-PV-0156-T): 0.71

Prestosuchus chiniquensis (UFRGS-PV-0152-T): 1.14
Prolacerta (BP/1/471): 3.80
Prolacerta (BP/1/4504): 2.93
Proterochampsa barrionuevoi (Dilkes and Arcucci, 2012: fig. 5a, b): 2.33
Proterosuchus fergusi (RC 59): 3.50
Proterosuchus fergusi (SAM-PK-K140): 2.39
Proterosuchus fergusi (SAM-PK-11208): 3.19
Proterosuchus fergusi (BP/1/3993): 3.03
Proterosuchus fergusi (TM 201): 3.03
Proterosuchus goweri (NMQR 880): ca. 3.64
Protorosaurus (USNM 442453, cast of NMK S 180): 2.59
Pseudochampsa ischigualastensis (PVSJ 567): 3.10
Riojasuchus tenuisceps (PVL 3827): 2.50
Sarmatosuchus (PIN 2865/68): 2.29
Shansisuchus shansisuchus (Young, 1964: figs. 8, 9): 1.07-1.33
Shansisuchus shansisuchus (Wang et al., 2013: fig. 2c): 1.30
Shansisuchus kuyeheensis (Cheng, 1980: fig. 24): ca. 1.57
Silesaurus opolensis (Dzik, 2003: fig. 6a): 2.29
Smilosuchus gregorii (UCMP 27200): 3.24
Smilosuchus adamanensis (Camp, 1930: fig. 11a): 4.32
Smilosuchus lithodendrorum (Camp, 1930: fig. 11c): 3.00
Tanystropheus longobardicus (Wild, 1973: fig. 10b): 2.44
Trilophosaurus buettneri (Spielmann et al., 2008: fig. 20a, TMM 31025-207): 2.58
Turfanosuchus dabanensis (IVPP V3237): 1.69
Vancleavea campi (USNM 508579 cast of GR 138): 1.75
Youngina (SAM-PK-K7578): 2.00

Discretization by the cluster analysis: (1) 0.71; (2) 1.07-2.00; (3) 2.22-3.80; (4) 4.15-4.68. (5%=0.20). *Paleorhinus magnoculus* was not included because of the extremely dorsoventraly compressed snout.

(29) Premaxilla, downturned main body: absent, alveolar margin sub-parallel to the main axis of the maxilla (0); slightly, in which the alveolar margin is angled at approximately 20º to the alveolar margin of the maxilla (1); strongly, prenarial process obscured by the postnarial process in lateral view (if the postnarial process is long enough) and postnarial process parallel or posteroventrally oriented with respect to the main axis of the premaxillary body (2) (modified from Dilkes, 1998: 6; Reisz et al., 2010: 10; Ezcurra et al., 2010: 4; Nesbitt, 2011: 8; Dilkes and Arcucci, 2012: 5, in part), ORDERED.

(30) Premaxilla, angle formed between the alveolar margin and the anterior margin of the premaxillary body in lateral view: acute or right-angled (0); obtuse (1) (New character). This character is innaplicable in taxa with a premaxilla modified as a beak.

(31) Premaxilla, lateral surface of the main body: smooth (0); one or two ventrally or posteroventrally oriented grooves restricted to the anterior end of the main body (1); one longitudinal groove slightly displaced ventrally or at the point of mid-height of the main body (2) (New character).

(32) Premaxilla, narial fossa: absent or shallow (0); expanded in the anteroventral corner of the naris (1) (Sereno, 1999; Nesbitt, 2011: 9; cf. Dilkes and Arcucci, 2012: 7). This character is inapplicable if the premaxilla does not participate in the border of the external naris.

(33) Premaxilla, peg on the posterior edge of the premaxillary body: absent (0); present (1) (New character).

(34) Premaxilla, prenarial process length: less than the anteroposterior length of the main body of the premaxilla (0); greater than the anteroposterior length of the main body of the premaxilla (1) (Nesbitt and Norell, 2006; Nesbitt, 2011: 1). This character is inapplicable in taxa that lack a prenarial process.

(35) Premaxilla, base of the prenarial process: anteroposteriorly shallow (0); anteroposteriorly deep (1) (New character). This character is inapplicable if the premaxilla does not participate in the border of the external naris.

(36) Premaxilla, postnarial process: absent (0); short, ends well anterior to the posterior margin of the external naris (1); well-developed, forms most of the border of the external naris or excludes the maxilla from participation in the external naris (2) (Laurin, 1991: F1; Reisz et al., 2010: 12; Nesbitt, 2011: cf. 2, 5,

24; Ezcurra et al., 2014: 12), ORDERED. This character is innaplicable in taxa with non-terminal external nares.

(37) Premaxilla, postnarial process: wide, plate-like (0); thin (1) (Gauthier, 1986; Nesbitt, 2011: 3). This character is not applicable to taxa that lack a postnarial process.

(38) Premaxilla, sharp dorsal flange at the base of the postnarial process delimiting the posteroventral border of the external naris: absent (0); present (1) (New character). This character is inapplicable if the premaxilla does not participate in the border of the external naris.

(39) Premaxilla, postnarial process: fits between the nasal and the maxilla or lies on the anterodorsal surface of the maxilla (0); overlaps the anterodorsal surface of the nasal (1); fits into slot of the nasal (2) (Parrish, 1993; modified from Nesbitt, 2011: 4). This character is not applicable to taxa that lack a postnarial process or it does not extend behind the external naris.

(40) Premaxilla, contact with prefrontal: absent (0); present, marginal (1); present, extensive (2) (Dilkes, 1998: 7; modified from Ezcurra et al., 2014: 114), ORDERED.

(41) Premaxilla, number of tooth positions: 10 or more (0); 5 or more (1); 4 (2); 3 (3); 2 (4); 1 or edentulous (5) (Laurin, 1991: G1; Reisz and Dilkes, 2003: 41; Müller, 2004: 152; Reisz et al., 2010: 8; Ezcurra et al., 2010: 86; Nesbitt, 2011: 6; Ezcurra et al., 2014: 8), ORDERED.

(42) Premaxilla, orientation of the tooth series or the occlusal surface of premaxilla in ventral view: approximately parasagittal (0); strongly transverse and anterior teeth covering each other in lateral view (1) (New character). This character is inapplicable in taxa without maxillary teeth.

(43) Premaxilla, lateroventrally opening anterior alveoli in mature individuals: absent (0); present (1) (New character). This character is inapplicable in taxa without maxillary teeth.

(44) Septomaxilla: present (0); absent (1) (Dilkes, 1998: 14; Müller, 2004: 87; Reisz et al., 2010: 18).

(45) Maxilla-nasal, maxillo-nasal tuberosity, delimiting anteriorly the antorbital fossa if present: absent (0); present (1) (New character).

(46) Maxilla-jugal, anguli oris crest: absent (0); present (1) (Benton, 1984; Butler et al., in press).

(47) Maxilla-jugal, anterior extension of the anguli oris crest: restricted to the main body of the jugal (0); extending onto the maxilla, but not the anterior process of the jugal (1) (Benton, 1984; Butler et al., in press). This character is innaplicable in taxa without an anguli oris crest.

(48) Maxilla, anterior extent: posterior to the anterior extent of the nasals (0); anterior to the nasals (1) (Sereno, 1991; Nesbitt, 2011: 19).

(49) Maxilla, length of the portion of the bone anterior to the antorbital fenestra versus the total length of the bone: 0.12-0.22 (0); 0.29-0.60 (1); 0.64-0.76 (2) (Clark et al., 2000; modified from Nesbitt, 2011: 14), CONTINUOUS, ORDERED. This character is not applicable in taxa that lack an antorbital fenestra.

Aetosauroides scagliai (PVL 2059): <0.62
Batrachotomus kupferzellensis (SMNS 52970): <0.41
Cerritosaurus binsfeldi (CA s/n): 0.76
Chalishevia (PIN 4366/1): <0.47
Chanaresuchus bonapartei (MCZ 4039): 0.49
Chanaresuchus bonapartei (MCZ 4037): 0.65
Chanaresuchus bonapartei (PVL 4586): 0.51
Chanaresuchus bonapartei (PVL 4575): 0.47
"*Chasmatosaurus*" *yuani* (IVPP V4067): 0.36
Dimorphodon (NHMUK R41212-13): 0.54

Erythrosuchus (BP/1/5207): 0.43
Euparkeria (SAM-PK-5867): 0.22
Euparkeria (SAM-PK-6047a): 0.17
Euparkeria (SAM-PK-13665): 0.16
Fugusuchus (GMB V313 unpublished picture): >0.33
Garjainia prima (PIN 2394/5): 0.35
Gracilisuchus (MCZ 4117): 0.12
Gualosuchus reigi (PULR 05): 0.53
Gualosuchus reigi (PVL 4576): 0.58
Guchengosuchus (IVPP V8808-1): 0.36
Herrerasaurus (PVSJ 407): 0.42
Heterodontosaurus (SAM-PK-K1332): 0.47
Jaxtasuchus salomoni (SMNS 91083): 0.60
Kalisuchus (QM F8998): <0.37
Lewisuchus (PULR 01): <0.35
Marasuchus lilloensis (PVL 3870): <0.41
Nicrosaurus kapffi (SMNS 4379: Hungerbühler, 1998: fig. 2.10): 0.56
Ornithosuchus (Sereno, 1991: fig. 11a): 0.35
Paleorhinus magnoculus (MNHN-ALM1): 0.64
Prestosuchus chiniquensis (UFRGS-PV-0152-T): 0.38
Prestosuchus chiniquensis (UFRGS-PV-0156-T): 0.43
Proterochampsa barrionuevoi (Dilkes and Arcucci, 2012: figs. 4, 5): 0.73
Proterosuchus alexanderi (NMQR 1484): 0.43
Proterosuchus fergusi (BP/1/3993): 0.39
Proterosuchus fergusi (BSPG 1934 VIII 514): 0.33
Proterosuchus fergusi (GHG 231): 0.32
Proterosuchus fergusi (RC 59): 0.34
Proterosuchus fergusi (RC 846): 0.36
Proterosuchus fergusi (SAM-PK-11208): 0.35
Proterosuchus fergusi (SAM-PK-K140): 0.36
Proterosuchus goweri (NMQR 880): 0.31
Pseudochampsa ischigualastensis (PVSJ 567): 0.67
Rhadinosuchus gracilis (BSPG AS XXV 50): 0.52
Riojasuchus tenuisceps (PVL 3827): 0.39
Shansisuchus shansisuchus (Wang et al., 2013: fig. 2a): 0.36
Silesaurus opolensis (ZPAL Ab III/361/26, 1218): ca. 0.29
Smilosuchus gregorii (UCMP 27200): 0.54
Smilosuchus adamanensis (Camp, 1930: fig. 11a): 0.47
Smilosuchus lithodendrorum (Camp, 1930: fig. 11c): 0.48
Tasmaniosaurus (UTGD 54655): >0.29
Tropidosuchus romeri (PVL 4606): 0.39
Turfanosuchus dabanensis (IVPP V3237): ca. 0.19

Discretization by the cluster analysis: (1) 0.12-0.22; (2) 0.29-0.60; (3) 0.64-0.76. (5%=0.03).

(50) Maxilla, posterior border of the subnarial foramen extending posteriorly as a groove on the lateral surface of the anterior process: absent (0); present (1) (New character). This character is not applicable in taxa that lack a subnarial foramen.

(51) Maxilla, anterior maxillary foramen: absent (0); present (1) (Dilkes, 1998: 17; Müller, 2004: 88; Modesto and Sues, 2004; Nesbitt, 2011: 31; Ezcurra et al., 2014: 120).

(52) Maxilla, neurovascular foramina on the lateral surface of the anterior and horizontal processes: laterally or lateroventrally facing (0); lateroventrally facing and extending ventrally as deep, well-defined grooves (1) (New character). This character is innaplicable in taxa lacking neurovascular foramina on the lateral surface of the maxilla.

(53) Maxilla, antorbital fossa on the lateral surface of the bone: absent or not exposed in lateral view (0); present on the ascending process of the maxilla, but not along the horizontal process of the maxilla (1); present on the ascending and horizontal processes of the maxilla, but not reaching the posteroventral corner of the fenestra (2); present on the ascending and horizontal processes of the maxilla, reaching the posteroventral corner of the opening (3) (modified from Benton, 2004; Dilkes and Sues, 2009: 3; Nesbitt, 2011: 137, in part; Dilkes and Arcucci, 2012: 3 and 4; Ezcurra et al., 2014: 119), ORDERED. This character is not applicable in taxa that lack an antorbital fenestra.

(54) Maxilla, anteroposterior length of the antorbital fossa anterior to the antorbital fenestra versus length of the antorbital fenestra: 0.09-0.23 (0); 0.28-0.43 (1); 0.90-0.94 (2); >2.00 (3) (modified from Sereno et al., 1994), CONTINUOUS, ORDERED. This character is inapplicable in taxa that lack an antorbital fossa or is not extended anterior to the antorbital fenestra.

Aetosauroides scagliai (PVL 2052): 0.21
Aetosauroides scagliai (PVL 2059): 0.18
Batrachotomus kupferzellensis (Gower, 1999: fig. 2a): 0.17
Cerritosaurus binsfeldi (CA s/n): 0.28
Dimorphodon (NHMUK R41212-13): 0.11
Erythrosuchus (BP/1/5207): 0.11
Euparkeria (SAM-PK-6047a): 0.10
Gracilisuchus (MCZ 4117): 0.23
Herrerasaurus (PVSJ 407): 0.09
Heterodontosaurus (SAM-PK-K1332): 3.00
Ornithosuchus (Sereno, 1991: fig. 11a): 0.43
Paleorhinus angustifrons (BSPG 1931 X 502): 0.18
Paleorhinus magnoculus (MNHN-ALM1): 0.15
Prestosuchus chiniquensis (UFRGS-PV-0156-T): 0.14
Proterochampsa barrionuevoi (Dilkes and Arcucci, 2012: figs. 4): 0.90-0.94
Riojasuchus tenuisceps (PVL 3827): 0.31
Shansisuchus shansisuchus (Wang et al., 2013: fig. 2a): 0.18
Tropidosuchus romeri (PVL 4601): 0.18
Turfanosuchus dabanensis (IVPP V3237): 0.12

Discretization by the cluster analysis: (1) 0.09-0.23; (2) 0.28-0.43; (3) 0.90-0.94. (5%=0.04). *Heterodontosaurus* was excluded from the cluster analysis because of a strongly reduced antorbital fenestra.

(55) Maxilla, secondary antorbital fossa anteriorly to the antorbital fossa and adjacent to the dorsal margin of the anterior process: absent (0); present (1) (New character). This character is not applicable in taxa that lack a secondary antorbital fenestra.

(56) Maxilla, ascending process: absent (0); posterodorsally oriented (1); sub-vertical anterior margin of the base of the process (2) (Reisz and Dilkes, 2003: 5; Reisz et al., 2010: 13; modified from Ezcurra et al., 2014: 13).

(57) Maxilla, anterodorsal margin at the base of the ascending process: convex or straight (0); concave (1) (Langer and Benton, 2006; Nesbitt, 2011: 25). This character is not applicable in taxa that lack an ascending process or possess a secondary antorbital fenestra.

(58) Maxilla, ascending process shape: tapers posterodorsally (0); remains the same width for its length (1) (Nesbitt, 2011: 29). This character is not applicable in taxa that lack an ascending process or an antorbital fenestra.

(59) Maxilla, contact with prefrontal: absent (0); present (1) (Reisz and Dilkes, 2003: 6; Müller, 2004: 179; Reisz et al., 2010: 14; Dilkes and Arcucci, 2012: 9 and 10; Ezcurra et al., 2014: 14).

(60) Maxilla, ventral margin of the antorbital fossa or fenestra (if the antorbital fossa is absent from the horizontal process of the maxilla) in the horizontal process: mainly sub-parallel to the alveolar margin of the bone (0); diagonal, anteroventrally-to-posterodorsally oriented in an angle close to 45º (1) (New character). This character is inapplicable in taxa that lack an antorbital fenestra or fossa.

(61) Maxilla, shape of the posterior portion of the bone ventral to the antorbital fenestra: tapers posteriorly (0); has a similar dorsoventral depth as the anterior portion ventral to the antorbital fenestra (1); expands dorsoventrally towards the distal end of the horizontal process with a concave ventral margin of the antorbital fenestra (2); expands dorsoventrally towards the distal end of the horizontal process with a straight ventral margin of the antorbital fenestra (3) (modified from Nesbitt, 2011: 27). This character is innaplicable in taxa that lack an antorbital fenestra.

(62) Maxilla, posterior end of the horizontal process distinctly ventrally deflected from the main axis of the alveolar margin: absent (0); present (1) (New character).

(63) Maxilla, triangular dorsal process with clear dorsal apex formed by discrete expansion of the posterior end of the horizontal process in lateral view: absent (0); present (1) (modified from Butler et al., 2014a).

(64) Maxilla, palatal process on the anteromedial surface of the bone: absent (0); present and both counterparts do not meet at the midline (1); present and both counterparts meet at the midline (2) (Parrish, 1993; Gower and Sennikov, 1997; Ezcurra et al., 2010: 101; modified from Nesbitt, 2011: 32; Dilkes and Arcucci, 2012: 13, in part), ORDERED.

(65) Maxilla, position of the palatal process: adjacent to the bases of the interdental plates (0); distinctly dorsal to the bases of the interdental plates (1) (New character). This character is innaplicable in taxa lacking a palatal process on the maxilla.

(66) Maxilla, alveolar margin in lateral view: concave, straight or gently convex (0); distinctly convex (1); sigmoid, anteriorly concave and posteriorly convex (2); sigmoid, anteriorly convex, starting close to mid-length, and posteriorly concave (3) (Dilkes, 1998: 16; modified from Ezcurra et al., 2014: 121).

(67) Maxilla, edentulous anterior portion of the ventral margin of the bone: absent (0); present (1) (New character).

(68) Maxilla, alveolar margin on the anterior third of the bone (anterior to the level of the anterior border of the antorbital fenestra if present): approximately aligned to the posterior half of the alveolar margin (0); distinctly upturned (1) (New character).

(69) Maxilla, posterior extension in mature individuals: level with or posterior to posterior orbital border (0); anterior to posterior orbital border but posterior to anterior orbital border (1); level with or anterior to anterior orbital border (2)

(deBraga and Rieppel, 1997; Müller, 2004: 127; modified from Ezcurra et al., 2014: 122), ORDERED.

(70) Maxilla, tooth plate: absent (0); present (1) (Dilkes, 1998: 60; Ezcurra et al., 2014: 124).

(71) Maxilla, number of tooth rows: single row (0); multiple rows (1) (Dilkes, 1998: 61; Ezcurra et al., 2014: 125).

(72) Maxilla, location of teeth: only on occlusal surface (0); on occlusal and lingual surfaces (1) (Dilkes, 1998: 63; Ezcurra et al., 2014: 126).

(73) Maxilla, number of tooth positions: 8-9 (0); 10-14 (1); 15-22 (2); 23-35 (3); 36-40 (4) (modified from Reisz and Dilkes, 2003: 28; Reisz et al., 2010: 15; Ezcurra et al., 2014: 15), ORDERED.

Acerosodontosaurus (Bickelmann et al., 2009; MNHN 1908-32-57): > 36
Aetosauroides scagliai (PVL 2059): ≥10
Amotosaurus (SMNS unnumbered): 25
Asperoris (NHMUK R36615; Nesbitt et al., 2013a: 8): ≥10
Azendohsaurus madagaskarensis (Flynn et al., 2010: 676): 14
Batrachotomus kupferzellensis (Gower, 1999: 15): 11
Boreopricea (Tatarinov, 1978: 510): 33
Cerritosaurus binsfeldi (CA s/n): 10-14
Chalishevia (PIN 4366/1): 12-13
Chanaresuchus bonapartei (Romer, 1971a: 13): 18
"*Chasmatosaurus ultimus*" (IVPP V2301): 13-14
"*Chasmatosaurus*" *yuani* (IVPP V2719): 29
Dimorphodon (NHMUK R41212-13): 8
Doswellia kaltenbachi (USNM 186989, based on the dentary tooth count): >25
Erythrosuchus (BP/1/5207): 11
Euparkeria (Ewer, 1965): 13
Fugusuchus (Cheng, 1980: fig. 22): 17-18
Garjainia prima (PIN 2394/5): 13-14
Gephyrosaurus (Evans, 1980: 225): 40
GHG 7433MI: 8-10
Gracilisuchus (MCZ 4117): 15
Gualosuchus reigi (PULR 05): 14
Gualosuchus reigi (PVL 4576): 14
Guchengosuchus (IVPP V8808-1): 14
Herrerasaurus (PVSJ 407): 17-18
Heterodontosaurus (AM unnumbered): 12
Heterodontosuarus (AM 4765): 13
Jaxtasuchus salomoni (SMNS 91083): 16

Jesairosaurus lehmani (ZAR 06): ca. 20-21
Kalisuchus (QM F8998): ≥14
Lewisuchus (PULR 01): 20
Macrocnemus bessanii (PIMUZ T4355): 26
Marasuchus lilloensis (PVL 3870): ca. 12
Nicrosaurus kapffi (SMNS 5727: Hungerbühler, 2000: table 1): 19-21
Ornithosuchus (NHMUK R2409): 9
Paleorhinus angustifrons (BSPG 1931 X 502): 16-17
Petrolacosaurus (Reisz, 1981: 12): 35
Planocephalosaurus (Fraser, 1982: 714): 17
Prestosuchus chiniquensis (UFRGS-PV-0156-T): 11
Prolacerta (Modesto and Sues, 2004): 24-25
Prolacertoides jimusarensis (IVPP V3233): ca. 19
Proterochampsa barrionuevoi (MACN-Pv 18165): 12
Proterochampsa nodosa (MCP 1694-Pv): 10
Proterosuchus alexanderi (NMQR 1484): 27
"*Proterosuchus fergusi*" (SAM-PK-591): >20
Proterosuchus fergusi (RC 846): 31
Proterosuchus goweri (NMQR 880): 29
Protorosaurus (Gottmann-Quesada and Sander, 2009: 141): 28 ± 1
Pseudochampsa ischigualastensis (PVSJ 567): ≥15 (but lower than 30)
Riojasuchus tenuisceps (PVL 3827): 8
Sarmatosuchus (PIN 2865/68, based on the dentary tooth count): ca. <18
Shansisuchus (Young, 1964; Wang et al., 2013): 10-13
Silesaurus opolensis (Dzik, 2003: 561): 11
Smilosuchus gregorii (UCMP 27200): 21
Smilosuchus adamanensis (Camp, 1930: 41): 23
Smilosuchus lithodendrorum (Camp, 1930: fig. 48): 21-22
Tanystropheus longobardicus (Wild, 1973: table 2): 14
Tasmaniosaurus (UTGD 54655): >21
Trilophosaurus buettneri (Spielmann et al., 2008: 27): 13
Tropidosuchus romeri (PVL 4606): ca. 12-13
Turfanosuchus dabanensis (IVPP V3237): ca. ≥13
Uralosaurus magnus (PIN 2973/71, based on dentary tooth count): <14
Vancleavea campi (Nesbitt et al., 2009: 820): 13
Youngina (Gow, 1975: 91): ca. 30

(74) Nasal, total length versus total length of the frontal: 0.68-0.79 (0); 0.92-1.46 (1); 1.78-1.91 (2); 2.04-2.07 (3); 2.26-2.78 (4); 2.96-3.09 (5) (Dilkes, 1998; Rieppel et al., 1999 in part; Reisz and Dilkes, 2003: 50 in part; Müller, 2004: 4, 8; modified from Reisz et al., 2010: 6, 22; Ezcurra et al., 2010: 9, in part; modified from Dilkes and Arcucci, 2012: 14; modified from Ezcurra et al., 2014: 6), CONTINUOUS, ORDERED.

Aetosauroides scagliai (PVL 2059): >1.57
Bentonyx (BRSUG 27200): 1.06
Boreopricea (Tatarinov, 1978: 1a; Benton and Allen, 1997): <0.94
Chanaresuchus bonapartei (MCZ 4039): 1.46
Chanaresuchus bonapartei (MCZ 4037): 1.19
Chanaresuchus bonapartei (PVL 4586): 1.45
"*Chasmatosaurus*" *yuani* (IVPP V4067): 2.58
Erythrosuchus (BP/1/5207): 1.42
Euparkeria (SAM-PK-13665): 1.26
Garjainia prima (PIN 2394/5): ca. 2.75
Gephyrosaurus (Evans, 1980: fig. 1): 0.77
GHG 7433MI: >1.81
Gracilisuchus (MCZ 4117): ca. 1.35
Gualosuchus reigi (PULR 05): 1.84
Gualosuchus reigi (PVL 4576): 2.04
Heterodontosaurus (Norman et al., 2011: fig. 12): 1.36
Mesosuchus (SAM-PK-6536): 0.79
Nicrosaurus kapffi (SMNS 5276: Hungerbühler, 1998: fig. 2.15): 2.26
Ornithosuchus (Sereno, 1991: fig. 11a): 1.36
Paleorhinus magnoculus (MNHN-ALM1): 1.23
Petrolacosaurus (Reisz, 1981: fig. 3): 0.68
Planocephalosaurus (Fraser, 1982: fig. 1c): 0.68
Prestosuchus chiniquensis (UFRGS-PV-0156-T): 3.08
Prolacerta (SAM-PK-K10797): 1.14
Proterochampsa barrionuevoi (Dilkes and Arcucci, 2012: 4b): >2.05
Proterochampsa nodosa (MCP 1694-Pv): >2.27
Proterosuchus alexanderi (NMQR 1484): >1.44
Proterosuchus fergusi (BP/1/3993): 3.09
Proterosuchus fergusi (GHG 231): 2.66
Proterosuchus fergusi (RC 846): 2.78
Protorosaurus (USNM 442453, cast of cast of NMK S 180): 1.84
Pseudochampsa ischigualastensis (PVSJ 567): ca. 2.46
Riojasuchus tenuisceps (PVL 3827): 2.07
Rhynchosaurus articeps (NHMUK R1236): 1.00
Shansisuchus shansisuchus (Wang et al., 2013: fig. 3b): 2.38
Smilosuchus lithodendrorum (Camp, 1930: fig. 2a): 1.05
Tanystropheus longobardicus (Wild, 1973: fig. 9a): 1.85
Turfanosuchus dabanensis (IVPP V3237): slightly >1.45
Vancleavea campi (USNM 508579 cast of GR 138): 0.79
Youngina (GHG K 106): 0.92

Discretization by the cluster analysis: (1) 0.68-0.79; (2) 0.92-1.46; (3) 1.78-1.91; (4) 2.04-2.07; (5) 2.26-2.78; (6) 2.96-3.09. (5%=0.12).

(75) Nasal, exposure (excluding descending process if present): largely dorsal element (0); nearly vertical contribution to the snout (1) (reworded from Reisz and Dilkes, 2003: 12; Reisz et al., 2010: 5; Ezcurra et al., 2014: 5).

(76) Nasal, shape of anterior margin at midline: strongly convex with anterior process (0); transverse with little convexity (1) (Dilkes, 1998: 13; Ezcurra et al., 2014: 127).

(77) Nasal, anterior portion in lateral view: below or at the same level as skull roof (0); elevated above skull roof, giving the skull a “Roman nose” appearance (1) (Gower, 1999; Bursatte et al., 2010b: 25).

(78) Nasal, dorsal surface around posterior margin of external naris: smooth or sculpturing of ridges and grooves present (0); depression around entire posterior margin that lacks sculpturing (1) (Dilkes and Arcucci, 2012: 8).

(79) Nasal, descending process, which results from the articulation of the postnasal process of the premaxilla on the anterodorsal surface of the nasal and has an extensive contact with the ascending process of the maxilla: anteroposteriorly narrow (0); anteroposteriorly very broad, being considerably broader than the ascending process of the maxilla (1) (New character). This character is scored inapplicable in taxa that lack a descending process.

(80) Nasal, dorsolateral margin of the anterior portion: smoothly rounded (0); distinct longitudinal ridge on the lateral edge (1) (Nesbitt, 2011: 35).

(81) Nasal, participation in the dorsal border of the antorbital fossa: absent (0); present (1) (Sereno et al., 1994; Nesbitt, 2011: 37). This character is inapplicable in taxa that lack an antorbital fossa.

(82) Lacrimal-postorbital, contact between bones: absent (0); present (1) (New character). This character is inapplicable in taxa that lost the lacrimal.

(83) Lacrimal, participation in the posterior border of the external naris: present (0); absent (1) (reworded from Laurin, 1991: B2; Reisz et al., 2010: 24; Ezcurra et al.,

2010: 6, in part; Ezcurra et al., 2014: 23). This character is innaplicable in taxa lacking a lacrimal.

(84) Lacrimal, exposure on the skull roof in dorsal view: absent or marginal (0); present (1) (Ezcurra et al., 2010: 166). This character is innaplicable in taxa lacking a lacrimal.

(85) Lacrimal, anterior process forming the entire or almost the entire dorsal border of the antorbital fenestra: absent (0); present (1) (New character). This character is not applicable in taxa that lack an antorbital fenestra or lacrimal.

(86) Lacrimal, antorbital fossa forming a distinct inset margin to the antorbital fenestra on the lateral surface of the bone: absent (0); present, but strongly restricted anteirorly (1); present and occuping almost half or more of the anteroposterior length of the ventral process (2) (Benton, 2004; modified from Ezcurra et al., 2010: 2; modified from Ezcurra et al., 2015b: 108). This character is not applicable in taxa that lack an antorbital fenestra or lacrimal.

(87) Lacrimal, naso-lacrimal duct: completely enclosed by the lacrimal (0); enclosed by the lacrimal and prefrontal (1) (New character).

(88) Lacrimal, naso-lacrimal duct position: opens on the posterolateral edge of lacrimal (0); opens on the posterior surface of the lacrimal (1) (Reisz and Dilkes, 2003: 19; cf. Müller, 2004: 129; Reisz et al., 2010: 25; Ezcurra et al., 2010: 8; Dilkes and Arcucci, 2012: 12, in part; modified from Ezcurra et al., 2014: 24). This character is inapplicable if the prefrontal encloses part of the naso-lacrimal duct.

(89) Jugal-quadratojugal, ventral margin in lateral view: straight or convex (0); concave, though nowhere dorsal to tooth row (1) (Reisz and Dilkes, 2003: 52;

Reisz et al., 2010: 42; Ezcurra et al., 2014: 41). Scored as inapplicable in taxa that lack the posterior process of the jugal.

(90) Jugal, anterior process shape: continuously tapering or subrectangular, being lower than the portion of the maxilla underneath it (0); subrectangular or slightly dorsoventrally expanded, being higher than the portion of the maxilla underneath it (1); with an ascending subprocess excluding the lacrimal from the anteroventral border of the orbit (2) (Gower and Sennikov, 1997; modified from Ezcurra et al., 2010: 99).

(91) Jugal, anterior process continuously dorsally curved: absent, straight or curved only at its proximal half (0); present (1) (New character).

(92) Jugal, ventral border of the orbit: gently concave (0); V-shaped (1) (New character). This character is innaplicable in taxa in which the jugal does not contribute to the border of the orbit.

(93) Jugal, anterior extension of the anterior process: anterior to the level of mid-length of the orbit (0); up to or posterior to the level of mid-length of the orbit (1) (reworded from deBraga and Rieppel, 1997; reworded from Müller, 2004: 128; modified and reworded from Ezcurra et al., 2014: 123).

(94) Jugal, participation of the anterior process in the border of the antorbital fenestra: present (0); absent, excluded by contact between the maxilla and lacrimal (1) (Clark et al., 2000; Ezcurra et al., 2010: 14; Nesbitt, 2011: 69). This character is not applicable in taxa that lack an antorbital fenestra or the anterior process of the jugal does not extend anteriorly to the level of mid-length of the orbit.

(95) Jugal, longitudinal ridge or bump(s) on the lateral surface of the main body: absent (0); present (1) (Sereno and Novas, 1993; Nesbitt, 2011: 75; modified from Dilkes and Arcucci, 2012: 21).

(96) Jugal with multiple pits on the lateral surface of its main body: absent (0); present (1) (Dilkes, 1995; Butler et al., in press).

(97) Jugal, length of the posterior process versus the height of its base: 0.49-1.27 (0); 1.59-3.77 (1); 4.07-5.37 (2) (modified from Parrish, 1992; Gower and Sennikov, 1997; Ezcurra et al., 2010: 98, cf. 150), CONTINUOUS, ORDERED.

Acerosodontosaurus (MNHN 1908-32-57): 1.27
Amotosaurus (SMNS 90601): <1.50
Azendohsaurus madagaskarensis (Flynn et al., 2010: fig. 13a): 1.59
Batrachotomus kupferzellensis (SMNS 52970): >2.58
Boreopricea (Tatarinov, 1978: 1b): 0.49
Cerritosaurus binsfeldi (CA s/n): 2.87
Chanaresuchus bonapartei (PVL 4586): 2.84
Chanaresuchus bonapartei (MCZ 4039): 2.68
"*Chasmatosaurus*" *yuani* (IVPP V4067): 5.37
Cuyosuchus (MCNAM PV 2669): >4.29
Erythrosuchus (BP/1/5207): 3.32
Euparkeria (SAM-PK-6047a): 3.17
Fugusuchus (Cheng, 1980: fig. 22): 3.19
Garjainia madiba (BP/1/5760): 3.76
Garjainia prima (PIN 2394/5): 3.77
Gephyrosaurus (Evans, 1980: fig. 14a): 1.81
Gracilisuchus (PULR 08): 3.64
Gracilisuchus (MCZ 4117): 2.23
Gualosuchus reigi (PULR 05): 2.90
Gualosuchus reigi (PVL 4576): 1.83
Herrerasaurus (PVSJ 407): 2.17
Heterodontosaurus (AM unnumbered): 0.85
Heterodontosaurus (SAM-PK-K337): 0.94
Jesairosaurus lehmani (ZAR 08): ca. 2.60
Lewisuchus (PULR 01): 3.64
Mesosuchus (SAM-PK-6536): 2.95
Nicrosaurus kapffi (NHMUK 42743): 4.91
Ornithosuchus longidens (NHMUK R3562): >3.42
Paleorhinus angustifrons (BSPG 1931 X 502): 4.75
Petrolacosaurus (Reisz, 1981: fig. 2): 0.62
Planocephalosaurus (Fraser, 1982: figs. 2a, 3b): 3.45-3.48
Prestosuchus chiniquensis (UFRGS-PV-0156-T): 3.07
Prolacerta (BP/1/5375): 2.64
Prolacerta (SAM-PK-K10797): 2.07

Prolacerta (Modesto and Sues, 2004: fig. 8a, BP/1/3575): 3.11
Proterochampsa barrionuevoi (Dilkes and Arcucci, 2012: fig. 5d): 1.91
"*Proterosuchus fergusi*" (SAM-PK-591): >1.35
Proterosuchus alexanderi (NMQR 1484): 4.07
Proterosuchus goweri (NMQR 880): ca. 4.32
Proterosuchus fergusi (RC 846): 4.51
Protorosaurus (USNM 442453, cast of cast of NMK S 180): 0.70
Rhynchosaurus articeps (NHMUK R1236): 2.15
Riojasuchus tenuisceps (PVL 3827): 2.27
Eohyosaurus wolvaardti (SAM-PK-K10159): 2.46
Sarmatosuchus (PIN 2865/68): >2.96
Shansisuchus shansisuchus (Young, 1964: fig. 12c): 2.48
Silesaurus opolensis (ZPAL AbIII/1930): >1.70
Smilosuchus gregorii (Camp, 1930: fig. 11b): 4.15
Smilosuchus adamanensis (Camp, 1930: fig. 11a): 3.45
Smilosuchus lithodendrorum (Camp, 1930: fig. 11c): 4.40
Tanystropheus longobardicus (PIMUZ T2189): 1.78
Tropidosuchus romeri (PVL 4606): 4.1
Turfanosuchus dabanensis (IVPP V3237): ca. 3.55
Vancleavea campi (USNM 508579 cast of GR 138): 2.37
Youngina (Gow, 1975: fig. 5): 2.43

Discretization by the cluster analysis: (1) 0.49-1.27; (2) 1.59-3.77; (3) 4.07-5.37. (5%=0.24).

(98) Jugal posterior process with a distinct lateroventral orientation with respect to the sagittal axis of the snout: absent (0); present (1) (Butler et al., in press).

(99) Jugal, distal half of the posterior process: tapering (0); subrectangular (1) (New character). The character is innaplicable if the posterior process of the jugal is forked by the quadratojugal.

(100) Jugal, posterior process forms entirely or almost entirely the ventral border of the infratemporal fenestra (it also applies in the lower temporal bar is incomplete): absent (0); present (1) (New character). This character is inapplicable in taxa that lack an infratemporal fenestra.

(101) Jugal, base of the posterior process with a semi-elliptical, ventral expansion in lateral view: absent (0); present (1) (reworded from Gower and Sennikov, 1997; Ezcurra et al., 2010: 97).

(102) Jugal, posterior process: lies dorsal to the anterior process of the quadratojugal (0); lies ventral to the anterior process of the quadratojugal (1); splits the anterior process of the quadratojugal (2); is splited by the anterior process of the quadratojugal (3) (Nesbitt, 2011: 71). This character is inapplicable to taxa that lack a quadratojugal or have an open lower temporal fenestra.

(103) Jugal, posterior termination of the posterior process: anterior to or at level with the posterior border of the infratemporal fenestra (0); posterior to the infratemporal fenestra (1) (Nesbitt, 2011: 72). This character is inapplicable in taxa that lack an infratemporal fenestra.

(104) Prefrontal, suture with the nasal: parasagittal, at least in its posterior third, or anterolateral (0); anteromedial (1) (Laurin, 1991: E1; Reisz et al., 2010: 33; modified from Ezcurra et al., 2014: 32).

(105) Prefrontal, subtriangular medial process: absent, nasal-frontal suture transversely broad (0); present, nasal-frontal suture strongly transversely reduced (1) (New character).

(106) Prefrontal, groove on the lateral surface of the main body opening into the orbital border: absent (0); present (1) (New character).

(107) Frontal, suture with the nasal: transverse (0); oblique, forming an angle of at least 60° with long axis of the skull and frontal(s) entering between both nasals (1); oblique, and nasal entering considerably between frontal(s) in a non-interdigitate suture (2) (deBraga and Rieppel, 1997; Müller, 2004: 154; Nesbitt, 2011: 43, in part; modified from Ezcurra et al., 2014: 128). This character is innaplicable if the nasal is received by a slot in the frontal.

(108) Frontal, orbital border in mature individuals: absent or anteroposteriorly short (0); anteroposteriorly long and forms most of the dorsal edge of the orbit (1) (Reisz and Dilkes, 2003: 13; Reisz et al., 2010: 26; Ezcurra et al., 2014: 25).

(109) Frontal, dorsal surface: flat or slightly depressed (0); with longitudinal ridge along midline (1) (Wu and Chatterjee, 1993; Nesbitt, 2011: 42).

(110) Frontal, suture with parietal: mostly transverse or parietals entering slightly between frontals on the median line, forming an obtuse-angled suture (0); parietals entering strongly between both frontals, forming an acute-angled suture (1); W-shaped suture (2) (Reisz and Dilkes, 2003: 4; Müller, 2004: 10; Reisz et al., 2010: 27; modified from Ezcurra et al., 2014: 26).

(111) Frontal, participates on the anteromedial corner of the supratemporal fossa: absent (0); present (1) (Rieppel et al., 1999; modified from Müller, 2004: 178; modified from Ezcurra et al., 2014: 129). This character is inapplicable in taxa that lack a supratemporal fossa or fenestra.

(112) Frontal, dorsal surface adjacent to sutures with the postfrontal (if present) and parietal: flat to slightly concave (0); possesses a longitudinal depression with deep pits (1) (Dilkes, 1998: 20; Ezcurra et al., 2014: 130).

(113) Frontal, longitudinal groove: longitudinally extended along most of the surface of the frontal (0); anterolaterally-to-posteromedially extended along the posterior half of the frontal (1) (Butler et al., in press). This character is innaplicable in taxa that lack a longitudinal depression with deep pits on the frontal.

(114) Frontal, ventral surface: hour-glass-shaped median longitudinal canal for the passage of the olfactory tract and olfactory bulb moulds on the anterior end of the bone (0); median longitudinal canal for the passage of the olfactory tract only slightly constricted, no olfactory bulb moulds and distinct semilunate

posteromedially-to-anterolaterally oriented ridge on the orbital roof, extending onto the prefrontal (1) (New character).

(115) Frontal, olfactory tract on the ventral surface of the frontal: maximum transverse constriction point well posterior to the moulds of the olfactory bulbs and posterolateral margin of the bulbs delimited by a low ridge (0); maximum transverse constriction of the olfactory tract immediately posterior to the moulds of the olfactory bulbs and posterolateral margin of the bulbs well delimited by a thick, tall ridge (1) (New character). This character is inapplicable in taxa that lack olfactory bulb moulds and constriction of the olfactory tract canal.

(116) Postfrontal: equivalent in size to postorbital (0); reduced to approximately less than half the dimensions of the postorbital (1); absent (2) (Benton, 1985; Nesbitt, 2011: 44, in part; Ezcurra et al, 2010: 10; Dilkes and Arcucci, 2012: 16, in part), ORDERED.

(117) Postfrontal, participation in the border of the supratemporal fenestra: absent (0); present (1) (modified from Laurin, 1991: A1, B3; Dilkes, 1998: 22; Müller, 2004: 89, 90; Reisz et al., 2010: 39; Ezcurra et al., 2014: 38, in part). Scored as inapplicable in taxa that lack postfrontal.

(118) Postfrontal, shape of dorsal surface: flat or slightly concave towards raised orbital rim (0); depression with deep pits (1) (Dilkes, 1998: 21; Ezcurra et al., 2014: 131). Scoring inapplicable in taxa that lack postfrontal.

(119) Postorbital-jugal, postorbital bar: composed both of the jugal and postorbital in nearly equal proportion (0); composed mostly by the postorbital (1) (Nesbitt, 2011: 67).

(120) Postorbital-squamosal, upper temporal bar: located approximately at level of the mid-height of the orbit (0); located approximately aligned to the dorsal border of the orbit (1) (New character).

(121) Postorbital-squamosal, contact: restricted to the dorsal margin of the elements (0); continues ventrally for much or most of the ventral length of the squamosal, but squamosal does not contact jugal (1); continues ventrally for much or most of the ventral length of the squamosal and squamosal contacts jugal (2) (modified from Nesbitt, 2011: 66), ORDERED.

(122) Postorbital, lateral boss adjacent to orbital margin: absent (0); present (1) (Reisz and Dilkes, 2003: 37; Reisz et al., 2010: 44; Ezcurra et al., 2014: 43).

(123) Postorbital, supratemporal fossa extending onto the ascending process: absent (0); present (1) (Gauthier, 1986; reworded from Nesbitt, 2011: 144). This character is not applicable in taxa that lack a supratemporal fossa medially to the supratemporal fenestra, or the supratemporal fenestra.

(124) Postorbital, posterior process extends close to or beyond the level of the posterior margin of the supratemporal fenestrae: absent (0); present (1) (Laurin, 1991: I1; Reisz and Dilkes, 2003: 23; Müller, 2004: 131; reworded from Reisz et al., 2010: 45; modified from Ezcurra et al., 2014: 44).

(125) Postorbital, extension of the ventral process: ends much higher than the ventral border of the orbit (0); ends close to or at the ventral border of the orbit (1) (Desojo et al., 2011: 112).

(126) Postorbital, ventral process in lateral view: continuously anteriorly curved or straight (0); distinctly anteriorly flexed (1) (New character).

(127) Postorbital, depression on the lateral surface of the ventral process: absent (0); present (1) (Wu et al., 2001; Ezcurra et al., 2010: 17; Dilkes and Arcucci, 2012: 24).

(128) Postorbital, anteriorly projecting, rounded spur on the anterior edge of the ventral process indicating the lower delimitation of the eye-ball: absent (0); present (1) (Benton and Clark, 1988; Rauhut, 2003).

(129) Squamosal, completely covering the quadrate in lateral view: present (0); absent (1) (New character).

(130) Squamosal, overhanging quadrate laterally: absent (0); present (1) (Benton, 2004; Ezcurra et al., 2010: 15). This character is inapplicable in taxa that the quadrate is completely covered by the squamosal in lateral view.

(131) Squamosal, anterior process forms most of the lateral border of the supratemporal fenestra: absent (0); present (1) (New character). This character is innaplicable in taxa lacking a supratemporal fenestra.

(132) Squamosal, anteroventral process: absent (0); present (1) (Reisz and Dilkes, 2003: 8; Reisz et al., 2010: 35; Nesbitt, 2011: 52; Ezcurra et al., 2014: 34, in part).

(133) Squamosal, transition between the anterior and ventral processes: sharp, posterodorsal border of the infratemporal fenestra with square outline (0); gentle, widely rounded posterodorsal border of the infratemporal fenestra (1) (New character). This character is inapplicable in taxa that lack a ventral process of the squamosal.

(134) Squamosal medial process: short, forming approximately half or less of the posterior border of the supratemporal fenestra (0); long, forming entirely or

almost entirely the posterior border of the supratemporal fenestra (1) (Butler et al., in press).

(135) Squamosal, posterior process length: does not extend posterior to the head of the quadrate (0); extends posterior to the head of the quadrate (1) (Nesbitt et al., 2009; Ezcurra et al., 2010: 157; Nesbitt, 2011: 48; Dilkes and Arcucci, 2012: 19). This character is inapplicable in taxa that the quadrate is completely covered by the squamosal in lateral view.

(136) Squamosal, posterior process shape: straight (0); ventrally curved (1) (Ezcurra et al., 2010: 165). This character is inapplicable in taxa that the quadrate is completely covered by the squamosal in lateral view.

(137) Squamosal, ventral process: present (0); absent (1) (New character).

(138) Squamosal, ventral process shape: anteroposteriorly broad and plate-like (0); anteroposteriorly narrow and strap-like (1) (Gauthier, 1986; Benton and Clark, 1988; Laurin, 1991: D2, E4; Reisz and Dilkes, 2003: 24; modified from Dilkes, 1998: 34 and Reisz et al., 2010: 37; Ezcurra et al., 2010: 151, in part; Nesbitt, 2011: 56, in part; modified from Ezcurra et al., 2014: 36, in part). This character is innaplicable in taxa that lack a ventral process in the squamosal.

(139) Squamosal, ventral process orientation: posteroventrally directed, vertical, or more than 45º from the vertical (0); anteroventrally directed at 45º or less (1) (modified from Ezcurra et al., 2010: 167). This character is inapplicable in taxa that lack a ventral process in the squamosal.

(140) Squamosal, ventral process forms more than half of the posterior border of the infratemporal fenestra: absent (0); present (1) (New character). This character is inapplicable in taxa that lack a ventral process in the squamosal.

(141) Squamosal, longitudinal ridge on the lateral surface of the ventral process: absent (0); present (1) (Nesbitt, 2011: 51). This character is inapplicable in taxa that lack a ventral process in the squamosal.

(142) Squamosal, posterodorsal portion with a supratemporal fossa: absent (0); present (1) (Nesbitt, 2011: 55). This character is innaplicable in taxa lacking a supratemporal fenestra.

(143) Quadratojugal: absent or fused to the quadrate (0); present (1) (modified from Reisz and Dilkes, 2003: 36; Reisz et al., 2010: 46; Ezcurra et al., 2014: 45).

(144) Quadratojugal, shape: L-shaped or strip-like bone (0); subtriangular (1) (Sereno, 1991; Nesbitt, 2011: 46). This character is inapplicable in taxa that lack a quadratojugal or infratemporal fenestra.

(145) Quadratojugal-jugal, infratemporal fossa marked by a sharp edge: absent (0); present (1) (Nesbitt et al., 2009; Nesbitt, 2011: 47, in part; Dilkes and Arcucci, 2012: 23 and 25). This character is inapplicable in taxa that lack a quadratojugal or an infratemporal fenestra.

(146) Quadratojugal, anterior process: absent, anteroventral margin of the bone rounded (0); incipient, short anterior prong on the anteroventral margin of the bone (1); distinctly present, in which the lower temporal bar is complete, but process finishes well posterior to the base of the posterior process of the jugal (2); distinctly present, in which the lower temporal bar is complete and participates in the posteroventral border of the infratemporal fenestra, and process finishes close to the base of the posterior process of the jugal (3) (Laurin, 1991: A2; Reisz and Dilkes, 2003: 3 and 9 and 11 in part; Reisz et al., 2010: 40; Ezcurra et al., 2010: 1, 18; Nesbitt, 2011: 70; Dilkes and Arcucci, 2012: 22, in part; modified from

Ezcurra et al., 2014: 39), ORDERED. This character is inapplicable in taxa that lack an infratemporal fenestra or quadratojugal.

(147) Quadratojugal, widely concave notch on the anterior margin of the ascending process: absent (0); present (1) (Dilkes and Arcucci, 2009; reworded from Dilkes and Arcucci, 2012: 26). This character is inapplicable in taxa that lack a quadratojugal, an anterior process of the quadratojugal or an infratemporal fenestra.

(148) Quadratojugal, posterior process: absent (0); present, but distal condyles of the quadrate broadly visible in lateral view (1); present, overlapping completely or almost completely the distal condyles of the quadrate in lateral view (2) (modified from Currie, 1995), ORDERED. This character is inapplicable in taxa that lack a quadratojugal.

(149) Supratemporal: broad element (0); slender, in parietal and squamosal trough (1); absent (2) (Dilkes, 1998; Reisz and Dilkes, 2003: 22; Müller, 2004: 21; Reisz et al., 2010: 52; Ezcurra et al., 2010: 13, in part; Nesbitt, 2011: 145, in part; Dilkes and Arcucci, 2012: 18, in part; Ezcurra et al., 2014: 51), ORDERED.

(150) Supratemporal, bifurcated medial border, in which a ventromedial process extends underneath the posterolateral process of the parietal: present (0); absent (1) (Butler et al., in press). This character is inapplicable in taxa lacking a supratemporal.

(151) Parietal, median contact between both parietals: suture present (0); fused with loss of suture (1) (Dilkes, 1998: 25; Nesbitt, 2011: 58; Ezcurra et al., 2014: 133).

(152) Parietal, extension over interorbital region: absent or marginal (0); present (1) (Reisz and Dilkes, 2003: 16; Reisz et al., 2010: 28; Ezcurra et al., 2014: 27).

(153) Parietal, separation of supratemporal fenestrae: broad, flat area (0); transversely thin, strip of flat bone (1); sagittal crest (2) (Laurin, 1991: G2; Müller, 2004: 13, in part; Reisz et al., 2010: 30; Nesbitt, 2011: 59; Ezcurra et al., 2014: 29, in part).

(154) Parietal, supratemporal fossa medial to the supratemporal fenestra: well exposed in dorsal view and mainly dorsally or dorsolaterally facing (0); poorly exposed in dorsal view and mainly laterally facing (1) (New character). This character is inapplicable in taxa that lack a supratemporal fossa.

(155) Parietal, pineal fossa on the median line of the dorsal surface: absent (0); present (1) (Parrish, 1992; Gower and Sennikov, 1997; Ezcurra et al., 2010: 100). The character should not be scored for early juveniles.

(156) Parietal, position of the pineal fossa: restricted to the parietal (0); extended along frontal and parietal (1) (New character). This character is innaplicable in taxa lacking a pineal fossa.

(157) Parietal, pineal foramen in dorsal view: considerably large (0); reduced to a small, circular pit (1); absent (2) (modified from Laurin, 1991: G3; Müller, 2004: 12; Reisz et al., 2010: 31; Ezcurra et al., 2010: 11, in part; Nesbitt, 2011: 63, in part; Ezcurra et al., 2014: 30).

(158) Parietal, position of the pineal foramen in dorsal view: completely enclosed by parietals in the anterior half of the bone (excluding posterolateral processes and anterior projections of the parietals if present) (0); completely enclosed by parietals close to mid-length or in the posterior half of the bone (excluding posterolateral processes and anterior projections of the parietals if present) (1); enclosed by both frontals and parietals (2) (Reisz and Dilkes, 2003: 17; Müller, 2004: 12; Reisz et al., 2010: 32; Ezcurra et al., 2010: 11, in part; modified from

from Ezcurra et al., 2014: 31). Scored as inapplicable in taxa that lack a pineal foramen.

(159) Parietal, distinct transverse emargination adjacent to the posterior margin of the bone in late ontogeny: absent (0); present (1) (Müller, 2004: 177; Ezcurra et al., 2014: 134).

(160) Parietal, posterolateral process: nearly vertical (0); ventrally inclined greater than 45º (1) (Heckert and Lucas, 1999; Nesbitt, 2011: 62).

(161) Parietal, posterolateral process with a strongly transversely convex dorsal margin elevated from the median line of the posterior margin of the skull roof: absent (0); present (1) (New character).

(162) Parietal, tuberosity on the posterior surface of the base of the posteroventral process: absent (0); present (1) (New character).

(163) Postparietal, size: sheet-like, both together not much narrower than the suproccipital (0); small, splint-like (1); absent as a separate ossification (2) (Laurin, 1991: E2, G5, J2; reworded from Reisz et al., 2010: 54; Ezcurra et al., 2010: 12, in part; Nesbitt, 2011: 146, in part; Dilkes and Arcucci, 2012: 17, in part; Ezcurra et al., 2014: 53), ORDERED.

(164) Postparietal, fusion between counterparts: absent (0); present (1) (New character). This character is inapplicable in taxa that lack postparietals. This character is inapplicable in taxa that lack a postparietal.

(165) Tabular: present (0); absent (1) (Laurin, 1991: E3; Reisz and Dilkes, 2003: 46; Reisz et al., 2010: 53; modified from Ezcurra et al., 2014: 52).

(166) Palpebral/s: absent (0); present (1) (Nesbitt, 2011: 147).

(167) Neomorphic bone (= septomaxilla of phytosaurs), separate ossification anterior to nasals and surrounded by the premaxilla on the dorsal surface of the snout: absent (0); present (1) (Sereno, 1991; reworded from Nesbitt, 2011: 150).

(168) Quadrate, shape: straight posteriorly (0); shallowly emarginated (1); with conch (2) (Laurin, 1991: E7, J3; Müller, 2004: 29 in part; Reisz et al., 2010: 55; Ezcurra et al., 2014: 54), ORDERED.

(169) Quadrate, angle between the posterior margins of the proximal and distal ends: 41-47º (0); 91-96º (1); 106-137º (2); 143-158º (3) (New character), CONTINUOUS, ORDERED. Inapplicable in taxa with a straight posterior margin of the quadrate.

Azendohsaurus madagaskarensis (UA 7-20-99-653): 108º
Batrachotomus kupferzellensis (SMNS 52970): 133º
Boreopricea (Tatarinov, 1978: fig. 1b): 118º
Cerritosaurus binsfeldi (CA s/n): 150º
Chanaresuchus bonapartei (MCZ 4039): 132º
Chanaresuchus bonapartei (PVL 4586): 136º
Chanaresuchus bonapartei (PVL 4575): 134º
"*Chasmatosaurus*" *yuani* (IVPP V4067): 155º
Doswellia kaltenbachi (USNM 214823): 117º
Erythrosuchus (BP/1/5207): 128º
Euparkeria (SAM-PK-6047a): 129º
Garjainia prima (PIN 2394/5): 136º
Gephyrosaurus (Evans, 1980: fig. 17d): 91º
Gracilisuchus (MCZ 4117): 158º
Gualosuchus (PVL 4576): 130º
Howesia (SAM-PK-5885): 108º
Herrerasaurus (PVSJ 407): 148º
Heterodontosaurus (SAM-PK-K337): 112º
Jesairosaurus lehmani (ZAR 06): 130º
Lewisuchus (PULR 01): 125º
Marasuchus lilloensis (Bonaparte, 1975: fig. 3): 110º
Mesosuchus (SAM-PK-6536): 116º
Nicrosaurus kapffi (SMNS 4379: Hungerbühler, 1998: fig. 2.10): 133º
Ornithosuchus (NHMUK R2409): ca. 140º
Paleorhinus angustifrons (BSPG 1931 X 502): 123º
Paliguana (AM 3585): 110º
Planocephalosaurus (Fraser, 1982: fig. 1a): 129º
Prestosuchus chiniquensis (UFRGS-PV-0156-T): 96º
Prolacerta (BP/1/471): 95º
Prolacerta (BP/1/2675): 126º

Prolacerta (BP/1/4504a): 107º
Prolacerta (BP/1/5375): 92º
Prolacerta (GHG 431): 114º
Prolacerta (SAM-PK-K10018): 136º
Prolacerta (SAM-PK-K10797): 106º
Proterosuchus alexanderi (NMQR 1484): 149º
Proterosuchus fergusi (BP/1/4016): 124º
Proterosuchus fergusi (SAM-PK-K140): 122º
Proterosuchus fergusi (SAM-PK-11208): 125º
Proterosuchus fergusi (RC 846): 126º
Proterosuchus fergusi (BSPG 1934 VIII 514): 120º
Proterosuchus fergusi (GHG 231): 126º
Proterosuchus goweri (NMQR 880): 149º
Protorosaurus (USNM 442453, cast of cast of NMK S 180): 137º
Riojasuchus tenuisceps (PVL 3827): 132º
Eohyosaurus wolvaardti (SAM-PK-K10159): 128º
Sarmatosuchus (PIN 2865/68): 121º
Shansisuchus shansisuchus (Young, 1964: fig. 13a): 130º
Silesaurus opolensis (ZPAL AbIII/1930): 133º
Smilosuchus gregorii (UCMP 27200): 123º
Smilosuchus adamanensis (Camp, 1930: fig. 11a): 135º
Smilosuchus lithodendrorum (Camp, 1930: fig. 11c): 137º
Tanystropheus longobardicus (Nosotti, 2007: fig. 43, PIMUZ T2484): 95º
Trilophosaurus buettneri (Spielmann et al., 2008: fig. 18a): 108º
Tropidosuchus romeri (PVL 4601): 126º
Tropidosuchus romeri (PVL 4606): 143º
Turfanosuchus dabanensis (IVPP V3237): 108º
Vancleavea campi (USNM 508579, cast of GR 138): 44º
Youngina (SAM-PK-K6205): 131º

Discretization by the cluster analysis: (1) 41-47º; (2) 91-97º; (3) 106-137º; (4) 143-158º. (5%=5.7).

(170) Quadrate, proximal head: does not have a sutural contact with the paraoccipital process of the opisthotic (0); has a sutural contact with the paraoccipital process of the opisthotic (1) (Nesbitt, 2011: 77).

(171) Quadrate, proximal head: partially exposed laterally (0); completely covered by the squamosal (1) (Sereno and Novas, 1993; Nesbitt, 2011: 78). This character is inapplicable in taxa that the quadrate is completely covered by the squamosal in lateral view.

(172) Quadrate, proximal end hooked posteriorly in lateral view: absent (0); present (1) (Nesbitt et al., 2013c).

(173) Quadrate, foramen on the medial wall of the quadrate foramen: absent (0); present (1) (New character).

(174) Vomer, shape: broad, plate-like bone, at least as transversely broad as the internal naris (0); stick-like bone, transversely narrower than the internal naris (1) (New character).

(175) Vomer, pair of vomeri in ventral view: subtriangular (0); hourglass-shaped, with a transverse constriction close to their mid-length, or slit-like (1) (New character).

(176) Vomer, contact with maxilla: absent (0); present (1) (Dilkes, 1998: 38; Müller, 2004: 92; Ezcurra et al., 2014: 135).

(177) Vomer, teeth: present, more than one row or no rows are distinguishable (0); present, mainly in a single row, but multiple teeth present immediately anterior to the contact with the pterygoid (1); present, single row along entire extension (2); absent (3) (Dilkes, 1998; modified from Ezcurra et al., 2010: 37; Dilkes and Arcucci, 2012: 37, in part), ORDERED.

(178) Palatine, transverse extension: narrow, subequal contribution of the palatine and pterygoid to or pterygoid main component of the palate posteriorly to the choanas (0); broad, the palatine is the main component of the palate posteriorly to the choanas and the anterior ramus of the pterygoid is splint-like (1) (taken from Liu et al., in press; new character for quantitative phylogenies). This character can be scored also from the shape of the anterior ramus of the pterygoid.

(179) Palatine, anterior processes forming the posterior border of the choana: subequal in anterior extension or anterolateral process longer (0); anteromedial process longer (1); single process (2) (New character).

(180) Palatine, teeth: present (0); absent (1) (Dilkes, 1998: 67; Müller, 2004: 99; Ezcurra et al., 2010: 38; Dilkes and Arcucci, 2012: 38; Ezcurra et al., 2014: 136).

(181) Pterygoids, contact with each other: present, anteriorly (0); absent, remain separate along their entire length (1) (Dilkes, 1998: 126; Ezcurra et al., 2010: 41; Ezcurra et al., 2014: 137).

(182) Pterygoid, anterior ramus (= palatal process): extends anterior to the anterior limit of the palatine (0); forms oblique suture with palatine but process ends before reaching anterior limit of palatine (1); forms transverse suture with palatine (2) (deBraga and Rieppel, 1997; Müller, 2004: 139; Ezcurra et al., 2014: 138).

(183) Pterygoid, anterior ramus (= palatal process) shape: transversely broad at its base, converging gradually with the transverse ramus (0); transversely narrow along its entire extension, converging in a right or acute angle with the transverse ramus, with the bone possessing an overall L-shape contour in ventral or dorsal view (1) (New character).

(184) Pterygoid, teeth on the ventral surface of the anterior ramus (= palatal process), excluding tiny palatal teeth if present: present in two distinct fields (= T2 and T3 of Welman, 1998) (0); present in three distinct fields (= T2, T3a and T3b) (1); present in three distinct fields (= T2a, T2b and T3) (2); present in one field that occupies most of the transverse width of the ramus (= T2 + T3) (3); present in only one posteromedially-to-anterolaterally field (= T2) (4); present in only one field adjacent to the medial margin of the ramus (= T3) (5); absent (6) (Dilkes, 1998: 68; Müller, 2004: 100; Ezcurra et al., 2010: 39, in part; Nesbitt, 2011: 175, in part; modified from Dilkes and Arcucci, 2012: 39; modified from Ezcurra et al., 2014: 139).

(185) Pterygoid, number of rows on palatal tooth series T2: more than two or do not dispose on distinct rows (0); two rows parallel to each other (1); single row (2)

(New character). This character is inapplicable if the tooth field T2 is subdivided in T2a and T2b.

(186) Pterygoid, number of rows on palatal tooth series T3: more than two or do not dispose on distinct rows (0); two parallel rows (1); single row (2) (New character). This character is inapplicable if the tooth field T3 is subdivided into T3a and T3b or it is absent.

(187) Pterygoid, most lateral row of teeth on the ventral surface of the anterior ramus (= palatal ramus) raised on a thick, posteromedially-to-anterolaterally oriented ridge: absent (0); present (1) (New character). This character is inapplicable if series T2 is absent.

(188) Pterygoid, a row of fang-like teeth on the medial edge of the anterior ramus (= palatal process) (= T4 of Welman, 1998): absent (0); present (1) (New character).

(189) Pterygoid, orientation of the lateral ramus: posterolaterally, forming an obtuse angle with the anterior ramus (0); laterally or anterolaterally, forming a right or acute angle with the anterior ramus (1) (New character).

(190) Pterygoid, lateral margin of the lateral ramus: posterolateral margin with an acute corner (0); posterolateral margin merges smoothly into anterolateral margin forming a smoothly convex lateral outline (1) (deBraga and Rieppel, 1997; Müller, 2004: 164; Ezcurra et al., 2014: 141).

(191) Pterygoid, teeth on lateral ramus: present, more than a single row or no rows recognizable (0); present, single row on the posterior edge (= T1 of Welman, 1998) (1); absent (2) (Laurin, 1991: E5; Reisz and Dilkes, 2003: 30; Müller, 2004: 163; Reisz et al., 2010: 49; Ezcurra et al., 2010: 40, in part; Nesbitt, 2011: 176: in part; Dilkes and Arcucci, 2012: 40, in part; modified from Ezcurra et al., 2014: 48), ORDERED.

(192) Ectopterygoid, body: arcs anteriorly (0); arcs anterodorsally (1) (Nesbitt, 2011: 87).

(193) Ectopterygoid, articulation with pterygoid: simple overlap between ectopterygoid and pterygoid (0); complex overlap between ectopterygoid and pterygoid (1) (Sereno and Novas, 1993; Dilkes, 1998: 142; Nesbitt, 2011: 84; Ezcurra et al., 2014: 142).

(194) Ectopterygoid, suture with pterygoid: transversely does not reach the posterolateral corner of the transverse flange (0); reaches the posterolateral corner of the transverse flange (1) (Dilkes, 1998: 42; Müller, 2004: 95; Ezcurra et al., 2010: 158; Nesbitt, 2011: 88, in part; modified from Ezcurra et al., 2014: 143).

(195) Ectopterygoid, contact with maxilla: absent (0); present (1) (Dilkes, 1998: 40; Müller, 2004: 94; Ezcurra et al., 2010: 19; Dilkes and Arcucci, 2012: 27; Ezcurra et al., 2014: 144).

(196) Ectopterigoid, posterior expansion in contact with jugal: absent (0); present (1) (Dilkes, 1998: 39; Ezcurra et al., 2014: 145).

(197) Supraoccipital, shape in occipital view: plate-like (0); inverted V-shaped (1) (Dilkes, 1995).

(198) Supraoccipital, participation in the dorsal border of the foramen magnum: absent (0); present (1) (Gower, 2002; Ezcurra et al., 2010: 152; Nesbitt, 2011: 126).

(199) Supraoccipital, posterior surface: smooth or with a low median ridge (0); with a prominent median, vertical peg (1) (Dilkes and Sues, 2009; Desojo et al., 2011: 94).

(200) Otoccipital, fusion between opisthotic and exoccipital: absent or partial (0); present (1) (Juul, 1994; Ezcurra et al., 2010: 22; Dilkes and Arcucci, 2012: 29)

(201) Opisthotic, contact between paraoccipital process and parietal immediately lateral to supraoccipital: absent (0); present (1) (Dilkes, 1998; Ezcurra et al., 2010: 31; Dilkes and Arcucci, 2012: 36).

(202) Opisthotic, paraoccipital processes orientation: extend laterally forming aproximatelly a 90° angle with the parasagittal plane (0); deflected posterolaterally at an angle of more than 20° from the transverse plane of the skull (1) (deBraga and Rieppel, 1997; Müller, 2004: 158; modified from Ezcurra et al., 2014: 146).

(203) Opisthotic, paraoccipital process attachment: ends freely (0); contacts supratemporal or quadrate and/or squamosal (Laurin, 1991: A4, E6; Reisz and Dilkes, 2003: 26; Reisz et al., 2010: 58; Ezcurra et al., 2014: 57).

(204) Opisthotic, fossa immediately lateral to the foramen magnum: absent (0); present (1) (taken from Gower and Sennikov, 1996; new character for quantitative phylogeny).

(205) Opisthotic, ventral ramus shape: club-shaped (0); pyramidal, with a tapering distal end (1); rod-like, with a cylindrical distal end and relatively thin (2); rod-like and very robust (3); plate-like (4) (Gower and Sennikov, 1996, 1997; Dilkes, 1998: 46; Ezcurra et al., 2010: 105 in part; modified from Ezcurra et al., 2014: 148).

(206) Opisthotic, ventral ramus: extends further laterally than the lateralmost edge of the exoccipital in posterior view (0); covered by the lateralmost edge of the exoccipital in posterior view (1) (Gower, 2002; Nesbitt, 2011: 111).

(207) Exoccipital, lateral surface: without subvertical crest (= metotic strut) (0); with clear crest (= metotic strut) present posterior to external foramina for hypoglossal nerve (CN XII) (1); with clear crest (= metotic strut) present anterior to the more

posterior external foramina for hypoglossal nerve (CN XII) (2) (Gower, 2002; Nesbitt, 2011: 114).

(208) Exoccipital, medial margin of their distal ends: no contact with its counterpart (0); contact with its counterpart to exclude basioccipital from the floor of the endocranial cavity (1) (Gower and Sennikov, 1996; Ezcurra et al., 2010: 32; Nesbitt, 2011: 115).

(209) Exoccipital, number of foramina for the hypoglossal nerve (CN XII): two (0); one (1) (Gower and Sennikov, 1996; Ezcurra et al., 2010: 23; Dilkes and Arcucci, 2012: 30).

(210) Pseudolagenar recess, between the ventral surface of the ventral ramus of the opisthotic and the basal tubera: present (0); absent (1) (Gower and Sennikov, 1996, 1997; Ezcurra et al., 2010: 111).

(211) Lagenar/cochlea recess: absent or short and strongly tapered (0); present and elongated and tubular (1) (Gower, 2002; Nesbitt, 2011: 118).

(212) Basioccipital-parasphenoid/parabasisphenoid, contact with each other in mature individuals: loose, overlapping suture (0); tightly sutured, sometimes by an interdigitated suture, or both bones fused with each other (1) (deBraga and Rieppel, 1997; Müller, 2004: 137; modified from Ezcurra et al., 2014: 151).

(213) Basioccipital-parasphenoid/parabasisphenoid, basal tubera: clearly separated from each other (0); partially connected to each other (1); medially expanded and nearly or completely connected (2) (modified from Nesbitt, 2011: 104) ORDERED.

(214) Basioccipital, position of the posterior margin of the occipital condyle: even with craniomandibular joint (0); anterior to craniomandibular joint (1); posterior

to craniomandibular joint (2) (Dilkes 1998: 51; Ezcurra et al., 2010: 27; Ezcurra et al., 2014: 157).

(215) Basioccipital, articular surface of the occipital condyle: concave (0); semi-spherical (1) (New character).

(216) Basioccipital, notochordal scar on the occipital surface of the occipital condyle: absent or developed as a small sub-circular pit (0); developed as a vertical furrow or a large sub-circular fossa that occupies approximately half of the height of the occipital surface of the condyle (1) (New character). This character is inapplicable in taxa with a concave articular surface of the occipital condyle.

(217) Basioccipital, occipital neck: present, distinctly separating the occipital condyle from the basioccipital body (0); absent or extremely short (1) (Ezcurra et al., 2010: 168).

(218) Basioccipital, shape of the basal tubera: rounded and anteroposteriorly elongated (0); bladelike and anteroposteriorly shortened (1) (Nesbitt, 2011: 106).

(219) Basioccipital, orientation of the basal tubera: lateroventral, basal tubera divergent from each other (0); ventral, basal tubera parallel with each other (1) (New character).

(220) Parasphenoid-basisphenoid/parabasisphenoid, exposure on the median line of the endocranial cavity floor: present (0); absent (1) (Gower and Sennikov 1996: 10, 1997; Ezcurra et al., 2010: 108).

(221) Parasphenoid/parabasisphenoid, orientation: horizontal (0); oblique, main axis posterodorsally-to-anteroventrally oriented (1) (Gower and Sennikov, 1996; Ezcurra et al., 2010: 28; Nesbitt, 2011: 97; Dilkes and Arcucci, 2012: 32).

(222) Parasphenoid/parabasisphenoid, posterodorsal portion: incompletely ossified (0); completely ossified (1) (New character).

(223) Parasphenoid/parabasisphenoid, intertuberal plate: absent (0); present and straight (1); present and arched anteriorly (2) (Gower and Sennikov, 1996, in part; Ezcurra et al., 2010: 29, in part; Nesbitt, 2011: 96; Dilkes and Arcucci, 2012: 33).

(224) Parasphenoid/parabasisphenoid, semilunar depression on the posterolateral surface of the bone: absent (0); present (1) (Gower and Sennikov, 1996; Ezcurra et al., 2010: 30; Nesbitt, 2011: 98; Dilkes and Arcucci, 2012: 34).This character is inapplicable in taxa that the posterodorsal portion of the parasphenoid/parabasisphenoid is not ossified, resulting in a non-ossified gap with the prootic.

(225) Parasphenoid/parabasisphenoid, recess (= median pharyngeal recess, = hemispherical sulcus, = hemispherical fontanelle): absent (0); present (1) (Nesbitt and Norell, 2006; Nesbitt, 2011: 100; Dilkes and Arcucci, 2012: 35).

(226) Parasphenoid/parabasisphenoid, position of the foramina for entrance of the cerebral branches of the internal carotid artery leading to the pituitary fossa: ventral (0); posterolateral (1); anterolateral (2) (Parrish, 1993; Dilkes, 1998: 45, in part; Ezcurra et al., 2010: 21, in part; Ezcurra et al., 2014: 150, in part; Nesbitt, 2011: 95; Dilkes and Arcucci, 2012: 28).

(227) Parasphenoid/parabasisphenoid, position of the foramina for the entrance of the cerebral branches of the internal carotids on the ventral surface of the bone: immediately medial or posteromedial to the base of the basipterygoid process (0); close to the suture between basioccipital and parabasisphenoid (1) (New character). This character is not applicable if foramina for the passage of the internal carotid artery open laterally.

(228) Parasphenoid/parabasisphenoid, shape of the cultriform process in lateral view: continuously tapering anteriorly, without dorsoventral constriction at its base (0); dorsoventrally compressed at its base (1) (Parrish, 1993; Juul, 1994; Gower and Sennikov, 1996, 1997: 13; Ezcurra et al., 2010: 110).

(229) Parasphenoid/parabasisphenoid, base of the cultriform process: relatively dorsoventrally short (0); tall, with the dorsal edge extending up between clinoid processes and ventral parts of the crista prootica (1) (Gower and Sennikov, 1996, 1997: 15; Ezcurra et al., 2010: 112).

(230) Basisphenoid/parabasisphenoid, anterior tympanic recess on the lateral side of the braincase: absent (0); present (1) (Makovicky and Sues, 1998; Rauhut, 2003; Nesbitt, 2011: 101).

(231) Basisphenoid/parabasisphenoid, parasphenoid crest: absent (0); present, thick crest running along the ventrolateral border of the basisphenoid body and converging between the bases of the basipterygoid processes (1) (New character).

(232) Basisphenoid/parabasisphenoid, pair of posterolaterally-to-anteromedially oriented thin ridges that extend onto the base of the ventral surface of the cultriform process: absent (0); present (1) (New character).

(233) Basisphenoid/parabasisphenoid, basipterygoid processes: short, with short articulating facets (0); long, with hemispherical articulating facets (1) (Reisz and Dilkes, 2003: 20; Müller, 2004: 96; Reisz et al., 2010: 51; modified from Ezcurra et al., 2014: 50).

(234) Basisphenoid/parabasisphenoid, orientation of basipterygoid processes: anteriorly or ventrally at their distal tips (0); posteriorly at their distal tips (1) (Dilkes, 1998; Ezcurra et al., 2010: 20; Nesbitt, 2011: 93).

(235) Prootic-supraoccipital, auricular recess: largely restricted to the prootic (0); extends onto internal surface of the supraoccipital (1) (Gower, 2002; Nesbitt, 2011: 133).

(236) Prootic-basisphenoid/parabasisphenoid, external foramina for passage of the abducens nerves (CN VI): only within basisphenoid (0); between prootic and basisphenoid (1); only within prootic (2) (Dilkes, 1998: 49, in part; Nesbitt, 2011: 122; Ezcurra et al., 2014: 156, in part).

(237) Prootic-basisphenoid/parabasisphenoid, external foramina for passage of the abducens nerves (CN VI): on the underside of a horizontal surface (0); on the anterior surface of the dorsum sella (1) (Gower, 2002; Nesbitt, 2011: 123).

(238) Prootic, extensive contact with parietal: absent (0); present (1) (deBraga and Rieppel, 1997; Müller, 2004: 160; Ezcurra et al., 2014: 155).

(239) Prootic, contact with its counterpart on the median line of the floor of the endocranial cavity: absent (0); present (1) (Gower and Sennikov, 1996: 9, 1997; Ezcurra et al., 2010: 107).

(240) Prootic, lateral surface: continuous and slightly convex (0); crista prootica present (1) (Gower and Sennikov, 1996, 1997: 8; Dilkes, 1998: 47; Ezcurra et al., 2010: 106 in part; Ezcurra et al., 2014: 153).

(241) Prootic, anterior inferior process: absent (0); present (1) (Dilkes, 1998: 48; Ezcurra et al., 2014: 154).

(242) Prootic, ridge on the lateral surface of the inferior anterior process ventral to the trigeminal foramen: present (0); absent (1) (Gower and Sennikov, 1996; Ezcurra et al., 2010: 24; Nesbitt, 2011: 94; Dilkes and Arcucci, 2012: 31). This character is scored as inapplicable in taxa that lack an anterior inferior process.

(243) Prootic, vestibule on the medial surface: incompletely ossified (0); almost completely ossified (1) (Gower, 2002; Nesbitt, 2011: 117).

(244) Laterosphenoid, ossification: absent (0); present (1) (Dilkes 1998: 50; Ezcurra et al., 2010: 26; Nesbitt, 2011: 92; Ezcurra et al., 2014: 149).

(245) Laterosphenoid, anterodorsal channel: absent (0); present (1) (Gower and Sennikov, 1996, 1997; Ezcurra et al., 2010: 109). Character inapplicable in taxa lacking an ossified laterosphenoid.

(246) Lower jaw, symphysis: formed largely by dentary (0), formed only by splenial (1) (Dilkes, 1998).

(247) Lower jaw, distinct dorsal process behind the alveolar margin: absent, with a slightly convex dorsal margin behind the alveolar portion (0); present, formed by a dorsally well-developed surangular (1); present, formed by a dorsally well-developed posterodorsal ramus of the dentary and sometimes a dorsally well-developed coronoid bone (2) (Rieppel et al., 1999; Müller, 2004: 36; Nesbitt, 2011: 158, in part; modified from Ezcurra et al., 2014: 158).

(248) Lower jaw, external mandibular fenestra: absent (0); present (1) (Dilkes, 1998: 76; Ezcurra et al., 2010: 42; Nesbitt, 2011: 138; Ezcurra et al., 2014: 166).

(249) Lower jaw, anteroposterior length of the external mandibular fenestra versus anteroposterior length of the dentary anterior to the fenestra: 0.07-0.36 (0); 0.44-0.53 (1); 0.71-0.88 (2) (Butler, 2005; modified from Nesbitt, 2011: 162; cf. Dilkes and Arcucci, 2012: 47), CONTINUOUS, ORDERED. This character is inapplicable in taxa that lack an external mandibular fenestra.

Batrachotomus kupferzellensis (Gower, 1999: fig. 18a): 0.36
Cerritosaurus binsfeldi (CA s/n): >0.39
Chanaresuchus bonapartei (PVL 4586): 0.51
Euparkeria (BP/1/5867): ca. 0.32
Erythrosuchus (BP/1/5207): 0.48
Garjainia prima (PIN 2394/5): ca. 0.20

Gracilisuchus (MCZ 4118): 0.21
Gualosuchus (PVL 4576): 0.71
Herrerasaurus (PVSJ 407): 0.53
Heterodontosaurus (SAM-PK-K1332): 0.16
Nicrosaurus kapffi (NHMUK 42744: Hungerbühler, 1998: fig. 2.26b): 0.51
Prestosuchus chiniquensis (UFRGS-PV-0152-T): 0.28
Proterochampsa nodosa (MCP 1694-Pv): 0.29
Proterosuchus alexanderi (NMQR 1484): 0.11
Proterosuchus fergusi (RC 59): 0.17
Proterosuchus fergusi (RC 846): 0.07
Proterosuchus fergusi (SAM-PK-11208): 0.13
Riojasuchus tenuisceps (PVL 3827): 0.88
Silesaurus opolensis (ZPAL AbIII/1930): 0.24
Smilosuchus gregorii (UCMP 27200): 0.44
Tropidosuchus romeri (PVL 4601): 0.47
Turfanosuchus dabanensis (IVPP V3237): ca. 0.20

Discretization by the cluster analysis: (1) 0.07-0.36; (2) 0.44-0.53; (3) 0.71-0.88. (5%=0.04).

(250) Lower jaw, Meckelian fossa orientation: dorsomedially (0); mostly dorsally due to greatly expanded prearticular resulting in a ventral border of the fossa situated dorsal to the half-height of the lower jaw at that level (1) (deBraga and Rieppel, 1997; Müller, 2004: 165; Ezcurra et al., 2014: 159).

(251) Dentary-splenial, mandibular symphysis length: positioned distally (0); present along one-third of the lower jaw (1) (Sereno, 1991; Nesbitt, 2011: 160).

(252) Dentary, minimum height of the bone versus length of the alveolar margin (including edentulous anterior end if present): 0.05-0.14 (0); 0.16-0.19 (1); 0.22-0.29 (2); 0.34-0.36 (3) (New character). CONTINUOUS, ORDERED.

Aetosauroides (PVL 2059): <0.09
Azendohsaurus madagaskarensis (FMNH PR 2751): 0.24
Batrachotomus (SMNS 80260): ca. 0.18
Chanaresuchus bonapartei (PVL 4575): 0.09
Chanaresuchus bonapartei (PVL 4586): 0.08
"*Chasmatosaurus ultimus*" (IVPP V2301): <0.14
"*Chasmatosaurus*" *yuani* (IVPP V36315): 0.16
Dimorphodon (NHMUK R41212-13): 0.11
Doswellia kaltenbachi (USNM 186989): 0.09
Euparkeria (SAM-PK-K8309): 0.16
Garjainia madiba (BP/1/7153): 0.26

Garjainia prima (PIN 2394/5-8, 5-9): ca. 0.22
Garjainia prima (PIN 951/30): 0.24
Gephyrosaurus (Evans, 1980: fig. 41a): 0.11
Gualosuchus (PVL 4576): 0.12
Herrerasaurus (MACN-Pv 18060): 0.19
Herrerasaurus (PVSJ 53): 0.24
Heterodontosaurus (AM unnumbered): 0.22
Heterodontosaurus (SAM-PK-K1332): 0.23
Nicrosaurus kapffi (NHMUK R42744): 0.05
Nundasuchus (Nesbitt et al., 2014: fig. 3a): <0.19
Paleorhinus sp. (ZPAL unnumbered): <0.04
Petrolacosaurus (Reisz, 1981: fig. 12): 0.10
Planocephalosaurus (Fraser, 1982: plate 70, fig. 2): 0.23
Prestosuchus chiniquensis (UFRGS-PV-0152-T): 0.22
Prolacerta (BP/1/471): 0.08
Proterosuchus alexanderi (NMQR 1484): 0.12
Proterosuchus fergusi (RC 846): 0.17
Proterosuchus fergusi (BSPG 1934 VIII 514): 0.13
Rhadinosuchus (BSPG AS XXV 50): 0.08
Riojasuchus (PVL 3827): 0.36
Sarmatosuchus (PIN 2865/68-11): 0.22
Shansisuchus shansisuchus (Young, 1964: fig. 17c): 0.22
Silesaurus (ZPAL Ab III/437/1): 0.16
Silesaurus (ZPAL AbIII/1930): 0.14
Smilosuchus gregorii (UCMP 27200): 0.08
Tanystropheus (Nosotti, 2007: fig. 49): 0.11
Trilophosaurus (Spielmann et al., 2008: fig. 28b): 0.29
Turfanosuchus dabanensis (IVPP V3237): 0.09
Uralosaurus (PIN 2973/1): ca. 0.27
Vancleavea campi (USNM 508579, cast of GR 138): 0.35

Discretization by the cluster analysis: (1) 0.05-0.14; (2) 0.16-0.19; (3) 0.22-0.29; (4) 0.34-0.36. (5%=0.015).

(253) Dentary, shape of the tooth bearing portion: mostly straight (0); distinctly dorsally curved for all or most of its anteroposterior length (1); ventrally curved or deflected (2) (modified from Nesbitt, 2011: 154, in part).

(254) Dentary, large foramina aligned in two distinct rows starting on the anteroventral corner of the bone: absent (0); present (1) (New character).

(255) Dentary, longitudinal groove approximately centred on the lateral surface: absent (0); present (1) (New character).

(256) Dentary, position of the Meckelian groove on the anterior half of the bone: dorsoventral centre of the dentary (0); restricted to the ventral border (1) (Nesbitt, 2011: 152).

(257) Dentary, dorsal margin of the anterior portion compared to the dorsal margin of the posterior portion: horizontal (in the same plane) (0); dorsally expanded (1) (modified from Nesbitt, 2011: 154).

(258) Dentary, posterodorsal extension posterior to the level of the alveolar margin: poorly developed (0); well developed, single process that may contribute to the anterodorsal border of the external mandibular fenestra (1); pair of processes (i.e. posterodorsal and posterocentral processes, in which the latter contributes to the anterodorsal border of the external mandibular fenestra) (2) (New character).

(259) Dentary, distal end of the posterocentral process (process that contributes to the anterodorsal border of the external mandibular fenestra): tapering (0); rounded (1) (New character). This character is considered inapplicable in taxa that lack a posterocentral process.

(260) Dentary, posteroventral process, which is a process adjacent to the ventral margin of the bone: absent (0); present, excluded from the border of the external mandibular fenestra (1); present, contributing to the border of the external mandibular fenestra (2) (reworded and modified from Nesbitt et al., 2009 and Nesbitt, 2011: 164).

(261) Posterior-most dentary teeth: on the anterior half of lower jaw (0); on the posterior half of lower jaw (1) (Langer and Schultz, 2000).

(262) Dentary, alveolar margin: present along entire length of the dentary (0); absent in the anterior portion (1) (Parrish, 1994; modified from Nesbitt, 2011: 166).

(263) Dentary, number of tooth rows: one (0); two (1); more than two (2) (Dilkes, 1998: 64; Ezcurra et al., 2014: 160), ORDERED.

(264) Dentary, occlusion with cranial teeth: single-sided overlap (0); flat occlusion (1); blade and groove (2) (Dilkes, 1998: 65; Ezcurra et al., 2014: 161).

(265) Surangular-angular, suture: even with lateral surface of mandible (0); elevated and separates dorsal concave area on surangular from concave area on angular (1) (Dilkes and Arcucci, 2012: 45).

(266) Surangular-angular, suture along the anterior half of the bones in lateral view: anteroposteriorly convex ventrally (0); anteroposteriorly concave ventrally (1) (New character).

(267) Surangular-articular, retroarticular process: absent (0); anteroposteriorly short, being poorly developed posteriorly to the glenoid fossa (1); anteroposteriorly long, extending considerably posterior to the glenoid fossa (2) (Laurin, 1991: B6, E10, J5; Reisz et al., 2010: 63; reworded from Ezcurra et al., 2014: 62; Ezcurra et al., 2015b: 109, in part), CONTINUOUS, ORDERED.

(268) Surangular-articular, retroarticular process: not upturned (0); upturned (1) (Dilkes 1998: 75; Müller, 2004: 101; Ezcurra et al., 2014: 167). This character is scored as inapplicable in taxa that lack a retroarticular process.

(269) Surangular, anterior extension: beyond coronoid eminence (0); posterior to reaching the anterior border of the coronoid eminence (1) (deBraga and Rieppel, 1997; Müller, 2004: 143; Ezcurra et al., 2014: 162).

(270) Surangular, lateral shelf: absent (0); present, low ridge near dorsal margin (1); present, presence of laterally or ventrolaterally projecting shelf with straight or gently convex lateral edge (2); present, presence of laterally projecting shelf with

strongly convex lateral edge (3) (deBraga and Rieppel, 1997; Müller, 2004: 166; Dilkes and Arcucci, 2012: 43, in part; Ezcurra et al., 2014: 163).

(271) Surangular, dorsal margin in lateral view: straight or gently convex (0); strongly convex (1) (Dilkes and Arcucci, 2012: 44).

(272) Surangular, anterior surangular foramen: absent (0); present (1) (Modesto and Sues, 2004: 145; Ezcurra et al., 2010: 43; Dilkes and Arcucci, 2012: 48; Ezcurra et al., 2014: 164).

(273) Surangular, posterior surangular foramen: absent (0); present (1) (Modesto and Sues, 2004: 146; Ezcurra et al., 2010: 44; Nesbitt, 2011: 163, in part; Dilkes and Arcucci, 2012: 49; Ezcurra et al., 2014: 165).

(274) Angular, lateral exposure in the lower jaw: wide (0); narrow (1) (Laurin, 1991: J4; Müller, 2004: 167; Reisz et al., 2010: 62; Ezcurra et al., 2014: 61).

(275) Angular, ventrolateral surface: continuous with lateral surface of angular (0); laterally projecting ridge present that separates lateral and ventral sides of the angular (1) (Dilkes and Arcucci, 2012: 46).

(276) Angular, posteroventral surface: ridged or keeled (0); transversely convex (1) (Reisz and Dilkes, 2003: 38; Reisz et al., 2010: 61; Ezcurra et al., 2014: 60; Ezcurra et al., 2015b: 110).

(277) Articular, foramen on the medial side: absent (0); present (1) (Nesbitt, 2011: 159).

(278) Articular, ventromedially directed process: absent (0); present (1) (Nesbitt, 2011: 157).

(279) Stape, shape: robust, with thick shaft (0); slender, rod-like shaft (1) (Laurin, 1991: E8; Reisz et al., 2010: 65; Ezcurra et al., 2014: 64).

(280) Stape, stapedial foramen piercing the columellar process: present (0); absent (1) (Laurin, 1991: E9; Reisz et al., 2010: 66; Ezcurra et al., 2014: 65).

(281) Teeth, posterior extent of mandibular and maxillary tooth rows: subequal (0); maxillary tooth extending further posteriorly (1) (Bennett, 1996; Ezcurra et al., 2010: 36).

(282) Teeth, tooth implantation: subthecodont (= protothecodont) (0); ankylothecodont (teeth fused to the bone at the base of the crown by bony ridges and the root can be discerned; there is tooth replacement) (1); pleurodont (2); acrodont (teeth fused to the bone in adults so that no root can be discerned; no tooth replacement) (3); thecodont (4) (Dilkes, 1998: 55; Laurin, 1991: G4; Müller, 2004: 38; modified from Reisz et al., 2010: 1; Ezcurra et al., 2010: 102 in part; Nesbitt, 2011: 174, in part; Ezcurra et al., 2014: 1).

(283) Teeth, maxillary and/or dentary tooth crowns: generally homodont (0); markedly heterodont (gross change in morphology) (1) (Parrish, 1993; Nesbitt, 2011: 167).

(284) Teeth, maxillary tooth crowns in labial view: all the tooth crowns possess a rather similar distal edge morphology along the entire alveolar margin (0); the distal edge of the posterior tooth crowns possess a distinct different morphology from those of the anterior tooth crowns, with the posterior edge usually convex (1) (modified from Sues et al., 2003; modified from Nesbitt, 2011: 15).

(285) Teeth, distal edge of the maxillary tooth crowns in labial view: concave along the entire alveolar margin (0); straight (1); convex in at least some anterior tooth crowns (2) (Reisz and Dilkes, 2003: 1; Reisz et al., 2010: 2; Ezcurra et al., 2010: 34, in part; Nesbitt, 2011: 173, in part; modified from Ezcurra et al., 2014: 2),

ORDERED. This character is not applicable to taxa with the posterior edge of the posterior tooth crowns different from those of the anterior tooth crowns.

(286) Teeth, serrations on the maxillary/dentary crowns: absent (0); distinctly present on the distal margin and usually apically restricted, low or absent on the mesial margin (1); present and distinct on both margins (2) (Dilkes, 1998; Reisz and Dilkes, 2003: 32; Reisz et al., 2010: 3; Ezcurra et al., 2010: 33, modified; Nesbitt, 2011: 168, in part, modified; Ezcurra et al., 2014: 3).

(287) Teeth, labiolingual compression of the marginal dentition: only distally or nowhere (0); present (1) (Dilkes, 1998; Reisz and Dilkes, 2003:1, 34; Reisz et al., 2010: 4; Ezcurra et al., 2010: 35; Ezcurra et al., 2014: 4).

(288) Teeth, multiple maxillary or dentary tooth crowns with longitudinal labial or lingual striations or grooves: absent (0); present (1) (New character).

(289) Teeth, multiple maxillary and dentary tooth crowns with extensive wear facets: absent (0); present (1) (Weishampel and Witmer, 1990; Nesbitt, 2011: 169)

(290) Teeth, multiple maxillary and dentary tooth crowns distinctly mesiodistally expanded above the root: absent (0); present (1) (Sereno, 1986; Nesbitt, 2011: 171).

(291) Hyoid apparatus, length and orientation of the ceratobranchial: short, directed to quadrate region (0); long, directed posteriorly and extending posteriorly beyond the quadrate condyles (1) (Reisz and Dilkes, 2003: 40; Reisz et al., 2010: 67; Ezcurra et al., 2014: 66).

(292) Cervical, dorsal, sacral and caudal vertebrae, notochordal canal piercing completely the centrum: present throughout ontogeny (0); absent in adults (1) (Laurin, 1991: F3; Reisz et al., 2010: 68; Ezcurra et al., 2014: 67).

(293) Cervical and dorsal vertebrae, at least one or more cervical or anterior dorsal with a parallelogram centra in lateral view, in which the anterior articular surface is situated higher than the posterior one: absent (0); present (1) (Bonaparte, 1975; Sereno, 1991; Novas, 1996; Ezcurra et al., 2010: 115; reworded from Ezcurra et al., 2014: 174).

(294) Cervical and dorsal vertebrae, one or more vertebrae with an accessory rib articular facet between the diapophysis and parapophysis in the cervico-dorsal transition: absent (0); present (1) (Parrish, 1992: 21).

(295) Cervical and dorsal vertebrae, anterior centrodiapophyseal lamina and/or paradiapophyseal lamina in posterior cervicals or anterior dorsals: absent (0); present (1) (Galton, 1990; Ezcurra et al., 2014: 180).

(296) Cervical and dorsal vertebrae, posterior centrodiapophyseal lamina in cervicals and/or anterior dorsals: absent (0); present (1) (Galton, 1990; Ezcurra et al., 2014: 181).

(297) Cervical and dorsal vertebrae, prezygodiapophyseal lamina in posterior cervicals and/or anterior dorsals: absent (0); present (1) (Bonaparte, 1986; Ezcurra et al., 2014: 182).

(298) Cervical and dorsal vertebrae, postzygodiapophyseal lamina in posterior cervicals and/or anterior dorsals: absent (0); present (1) (Coria and Salgado, 2000; Ezcurra et al., 2014: 183).

(299) Cervical and dorsal vertebrae, thick, mainly vertical tuberosity immediately below the transverse process, but both structures are not connected with each other, in posterior cervicals and anterior dorsals: absent (0); present (1) (New character).

(300) Cervical and dorsal vertebrae, fan-shaped neural spine in lateral view: absent (0); present (1) (New character).

(301) Cervical and dorsal vertebrae, gradual transverse expansion of the distal half of the neural spine: absent (0); present, but lacking distinct mammillary processes on the lateral surface of the neural spine (1); present, with distinct mammillary processes on the lateral surface of the neural spine (2) (modified from Laurin, 1991: H3; Reisz et al., 2010: 76; Ezcurra et al., 2014: 75).

(302) Cervical and dorsal vertebrae, spine table on the distal end of the postaxial neural spines (not mammillary process): absent (0); present in cervicals, but not in dorsals (1); present in dorsal, but not in cervicals (2); present in both cervicals and dorsals (3) (modified from Dilkes, 1998; Ezcurra et al., 2010: 49, in part; Nesbitt, 2011: 191 and 197, in part; Dilkes and Arcucci, 2012: 53 and 54).

(303) Cervical and dorsal vertebrae, distal surface of transverse expansion of the neural spine: convex (0); approximately flat (1) (modified from Dilkes, 1998; Ezcurra et al., 2010: 49, in part; Nesbitt, 2011: 197, in part). This character is innaplicable in taxa that lack a transverse expansion of the distal end of the neural spine or possess mammillary processes.

(304) Cervical and dorsal vertebrae, outline of the spine tables in dorsal view: sub-oval or sub-rectangular (0); sub-triangular or heart-shaped (1) (Gauthier, 1984; modified from Nesbitt, 2011: 191). Character inapplicable in taxa that lack spine tables.

(305) Cervical vertebrae, number of vertebrae in the neck: less than eight (0); eight to ten (1); more than ten (2) (modified from Gauthier, 1986), ORDERED.

(306) Cervical vertebrae, atlantal articulation facet in the axial intercentrum: saddle-shaped (0); concave with upturned lateral borders (1) (Gauthier, 1986; Nesbitt, 2011: 178).

(307) Cervical vertebrae, ventral surface of the centrum in anterior cervicals: transversely convex (0); with a low median longitudinal keel (1); with a median longitudinal keel that extends ventral to the centrum rim in at least one anterior cervical (2) (modified from Nesbitt, 2011: 190), ORDERED.

(308) Cervical vertebrae, height of neural spine of the axis: dorsoventrally tall (0); strongly dorsoventrally short (1) (New character).

(309) Cervical vertebrae, shape of the neural spine of the axis: expanded posterodorsally or the height of the anterior portion is equivalent to the posterior height (0); expanded anterodorsally (1) (modified from Nesbitt, 2011: 179).

(310) Cervical vertebrae, dorsal margin of the neural spine of the axis: dorsally convex (0); mostly straight or dorsally concave (1) (Makovicky and Sues, 1998).

(311) Cervical vertebrae, lengthes of the fourth or fifth cervical centra versus the heights of their anterior articular surfaces: 0.63-2.67 (0); 2.92-4.12 (1); 6.09-6.80 (2); 14.16-14.33 (3) (Laurin, 1991: H1; modified from Senter, 2004: 28, Müller, 2004: 174, and Reisz et al., 2010: 69; Ezcurra et al., 2010: 47 and 103, in part; Nesbitt, 2011: 181 and 183, in part; cf. Dilkes and Arcucci, 2012: 51; modified from Ezcurra et al., 2014: 68), CONTINUOUS, ORDERED.

Aetosauroides scagliai (PVL 2059): 1.35
Aetosauroides scagliai (PVL 2091): 0.91
Amotosaurus (SMNS 50830): 6.09-6.80
Azendohsaurus madagaskarensis (UA-7-20-99-653): 2.67-2.92
Batrachotomus kupferzellensis (SMNS 80288, middle cervical): 0.82
Batrachotomus kupferzellensis (SMNS cast of MHI 1895, fifth cervical): 0.97
Boreopricea (Benton and Allen, 1997: fig. 6a, PIN 3708/1): 1.92-2.00
Chanaresuchus bonapartei (MCZ 4037): 1.03
Chasmatosuchus rossicus (PIN 3200/217): 1.62
Doswellia kaltenbachi (Weems, 1980: table 3): 2.46

Eryrhtosuchus (BP/1/4680, Gower, 2003: table 1): 0.63-0.72
Eryrhtosuchus (SAM-PK-K3028, Gower, 2003: table 1): 0.70
Euparkeria (SAM-PK-5867): 1.45
Euparkeria (UMZC T692): 1.09-1.48
Gamosaurus (PIN 3361/13): 1.92
Garjainia madiba (BP/1/5360): 0.89
Garjainia prima (PIN 2394/5-12, 5-13): 1.07-1.11
Gephyrosaurus (Evans, 1980: fig. 4): 1.20
Gracilisuchus (PULR 08): 1.76-1.95
Gracilisuchus (MCZ 4118): 1.41
Gualosuchus (PVL 4576): 1.16-1.24
Herrerasaurus (MACN-Pv 18060): 2.23-2.63
Herrerasaurus (PVSJ 373): 1.82
Heterodontosaurus (SAM-PK-K1332): 1.50-1.53
Jaxtasuchus salomoni (SMNS 91083): 2.98
Jesairosaurus lehmani (ZAR 07): <2.00
Lewisuchus (PULR 01): 2.31
Macrocnemus bessanii (PIMUZ T4822): 3.70-4.12
Marasuchus lilloensis (PVL 3870): 1.56-1.87
Marasuchus lilloensis (PVL 3872): 1.51-2.00
Mesosuchus (SAM-PK-5882, fourth cervical): 2.01
Nundasuchus (Nesbitt et al., 2014: fig. 4c): 0.87
Petrolacosaurus (Reisz, 1981: fig. 14): 2.05-2.41
Prestosuchus chiniquensis (UFRGS-PV-0152-T): 1.39
Prolacerta (BP/1/2675): 3.29-3.50
Proterochampsa barrionuevoi (Dilkes and Arcucci, 2012: fig. 11c): 1.56
Proterosuchus alexanderi (NMQR 1484): 1.38-1.53
Proterosuchus fergusi (BP/1/3993): 1.73
Proterosuchus fergusi (SAM-PK-11208): 1.67
Protorosaurus (BSPG AS VII 1207; BSPG 1995 I 5, cast of WMsN P 47361): 3.12-3.24
Rhynchosaurus articeps (Benton, 1990: fig. 8b): 1.81
Riojasuchus tenuisceps (PVL 3827): 1.07-1.16
Sarmatosuchus (PIN 2865/68): 0.94-1.08
Shansisuchus kuyeheensis (Cheng, 1980: fig. 25): 0.85
Shansisuchus shansisuchus (Wang et al., 2013: fig. 4a): 0.77
Silesaurus opolensis (Piechowski and Dzik, 2010: fig. 4e, f): 2.29-2.50
Smilosuchus gregorii (Camp, 1930: plate III): 0.75-0.77
Tanystropheus longobardicus (PIMUZ T2818, fourth cervical): 14.25
Trilophosaurus buettneri (Spielmann et al., 2008: appendix 10): 1.84-2.50
Tropidosuchus romeri (PVL 4601): 2.07-2.15

Discretization by the cluster analysis: (1) 0.63-2.67; (2) 2.92-4.12; (3) 6.09-6.80; (4) 14.16-14.33. (5%=0.17). *Amotosaurus* and *Tanystropheus* were not included in the cluster analysis and the 5% variation calculation.

(312) Cervical vertebrae, diapophysis and parapophysis of anterior to middle cervical postaxial vertebrae: single facet or both situated on the same process (0); situated

on different processes and well separated (1); situated on different processes and nearly touching (2) (modified from Nesbitt, 2011: 184).

(313) Cervical vertebrae, longitudinal lamina or tuberosity extended posteriorly from the base of the transverse process in postaxial anterior and middle cervicals: absent or poorly developed, not well laterally developed (0); strongly developed, flaring laterally as a prominent and thick, wing-like shelf (1) (New character).

(314) Cervical vertebrae, posterior portion of the neural arch ventral to the postzygapophysis in postaxial cervicals: smooth (0); with a shallow, posterolaterally facing fossa (1) (New character).

(315) Cervical vertebrae, epipophysis in anterior postaxial cervicals: absent (0); present (1) (Gauthier, 1986; Nesbitt, 2011: 186).

(316) Cervical vertebrae, epipophysis in the sixth to last cervical vertebrae: absent (0); present (1) (Sereno et al., 1993; Nesbitt, 2011: 187). This character applies to the anterior dorsals in taxa with less than nine cervical vertebrae.

(317) Cervical vertebrae, excavation immediately lateral to the base of postaxial cervical neural spines: absent (0); shallow (1); represented by a deep pocket or pit (2) (modified from Reisz and Dilkes, 2003: 47; Reisz et al., 2010: 71; Ezcurra et al., 2014: 70), ORDERED.

(318) Cervical vertebrae, shape of the postaxial neural spines in lateral view: sub-triangular (0); rectangular (1) (Laurin, 1991: C1; Reisz et al., 2010: 72; Ezcurra et al., 2014: 71).

(319) Cervical vertebrae, distinct longitudinal lamina extending along the lateral surface of the centrum at mid-height in anterior and middle postaxial cervical vertebrae: absent (0); present (1) (Ezcurra et al., 2014: 169).

(320) Cervical vertebrae, longitudinal lamina connecting the prezygapophysis and postzygapophysis in the third cervical neural arch: absent (0); present (1) (Ezcurra et al., 2014: 170).

(321) Cervical vertebrae, shape of postaxial anterior cervical neural spines: tall, with height and length approximately equal or larger (0); long and low, with height lower than length (1) (Dilkes, 1998: 82; Ezcurra et al., 2014: 171).

(322) Cervical vertebrae, anterior and middle postaxial cervical neural spines with an anterior overhang: absent (0); present (1) (Senter, 2004: 30; Ezcurra et al., 2014: 172).

(323) Cervical vertebrae, position of the mammillary processes of the neural spines along the neck: present from the fourth presacral (0); present from the fifth presacral (1); present from the sixth or seventh presacral (2); present from the eighth or ninth presacral (3) (New character), ORDERED. Character inapplicable in taxa that lack mammillary processes.

(324) Cervical vertebrae, postaxial cervical intercentra: present (0); absent (1) (Dilkes, 1998: 79; Müller, 2004: 43; Ezcurra et al., 2010: 45; Nesbitt, 2011: 177, in part; Dilkes and Arcucci, 2012: 50, in part; Ezcurra et al., 2014: 168).

(325) Cervical and dorsal ribs, tuberculum in posterior cervical or anterior dorsal ribs: short (0); long and distinct (1) (Ezcurra et al., 2010: 92).

(326) Cervical and dorsal ribs, at least one rib of the cervico-dorsal transition with a thin lamina webbing tuberculum and capitulum: absent (0); present (1) (New character). This character is inapplicable in taxa with holocephalous ribs or poorly differnciated tuberculum and capitulum.

(327) Cervical ribs, shape: short, being less than two times the length of its respective vertebra, and tapering at a high angle to the neck (0); short, being less than two

times the length of its respective vertebra, and shaft parallel to the neck (1); very long, being two times the length of its respective vertebra, and parallel to the neck (2) (Gauthier, 1986; Benton and Clark, 1988; Juul, 1994; Dilkes, 1998: 77; Müller, 2004: 102; Ezcurra et al., 2010: 116 in part; Nesbitt, 2011: 196, in part; Ezcurra et al., 2014: 173).

(328) Cervical ribs, accessory process on anterolateral surface of anterior cervical ribs: absent (0); present (1) (Laurin, 1991: H4; Müller, 2004: 48; Reisz et al., 2010: 77; Ezcurra et al., 2014: 76).

(329) Dorsal vertebrae, length of the centrum versus height of the centrum in anterior dorsals: 0.45-1.10 (0); 1.18-2.00 (1); 2.19-2.74 (2) (Sereno, 1999; modified from Ezcurra et al., 2014: 176), CONTINUOUS, ORDERED.

Acerosodontosaurus (MNHN 1908-32-57): 1.71
Aenigmastropheus (UMZC T836): 1.35
Aetosauroides scagliai (PVL 2052): 0.92-0.93
Aetosauroides scagliai (PVL 2059): 1.28-1.34
Aetosauroides scagliai (PVL 2073): 1.10
Amotosaurus (SMNS 54784b): 1.93
Archeopelta arborensis (CPEZ-239a): 0.88
Azendohsaurus madagaskarensis (UA 8-26-98-250): 1.38
Azendohsaurus madagaskarensis (UA 8-26-98-265): 1.51
Batrachotomus kupferzellensis (SMNS 80309): 1.09
Batrachotomus kupferzellensis (SMNS 80296): 1.18
Boreopricea (PIN 3708/1): 1.56-1.67
Chalishevia (PIN 4188/98): 0.95
Chanaresuchus bonapartei (MCZ 4037): 1.04-1.19
Chanaresuchus bonapartei (PVL 4575): 1.60
"*Chasmatosaurus*" *yuani* (IVPP V2719): 1.27
Cuyosuchus (MCNAM PV 2669): 1.25-1.39
"*Dongusia colorata*" (PIN 268/2): 1.10
Doswellia kaltenbachi (Weems, 1980: table 4): 1.93-2.00
Eorasaurus olsoni (PIN 156/100): ca. 1.65
Erythrosuchus (NHMUK R3592 large, Gower, 2003: table 1): 0.55
Erythrosuchus (BP/1/4680, Gower, 2003: table 1): 0.48
Erythrosuchus (SAM-PK-Kun-no, Gower, 2003: table 1): 0.45-0.60
Euparkeria (UMZC T692): 1.39-1.89
Herrerasaurus (PVSJ 373): 1.02-1.30
Jaxtasuchus salomoni (SMNS 91352): 1.66
Jesairosaurus lehmani (ZAR 10): 2.45
Garjainia madiba (BP/1/7135): 1.08

Garjainia prima (PIN 2394/5-14, 5-16): 0.80-0.96
Gracilisuchus (MCZ 4118): 1.48-1.50
Gualosuchus (PVL 4576): 0.95
Lewisuchus (PULR 01): 1.73-1.85
Macrocnemus bessanii (PIMUZ T2472): 1.40-1.53
Macrocnemus bessanii (PIMUZ T4355): 1.52-1.62
Marasuchus lilloensis (PVL 3870): 1.90-2.19
Marasuchus lilloensis (PVL 3872): 1.32-1.71
Mesosuchus (SAM-PK-6046: second vertebra of the axial series): 1.26
Nicrosaurus kapffi (SMNS 12671): 0.89
Noteosuchus (Carroll, 1976: fig. 2, anteriormost preserved vertebra): 2.60
Petrolacosaurus (Reisz, 1981: fig. 15a, b): 1.76
Prestosuchus chiniquensis (UFRGS-PV-0152-T): 0.90-0.93
Prolacerta (BP/1/2675, first and second dorsals): 1.78
Proterosuchus alexanderi (NMQR 1484): 1.00
Proterosuchus fergusi (SAM-PK-K140): 0.96-1.01
Protorosaurus (BSPG 1995 I 5, cast of WMsN P 47361; ZMR MB R2172): 1.70-1.73
Pseudochampsa ischigualastensis (PVSJ 567): 1.40
Rhynchosaurus articeps (SHYMS 2): 1.83
Riojasuchus tenuisceps (PVL 3827): 0.84-0.92
SAM P41754: 1.23
Shansisuchus kuyeheensis (Cheng, 1980: fig. 26): 1.00-1.10
Shansisuchus shansisuchus (Wang et al., 2013: fig. 4a): 0.72
Shansisuchus shansisuchus (Young, 1964: fig. 23a-c): 0.68-0.84
Silesaurus opolensis (Piechowski and Dzik, 2010: fig. 6b, c): 1.50-1.67
Smilosuchus gregorii (UCMP 26699): 0.89-0.98
Tanystropheus longobardicus (PIMUZ T2817, first to third dorsal): 2.39-2.74
Tasmaniosaurus (UTGD 54655, anterior-middle dorsal): 1.29
Trilophosaurus buettneri (Spielmann et al., 2008: appendix 10, postaxial vertebrae 8-11): 1.23-1.79
Tropidosuchus romeri (PVL 4601, 12-13th presacral): 1.34-1.51
Vancleavea campi (Nesbitt et al., 2009: fig. 11b): 1.67
Youngina (BP/1/3859): 1.77-1.85

Discretization by the cluster analysis: (1) 0.45-1.10; (2) 1.18-2.00; (3) 2.19-2.74. (5%=0.11). In this case, the difference between ranges of the states (0) and (1) is lower than the variation of 5%, but it was discretized to capture the information provided by the anteroposteriorly short vertebrae of some erythrosuchids and suchians.

(330) Dorsal vertebrae, length of the centrum versus height of the centrum in posterior dorsals: 0.66-1.39 (0); 1.48-1.86 (1); 1.95-2.04 (2); 2.39-2.46 (3) (modified from Ezcurra et al., 2010: 87), CONTINUOUS, ORDERED.

Acerosodontosaurus (MNHN 1908-32-57): 1.50
Aetosauroides scagliai (PVL 2073, dorsals 14-16): 1.38-1.54

Amotosaurus (SMNS 54783): 1.60-1.95
Archeopelta arborensis (CPEZ-239a): 1.31
Azendohsaurus madagaskarensis (UA 8-29-98-325): 0.97
Azendohsaurus madagaskarensis (UA 7-20-99-654): 1.02
Azendohsaurus madagaskarensis (UA 8-27-98-270): 0.77
Batrachotomus kupferzellensis (SMNS 80300): 1.14
Chanaresuchus bonapartei (MCZ 4037): 1.23-1.35
"*Chasmatosaurus*" *yuani* (IVPP V2719): 1.28-1.31
Chasmatosuchus rossicus (PIN 3200/212): 1.16
Cuyosuchus (MCNAM PV 2669): 1.18-1.21
Dimorphodon (NHMUK R41212-13): 1.38-1.48
Doswellia kaltenbachi (Weems, 1980: table 4): 1.86-2.00
Erythrosuchus (NHMUK R3592 large, Gower, 2003: table 1): 0.83
Erythrosuchus (NHMUK R3592 small, Gower, 2003: table 1): 0.78
Erythrosuchus (SAM-PK-905, Gower, 2003: table 1): 0.79
Euparkeria (SAM-PK-6047A): 1.26-1.48
Garjainia madiba (BP/1/6232aj): 1.00
Garjainia prima (Huene, 1960: plate 13, figs. 13, 14): 1.00-1.23
Gephyrosaurus (Evans, 1980: fig. 7): 2.39
Gracilisuchus (MCZ 4118): 1.30-1.39
Gualosuchus (PVL 4576): 1.39-1.49
Herrerasaurus (MACN-Pv 18060): 0.85
Herrerasaurus (MCZ 7064): 0.66
Herrerasaurus (PVSJ 373): 0.85
Heterodontosaurus (AM unnumbered): 1.49-1.70
Howesia (SAM-PK-5886): 1.25-1.36
Jesairosaurus lehmani (ZAR 12): 1.84-2.04
Jesairosaurus lehmani (ZAR 14): 1.27
Lagerpeton chanarensis (PVL 4625): 1.54-2.42
Lewisuchus (PULR 01): 2.03
Macrocnemus bessanii (PIMUZ T4822): 2.46
Marasuchus lilloensis (PVL 3870): 1.59-1.77
Mesosuchus (SAM-PK-6046): 1.18-1.38
Noteosuchus (AM 3591, tenth vertebra of preserved series): 1.67
Nundasuchus (Nesbitt et al., 2014: fig. 4o): 0.83-0.91
Ornithosuchus (Walker, 1964: fig. 8j): 1.67
Petrolacosaurus (Reisz, 1981: fig. 15e): 1.32-1.33
Planocephalosaurus (Fraser and Walkden, 1984: fig. 7b): 1.96
Prestosuchus chiniquensis (UFRGS-PV-0152-T): 0.87-0.93
Prolacerta (BP/1/2675, 20th presacral): 1.70
Proterochampsa barrionuevoi (Trotteyn, 2010: fig. 5): 1.60
Protorosaurus (BSPG 1995 I 5, cast of WMsN P 47361): 1.38
Pseudochampsa ischigualastensis (PVSJ 567): 1.73
Riojasuchus tenuisceps (PVL 3827): 1.00-1.01
Sarmatosuchus (PIN 2865/68-23, 68-24): 0.87-0.94
Shansisuchus shansisuchus (Young, 1964: fig. 23a-c): 1.07-1.26
Silesaurus opolensis (Piechowski and Dzik, 2010: fig. 7e-f): 1.48-1.58
Smilosuchus gregorii (UCMP 26699): 0.85-0.94
Trilophosaurus buettneri (Spielmann et al., 2008: appendix 10, presacral vertebrae 21-24): 1.36-1.79

Tropidosuchus romeri (PVL 4601, 21th presacral): 1.72
Youngina (BP/1/3859): 1.73

Discretization by the cluster analysis: (1) 0.66-1.39; (2) 1.48-1.86; (3) 1.95-2.04; (4) 2.39-2.46. (5%=0.09).

(331) Dorsal vertebrae, ventral surface of middle and posterior centra: transversely convex (0); ridged, with slightly swollen sides (1); single keel (2); double keel (3) (Laurin, 1991: H2; Reisz and Dilkes, 2003: 44; Reisz et al., 2010: 74; Ezcurra et al., 2014: 73).

(332) Dorsal vertebrae, lateral fossa on the centrum below the neurocentral suture: absent (0); present, but not well-rimmed (1); present and well-rimmed (2) (Gauthier, 1986; modified from Ezcurra et al., 2010: 88), ORDERED.

(333) Dorsal vertebrae, subcentral foramen in the lateral surface of the centra: absent (0); present (1) (Ezcurra et al., 2014: 177).

(334) Dorsal vertebrae, diapophysis and parapophysis in anterior dorsals: close to the body of the midline (0); expanded on stalks (1) (Nesbitt, 2011: 199).

(335) Dorsal vertebrae, ratio between transverse width of diapophysis and length of the centrum in anterior dorsals: <0.70 (0); >0.75 (1) (Ezcurra et al., 2014: 178).

(336) Dorsal vertebrae, development of the transverse processes in middle and posterior dorsals: short (0); moderately long (1); extremely long, being considerably broader than their respective centra (2) (Laurin, 1991: F5; Reisz et al., 2010: 75; modified from Ezcurra et al., 2014: 74).

(337) Dorsal vertebrae, zygapophyses close to each other medially, respectively, in anterior-middle dorsals: absent, zygapophyses laterally divergent beyond the lateral margin of the centrum (0); present, zygapophyses mainly oriented in the parasagittal plane (1) (Ezcurra et al., 2014: 185).

(338) Dorsal vertebrae, hyposphene-hypantrum accessory intervertebral articulation: absent (0); present (1) (Gauthier, 1986; Juul, 1994; Ezcurra et al., 2010: 117; Nesbitt, 2011: 195).

(339) Dorsal vertebrae, zygosphene-zygantrum articulation: absent (0); present (1) (Rieppel et al., 1999; Müller, 2004: 44; Ezcurra et al., 2014: 186).

(340) Dorsal vertebrae, dorsally opening pit lateral to the base of the neural spine: absent (0); shallow (1); developed as a deep pit (2) (Dilkes 1998: 84; Müller, 2004: 103, in part; Ezcurra et al., 2010: 48; Dilkes and Arcucci, 2012: 52; Ezcurra et al., 2014: 184), ORDERED.

(341) Dorsal vertebrae, anterior and middle dorsal neural spines: sub-rectangular, with the anterior margin vertical, anterodorsally or slightly posterodorsally inclined (0); sub-triangular, with the anterior margin strongly posterodorsally oriented (1) (Ezcurra et al., 2014: 179).

(342) Dorsal vertebrae, position of middle dorsal neural spines: situated at mid-length between the zygapophyses (0); posteriorly displaced from mid-length between the zygapophyses (1) (Ezcurra et al., 2010: 90; Dilkes and Arcucci, 2012: 55).

(343) Dorsal vertebrae, position of the mammillary processes of the neural spines in the trunk: extend up to the tenth presacral (0); extend up to the eleventh presacral (1); extend up to the twelfth presacral (2); extend up to the thirteenth presacral (3); extend up to the sixteenth presacral (4) (New character), ORDERED. This character is inapplicable in taxa that lack mammillary processes.

(344) Dorsal vertebrae, intercentra: present (0); absent (1) (Rieppel et al., 1999; Müller, 2004: 42; Ezcurra et al., 2010: 46; Dilkes and Arcucci, 2012: 50, in part; Ezcurra et al., 2014: 175).

(345) Dorsal ribs, angle between heads and shaft in anterior dorsal ribs: close to 90º (0); low, gentle posteroventral bowing of the base of the shaft (1) (Dilkes and Sues, 2009; Ezcurra et al., 2010: 51; Dilkes and Arcucci, 2012: 57). This character is inapplicable in taxa that the cervical rib is directed in a high angle to the neck.

(346) Dorsal ribs, proximal end of middle dorsal ribs: dichocephalous (0); holocephalous (1) (Laurin, 1991: D3; Reisz et al., 2010: 79; Ezcurra et al., 2010: 52; Dilkes and Arcucci, 2012: 58; Ezcurra et al., 2014: 78).

(347) Sacral vertebrae-sacral ribs, ratio between the width of the neural arch + ribs of the first primordial sacral and the length of the neural arch across the zygapophyses: less than three times (0); three times or more (1) (Desojo et al., 2011: 95).

(348) Sacral vertebrae, number: two (0); three (1); four or more (2) (Reisz and Dilkes, 2003: 48; Reisz et al., 2010: 80; Nesbitt, 2011: 205, 206 and 207; Ezcurra et al., 2014: 79), ORDERED.

(349) Sacral ribs: almost entirely restricted to a single sacral vertebra (0); shared between two sacral vertebrae (1) (Nesbitt, 2011: 208).

(350) Sacral ribs, second rib: not bifurcate distally (0); bifurcate distally with posterior process pointed bluntly (1); bifurcate distally with posterior process truncated sharply (2) (Dilkes, 1998: 87; Müller, 2004: 105; Ezcurra et al., 2010: 53, in part; Nesbitt, 2011: 203, in part; Dilkes and Arcucci, 2012: 59, in part; Ezcurra et al., 2014: 187).

(351) Sacral and caudal vertebrae, transverse processes and ribs of sacral and/or anterior caudal vertebrae in mature individuals: not fused to each other (0); fused

to each other (1) (Rieppel et al., 1999; Müller, 2004: 50; Ezcurra et al., 2014: 188).

(352) Caudal vertebrae, length of the transverse process + rib versus length across zygapophyses in anterior caudal vertebrae: 0.29-0.41 (0); 0.62-1.18 (1); 1.51-1.68 (2); 2.20-2.72 (3) (Dilkes, 1998: 89; Dilkes and Arcucci, 2012: 56, in part; modified from Ezcurra et al., 2014: 191), CONTINUOUS, ORDERED.

Aetosauroides scagliai (PVL 2052): >1.12
Amotosaurus (SMNS 90600): ca. 1.62
Azendohsaurus madagaskarensis (UA 8-25-98-220): 0.67
Azendohsaurus madagaskarensis (UA 8-29-97-169): 0.62
Chanaresuchus bonapartei (PVL 4575): 1.68
"*Chasmatosaurus*" *yuani* (Young, 1936: fig. 6): 2.20
Cuyosuchus (MCNAM PV 2669): 0.85-1.08
Doswellia kaltenbachi (USNM 244214): 2.72
Gracilisuchus (PVL 4597): 0.72-0.81
Herrerasaurus (PVL 2566: first caudal): 1.04
Jesairosaurus lehmani (ZAR 09): 0.79
Macrocnemus bessanii (PIMUZ T4355): ca. 1.64
Marasuchus lilloensis (PVL 3871): ca. 0.65
Mesosuchus (SAM-PK-7416: first caudal): ca. 1.51
Noteosuchus (AM 3591, first and second caudal): 1.53-1.58
Petrolacosaurus (Reisz, 1981: fig. 15h, i): 2.46
Prolacerta (Gow, 1975: fig. 22, 1st-2nd caudals): 0.80-1.01
Proterosuchus alexanderi (NMQR 1484): 0.71-0.89
Protorosaurus (BSPG 1995 I 5, cast of WMsN P 47361): 0.35
Pseudochampsa ischigualastensis (PVSJ 567): 1.18
Silesaurus opolensis (Dzik, 2003: fig. 12a): 0.92
Tanystropheus longobardicus (Wild, 1973: fig. 59d): >0.92
Trilophosaurus buettneri (Spielmann et al., 2008: fig. 50): 0.74
Tropidosuchus romeri (PVL 4601, third caudal): ca. 1.45
Youngina (BP/1/3859): 1.15

Discretization by the cluster analysis: (1) 0.29-0.41; (2) 0.62-1.18; (3) 1.53-1.68; (4) 2.20-2.72. (5%=0.12).

(353) Caudal vertebrae, distal end of the transverse processes of anterior caudals: tapering or squared (0); anteroposteriorly expanded (1) (modified from Dilkes and Arcucci, 2009; modified from Dilkes and Arcucci, 2012: 56).

(354) Caudal vertebrae, neural spine height versus anteroposterior length at its base in anterior caudals: 0.84-2.21 (0); 2.36-2.65 (1); 2.92-3.05 (2); 3.42-3.54 (3) (Dilkes, 1998: 88; Müller, 2004: 106; modified from Ezcurra et al., 2014: 189), CONTINUOUS, ORDERED.

Aetosauroides scagliai (PVL 2073): >1.00
Azendohsaurus madagaskarensis (UA 8-29-97-169): 1.36
Batrachotomus kupferzellensis (SMNS 80337): 3.42
Chanaresuchus bonapartei (PVL 4575): 1.49
"*Chasmatosaurus*" *yuani* (IVPP V4067): 2.09
Cuyosuchus (MCNAM PV 2669): 1.94-2.46
Dorosuchus (PIN 1579/64): >1.15
Erythrosuchus (NHMUK R3592, Gower, 2003: table 1): >1.25
Euparkeria (SAM-PK-K8050): 2.21-2.36
Doswellia kaltenbachi (Weems, 1980: table 5): 0.47-0.53
Garjainia madiba (BP/1/5360): >1.30
Garjainia prima (Huene, 1960: plate 13, fig. 17): 1.94
Gracilisuchus (PVL 4597): 1.68
Heterodontosaurus (SAM-PK-K1332): 2.03
Howesia (SAM-PK-5886): 2.65-2.98
Jesairosaurus lehmani (ZAR 09): 1.61-1.74
Lagerpeton chanarensis (PVL 4625): 1.47
Lewisuchus (PULR 01): 0.84
Mesosuchus (SAM-PK-6046: second to fourth caudal): 2.99-3.54
Nicrosaurus kapffi (SMNS 12671): 2.98
Noteosuchus (AM 3591): 2.11
Ornithosuchus (Walker, 1964: fig. 8j, 2^{nd}-4^{th} caudal): 1.81-2.05
Ornithosuchus (Walker, 1964: fig. 8l, 1^{st}-2^{nd} caudal): 1.45-1.81
Petrolacosaurus (Reisz, 1981: fig. 15h): 1.22
Prestosuchus chiniquensis (UFRGS-PV-0152-T): 1.61
Prolacerta (Gow, 1975: fig. 22, 1^{st}-2^{nd} caudals): 1.51-1.54
Proterosuchus alexanderi (NMQR 1484): 1.52-1.96
Protorosaurus (BSPG 1995 I 5, cast of WMsN P 47361): 2.13
Rhynchosaurus articeps (BATGM M20a: caudals 1-5): 1.52-2.56
Silesaurus opolensis (Dzik, 2003: fig. 12a): 1.50
Smilosuchus gregorii (UCMP 26699): 2.44-2.53
Tanystropheus longobardicus (Wild, 1973: fig. 59a): 1.48
Trilophosaurus buettneri (Spielmann et al., 2008: fig. 50e, h): 1.60-2.14
Tropidosuchus romeri (PVL 4601, first and second caudals): 0.96-1.07
Turfanosuchus dabanensis (IVPP V3237): 1.91
Youngina (Currie, 1981: fig. 1d): 1.19

Discretization by the cluster analysis: (1) 0.84-2.21; (2) 2.36-2.65; (3) 2.92-3.05; (4) 3.42-3.54. (5%=0.13).

(355) Caudal vertebrae, accessory laminar process on the anterior face of the neural spine on middle caudals: absent (0); present (1) (Benton and Clark, 1988; Nesbitt, 2011: 210).

(356) Caudal vertebrae, prezygapophysis of posterior caudals: not elongated (0); elongated more than a quarter of the adjacent centrum (1) (Gauthier, 1986; Nesbitt, 2011: 211).

(357) Chevrons, distal anteroposterior width of anterior and middle haemal spines in lateral view: equivalent to proximal width (0); longer than proximal width (= paddle-like haemal spine) (1) (Dilkes, 1998: 91; Müller, 2004: 108; modified from Ezcurra et al., 2014: 192).

(358) Gastralia: present, forming an extensive ventral basket with closely packed elements (0); present, well separated (1); absent (2) (Dilkes, 1998: 92, in part; Müller, 2004: 109, in part; Nesbitt, 2011: 412; Ezcurra et al., 2014: 193, in part).

(359) Scapula-coracoid, both bones fuse with each other in mature individuals: present, without a complete line of suture (0); absent (1) (Rowe, 1989).

(360) Scapula-coracoid, notch on the anterior margin at level of the suture between both bones: absent (0); present (1) (Benton, 2004; Ezcurra et al., 2010: 57; Nesbitt, 2011: 221).

(361) Scapula-coracoid, glenoid fossa orientation: posterolateral (0); posteroventral (1) (Fraser et al., 2002; Nesbitt, 2011: 227).

(362) Scapula, total length of the scapula versus minimum anteroposterior width of the scapular blade: 1.23-2.61 (0); 3.25-6.73 (1); 7.92-10.45 (2) (Benton, 1985; modified from Ezcurra et al., 2010: 58; cf. Nesbitt, 2011: 218; cf. Dilkes and Arcucci, 2012: 63), CONTINUOUS, ORDERED.

Aetosauroides scagliai (PVL 2073): 5.02
Amotosaurus (SMNS 50830): 1.46

Amotosaurus (SMNS 54810): 1.33
Azendohsaurus madagaskarensis (UA 9-8-98-501): 4.88
Batrachotomus kupferzellensis (SMNS 80271): 6.36
Chanaresuchus bonapartei (PVL 4575): 7.92
Chanaresuchus bonapartei (MCZ 4035): 8.97
"*Chasmatosaurus*" *yuani* (IVPP V2719): ca. 2.04
Dimorphodon (NHMUK R41212-13): ca. 8.80
Erythrosuchus (SAM-PK-905): 5.60
Erythrosuchus (NHMUK R3592): 5.90
Euparkeria (SAM-PK-5867): 4.44
Garjainia madiba (BP/1/7152): 4.45
Garjainia prima (PIN 2394/5-32, 5-33): 3.73-3.74
Garjainia prima (Huene, 1960: table 14, fig. 10): 4.17
Gracilisuchus (PULR 08): >5.62
Gualosuchus (PVL 4576): >6.46
Guchengosuchus (Peng, 1991: fig. 7): 5.28
Herrerasaurus (PVSJ 053): 8.64
Heterodontosaurus (SAM-PK-K1332): 9.79
Jesairosaurus lehmani (ZAR 09): > 7.00
Lewisuchus (PULR 01): ca. 9.10
Macrocnemus bessanii (PIMUZ T4355): 1.47
Mesosuchus (SAM-PK-6536): >3.56
Nundasuchus (Nesbitt et al., 2014: table 1): 5.32
Ornithosuchus (Walker, 1964: fig. 9f): 8.76
Planocephalosaurus (Fraser and Walkden, 1984: fig. 13a): ca. 5.10
Prestosuchus chiniquensis (UFRGS-PV-0629-T): 4.87
Prolacerta (BP/1/2675): ca. 1.79
Proterosuchus alexanderi (NMQR 1484): 2.13
Protorosaurus (BSPG 1995 I 5, cast of WMsN P 47361): 2.61
Rhynchosaurus articeps (SHYMS 2): 4.69
Sarmatosuchus (PIN 2865/68): 2.10
Shansisuchus kuyeheensis (Cheng, 1980: fig. 27): 5.47
Shansisuchus shansisuchus (Young, 1964: fig. 26a): 6.08
Shansisuchus shansisuchus (Young, 1964: fig. 26b): 6.00
Shansisuchus shansisuchus (Young, 1964: fig. 26b): 5.81
Shansisuchus shansisuchus (Young, 1964: fig. 26d): 5.96
Silesaurus opolensis (Dzik, 2003: fig. 9a): 10.45
Smilosuchus gregorii (UCMP 26699): 6.29
Tanystropheus longobardicus (Nosotti, 2007: fig 20): 1.40
Tanystropheus longobardicus (Wild, 1973: plate 17): 1.23
Trilophosaurus buettneri (Spielmann et al., 2008: 65b): >6.15
Tropidosuchus romeri (PVL 4601): 6.73
Vancleavea campi (Nesbitt et al., 2009: fig. 12): 4.46
Youngina (BP/1/3859): 3.25

Discretization by the cluster analysis: (1) 1.23-2.61; (2) 3.25-6.73; (3) 7.92-10.45. (5%=0.46).

(363) Scapula, large fenestra between scapula and coracoid immediately anterior to the glenoid region: absent (0); present (1) (New character).

(364) Scapula, anterior margin of the scapular blade in lateral view: straight or convex along entire length (0); distinctly concave (1) (deBraga and Reisz, 1995: 27; Gower and Sennikov, 1997; Reisz et al., 2010: 86; Ezcurra et al., 2010: 104; Nesbitt, 2011: 217; modified from Ezcurra et al., 2014: 85).

(365) Scapula, supraglenoid foramen: absent (0); present (1) (Reisz and Dilkes, 2003: 29; Reisz et al., 2010: 87; Ezcurra et al., 2014: 86).

(366) Scapula, teardrop-shaped tuber on the posterior edge, just dorsal of the glenoid fossa: absent (0); present (1) (Nesbitt, 2011: 219).

(367) Scapula, diagonal ridge adjacent to the anterior margin on the medial surface of the scapular blade: absent (0); present (1) (New character).

(368) Scapula, acromion process: in about the same plane as the ventral edge of the scapula (0); distinctly raised above the ventral edge of the scapula (1) (Nesbitt, 2011: 220).

(369) Scapula, acromion process: gently raised from the anterior margin of the scapular blade (0); sharply raised in an angle close to 90º from the anterior margin of the scapular blade (1) (Novas, 1992).

(370) Coracoid, anterior border in lateral view: rounded (0); distinctly hooked (1) (Sereno, 1991; Nesbitt, 2011: 226).

(371) Coracoid, posterior border in lateral view: unexpanded posteriorly (0); expanded posteriorly - the entire border, not only the posteroventral region as is the case in the postglenoid process - and, as a result, the scapular girdle acquires an L-shape in lateral view (1) (New character).

(372) Coracoid, subglenoid lip: as developed as or less developed than the supraglenoid lip on the scapula (0); more posteriorly extended than the supraglenoid lip on the scapula (1) (New character).

(373) Coracoid, biceps process on the lateral surface: absent or small (0); large (1) (Laurin, 1991: H5; Reisz et al., 2010: 88; Nesbitt, 2011: 225; Ezcurra et al., 2014: 87).

(374) Coracoid, postglenoid process separated from the glenoid fossa by a notch: absent (0); present (1) (Clark et al., 2004; modified from Nesbitt, 2011: 222; modified from Dilkes and Arcucci, 2012: 64).

(375) Coracoid, postglenoid process shape: rounded posterior margin in lateral view (0); tapering posterior margin in lateral view (1) (New character). This character is innaplicable in taxa that lack a postglenoid process.

(376) Cleithrum: present (0); absent (1) (Laurin, 1991: E11; Reisz et al., 2010: 85; Ezcurra et al., 2014: 84).

(377) Interclavicle: present (0); absent (1) (Gauthier, 1986; Benton, 2004; Ezcurra et al., 2010: 54, in part; Nesbitt, 2011: 214).

(378) Interclavicle, anterior process: present (0); absent (1) (Laurin, 1991: J6; deBraga and Reisz, 1995: 26; Müller, 2004: 55; Reisz et al., 2010: 82; Ezcurra et al., 2010: 54, in part; Dilkes and Arcucci, 2012: 61, in part; Ezcurra et al., 2014: 81).

(379) Interclavicle, anterior margin with a median notch: absent (0); present (1) (modified from Dilkes, 1998: 97; Müller, 2004: 111; Ezcurra et al., 2010: 55; Dilkes and Arcucci, 2012: 61, in part; Ezcurra et al., 2014: 195).

(380) Interclavicle, lateral processes: well developed (0); reduced or absent (1) (modified from Gauthier, 1984; modified from Nesbitt, 2011: 215; cf. Dilkes and Arcucci, 2012: 60).

(381) Interclavicle, webbed between lateral and posterior processes: present, proximal half of the bone sub-triangular or diamond-shaped (0); absent, rather sharp angles between processes (1) (Laurin, 1991: J6; Reisz et al., 2010: 83; Ezcurra et al., 2014: 82).

(382) Interclavicle, transverse width at mid-length of the posterior process versus the length of the posterior process: 0.07-0.14 (0); 0.20-0.27 (1) (Laurin, 1991: J6; Reisz et al., 2010: 84; modified from Ezcurra et al., 2014: 83), CONTINUOUS, ORDERED.

Aetosauroides scagliai (PVL 2073): 0.11
Azendohsaurus madagaskarensis (UA 8-27-98-271): 0.08
"*Chasmatosaurus*" *yuani* (IVPP V4067): 0.22
Doswellia kaltenbachi (USNM 244214): 0.14
Euparkeria (SAM-PK-5867): <0.09
Garjainia prima (PIN 2394/5-34): 0.21
Jesairosaurus lehmani (ZAR 09): 0.10
Macrocnemus bessanii (PIMUZ T4355): 0.09
Mesosuchus (SAM-PK-6536): 0.10
Nicrosaurus kapffi (SMNS 5705/1): 0.27
Petrolacosaurus (Reisz, 1981: fig. 17b): 0.11
Prestosuchus chiniquensis (UFRGS-PV-0152-T): 0.20
Prolacerta (BP/1/2675): 0.08
Proterosuchus alexanderi (NMQR 1484): 0.25
Proterosuchus fergusi (GHG 363): 0.24
Protorosaurus (Gottmann-Quesada and Sander, 2009: fig. 19): <0.17
Rhynchosaurus articeps (NHMUK R1239): 0.11
Tasmaniosaurus (UTGD 54655): 0.07
Trilophosaurus buettneri (Gregory, 1945: fig. 8b): 0.13
Youngina (SAM-PK-K7710): 0.13

Discretization by the cluster analysis: (1) 0.07-0.14; (2) 0.20-0.27 (5%=0.01).

(383) Interclavicle, posterior ramus: little change in width along entire length (0); gradual transverse expansion present (1) (Dilkes, 1998: 98; Müller, 2004: 112; Ezcurra et al., 2010: 56; Dilkes and Arcucci, 2012: 62; Ezcurra et al., 2014: 196).

(384) Clavicle, articulation with interclavicle: on the anteroventral surface of the interclavicle (0); on the anterodorsal surface of the interclavicle (1); into a deep

socket (2) (Rieppel et al., 1999; Müller, 2004: 53; reworded and modified from from Ezcurra et al., 2014: 194).

(385) Sternum: not mineralized (0); mineralized (bone or calcified cartilage) (1) (Laurin, 1991: A5; Müller, 2004: 81; Reisz et al., 2010: 81; Ezcurra et al., 2014: 80). Scored as missing data in taxa without sufficiently articulated specimens.

(386) Forelimb-hindlimb, length ratio: >0.55 (0); <0.55 (1) (modified from Gauthier, 1984; Nesbitt, 2011: 212).

(387) Humerus, torsion between proximal and distal ends: approximately 45° or more (0); 35° or less (1) (Müller, 2004: 145; modified from Ezcurra et al., 2014: 197).

(388) Humerus, transverse width of the proximal end versus total length of the bone in mature individuals: 0.20-0.41 (0); 0.46-0.54 (1); 0.57-0.70 (2) (modified from Nesbitt, 2007; modified from Nesbitt, 2011: 236), CONTINUOUS, ORDERED.

Aetosauroides scagliai (PVL 2073): 0.34
Aetosauroides scagliai (PVL 2091): 0.58
Amotosaurus (SMNS 54783): 0.22
Azendohsaurus madagaskarensis (UA 7-13-99-578): 0.53
Azendohsaurus madagaskarensis (UA 8-29-97-151): 0.53
Batrachotomus kupferzellensis (SMNS 80276): 0.41
Chanaresuchus bonapartei (PVL 4575): 0.38
"*Chasmatosaurus*" *yuani* (IVPP V2719): 0.48
"*Chasmatosaurus*" *yuani* (IVPP V4067): 0.50
Cuyosuchus (MCNAM PV 2669): 0.41
Dimorphodon (Padian, 1983: table 1, YPM 350): 0.37
Erythrosuchus (SAM-PK-905): 0.70
Euparkeria (SAM-PK-5867): 0.37
Euparkeria (SAM-PK-7696): 0.46
Euparkeria (SAM-PK-8050): 0.38
Euparkeria (SAM-PK-13666): 0.35
Garjainia madiba (BP/1/5360): 0.63
Garjainia prima (PIN, *G. triplicostata*): 0.57
Gracilisuchus (CRILAR #079-2011): 0.23
Gualosuchus (PVL 4576): 0.35
Herrerasaurus (MACN-PV 18060): 0.29
Heterodontosaurus (SAM-PK-K1332): 0.25
Jaxtasuchus salomoni (SMNS 91002): 0.31
Jesairosaurus lehmani (ZAR 09): 0.39
Koilamasuchus (MACN-Pv 18119): >0.41
Lewisuchus (PULR 01): ca. 0.28

Macrocnemus bessanii (PIMUZ T2472): 0.21
Marasuchus lilloensis (PVL 3871): >0.18
Nicrosaurus kapffi (SMNS unnumbered): 0.38
Nundasuchus (Nesbitt et al., 2014: table 1): 0.54
Petrolacosaurus (Reiz, 1981: 43): 0.27
Prestosuchus chiniquensis (UFRGS-PV-0152-T): 0.38
Prolacerta (BP/1/2675): 0.32
Proterochampsa barrionuevoi (Trotteyn, 2011: table 2): 0.41
Protorosaurus (Gottmann-Quesada and Sander, 2009: appendix I, FG 2666/2004b): 0.20
Protorosaurus (Gottmann-Quesada and Sander, 2009: appendix I, WMsN P 47361): 0.33
Rhynchosaurus articeps (NHMUK R1239): 0.38
Riojasuchus tenuisceps (PVL 3826): 0.46
Shansisuchus kuyeheensis (Cheng, 1980: fig. 28): 0.57
Shansisuchus shansisuchus (Young, 1964: table 7, 27a): 0.60
Shansisuchus shansisuchus (Young, 1964: table 7, 27b): 0.60
Shansisuchus shansisuchus (Young, 1964: table 7, 27c): 0.58
Shansisuchus shansisuchus (Young, 1964: table 7, 27d): 0.62
Silesaurus opolensis (Dzik, 2003: fig. 9b): 0.22
Smilosuchus gregorii (USNM 18313): 0.34
Tanystropheus longobardicus (PIMUZ T2817): 0.20
Tanystropheus longobardicus (Nosotti, 2007: fig. 7): 0.20
Trilophosaurus buettneri (Spielmann et al., 2008: fig. 66a): 0.31
Tropidosuchus romeri (PVL 4601): 0.24
Turfanosuchus dabanensis (IVPP V3237): 0.39
Vancleavea campi (Parker and Barton, 2008: fig. 8.4): 0.28
Youngina (BP/1/3859): 0.32

Discretization by the cluster analysis: (1) 0.20-0.41; (2) 0.46-0.54; (3) 0.57-0.70. (5%=0.025).

(389) Humerus, proximal articular surface in proximal view: subrectangular to crescent-shape (0); sub-oval (1) (modified from Bonaparte, 1991).

(390) Humerus, proximal articular surface: continuous with the deltopectoral crest (0); separated by a gap from the deltopectoral crest (1) (Nesbitt, 2011: 233).

(391) Humerus, proximal end in anterior view: approximately symmetric (0); medially expanded, being asymmetric (1) (New character).

(392) Humerus, internal tuberosity distinctly separated from the proximal articular surface: absent (0); present (1) (New character).

(393) Humerus, shape of the deltopectoral crest in lateral view: rounded or subtriangular (0); subrectangular or trapezoidal (1) (modified from Sereno, 1991; Juul, 1994; Ezcurra et al., 2010: 118).

(394) Humerus, length of the deltopectoral crest versus total length of the bone in mature individuals: 0.16-0.18 (0); 0.24-0.28 (1); 0.30-0.34 (2); 0.36-0.38 (3); 0.40-0.43 (4); 0.46-0.49 (5); 0.52-0.55 (6) (modified from Benton, 1990; Juul, 1994; modified from Ezcurra et al., 2010: 119; modified from Nesbitt, 2011: 230), CONTINUOUS, ORDERED.

Aetosauroides scagliai (PVL 2073): 0.33
Aetosauroides scagliai (PVL 2091): 0.30
Azendohsaurus madagaskarensis (UA 8-29-97-151): 0.30
Batrachotomus kupferzellensis (SMNS 80276): 0.46
Chanaresuchus bonapartei (PVL 4575): 0.31
"*Chasmatosaurus*" *yuani* (IVPP V2719): 0.37
"*Chasmatosaurus*" *yuani* (IVPP V4067): 0.42
Cuyosuchus (Rusconi, 1951: fig. 38c): 0.48
Dimorphodon (Padian, 1983: fig. 8, YPM 350): 0.46
Erythrosuchus (SAM-PK-905): 0.55
Euparkeria (SAM-PK-5867): 0.38
Garjainia madiba (BP/1/5360): 0.43
Garjainia prima (PIN, *G. triplicostata*): 0.48
Gracilisuchus (CRILAR #079-2011): 0.49
Herrerasaurus (MACN-PV 18060): 0.52
Heterodontosaurus (SAM-PK-K1332): 0.42
Jaxtasuchus salomoni (SMNS 91002): 0.36
Lewisuchus (PULR 01): >0.37
Marasuchus lilloensis (PVL 3871): ca. 0.40
Nicrosaurus kapffi (SMNS unnumbered): 0.32
Nundasuchus (Nesbitt et al., 2014: fig. 7b): 0.43
Petrolacosaurus (Reisz, 1981: fig. 19): 0.17
Prestosuchus chiniquensis (UFRGS-PV-0152-T): 0.34
Prolacerta (BP/1/2675): 0.27
Proterochampsa barrionuevoi (Trotteyn, 2011: fig. 9): 0.25
Protorosaurus (BSPG 1995 I 5, cast of WMsN P 47361): 0.26
Rhynchosaurus articeps (NHMUK R1239): 0.34
Riojasuchus tenuisceps (PVL 3826): 0.43
Silesaurus opolensis (Dzik, 2003: fig. 9b): 0.38
Shansisuchus kuyeheensis (Cheng, 1980: fig. 28): 0.46
Shansisuchus shansisuchus (Young, 1964: table 7, 27a): 0.40
Shansisuchus shansisuchus (Young, 1964: table 7, 27b): 0.40
Shansisuchus shansisuchus (Young, 1964: table 7, 27c): 0.42
Shansisuchus shansisuchus (Young, 1964: table 7, 27d): 0.48

Smilosuchus gregorii (USNM 18313): 0.28
Trilophosauurs buettneri (Spielmann et al., 2008: fig. 66d): 0.24
Turfanosuchus dabanensis (IVPP V3237): 0.37
Vancleavea campi (Parker and Barton, 2008: fig. 8.4): 0.33
Youngina (SAM-PK-K7710): 0.28

Discretization by the cluster analysis: (1) 0.16-0.18; (2) 0.24-0.28; (3) 0.30-0.34; (4) 0.36-0.38; (5) 0.40-0.43; (6) 0.46-0.49; (7) 0.52-0.55. (5%=0.02).

(395) Humerus, transverse width of the distal end versus total length of the bone in mature individuals: 0.15-0.17 (0); 0.20-0.46 (1); 0.49-0.57 (2) (modified from Ezcurra et al., 2010: 93; modified from Nesbitt, 2011: 235), CONTINUOUS, ORDERED.

Aetosauroides scagliai (PVL 2073): 0.33
Aetosauroides scagliai (PVL 2091): 0.40
Amotosaurus (SMNS 54783): 0.20
Azendohsaurus madagaskarensis (UA 7-13-99-578): 0.44
Batrachotomus kupferzellensis (SMNS 80276): 0.32
Chanaresuchus bonapartei (PVL 4575): 0.27
"*Chasmatosaurus*" *yuani* (IVPP V2719): 0.54
"*Chasmatosaurus*" *yuani* (IVPP V4067): 0.56
Cuyosuchus (MCNAM PV 2669): 0.34
Dimorphodon (Padian, 1983: table 1, YPM 350): 0.22
Erythrosuchus (SAM-PK-905): 0.57
Euparkeria (SAM-PK-5867): 0.32
Euparkeria (SAM-PK-8050): 0.34
Garjainia madiba (BP/1/5360): 0.50
Garjainia prima (PIN, *G. triplicostata*): 0.52
Gephyrosaurus (Evans, 1980: fig. 18a): ca. 0.35
Gracilisuchus (CRILAR #079-2011): 0.23
Gualosuchus (PVL 4576): 0.26
Herrerasaurus (MACN-PV 18060): 0.28
Heterodontosaurus (SAM-PK-K1332): 0.23
Howesia (Broom, 1906: plate XL, fig. 13, SAM-PK-5885): <0.37
Jaxtasuchus salomoni (SMNS 91002): 0.23
Jesairosaurus lehmani (ZAR 09, large specimen): 0.23
Jesairosaurus lehmani (ZAR 09, small specimen): 0.30
Koilamasuchus (MACN-Pv 18119): 0.41
Macrocnemus bessanii (PIMUZ T4355): 0.26
Marasuchus lilloensis (PVL 3871): 0.16
Nicrosaurus kapffi (SMNS unnumbered): 0.31
Nundasuchus (Nesbitt et al., 2014: table 1): 0.40
Petrolacosaurus (Reiz, 1981: 43): 0.29
Prestosuchus chiniquensis (UFRGS-PV-0152-T): 0.32
Prolacerta (BP/1/2675): 0.34

Proterochampsa barrionuevoi (Trotteyn, 2011: table 2): 0.36
Protorosaurus (Gottmann-Quesada and Sander, 2009: appendix I, FG 2666/2004b): 0.35
Protorosaurus (Gottmann-Quesada and Sander, 2009: appendix I, NHMW 1943I4): 0.36
Protorosaurus (Gottmann-Quesada and Sander, 2009: appendix I, WMsN P 47361): 0.52
Rhynchosaurus articeps (NHMUK R1239): 0.49
Riojasuchus tenuisceps (PVL 3826): 0.28
Shansisuchus kuyeheensis (Cheng, 1980: fig. 28): 0.46
Shansisuchus shansisuchus (Young, 1964: table 7, 27a): 0.43
Shansisuchus shansisuchus (Young, 1964: table 7, 27b): 0.46
Shansisuchus shansisuchus (Young, 1964: table 7, 27c): 0.50
Shansisuchus shansisuchus (Young, 1964: table 7, 27d): 0.46
Silesaurus opolensis (Dzik, 2003: fig. 9b): 0.16
Smilosuchus gregorii (USNM 18313): 0.31
Tanystropheus longobardicus (Nosotti, 2007: fig. 7): 0.22
Trilophosauurs buettneri (Spielmann et al., 2008: appendix 10, TMM 31025-849): 0.31
Trilophosauurs buettneri (Spielmann et al., 2008: appendix 10, TMM 31025-690): 0.27
Trilophosauurs buettneri (Spielmann et al., 2008: appendix 10, TMM 31025-926): 0.34
Trilophosauurs buettneri (Spielmann et al., 2008: appendix 10, TMM 31025-66X): 0.34
Trilophosauurs buettneri (Spielmann et al., 2008: appendix 10, TMM 31025-140): 0.34
Tropidosuchus romeri (PVL 4601): 0.22
Turfanosuchus dabanensis (IVPP V3237): 0.25
Youngina (BP/1/3859): 0.42

Discretization by the cluster analysis: (1) 0.15-0.17; (2) 0.20-0.46; (3) 0.49-0.57. (5%=0.02).

(396) Humerus, entepicondyle size in mature individuals: moderately large (0); strongly developed (1) (Laurin, 1991: I2; Reisz et al., 2010: 90; Ezcurra et al., 2014: 89).

(397) Humerus, entepicondylar foramen: present (0); absent (1) (Laurin, 1991: F6; Reisz et al., 2010: 91; Ezcurra et al., 2014: 90).

(398) Humerus, ectepicondylar region: foramen present (0); foramen absent, supinator process and groove present (1); supinator process, groove or foramen absent (2) (Laurin, 1991: J7; Müller, 2004: 64, 176; Reisz et al., 2010: 92; Nesbitt, 2011:

234, in part; Dilkes and Arcucci, 2012: 65, in part; modified from Ezcurra et al., 2014: 91).

(399) Humerus, capitellum (radial condyle) and trochlea (ulnar condyle): ball-shaped structures distinct from the ectepicondyle and entepicondyle (0); absent or incipient (1) (Rieppel et al., 1999 and Müller, 2004: 63; modified from Ezcurra et al., 2014: 198).

(400) Humerus, trochlea (ulnar condyle) situated approximately at mid-width on the distal end of the bone: present (0); absent, being considerably laterally displaced (1) (Ezcurra et al., 2014: 199). This character is inapplicable for taxa that lack or have incipient radial and ulnar condyles.

(401) Ulna, olecranon process: absent, not ossified or very low (0); prominent but lower than its anteroposterior depth at base (1); strongly developed, being higher than its anteroposterior depth at base (2) (Laurin, 1991: C2; deBraga and Rieppel, 1997; Müller, 2004: 147; modified from Reisz et al., 2010: 95; Ezcurra et al., 2014: 94), ORDERED.

(402) Ulna, olecranon process in lateral view: tapering toward its distal end (0); subrectangular or slightly expanded towards its distal end (1) (Ezcurra et al., 2014: 201). This character is inapplicable in taxa without an olecranon process (e.g. *Macrocnemus*).

(403) Ulna, olecranon process as a separate ossification: absent (0); present (1) (Laurin, 1991: C2; Ezcurra et al., 2014: 200).

(404) Ulna, lateral tuber (= radius tuber) on the proximal portion: absent (0); present (1) (Nesbitt, 2011: 237; Dilkes and Arcucci, 2012: 67).

(405) Ulna, distal end in posterolateral view: rounded and convex (0); squared off where the distal surface is nearly flat (1) (Nesbitt, 2011: 238; Dilkes and Arcucci, 2012: 66).

(406) Radius, total length versus total length of the humerus: 0.62-0.66 (0); 0.69-0.92 (1); 0.95-0.97 (2); 1.14-1.17 (3) (Laurin, 1991: A6, H7; Reisz et al., 2010: 93; modified from Nesbitt, 2011: 241; modified from Ezcurra et al., 2014: 92), CONTINUOUS, ORDERED.

Aetosauroides scagliai (PVL 2059): 0.90
Aetosauroides scagliai (PVL 2073): 0.73
Boreopricea (Benton and Allen, 1997: 941, 942): 0.79
Chanaresuchus bonapartei (Romer, 1972e: 12): 0.92
"*Chasmatosaurus*" *yuani* (Young, 1978: table 1; IVPP V4067): 0.76
Erythrosuchus (SAM-PK-905): 0.75
Euparkeria (SAM-PK-5867): 0.84
Euparkeria (SAM-PK-13666): 0.83
Herrerasaurus (PVSJ 407): 0.92
Heterodontosaurus (SAM-PK-K1332): 0.70
Macrocnemus bessanii (Rieppel, 1989b: table 2, PIMUZ T2477): 0.95
Macrocnemus bessanii (Rieppel, 1989b: table 2, PIMUZ T2472): 0.92
Macrocnemus bessanii (Rieppel, 1989b: table 2, PIMUZ T4355): 0.96
Marasuchus lilloensis (PVL 3871): >0.72
Ornithosuchus (Huene, 1914: 17): 0.79
Petrolacosaurus (Reisz, 1981: 45): 0.92
Prolacerta (Gow, 1975: 111, BP/1/2675): 0.88
Proterochampsa barrionuevoi (Trotteyn, 2011: table 2): 0.76
Protorosaurus (Gottmann-Quesada and Sander, 2009: appendix I, FG 2666/2004b): 0.84
Protorosaurus (Gottmann-Quesada and Sander, 2009: appendix I, NHMW 1943I4): 0.79
Protorosaurus (Gottmann-Quesada and Sander, 2009: appendix I, WMsN P 47361): 0.86
Rhynchosaurus articeps (NHMUK R1238): 0.71
Rhynchosaurus articeps (SHYMS 6): 0.84
Riojasuchus tenuisceps (Bonaparte, 1971): ca. 0.75
Silesaurus opolensis (ZPAL Ab III/361): 1.16
Tanystropheus longobardicus (Nosotti, 2007: table 6, MSNM BES SC 1018): 0.66
Tanystropheus longobardicus (Nosotti, 2007: table 4, MSNM BES SC 265): 0.70
Trilophosaurus buettneri (Spielmann et al., 2008: fig. 72d, appendix 10, TMM 31025-140): 0.81
Tropidosuchus romeri (Arcucci, 1990: 373): 0.78
Vancleavea campi (Nesbitt et al., 2009: fig. 13): 0.62
Youngina (Gow, 1975: 97): 0.78

Youngina (SAM-PK-K7710): 0.70

Discretization by the cluster analysis: (1) 0.62-0.66; (2) 0.69-0.92; (3) 0.95-0.97; (4) 1.14-1.17. (5%=0.03).

(407) Radius, length in comparisons with that of the ulna: shorter (0); longer or subequal (1) (Rieppel et al., 1999, Müller, 2004: 66; Ezcurra et al., 2014: 202). The olecranon process of the ulna should not be taken into account if present.

(408) Radius, shape: straight (0); twisted in lateral view (1) (Laurin, 1991: I3; Reisz et al., 2010: 94; Ezcurra et al., 2014: 93).

(409) Radius, distal end: unexpanded or poorly anteroposteriorly expanded (0); strongly anteroposteriorly expanded (1) (New character).

(410) Carpals, perforating foramen between intermedium and ulnare: present (0); absent (1) (New character). This character is innaplicable in taxa that lack an intermedium.

(411) Carpals, medial centrale carpi: present (0); absent (1) (Laurin, 1991: F7; Reisz et al., 2010: 96; Ezcurra et al., 2014: 95).

(412) Carpals, lateral centrale carpi: large (0); small or absent (1) (Laurin, 1991: E12; Reisz et al., 2010: 97; Ezcurra et al., 2014: 96).

(413) Carpals, pisiform: present (0); absent (1) (New character).

(414) Manus, longest metacarpal + digit: longer than humeral length (0); subequal to shorter than humeral length (1) (Senter, 2004: 51; Ezcurra et al., 2014: 203).

(415) Metacarpus, length of the longest metacarpal versus length of the longest metatarsal: 0.34-0.39 (0); 0.43-0.45 (1); 0.54-0.98 (2) (modified from Nesbitt, 2011: 245), CONTINUOUS, ORDERED.

Amotosaurus (SMNS 54783): 0.34
Boreopricea (Tatarinov, 1978: fig. 2): 0.74
GHG 7433MI: 0.39
Herrerasaurus (PVSJ 373): 0.38

Heterodontosaurus (SAM-PK-K1332): 0.34
Jaxtasuchus salomoni (SMNS 91352): 0.58
Macrocnemus bessanii (PIMUZ T2472): 0.43
Noteosuchus (AM 3591): 0.45
Proterosuchus fergusi (SAM-PK-K140): 0.59
Protorosaurus (Gottmann-Quesada and Sander, 2009: appendix I, Nat. Kab. 191): 0.97
Tanystropheus longobardicus (Nosotti, 2007: tables 5, 6, MSNM BES SC 1018): 0.38
Trilophosaurus buettneri (Spielmann et al., 2008: figs.74a, 91a): 0.59
Vancleavea campi (Nesbitt et al., 2009: 831, 836): 0.75
Youngina (based on extrapolations between the forelimb of BP/1/3859 and the hindlimb of SAM-PK-K7710d): 0.54

Discretization by the cluster analysis: (1) 0.34-0.39; (2) 0.43-0.45; (3) 0.54-0.59; (4) 0.74-0.75; (5) 0.95-0.98. (5%=0.03). The last three clusters were merged together because the last two were restricted to a single terminal.

(416) Metacarpus, proximal ends: overlap (0); abut one another without overlapping

(1) (Sereno and Wild, 1992; Nesbitt, 2011: 246).

(417) Metacarpus, width of the distal end of the metacarpal I versus its total length:

0.26-0.33 (0); 0.36-0.45 (1); 0.48-0.53 (2); 0.58-0.64 (3); 0.73-0.75 (4) (modified

from Bakker and Galton, 1974; modified from Nesbitt, 2011: 251),

CONTINUOUS, ORDERED.

Acerosodontosaurus (MNHN 1908-32-57): 0.44
Amotosaurus (SMNS 54783): 0.26
Azendohsaurus madagaskarensis (UA 7-16-99-607): 0.53
Dimorphodon (NHMUK R41212-13): <0.12
Erythrosuchus (NHMUK R3592): 0.74
Euparkeria (SAM-PK-13666): 0.52-0.60
Herrerasaurus (PVSJ 373): 0.40
Herrerasaurus (PVSJ 380): 0.50
Heterodontosaurus (SAM-PK-K1332): 0.31
Jaxtasuchus salomoni (SMNS 91352): 0.64
Noteosuchus (AM 3591): 0.48
Ornithosuchus (Walker, 1964: fig. 10f): 0.33
Petrolacosaurus (Reisz, 1981: 0.48
Prolacerta (BP/1/2675): 0.36
Proterosuchus fergusi (SAM-PK-K140): 0.50
Protorosaurus (BSPG 1995 I 5, cast of WMsN P 47361): 0.50
Rhynchosaurus articeps (SHYMS 4): 0.43
Rhynchosaurus articeps (SHYMS 6): 0.39
Riojasuchus tenuisceps (PVL 3827): 0.37

Shansisuchus shansisuchus (Young, 1964: table 9): 0.58-0.63
Tanystropheus longobardicus (Nosotti, 2007: fig. 23, MSNM BES SC 1018): 0.38
Trilophosaurus buettneri (Spielmann et al., 2008: fig. 74a): 0.50
Vancleavea campi (Nesbitt et al., 2009: fig. 13): 0.45
Youngina (BP/1/3859): 0.42

Discretization by the cluster analysis: (1) 0.26-0.33; (2) 0.36-0.45; (3) 0.48-0.53; (4) 0.58-0.64; (5) 0.73-0.75. (5%=0.02).

(418) Metacarpus, extensor pits on the dorsodistal portion of the metacarpals I-III: absent or shallow and symmetrical (0); deep and asymmetrical (1) (Sereno et al., 1993; Nesbitt, 2011: 250).

(419) Metacarpus, metacarpal IV: longer than metacarpal III (0); equal or shorter than metacarpal III (1) (deBraga and Rieppel, 1997; Müller, 2004: 148; Nesbitt, 2011: 260; Ezcurra et al., 2014: 204).

(420) Manual digits, unguals of manual digits I-III: blunt on at least digits II and III (0); trenchant on digits I-III (1) (Gauthier, 1986; Nesbitt, 2011: 257).

(421) Manual digits, second phalanx of manual digit II: shorter than the first phalanx of manual digit II (0); longer than the first phalanx of manual digit II (1) (Gauthier, 1986; Nesbitt, 2011: 255).

(422) Manual digits, number of phalanges in digit IV: five (0); four (1); three or less (2) (Gauthier, 1986; Benton and Clark, 1988; Sereno, 1993; Ezcurra et al., 2010: 120; cf. Nesbitt, 2011: 258), ORDERED.

(423) Pelvic girdle, acetabulum: completely closed (0); perforated (1) (Gauthier, 1986; Laurin, 1991: J8; Juul, 1994; Reisz et al., 2010: 98; modified from Ezcurra et al., 2010: 124; cf. Nesbitt, 2011: 273; Ezcurra et al., 2014: 96).

(424) Pelvic girdle, acetabulum orientation: mainly laterally facing (0); lateroventrally or mainly ventrally facing (1) (Benton and Clark, 1988; Juul, 1994; Ezcurra et al., 2010: 123; Nesbitt, 2011: 270).

(425) Pelvic girdle, acetabular antitrochanter: absent (0); present (1) (Sereno and Arcucci, 1993; Ezcurra et al., 2010: 125; Nesbitt, 2011: 274).

(426) Ilium, maximum height of the ilium versus length of the femur: 0.11-0.14 (0); 0.24-0.26 (1); 0.29-0.47 (2); 0.54-0.57 (3) (New character), CONTINUOUS, ORDERED.

Acerosodontosaurus (MNHN 1908-32-57): 0.33
Aetosauroides scagliai (PVL 2073): 0.39
Archeopelta arborensis (CPEZ-239a): 0.43
Chanaresuchus bonapartei (Romer, 1972e: plate 1): 0.38
Cuyosuchus (MCNAM PV 2669): <0.38
Dimorphodon (NHMUK R1034): 0.12
Dorosuchus (PIN 1579/61): 0.47
Lagerpeton chanarensis (PVL 4619): 0.26
Gracilisuchus (PVL 4597): ca. 0.24-0.30
Herrerasaurus (PVL 2566): 0.37
Heterodontosaurus (AM unnumbered): 0.25
Heterodontosaurus (SAM-PK-K1332): 0.30
Macrocnemus bessanii (PIMUZ T2472): 0.24
Macrocnemus bessanii (Besano II specimen): 0.25
Marasuchus lilloensis (PVL 3870): 0.31
Mesosuchus (Haughton, 1921: 86, 87; SAM-PK-6046): 0.56
Noteosuchus (Carroll, 1976: figs. 2, 3): 0.38
Ornithosuchus (NHMUK R3561): 0.34
Prestosuchus chiniquensis (UFRGS-PV-0629-T): 0.47
Prolacerta (BP/1/2676): 0.41
Riojasuchus tenuisceps (PVL 3828): 0.35
Silesaurus opolensis (ZPAL Ab III/361): >0.28
Tanystropheus longobardicus (Nosotti, 2007: fig. 27, MSNM BES SC 1018): 0.29
Trilophosaurus buettneri (Spielmann et al., 2008: fig. 76a, appendix 10: TMM 31025-140): >0.31
Turfanosuchus dabanensis (IVPP V3237): ca. 0.40
Youngina (BP/1/3859): 0.40

Discretization by the cluster analysis: (1) 0.11-0.14; (2) 0.24-0.26; (3) 0.29-0.47; (4) 0.54-0.57. (5%=0.022).

(427) Ilium, laterally deflected iliac blade: absent (0); present (1) (Dilkes and Sues, 2009; Desojo et al., 2011: 96).

(428) Ilium, preacetabular process: absent or incipient (0); present, being considerably anteroposteriorly shorter than its dorsoventral height (1); present, being longer

than two thirds of its height and not extending beyond the level of the anterior margin of the pubic peduncle (2); present and extending beyond the level of the anterior margin of the pubic peduncle (3) (modified from Dilkes, 1998; Rieppel et al., 1999; Müller, 2004: 67; Ezcurra et al., 2010: 61, in part; Nesbitt, 2011: 268 and 269; Dilkes and Arcucci, 2012: 68, in part; Ezcurra et al., 2014: 205), ORDERED.

(429) Ilium, preacetabular process in lateral view: semicircular (0); subtriangular or finger-like (1) (New character). This character is inapplicable in taxa that lack a preacetabular process.

(430) Ilium, lateral crest dorsal to the supraacetabular crest/rim: absent (0); present and divides the preacetabular process from the postacetabular process (1); confluent with the anterior extent of the preacetabular process (2) (Nesbitt, 2011: 265).

(431) Ilium, length of the postacetabular process versus anteroposterior length of the acetabulum: 0.31-0.63 (0); 0.79-1.24 (1); 1.31-1.37 (2); 1.49-1.55 (3) (modified from Dilkes, 1998: 102; Müller, 2004: 113 in part; Ezcurra et al., 2010: 94 in part; Ezcurra et al., 2014: 206), CONTINUOUS, ORDERED.

Acerosodontosaurus (MNHN 1908-32-57): 1.24
Aetosauroides scagliai (PVL 2059): 0.31
Aetosauroides scagliai (PVL 2073): 0.35
Amotosaurus (SMNS 90544): 1.08
Azendohsaurus madagaskarensis (UA 8-30-98-375): 1.04
Azendohsaurus madagaskarensis (UA 9-5-98-448): 1.03
Azendohsaurus madagaskarensis (UA 8-29-97-155): 0.98
Batrachotomus kupferzellensis (SMNS 80273): 1.13
Chanaresuchus bonapartei (MCZ 4035): 0.85
"*Chasmatosaurus*" *yuani* (Young, 1936: fig. 10): ca. 0.92
Cuyosuchus (Rusconi, 1951: fig. 31a): 0.91
Dimorphodon (NHMUK R1034): 1.18
Dorosuchus (PIN 1579/61): 1.03
Doswellia kaltenbachi (USNM 244214): 1.22
Erythrosuchus (NHMUK R3592): 0.87
Erythrosuchus (SAM-PK-905): 0.90

Euparkeria (SAM-PK-7696): 1.21
Garjainia madiba (BP/1/5525): 1.19
Garjainia prima (PIN, *G. triplicostata*): 0.98
Gracilisuchus (PVL 4597): 1.11
Herrerasaurus (PVL 2566): 0.79
Herrerasaurus (MCZ 4381): 0.94
Herrerasaurus (MLP-61-VIII-2-2): 0.94
Heterodontosaurus (SAM-PK-K1332): 1.19
Howesia (NHMUK R5872, cast of SAM-PK-5886): ca. 0.92
Koilamasuchus (MACN-Pv 18119): 0.55-0.85
Lagerpeton chanarensis (PVL 4619): 0.89
Macrocnemus bessanii (Besano II specimen): 1.00
Marasuchus lilloensis (PVL 3870): 0.89
Mesosuchus (SAM-PK-7416): 0.82
Noteosuchus (AM 3591): 1.11
Ornithosuchus (Walker, 1964: fig. 11f): 1.00
Petrolacosaurus (Reisz, 1981: fig. 18): 1.00
Prestosuchus chiniquensis (UFRGS-PV-0152-T): 0.96
Prestosuchus chiniquensis (UFRGS-PV-0629-T): 0.96
Prolacerta (BP/1/2676): >1.07
Planocephalosaurus (Fraser and Walkden, 1984: fig. 17b): 0.92
Riojasuchus tenuisceps (PVL 3827): 1.36
Riojasuchus tenuisceps (PVL 3828): 1.52
Shansisuchus shansisuchus (Young, 1964: fig. 30b): 1.34
Silesaurus opolensis (ZPAL Ab III/361): 0.97
Smilosuchus gregorii (UCMP 26699): 1.03
Tanystropheus longobardicus (Nosotti, 2007: fig. 24, MSNM BES SC 1018): 1.32
Trilophosaurus buettneri (Spielmann et al., 2008: fig. 76a): 0.82
Turfanosuchus dabanensis (IVPP V3237): 1.34
Vancleavea campi (Nesbitt et al., 2009: fig. 14b): 0.63
Youngina (BP/1/3859): 0.45

Discretization by the cluster analysis: (1) 0.31-0.63; (2) 0.79-1.24; (3) 1.31-1.37; (4) 1.49-1.55. (5%=0.06).

(432) Ilium, main axis of the postacetabular process in lateral or medial view: posterodorsally oriented (0); mainly posteriorly oriented (1) (New character).

(433) Ilium, caudifemoralis brevis muscle origin on the lateroventral surface of the postacetabular process: not dorsally or laterally rimed by a brevis shelf (0); dorsally rimed by a brevis shelf, but lacking a brevis fossa (1); dorsolaterally rimed by a brevis shelf and with a lateroventrally facing brevis fossa (2); laterally

rimed by a brevis shelf and with a ventrally facing brevis fossa (3) (Gauthier, 1986; Juul, 1994; Ezcurra et al., 2010: 121, 122; Nesbitt, 2011: 271, in part).

(434) Ilium, dorsal margin of the iliac blade: convex (0); mostly straight (1); concave (2) (modified from Dilkes, 1998; modified from Ezcurra et al., 2010: 60).

(435) Ilium, angle between anterior margin of the pubic peduncle and longitudinal axis across pubic and ischiadic peduncles: lower than 45º (0); equal or higher than 45º (1) (Ezcurra et al., 2010: 95).

(436) Ilium, posteriorly projected heel on the posterior margin of the ischiadic peduncle in lateral view: absent (0); present, the dorsal margin of which is set at 45º or less to the longitudinal axis of the bone (1) (Ezcurra et al., 2010: 96).

(437) Pubis-ischium, contact: present and extended ventrally (0); present and reduced to a thin proximal contact (1) (Nesbitt, 2011: 287).

(438) Pubis-ischium, thyroid fenestra: absent (0); present (1) (Rieppel et al., 1999; Müller, 2004: 68; Ezcurra et al., 2014: 208).

(439) Pubis, total length versus anteroposterior length of the acetabulum: 0.95-2.58 (0); 2.84-3.43 (1); 3.94-4.87 (2) (modified from Sereno, 1991; Juul, 1994; Weinbaum and Hungerbühler, 2007; Ezcurra et al., 2010: 126, 169; cf. Nesbitt, 2011: 278), CONTINUOUS, ORDERED.

Acerosodontosaurus (Currie, 1980: fig. 7): 1.82
Aetosauroides scagliai (PVL 2052): 2.19
Aetosauroides scagliai (PVL 2073): 2.14
Amotosaurus (SMNS 50830): ca. 2.17
Chanaresuchus bonapartei (PVL 4575): 1.86
Cuyosuchus (Rusconi, 1951: fig. 37): 2.47
Dimorphodon (NHMUK R1034): ca. 1.00
Doswellia kaltenbachi (USNM 244214): 1.75
Erythrosuchus (SAM-PK-905): 1.52
Euparkeria (SAM-PK-7696): 2.27
Garjainia prima (PIN, *G. triplicostata*): 1.97
Gracilisuchus (PVL 4597): 2.37
Herrerasaurus (MCZ 4381): 3.43
Herrerasaurus (PVL 2566): 4.22

Heterodontosaurus (SAM-PK-K1332): 4.87
Howesia (SAM-PK-5886): 1.65
Lagerpeton chanarensis (PVL 4619): 1.58
Macrocnemus bessanii (Besano II specimen): 1.44
Marasuchus lilloensis (PVL 3870): 2.84
Mesosuchus (SAM-PK-7416): 1.66
Mesosuchus (SAM-PK-6046): ca. 1.35
Noteosuchus (Carroll, 1976: figs. 1, 3h): 1.69
Ornithosuchus (Walker 1964: fig. 11f): 3.94
Petrolacosaurus (Reisz, 1981: fig. 18): 2.16
Planocephalosaurus (Fraser and Walkden, 1984: fig. 16): 2.58
Prestosuchus chiniquensis (UFRGS-PV-0629-T): 2.36
Prolacerta (BP/1/2676): 2.01
Riojasuchus tenuisceps (PVL 3827): 3.40
Silesaurus opolensis (ZPAL Ab III/361): 4.72
Smilosuchus gregorii (Long and Murry, 1995: fig. 31a): 1.61
Tanystropheus longobardicus (Nosotti, 2007: fig. 24, MSNM BES SC 1018): 2.34
Trilophosaurus buettneri (Spielmann et al., 2008: figs. 76a, 78a): 1.39
Tropidosuchus romeri (PVL 4601): 1.92
Turfanosuchus dabanensis (IVPP V3237): 3.06
Youngina (BP/1/3859): 1.20

Discretization by the cluster analysis: (1) 1.20-2.58; (2) 2.84-3.43; (3) 3.94-4.87. (5%=0.18).

(440) Pubis, anterior and posterior portions of the acetabular margin: continuous (0); recessed (1) (Sereno, 1991; Ezcurra et al., 2010: 127; Nesbitt, 2011: 286)

(441) Pubis, tuberosity for the attachment of the ambiens muscle in mature individuals: prominent (0); incipient or absent (1) (Hutchinson, 2001; Ezcurra et al., 2010: 62; Dilkes and Arcucci, 2012: 69).

(442) Pubis, shaft orientation: anteroventral (0); vertical or posteroventral (1) (Benton, 1985; Juul, 1994; Ezcurra et al., 2010: 128; Nesbitt, 2011: 279).

(443) Pubis, form of the shaft (= pubic tubercle, = pectineal tuberosity): plate-like (0); rod-like and curved posteriorly (1); rod-like and straight (2) (Ezcurra, 2006; Ezcurra et al., 2010: 154).

(444) Pubis, anterior apron: absent (0); present (1) (Dilkes, 1998: 104; Ezcurra et al., 2014: 209).

(445) Pubis, transverse width of conjoined aprons versus total length of the bone: 0.27-0.59 (0); 0.77-0.97 (1); 1.12-1.28 (2); 1.48-1.94 (3) (modified from Cooper, 1984; Ezcurra et al., 2010: 155), CONTINUOUS, ORDERED. This character is not applicable in taxa that lack an anterior pubic apron.

Aetosauroides scagliai (PVL 2052): 0.86
Aetosauroides scagliai (PVL 2073): 0.77
Azendohsaurus madagaskarensis (UA 8-30-98-375): 0.97
Batrachotomus kupferzellensis (SMNS 80269): 0.34
Chanaresuchus bonapartei (PVL 4575): 1.80
Cuyosuchus (MCNAM PV 2669): >0.85
Doswellia kaltenbachi (USNM 244214): 1.69
Erythrosuchus (NHMUK R3592): 0.88
Erythrosuchus (SAM-PK-905): 0.96
Garjainia prima (PIN, *G. triplicostata*): 1.12
Gracilisuchus (PVL 4597): 0.27
Herrerasaurus (PVL 2566): 0.41
Lagerpeton chanarensis (PVL 4619): 1.68
Marasuchus lilloensis (PVL 3870): 0.56
Mesosuchus (SAM-PK-6046): 1.94
Noteosuchus (Carroll, 1976: fig. 1): 1.54
Nundasuchus (Nesbitt et al., 2014: fig. 8b): slightly above 1.07
Ornithosuchus (Walker, 1964: fig. 11h): 0.47
Prestosuchus chiniquensis (UFRGS-PV-0629-T): 0.43
Riojasuchus tenuisceps (PVL 3827): 0.59
Shansisuchus shansisuchus (Young, 1964: fig. 29e): 1.13
Silesaurus opolensis (Dzik, 2003: fig. 12d): 0.49
Smilosuchus gregorii (UCMP 26699): 1.28
Tropidosuchus romeri (PVL 4601): 1.48
Turfanosuchus dabanensis (IVPP V3237): ca. 0.52

Discretization by the cluster analysis: (1) 0.27-0.59; (2) 0.77-0.97; (3) 1.12-1.28; (4) 1.48-1.94. (5%=0.08).

(446) Pubis, pectineal process: absent (0); present (1) (Ezcurra et al., 2014: 207).

(447) Pubis, distal end in lateral or medial view: unexpanded (0); gradually expanded anteroposteriorly relative to the shaft (1); sharply expanded anteroposteriorly relative to shaft, forming a pubic boot (2) (Gauthier, 1986; modified from Nesbitt, 2011: 283). This character is inapplicable in taxa that lack a rod-like pubic shaft.

(448) Pubis, transverse width of the distal portion: nearly as broad as the proximal width (0); significantly narrower than the proximal width (1) (Galton, 1976;

Nesbitt, 2011: 289). This character is inapplicable in taxa that lack a rod-like pubic shaft.

(449) Ischium, total length versus anteroposterior length of the acetabulum: 1.04-1.24 (0); 1.55-2.50 (1); 2.72-3.24 (2); 4.31-4.48 (3) (Benton, 2004; modified from Ezcurra et al., 2010: 63; cf. Nesbitt, 2011: 282, 298; cf. Dilkes and Arcucci, 2012: 70), CONTINUOUS, ORDERED.

Aetosauroides scagliai (PVL 2052): 1.79
Aetosauroides scagliai (PVL 2073): 1.77
Amotosaurus (SMNS 50830): ca. 2.17
Chanaresuchus bonapartei (MCZ 4035): 1.65
Cuyosuchus (MCNAM PV 2669): >2.63
Doswellia kaltenbachi (USNM 244214): 1.66
Erythrosuchus (SAM-PK-905): 1.90
Euparkeria (SAM-PK-7696): 2.72
Garjainia madiba (BP/1/5525): 2.40
Garjainia prima (PIN, *G. triplicostata*): 2.43
Gephyrosaurus (Evans, 1981: fig. 20): ca. 2.00
Gracilisuchus (PVL 4597): 1.99-2.36
Herrerasaurus (MCZ 4381): 1.64
Heterodontosaurus (SAM-PK-K1332): 4.4
Howesia (NHMUK R5872, cast of SAM-PK-5886): ca. 1.79
Lagerpeton chanarensis (PVL 4619): 2.17
Macrocnemus bessanii (Besano II specimen): 1.55
Marasuchus lilloensis (PVL 3870): 2.18
Mesosuchus (SAM-PK-6046): 1.24
Noteosuchus (Carroll, 1976: figs. 1, 3h): 2.31
Ornithosuchus (Walker, 1964: fig. 11g): 2.96
Petrolacosaurus (Reisz, 1981: fig. 18): 2.72
Planocephalosaurus (Fraser and Walkden, 1984: fig. 16): 2.35
Prestosuchus chiniquensis (UFRGS-PV-0629-T): 2.24
Prolacerta (BP/1/2676): 1.92
Rhynchosaurus articeps (SHYMS 5): 1.58
Silesaurus opolensis (ZPAL Ab III/361): 3.24
Smilosuchus gregorii (Long and Murry, 1995: fig. 31a): 2.03
Tanystropheus longobardicus (Nosotti, 2007: fig. 25, MSNM BES SC 1018): 2.50
Trilophosaurus buettneri (Spielmann et al., 2008: fig. 82a): 1.66
Tropidosuchus romeri (PVL 4601): 1.71
Vancleavea campi (Nesbitt et al., 2009: fig. 14b, c): 2.43
Youngina (BP/1/3859): 1.04

Discretization by the cluster analysis: (1) 1.04-1.24; (2) 1.55-2.50; (3) 2.72-3.24; (4) 4.31-4.48. (5%=0.17).

(450) Ischium, proximal articular surface: articular surface with the ilium and pubis continuous (0); articular surfaces with the ilium and pubis separated by a fossa (1); articular surfaces with the ilium and pubis separated by a non-articulating notched surface (2) (Irmis et al., 2007; Nesbitt, 2011: 297), ORDERED.

(451) Ischium, longitudinal groove on the dorsal surface of shaft: absent (0); present (1) (Yates, 2003).

(452) Ischium, medial contact with antimere: restricted to the medial edge (0); extensive contact but the dorsal margins are separated (1) (Nesbitt, 2011: 291).

(453) Ischium, cross section of the distal portion: plate-like (0); semicircular or subtriangular (1) (Sereno, 1999; modified from Nesbitt, 2011: 293).

(454) Femur, total length versus total length of the humerus: 0.92-0.97 (0); 1.15-1.56 (1); 1.62-1.74 (2); 1.86-1.96 (3) (Laurin, 1991: C3; Reisz et al., 2010: 104; cf. Ezcurra et al., 2010: 59; cf. Nesbitt, 2011: 231; modified from Ezcurra et al., 2014: 103), CONTINUOUS, ORDERED.

Aetosauroides scagliai (PVL 2073): 1.62
Boreopricea (Tatarinov, 1978: 511; Benton and Allen, 1997: 941, 942): 1.19-1.25
Chanaresuchus bonapartei (PVL 4575): 1.63
Chanaresuchus bonapartei (MCZ 4035): 1.51
"*Chasmatosaurus*" *yuani* (IVPP V2719): 1.50
"*Chasmatosaurus*" *yuani* (table 1, IVPP V4067): 1.38
Cuyosuchus (MCNAM PV 2669): >1.31
Dimorphodon (Padian, 1983: table 1, YPM 9182): 0.94
Euparkeria (SAM-PK-5867): 1.47
Euparkeria (SAM-PK-7696): 1.31
Gualosuchus (PVL 4576): 1.46
Herrerasaurus (MACN-Pv 18060): 1.86-1.96
Heterodontosaurus (SAM-PK-K1332): 1.35
Jaxtasuchus salomoni (SMNS 91002): 1.62
Macrocnemus bessanii (Rieppel, 1989b: table 2, PIMUZ T2477): 1.32
Macrocnemus bessanii (Rieppel, 1989b: table 2, PIMUZ T2472): 1.25
Macrocnemus bessanii (Rieppel, 1989b: table 2, PIMUZ T4355): 1.23
Marasuchus lilloensis (PVL 3871): 1.44
Nundasuchus (Nesbitt et al., 2014: table 1): 1.37
Petrolacosaurus (Peabody, 1952: table 4, estimated femoral length of 1427 based on the ratio between the radii of 1427 and 1428): 1.15
Prestosuchus chiniquensis (UFRGS-PV-0152-T): 1.53

Proterochampsa barrionuevoi (Trotteyn, 2011: table 2): 1.67
Protorosaurus (Gottmann-Quesada and Sander, 2009: appendix I, BSPG AS VII 1207): 1.55
Protorosaurus (Gottmann-Quesada and Sander, 2009: appendix I, NHMW 1943I4): 1.41
Tanystropheus longobardicus (Nosotti, 2007: tables 4, 5, MSNM BES SC 265): 1.44
Tanystropheus longobardicus (Wild, 1973: plate 7, specimen g): 1.53
Tanystropheus longobardicus (Wild, 1973: plate 7, specimen a): 1.42
Tanystropheus longobardicus (PMIUZ T2817): 1.45
Trilophosauurs buettneri (Spielmann et al., 2008: appendix 10, TMM 31025-140): 1.21
Tropidosuchus romeri (PVL 4601): 1.40
Turfanosuchus dabanensis (IVPP V3237): 1.56
Vancleavea campi (Nesbitt et al., 2009: figs. 13, 15): 1.74
Youngina (BP/1/3859): 1.48

Discretization by the cluster analysis: (1) 0.92-0.97; (2) 1.15-1.56; (3) 1.62-1.74; (4) 1.86-1.96. (5%=0.05).

(455) Femur, minimum transverse width versus minimum transverse width of the humerus: 0.93-0.98 (0); 1.08-1.32 (1); 1.46-1.80 (2); 1.93-2.00 (3) (deBraga and Reisz, 1995: 38; Reisz et al., 2010: 105; modified from Ezcurra et al., 2014: 104), CONTINUOUS, ORDERED.

Acerosodontosaurus (MNHN 1908-32-57): 1.14
Aetosauroides scagliai (PVL 2052): 1.67
Aetosauroides scagliai (PVL 2073): 1.73
Boreopricea (Benton and Allen, 1997: fig. 2): 1.46
Chanaresuchus bonapartei (PVL 4575): 2.00
"*Chasmatosaurus yuani*" (IVPP V2719): 1.24
"*Chasmatosaurus yuani*" (IVPP V4067): 1.08-1.18
Cuyosuchus (MCNAM PV 2669): 1.24
Euparkeria (SAM-PK-5867): 1.53
Euparkeria (SAM-PK-7696): 1.65
Gracilisuchus (CRILAR #079-2011): 0.95
Gualosuchus (PULR 05): 1.57
Heterodontosaurus (SAM-PK-K1332): 1.29
Jaxtasuchus salomoni (SMNS 91002): 1.93
Macrocnemus bessanii (PIMUZ T2472): 1.80
Macrocnemus bessanii (PIMUZ T4355): 1.29
Marasuchus lilloensis (PVL 3871): 1.57
Nundasuchus (Nesbitt et al., 2014: table 1): 1.32
Prestosuchus chiniquensis (UFRGS-PV-0152-T): 1.59
Proterochampsa barrionuevoi (Trotteyn, 2011: fig. 3): ca. 1.09
Rhynchosaurus articeps (NHMUK R1239): 1.50

Riojasuchus tenuisceps (PVL 3828): 1.70
Tanystropheus longobardicus (Nosotti, 2007: plate IV, MSNM BES SC 1018): 1.18
Trilophosauurs buettneri (Spielmann et al., 2008: appendix 10, TMM 31025-140): 1.13
Turfanosuchus dabanensis (IVPP V3237): 1.46
Vancleavea campi (Nesbitt et al., 2009: figs. 13, 15): 1.21
Youngina (SAM-PK-K7710): 1.09

Discretization by the cluster analysis: (1) 1.08-1.32; (2) 1.46-1.80; (3) 1.93-2.00. (5%=0.05).

(456) Femur, proximal articular surface: well ossified, being flat or convex (0); partially ossified, being concave and sometimes with a circular pit (1) (New character).

(457) Femur, femoral head: not distinctly offset from the shaft (0); distinctly offset from the shaft (1) (Gauthier, 1986; Juul, 1994; Ezcurra et al., 2010: 129).

(458) Femur, femoral head orientation (long axis of the femoral head angle with respect to the transverse axis through the femoral condyles Parrish, 1986): anterior (60º-90º) (0); anteromedial (20º-60º) (1) (Benton and Clark, 1988; Nesbitt, 2011: 305; Dilkes and Arcucci, 2012: 75).

(459) Femur, proximal articular surface (= posterolateral portion of the head sensu Nesbitt 2011): limited to the proximal surface of the bone (0); extends under the proximal surface of the bone (1) (reworded from Sereno and Arcucci, 1993; Ezcurra et al., 2010: 130; Nesbitt et al., 2011: 313).

(460) Femur, proximal surface: rounded and smooth (0); transverse groove present (1) (modified from Ezcurra, 2006; modified from Nesbitt, 2011: 314).

(461) Femur, posteromedial tuber (= anteromedial tuber of Nesbitt, 2011) on the femoral head: absent (0); present (1) (Gauthier, 1986; modified from Nesbitt, 2011: 300; modified from Dilkes and Arcucci, 2012: 73).

(462) Femur, posterior tuber (= posteromedial tuber of Nesbitt, 2011) on the femoral head: present (0); absent (1) (Novas, 1996; Ezcurra et al., 2010: 156; Nesbitt, 2011: 301; Dilkes and Arcucci, 2012: 74). This character is inapplicable in taxa in which the internal trochanter reaches the proximal margin of the bone.

(463) Femur, anterior tuber (= anterolateral tuber of Nesbitt, 2011) on the femoral head: present as an expansion (0); absent (1) (Sereno and Arcucci, 1994; Nesbitt, 2011: 302).

(464) Femur, intertrochanteric fossa (= trochanteric fossa of Novas, 1996) on the ventral/posterior surface of the proximal end: present (0); absent (1) (modified from Novas, 1996; Benton, 2004; Ezcurra et al., 2010: 65, 131; Dilkes and Arcucci, 2012: 72).

(465) Femur, dorsolateral trochanter on the anterolateral surface of the proximal end: absent (0); present (1) (Chatterjee, 1987; Nesbitt, 2011: 307). This character is innaplicable in taxa with a wing-like anterior trochanter that extends proximally close to the greater trochanter.

(466) Femur, transition between femoral head and shaft: smooth (0); notch (1); concave emargination (2) (Sereno and Arcucci, 1994; Novas, 1996; Nesbitt, 2011: 304).

(467) Femur, anterior trochanter (= lesser or minor trochanter) (= iliofemoralis cranialis muscle insertion): absent (0); present (1) (Gauthier, 1986; Novas, 1992; Juul, 1994; Ezcurra et al., 2010: 132; Nesbitt, 2011: 308, in part; Dilkes and Arcucci, 2012: 76).

(468) Femur, trochanteric shelf (= iliofemoralis externus muscle insertion): absent (0); present in mature individuals (1) (Gauthier, 1986; Novas, 1996; Ezcurra et al., 2010: 133; Nesbitt, 2011: 311).

(469) Femur, attachment of the caudofemoralis musculature on the posterior surface of the bone: not in a distinct structure (0); on internal trochanter, bladelike with a distinct asymmetric apex located medially (1); on fourth trochanter, low and without a distinct medial asymmetrical apex (2) (modified from Juul, 1994; modified from Ezcurra et al., 2010: 64; Nesbitt, 2011: 315 and 316, in part; Dilkes and Arcucci, 2012: 71, in part).

(470) Femur, position of the internal trochanter: reaches the proximal articular surface of the bone (0); well separated distally from the proximal articular surface of the bone (1) (New character). This character is innaplicable in taxa that lack a fourth trochanter.

(471) Femur, fourth trochanter shape: moundlike and rounded (0); sharp flange (1) (Gauthier, 1986; modified from Nesbitt, 2011: 316). Scored as inapplicable in taxa that lack a fourth trochanter.

(472) Femur, fourth trochanter in medial or lateral view: symmetrical, with the proximal and distal margins forming similar low-angle slopes to the shaft (0); asymmetrical, with the distal margin forming a steeper angle to the shaft (1) (Langer and Benton, 2006; Nesbitt, 2011: 317). Scored as inapplicable in taxa that lack a fourth trochanter.

(473) Femur, fourth trochanter: restricted to the proximal half of the shaft and low (0); distally extended beyond mid-shaft and well posteriorly developed (1) (New character). Scored as inapplicable in taxa that lack a fourth trochanter.

(474) Femur, bone wall thickness at or near midshaft: thickness/diameter >0.3 (0); thin, thickness/diameter <0.3 (1) (Nesbitt, 2011: 323).

(475) Femur, shaft: diameter constant or widening distally (0); diameter distally narrowed (1) (Senter, 2004: 61; Ezcurra et al., 2014: 210).

(476) Femur, distal transverse width versus total length: 0.08-0.11 (0); 0.13-0.24 (1); 0.26-0.36 (2); 0.39-0.41 (3) (Reisz and Dilkes, 2003: 21; Reisz et al., 2010: 103; modified from Ezcurra et al., 2014: 102), CONTINUOUS, ORDERED.

Aetosauroides scagliai (PVL 2073): 0.26-0.27
Archeopelta arborensis (CPEZ-239a): 0.26
Azendohsaurus madagaskarensis (UA 9-8-98-502): 0.29
Batrachotomus kupferzellensis (SMNS 52970): 0.24
Boreopricea (Benton and Allen, 1997: 942): 0.22
Chanaresuchus bonapartei (PVL 4575): 0.16
Chanaresuchus bonapartei (MCZ 4035): 0.20
"*Chasmatosaurus*" *yuani* (IVPP V2719): 0.31
"*Chasmatosaurus*" *yuani* (IVPP V4067): 0.32
Cuyosuchus (MCNAM PV 2669): <0.29
Dimorphodon (Padian, 1983: table 1, YPM 9182): 0.14
Dongosuchus (PIN 952/15-1): 0.18
Dongosuchus (PIN 952/15-2): 0.18
Dorosuchus (PIN 1579/61): 0.27
Doswellia kaltenbachi (USNM 186989): ca. 0.18
Erythrosuchus (NHMUK R3592): 0.40
Euparkeria (SAM-PK-5867): 0.19
Euparkeria (SAM-PK-5867): 0.24
Euparkeria (SAM-PK-6047B): 0.27
Euparkeria (SAM-PK-7868): 0.20
Garjainia madiba (BP/1/5767): 0.32
Garjainia prima (PIN, *G. triplicostata*): 0.34
Gracilisuchus (PVL 4597): 0.08
Gualosuchus (PULR 05): ca. 0.24
Gualosuchus (PVL 4576): ca. 0.22
Herrerasaurus (MACN-Pv 18060): 0.17
Herrerasaurus (PVL 2566): 0.22
Herrerasaurus (PVSJ 373): 0.21
Lagerpeton chanarensis (MCZ 4121): 0.20
Lagerpeton chanarensis (PVL 4619): 0.21
Marasuchus lilloensis (PVL 3870): 0.15
Mesosuchus (SAM-PK-7416): 0.31
Noteosuchus (Carroll, 1976: fig. 5b): 0.29
Nundasuchus (Nesbitt et al., 2014: table 1): 0.30
Ornithosuchus (Walker, 1964: fig. 12c): 0.18
Petrolacosaurus (Reisz, 1981: 45): 0.30
Prestosuchus chiniquensis (UFRGS-PV-0152-T): 0.23
Prolacerta (BP/1/2676): 0.23
Proterosuchus fergusi (SAM-PK-K140): 0.36
Proterochampsa barrionuevoi (Trotteyn, 2011: table 2): 0.18
Protorosaurus (SMNS 55387, cast of Simon/Bartholomäus specimen): 0.23
Riojasuchus tenuisceps (PVL 3827): 0.33
Riojasuchus tenuisceps (PVL 3828): 0.24
Shansisuchus shansisuchus (Young, 1964: table 8, 31a): 0.30

Shansisuchus shansisuchus (Young, 1964: table 8, 31b): 0.28
Shansisuchus shansisuchus (Young, 1964: table 8, 31c): 0.32
Silesaurus opolensis (ZPAL Ab III/361/25): 0.16
Smilosuchus gregorii (Long and Murry, 1995: fig. 36b): 0.20
Tanystropheus longobardicus (SMNS unnumbered): 0.13
Trilophosauurs buettneri (Spielmann et al., 2008: appendix 10, TMM 31025-140): 0.21
Trilophosauurs buettneri (Spielmann et al., 2008: appendix 10, TMM 31025-694): 0.21
Trilophosauurs buettneri (Spielmann et al., 2008: appendix 10, TMM 31025-067): 0.15
Trilophosauurs buettneri (Spielmann et al., 2008: appendix 10, TMM 31025-826): 0.19
Trilophosauurs buettneri (Spielmann et al., 2008: appendix 10, TMM 31025-67-RR): 0.18
Tropidosuchus romeri (PVL 4601): 0.13
Turfanosuchus dabanensis (IVPP V3237): 0.19
Vancleavea campi (AMNH 30884, cast): 0.22
Youngina (BP/1/3859): 0.11

Discretization by the cluster analysis: (1) 0.08-0.11; (2) 0.13-0.24; (3) 0.26-0.36; (4) 0.39-0.41. (5%=0.02).

(477) Femur, distal condyles: prominent, strong dorsoventral expansion (in sprawling orientation) restricted to the distal end (0); not projecting markedly beyond shaft and expand gradually if there is any expansion (1) (Gauthier et al., 1988; Nesbitt, 2011: 318; Dilkes and Arcucci, 2012: 77).

(478) Femur, distal articular surface: uneven, fibular condyle projecting distally distinctly beyond tibial condyle (0); both condyles prominent distally and approximately at same level (1); both condyles do not project distally (distal articular surface concave or almost flat) (2) (Gauthier et al., 1988; Laurin, 1991: B8; modified from Rieppel et al., 1999, and Müller, 2004: 72; Reisz et al., 2010: 102; Ezcurra et al., 2010: 160 in part; Ezcurra et al., 2014: 101).

(479) Femur, anterior extensor groove: absent, posterior margin of the bone straight or convex in distal view (0); present, posterior margin of the bone concave in distal view (1) (Rauhut, 2003).

(480) Femur, surface between the lateral condyle and crista tibiofibularis on the distal surface: smooth (0); deep groove (1) (Rowe, 1989; Nesbitt, 2011: 322).

(481) Tibia, total length versus total length of the femur: 0.46-0.51 (0); 0.60-0.65 (1); 0.70-1.27 (2); 1.41-1.46 (3) (Benton, 2004; modified from Ezcurra et al., 2010: 66; modified from Nesbitt, 2011: 299), CONTINUOUS, ORDERED.

Aetosauroides scagliai (PVL 2052): <0.95
Aetosauroides scagliai (PVL 2073): >0.74
Amotosaurus (SMNS 54810): 1.03
Boreopricea (PIN 3708/1 and Tatarinov, 1978: 511): 0.80
Chanaresuchus bonapartei (MCZ 4035): 0.74
Chanaresuchus bonapartei (PVL 4575): 0.74
"*Chasmatosaurus*" *yuani* (IVPP V2719): 0.88
"*Chasmatosaurus*" *yuani* (IVPP V4067): 0.63
Cuyosuchus (MCNAM PV 2669): <0.79
Dimorphodon (Padian, 1983: table 1, YPM 9182): 1.44
Dorosuchus (PIN 1579/61): 0.74
Euparkeria (SAM-PK-5867): 0.86
Euparkeria (SAM-PK-7696): 0.81
Euparkeria (SAM-PK-7707): 0.83
Gracilisuchus (PVL 4597): 0.91
Gualosuchus (PVL 4576): 0.74
Herrerasaurus (MACN-Pv 18060): 0.90
Herrerasaurus (PVL 2566): 0.87
Herrerasaurus (PVSJ 373): 0.91
Heterodontosaurus (SAM-PK-K1332): 1.14
Jaxtasuchus salomoni (SMNS 91352): 0.72
Jesairosaurus lehmani (ZAR 15): <0.98
Lagerpeton chanarensis (PULR 06): 1.19
Lagerpeton chanarensis (PVL 4619): 1.17
Macrocnemus bessanii (Rieppel, 1989b: table 2, AIII/208): 1.01
Macrocnemus bessanii (Rieppel, 1989b: table 2, PIMUZ T2477): 1.06
Macrocnemus bessanii (Rieppel, 1989b: table 2, PIMUZ T2472): 1.08
Macrocnemus bessanii (Rieppel, 1989b: table 2, PIMUZ T4355): 1.11
Macrocnemus bessanii (Peyer, 1937: 91, Alla Cascina): 0.97
Macrocnemus bessanii (Peyer, 1937: 91, Besano II): 0.99
Macrocnemus bessanii (Peyer, 1937: 94, Tre Fontane 1936): 1.05-1.06
Marasuchus lilloensis (PVL 3870): 1.11-1.19
Marasuchus lilloensis (PVL 3871): 1.22-1.27
Mesosuchus (Haughton, 1921: 87, SAM-PK-6046): 0.98
Mesosuchus (Dilkes, 1998: 518, SAM-PK-7416): 0.83
Noteosuchus (Carroll, 1976: 48): 0.90
Nundasuchus (Nesbitt et al., 2014: table 1, length of fibula instead of tibia): 0.71
Petrolacosaurus (Peabody, 1952: table 4 for KUMNH 1428): 1.16
Prestosuchus chiniquensis (UFRGS-PV-0629-T): 0.82
Prolacerta (Gow, 1975: 111, BP/1/2676): 1.07

Proterochampsa barrionuevoi (Trotteyn, 2011: table 2): 0.70
Protorosaurus (Gottmann-Quesada and Sander, 2009: appendix I, IPB R 535): 0.89
Protorosaurus (Gottmann-Quesada and Sander, 2009: appendix I, Nat. Kab. 191): 0.87
Protorosaurus (Gottmann-Quesada and Sander, 2009: appendix I, NHMW 1943I4): 0.93
Protorosaurus (Gottmann-Quesada and Sander, 2009: appendix I, Simon/Bartholomäus specimen): 0.91
Pseudochampsa ischigualastensis (PVSJ 567): 0.83-0.89
Rhynchosaurus articeps (SHYMS 5): 0.96
Riojasuchus tenuisceps (PVL 3827): 0.83
Silesaurus opolensis (Dzik, 2003: fig. 3): ca. 0.91
Tanystropheus longobardicus (Nosotti, 2007: table 5, MSNM BES SC 265): 0.85-0.88
Tanystropheus longobardicus (PIMUZ T2817): 0.74
Tasmaniosaurus (UTGD 54655): <0.89
Trilophosauurs buettneri (Spielmann et al., 2008: fig. 85b): 0.82
Tropidosuchus romeri (PVL 4601): 0.92
Vancleavea campi (Nesbitt et al., 2009: fig. 15): 0.48
Youngina (SAM-PK-K7710a): 1.00
Youngina (SAM-PK-K7710b): 0.95
Youngina (SAM-PK-K7710d): 0.95
Youngina (SAM-PK-K7710e): 1.00

Discretization by the cluster analysis: (1) 0.46-0.51; (2) 0.60-0.65; (3) 0.70-1.27; (4) 1.41-1.46. (5%=0.05).

(482) Tibia, distinctly anteriorly projected process beyond the articular portion for the femur on the proximal end (= cnemial crest): absent or just a slightly bump (0); present and anteriorly straight (1); present and curved anterolaterally (2) (Gauthier, 1986; Benton and Clark, 1988; Juul, 1994; Ezcurra et al., 2010: 134, in part; Nesbitt, 2011: 328).

(483) Tibia, proximal surface of the lateral condyle: convex or flat (0); depressed (1) (Nesbitt, 2011: 330; Dilkes and Arcucci, 2012: 80).

(484) Tibia, lateral posterior condyle of the proximal end: offset anteriorly from the medial posterior condyle (0); level with the medial posterior condyle at its posterior border (1) (Langer and Benton, 2006; Nesbitt, 2011: 331).

(485) Tibia, lateral surface of the proximal half: smooth (0); with a longitudinal crest (= fibular crest) (1) (Gauthier, 1986; Nesbitt, 2011: 333).

(486) Tibia, posterolateral process (= lateral malleolus) in the distal end: absent (0); present (1) (Novas, 1992; Juul, 1994; reworded from Ezcurra et al., 2010: 135; Nesbitt, 2011: 334). This character is inapplicable if the distal ends of tibia and fibula are fused to each other.

(487) Tibia, posterior surface of the distal end: rounded (0); distinct proximodistally oriented ridge present (1) (Nesbitt, 2011: 336).

(488) Tibia, posterior side of the distal portion: smooth and featureless (0); dorsoventrally oriented groove or gap (1) (Nesbitt, 2011: 337; Dilkes and Arcucci, 2012: 78).

(489) Tibia, lateral side of the distal portion: smooth/rounded (0); proximodistally oriented groove (1) (Novas, 1996; Nesbitt, 2011: 338; Dilkes and Arcucci, 2012: 79). This character is inapplicable if the distal ends of tibia and fibula are fused to each other.

(490) Fibula, proximal end in proximal view: round or slightly elliptical (0); transversely compressed (1) (Nesbitt, 2011: 341).

(491) Fibula, anterior edge of the proximal portion: rounded (0); tapers to a point and arched anteromedially (1) (Nesbitt, 2011: 342).

(492) Fibula, proximal portion in lateral view: symmetrical or nearly symmetrical (0); posterior part expanded posteriorly (1) (Nesbitt, 2011: 343).

(493) Fibula, transverse width at mid-length: subequal to transverse width of the tibia (0); distinctly narrower than transverse width of the tibia (1) (Gauthier, 1986; Juul, 1994; reworded from Ezcurra et al., 2010: 136).

(494) Fibula, area of attachment of the iliofibularis muscle: not on a prominent process (0); on a low, distinct tubercle (1); on a hypertrophied tubercle (2) (modified from Benton, 2004; modified from Ezcurra et al., 2010: 67; Nesbitt, 2011: 339, in part), ORDERED.

(495) Fibula, location of the attachment site of the iliofibularis muscle: near the proximal portion (0); near the midpoint between the proximal and distal ends (1) (Sereno, 1991; Nesbitt, 2011: 340).

(496) Fibula, distal end in lateral view: angled anterodorsally (asymmetrical) (0); rounded or flat (symmetrical) (1) (Nesbitt, 2011: 345).

(497) Proximal tarsals, articulation between astragalus and calcaneum: roughly flat (0); concavoconvex with concavity on the calcaneum (1); concavoconvex with concavity on the astragalus (2); fused (3) (Laurin, 1991: F8; Sereno, 1991; Müller, 2004: 171; Reisz et al., 2010: 107; Nesbitt, 2011: 368 and 370; Ezcurra et al., 2014: 106, in part).

(498) Proximal tarsals, foramen for the passage of the perforating artery between the astragalus and calcaneum (= perforating foramen): present (0); absent (1) (Rieppel et al., 1999; Müller, 2004: 74; Ezcurra et al., 2010: 68; Nesbitt, 2011: 369; Dilkes and Arcucci, 2012: 81; Ezcurra et al., 2014: 212).

(499) Astragalus, crural facets: separated by a non-articular surface (0); continuous (1) (Sereno and Arcucci, 1990; Sereno, 1991; Ezcurra et al., 2010: 69; Nesbitt, 2011: 365; Dilkes and Arcucci, 2012: 82).

(500) Astragalus, tibial facet: concave or flat (0); divided into distinct posteromedial and anterolateral basins (1) (Sereno, 1991; Ezcurra et al., 2010: 73; Nesbitt, 2011: 366; Dilkes and Arcucci, 2012: 86).

(501) Astragalus, ascending process (= anterior ascending process): absent (0); present, occupying most of the anteroposterior depth of the astragalus (1); present, restricted to the anterior half of the astragalar depth (2) (Gauthier, 1986; Novas, 1989; Ezcurra et al., 2010: 137; Nesbitt, 2011: 356) ORDERED.

(502) Astragalus, anterior hollow: shallow depression (0); reduced to a foramen (= extensor canal) or absent (1) (Nesbitt, 2011: 357).

(503) Astragalus, posterior groove: present (0); absent (1) (Sereno, 1991; Gower, 1996; Ezcurra et al., 2010: 138; Nesbitt, 2011: 363)

(504) Astragalus, anteromedial corner in proximal view: obtuse (0); acute (1) (Bonaparte, 1976; Sereno, 1991; Juul, 1994; Ezcurra et al., 2010: 139; Nesbitt, 2011: 361).

(505) Astragalus, dorsolateral margin: overlaps the anterior and posterior portions of the calcaneum equally (0); posterior corner dorsally overlaps the calcaneum much more than the anterior portion (1) (Nesbitt et al., 2009; Ezcurra et al., 2010: 161; Nesbitt, 2011: 360).

(506) Astragalus, articulation with distal tarsal 4: poorly defined (0); well defined (1) (deBraga and Rieppel, 1997; Müller, 2004: 150; modified from Ezcurra et al., 2014: 213).

(507) Calcaneum, articular facet for the astragalus: lies completely medial to the fibular facet (0); lies partially ventral to the fibular facet (1) (Parrish, 1993; Nesbitt, 2011: 358).

(508) Calcaneum, calcaneal tuber: absent or incipient (0); prominent (1) (Gauthier, 1986; Laurin, 1991: F9; Sereno, 1991; Juul, 1994; Müller, 2004: 75; Reisz et al., 2010: 109; Ezcurra et al., 2010: 142; Nesbitt, 2011: 373; Ezcurra et al., 2014: 108).

(509) Calcaneum, orientation of calcaneal tuber: lateral (0); deflected between 21º-49º posterolaterally (1); between 50º-90º posteriorly (2) (Sereno, 1991; Ezcurra et al., 2010: 70, in part; Nesbitt, 2011: 377; Dilkes and Arcucci, 2012: 83), ORDERED. This character is inapplicable in taxa that lack or have an incipient a calcaneal tuber.

(510) Calcaneum, proportions of calcaneal tuber at the midshaft: taller than broad (0); about the same or broader than tall (1); just less than twice the transverse width of the fibular facet (2) (Sereno, 1991; Ezcurra et al., 2010: 74, in part; Nesbitt, 2011: 376; Dilkes and Arcucci, 2012: 87, in part). This character is inapplicable in taxa that lack or have an incipient a calcaneal tuber.

(511) Calcaneum, calcaneal tuber distal end: rounded and unexpanded (0); flared, dorsally and/or ventrally (1) (Sereno, 1991; reworded from Ezcurra et al., 2010: 75; Nesbitt, 2011: 374; Dilkes and Arcucci, 2012: 88). This character is inapplicable in taxa that lack or have an incipient a calcaneal tuber.

(512) Calcaneum, calcaneal tuber distal end in proximal or distal view: tapering or squared (0); expanded (1) (New character). This character is inapplicable in taxa that lack or have an incipient a calcaneal tuber.

(513) Calcaneum, distal surface of calcaneal tuber with a vertical median depression: absent (0); present (1) (Parrish, 1993; Juul, 1994; Ezcurra et al., 2010: 143; Nesbitt, 2011: 375). This character is inapplicable in taxa that lack or have an incipient a calcaneal tuber.

(514) Calcaneum, ventral notch between the main body and the calcaneal tuber: absent (0); present (1) (New character). This character is inapplicable in taxa that lack or have an incipient a calcaneal tuber.

(515) Calcaneum, ventral articular surface for distal tarsal 4 and the distal end of the calcaneal tuber: continuous (0); separated by a clear gap (1); separated by a gap with a laterally and mediall delimited ventral fossa (2) (Nesbitt, 2011: 371), ORDERED. This character is inapplicable in taxa that lack or have an incipient a calcaneal tuber.

(516) Calcaneum, fibular facet: slightly convex or flat (0); hemicylindrical (1); concave (2) (modified from Novas, 1989; Parrish, 1993; Juul, 1994; modified from Ezcurra et al., 2010: 72, 140; Nesbitt, 2011: 378; Dilkes and Arcucci, 2012: 85).

(517) Calcaneum, articular facets for the fibula and astragalus: connected by a continuous surface (0); separated (1) (Nesbitt, 2011: 372).

(518) Calcaneum, articular surfaces for fibula and distal tarsal 4: separated by a non-articular surface (0); continuous (1) (Sereno, 1991; Ezcurra et al., 2010: 71; Nesbitt, 2011: 380; Dilkes and Arcucci, 2012: 84).

(519) Calcaneum, transverse width of the distal articular surface versus transverse width of the astragalus: 0.28-0.33 (0); 0.41-0.48 (1); 0.54-1.22 (2) (modified from Sereno, 1991; Juul, 1994; Ezcurra et al., 2010: 141), CONTINUOUS, ORDERED.

Aetosauroides scagliai (PVL 2052): 1.05
Aetosauroides scagliai (PVL 2073): 1.03
Amotosaurus (SMNS 54783a): 0.85
Azendohsaurus madagaskarensis (UA 8-25-98-231): 0.61
Erythrosuchus (NHMUK R3592): 0.58
Euparkeria (UMZC T692): 0.48
Gracilisuchus (PVL 4597): 0.89
Herrerasaurus (PVSJ 373): 0.30
Howesia (Carroll, 1976: fig. 8): 0.56
Macrocnemus bessanii (PIMUZ T4822): 1.20
Macrocnemus bessanii (Rieppel, 1989b: fig. 8c, PIMUZ T2473): 1.08
Marasuchus lilloensis (Sereno and Arcucci, 1994: fig. 11): 0.42
Mesosuchus (SAM-PK-7416): 0.55
Nundasuchus (Nesbitt et al., 2014: fig. 12a): 0.63

Petrolacosaurus (Reisz, 1981: fig. 24): 0.87
Prestosuchus chiniquensis (UFRGS-PV-0152-T): 0.64
Prolacerta (BP/1/2676): 0.56
Proterosuchus alexanderi (NMQR 1484): 0.44
Protorosaurus (SMNS 55387, cast of the Simon/Bartholomäus specimen): 0.75
Riojasuchus tenuisceps (PVL 3827): 0.73
Silesaurus opolensis (ZPAL Ab III/361/20): 0.41
Smilosuchus gregorii (USNM 18313): 0.54
Tanystropheus longobardicus (Nosotti, 2007: fig. 63, PIMUZ T2480): 0.58
Trilophosauurs buettneri (Spielmann et al., 2008: fig. 91b): 0.71
Tropidosuchus romeri (PVL 4601): 0.44
Vancleavea campi (Nesbitt et al., 2009: fig. 17): 0.46
Youngina (Broom, 1921: fig. 20): 0.74

Discretization by the cluster analysis: (1) 0.28-0.33; (2) 0.41-0.48; (3) 0.54-1.22. (5%=0.045).

(520) Distal tarsals, medial pedal centrale: present and does not contact tibia (0); present and contacts the tibia (1); absent as a separate ossification (2) (deBraga and Rieppel, 1997; Dilkes 1998: 117; Müller, 2004: 151; Ezcurra et al., 2010: 77, in part; Nesbitt, 2011: 381, in part; Dilkes and Arcucci, 2012: 89, in part; modified from Ezcurra et al., 2014: 214), ORDERED.

(521) Distal tarsals, distal tarsal 1: present (0); absent (1) (Gauthier, 1984; Dilkes, 1998; Rieppel et al., 1999; Müller, 2004: 76; Ezcurra et al., 2010: 78, in part; Nesbitt, 2011: 346, in part; Dilkes and Arcucci, 2012: 90, in part; Ezcurra et al., 2014: 215).

(522) Distal tarsals, distal tarsal 2: present (0); absent (1) (Gauthier, 1984; Dilkes, 1998; Ezcurra et al., 2010: 78, in part; Nesbitt, 2011: 346, in part; Dilkes and Arcucci, 2012: 90, in part).

(523) Distal tarsals, distal tarsal 4 transverse width: broader than distal tarsal 3 (0); subequal to distal tarsal 3 (1) (Sereno, 1991; Juul, 1994; Ezcurra et al., 2010: 144; Nesbitt, 2011: 347; Dilkes and Arcucci, 2012: 91).

(524) Distal tarsals, articular facet for metatarsal V on distal tarsal 4: more than half of the lateral surface of the bone (0); less than half of the lateral surface of the bone (1) (Sereno, 1991, in part; Ezcurra et al., 2010: 145, in part; Nesbitt, 2011: 348; Dilkes and Arcucci, 2012: 92, in part).

(525) Distal tarsals, proximal surface of distal tarsal 4: flat (0); distinct, proximally raised region on the posterior portion (= heel of Sereno and Arcucci, 1994) (1) (Nesbitt, 2011: 353).

(526) Distal tarsals, distal tarsal 5: present (0); absent (1) (Laurin, 1991: E13; Reisz et al., 2010: 112; Ezcurra et al., 2014: 111).

(527) Pes, foot length (articulated fourth metatarsal and digit) versus tibia-fibula length: >1 (0); <1 (1) (deBraga and Reisz, 1995: 33, 42; Reisz et al., 2010: 106; cf. Ezcurra et al., 2010: 80; Ezcurra et al., 2014: 105).

(528) Metatarsus, configuration: metatarsals diverging from ankle (0); compact, metatarsals I–IV tightly bunched (1) (Gauthier, 1986; Benton, 2004; Ezcurra et al., 2010: 79; Nesbitt, 2011: 382; Dilkes and Arcucci, 2012: 93).

(529) Metatarsus, metatarsals overlapping proximally: absent (0); present (1) (deBraga and Reisz, 1995: 43; Reisz et al., 2010: 110; Ezcurra et al., 2014: 109).

(530) Metatarsus, length of the longest metatarsal versus length of the tibia: 0.20-0.23 (0); 0.29-0.32 (1); 0.37-0.59 (2); 0.62-0.65 (3) (Sereno, 1991; modified from Nesbitt, 2011: 383; modified from Dilkes and Arcucci, 2012: 94), CONTINUOUS, ORDERED.

Aetosauroides scagliai (PVL 2052): 0.46
Amotosaurus (SMNS 54783): 0.37
Boreopricea (Benton and Allen, 1997: 943, 944): 0.65
Chanaresuchus bonapartei (Romer, 1972e: fig. 2): 0.55
Dimorphodon (Padian, 1983: table 1, YPM 350): 0.31
Euparkeria (SAM-PK-7696): 0.43
Gracilisuchus (PVL 4597): 0.43
Herrerasaurus (PVSJ 373): 0.52

Heterodontosaurus (SAM-PK-K1332): 0.53
Jaxtasuchus salomoni (SMNS 91352): 0.59
Lagerpeton chanarensis (PULR 06): 0.53
Lagerpeton chanarensis (PVL 4619): 0.53
Macrocnemus bessanii (Rieppel, 1989b: table 2, A III/208): 0.52
Macrocnemus bessanii (Rieppel, 1989b: table 2, PIMUZ T2473): 0.42
Macrocnemus bessanii (Rieppel, 1989b: table 2, PIMUZ T2477): 0.52
Macrocnemus bessanii (Rieppel, 1989b: table 2, PIMUZ T2472): 0.47
Macrocnemus bessanii (Rieppel, 1989b: table 2, PIMUZ T4355): 0.45
Macrocnemus bessanii (Peyer, 1937: 91, Alla Cascina specimen): 0.54
Macrocnemus bessanii (Peyer, 1937: 94, Tre Fontane specimen 1936): 0.51
Marasuchus lilloensis (PVL 3870): 0.56
Marasuchus lilloensis (PVL 3871): 0.58
Mesosuchus (SAM-PK-7416): 0.53
Noteosuchus (AM 3591): 0.48
Nundasuchus (Nesbitt et al., 2014: table 1, fibula used instead of tibia): 0.43
Petrolacosaurus (Peabody, 1952: fig. 6a): 0.43
Prestosuchus chiniquensis (UFRGS-PV-0152-T): 0.41
Prolacerta (BP/1/2676): 0.38
Proterochampsa barrionuevoi (Trotteyn, 2011: table 2): >0.50
Protorosaurus (Gottmann-Quesada and Sander, 2009: appendix I, IPB R 535): 0.54
Protorosaurus (Gottmann-Quesada and Sander, 2009: appendix I, Nat. Kab. 191): 0.21
Protorosaurus (Gottmann-Quesada and Sander, 2009: appendix I, NHMW 1943I4): 0.45-0.51
Protorosaurus (Gottmann-Quesada and Sander, 2009: appendix I, Simon/Bartholomäus specimen): 0.47
Pseudochampsa ischigualastensis (PVSJ 567): 0.39-0.43
Rhynchosaurus articeps (SHYMS 5): 0.51
Rhynchosaurus articeps (NHMUK R1238): 0.52
Riojasuchus tenuisceps (PVL 3827): 0.45
Silesaurus opolensis (Dzik, 2003: fig. 4): 0.51
Tanystropheus longobardicus (Nosotti, 2007: table 5, MSNM BES SC 1018): 0.51
Tanystropheus longobardicus (Nosotti, 2007: table 5, MSNM BES SC 265): 0.50-0.51
Tasmaniosaurus (UTGD 54655): >0.41
Trilophosauurs buettneri (Spielmann et al., 2008: figs. 85b, 91a): 0.43
Tropidosuchus romeri (PVL 4601): 0.49
Tropidosuchus romeri (PVL 4606): 0.52
Vancleavea campi (Nesbitt et al., 2009: fig. 15): 0.63
Youngina (Smith and Evans, 1996: table 1, SAM-PK-K7710a): 0.54
Youngina (Smith and Evans, 1996: table 1, SAM-PK-K7710d): 0.50

Discretization by the cluster analysis: (1) 0.20-0.23; (2) 0.29-0.32; (3) 0.37-0.59; (4) 0.62-0.65. (5%=0.022).

(531) Metatarsus, metatarsals I and V mid-shaft diameters: subequal or greater (0); lower (1) than those of metatarsals II–IV (Sereno, 1991; Juul, 1994; Ezcurra et al., 2010: 146, 162; Nesbitt, 2011: 384).

(532) Metatarsus, length of metatarsal I versus metatarsal III: 0.17-0.21 (0); 0.27-0.33 (1); 0.38-0.42 (2); 0.46-0.79 (3); 0-93-0.97 (4) (modified from Sereno, 1991; Dilkes 1998: 123; Müller, 2004: 173; Modesto and Sues, 2004: 123; cf. Ezcurra et al., 2010: 147; modified from Nesbitt, 2011: 387; modified from Ezcurra et al., 2014: 216), CONTINUOUS, ORDERED.

Aetosauroides scagliai (PVL 2052): 0.69-0.74
Amotosaurus (SMNS 54783a): 0.58
Azendohsaurus madagaskarensis (UA 7-13-99-576): 0.68
Azendohsaurus madagaskarensis (UA 8-28-98-295): 0.65
Chanaresuchus bonapartei (Romer, 1972e: fig. 2): 0.42
Dimorphodon (Nesbitt, 2011: character 387): ≥0.85
Euparkeria (SAM-PK-7696): 0.63
Euparkeria (SAM-PK-8309): 0.56
GHG 7433MI: ca. 0.61
Gracilisuchus (PVL 4597): 0.79
Herrerasaurus (PVSJ 373): 0.61
Heterodontosaurus (SAM-PK-K1332): 0.56
Lagerpeton chanarensis (PULR 06): 0.17
Lagerpeton chanarensis (PVL 4619): 0.20
Macrocnemus bessanii (Peyer, 1937: 91, Alla Cascina specimen): 0.46
Macrocnemus bessanii (Peyer, 1937: 93, Besano III specimen): 0.75
Macrocnemus bessanii (Peyer, 1937: 94, Tre Fontane specimen 1936): 0.56-0.57
Macrocnemus bessanii (PIMUZ T4822): 0.46
Macrocnemus bessanii (PIMUZ T4355): 0.56
Marasuchus lilloensis (PVL 3870): 0.50
Mesosuchus (SAM-PK-7416): 0.41
Noteosuchus (AM 3591): 0.39
Nundasuchus (Nesbitt et al., 2014: table 1): 0.63
Petrolacosaurus (Reisz, 1981: fig. 24a): 0.56
Prolacerta (BP/1/2676): 0.72
Proterosuchus fergusi (SAM-PK-K140): 0.47
Protorosaurus (Gottmann-Quesada and Sander, 2009: appendix I, Nat. Kab. 191): 0.53
Protorosaurus (Gottmann-Quesada and Sander, 2009: appendix I, NHMW 1943I4): 0.47-0.48
Protorosaurus (Gottmann-Quesada and Sander, 2009: appendix I, NMK S180): 0.53
Protorosaurus (Gottmann-Quesada and Sander, 2009: appendix I, NMK S180): 0.54

Protorosaurus (Gottmann-Quesada and Sander, 2009: appendix I, PSM 7): 0.56
Protorosaurus (Gottmann-Quesada and Sander, 2009: appendix I, Simon/Bartholomäus specimen): 0.51
Pseudochampsa ischigualastensis (PVSJ 567): 0.32-0.33
Rhynchosaurus articeps (SHYMS 5): 0.42
Rhynchosaurus articeps (NHMUK R1238): 0.38
Riojasuchus tenuisceps (PVL 3827): 0.60
Tanystropheus longobardicus (Nosotti, 2007: table 5, MSNM BES SC 1018): 0.74
Tanystropheus longobardicus (Nosotti, 2007: table 5, MSNM BES SC 265): 0.66
Trilophosauurs buettneri (Spielmann et al., 2008: fig. 91a): 0.52
Tropidosuchus romeri (PVL 4601): 0.28
Tropidosuchus romeri (PVL 4606): 0.27
Vancleavea campi (Nesbitt et al., 2009: 836): 0.71-0.95
Youngina (Smith and Evans, 1996: table 1, SAM-PK-K7710b): 0.40
Youngina (Smith and Evans, 1996: table 1, SAM-PK-K7710d): 0.40
Youngina (Broom, 1921: fig. 20): 0.55

Discretization by the cluster analysis: (1) 0.17-0.21; (2) 0.27-0.33; (3) 0.38-0.42; (4) 0.46-0.79; (5) 0-93-0.97. (5%=0.04).

(533) Metatarsus, anteromedial portion of the shaft of the metatarsal I: smooth or slight ridge (0); distinct, rugose ridge present (1) (Nesbitt, 2011: 386).

(534) Metatarsus, length of the metatarsal II versus length of the metatarsal IV: 0.52-0.56 (0); 0.60-0.85 (1); 0.90-1.02 (2); 1.06-1.15 (3) (Gauthier, 1986; modified from Nesbitt, 2011: 395), CONTINUOUS, ORDERED.

Aetosauroides (PVL 2073): 0.98
Aetosauroides (PVL 2052): 0.95
Amotosaurus (SMNS 54783a): 0.76
Amotosaurus (SMNS 90563): 0.83
Azendohsaurus madagaskarensis (Nesbitt unpublished data): 0.83
Chanaresuchus bonapartei (Romer, 1972e: fig. 2f): 0.79
Dimorphodon (NHMUK R): 1.06
Erythrosuchus (BP/1/2096): 1.15
Euparkeria (GPIT 1681/1): 0.85
Euparkeria (SAM-PK-K8309): 0.91
GHG 7433MI: 0.84
Gracilisuchus (PVL 4597): 0.97
Herrerasaurus (PVSJ 373): 0.99
Heterodontosaurus (SAM-PK-K1332): 0.97
Lagerpeton (PULR 06): 0.52
Lagerpeton (PVL 4619): 0.53
Macrocnemus (PIMUZ T4822): 0.67
Macrocnemus (PIMUZ T4355): 0.73

Macrocnemus (PIMUZ T2472): 0.71
Marasuchus (PVL 3870): 0.90
Marasuchus (PVL 3871): 0.93
Mesosuchus (SAM-PK-7416): 0.63
Noteosuchus (AM 3591): 0.63
Ornithosuchus (NHMUK R2410): 1.00
Petrolacosaurus (Reisz, 1981: fig. 21): 0.56
Proterosuchus fergusi (SAM-PK-K140): 0.77
Protorosaurus (Gottmann-Quesada and Sander, 2009: appendix 1, IPB R 535): 0.61-0.67
Protorosaurus (Gottmann-Quesada and Sander, 2009: appendix 1, Nat. Kab. 191): 0.74
Protorosaurus (Gottmann-Quesada and Sander, 2009: appendix 1, NHMW 1974/1635): 0.63-0.68
Protorosaurus (Gottmann-Quesada and Sander, 2009: appendix 1, NMK S 180): 0.64
Protorosaurus (Gottmann-Quesada and Sander, 2009: appendix 1, NMK S182): 0.68
Prolacerta (Gow, 1975: fig. 24g): 0.75
Rhynchosaurus articeps (NHMUK R1238): 0.72
Pseudochampsa (PVSJ 567): 1.02
Riojasuchus (PVL 3827): 0.93
Silesaurus (ZPAL AbIII/363): 1.00
Tanystropheus (Nosotti, 2007: table 7): 0.95
Trilophosaurus (Spielmann et al., 2008: fig. 91a): 0.71
Tropidosuchus (PVL 4601): 0.84
Tropidosuchus (PVL 4606): 0.82
Youngina (SAM-PK-K7710a): 0.60
Youngina (SAM-PK-K7710d): 0.61

Discretization by the cluster analysis: (1) 0.52-0.56; (2) 0.60-0.85; (3) 0.90-1.02; (4) 1.06-1.15. (5%=0.031).

(535) Metatarsus, metatarsal II midshaft diameter: less than or equal to the midshaft diameter of the metatarsals I-IV (0); more than the midshaft diameter of metatarsal I (1) (Nesbitt et al., 2009; Nesbitt, 2011: 388; Dilkes and Arcucci, 2012: 95).

(536) Metatarsus, metatarsal IV mid-shaft diameter: subequal to (0); lower than (1) that of metatarsal III (Nesbitt et al., 2009; Ezcurra et al., 2010: 163; Nesbitt, 2011: 394; Dilkes and Arcucci, 2012: 96).

(537) Metatarsus, length of metatarsal IV versus length of metatarsal III: 0.85-1.00 (0); 1.04-1.08 (1); 1.11-1.28 (2); 1.31-1.34 (3) (Laurin, 1991: F10; Reisz et al., 2010: 111; Ezcurra et al., 2010: 164; modified from Nesbitt, 2011: 393; modified from Dilkes and Arcucci, 2012: 97; modified from Ezcurra et al., 2014: 110), CONTINUOUS, ORDERED.

Aetosauroides scagliai (PVL 2052): 1.00
Amotosaurus (SMNS 54783a): 1.15
Azendohsaurus madagaskarensis (UA 7-13-99-576): 1.07
Azendohsaurus madagaskarensis (UA 8-28-98-295): 1.08
Boreopricea (Benton and Allen, 1997: 944): 1.04
Chanaresuchus bonapartei (Romer, 1972e: fig. 2): 0.95
Dimorphodon (Padian, 1983: table 1, YPM 350): 0.98
Erythrosuchus (BP/1/2096): 0.94
Euparkeria (SAM-PK-7696): 1.06
Euparkeria (SAM-PK-8309): 0.91
GHG 7433MI: ca. 1.00
Gracilisuchus (PVL 4597): 0.95
Herrerasaurus (PVSJ 373): 0.87
Heterodontosaurus (SAM-PK-K1332): 0.90
Lagerpeton chanarensis (PULR 06): 1.12
Lagerpeton chanarensis (PVL 4619): 1.13
Macrocnemus bessanii (Peyer, 1937: 91, Alla Cascina specimen): 1.16
Macrocnemus bessanii (Peyer, 1937: 94, Tre Fontane specimen 1936): 1.17-1.19
Macrocnemus bessanii (PIMUZ T4822): 1.16
Macrocnemus bessanii (PIMUZ T4355): 1.13
Marasuchus lilloensis (PVL 3870): 0.99
Marasuchus lilloensis (PVL 3871): 0.89
Mesosuchus (SAM-PK-7416): 1.18
Noteosuchus (AM 3591): 1.22
Petrolacosaurus (Reisz, 1981: fig. 24a): 1.26
Prolacerta (BP/1/2676): 1.24
Proterosuchus fergusi (SAM-PK-K140): 1.11
Protorosaurus (Gottmann-Quesada and Sander, 2009: appendix I, IPB R 535): 1.23-1.33
Protorosaurus (Gottmann-Quesada and Sander, 2009: appendix I, Nat. Kab. 191): 1.00
Protorosaurus (Gottmann-Quesada and Sander, 2009: appendix I, NHMW 1943I4): 1.16-1.24
Protorosaurus (Gottmann-Quesada and Sander, 2009: appendix I, NMK S180): 1.16
Protorosaurus (Gottmann-Quesada and Sander, 2009: appendix I, PSM 7): 1.26
Protorosaurus (Gottmann-Quesada and Sander, 2009: appendix I, Simon/Bartholomäus specimen): 1.20
Pseudochampsa ischigualastensis (PVSJ 567): 0.85-0.92
Rhynchosaurus articeps (SHYMS 5): 1.13

Rhynchosaurus articeps (NHMUK R1238): 1.17
Riojasuchus tenuisceps (PVL 3827): 0.93
Silesaurus opolensis (ZPAL AbIII/361): 0.85
Tanystropheus longobardicus (Nosotti, 2007: table 5, MSNM BES SC 1018): 0.96
Trilophosauurs buettneri (Spielmann et al., 2008: fig. 91a): 1.22
Tropidosuchus romeri (PVL 4601): 0.96
Tropidosuchus romeri (PVL 4606): 0.99
Youngina (Smith and Evans, 1996: table 1, SAM-PK-K7710a): 1.18
Youngina (Smith and Evans, 1996: table 1, SAM-PK-K7710d): 1.20
Youngina (Broom, 1921: fig. 20): 1.28

Discretization by the cluster analysis: (1) 0.85-1.00; (2) 1.04-1.08; (3) 1.11-1.28; (4) 1.31-1.34. (5%=0.024).

(538) Metatarsus, distal articular surface of metatarsal IV: broader than deep (nearly symmetrical) (0); as broad as deep as or deeper than broad (asymmetrical) (1) (Sereno, 1999; Nesbitt, 2011: 391).

(539) Metatarsus, dorsal prominence separated from the proximal surface by a concave gap in metatarsal V: absent (0); present (1) (Nesbitt, 2011: 397).

(540) Metatarsus, metatarsal V with a hook-shaped proximal end: absent, articular face for distal tarsal 4 aligned to the medial margin of the shaft (0); present, with a gradually medially curved proximal process (1); present, with a sharply medially flexed proximal process and, as a result, the metatarsal acquires a L-shape in dorsal or ventral view (2) (Laurin, 1991: E14; Sereno, 1991; Juul, 1994; Müller, 2004: 80; Reisz et al., 2010: 113; Ezcurra et al., 2010: 148; Nesbitt, 2011: 398; Dilkes and Arcucci, 2012: 98; modified from Ezcurra et al., 2014: 112).

(541) Metatarsus, metatarsal V lateral plantar tubercle in mature individuals: absent (0); present (1) (Ezcurra et al., 2014: 217).

(542) Metatarsus, metatarsal V medial plantar tubercle in mature individuals: absent (0); present (1) (deBraga and Rieppel, 1997; Müller, 2004: 172; Ezcurra et al., 2014: 218).

(543) Pedal digits, length of digit III versus length of digit IV: 0.64-0.77 (0); 0.82-0.83 (1); 0.87-1.44 (2) (Dilkes, 1998: 124; Ezcurra et al., 2010: 81; modified from Ezcurra et al., 2014: 219), CONTINUOUS, ORDERED.

Amotosaurus (SMNS 54783b): 0.83
Azendohsaurus madagaskarensis (UA 8-25-98-231): ca. 0.94
Chanaresuchus bonapartei (Romer, 1972e: fig. 2): 1.42
Heterodontosaurus (SAM-PK-K1332): ca. 1.00
Lagerpeton chanarensis (PVL 4619): 0.87
Petrolacosaurus (Peabody, 1952: fig. 9): 0.64
Prolacerta (BP/1/2676): 1.06
Protorosaurus (SMNS 55387, cast of Simon/Bartholomäus specimen): 0.77
Protorosaurus (NHMW 1943I4): 0.82
Rhynchosaurus articeps (SHYMS 5): 0.82
Tanystropheus longobardicus (Nosotti, 2007: table 5, MSNM BES SC 1018): 0.90
Tanystropheus longobardicus (PIMUZ T2817): 0.88
Trilophosauurs buettneri (Spielmann et al., 2008: fig. 91a): 0.73
Youngina (Smith and Evans, 1996: fig. 8a): 0.72

Discretization by the cluster analysis: (1) 0.64-0.77; (2) 0.82-0.83; (3) 0.87-1.44. (5%=0.04). Values between 0.87 and 1.44 were merged together because they were not informative discretized separately.

(544) Pedal digits, phalanges on pedal digit V: present and “fully” developed first phalanx (0); present and “poorly” developed first phalanx (1); absent (2) (Gauthier, 1984; Juul, 1994; Ezcurra et al., 2010: 82; Nesbitt, 2011: 399; Dilkes and Arcucci, 2012: 99, in part), ORDERED.

(545) Pedal digits, ratio of lengths of pedal digits V and I: 0.30-0.85 (0); 1.37-3.07 (1) (Juul, 1994; modified from Ezcurra et al., 2010: 83; modified from Dilkes and Arcucci, 2012: 100), CONTINUOUS, ORDERED. This character is inapplicable in taxa lacking digit V.

Amotosaurus (SMNS 54783a): 1.84
Azendohsaurus madagaskarensis (UA 8-25-98-231): 1.45
Euparkeria (SAM-PK-8309): 0.78
Herrerasaurus (PVSJ 373): 0.37
Macrocnemus bessanii (PIMUZ T4822): 1.73
Petrolacosaurus (Peabody, 1952: fig. 9): 1.91
Prolacerta (BP/1/2676): 1.87

Protorosaurus (SMNS 55387, cast of Simon/Bartholomäus specimen): 1.42
Protorosaurus (NHMW 1943I4): 1.86
Protorosaurus (Gottmann-Quesada and Sander, 2009: fig. 24, PSM 7): 1.44
Tanystropheus longobardicus (Nosotti, 2007: table 5, MSNM BES SC 265): 3.07
Tanystropheus longobardicus (Nosotti, 2007: table 5, MSNM BES SC 1018): 2.90
Trilophosauurs buettneri (Spielmann et al., 2008: fig. 91a): 1.74
Youngina (Smith and Evans, 1996, fig. 8a): 2.11

Discretization by the cluster analysis: (1) 0.30-0.85; (2) 1.37-3.07. (5%=0.135).

(546) Foot, phalanx V-1: subequal or shorter than other non-ungual phalanges (0); metatarsal-like, considerably longer than other non-ungual phalanges (1) (taken from Fraser and Rieppel, 2006; new character for quantitative phylogenetic analysis). This character is inapplicable in taxa lacking a fifth digit.

(547) Pedal digits, pedal unguals: weakly transversely compressed, rounded and triangular in cross-section (0); dorsolaterally compressed (1); strongly transversely compressed, with a sharp dorsal keel (2) (Sereno, 1991; Nesbitt, 2011: 400).

(548) Osteoderms, dorsal osteoderms: absent (0); present, one row (1); present, two rows (2); present, more than two rows (3) (Bennett, 1996; modified from Ezcurra et al., 2010: 84; Nesbitt, 2011: 401 and 402; Dilkes and Arcucci, 2012: 101 and 102), ORDERED.

(549) Osteoderms, sculpture on their external surface: absent (0); present (1) (Parrish, 1993; Ezcurra et al., 2010: 149). This character is inapplicable in taxa that lack osteoderms.

(550) Osteoderms, coarse and incised ornamentation composed of central regular pits of subequal size and contour on the external surface of the dorsal osteoderms: absent (0); present (1) (Desojo et al., 2011: 91). This character is inapplicable in taxa that lack osteoderms or sculpture on the external surface of the osteoderms.

(551) Osteoderms, dorsal prominence in paramedian osteoderms: absent (0); longitudinal keel, extending along all or most of the anteroposterior length of the osteoderm as a transversely compressed flange (1); blunt, anteroposteriorly restricted eminence (2) (modified from Schoch and Sues, 2013: 116).

(552) Osteodemrs, paramedian osteoderms: thin (0); very thick (1) (Desojo et al., 2011: 90). This character is inapplicable in taxa that lack osteoderms.

(553) Osteoderms, relation between paramedian dorsal osteoderms and presacral vertebrae: one to one (includes pairs) (0); more than one osteoderm (1) (Gauthier, 1986; Benton and Clark, 1988; Nesbitt, 2011: 410). This character is inapplicable in taxa that lack osteoderms.

(554) Osteoderms, dorsal osteoderm alignment dorsal to the dorsal vertebrae: staggered (0); one to one (1) (Nesbitt, 2011: 411). This character is inapplicable in taxa that lack osteoderms or have a single row of osteoderms.

(555) Osteoderms, dimensions of presacral dorsal osteoderms: square-shaped, about equal dimensions (0); longer than wide (1); wider than long (2) (Nesbitt, 2011: 407). This character is inapplicable in taxa that lack osteoderms.

(556) Osteoderms, unornamented anterior articular lamina in paramedian osteoderms: absent (0); present (1) (Desojo et al., 2011: 92). This character is inapplicable in taxa that lack osteoderms.

(557) Osteoderms, anterior edge of paramedian presacral dorsal osteoderms: straight or rounded (0); with a distinct anterior process (= leaf shaped) (1) (Clark et al., 2000; Nesbitt, 2011: 403). This character is inapplicable in taxa that lack osteoderms.

(558) Osteoderms, presacral paramedian osteoderms with a distinct longitudinal bend near the lateral edge: absent (0); present (1) (Clark et al., 2000; Nesbitt, 2011: 404). This character is inapplicable in taxa that lack osteoderms.

(559) Osteoderms, appendicular osteoderms: absent (0); present (1) (Heckert and Lucas, 1999; Nesbitt, 2011: 405).

(560) Osteoderms, ventral osteoderms: absent (0); present, scattered, not forming a carapace (1); present, forming a carapace (2) (Heckert and Lucas, 1999; Ezcurra et al., 2010: 85; Nesbitt, 2011: 409, in part; Dilkes and Arcucci, 2012: 103, in part).

Appendix 9

TNT file of the data matrix of Chapter 5

xread
560 95
Petrolacosaurus_kansensis 0000110000010-000010100000020000010---0[1
2]10000-0--10---0--0--000-0001000300000-0-000--0000000-0000-?03?1001100-0-
000000000-000000-0000--000?001??3??11010-0-010000000000-0-
0?000100000000000110?000001000100?0000??0000-10?00?2?0?????100[0
1]?????????0-000-000010101-01000010-00100000000000000000100000?00000020--
001011000?00110010100-0110200000???2[0
1]11001000?030000?00?0?0010100?1000-
0001000000000?100001001012?000110000000?020000000?000010011100000020-
10-20?001?0000?????000011---??2001?200?00000??000?00000000??000-------
000200001000012O3?0002?10??001000----------00
Acerosodontosaurus_piveteaui 0?0?????????0-
?0?0????????????????????????????-???--?????--0???0??10004???????-010--
0011000-
??00000?0????1?1???000??00????00?0????????0001???????????1??????????????0-
??0????????????????????0???0??
00-????2?????????00??10??0?????00??00000000?0000?10000000--
???????????001???0-?0?0011?01000000001-
001????1??????0????????????????????0??????????????????????101000-
?00?1100000??0100???00?200-01000000?001020-00-????0?1?000??-??000010---
?0??1???0?????????0??0---
-------00
Youngina_capensis ?0000-0000010-000011?000000101O0?11110-0300000-1--00--
-00-0--00??0001000310000-0-010--??10100-10100000000001101-0-000100100-
10000101010000001001002001101O-0-
010000000002000?000001000000100101000?00100011010001100000-1000002-
0000001000?000001000-000-00?010?[0 1]??0?0000110?0000001?0001000[0 1]0[0
1]000?00?10000000--0?0????00000010000-00-0?11000000000001-001?002[0
1]10000120101O0?0?0001100-?000010001000000011101000-
00?1110?00102010000000200-000001100001020-00-0010011000000-0100??10---
?00111?200?00??????0??100000????000-------0002000010000120[2
3]01002?00000010?10-001-200000
Paliguana_whitei ??000-01????0-?000???0????????????????0????????-???--
?????--???????1?????0?????-0??--???0100-?0??????????0?10?00-
??10000?010000010????????1000??????2-??00????00002-
1??22?0?????????0?????????2????????????????????????0????????????????????????
??0-??0-
?0??00???????00???0?0?????????????200000????????????????????????????????
??
??
??
?

Planocephalosaurus_robinsonae 0?000-0?00000-00?0?01000000201000100---
0210?00-?--10---1011--000-0001000200000-0-010--??00001-0010010?0000010100-
??11000200000001000010001010000-----2-10010-0100??2-
10022?00?000011001012-000020?0?0???0????????0??0010-
10??0?0?000???101????????????0[2 3]0-?02200?01??0000--2010000-
01????130020[0 1]000?00?00000000--
???001?00??001???0?01?00?2?00000001011?001?0021???00??0001010000101100-
101?01??0??0???0????100??????????????????????????000?00-010010101000000-0--
10??0????0???-???00010---?0?1???????0???????????3100001??1?0-------
0?0??????????????????0111?????????????????
Gephyrosaurus_bridensis 0?00110100010-0000?00000000101000100---0110?00-
1--10---1001--000-0001000400000-0-010--0000001-0010000-0000110000-
00110002000000010001010000000[0 1]000-02-10010-01000?2-
10021000?000011001011-0010200010???0??????000??0010-
10000?0?000??01010?00????????020-000200101-[1
2]10000120100101010??120020001 0?00?000000?????000?0000000000?0?01?00?
3001000001011?001?0011?0??01[0 1]0?0?0?100???11?0-
100001??0??0???0???1100??????????????????????????0?0?00-0?0000001???000-1--
???00??00?0?????000011---?0?1???????0?????0?000?310000?0?1?0-------
0?0?????00?????????????1111?[0 1]???????????????
Aenigmastropheus_parringtoni
??
??
??
??0101110000[0
2]???????????0?001??????????1???100?1000????????????????????????????????????
??????????????????111002000??
??
??????????????????????????????
Protorosaurus_speneri?0000-0000010-010011??0000020100?10110-0300?00-1--10--
-1??0--00??0001000320000-0-01?--0000000-000?100-00000100-0-??0000000-
0100010001?10000000??????2-[0 1]02-0-[0 1 2]?1000??10012?00????2??????[0
1]????????????010?011010???????0????????????????????????????000-
?0?20000???10000020000?0001?????000[0 1]00000?11011110020--0?[0
1]0011?0000[0
1]10011311?2110?10001?001010101?00000000?1000000110?0000110-
?0000000?0010?00001[1 2]11101201?01100000011202?0010????0[0
1]?0?000??00??1?20-?0-????01?00?0??-???0??10---
?1101??20???000???010??2000001??000-------00020000001001[0 2]030100[0 2
3]?1100[0 1]01000----------00
Amotosaurus_rotfeldensis 0-?0100?????????10????[0
1]0?0??????????????110?00-
????0???110???00??000?0003????????0???????0000?000?000-
0?0?1?0??20?
0?003--00102?????????????????????0????????0?0?0?????0?00???????????000-
00?200?01?0?0000??0000???0?????10001001?0111?1100?100--
1??111200?00010?11-11?211[1 2]00?001???001-[0
1]010002?20????01?001000?0000?00-?????????1??0?000??10??1-1?[0
1]?0?100?????000?????0???0100111000010011 00-0--10??0???0???????000010---

?1??1??20?????????01????0??0????0?0-------00022101??1111203?1002?01??1?11[0
1]0----------00
Macrocnemus_bassanii 00000-0100010-
0000?10?0000120000?002100010??00-?--1?---1101--00??00010003?0?0?-?-0?0--
???0000-00???????000110100-0100010000010010?00????????0????????01200-2-
100????0?1???0?00?0??0???0??
???????????000-?0?0?000????0000????00?00???????000000000111?1?100100--
1??1111?0?11011111-[0 1]1?21130?0001000001-
1010102120?00101?001?00?0??0?00-10110000000?0??00??10111-0-000[1
2]100????110?000000?01010011101[0 1]01001020-00?10??01[1 2]?0?0?????00000-
---?1??1??2???00??0??010??0000001??000-------
00021100001111203?1002?1211?01000----------00
Tanystropheus_longobardicus 0-000-0100010-0[0
1]1001?00000120000?002100010??00-0--00---1101--000-3001000120000-0-010--
0000100-001?000-0010111000-01110[0 1]01000[0 1]0001000-1001----00-----
??11200-0[0 2]100?2-10011000?0[0 1]0201[0 1]000[5 6]-2-
010200??001010100???00?00?01?10?????????0??0000?????10??0-000-?00200001-
0100001200000000l?01110[0 1][0 1][0 1 2]0010[0 1]111011110100--
2?1111300011011011-11?212?200001000001-10[0 1]000?1[1 2 3]10001011001[0
1]00?0000?00-10???0?0?0010??00??10111-0-0?0[0
1]10001111001010010?02010021120[0 1]01001100-0--10??011100000-01000010---
?11011020???000???000?10000001??100-------
00022110001111203?2000?0110201100----------00
Jesairosaurus_lehmani 0?000-00????0-?000[1 2
3]1?000?0140???????????100?00-?-?10--?1001--00??00010002???????-010--
??00001-0010000-0???[0 1]101-0-??0100020-1100?100000000000????????2-010-0-
00000???10?12?00????????0?03--
00102?????0?0??11????????0?1??1???0?0?0?????????????????????000-00?210?01-
0???00120000??101?????[0 4]0010???01???00?0?000--1?[1 2]0000????001???0-
?????200[0 1]00000??[0 1]01-10?00??1100???00?0201???0101?00-
10110001?1?10??00??10101-?????????????????????????0??0[1 2][0
1]0?1000000?01100-0--?0?00???0???????????0----?0?????[0 1
2]????????1?110???0----------
00
Azendohsaurus_madagaskarensis 0?000-0110010-0100112000001100101--
20000200?00-0--10---1[0 1]00--100-00010001?000?-0-01?----00000-0010000-
0??01100011??000000011100010l0?0?00000011000-1??00000-0210002-
10?12001001020101102-
1001010000001010010200001011010000?012??????0??00???0?11??10000-
002200101?010000?1??01?1001?01111002210011?11011110000--100001[0
1]20011?10011-11?[1 2]110000101110101-10000001100001[0
1]1101010000000000-?0000l010?01100000211110110011[0
1]??000001??0201110000?020011000[0 1]00?000111000?0?00??000000001000011-
--
?020010?00100000100?0?0200000000001100000000020000001?01?030100100210
201000----------00
Trilophosaurus_buettneri ??000-0100010-0[0 1]010?21001-120001??02000?50-
000-0-010---1101--10??01010001?1000-0-010--???1001-00?0?-??-010110000-
??00000001?000010?0-1001----11?-?-?2-00200-??10002-10012001?????1?1??06---
0??????1?0101001030000101111000?010??00???0000???????????020-

102210?01?0110001101000000??0111100200000?11000110000--
0?1000010011?10001-01?111[0 1]000-11000001-00100001100001?000[1
2]010000001000-100000011?0100001011111011001011000100120200110000[2
3]00-0110[0 1]0000001000-1--10000110000010010000011---
?0100002001000001001O?0200000??000110000000002000000100120 3?1002?02??0
01000----------00
Noteosuchus_colletti
??
??
??
??1???????0?[0
1]??????????????????????????21000??1????01?0?100021200?0?0?????????????????
????????????????????????????????0????0001?1?2?00010??200-0110[0
1]000000??2????01??00??100000-01000010---
?020110200100000??01???200000?000010000000000?[0
1]000001?01202?1002?1210?0?000----------00
Mesosuchus_browni 0000100110210-0010101000201111001--21001400?00-0-010-
--1001--00100101010?00000-0-010--0100000-0010000-
00001000010??10101001000101000000000001001000-20010010-0010002-
100120000001100000000000112010110100011120 0?01?10110100?0101000??0010
0?????110?0-000-00?000?01-[1
2]00210021011001010???0400200010?11?00000000--1?1000010010010000-
1??1110000?010??101-0010001120[2 3]??00000[1 2]0100?0000?00-
10100001000?????????1111-0-
00??1000?????0?00?0?0003010010000100001011301000000??100000-01000010---
?020110200100000 10?10?12000000?000100000000002100000 1?012020100 2?12?0?
0?000----------00
Howesia_browni 0?00100010?????[0 1]10[0 1]??00??????????????1?????0-
????????[1 2]??1??00??1??1111-?0100?0?010????00000?01?0000-00001000-
10001010?00-000?01000?0000000?0??????0?102-0-1??00?2-1?0120?0?????0?00[0
1]00100010201001010 0?1?1????0???01???00?0?0?000???0000?????????0-?[0 1]0-
????????1????21??21??1?01???????10020001 0?1?????????????[1
2]000??????????????????0?00??1???1???0??00021?0[1
2]0?0011??0?00??00??????01001?????1???????[0
1]01??????????????????????????0?0?0100100000000001021?11010??0???0?000-
0??00010---
?0?011??00100000?0010?120000?0?00010?000000002100000 1?01?0???00??12???0
?0?0----------??
SAM_PK_K10159 ??00??00???????010[0
1]??????????????????????????11?????????????0???1??1111-
??????????????100000?0110000-0???????-??00[0 1]??0100-
100101000000000010010010200 1?2-????1??02-1??1200000??2???0??[0 2
5]???0????????0?0??11??00-???1????1-
[1
2]??21002101 1?1101?????1??2000101??
??
??
??
Rhynchosaurus_articeps 0000100010210-00200010-12-1-2-000--200025--
?0111-010---1001--00??1101111-10100-0-010--0100100-0011000-00000000-

11??1000100-1001010000100000000100102011102-0-2-10002-
1001?00000??30?10006---
0102??1111??001????????0?01??0???01??000??00000???0?1?????110-?0?100001-
[1 2]0122002?0?10010100??010020001011??00000000--1?????0?0?0?010000-
11???1?000?0100000?-1??00021?0[0
1]0?00100101?0?0000001110100001000102?0000221111-
0?00011000???1?01?0?010?0?0100?001[0 1]000?010?0-
0??10??0?2?0????????00010---00??[0
1]??20???0000???1????2?000?0??0?10?0??00000?100?0??001202?1002?11?01??000-
---------00
Bentonyx_sidensis 0?000-0010210-00200010-12-1-2-000--200025--?0101-010---
100?--00??1?01111-10100-0-010--01?1000-00?1?????0000000-11??1010100-
100101000?10?00???0??????11102-0-2-10002-1001?000?01130?10006---
01?2?????1???011?[0 2]0???1?10110000?010?0?????0100???????????110-
?0?100?01-
??122????0?1??????????1??200010??
??
??
??
Eorasaurus_olsoni
??
??
??
??11?11100??[0
2]?????????100?0[0
1]11????011??1?????1?1???
??
??
???????????
Prolacertoides_jimusarensis 0??0??0?00?10-???????00??????????????0????00-?-
???--?1000--0???2?010002?00?0?0-010--???0000-
?????????010??
??00?30?10?0????01??00000??
??????????????????????????????????[0
4]??1000??
??
??
??
Prolacerta_broomi 00000-0100010-000011100120121O?00?021000100000-?-010-
--10?0--000-000100031000?-0-010--0000100-00100[0 1]0-[0 1]000110100-
0010000000000001010000000000001000-11101[0 2][0 1]0-[0 1 2]010002-1001[1
2]000010000101000000110101l0?0100011000100000011O[0
1]000002100010000000100011000-000-000010001-
000000021000111010011110000100011111O100020--101101120000[0
1]101113011[1 2]11100000110010120010001110O?0??0000000000000100-
10110001O?00000000110111-0-0??1100??0?1?01000?000020100[1 2
3]0101100001020-01-10000??100000-01000010---
0010010200100000l??10?12000000?000100000?000021000001101203010O2?12??2
01000----------00

K_australiensis_holotype
???00??1?????????01??
??100-??[0
1]00?00?00????101000?0000?0?1000-1[0 1]?0101100010002-
1?????0????????????????????????????0???0???????0????????0?2?000???0000??????
????????????????????????0?2??0??1??
??
??
??
????????
K_australiensis_combined ???00-?1????0-???01????????????????????????0-?-
???--?100?--0???[0 3]??[0 1]00????????0-???--???????-?????????0?????100-??[0
1]00?00?00????101000?0000?0?1000-1[0 1]?0101100010002-
1?????0????????????????????????????0???0???????0????????0?2?000???0000??????
????????????????????????0?2??0??1??
??
??
??
????????
Boreopricea_funerea ??000-0?00010-00?0[0 1]01000?01201???11210-010??00-?-
??0---1001--00??000100?3[0 1]000?-0-010--??-0000-0000000-00000100?0-
0?000?000?0100010????00??????1000-???000???10100?2-1?012?00?1?0[0 1
2]0?????000??012??000?????????????????1?????????????????????????????000-
?0?2?0?01-?0000??10?00??001????0[0 2 4]000000?0?11?10000020--
??0???020011010?1031???11?00000100010141?1?????????0????0?0?000000??????
0???0???100?00000??0111-0-
0??1100????02??0?000?????????????????????????????????12?0???????????????010
???2?0??????1?01??02??00????0010000000000?1??000?00130?0?00101210?0?00??
??????????
Archosaurus_rossicus_holotype
????????00?1?????????????????220010?1201??101????????????????????????
??
??
??1?????????????????
??
??
??
????????????????????????
'Proterosuchus_ferugsi' ??0?????????100???????[0
1]?????????????????????0??????????-100?020???0?0?0??[2
3]?0?????????????????0????[1
2]0??0??
?11?[1
2]01?100000?100101101??
???????????0?????????????????1000????01????????????????????????????????????
??
??
??
Proterosuchus_fergusi[0 1]?000-0100011002102111012112200101120100101000-
010[0 1]00--100002001000000003[4 5]0000-0-010110000100000201100[0

1]000000000-??10001000100001010100000010010[0 1][0 1]-2110[0 1]0[0 1]11[1
2]11000011001200001???0101000000100101101000011100001?0000110101?01210
000000101?101?11?01?001000111O?02100000012101011001101111000110001111
100[0 1]0020--10[0 1]001010[0 1]00[1 2]10000201?210?010011110[1 2]01[0
2]001??0?1????0?0??????????????????01101100?????????????????01000?100100??2
02000????????????????????????????????????100010-01000010---
0020110?001?????????????000000000100?????000?1000001?01?03010020?2?0?0?
000??--------00
Proterosuchus_goweri[0 1]?000-010001100210[2 3]1[0
1]00121122?010?1??1?0101000-010?00--1?000200102100000 3?00???0-
01011000??0??0020?10??0000?0000-
00100?1000??00010?01???000?001???????0000111010000 11??13000011120??1000
[0
1]?01???01?0101001110 3001?0?00110101?012100000010 1???1?110?10??????????
??????????????????????11?1????1??0??
??
??0010??
??100?0?0???
Proterosuchus_alexanderi ?0001001?0??1002102??[0
1]01????2??????????0?????0-?1?????-1?00?20???0?0?0003[2 3 4
5]0????0?0?0?????01000??20110-0000000000-
??10001000100?0101010000001001000-2110000112-
10000110?1300001????????000001001?11?1010011100001?0?00110101?0?2?0????
?0101???1?11??10001000011?00210000001210 00?10??10??1[0
4]000110001111?0000020--
1?0000010?00110000101121 0??1?0110?01014?0?000211001?10?0000000?0000000
-1011011000???0?100???????010?0??????????????????000?0100?1??0000?01020-00-
?0000??10?010-01000010---
0???????????0000???1??120000000000100000100001100000 1?01?0?0?00??1200?0
?0?0----------?0
'Chasmatosaurus'_yuani 1?000-010001100210?11001?11[2
3]20110112010010 1?00-011000--10000200100100000340000-0-
01011??0010000020110-1000000000-??10001000100001010 10??0001001000-
2???0000-2-100?[0 1]110?130?0010?20??1?0[0
2]?0??001?11?1?????11?30?1?0??1110000?0?210?????0????????????001?001110
00210?000002102?11001????1[1 4]00011000?1??10001020--??[1
2]?????????01???0[0 1]???[1 2]?100[0 1]0??1000[1 2]0131010000130010?[0
1]000000???0000?00-1010011000001001 01[3 4]21011-[0
1]10001100??????0?0?0??000?010011000000?01020-01-?0?0011100010-01000010-
--?020110[1 2]0010000010010?120??0?0??0010011000000?[0
1]000001?01?????????12??????000---------00
'Chasmatosaurus_ultimus'
2??0????????1?????????????????????????????????????003??????010?210?1?
0001???
??????????????????????????????111?11110????????????11?????????????????????
??????????????????????????00???0010101[1 2]???000?????????????????14000[1
2]1000???
??
??
??

Ankistrodon_indicus [0
1]??
??
??
??1??0110?0??????????????????????
??
??
??
????????????????????
Tasmaniosaurus_triassicus
0?0?????????100???????????1?10?????20???10??????[1 2]?????-
10??0100??0???000[2
3]???????????1?????????????????????1?0???00????????????????????????????????
??0?[0 2]???2-
?0??01?????????????????????????1??
??????????0????0?0??002???000?????????????????11000[1
2]10?0?1??1010????????????????????????????????1??1????1??10??????????????1[0
1]?????????????????01100010??
??[0 1
2]??[2
3]0???????02?????????????????????
Blomosuchus_georgii
??
??
??0?????????12100
0?000101?[1
2]??
??
??
??
?????????????????
Vonhuenia_fredericki
??
??
??
??111101100101
-?????????0??11????-
??
??
??
???
C_rossicus_combined
??
??
??
??11111110?101
-??1???011[0 1]00210?00-
0?????001???1?001??
??

??
????
Chasmatosuchus_magnus
??
??
??
??11???1???????
??1????11?0?210?00-
??
??
??
???
Gamosaurus_lozovskii
??
??
??
??11?11111?????
??1???0110002?0??
??
??
????????????????????????
C_magnus_combined
??
??
??
??11?11111?????
??1???011000210?00-
??
??
??
???
Chasmatosuchus_vjushkovi [0
1]????????00??????????????????220010?0201??10????????????????????????????????????
??
??
??1???[1
2]1??
??
??
??
SAM_P41754_Long_Reef
??
??
??
??1??1010001[2
3]10????????????????????????????1?21011?10020????????????????????????????????????
??
??
????????????????????????????????

Koilamasuchus_gonzalezdiazi
??
??
??
??0?[0
1]?????????????????????????1??????20??
?????????1[1 2]??0???10??1-?????????????????????0???021?[0
1]1?000??
??[2 3]0-10?11010??
Kalisuchus_rewanensis_holotype 2?00????????10??????????????2??????[1
2]????????0???[0 1]?000-?[1 2]???0???10000?000[2 3 4]???????-
??
??
??1??0210?0????????????????????????
??
??
??
???????????????
Fugusuchus_hejiapanensis ??000-00?0??100210[2
3]1?10????????????????0????00-?[1 2]??00--10000200??0?010002?0?0?-
000?011??0000001010011??000200?-0-
??10001000100010?01??0000100??????????0-0-2-
100?011?????0??????01?????????????????1000111?10001100011100 01?10000100
0100??0??110??1000?10?0????????????????
??
??????????????????0?00??100??
??
????????????????????
Sarmatosuchus_otschevi 2?000-0?0001?????0[2
3]???????1220110?0201??10????????????????????????????0???[1
2]??????????????????00??00[1
2]0??1???????0????00?????0???????10?01?000001001?????????????????1????????120
001????010??00?000002?????0?0111?00001?0011110000?1111000?000000??0??11
0???0[0 1]???0211001????000?????????????????10??21000?111101110101-[1
2]?1001010000[0 1]10000-01????0001??1110?0?-
???????????0????100000000000000-
??????????????????????????01000??
??
????????????????????????????????
Guchengosuchus_shiguaiensis ??001001?00?101???[2 3]??1[0
1]?????????????2??20????0??010010-01-??020?10001[0
1]0001?0000000?1?????????????????????????10-0-00[0 1]?0????-
????????????????????????????000-0-2-1010[0 1]?1????????????0????06---
00?2?????0?1?11?0????????????????????????????0??1?1100?????????????????????
?0?1??20??????1???10002100 0?111?111?0100-??1????[1 2]0000110?01-?11[1
2]1????????11020?-
?00?????????????1?01?100?????????????????????1????????011??0?0???101?????????
??
??

Cuyosuchus_huenei
???0?????????????0??
??????????????????????????1020??0??
??1????????????????????????????
??1111111001
01-?????????0?011????-?1???10010011100201-??00?02110[0 1]0??[0
1]1?0?0?????000000-???????????1000000510111-0100???0?????????????0?0[0 1
2]011011010000000021?000[2 3]?000[1 2 3]110?000001?0??[0 1]?---?0[0 1
2]1110[0 1
2]001000001000111???10?????
????[1 2]
GHG_7433MI 2?000-
01????1??130?100?1?0001[2 3 4
5]?????0????????????????????????????[0 1]?0000-
??100?10101?0????????????????????????000111??101?????????????????????????0
00??0??[0
1]00?1????000?????????????????4??021000111??????0??????????????????11????????
????010??11??1???10????????????0?????????????????????????????01?0000????121-
010????011????00?????????????????????00?0?021?010?0000????????????????????
??????001????????????01?????????????????????????????01?03?1010??????????0?---
------0?
Garjainia_prima 2?000001000110021021210120111020000200201001l0-
011011--200?13001001110001400001000l0011-02010110100100100100l000-1-
100010101000110001000000100100202l-?00111??1010[1 2]?100120000????0?[0
1]??0[0
6]220000201111000111113001100101100001111100000001010201111001100l000
210001201000001110300000l?1??1[1 4]000210?0?111111110101-
1?2001010100111000-?1??100010111100101-?0000000?00???[0
1]1101010010000000-?0???0110??1200001521111-
01001??01?????????????000?0100111001000000212010l0?00??100010-01000010--
-
?020210?00100000100001?101????????0100000100001????????01?????????????????
?0?---------??
Garjainia_madiba_holotype
??00????????????10??
???????????0????????????10100?00?????????0-
??10001?10?0001?????????????????1??[2
3]??0?0??1?1?????????????????
??
??
??
??
??
??????????????????????????????
Garjainia_madiba_combined 2?00??[0 1]100011???10???????01210200?020[0
1]??100????????1[0 1]??[1
2]???????100?1?000???0?????0??????0?????101001001??1?????????10001?10?0001
?????????????????100[2
3]02?????1????1?11??1????0?0????????????????????????0?0??1?130?110000?1000
011111000?000101????111?0??0????021000[0 1]????0000?11?[2 3]??1?0111???[1
4]00021000?111101000101-??[1 2]???010????11???-?1???00?10??11??101-

?0???00????1???1?010100110?0000-???????????1200001421111-
01001?????????????????0?0?0000110?0100?001[1 2]1??1?10000??100010-
01000010---
0020110?00100000???
??????????
Erythrosuchus_africanus 2?000-
000001110210211100101110201002002010?10-0100110-
200002001131120001100000010100 1??020101101001[0 1]010010000-0-1-
1000101-100001000000000001101002022-000-112-101111100120001????0?10006---
00020?10100011110410111011110000011?110000100000021111110110011 00?0000
120100000111030010011 1??1400021000?111111100101-102???010100110000-
0111100[0 2]10011110201-00000000?0?00[0 1]01101010011000000-
??????????01200001621111-
010011101??????040????000?011011000100001021101010000??100010001000011-
--
0030210?00100000100 01?00110000000100010000002211000 1?01?0?0300000210
???0000---------??
Shansisuchus_shansisuchus 2?000-000001101210312 10??01110001002[0
1]020100?10-011012012-00110011011000014000010101000??0[1
2]000?1010010010001000-0-1-1000100-?000110?00?00000100100[2 3]02??000-
102-10001110012?00?????0?1??06---
01?2?????001111?040?1110?1110?00?11?1?0??10??00?2111111?11001?002000012
0[1 2]?00000110300?001?????400[0 1]21000?11?11?1?0101-???0010?0??0010??0-
?1?2?00010111100?01-000?0000?????0?11010100?1000000-???????????120000?[4
5][1 2]01[1 2]1-
0?001??01??????030?00?0?0?01102100 1000?0102120?0?0?00??000??000?00001?--
-
??2111??00100000101???1010000?000010011000000?????????01?????????02?????
?00?---------??
Shansisuchus_kuyeheensis
??????????????????????????120?110001?0?????10???????10?????????????[0 1
3]?1?00??
??
??????????????????????????????????????00?1????000?????????????????[0 2
4]???????0?1??11??????????1???010?????0?????????0???00?11?0??1???0??????????
??1?01010???000000-???????????120000?5101?1-
??
??
????
Chalishevia_cothurnata 2?000-???00?101???????[0 1]1[1
2]???????????2??20????1??0?1012?12-
??12??10211?0001??00010??1???
??????????1????2?????????????????????01?0?00????????????????????????????????
??00?0????????4??02
1000?1??110?????????1????1000?0?0?????????0?010???1?0????????????????????
??
??
??
'Dongusia_colorata'
??

??
??
??1??11110?????
??????????????????????????0??2000?01010??
??
??
????????????????????????
Uralosaurus_holotype
??
??
??????????????????????????????0????06---
0002??
??
??
??
??
Uralosaurus_combined
2??
?1??
??????????????????????????????0????06---
0002??0????0210001????00
0?????????????????4???21??
??
??
??
Vancleavea_campi 2000100-00110-0100101?1100110000010200001???00-0--00--
-1001--0-1?010000?100000-0------??00000-0110000?0000-?02-0-??2--0100--
000010-0111000000-1002022-000-0-??00002-
101100100????????????????????????0?1??11???00??000110000?????????????????1
??1??1?00???03200?01-[1 2]0000001100???001????1401-21000?1????00?000--
??1????1??1?010???-1????1?3100?1?00[0 1]0?-
??0?00?????00?211010100010?????????????????000?00002?0121-
1?0000100?????2?101???000?00-00101000??0????????10?002100000000100000----
00111100101000001 00???10100001000011000000000121 10??1?0?30[3
4]0????000???????30-101?001?12
Asperoris_mnyama 2?001000?0011?0?1????1[0 1]000110000?020020200?0????-
01[0 1]?-10??0??011[0 3]00?000??00?000?01????????????????????0?01012-0-
00??0????-?????????????????????????????000-0-[1 2]?1001[0 1]-
??
??????????????????????????????????4????1??0????????????????????????????????
??
??
??
???????
Euparkeria_capensis 2000[0 1]0010000100110112100[0
2]011010001020000200100-000[0 1]010-10000200100001000110000000010111-
000000001001000000110100-??100010000000010000010010000 1002022-01000-2-
100001100120000110211011002000102010010101001040000001011000 0?1101000
10001000111?11101?00100011000020[1
2]000000210201110110??140002100011101111001 01-10100001 0?00110000-

010211[0 1]0100011??101-00000001??[0 1]00?01001010?0000000-
10????000001[0 1]0010?310121-000001100??????0[2
3]010??00??011011010000001011?000200001200100000100002-00000[1
2]1100200100000001?0?021100000000111100100001211000 1?012030[1 2]00[0
1]?01?0?000[0 1]20-1010101100
Dorosuchus_neoetus
??
??
??0111?1?04001?0?11?10000?110?
000??000000???11100????????????????????????????????1????????????1????????
??00?1????????????????????????????
??0?020100110100????????????????????
??00100000100002-
000?021110200100000??
??????????????????
Dongusuchus_efremovi
??
??
??
??
??
??
??
??00101
000100002-
0000011110??
??????????????????
Proterochampsa_barrionuevoi ?21[0
1]202000111001?031101001121001 0?021000100100-?2-0?12-
100100001?0?020001[3 4 5]000000001000?-000000001000000000[0 1]100-0-??2--
0100-000001000100000010010022-000-0-2-10002-10?1?0?0011020?001042-
10102?10110101111040 0?01?10111001?0?20001??000000????????1?001?00?0001?
1010?000?0-03100000?0???4000[1 2]10?0?10?0000?000--[0 1]?2100010???010?00-
11?[1 2]??1000?1110000?-10000?01???0??00?0?0100??0000?0-
??????????0100000?1101[1 2]1-0-
???11??????????????0?????????????00?????????????????1001?????1?0002-
?00?01121?2100000011??10??2?100?0??0?????????????????????1[2
3]??????????????????00----------00
Proterochampsa_nodosa
2?11202000111001103120 10?11?10?1??021000100?00-?????0--
10010000??0?020001[4 5]000100-01000??00000000?0?00?0000?100-0-?????0100-
?000010001?00?00??0100[2 3]022-?00-
????1000??1001?00001??20????0????0????????0???111?????????????????????????
??????????????????001000?000????1?0?00?0-
031??000?0???4000?00?0??
??
??
??
Tropidosuchus_romeri ?000202100111[0 1]0010[1
2]1?0100???00010102?000100?00-11-0000-
10010100??0?0100?1?0001?0001010??0000011020000000000010000-??2--
01000010101010[0 1]0000001011012122-0?000-2-1000??1001[2 3]0000????01?1[0

1]00221010?????0?0??110400??1?10111000?0?2?000???0000???????????0011?0?
201?0????0?01?2??3????11?0???[0 2 4]000[1 2]1000?11?00000100--
10200?010?00010001-11???110100?11??001-10?00001[1
2]1000??110101??0?0000?0-?0?????????10??00??10111-
0?0??11?????????????????000?0110????000000101130001O?001?0010000??00002-
000?01111?2100000011011101211000100001101000000012110001[0
1]0120101110000???2--010-101-0??00?
Cerritosaurus_binsfeldi ??0020200011110110[1 2
3]11010??1110?1?10210?01???00-12?0011-
10?10100??000100?1?0001?0001002??000000101000000000001??-0-??2--0100-
010101010??1100010110031?2-0?0-0-2-
100???10013000?????????????????????????0???111?????????????????????????????
?????????????11???2??????????00?11?3???001?????[0 2 4]00[0
1]01000?????????0????1?????????000?????????????????10??0????0?????????????
??
??
??
??????????????????????????????10-???-1?????
Gualosuchus_reigi 2?0021210011110210[2 3]1002000121001010210001O0?00-
11-000--100103001001010001[2 3]0001-0-01000??0100001010000000000010000-
002--01000000111010[0 1]?110001011002122-00010-2-10002-
100120000110201O1?00221010201111O?01?110?0?0???10111000?0?2?0?????00???
??????????0012000201?010100001?100300001100??1400001000?11?00000000--
102000010?00010000-11?2?0[0 1]0100?1???001-100???????????0100[1 2]010001[0
1]00010-???????????10?010??10121-
??1200100000100002-
001?0[1
2]11102100000011011O?1??????????????????0????????????1??????????????????010
-011-10000?
Chanaresuchus_bonapartei 21[0 1]0212[0 1]00111002103100200O1[2
3]100101021000100100-1[1 2]-000--100101001001010002100O1-0-01002?-
0100001010000000000010200-??2--010000001[0 1]10100011000101101212200010-
2-10002-100120000110200O1[0
1]00221000O?10110101011110200O?10101110000012100O???0000???1???1?1?001100
02010010100001?110300[0 1]01100??1400011000?10011000000--10200[0
1]010?00010000-11?2?[0 1]0010011100001-100001012100?0?1102010001000010-
??????????01000100210121-
?????1?????????????????000201101001000000101130001000O[1
2]300100000100002-
001001111?2100000011011O?12110000000011010000000?2111?01101202011107O
0??22--010-011-000000
Pseudochampsa_ischigualastensis ?110212100111107O[1 2
3]1?0200012100107O2100?10??00-?2-000--10??0100??0101000[2 3]40001?0-
0???0??01000010?0?00?0000010000-??2--010000?01110101000000101101212200-
?0010-2-
10?0??1001?00001???0????00221010200??1?????110??0??1?10111000?0?1?000???
0000?????1?????00???0??0??????0000??0-???????1?0??1400001000????0000???[0
1]??1?[1 2]?????0?00??0????11?2?11010??1000001-
100?0??111?0000000?0?00??0000?0-
1?????????????0000?????????????????????????????????????1???0?????????011?000???

?????0????????0002-000????????21??00?011?110?1???0000??0?1[0
1]????0???????????101201?2110?00??????010-01?-100000
Rhadinosuchus_gracilis ??0021??00111?0????????2???1?1??1?10????0[1
2]0??0??11??02?-10??0000??0?0?00???0001?00?1??2???[0
1]??10?[2 3]1[1
2]??1??40??0??????????????
??????????????????1?????0????00211?0????000??????????????????14?0[0
1]21000?1?????????????????????????????????????[1
2]1????????????????????????????0??
??
??
??01??????????????????10-
01??0000??
Archeopelta_arborensis
??
??
??0111?0?04100?1?10?10100?110?
001??000?1??1??110??1???????0
00--?????????????????????????00000?1?1???01-
1??1???0??10110????????????????????????
??0??211???0?00?00?????????????00??00100001100002-
000?02011??101??
?[2 3]110110210???
Tarjadia_ruthae
????20?1??
??00????????????????????????????
???0?0??00?1???0????????????????????
??10?????????0?????????????1??1??????
[2
3]1????????????????????????????010??2?000????????????????????????????????????
??
???????????002-
0000??
[2 3]1101??2101??
Jaxtasuchus_salomoni[0 1]??020??????1????0????[0
1]?????????????????????0???100-
1??100?000010000?0002??0?
??0????0????0????????0?11????
???01?????110????????????????????????????????1?????????????????1???????0?1????
?400001100?11???????0[0 2]??1?[0 1]???1[1 2]000?010?11-???[1 2]?1?[2
3]10?????????-11??????????0????????????????????????????????1000110310111-0-
??0?000?????2?300????????????????????????????????????2300100?00??0??2-
000?0?10102?0?00?011?00001?????????????????????????????0????0120???00??0000?
1?00311201?010110
Doswellia_kaltenbachi 2?1020[0 1]0????????-13????????????????????????0-
??????????????0??????0000[3 4]????????0??????11?0??00-0--0--??????0-0-??2---
100-0-0-0100-1110000-001----22-000-0-??00002-
1??120000????0????000210112010110111111020001 1?10011000?010?001???0000?
??????????000-?0020000[1 2]???000012000100001001114??0?0????11?000000101-
1??10?010000011011-10?[1 2]11[1 2]010012100000-1101110?3000?1[0
1]????????????????????00000012??000?111010

000000001011300010000???01???????0????????011?1?????????????????????????
??31120?1[0 2]101?0
Paleorhinus_spp. 2?10101001111000101200000014000-00--1-00000100-12-0-
10-10100200102002000210000-0001002??100001102000011000[0 1 2]100-0-
001000100-0[0 1]0[0 1]0111000110010011[0 1]02022-000-0-2-10002-
10112100011131210116---0[0 1]020111101010110400l?1?10110000?0?[0 1]?[0
1]?????0000?????????1?0[0 2]1?110001?1[1 2]0??0000?11?2000001?111?401-
21000??
??
??
??
??
Nicrosaurus_kapffi 2?10101001111000001230000012000-00--0-00000?00-11-
000--10100200102002000240?10-0-[0 1]1000??100-010020000110000100-0-
??1000100-11000100000110010001102022-000-0-[1 2]110002-
10112100011131210116---000201111010101104001??011110000?000?0[1 2]-
???0000?????11????011111000101102100000101201000l?1??0401-[1 2][0
1]000?11?1111000310???????100?001??00-1????0??1011?11000?-
1??????1?02????????????????????????00?1011??010001012111l1-[1
2]?000??00100001100002-
000?0?101??00100000101?210??
??????????????
Smilosuchus_spp. ??10101001111000001220000l[2 3]000-00--0-00000?00-11-
0-0--10000100102002000[2 3]10000-0-11000??100-0100[1 2]0010110000100-0-
001000100-11000100000110111001102022-000-0-2-10002-
10112100?11131210116---000201111010101104001011201000?010001-
010000??1?0?11??1?011111000101102100000110200010l1?1?1401-
20100?110111100031[0 1]1?100101000001??00-11?2100010111010001-
10010001??110?01001010010010100-?00010?1??01000110111111-
1?000?100?????????????000?011011010000001021200010000??00100000100002-
0000011010?00100000001?2101110000000011111001101221l??01?0??0?1????00?
??????2210010?0000?0
Ornithosuchus_longidens
2?001001000110021?011110001121100000210103001?00-01-0031-
10100100?000100001000000001101???2000000[1 2]001000-00010000-
??100010111000010001011000101100302201-01000-2-10002-10?1[2
3]000010131110?16---
0002011110?0?011???1?001?01?201?0????
0000?1?030?1????????40002100l?1??11110003l????????10??0010??0-
11????10101?1??0?0?-
1?0?10????010?010020100?10001111102????1?001??0110??0121-
000??1100??????00?????10020110110100002110110000222?00??00101100100102-
000?0110?0??11000????1?2?02???0??????12?110??00???????????1?0???00????????
??220-[0 1]001100[0 1]00
Riojasuchus_tenuisceps 2?00?-
000001110210112100011221?00002101030l?00-01-0?31-
10100000?2?000100003001000001101??020000001001000000?2100-0-
??100010000000010000011000100100302201-010-0-2-00002-10012000011131110[0
1]16---
00020?1110?0?011040???1?11110000?01001????00000???1?1???1?001201321??00
020000001003l?1001?111140002100l?100000000031010200101000001000l-1??[1

2]?00000111100001-
100011?1?0?0???100?0?00?11?01111?????????01100110410121-
100111??11?????010????1002011[0 2][2
3]10200001110110000?20???201100100100102-000?0[1
2]10002111000100011210211100001001211101100122110011?012030200000100?[
0 1]?0220-000120000?
Nundasuchus_songeaensis
2???
??
??????????????????????????????????3--
001?2???0????0[0
1]11100????000??21?20?0????????4???21000?11?1101000311?0????010?0??10??0-
11????0[0 3]10??1110?01-
1?00?001????0101?010100?10000110?01010??1??110011?410111-
??????????????????????1?????????????0??10112000?????1100101?00100002-
000002101020110001000 1?2001110000000011111001101 22???01??012031?00?011
???0?0220-10100011?0
Turfanosuchus_dabanensis ?0001001?001100010?1[1
2]?000011010000021020100?00-00?0020-10000001??0011000[1 2][1 2 3 4
5]001001101111??0100011010010 0?000111100-
??10001011001101001 0?1100100010?20?2-00[0 2]10-
??1000??100120000????1????13--
?01?2????????1?1?0402?01?10?10000?1100100??00?00?21??110???0010000101?0?
0[1 2]000001110 20?0001?????40?021000?110?111010310??[1 2]000??00?0010??1-
?1??????20??11?0101-
???00001??0000????????1?????????????????????1000000310111-
100????0?????????????00?2021020010??01010110000?????12001?0100?00002-
000?011010?01100010101????1111001 0?001221110[1
2]101?????????01?0???????01???????20-101?0011??
Gracilisuchus_stipanicicorum2?001[0 1]11000110001011[1
2]000001101000002102020 0?00-00-0020-2[0
1]000101200011000210000011011 11??0100011010-1031000110000-
??10001111100101100-011001-011002022-01010-2-1000[1
2]?100130100????1??0?16---0102011010101011040?[0 1]???00???????1?001[1 2]-
???0000?????1???1?001000?10100200000001110200000110??1400[0
1]21000?11?111101031010 10?1010100210001-11?11100200?1000101-
10000001100000[0 1]???[1 2]?1?????????????????????1000001510121-
??????????????????????????00[1
2]021011000000001021000 01?000?000100100?00002-00000011102[1
2]?100010???1100111100000000122111021012 2???01??012030200000100?0?0020-
10100011??
Aetosauroides_scagliai 2?0011000001100??????100001[2 3
4]0?0?00?21000100?0??0[0 1]-0030-110001?1??000?000?[2 3 4 5]0001-10?110[1
2]???????1?????????000[0 1]100-0-??[0 1]???0??-?????????????????????????000-
????110?????????????????1????1[4 6]?-
?01?????????????????0????0?1000?????????????????????????????21???01?10?1?2?
100?????????????????14??0210???1?01111000 2101?100?010?0?010100-11?[1 2]?[0
1][0 1]020011000001-10000001[1 2 3]????1?1?010?00?10??0????01010000?01[0
2]00010211111-
100111100??????0??????0102031000010000001011100010000220010010010000 2-

000002101020110001010112101111000000012211101111221100 11?012030200000
100?????2102001200012
Batrachotomus_kupferzellensis
2?001001?0011002102?2100101101010?011000200?10-0[0 1]00130-
110001?02100110001?0011-11010011-01000?1010?00?0000101000-
0010001011001101 00?0011000?101002022-00110-2-10012-1?0120000??1??11???6-
--000201101011101?0401110110?100100110012-
??00001121?11111??0010001001012?2000001110200 10??11??140?021000?111111
100031[0 1]??2001010000010000-11?[1 2]1[0 1]0020001010101-
?0001001??31?001?01010101 0?00110?????????01000010510111-
11011??00?????????????010?021111010110?01021002 0?0010??00101100100002-
0000011010?01100010001?21011?1?????11221100?111????????01?0???????1200
????220-10011011??
Prestosuchus_chiniquensis 2000100100011102102121000 01[0
1]01000021000200?00-01-0020-
10100101210011000150011000010 01??0100010010010010000000000-
??10001011000011011001100001010 02 2-00010-2-10012-
100110000????1110?16---01020?1?1010101104011[0 1]1?10110000?110012-
0000001??11?111?1?0010002000012020000011102001001111114000210 0?11?111
10003101 0?000010000010000-11?[1 2]100020001010001-
10000001?001?0011010101010000110?0101011???1000010210111-
1101???00?????????????0102021011020110001021002110011120010110010000 2-
000?011010201100010001121011110000000122110021112211 00?1?0120?0?00?01[
1 2]???0?0220-1011001100
Dimorphodon_macronyx ?[1 2]00??0?000110021 0?22?0000-
3000001111000200?00-11-0?20-11000100??000200?0??00?0??01002???2000000-----
---????1??????????0000??00?010?01?1-0000??10?2-
1?????????????????001???0???
??????????????????????00??0001?100???1000??????0?????????0[0 2 4]10[0
1]01000?1????????00--??1???????????????-11????[0 1]010??11?0???-
10?????????01??00020000?10?1110-??????????010?11105101201?????????????0?0-
011110?10031010021000001 12??00??0???0?01100100?00000----10111?0300?0-00-
??110?0311?0111???0-------??1?2111101?1?1040300011100?0?000----------00
Lagerpeton_chanarensis
??
??
??
??1?????????0--
??????????????????????????[1
3]?????????????1??00001??0??
??????????????????001102101002000000001130001 0000??01110101100002-
100?011111210100000101110131110111 00-0-------2-1-
211111101120000002 0000022--0?????????????
Marasuchus_lilloensis[0 1]???????????10????????????????????????????????[0
1]???????1?0??0????0?0?0001??
?????0????10????????????????????????????????12000????????????????????????0?01
????411101?10???000?010002-
?0000???????1110?????????????????????????????????400021??0?1101000010
0--102001010?00010010-1????[1 2]10100??1??001-
1?00000111?000?001?0?00?10001110??????????01?1?110400121-1001?[1 2

3]10??????????????012021010020010110011000011000120011010000011 2-
000?011100210001001101 10?02110110100012000001001121111111112030200000
000?2--00----------0?
Lewisuchus_admixtus[0 1]?00????????11??10[1 2]???0?0??????????????????0???[0
1]-002??10??0000[1 2]0000?0002????????0????????00??1010-
0031??????????????0??01?001110????10000?0?100202?????????????????120000
?????????05-2-0102101?10111?110401001110110000010002-
00100000?11?11101??01??????????????0020??0?000??11??400[0
1]21000?11?11110100--11100001 0?000100??-110??120100011??001-
10????????0????0012010001000111?????????10?01?0[3 4 5 6]?0?21-
??
???10?01001???10-000-
10?00?
Silesaurus_opolensis 0?000-01?00?1????0?????0001200000??2100?200?0??01-
003??[1 2]???000021000100 01??000-??01?????1?00001010??0?????110100-
00???0?0??101?010?00?1101010?1002?2??0?010-2-100?2-1?0120000????????[0
1]06---
0102?01??0?1??110411?011?0110000?0100000001000012 1??1110??001000100011
20101000121 01??010100???100221111?11?11110000--111000010000011010-
11?2111010001110001-10001101100001[0
1]0?120100?10?01111?????????000001003001 21-0-??13100?????????????000[2
3]021210220010210011000121?10??00101110011112-
000101110021011100111111012110211100 00-------
20112???1???1021??2000100???2--10----------00
Heterodontosaurus_tucki 00000-
01?00110000020210101110001000200013001 00-01-00[2 3]3-
100000002001010001100 00-1001012??1100011000010000001100 10-002--
1100100010100000110010001102022-00210-2-11002-11?1200001??3????1?6---
010210???0111?110411001?10010000?010002-
??10000???1?111?1?021000210010111100101201211100100??041012[0
1]110?11?00000000--110001010?10010000-11??0?1?101111?0001-
100?20?1?0000121?120100?10?0?10-11-------0110?11?0410121-100101100-
100101011112101[1 2]03101100101020112--00-32?1011011?0?0??-?102-
110?0?1?0?22001110?1101101311?2111?0-0-------
201?211110101021302000100??22--00----------00
Herrerasaurus_ischigualastensis 2?000-
0100011011002121001011000100020000200?00-0100120010000000[1
2]130010002?0000-0001102??0100001010-0030000?10010-002--0[0
1]00110010100000000000001002022-00010-2-10002-10?130000????1????06---
01?210?010111011040?0???11110000?010?12-???0000???1?????1?001100[1
2]00110202000001[1 2]102001001?[0
1]111400021000?11?11110002001120010100 11[0 1]10010-11?2?[0
1]00100?1110001-
100000011??01000?120000011?01111?????????11001111610121-100101100-
111001[1 2]111121012021211120010[1 2]101210021121113?01110100012112-
010?01110[0 1]220[0 1]011011101101211021110000-------
2010211110101121302000110 00?10000----------00
;
ccode + 0 1 6 8 9 16 18.20 27 28 35 39 40 48 52 63 68 72 73 115 120 145 147 148
162 167 168 176 190 212 248 251 262 266 284 304 306 310 316 322 328 329 331

```
339 342 347 351 353 361 381 385 387 393 394 400 405 414 416 421 425 427 430
438 444 448 449 453 454 475 480 493 500 508 514 518 519 529 531 533 536
542.544 547 *;
proc /;
```

Appendix 10

Synapomorphy lists of the clades recovered in the phylogenetic analysis 3 of Chapter 5.

Younginiformes Romer, 1945

New definition. All taxa more closely related to *Youngina capensis* Broom, 1914 than to *Varanus niloticus* (Linnaeus, 1758), *Crocodylus niloticus* Laurenti, 1768 or *Passer domesticus* Linnaeus, 1758 (stem-based).

Temporal range. Latest Middle–Late Permian (Capitanian−Changhsingian, *Youngina capensis*; Rubidge et al., 2013).

Synapomorphies. Jugal-quadratojugal ventral margin concave in lateral view (88:0→1); parietals entering strongly between both frontals, forming an acute-angled suture (110:0→1); ulna without, or with not ossified or very low, olecranon process (401:2→0); radius twisted in lateral view (408:0→1); and distal end width of the metacarpal I versus its total length = 0.36−0.45 (417:2→1).

Sauria Gauthier, 1984

Definition. The most recent common ancestor of Lepidosauria and Archosauria and all of its descendants (Gauthier et al., 1988).

Temporal range. Middle Late Permian (middle Wuchiapingian, *Protorosaurus speneri*; Ezcurra et al., 2014) to Recent (*Passer domesticus*).

Synapomorphies. Ascending process of the maxilla posterodorsally oriented (56:0→1); anterior process of the quadratojugal absent (146:2→0); supratemporal bone absent (149:1→2); parietal extension over interorbital region absent or marginal

(152:1→0); postparietal bone absent as a separate ossification (163:0→2); tabular bone absent (165:0→1); quadrate shallowly emarginated posteriorly (168:0→1); parasphenoid/parabasisphenoid intertuberal plate absent (223:2→0); dentary without large foramina aligned in two distinct rows starting on the anteroventral corner of the bone (254:1→0); retroarticular process of the surangular-articular anteroposteriorly long, extending considerably posterior to the glenoid fossa (267:1→2); distal edge of the maxillary tooth crowns straight (285:0→1); posterior cervical or anterior dorsal ribs with long and distinct tuberculum (0→1); scapular blade with distinctly concave anterior margin in lateral view (364:0→1); cleithrum absent (376:0→1); articular facet for metatarsal V on distal tarsal 4 occupies more than half of the lateral surface of the bone (524:1→0); and metatarsal V with a hook-shaped, gradually medially curved proximal end (540:0→1).

Lepidosauromorpha Gauthier, 1984

Definition. *Sphenodon* and squamates and all saurians sharing a more recent common ancestor with them than they do with crocodiles and birds (Gauthier et al., 1988).

Temporal range. Early Triassic (Induan–early Olenekian, *Paliguana whitei*; Damiani et al., 2000; Rubidge, 2005; Lucas, 2010) to Recent (*Varanus niloticus*).

Synapomorphies. Postfrontal reduced to approximately less than half the dimensions of the postorbital (116:0→1); quadrate with conch (168:1→2); and maxillary tooth crowns with convex distal edge in labial view in at least some anterior crowns (285:1→2).

Lepidosauria/Rhynchochephalia (*Gephyrosaurus bridensis* + *Planocephalosaurus robinsonae*)

Temporal range. Late Triassic (Rhaetian, *Planocephalosaurus robinsonae*; Whiteside and Marshall, 2008) to Recent (*Sphenodon punctatus*).

Synapomorphies. Jugal with anterior extension of the anterior process up to or posterior to the level of mid-length of the orbit (93:0→1); postfrontal with participation in the border of the supratemporal fenestra (117:0→1); parietal with poorly exposed supratemporal fossa in dorsal view and mainly laterally facing (154:0→1); and basioccipital with posterior margin of the occipital condyle anterior to craniomandibular joint (214:0→1).

Archosauromorpha Huene, 1946

Definition. *Protorosaurus* and all other saurians that are related more closely to *Protorosaurus* than to Lepidosauria (Dilkes, 1998).

Temporal range. Middle Late Permian (middle Wuchiapingian, *Protorosaurus speneri*; Ezcurra et al., 2014) to Recent (*Passer domesticus*).

Synapomorphies. At least one or more cervical or anterior dorsal with a parallelogram centrum in lateral view, in which the anterior articular surface is situated higher than the posterior one (293:0→1); cervical or anterior dorsal vertebrae with posterior centrodiapophyseal lamina (296:0→1); posterior cervical or anterior dorsal vertebrae with prezygodiapophyseal lamina (297:0→1); and humerus without entepicondylar foramen (397:0→1).

Unnamed clade (*Protorosaurus speneri* + Archosauria)

Temporal range. Middle Late Permian (middle Wuchiapingian, *Protorosaurus speneri*; Ezcurra et al., 2014) to Recent (*Passer domesticus*).

Synapomorphies. Cervical, dorsal, sacral and caudal vertebrae without a notochordal canal piercing the centrum in adults (292:0→1).

Unnamed clade (*Trilophosaurus buettneri* + Archosauria)

Temporal range. Late Permian (Wuchiapingian, *Eorasaurus olsoni*, youngest boundary of the biostratigraphic range; Ezcurra et al., 2014) to Recent (*Passer domesticus*).

Synapomorphies. Main body of the premaxilla forms half or more than half of snout in front of the posterior border of the external naris (27:0→1); postnarial process of the premaxilla forms most of the border of the external naris or excludes the maxilla from participation in the external naris (36:1→2); anterior extent of the maxilla posterior to the anterior extent of the nasals (48:1→0); ventral ramus of the opisthotic rod-like, with a cylindrical distal end and relatively thin (205:1→2); anterior postaxial cervical vertebrae with epipophysis (315:0→1); sixth to last cervical vertebrae with epipophysis (316:0→1); scapula without supraglenoid foramen (365:1→0); subglenoid lip of the coracoid as developed as or less developed than the supraglenoid lip on the scapula (372:1→0); olecranon process of the ulna prominent but lower than its anteroposterior depth at base (401:2→1); main axis of the postacetabular process of the ilium mainly posteriorly oriented in lateral or medial view (432:0→1); and metatarsal V with a hook-shaped, sharply medially flexed proximal end and, as a result, the metatarsal acquires a L-shape in dorsal or ventral view (540:1→2).

Unnamed clade (*Prolacertoides jimusarensis* + *Trilophosaurus buettneri*)

Temporal range. Earliest Triassic (Induan, *Prolacertoides jimusarensis*; Lucas, 2010) to Late Triassic (*Trilophosaurus buettneri*).

Synapomorphies. 15–22 tooth positions in the maxilla (73:3→2); and prefrontal with a subtriangular medial process that reduces transversely the nasal-frontal suture (105: 0→1).

Unnamed clade (*Azendohsaurus madagaskarensis* + *Trilophosaurus buettneri*)

Temporal range. Late Middle Triassic (*Azendohsaurus madagaskarensis*; Flynn et al., 1999, 2000) to Late Triassic (*Trilophosaurus buettneri*).

Synapomorphies. Posterior end of the horizontal process of the maxilla distinctly ventrally deflected from the main axis of the alveolar margin (62:0→1); 10–14 tooth positions in the maxilla (73:2→1); tooth attachment: ankylothecodont (282:0→1); and distal edge of the maxillary tooth crowns convex in labial view in at least some anterior teeth (285:1→2).

Unnamed clade (Tanystropheidae + Archosauria)

Temporal range. Late Permian (Wuchiapingian, *Eorasaurus olsoni*, youngest boundary of the biostratigraphic range; Ezcurra et al., 2014) to Recent (*Passer domesticus*).

Synapomorphies. 5 or more tooth positions in the premaxilla (41:2→1); maxilla contacts prefrontal (59:0→1); interclavicle without anterior process (378:0→1); anterior margin of the interclavicle with a median notch (379:0→1); entepicondyle of the humerus moderately large in mature individuals (396:1→0); capitellum (radial condyle) and trochlea (ulnar condyle) of the humerus absent or incipient (399:0→1); olecranon process of the ulna absent, not ossified or very low (401:1→0); proximal articular surface of the femur partially ossified, being concave and sometimes with a

circular pit (456:0→1); and medial pedal centrale present and contacts the tibia (520:0→1).

Tanystropheidae Gervais, 1858

Definition. The most recent common ancestor of *Macrocnemus*, *Tanystropheus* and *Langobardisaurus* and all of its descendants (node-based) (Dilkes, 1998).

Temporal range. Early Triassic (Induan–Olenekian, *Augustaburiania vatagini*; Sennikov, 2011) to Late Triassic (Norian, *Tanytrachelos ahynis*; Fraser et al., 1996).

Synapomorphies. Prenarial process of the premaxilla less than the anteroposterior length of the main body of the premaxilla (34:1→0); anterodorsal margin of the maxilla concave at the base of the ascending process (57:0→1); maximum transverse constriction of the olfactory tract on the frontals immediately posterior to the moulds of the olfactory bulbs and posterolateral margin of the bulbs well delimited by a thick, tall ridge (115:0→1); parietal extends over interorbital region (152:0→1); cervical and dorsal vertebrae with fan-shaped neural spine in lateral view (300:0→1); neural spine of the axis strongly shortened dorsoventrally (308:0→1); neural spine of the axis anterodorsally expanded (309:0→1); length of the fourth and fifth cervical centrum versus the height of their anterior articular surface = 2.92–4.12 (311:0→1); length of the centrum versus height of the centrum in posterior dorsals = 1.48–2.04 (330:0→1/2); length of the transverse process + rib versus length across zygapophyses in anterior caudal vertebrae = 1.51–1.68 (352:1→2); scapula and coracoid do not fuse with each other in mature individuals (359:0→1); total length of the scapula versus minimum anteroposterior width of the scapular blade = 1.23–2.61 (362:1→0); large fenestra between scapula and coracoid immediately anterior to the glenoid region (363:0→1); lateroventral surface of the postacetabular process of the

ilium with a brevis shelf, but lacking a brevis fossa (433:0→1); thyroid fenestra between pubis and ischium (438:0→1); diameter of the femoral shaft distally narrowed (475:0→1); articulation between astragalus and calcaneum roughly flat (497:2→0); distal tarsal 1 absent (521:0→1); foot length (articulated fourth metatarsal and digit) less than tibia-fibula length (527:0→1); and metatarsals I–IV tightly bunched (528:0→1).

Unnamed clade (*Amotosaurus rotfeldensis* + *Tanystropheus longobardicus*)

Temporal range. Early Middle Triassic (Anisian, *Amotosaurus rotfeldensis*; Fraser and Rieppel, 2006) to latest Middle–earliest Late Triassic (*Tanystropheus* cf. *Tanystropheus longobardicus*; Rieppel et al., 2010).

Synapomorphies. Orbit with elevated rim restricted to the ascending process of the jugal and sometimes also onto the ventral process of the postorbital (17:0→1); multiple maxillary or dentary tooth crowns with longitudinal labial or lingual striations or grooves (288:0→1); lengthes of the fourth or fifth cervical centra versus the heights of their anterior articular surfaces = 6.09–6.80 (311:1→2); length of the longest metacarpal versus length of the longest metatarsal = 0.34–0.39 (415:1→0); pubic shaft vertically or posteroventrally oriented (442:0→1); medial pedal centrale absent as a separate ossification (520:1→2); metatarsal V without a dorsal prominence separated from the proximal surface by a concave gap (539:1→0); metatarsal V with a hook-shaped, gradually medially curved proximal process (540:2→1); and pedal phalanx V-1 metatarsal-like, being considerably longer than other non-ungual phalanges (546:0→1).

Unnamed clade (*Boreopricea funerea* + Archosauria)

Temporal range. Late Permian (Wuchiapingian, *Eorasaurus olsoni*, youngest boundary of the biostratigraphic range; Ezcurra et al., 2014) to Recent (*Passer domesticus*).

Synapomorphies. Posterior margin of the occipital condyle anterior to craniomandibular joint (214:0→1); posterior-most dentary teeth on the anterior half of lower jaw (261:1→0); cervical or anterior dorsal vertebrae without a posterior centrodiapophyseal lamina (296:1→0); and anterior and middle postaxial cervical neural spines without an anterior overhang (322:1→0).

Unnamed clade (*Jesairosaurus lehmani* + Archosauria)

Temporal range. Late Permian (Wuchiapingian, *Eorasaurus olsoni*, youngest boundary of the biostratigraphic range; Ezcurra et al., 2014) to Recent (*Passer domesticus*).

Synapomorphies. Narrow lateral exposure of the angular in the lower jaw (274:0→1); and sixth to last cervical vertebrae without epipophysis (316:1→0).

Unnamed clade (Rhynchosauria + Archosauria)

Temporal range. Late Permian (Wuchiapingian, *Eorasaurus olsoni*, youngest boundary of the biostratigraphic range; Ezcurra et al., 2014) to Recent (*Passer domesticus*).

Synapomorphies. Main body of the premaxilla slightly downturned, in which the alveolar margin is angled at approximately 20º to the alveolar margin of the maxilla (29:0→1); postfrontal reduced to approximately less than half the dimensions of the postorbital (116:0→1); ventral process of the postorbital ends much higher than the ventral border of the orbit (125:1→0); supratemporal present (149:2→1); tooth

bearing portion of the dentary mostly straight (253:2→0); suture along the anterior half of the surangular and angular anteroposteriorly convex ventrally in lateral view (266:1→0); retroarticular process of the lower jaw upturned (268:0→1); tooth implantation ankylothecodont (282:0→1); and intercentra in the dorsal series (344:1→0).

Rhynchosauria Osborn, 1903

Previous definition. The most recent common ancestor of *Mesosuchus* and *Howesia* and all of its descendants (node-based) (Dilkes, 1998).

New definition. All taxa more closely related to *Rhynchosaurus articeps* Owen, 1842 than to *Trilophosaurus buettneri* Case, 1928, *Prolacerta broomi* Parrington, 1935 or *Crocodylus niloticus* Laurenti, 1768 (stem-based). A new definition for Rhynchosauria is proposed because in the phylogenetic hypothesis recovered here the previous definition will exclude *Noteosuchus colletti* from the clade, and this species has been historically considered as a rhynchosaur (Watson, 1912; Broom, 1925; Carroll, 1976; Dilkes, 1998; Ezcurra et al., 2014).

Temporal range. Earliest Triassic (Indian–early Olenekian, *Noteosuchus colletti*; Rubidge, 2005) to middle Late Triassic (early Norian, *Hyperodapedon* spp; Martínez et al., 2011).

Synapomorphies. Length of the transverse process + rib versus length across zygapophyses in anterior caudal vertebrae = 1.51–1.68 (352:1→2); and length of metatarsal I versus length of metatarsal III = 0.38–0.42 (532:3→2).

Unnamed clade (*Mesosuchus browni* + Rhynchosauridae)

Temporal range. Early Middle Triassic (early Anisian, *Mesosuchus browni*; Rubidge, 2005) to middle Late Trassic (early Norian, *Hyperodapedon* spp; Martínez et al., 2011).

Synapomorphies. Neural spine height versus anteroposterior length at its base in anterior caudal vertebrae = 2.36–2.65 (354:0→1); and main axis of the postacetabular process of the ilium posterodorsally oriented in lateral or medial view (432:1→0):

Unnamed clade (*Howesia* + Rhynchosauridae)

Temporal range. Early Middle Triassic (early Anisian, *Howesia browni*; Hancox, 2000) to middle Late Trassic (early Norian, *Hyperodapedon* spp; Martínez et al., 2011).

Synapomorphies. Supratemporal fossa immediately medial and anterior to the supratemporal fenestra on the dorsal surface of the skull roof absent (8:1→0); alveolar margin of the maxilla distinctly convex in lateral view (66:0→1); maxilla with tooth plate (70:0→1); teeth on occlusal and lingual surfaces of the maxilla (72:0→1); anterior margin of the nasals transverse, with little convexity, at midline (76:0→1); parietals with sagittal crest between supratemporal fenestrae (153:0→2); scapula and coracoid do not fuse (359:0→1).

Unnamed clade (*Eohyosaurus wolvaardti* + Rhynchosauridae)

Temporal range. Early Middle Triassic (early Anisian, *Eohyosaurus wolvaardti*; Hancox, 2000) to middle Late Trassic (early Norian, *Hyperodapedon* spp; Martínez et al., 2011).

Synapomorphies. Maxilla and jugal with anguli oris crest (46:0→1); and posterior process of the postorbital extends close to or beyond the level of the posterior margin of the supratemporal fenestrae (124:0→1).

Rhynchosauridae Huxley, 1859

Definition. The most recent common ancestor of *Rhynchosaurus*, *Stenaulorhynchus*, *Scaphonyx* and *Hyperodapedon* and all of its descendants (node-based) (Dilkes 1998).

Temporal range. Early Middle Triassic (Anisian, *Rhynchosaurus articeps*; Benton, 1990) to middle Late Trassic (early Norian, *Hyperodapedon* spp; Martínez et al., 2011).

Synapomorphies. Orbit with well-developed elevated rim along the jugal, postorbital, frontal, prefrontal and lacrimal (17:1→2); posterior process of the jugal with a distinct lateroventral orientation with respect to the sagittal axis of the snout (98:0→1); medial process of the squamosal long, forming entirely or almost entirely the posterior border of the supratemporal fenestra (134:0→1); teeth absent in the vomer (177:2→3); teeth absent in the ventral surface of the anterior ramus of the pterygoid (184:0→6); inverted V-shaped supraoccipital in occipital (197:0→1); distinct dorsal process behind the alveolar margin of the lower jaw present and formed by a dorsally well-developed surangular (247:0→1); and blade and groove occlusion between dentary and cranial teeth (264:1→2).

Unnamed clade (Prolacertidae + Archosauria)

Temporal range. Late Permian (Wuchiapingian, *Eorasaurus olsoni*, youngest boundary of the biostratigraphic range; Ezcurra et al., 2014) to Recent (*Passer domesticus*).

Synapomorphies. Maxilla without contact with prefrontal (59:1→0); row of fang-like teeth on the medial edge of the anterior ramus of the pterygoid (= T4 of Welman, 1998) (188:0→1); suture between pterygoid and ectopterygoid reaches the posterolateral corner of the transverse flange of the pterygoid (194:0→1); ventral ramus of the opisthotic club-shaped (205:2→0); pseudolagenar recess between the ventral surface of the ventral ramus of the opisthotic and the basal tubera (210:1→0); intertuberal plate present and arched anteriorly in the parabasisphenoid (223:0→2); posterior surangular foramen present (273:0→1); distal edge of the maxillary tooth crowns concave in labial view along the entire alveolar margin (285:1→0); labiolingual compression of the marginal dentition (287:0→1); gradual transverse expansion of the distal half of the cervical and dorsal neural spines with distinct mammillary processes on the lateral surface (301:0→2); postaxial cervical intercentra (324:1→0); zygapophyses mainly oriented in the parasagittal plane in anterior–middle dorsal vertebrae (337:0→1); total length of the scapula versus minimum anteroposterior width of the scapular blade = 1.23–2.61 (362:1→0); anterior margin of the scapular blade straight or convex along its entire length in lateral view (364:1→0); and length of digit III versus length of digit IV = 0.87–1.44 (543:1→2).

Prolacertidae Parrington, 1935

New definition. All taxa more closely related to *Prolacerta broomi* Parrington, 1935 than to *Protorosaurus speneri* Meyer, 1832, *Tanystropheus longobardicus* (Bassani, 1886), *Proterosuchus fergusi* Broom, 1903 or *Euparkeria capensis* Broom, 1913 (stem-based).

Temporal range. Early Triassic (*Prolacerta broomi*; Rubidge, 2005).

Synapomorphies. Parietals strongly entering between both frontals, forming an acute-angled suture (110:0→1).

Comments. This result supports previous claims of very close affinities or even synonymy between *Prolacerta broomi* and *Kadimakara australiensis* (Bartholomai, 1979; Borsuk-Białynicka and Evans, 2009; Evans and Jones, 2010). *Kadimakara australiensis* possesses a median subrectangular fossa on the posterior half of the parietals that is separated from the margins of the supratemporal fossae by broad flat surfaces (QM F6710). By contrast, *Prolacerta broomi* lacks a fossa on the posterior half of the parietals or possesses a median fossa that is confluent with the margins of the supratemporal fossae (BP/1/471, 2675, 4504a, 5375; GHG 431; SAM-PK-K10797; UMCZ 2003.41R). As a result, the morphology of the dorsal surface of the parietals allows these closely related species to be distinguished from each other.

Unnamed clade (*Tasmaniosaurus triassicus* + Archosauria)

Temporal range. Latest Permian (Changhsingian, *Archosaurus rossicus*; Rubidge, 2005; Sennikov and Golubev, 2012) to Recent (*Passer domesticus*).

Synapomorphies. Antorbital fenestra present (13:0→1); postnarial process of the premaxilla wide and plate-like (37:1→0); pineal foramen absent (157:0→2); postparietal present (163:2→0); dentary with posterodorsal and posterocentral processes (258:1→2); serrations on the maxillary and dentary crowns (286:0→1/2); and lateral fossa on the centrum below the neurocentral suture in dorsal vertebrae (0→1).

Comments. *Tasmaniosaurus triassicus* was originally interpreted as a proterosuchid archosauriform, but is recovered here as the sister taxon of Archosauriformes. As a result, character states usually considered as synapomorphic of Archosauriformes are

optimized here as apomorphic of this more inclusive clade (e.g. antorbital fenestra, serrated teeth; Dilkes, 1998; Nesbitt, 2011).

Archosauriformes Gauthier, Kluge and Rowe, 1988

Definition. The least inclusive clade containing *Crocodylus niloticus* Laurenti, 1768, and *Proterosuchus fergusi* Broom, 1903 (node-based) (Nesbitt, 2011).

Temporal range. Latest Permian (Changhsingian, *Archosaurus rossicus*; Rubidge, 2005; Sennikov and Golubev, 2012) to Recent (*Passer domesticus*).

Synapomorphies. Interdental plates present, but restricted to the anterior end of the dentary (1:0→1); orbital border of the frontal absent or anteroposteriorly short in mature individuals (108:1→0); and tooth bearing portion of the dentary distinctly dorsally curved for all or most of its anteroposterior length (253:0→1).

Proterosuchidae Huene, 1908

Definition. All taxa more closely related to *Proterosuchus fergusi* Broom, 1903 than to *Erythrosuchus africanus* Broom, 1905, *Crocodylus niloticus* Laurenti, 1768 or *Passer domesticus* Linnaeus, 1758 (stem-based) (Ezcurra et al., 2013).

Temporal range. Latest Permian (Changhsingian, *Archosaurus rossicus*; Rubidge, 2005; Sennikov and Golubev, 2012) to earliest Triassic (Induan–?early Olenekian: *Proterosuchus fergusi*: Rubidge, 2005).

Synapomorphies. Alveolar margin of the premaxilla does not reach the contact with the maxilla and forms a diastema (= subnarial gap) (26:0→1); base of the prenarial process of the premaxilla anteroposteriorly deep (35:0→1); lateroventrally opening anterior alveoli in the premaxilla in mature individuals (43:0→1); maxilla extends level to or posterior to posterior orbital border in mature individuals (69:1→0); length

of the posterior process of the jugal versus the height of its base = 4.07–5.37 (97:1→2); distal half of the posterior process of the jugal subrectangular (99:0→1); transverse suture between nasals and frontals (107:1→0); pineal fossa on the median line of the dorsal surface of the parietal (155:0→1); basipterygoid process of the parabasisphenoid posteriorly oriented at its distal tip (234:0→1); prezygodiapophyseal lamina absent in posterior cervical or anterior dorsal vertebrae (297:1→0); interclavicle with rather sharp angles between lateral and posterior processes (381:0→1); posterior ramus of the interclavicle with little change in width along its entire length (383:1→0); and proximal surface of the femur with transverse groove (460:0→1).

Unnamed clade (*Proterosuchus alexanderi* + *Proterosuchus goweri* + *"Chasmatosaurus" yuani*)

Temporal range. Earliest Triassic (Induan–?early Olenekian: *Proterosuchus alexanderi*: Rubidge, 2005).

Synapomorphies. Angle between the posterior margins of the proximal and distal ends of the quadrate = 143–158º (169:2→3); mammillary processes of the neural spine of cervical vertebrae present from the fifth presacral (323:2→1); zygapophyses of dorsal vertebrae laterally divergent beyond the lateral margin of the centrum (337:1→0); and mammillary processes of the neural spine of dorsal vertebrae extend up to the thirteenth presacral (343:2→3).

Unnamed clade (*Proterosuchus goweri* + *"Chasmatosaurus" yuani*)

Temporal range. Earliest Triassic (Induan–?early Olenekian: *Proterosuchus goweri*: Rubidge, 2005).

Synapomorphies. Ventral ramus of the opisthotic rod-like and very robust (205: 0→3).

Unnamed clade (*Fugusuchus hejiapanensis* + Archosauria)

Temporal range. Late Early Triassic (late Olenekian, *Garjainia prima*; Gower and Sennikov, 2000) to Recent (*Passer domesticus*).

Synapomorphies. Dorsal surface of the skull roof without supratemporal fossa immediately medial or anterior to the supratemporal fenestra (8:1→0); 15–22 tooth positions in the maxilla (73:3→2); fusion between opisthotic and exoccipital (200:0→1); basal tubera of the basioccipital partially connected to each other (213:0→1); occipital neck of the basioccipital distinctly separating the occipital condyle from the basioccipital body (217:1→0); and intertuberal plate of the parabasisphenoid straight (223:2→1).

Unnamed clade (*Sarmatosuchus otschevi* + Archosauria)

Temporal range. Late Early Triassic (late Olenekian, *Garjainia prima*; Gower and Sennikov, 2000) to Recent (*Passer domesticus*).

Synapomorphies. Basioccipital and parabasisphenoid tightly sutured, sometimes by an interdigitated suture, or both bones fused with each other in mature individuals (212:0→1); and parabasisphenoid oblique, with a posterodorsally-to-anteroventrally oriented main axis (221:0→1).

Unnamed clade (Erythrosuchidae + Archosauria)

Temporal range. Late Early Triassic (late Olenekian, *Garjainia prima*; Gower and Sennikov, 2000) to Recent (*Passer domesticus*).

Synapomorphies. Anteroposterior length of the main body of the premailla versus its maximum dorsoventral height = 1.07–2.00 (28:2→1); transition between the anterior and ventral processes of the squamosal sharp and the posterodorsal border of the infratemporal fenestra with square outline (133:1→0); ventral ramus of the opisthotic plate-like (205:0→4); external foramina for passage of the abducens nerves (CN VI) on the anterior surface of the dorsum sella (237:0→1); dentary without large foramina aligned in two distinct rows starting on the anteroventral corner of the bone (254:1→0); posterior centrodiapophyseal lamina in cervical or anterior dorsal vertebrae (296:0→1); total length of the scapula versus minimum anteroposterior width of the scapular blade = 3.25–6.73 (362:0→1); and anterior margin of the scapular blade distinctly concave in lateral view (364:0→1).

Erythrosuchidae Watson, 1917

Definition. All taxa more closely related to *Erythrosuchus africanus* Broom, 1905 than to *Proterosuchus fergusi* Broom, 1903, or *Passer domesticus* Linnaeus, 1758 (stem-based) (Ezcurra et al., 2010).

Temporal range. Late Early Triassic (late Olenekian, *Garjainia prima*; Gower and Sennikov, 2000) to early Late Triassc (late Carnian–early Norian, *Cuyosuchus huenei*; Spalletti et al., 2008).

Synapomorphies. Alveolar margin on the anterior third of the maxilla (anterior to the level of the anterior border of the antorbital fenestra) distinctly upturned (68:0→1); teeth absent from the ventral surface of the anterior ramus of the pterygoid (184:0→6); articular with a ventromedially directed process (278:0→1); and distal end of the radius strongly anteroposteriorly expanded (409:0→1).

Synapomorphies present in only some trees. Jugal with a longitudinal ridge or bump(s) on the lateral surface of its main body (95:0→1); dorsally opened pit lateral to the base of the neural spine of dorsal vertebrae developed as a deep pit (340:1→2); length of the deltopectoral crest of the humerus versus total length of the bone in mature individuals = 0.46–0.49 (394:3→5); and transverse width of the fibula at mid-length subequal to transverse width of the tibia (493:1→0).

Unnamed clade (*Shansisuchus shansisuchus* + *Garjainia prima*)

Temporal range. Late Early Triassic (late Olenekian, *Garjainia prima*; Gower and Sennikov, 2000) to late Middle Triassic (Ladinian, *Chalishevia cothurnata*; Gower and Sennikov, 2000).

Synapomorphies. Length of the centrum versus height of the centrum in anterior dorsals = 0.45–1.10 (329:1→0); transverse processes and ribs of sacral and/or anterior caudal vertebrae not fused to each other in mature individuals (351:1→0); and transverse width of the proximal end of the humerus versus total length of the bone in mature individuals = 0.57–0.70 (388:0→2).

Synapomorphies present in only some trees. Maxillo-nasal tuberosity delimiting anteriorly the antorbital fossa (45:0→1); anterior margin of the base of the ascending process of the maxilla sub-vertical (56:1→2); edentulous anterior portion of the ventral margin of the maxilla (67:0→1); ventral surface of the frontal with a median longitudinal canal for the passage of the olfactory tract only slightly constricted and without olfactory bulb moulds and distinct semilunate posteromedially-to-anterolaterally oriented ridges on the orbital roof (114:0→1); pineal fossa on the median line of the dorsal surface of the parietal (155:0→1); and lateral surface of the

surangular with a laterally projecting shelf that possesses a strongly convex lateral edge (270:2→3).

Unnamed clade (*Erythrosuchus africanus* + *Garjainia prima*)

Temporal range. Late Early Triassic (late Olenekian, *Garjainia prima*; Gower and Sennikov, 2000) to early Middle Triassic (early Anisian, *Erythrosuchus africanus*; Rubidge, 2005).

Synapomorphies. Lateral surface of the premaxilla with a longitudinal groove slightly displaced ventrally or at the point of mid-height of the main body (31:0→2); ventral surface of the centrum in anterior cervical vertebrae with a median longitudinal keel that extends ventral to the centrum rim in at least one vertebra (307:1→2); transverse width of the distal end of the humerus versus total length of the bone in mature individuals = 0.49–0.57 (395:1→2); and entepicondyle of the humerus strongly developed in mature individuals (396:0→1).

Synapomorphies present in only some trees. V-shaped ventral border of the orbit formed by the jugal (92:0→1); lateral surface of the main body of the prefrontal with a groove that opens into the orbital border (106:0→1); transverse suture between nasal and frontal (107:1→0); lateral boss adjacent to orbital margin of the postorbital (122:0→1); suture between surangular and angular along the anterior half of the bones anteroposteriorly concave ventrally in lateral view (266:0→1); posterior portion of the neural arch ventral to the postzygapophysis in postaxial cervicals with a shallow, posterolaterally facing fossa (314:0→1); posteriorly projected heel on the posterior margin of the ischiadic peduncle of the ilium present in lateral view, the dorsal margin of which is set at 45º or less to the longitudinal axis of the bone (436:0→1); and distal condyles of the femur with a prominent, strong dorsoventral

expansion (in sprawling orientation) restricted to the distal end of the bone (477:1→0).

***Garjainia* (*Garjainia prima* + *Garjainia madiba* + GHG 7433MI)**

Temporal range. Late Early Triassic (late Olenekian, *Garjainia prima* and *Garjainia madiba*; Gower and Sennikov, 2000; unknown exact age for GHG 7433MI).

Synapomorphies. Supratemporal fossa immediately medial or anterior to the supratemporal fenestra on the dorsal surface of the skull roof (8:0→1); and posterior portion of the maxilla ventral to the antorbital fenestra expands dorsoventrally towards the distal end of the horizontal process with a straight ventral margin of the antorbital fenestra (61:2→3).

Synapomorphies present in only some trees. Fossa immediately lateral to the foramen magnum on the occipital surface of the opisthotic (204:0→1); ventral ramus of the opisthotic rod-like and very robust (205:4→3); basal tubera of the basioccipital clearly separated from each other (213:1→0); ventral surface of the parabasispheniod with a pair of posterolaterally-to-anteromedially oriented thin ridges that extend onto the base of the cultriform process (232:0→1); basipterygoid processes of the parabasisphenoid oriented posteriorly at their distal tips (234:0→1); distinct longitudinal lamina extending along the lateral surface of the centrum at mid-height in anterior and middle postaxial cervical vertebrae (319:0→1); shallow dorsally opening pit lateral to the base of the dorsal neural spines (340:2→1); semicircular preacetabular process of the ilium in lateral view (429:1→0); and prominent tuberosity for the attachment of the ambiens muscle in the pubis of mature individuals (441:1→0).

Unnamed clade (*Dorosuchus neoetus* + *Asperoris mnyama* + Archosauria)

Temporal range. Late Early Triassic (latest Olenekian, *Ctenosauriscus koeneni*; Butler et al., 2011) to Recent (*Passer domesticus*).

Synapomorphies. Suture between premaxilla and maxilla as simple continuous contact (24:1→0); premaxilla and maxilla without subnarial foramen between them (25:2→0); premaxilla without a downturned main body - alveolar margin of premaxilla is sub-parallel to the main axis of the maxilla (29:1→0); four tooth positions in the premaxilla (41:1→2); parabasisphenoid without intertuberal plate (223:1→0); proximal articular surface of the femur well ossified, being flat or convex (456:1→0); femoral head anteromedially orientated, 20º–60º with respect to the transverse axis through the femoral condyles (458:0→1); and attachment of the caudofemoralis musculature on the posterior surface of the femur placed on a fourth trochanter (469:1→2).

Unnamed clade (*Euparkeria capensis* + Archosauria)

Temporal range. Late Early Triassic (latest Olenekian, *Ctenosauriscus koeneni*; Butler et al., 2011) to Recent (*Passer domesticus*).

Synapomorphies. Orbital border of the frontal anteroposteriorly long and forms most of the dorsal edge of the orbit in mature individuals (108:0→1); basal tubera of the basioccipital clearly separated from each other (213:1→0); and prootic without ridge on the lateral surface of the inferior anterior process ventral to the trigeminal foramen (242:0→1).

Unnamed clade (Proterochampsia + Archosauria)

Temporal range. Late Early Triassic (latest Olenekian, *Ctenosauriscus koeneni*; Butler et al., 2011) to Recent (*Passer domesticus*).

Synapomorphies. Posterior process of the jugal does not form entirely or almost entirely the ventral border of the infratemporal fenestra (100:1→0); postparietal absent as a separate ossification (163:0/1→2); absence of pseudolagenar recess between the ventral surface of the ventral ramus of the opisthotic and the basal tubera (210:0→1); parabasisphenoid horizontal (221:1→0); minimum height of the dentary versus length of the alveolar margin (including edentulous anterior end if present) = 0.05–0.14 (252:1→0); posterior surangular foramen (273:1→0); cervical and dorsal vertebrae without gradual transverse expansion of the distal half of the neural spine (301:1→0); absence of excavation immediately lateral to the base of postaxial cervical neural spines (317:1→0); absence of postaxial cervical intercentra (324:0→1); absence of dorsally opening pit lateral to the base of the dorsal neural spines (340:1→0); absence of dorsal intercentra (344:0→1); and large biceps process on the lateral surface of the coracoid (373:0→1).

Proterochampsia Bonaparte, 1971

Definition. The most inclusive clade containing *Proterochampa barrionuevoi* Reig, 1959, but not *Euparkeria capensis* Broom, 1913, *Erythrosuchus africanus* Broom, 1905, *Passer domesticus* Linnaeus, 1758, or *Crocodylus niloticus* Laurenti, 1768 (stem-based) (Nesbitt, 2011).

Temporal range. Late Middle Triassic (Ladinian, *Jaxtasuchus salomoni*; Schoch and Sues, 2013) to Late Triassic (late Norian, *Doswellia sixmilensis*; Heckert et al., 2012).

Synapomorphies. External naris dorsally directed (11:0→1); dorsoventral height of the snout at the level of the anterior tip of the maxilla versus dorsoventral height at the

level of the anterior border of the orbit = 0.38–0.53 (21:2→1); lateral margin of the snout anterior to the prefrontal formed by the nasal and maxilla with gently rounded transition along the maxilla from the lateral to dorsal side of rostrum (23:0→1); 5 or more tooth positions in the premaxilla (41:2→1); maxilla contacts prefrontal (59:0→1); transition between the anterior and ventral processes of the squamosal gentle, widely rounded posterodorsal border of the infratemporal fenestra (133:0→1); lateral row of teeth on the ventral surface of the anterior ramus (= palatal ramus) of the pterygoid raised on a thick, posteromedially-to-anterolaterally oriented ridge (187:0→1); tooth bearing portion of the dentary ventrally curved or deflected (253:1→2); cervical and anterior dorsal vertebrae without posterior centrodiapophyseal lamina (296:1→0); posterior cervical and anterior dorsal vertebrae without prezygodiapophyseal lamina (297:1→0); posterior cervical and anterior dorsal vertebrae without postzygodiapophyseal lamina (298:1→0); transverse width of conjoined pubic aprons versus total length of the bone = 1.48–1.94 (445:2→3); tibia with straight cnemial crest (482:0→1); metatarsal V without a hook-shaped proximal end (540:1→0); and phalanges on pedal digit V present and with a "poorly" developed first phalanx (544:0→1).

Doswelliidae Weems, 1980

Definition. The most inclusive clade that contains all archosauromorphs more closely related to *Doswellia kaltenbachi* Weems, 1980 than to *Proterochampsa barrionuevoi* Reig 1959, *Erythrosuchus africanus* Broom, 1905, *Caiman latirostris* Daudin, 1802, or *Passer domesticus* Linnaeus, 1758 (stem-based) (Desojo et al., 2011).

Temporal range. Late Middle Triassic (Ladinian, *Jaxtasuchus salomoni*; Schoch and Sues, 2013) to Late Triassic (late Norian, *Doswellia sixmilensis*; Heckert et al., 2012).

Synapomorphies. Posterior extension of the maxilla level with or posterior to posterior orbital border in mature individuals (69:1→0); medial process of the squamosal long, forming entirely or almost entirely the posterior border of the supratemporal fenestra (134:0→1); parietal without distinct transverse emargination adjacent to the posterior margin of the bone in late ontogeny (159:1→0); posterior surface of the supraoccipital with a prominent median, vertical peg (199:0→1); total length of the femur versus total length of the humerus = 1.62–1.74 (454:1→2); proximal portion of the fibula symmetrical or nearly symmetrical in lateral view (492:1→0); more than two rows of dorsal osteoderms (548:1/2→3); presacral dorsal osteoderms square-shaped (555:1→0); and presence of appendicular osteoderms (559:0→1).

Unnamed clade (*Doswellia kaltenbachi* + *Tarjadia ruthae*)

Temporal range. Late Middle Triassic (Ladinian, *Jaxtasuchus salomoni*; Schoch and Sues, 2013) to Late Triassic (late Norian, *Doswellia sixmilensis*; Heckert et al., 2012).

Synapomorphies. Retroarticular process of the surangular and articular not upturned (268:1→0); transverse processes in middle and posterior dorsal vertebrae extremely long, being considerably broader than their respective centra (336:1→2); internal tuberosity of the humerus distinctly separated from the proximal articular surface of the bone (392:0→1); ilium with a laterally deflected iliac blade (427:0→1); ilium with convex dorsal margin of the iliac blade (434:1→0); external surface of the osteoderms sculptured (549:0→1); and unornamented anterior articular lamina in paramedian osteoderms (556:0→1).

Unnamed clade (*Jaxtasuchus salomoni* + *Doswellia kaltenbachi*)

Temporal range. Late Middle Triassic (Ladinian, *Jaxtasuchus salomoni*; Schoch and Sues, 2013) to Late Triassic (late Norian, *Doswellia sixmilensis*; Heckert et al., 2012).

Synapomorphies. Basioccipital with notochordal scar on the occipital surface of the occipital condyle developed as a vertical furrow or a large sub-circular fossa that occupies approximately half of the height of the condyle surface (216:0→1); and blunt anteroposteriorly restricted eminence in paramedian osteoderms (551:0→2).

Unnamed clade (*Tarjadia ruthae* + *Archeopelta arborensis*)

Temporal range. Late Middle−early Late Triassic (Ladinian-early Carnian, *Tarjadia ruthae* and *Archeopelta arborensis*; Desojo et al., 2011).

Synapomorphies. Very thick paramedian osteoderms (552:0→1); and presacral dorsal osteoderms wider than long (555:0→2).

Proterochampsidae Sill, 1967

Definition. The least inclusive group that is composed of *Chanaresuchus bonapartei* Romer, 1971a and *Proterochampsa barrionuevoi* Reig, 1959 but not *Euparkeria capensis* Broom, 1913, *Doswellia kaltenbachi* Weems, 1980, *Passer domesticus* Linnaeus, 1758 nor *Crocodylus niloticus* Laurenti, 1768 (node-based) (Trotteyn, 2011).

Temporal range. Late Middle−early Late Triassic (Ladinian–early Carnian, *Chanaresuchus bonapartei*; Desojo et al., 2011) to middle Late Triassic (middle Norian, *Proterochampsa barrionuevoi*; Martínez et al., 2011).

Synapomorphies. Dorsal orbital margin with a shelf/ridge elevated above skull table that extends along the lateral surface of the lacrimal, prefrontal, frontal and postorbital (7:0→2); premaxilla with a slightly downturned main body, in which the alveolar

margin is angled at approximately 20º to the alveolar margin of the maxilla (29:0→1); narial fossa expanded in the anteroventral corner of the naris (32:0→1); total length of the nasal versus total length of the frontal = 1.78–2.78 (74:1→2/3/4); ventral process of the squamosal forms more than half of the posterior border of the infratemporal fenestra (140:0→1); basioccipital with notochordal scar on the occipital surface of the occipital condyle developed as a vertical furrow or a large sub-circular fossa that occupies approximately half of the height of the condyle surface (216:0→1); parabasisphenoid with anteriorly arched intertuberal plate (223:0→2); ventral surface of the centrum in anterior cervical vertebrae with a median longitudinal keel that extends ventral to the centrum rim in at least one anterior cervical (307:1→2); and lateral posterior condyle of the proximal end of the tibia offset anteriorly from the medial posterior condyle (484:1→0).

***Proterochampsa* (*Proterochampsa barrionuevoi* + *Proterochampsa nodosa*)**

Temporal range. Early to middle Late Triassic (late Carnian to middle Norian, *Proterochampsa barrionuevoi*; Martínez et al., 2011).

Synapomorphies. Strongly dorsoventrally compressed skull with mainly dorsally facing antorbital fenestrae and orbits (3:0→1); alveolar margin of the premaxilla does not reach the contact with the maxilla and forms a diastema (= subnarial gap) (26:0→1); posterior extension of the maxilla level with or anterior to anterior orbital border in mature individuals (69:1→2); tooth bearing portion of the dentary mostly straight (253:2→0); retroarticular process of the lower jaw absent (267:1→0); and posteroventral surface of the angular ridged or keeled (276:1→0).

Unnamed clade (*Cerritosaurus binsfeldi* + Rhadinosuchinae)

Temporal range. Late Middle−early Late Triassic (Ladinian–early Carnian, *Chanaresuchus bonapartei*; Desojo et al., 2011) to middle Late Triassic (middle Norian, *Rhadinosuchus gracilis*; Martínez et al., 2011).

Synapomorphies. Anterior margin of the antorbital fenestra nearly pointed (14:0→1); longitudinal ridge on the lateral surface of the main body of the jugal (95:0→1); depression on the lateral surface of the ventral process of the postorbital (127:0→1); anterior process of the squamosal forms most of the lateral border of the supratemporal fenestra (131:0→1); posterodorsal portion of the squamosal with a supratemporal fossa (142:0→1); widely concave notch on the anterior margin of the ascending process of the quadratojugal (147:0→1); and anteroposterior length of the external mandibular fenestra versus anteroposterior length of the dentary anterior to the fenestra = 0.44–0.53 (249:0→1).

Unnamed clade (*Tropidosuchus romeri* + Rhadinosuchinae)

Temporal range. Late Middle−early Late Triassic (Ladinian–early Carnian, *Chanaresuchus bonapartei*; Desojo et al., 2011) to middle Late Triassic (middle Norian, *Rhadinosuchus gracilis*; Martínez et al., 2011).

Synapomorphies. Supratemporal fossa immediately medial or anterior to the supratemporal fenestra on the dorsal surface of the skull roof (8:0→1); antorbital fossa absent from the lateral surface of the maxilla (53:1→0); infratemporal fossa marked by a sharp edge on the quadratojugal (145:0→1); suture between surangular and angular elevated and separates dorsal concave area on surangular from concave area on angular (265:0→1); and ventrolateral surface of the angular with a laterally projecting ridge that separates the lateral and ventral sides of the angular (275: 0→1).

Rhadinosuchinae Hoffstetter, 1955

Definition. All archosauriforms more closely related to *Rhadinosuchus gracilis* Huene, 1938 and *Chanaresuchus bonapartei* Romer, 1971a than to *Cerritosaurus binsfeldi* Price, 1946, *Tropidosuchus romeri* Arcucci, 1990, and *Doswellia kaltenbachi* Weems, 1980 (stem-based) (Ezcurra et al., 2015b).

Temporal range. Late Middle−early Late Triassic (Ladinian–early Carnian, *Chanaresuchus bonapartei*; Desojo et al., 2011) to middle Late Triassic (middle Norian, *Rhadinosuchus gracilis*; Martínez et al., 2011).

Synapomorphies. Dermal sculpturing on the dorsal surface of the skull roof consists of shallow or deep pits scattered across surface and/or low ridges (5:0→1); lateral margin of the snout anterior to the prefrontal formed by the nasal and maxilla with sharp edge along the maxilla between the lateral and dorsal sides of this bone (= box-like snout of Kischlat, 2000) (23:1→2); anterior process of the jugal subrectangular or slightly dorsoventrally expanded, being higher than the portion of the maxilla underneath it (90:0→1); anteriorly projecting, rounded spur on the anterior edge of the ventral process of the postorbital indicating the lower delimitation of the eye-ball (128:0→1); and very thick paramedian osteoderms (552:0→1).

Unnamed clade (*Gualosuchus reigi* + *Chanaresuchus bonapartei*)

Temporal range. Late Middle−early Late Triassic (Ladinian–early Carnian, *Chanaresuchus bonapartei*; Desojo et al., 2011) to middle Late Triassic (middle Norian, *Rhadinosuchus gracilis*; Martínez et al., 2011).

Synapomorphies. Posterior process of the squamosal ventrally curved (136:0→1); proximal end of the humerus medially expanded, being asymmetric in anterior view

(391:0→1); and fourth trochanter of the femur distally extended beyond mid-shaft and well posteriorly developed (473:0→1).

Unnamed clade (*Chanaresuchus bonapartei* + *Rhadinosuchus gracilis*)

Temporal range. Late Middle−early Late Triassic (Ladinian–early Carnian, *Chanaresuchus bonapartei*; Desojo et al., 2011) to middle Late Triassic (middle Norian, *Rhadinosuchus gracilis*; Martínez et al., 2011).

Synapomorphies. Antorbital fossa forming a distinct inset margin to the antorbital fenestra on the lateral surface of the lacrimal and occuping almost half or more of the anteroposterior length of the ventral process of the lacrimal (86:0→2); and squared presacral dorsal osteoderms (555:1→0).

Archosauria Cope, 1869

Definition. The least inclusive clade containing *Crocodylus niloticus* Laurenti, 1768, and *Passer domesticus* Linnaeus, 1758 (node-based) (Sereno, 2005).

Temporal range. Late Early Triassic (latest Olenekian, *Ctenosauriscus koeneni*; Butler et al., 2011) to Recent (*Passer domesticus*).

Synapomorphies. Supratemporal fossa extending onto the ascending process of the postorbital (123:0→1); vomer without teeth (177:2→3); pterygoid without teeth on the ventral surface of the anterior ramus (= palatal process) (184:0→6); foramina for entrance of the cerebral branches of the internal carotid artery anterolaterally placed on the parabasisphenoid (226:0→2); internal tuberosity of the humerus distinctly separated from the proximal articular surface (392:0→1); olecranon process of the ulna prominent but lower than its anteroposterior depth at base (401:0→1); ventral articular surface of the calcaneum for distal tarsal 4 and the distal end of the calcaneal

tuber separated by a clear gap (515:0→1); articular surfaces for fibula and distal tarsal 4 in the calcaneum continuous (518:0→1); length of the metatarsal II versus length of the metatarsal IV = 0.90–1.02 (534:1→2); and relation between paramedian dorsal osteoderms and presacral vertebrae one to one (553:1→0).

Synapomorphy present in only some trees. Hyposphene-hypantrum accessory intervertebral articulation in dorsal vertebrae (338:0→1).

Pseudosuchia Zittel, 1887−1980

Definition. The most inclusive clade containing *Crocodylus niloticus* Laurenti, 1768, but not *Passer domesticus* Linnaeus, 1758 (stem-based) (Sereno, 2005).

Temporal range. Late Early Triassic (latest Olenekian, *Ctenosauriscus koeneni*; Butler et al., 2011) to Recent (*Crocodylus niloticus*).

Synapomorphies. Posttemporal fenestra smaller than the supraoccipital but does not develop as a small foramen (19:2→1); posterior process of the squamosal ventrally curved (136:0→1); anterior ramus (= palatal process) of the pterygoid transversely narrow along its entire extension, converging in a right or acute angle with the transverse ramus, with the bone possessing an overall L-shape contour in ventral or dorsal view (183:0→1); posteroventral process of the dentary contributes to the border of the external mandibular fenestra (260:1→2); articular with a ventromedially directed process (278:0→1); spine tables on the distal ends of the postaxial cervical and dorsal neural spines (302:0→3); length of the centrum versus height of the centrum in anterior dorsal vertebrae = 0.45–1.10 (329:1→0); distal articular surface of the femur uneven, fibular condyle projecting distally distinctly beyond tibial condyle (478:1→0); area of attachment of the iliofibularis muscle in the fibula placed on a hypertrophied tubercle (494:0/1→2); calcaneal tuber approximately as broad as or

broader than tall at midshaft (510:0→1); calcaneal tuber with a expanded distal end in proximal or distal view (512:0→1); transverse width of the distal articular surface of the calcaneum versus transverse width of the astragalus 0.54–1.22 (519:1→2); and pedal unguals strongly transversely compressed, with a sharp dorsal keel (547:0→2).

Phytosauria Meyer, 1861

Definition. The most inclusive clade containing *Rutiodon carolinensis* (Emmons, 1856) but not *Aetosaurus ferratus* Fraas, 1877, *Rauisuchus tiradentes* Huene, 1942, *Prestosuchus chiniquensis* Huene, 1942, *Ornithosuchus longidens* Huxley, 1877, and *Crocodylus niloticus* Laurenti, 1768 (stem-based) (Sereno, 2005).

Temporal range. Early Late Triassic (late Carnian–earliest Norian, *Parasuchus hislopi*; Langer, 2005) to latest Triassic (late Norian–?Rhaetian, *Redondasaurus*; Hunt and Lucas, 1993).

Synapomorphies. Strongly dorsoventrally compressed skull with mainly dorsally facing antorbital fenestrae and orbits (3:0→1); dorsal orbital margin of the frontal elevated above skull table (7:0→1); external naris non-terminal, considerably posteriorly displaced, but posterior rim of the naris well anterior to the anterior border of the orbit (10:0→1); external naris dorsally directed (11:0→1); antorbital length versus total length of the skull = 0.70–0.76 (20:1→2); snout transversely broader than or as broad as dorsoventrally tall at the level of the anterior border of the orbit (22:1→0); 10 or more tooth positions in the premaxilla (41:2→0); maxilla extends anterior to the nasals (48:0→1); alveolar margin of the maxilla sigmoid, anteriorly concave and posteriorly convex, in lateral view (66:0→2); posterior extension of the maxilla level with or anterior to anterior orbital border in mature individuals (69:1→2); number of maxillary tooth positions 15–22 (73:1→2); length of the

posterior process of the jugal versus the height of its base = 4.07–5.37 (97:1→2); posterior process of the jugal lies ventral to the anterior process of the quadratojugal (102:0→1); ventral process of the squamosal anteroventrally directed at 45º or less (139:0→1); neomorphic bone as a separate ossification anterior to nasals and surrounded by the premaxilla on the dorsal surface of the snout (167:0→1); proximal head of the quadrate has a sutural contact with the paraoccipital process of the opisthotic (170:0→1); palatine with a single anterior process forming the posterior border of the choana (179:1→2); Meckelian fossa of the lower jaw mostly dorsally oriented due to greatly expanded prearticular resulting in a ventral border of the fossa situated dorsal to the half-height of the lower jaw at that level (250:0→1); mandibular symphysis present along one-third of the lower jaw (251:0→1); tooth bearing portion of the dentary mostly straight (253:1→0); dorsal margin of the anterior portion of the dentary dorsally expanded compared to the dorsal margin of the posterior portion (257:0→1); and distal edge of the posterior maxillary tooth crowns with a distinct different morphology from those of the anterior tooth crowns, with the posterior edge usually convex in labial view (284:0→1).

Pseudopalatinae Long and Murry, 1995

Definition. The last common ancestor of *Nicrosaurus kapffi* (Meyer, 1860), *Mystriosuchus westphali* Hungerbühler and Hunt, 2000, *Machaeroprosopus pristinus* (Mehl, 1928), *Redondasaurus gregorii* Hunt and Lucas, 1993, and all descendants of that ancestor (node-based) (Parker and Irmis, 2006).

Temporal range. Middle Late Triassic (Norian, *Nicrosaurus kapffi*; Stocker and Butler, 2013) to latest Triassic (late Norian–?Rhaetian, *Redondasaurus*; Hunt and Lucas, 1993).

Synapomorphies. Orbit rim elevation absent or incipient (17:1→0); postnarial process of the premaxilla wide, plate-like (37:1→0); antorbital fossa on the lateral surface of the maxilla absent or not exposed in lateral view (53:1→0); posterior process of the postorbital extends close to or beyond the level of the posterior margin of the supratemporal fenestrae (124:0→1); basal tubera of the basioccipital partially connected to each other (213:0→1); and distinct dorsal process behind the alveolar margin of the lower jaw formed by a dorsally well-developed surangular (247:0→1).

Unnamed clade (*Nundasuchus songeaensis* + Suchia)

Temporal range. Late Early Triassic (latest Olenekian, *Ctenosauriscus koeneni*; Butler et al., 2011) to Recent (*Crocodylus niloticus*).

Synapomorphies. Coracoid with postglenoid process, separated from the glenoid fossa by a notch (374:0→1); transverse width of the proximal end of the humerus versus total length of the bone in mature individuals = 0.46–0.54 (388:0→1); proximal surface of the lateral condyle of the tibia depressed (483:0→1); posterior side of the distal portion of the tibia with a dorsoventrally oriented groove or gap (488:0→1); and proximal surface of the distal tarsal 4 with a distinct, proximally raised region on the posterior portion (= heel of Sereno and Arcucci, 1994) (525:0→1).

Unnamed clade (Ornithosuchidae + Suchia)

Temporal range. Late Early Triassic (latest Olenekian, *Ctenosauriscus koeneni*; Butler et al., 2011) to Recent (*Crocodylus niloticus*).

Synapomorphies. Dorsal vertebrae without hyposphene-hypantrum accessory intervertebral articulation (338:1→0); transverse width of conjoined pubic aprons

versus total length of the bone = 0.27–0.97 (445:2→0/1); tibial facet of the astragalus divided into distinct posteromedial and anterolateral basins (500:0→1); calcaneal tuber posteriorly oriented, between 50º–90º (509:1→2); and dorsal osteoderms aligned one to one dorsal to the dorsal vertebrae (554:0→1).

Ornithosuchidae Huene, 1908

Definition. *Ornithosuchus longidens* (Huxley, 1877), *Riojasuchus tenuisceps* Bonaparte, 1967, *Venaticosuchus rusconii* Bonaparte, 1970 and all descendants of their most recent common ancestor (node-based) (Sereno, 1991).

Temporal range. Early Late Triassic (late Carnian to earliest Norian, *Venaticosuchus rusconi*; Martínez et al., 2011) to middle Late Triassic (middle Norian, *Riojasuchus tenuisceps*; Kent et al., 2014).

Synapomorphies. Alveolar margin of the premaxilla does not reach the contact with the maxilla and forms a diastema (= subnarial gap) (26:0→1); slightly downturned main body of the premaxilla, alveolar margin is angled at approximately 20º to the alveolar margin of the maxilla (29:0→1); postnarial process of the premaxilla overlaps the anterodorsal surface of the nasal (39:0→1); three tooth positions in the premaxilla (41:2→3); anteroposterior length of the antorbital fossa anterior to the antorbital fenestra versus length of the antorbital fenestra = 0.28–0.43 (54:0→1); eight to nine tooth positions in the maxilla (73:1→0); ventral process of the squamosal forms more than half of the posterior border of the infratemporal fenestra (140:0→1); anterior process of the quadratojugal distinctly present, in which the lower temporal bar is complete and participates in the posteroventral border of the infratemporal fenestra, and process finishes close to the base of the posterior process of the jugal (146:2→3); parietal extends over interorbital region (152:0→1); lateral

ramus of the pterygoid posterolaterally oriented, forming an obtuse angle with the anterior ramus (189:1→0); mandibular symphysis present along one-third of the lower jaw (251:0→1); tooth bearing portion of the dentary ventrally curved or deflected (253:1→2); surangular with a laterally projecting shelf that possesses a strongly convex lateral edge (270:2→3); three sacral vertebrae (348:0→1); ectepicondylar region of the humerus without supinator process, groove or foramen (398:1→2); perforated acetabulum (423:0→1); total length of the pubis versus anteroposterior length of the acetabulum = 2.84–3.43 (439:0→1); anterior and posterior portions of the acetabular margin of the pubis recessed (440:0→1); ischium with articular surfaces with the ilium and pubis separated by a non-articulating concave surface (450:0→2); femur with anterior trochanter (467:0→1); articulation between astragalus and calcaneum concavoconvex with concavity on the astragalus (497:1→2); and fibular facet of the calcaneum slightly convex (516:1→0).

Suchia Krebs, 1974

Definition. The least inclusive clade containing *Aetosaurus ferratus* Fraas, 1877, and *Rauisuchus tiradentes* Huene, 1942, *Prestosuchus chiniquensis* Huene, 1942, *Crocodylus niloticus* Laurenti, 1768 (node-based) (Nesbitt, 2011).

Temporal range. Late Early Triassic (latest Olenekian, *Ctenosauriscus koeneni*; Butler et al., 2011) to Recent (*Crocodylus niloticus*).

Synapomorphies. Triangular dorsal process with clear dorsal apex formed by discrete expansion of the posterior end of the horizontal process of the maxilla in lateral view (63:0→1); dorsolateral margin of the anterior portion of the nasal with distinct longitudinal ridge on the lateral edge (80:0→1); dorsal vertebrae with well-rimed lateral fossa on the centrum below the neurocentral suture (332:1→2); zygapophyses

mainly oriented in the parasagittal axis and close to each other medially, respectively, in anterior–middle dorsal vertebrae (337:1→0); proximal end of the humerus approximately symmetric in anterior view (391:1→0); preacetabular process of the ilium longer than two thirds of its height and does not extend beyond the level of the anterior margin of the pubic peduncle (428:1→2); calcaneal tuber midshaft just less than twice the transverse width of the fibular facet (510:1→2).

Unnamed clade (*Koilamasuchus gonzalezdiazi* + Loricata)

Temporal range. Late Early Triassic (latest Olenekian, *Ctenosauriscus koeneni*; Butler et al., 2011) to Recent (*Crocodylus niloticus*).

Synapomorphies. Anterior edge of paramedian presacral dorsal osteoderms with a distinct anterior process (= leaf shaped) (557:0→1).

Unnamed clade (Gracilisuchidae + Loricata)

Temporal range. Late Early Triassic (latest Olenekian, *Ctenosauriscus koeneni*; Butler et al., 2011) to Recent (*Crocodylus niloticus*).

Synapomorphies. Transverse width of the proximal end of the humerus versus total length of the bone in mature individuals = 0.20–0.41 (388:1→0); and presacral paramedian osteoderms with a distinct longitudinal bend near the lateral edge (558:0→1).

Gracilisuchidae Butler et al., 2014a

Definition. The most inclusive clade containing *Gracilisuchus stipanicicorum* Romer, 1972b, but not *Ornithosuchus longidens* (Huxley, 1877), *Aetosaurus ferratus* Fraas, 1877, *Poposaurus gracilis* Mehl, 1915, *Postosuchus kirkpatricki* Chatterjee, 1985,

Rutiodon carolinensis (Emmons, 1856), *Erpetosuchus granti* Newton, 1894, *Revueltosaurus callenderi* Hunt, 1989, *Crocodylus niloticus* (Laurenti, 1768), or *Passer domesticus* Linnaeus, 1758 (stem-based) (Butler et al., 2014a).

Temporal range. Early Middle Triassic (Anisian, *Turfanosuchus dabanensis*) to late Middle−early Late Triassic (Ladinian−earliest Carnian, *Gracilisuchus stipanicicorum*) (Butler et al., 2014a).

Synapomorphies. Postnarial process of the premaxilla fits into slot of the nasal (39:0→2); length of the portion of the maxilla anterior to the antorbital fenestra versus the total length of the bone = 0.12–0.22 (49:1→0); antorbital fossa on the lateral surface of the maxilla present on the ascending and horizontal processes, but does not reach the posteroventral corner of the fenestra (53:3→2); anterior process of the lacrimal forms the entire or almost the entire dorsal border of the antorbital fenestra (85:0→1); ventral process of the squamosal anteroventrally directed at 45º or less (139:0→1); cervical and dorsal vertebrae with fan-shaped neural spine in lateral view (300:0→1); anterior and middle postaxial cervical neural spines with an anterior overhang (322:0→1); and internal tuberosity of the humerus not distinctly separated from the proximal articular surface (392:1→0).

Unnamed clade (“*Chasmatosaurus ultimus*” + Loricata)

Temporal range. Late Early Triassic (latest Olenekian, *Ctenosauriscus koeneni*; Butler et al., 2011) to Recent (*Crocodylus niloticus*).

Synapomorphies. Palatal process of the maxilla distinctly dorsally placed from the base of the interdental plates (65:0→1); and dorsal margin of the anterior portion of the dentary dorsally expanded compared to the dorsal margin of the posterior portion (257:0→1).

***Prestosuchus chiniquensis* + *Batrachotomus kupferzellensis* (?= Paracrocodylomorpha)**

Temporal range. Late Early Triassic (latest Olenekian, *Ctenosauriscus koeneni*; Butler et al., 2011) to Recent (*Crocodylus niloticus*).

Synapomorphies. Minimum height of the dentary versus length of the alveolar margin (including edentulous anterior end if present) = 0.16–0.19 (252:0→1); and tooth bearing portion of the dentary mostly straight (253:1→0).

Ornithodira Gauthier, 1986

Definition. The least inclusive clade containing *Pterodactylus antiquus* Sömmerring, 1812, and *Passer domesticus* Linnaeus, 1758 (node-based) (Nesbitt, 2011).

Temporal range. Early Middle Triassic (Anisian, *Asilisaurus kongwe*; Nesbitt et al., 2010) to Recent (*Passer domesticus*). The presence of probable dinosauromorph footprints in the Olenekian may pull back the temporal range of ornithodirans into the late Early Triassic (Brusatte et al., 2011).

Synapomorphies. Scapula and coracoid fused with each other without line of suture in mature individuals (359:1→0); total length of the scapula versus minimum anteroposterior width of the scapular blade = 7.92–10.45 (362:1→2); pelvic girdle with acetabular antitrochanter (425:0→1); preacetabular process of the ilium longer than two thirds of its height and does not extend beyond the level of the anterior margin of the pubic peduncle (428:1→2); dorsal margin of the iliac blade concave (434:1→2); thin femoral bone wall thickness at or near midshaft, thickness/diameter <0.3 (474:0→1); anterior hollow of the astragalus reduced to a foramen (= extensor canal) or absent (502:0→1); astragalus without posterior groove (503:0→1);

anteromedial corner of the astragalus acute in proximal view (504:0→1); calcaneal tuber absent or incipient (508:1→0); distal tarsal 4 transverse width subequal to distal tarsal 3 (523:0→1); articular facet for metatarsal V on distal tarsal 4 less than half of the lateral surface of the bone (524:0→1); compact metatarsus, metatarsals I–IV tightly bunched (528:0→1); and dorsal osteoderms absent (548:1/2→0).

Dinosauromorpha Benton, 1985

Definition. The most inclusive clade containing *Passer domesticus* Linnaeus, 1758, but not *Pterodactylus antiquus* Sömmerring, 1812, *Ornithosuchus longidens* Huxley, 1877, *Crocodylus niloticus* Laurenti, 1768 (stem-based) (Sereno, 2005).

Temporal range. Early Middle Triassic (Anisian, *Asilisaurus kongwe*; Nesbitt et al., 2010) to Recent (*Passer domesticus*). The presence of probable dinosauromorph footprints in the Olenekian may pull back the temporal range of dinosauromorphs into the late Early Triassic (Brusatte et al., 2011).

Synapomorphies. Pubis with prominent tuberosity for the attachment of the ambiens muscle in mature individuals (441:1→0); proximal articular surface of the femur (= posterolateral portion of the head sensu Nesbitt 2011) extends under the proximal surface of the bone (459:0→1); tibia with anteriorly straight, distinct cnemial crest (482:0→1); metatarsal V without a hook-shaped proximal end (540:1→0); and pedal digit V absent (544:0→2).

Dinosauriformes Novas, 1992

Definition. The least inclusive clade containing *Passer domesticus* Linnaeus, 1758, and *Marasuchus lilloensis* (Romer, 1972c) (node-based) (Sereno, 2005).

Temporal range. Early Middle Triassic (Anisian, *Asilisaurus kongwe*; Nesbitt et al., 2010) to Recent (*Passer domesticus*).

Synapomorphies. Contact between pubis and ischium reduced to a thin proximal articulation (437:0→1); total length of the pubis versus anteroposterior length of the acetabulum = 2.84–3.43 (439:0→1); anterior and posterior portions of the acetabular margin of the pubis recessed (440:0→1); transverse width of conjoined pubic aprons versus total length of the bone = 0.27–0.59 (445:2→0); ischium with proximal articular surfaces with the ilium and pubis separated by a fossa (450:0→1); femur with intertrochanteric fossa (= trochanteric fossa of Novas, 1996) on the posterior surface of the proximal end (464:1→0); femur with anterior trochanter (467:0→1); femur with trochanteric shelf (468:0→1); femur without anterior extensor groove in the distal end (479:1→0); tibia with posterolateral process (= lateral malleolus) in the distal end (486:0→1); lateral side of the distal portion of the tibia with a proximodistally oriented groove (489:0→1); and astragalus with ascending process (501:0→1).

Unnamed clade (Silesauridae + Dinosauria)

Temporal range. Early Middle Triassic (Anisian, *Asilisaurus kongwe*; Nesbitt et al., 2010) to Recent (*Passer domesticus*).

Synapomorphies. Posterior surface of the supraocciptial with a prominent median, vertical peg (199:0→1); anterior tympanic recess on the lateral side of the braincase (230:0→1); atlantal articulation facet in the axial intercentrum concave with upturned lateral borders (306:0→1); total length of the pubis versus anteroposterior length of the acetabulum = 3.94–4.87 (439:1→2); transverse width of the distal portion of the pubis significantly narrower than the proximal width (448:0→1); extensive medial

contact between ischia but the dorsal margins are separated (452:0→1); dorsolateral trochanter on the anterolateral surface of the proximal end of the femur (465:0→1); anterior edge of the proximal portion of the fibula tapers to a point and arched anteromedially (491:0→1); ascending process of the astragalus restricted to the anterior half of the astragalar depth (501:1→2); metatarsals I and V mid-shaft diameters lower than those of metatarsals II–IV (531:0→1); and distal articular surface of metatarsal IV as broad as deep as or deeper than broad (asymmetrical) (538:0→1).

Silesauridae Langer et al., 2010a

Definition. All archosaurs closer to *Silesaurus opolensis* Dzik, 2003, than to *Heterodontosaurus tucki* Crompton and Charig, 1962 and *Marasuchus lilloensis* (Romer, 1972c) (stem-based) (Langer et al., 2010a).

Temporal range. Early Middle Triassic (Anisian, *Asilisaurus kongwe*; Nesbitt et al., 2010) to late Late Triassic (middle Norian, *Eucoelophysis baldwini*; Ezcurra, 2006).

Synapomorphies. Dorsal margin of the neural spine of the axis dorsally convex (310:1→0); and ratio between transverse width of the diapophysis and length of the centrum in anterior dorsal vertebrae <0.70 (335:1→0).

Dinosauria Owen, 1842

Definition. The least inclusive clade containing *Triceratops horridus* (Marsh, 1889) and *Passer domesticus* Linnaeus, 1758 (node-based) (Sereno, 2005).

Temporal range. Early Late Triassic (late Carnian to earliest Norian, *Herrerasaurus ischigualastensis*; Martínez et al., 2011) to Recent (*Passer domesticus*).

Synapomorphies. Elevated rim of the orbit absent or incipient (17:1→0); anteroposterior length of the main body of the premaxilla versus its maximum dorsoventral height = 1.07–2.00 (28:2→1); narial fossa of the premaxilla expanded in the anteroventral corner of the naris (32:0→1); postnarial process of the premaxilla wide, plate-like (37:1→0); frontal participates on the anteromedial corner of the supratemporal fossa (111:0→1); lower jaw with posterior surangular foramen (273:0→1); epipophysis in anterior postaxial cervical vertebrae (315:0→1); Forelimb-hindlimb length ratio <0.55 (386:0→1); perforated acetabulum (423:0→1); main axis of the postacetabular process of the ilium mainly posteriorly oriented in lateral or medial views (432:0→1); pubic shaft vertically or posteroventrally oriented (442:0→1); pubic shaft rod-like and straight (443:0→1); articular surface with the ilium and pubis in the proximal end of the ischium separated by a non-articulating concave surface (450:1→2); fourth trochanter asymmetrical, with the distal margin forming a steeper angle to the shaft in medial or lateral view (472:0→1); cnemial crest of the proximal end of the tibia anterolaterally curved (482:1→2); posterior surface of the distal end of the tibia with a distinct proximodistally oriented ridge (487:0→1); and proximal portion of the fibula symmetrical or nearly symmetrical in lateral view (492:1→0).